

NASA CR-134991

(NASA-CR-134991) ASSESSMENT OF NDE
RELIABILITY DATA Final Report, Jul. 1974 -
Sep. 1975 (General Dynamics/Fort Worth)
HC \$11.75 CSCI 14D

N76-33525

Unclas
G3/38 05376

ASSESSMENT OF NDE RELIABILITY DATA

B. G. W. Yee, F. H. Chang,
J. C. Couchman and G. H. Lemon

General Dynamics
Fort Worth Division
Fort Worth, Texas

and

P. F. Packman

Vanderbilt University
Nashville, Tennessee \

Prepared for

NATIONAL AERONAUTICS AND SPACE ADMINISTRATION

NASA Lewis Research Center
Contract NAS-3-18907

REPRODUCED BY
NATIONAL TECHNICAL
INFORMATION SERVICE
U. S. DEPARTMENT OF COMMERCE
SPRINGFIELD, VA. 22161

N O T I C E

THIS DOCUMENT HAS BEEN REPRODUCED FROM THE BEST COPY FURNISHED US BY THE SPONSORING AGENCY. ALTHOUGH IT IS RECOGNIZED THAT CERTAIN PORTIONS ARE ILLEGIBLE, IT IS BEING RELEASED IN THE INTEREST OF MAKING AVAILABLE AS MUCH INFORMATION AS POSSIBLE.

1. Report No. NASA CR-134991		2. Government Accession No.		3. Recipient's Catalog No.	
4. Title and Subtitle ASSESSMENT OF NDE RELIABILITY DATA				5. Report Date October 1976	
				6. Performing Organization Code	
7. Author(s) B. G. W. Yee, F. H. Chang, J. C. Couchman and G. H. Lemon of General Dynamics and P. F. Packman, Vanderbilt University				8. Performing Organization Report No.	
9. Performing Organization Name and Address General Dynamics/Fort Worth Division Fort Worth, Texas and Vanderbilt University, Nashville, Tennessee				10. Work Unit No. YHG 6780	
				11. Contract or Grant No. NAS3-18907	
12. Sponsoring Agency Name and Address National Aeronautics and Space Administration Washington, D. C. 20546				13. Type of Report and Period Covered Contractor Report July 1974 - Sept 1975	
				14. Sponsoring Agency Code	
15. Supplementary Notes Project Manager, S. J. Klima, Materials & Structures Division NASA Lewis Research Center, Cleveland, Ohio					
16. Abstract Twenty sets of relevant NDE reliability data have been identified, collected, compiled, and categorized. Three relevant on-going programs are being monitored for future usage. A criterion for the selection of data for statistical analysis considerations has been formulated. A model to grade the quality and validity of the data sets has been developed. Data input formats, which record the pertinent parameters of the defect/specimen and inspection procedures, have been formulated for each NDE method. A comprehensive computer program has been written to calculate the probability of flaw detection at several confidence levels by the binomial distribution. This program also selects the desired data sets for pooling and tests the statistical pooling criteria before calculating the composite detection reliability. Probability of detection curves at 95 and 50 percent confidence levels have been plotted for individual sets of relevant data as well as for several sets of merged data with common sets of NDE parameters.					
17. Key Words (Suggested by Author(s)) NDE Reliability Probability of Detection Confidence Level Fatigue Cracks				18. Distribution Statement Unclassified	
19. Security Classif. (of this report) Unclassified		20. Security Classif. (of this page) Unclassified			

* For sale by the National Technical Information Service, Springfield, Virginia 22151

ASSESSMENT OF NDE RELIABILITY DATA

B. G. W. Yee, F. H. Chang,
J. C. Couchman and G. H. Lemon

General Dynamics
Fort Worth Division
Fort Worth, Texas

and

P. F. Packman
Vanderbilt University
Nashville, Tennessee

Final Report

Prepared for
NATIONAL AERONAUTICS & SPACE ADMINISTRATION
Lewis Research Center
Cleveland, Ohio

Contract NAS 3-18907

Foreword

This final report covers the work performed under Contract NAS-3-18907 from July 1974 to September 1975. The study was accomplished by General Dynamics Corporation, Fort Worth Division, Fort Worth, Texas and Vanderbilt University, Nashville, Tennessee. The program was managed by Dr. B. G. W. Yee of General Dynamics, with Dr. J. C. Couchman and Dr. F. H. Chang serving as principal investigators. Valuable contributions were made to the development of the statistical analysis by Dr. G. H. Lemon and computer programming by J. S. Kunselman and T. Walker. Dr. P. F. Packman of Vanderbilt University served as associate program manager. The program was under the technical direction of Mr. S. J. Klima, NASA Lewis Research Center, Cleveland, Ohio.

Participants in this program are indebted to many people in the NDE community for furnishing data to this program and for providing consultation.

Thank you!

TABLE OF CONTENTS

<u>Section</u>	<u>Page</u>
SUMMARY	vii
I INTRODUCTION	1
II ACQUISITION OF INFORMATION	2
2.1 Acquisition of NDE Reliability-Related Data	2
2.2 Bibliography	2
2.3 On-Going Programs	5
III SCREENING AND SEPARATION OF DATA BY NDE METHOD AND MATERIAL	6
3.1 Criterion for Selection of Data for Statistical Analysis	6
3.2 Separation and Categorization of Data Sets	7
IV STATISTICAL DETERMINATION OF NDE RELIABILITY	13
4.1 Introduction	13
4.2 Application of Binomial Distribution	13
4.2.1 Confidence Interval Estimates of the True Probability of Detection	14
4.2.2 Sample Size Determination	16
4.3 Comparison of Alternative Statistical Procedures	17
4.4 Data Cumulation Methods	19
V RESULTS	21
VI DISCUSSION OF RESULTS	29
6.1 Effects of Material, Source, and Inspection Parameters	30
6.2 Statistical Analysis Procedures	33
6.3 Data Deficiencies	34
6.4 Application to Fracture Mechanics	35
6.5 Optimum Demonstration Program	37

TABLE OF CONTENTS
(CONTINUED)

<u>Section</u>	<u>Page</u>
VII CONCLUSIONS	43
APPENDICES	
A - A Model to Grade the Quality and Validity of Data Sets	A-1 thru A-5
B - Data Pooling	B-1 thru B-4
C - NASA. FTN Computer Code	C-1 thru C-46
D - NDE Reliability Plots	D-1 thru D-344

LIST OF FIGURES

<u>Figure No.</u>		<u>Page</u>
6-1	Differential and Integral Crack Length Distribution Function for the Martin Marietta NDE Demonstration Program	36
6-2	Conditions for Success in Selecting a Sample Size that will Potentially Demonstrate POD90(CL95)	38

LIST OF TABLES

<u>Table No.</u>		<u>Page</u>
3-1	Status and Category of Data Considered for NDE Reliability Assessment	8
3-2	Data Grouping According to Specimen Thickness and Complexity	9
4-1	POD Estimation Method Comparisons	18
5-1	Summary of NDE Data Statistically Analyzed	22
5-2	List of Alloys with Valid Data	28
6-1	Interval Sample Size and Successes Required to Achieve POD90(CL95)	33

SUMMARY

The overall objective of this program is to assess available nondestructive testing data for the determination of the sensitivity and reliability of state-of-the-art production NDE methods for flaw detection on metallic materials. This program was separated into four different tasks. They were:

- | | |
|----------|---|
| Task I | Acquisition of Information |
| Task II | Screening and Separation of Data by NDE Method and Material |
| Task III | Statistical Determination of NDE Reliability |
| Task IV | Reporting |

Twenty sets of relevant NDE reliability data have been identified, collected, compiled, and categorized. Three relevant on-going programs have also been identified. A criterion for the selection of data for statistical analysis considerations has been formulated. A model to grade the quality and validity of the data sets has been developed. Data input formats, which record the pertinent parameters of the defect/specimen and inspection procedures, have been formulated for each NDE method. A comprehensive computer program has been written to calculate the probability of flaw detection at several confidence levels by the binomial distribution. This program also selects the desired data sets for pooling, and tests the statistical pooling criteria before calculating the composite detection reliability. Probability of detection curves at 95 and 50 percent confidence levels have been plotted by NDE technique and material type for individual sets of data as well as for merged data.

I. INTRODUCTION

In order to apply linear-elastic fracture mechanics to structural design, NDE has to show at a high level of confidence that no flaw larger than a specific size exists in the structure. To establish the minimum detectable flaw size, many companies and organizations have conducted NDE demonstration programs. Most of these demonstration programs have been conducted in the production and field-service environment, but some have been conducted in the laboratory environment.

The results obtained from demonstration programs are lacking in universal agreement. This lack of agreement is not surprising because each company or organization may use a different NDE procedure, different personnel, different procedures and parameters to generate the test flaws, different flaws and material types, and even different statistical analysis procedures. There appears to be a need to (1) collect much of the available NDE reliability data, (2) closely examine all the parameters that could affect the detection reliability, (3) compare the parameters used by each organization to obtain the data, and (4) attempt to identify the parameters that most likely cause observable differences in detection reliability. It appears worthwhile to obtain a composite detection reliability for each NDE method, material type, and flaw type by pooling data obtained from several sources. At the same time, the merits and shortcomings of several statistical analysis procedures should be carefully examined and the procedure most suitable for the analysis of NDE reliability data should be selected. Any needs for improved methods should be identified.

The program reported on in this document was intended to collect all available NDE data, screen and separate the data by NDE method and material, perform statistical analyses, and evaluate the state-of-the-art in NDE reliability.

II. ACQUISITION OF INFORMATION

The acquisition of NDE reliability related data, identification of on-going programs, and preparation of a bibliography of the acquired data is discussed in this section.

2.1 Acquisition of NDE Reliability Related Data

Twenty-three sets of potentially useful data have been identified during this program and twenty sets were acquired. Three sets of data involve on-going programs and the data were not made available for inclusion in this study. Of the twenty sets of data received, only seven sets were statistically analyzed. The thirteen sets of data that were not statistically analyzed were rejected because they did not satisfy the selection criterion discussed in Section III of this report or the owner refused to permit the data to be used.

2.2 Bibliography

The twenty sets of NDE reliability related data that have been acquired are listed below. Some of the references are private data in which case only company or committee report numbers are available. Several references to government funded programs, which have not been published can only be identified by sponsoring agencies and the name of an individual at the company where the work was conducted. Copies of these data can be obtained by either contacting an individual within the sponsoring agency or an individual associated with the company.

References

1. Pettit, D. E. and Hoepfner, D. W., "Fatigue Flaw Growth and NDI Evaluation for Preventing Through Cracks in Spacecraft Tankage Structures," NASA CR-128600 (NAS-9-11722), September 25, 1972, Lockheed, CA.
2. Rummel, W. D., Todd, P. H. Jr., Frecska, S. A. and Rathke, R. A., "The Detection of Fatigue Cracks by Non-destructive Test Methods," NASA CR-2369 (NAS-9-12276), February 1974, Martin Marietta.
3. Packman, P. F., et al, "The Applicability of Fracture Mechanics Nondestructive Testing Design Criterion," AFML-TR68-32, May 1968.
4. Anderson, R. T., Delacy, T. J., and Stewart, R. C., "Detection of Fatigue Cracks by Nondestructive Testing Methods," NASA CR-128946 (NAS-9-12326), March 1973.
5. Buchanan, R. A., "Analysis of Test Data on PVRC specification No. 3, Ultrasonic Examination of Forgings, Revisions I and II, January 14, 1974 (PVRC Committee on ND Examination of Mat. for Pressure Components, PVRC Welding Research Council).
6. Buchanan, R. A., and Talbot, T. F., "Analysis of ND Examination of PVRC Plate-Weld Specimen 251J," May 21, 1973. (PVRC Committee on ND Examination of Mat. for Pressure Components, PVRC WRC).
7. Yee, B. G. W., et al, "Evaluation and Optimization of the Advanced Signal Counting Technique on Weldments," General Dynamics/FWD, FZM-5917, January 31, 1972.
8. Bishop, C. R., "Nondestructive Evaluation of Fatigue Cracks," Rockwell International-Space Division SD73-SH-0219 (NAS-9-14000), September 1973.
9. Sattler, F. J., "Nondestructive Flaw Definition Techniques for Critical Defect Determination," NASA-CR-72602 (NAS-3-11221), January 1970.

10. Southworth, H. L., Steele, N. W., Torelli, P. P., et al, "Practical Sensitivity Limits of Production Nondestructive Testing Methods in Aluminum and Steel," AFML-TR-74-241, November 1974.
11. Moyzis, J. W., Jr., "Reliability of Airframe Inspections at the Depot Maintenance Level," Boeing, Wichita, Kansas. (Eddy current inspection of bolt holes in KC-135A wings). Boeing No. 1554, (No date).
12. Hannah, K. J., Cross, B. T., and Tooley, W. M., "Development of the Ultrasonic Delta Technique for Aluminum Welds and Materials," NASA CR-61952 (NAS 8-18009), May 15, 1968.
13. Sproat, W. H., "Reliability Analysis of C-5A Pylon Inspection," Lockheed-Georgia Internal Document No. LG-72-ER0107, (No date).
14. Sproat, W. H., "Reliability Evaluation of Nondestructive Inspection Methods Using C-130 Wing Boxes," Lockheed-Georgia Internal Document No. LG-72-ER0107, (No date).
15. Lord, R. J., "Evaluation of the Reliability and Sensitivity of NDT Methods for Titanium Alloys," AFML-TR-73-107, June 1974.
16. B-1 USAF/Rockwell International NDI Demonstration Program, E. L. Caustin, Director of Quality & Reliability Assurance, Los Angeles Division, (Set of Reports) 1972-1973.
17. A10 USAF/Fairchild Hiller NDI Demonstration Program, Ted Renshaw of Fairchild Hiller, (Set of Reports), Sept. 1973.
18. F-111 USAF/General Dynamics NDI Human Factors Study Program. Bill Kloster of General Dynamics, Fort Worth Division, (Set of Reports) 1971.
19. AFML Round Robin Results on (1) Delta Scan and (2) Magnetic Particle, Lee Gulley, AFML, WPAFB, Dayton, Ohio, March 1971.
20. Raatz, C. F., Senske, R. A. Woodmansee, W. E., et al. "Detection of Cracks Under Installed Fasteners," AFML-TR-74-80, April 1974.

2.3 On-Going Programs

There are several on-going programs that are currently known. Of these, only three are government funded and their results will be available to the public for analysis. The data from the privately funded programs may never be made available for public analysis.

The three government funded on-going programs are:

1. Crack detection reliability on welded plates and structures, Martin Marietta, Ward Rummel, sponsored by NASA/Johnson Space Center, NAS 9-13578.
2. Crack detection reliability on actual aircraft structures at the depot level, Lockheed, GA., W. Lewis, sponsored by Kelly Air Force Base.
3. Crack detection reliability on bolt holes on F-111 fatigue tested structures, General Dynamics, Fort Worth Division, B. G. W. Yee, Sponsored by SMALC.

III. SCREENING AND SEPARATION OF DATA BY NDE METHOD AND MATERIAL

This section describes the development of data selection criteria, separation and categorization of data, development of a model to grade quality of the data, and the development of a data input format for each NDE method.

3.1 Criteria for Selection of Data for Statistical Analysis

All of the reliability related NDE data are not necessarily suitable for statistical analysis. Some are lacking in the documentation of certain key pertinent parameters, such as the defect dimension, defect type, NDE method, etc. Statistical analysis of data when the key pertinent parameters are not documented would be marginal in value. A data selection criteria is needed to screen the data and prejudge the suitability of the data for statistical analysis. Such a criteria is necessarily subjective because it involves human judgment of data value or usefulness. It is felt that such a subjective criteria will still be useful to screen out data having marginal statistical value and to eliminate lost time in processing the data.

To be eligible for statistical analysis, a set of data must satisfy the following conditions:

- a) An NDE procedure or specification must accompany the data which clearly describes the equipment and the parameters used so that the data may be reproduced in other facilities (assuming the same equipment or its equivalent is used).
- b) The defect dimensions and specimen geometry must be well documented so that data may be statistically analyzed and compared to defect detection in the proper defect size range. When artificial methods of defect fabrication are used, at least ten percent (10%) of all defects in a given set must be destructively tested to obtain the defect dimensions. For methods that are used to produce multiple defects in a specimen or methods that are questionable for producing controllable defect dimensions, at least fifty percent (50%) of all defects in a given set must be destructively tested to verify the defect dimensions.

The model that was developed to grade the quality of the data was very subjective. It consisted of assigning weighting factors and summing up the weighting factors to obtain an overall factor that is an index of data quality. The model is included in Appendix A.

Data pooling tests that were coded in the NASA data processing code (reproduced in Appendix B) provided a means for isolating input errors and identifying any data set that may be suspect. The tests are derived from binomial statistics equations which are developed in the next section.

The computer code developed for processing the NDE reliability data is described in Appendix C. Included is a complete description of data input formats and parameter keys.

3.2 Separation and Categorization of Data Sets

The twenty sets of data listed in the Bibliography in Subsection 2.2 can be separated into three categories. Table 3-1 describes the data separated into the three categories and the status of these data sets. The first category is the data that appear to satisfy the criteria discussed in Subsection 3.1, and they will be considered for statistical analysis. There are seven (7) sets of data in this category. The second category is data that probably could be used if permission to use the data is granted by the rightful owner of the data. There are two sets of data in this category. The third category is the data that are either lacking in the inspection procedure documentation or defect dimension documentation. There are eleven sets of data in this category. The data sets in each of the three categories are presented in Table 3-1.

A large majority of the data were obtained on thin flat plates which contain fatigue cracks or weld defects. There are few sets of data that were obtained with relatively complex shaped specimens such as a T, I, or H shape. In order to gain a better understanding of the availability of data on material type, defect type, and specimen complexity, a table (Table 3-2) is constructed to categorize the data sets according to test specimen complexity. Within each data set, a brief description of the material type, NDE methods, and defect type is presented.

The materials and shapes for which valid data were obtained and statistical analysis results are computed are tabulated later in Section V (RESULTS).

Table 3-1 STATUS AND CATEGORY OF DATA
CONSIDERED FOR NDE RELIABILITY ASSESSMENT

Data that satisfy the criteria discussed in Subsection 3.1 and were statistically analyzed	Data that lack owner permission use	Data that were not statistically analyzed due to the lack of sufficient inspection procedure or defect dimension documentation or both
<u>References:</u> 2 3 4 8 10 11 16	<u>References:</u> 5 Pressure Vessel Research Committee approval needed before data can be used 6 Same as 5 above	<u>References:</u> 1 7 9 12 13 14 15 17 18 19 20

Table 3-2 Data Grouping According to Specimen Thickness and Complexity

Flat Plates and Simple Shape	Cylindrical, I, H, T and other Moderately Complex Shapes	Actual Aircraft Structures
<p>References:</p> <p>1 2219-T87 Al up to 1 cm thick</p> <ul style="list-style-type: none"> o Cracks in plates and welded plates o Ultrasonics, penetrant, eddy current, and X-ray o Laboratory environment <p>2 2219-T87 Al up to 1 cm thick</p> <ul style="list-style-type: none"> o Fatigue cracks in flat plates o Ultrasonic, penetrant, eddy current, and X-ray o Laboratory environment (mostly) <p>4 2219-T87 Al up to 1 cm thick</p> <ul style="list-style-type: none"> o Fatigue cracks in flat plates o Ultrasonic, penetrant, eddy current, and X-ray o Laboratory environment (mostly) 	<p>References:</p> <p>3 7075-T6511 Al</p> <ul style="list-style-type: none"> o Fatigue cracks in cylindrical tubes o Ultrasonic, penetrant, and X-ray <p>4300 V Steel</p> <ul style="list-style-type: none"> o Fatigue cracks in cylindrical tubes o Ultrasonics, penetrant, X-ray, and magnetic particle o Laboratory environment <p>10 2024 Al</p> <ul style="list-style-type: none"> o Forged defects o Ultrasonic, penetrant, eddy current, X-ray o Production environment <p>4340 M Steel</p> <ul style="list-style-type: none"> o Forged defects o Ultrasonics, penetrant eddy current, X-ray, and magnetic particles o Production environment <p>Some grinding cracks and hydrogen embrittlement cracks</p>	<p>References:</p> <p>11 7178-T651 Al</p> <ul style="list-style-type: none"> o Naturally occurring fatigue cracks in bolt holes o Eddy current o Laboratory and depot level <p>13 6Al-4V-Ti and 7075-T6Al</p> <ul style="list-style-type: none"> o Fatigue cracks off C-5A Pylon (actual and simulated) o Ultrasonics and X-ray <p>14 7075-T6 Al</p> <ul style="list-style-type: none"> o Fatigue cracks off C-130 wing boxes (actual and simulated) o Ultrasonics and eddy current <p>20 KC-135 lower wing skin panel and laboratory specimens with fatigue cracks under installed fastener</p> <ul style="list-style-type: none"> o Ultrasonic o Laboratory and field environment

Table 3-2 (Continued)

Flat Plates and Simple Shape	Cylindrical, I, H, T and other Moderately Complex Shapes	Actual Aircraft Structure
<p>5 Steel forging up to 25 cm thick</p> <ul style="list-style-type: none"> o Induced and naturally occurring defects o Ultrasonics o Laboratory environment <p>6 Steel welded-plates up to 28 cm thick</p> <ul style="list-style-type: none"> o Induced weld defects o Ultrasonics and X-ray o Laboratory environment <p>7 2219-T87 welded plates of 0.62 and 1.25 cm thick</p> <ul style="list-style-type: none"> o All types of weld defects o Ultrasonic and X-ray <p>8 2219-T87 Al up to 1 cm thick</p> <ul style="list-style-type: none"> o Fatigue cracks in flat plates o Ultrasonic, penetrant, eddy current, and X-ray o Production environment (mostly) <p>9 2219-T87 and 2014-T6Al up to 2.5 cm thick 6Al-4V-Ti and 5Al-2.5 Sn Ti up to 1½ cm thick</p> <ul style="list-style-type: none"> o Fatigue cracks in flat plates weld defects in plates 	<p>15 6Al-4V-Ti</p> <ul style="list-style-type: none"> o Induced forging defects o Ultrasonics, penetrant X-ray o Most production environment <p>18 D6ac Steel</p> <ul style="list-style-type: none"> o Induced forging defects o Ultrasonics, magnetic particle and rubber o Production environment 	

Table 3-2 (Continued)

Flat Plates and Simple Shape	Cylindrical, I, H, T and other Moderately Complex Shapes	Actual Aircraft Structure
<ul style="list-style-type: none"> o Ultrasonic, penetrant, X-ray, and eddy current o Laboratory environment <p>12 2219-T87 Welded plates of 1.25 and 2.5 cm thick</p> <ul style="list-style-type: none"> o All types of weld defects o Ultrasonic and X-ray <p>16 6Al-4V-Ti up to 13 cm thick</p> <ul style="list-style-type: none"> o Ultrasonic o Flat bottom holes and induced defects <p> 6Al-4V-Ti Diffusion Bonded thin plates</p> <ul style="list-style-type: none"> o Induced defects o Penetrant <p> Al Samples</p> <ul style="list-style-type: none"> o Fatigue cracks in flat plates o Penetrant <p> 6Al-4V-Ti</p> <ul style="list-style-type: none"> o Fatigue cracks in flat plates o Penetrant <p> Steel</p> <ul style="list-style-type: none"> o Induced weld defects o Ultrasonics 		

Table 3-2 (Continued)

Flat Plates and Simple Shape	Cylindrical, I, H, T and other Moderately Complex Shapes	Actual Aircraft Structure
<p>Al, Ti, and Steel Plates (multiple)</p> <ul style="list-style-type: none"> o Cracks in fastener holes o Eddy current <p>All in production environment</p> <p>17 Similar to those described in Reference 16</p> <p>19 o D6ac Steel Plate Delta Scan Ultrasonics</p>		<p>19 o D6ac, 4340, and other Steel Alloys Actual Aircraft Structure Magnetic Particle</p>

IV STATISTICAL DETERMINATION OF NDE RELIABILITY

This section describes the binomial statistical method, cumulative schemes, statistical pooling procedure, and digital computer code for computing NDE reliability.

4.1 Introduction

There are four possible outcomes from any nondestructive inspection of an item: (1) detection of a defect that is present, (2) non-detection of a defect that is present, (3) detection of a defect that is not present (false indication), and (4) non-detection of a defect that is not present. Because of these four possible outcomes, any single inspection may be called a quadrinomial event. Although it is recognized that false indications of defects and true indications of non-defective items (cases 3 and 4) are of practical significance to both the manufacturer and the customer, it is beyond the scope of this investigation to develop a straightforward statistical method for handling the quadrinomial event.

Preliminary indications show that most NDE reliability investigations have neglected to report information concerning either false indications of defects, or true indications that specimens contained no intentionally induced flaws. However, the data input format discussed in the previous section provides for storage of information concerning false indications for future use when more of these data become available.

Cases (1) and (2) involve either a detection or non-detection of a defect that is known to exist. This event can best be described statistically by applying the binomial distribution. The Normal, Chi-square, and Poisson distributions are sometimes used as approximations to the binomial. Their applicability to the problem of NDE reliability is to be considered in the later sections of this report.

4.2 Application of Binomial Distribution

An event that has only two possible outcomes is referred to as a binomial event. Suppose, for example, an experiment in NDE is performed where N specimens, all containing identical

flaws, are routed through an ultrasonic inspection system. Suppose further, that the system capability does not change throughout the entire inspection process, i.e., each specimen is evaluated independently of the others. Let p equal the true, (but as yet unknown) probability of detecting each flaw and $q=1-p$ be the probability of missing each flaw. Assuming p remains the same for all specimens, the random variable X can be defined as being the number of flaws that are detected in any given experiment. X , then, is referred to as a binomial random variable with parameters N and p . Its possible values are $0, 1, 2, \dots, N$. Equivalently, it can be said that X has a binomial distribution. The probability of obtaining any one of the $N+1$ possible values of X from such an experiment is described by the following equation:

$$P(X=n) = \binom{N}{n} p^n q^{N-n}, \quad n=0,1,\dots,N \quad (1)$$

where $\binom{N}{n} = \frac{N!}{n!(N-n)!}$.

The sum of all the possible values for equation (1) is equal to unity and can be written as follows:

$$(p+q)^N = \sum_{n=0}^N \binom{N}{n} p^n q^{N-n} = 1 \quad (2)$$

The probability of detecting n or more flaws can be found by summing equation (1) over all the values of X for which $X \geq n$. Thus,

$$P(X \geq n) = \sum_{i=n}^N \binom{N}{i} p^i q^{N-i}. \quad (3)$$

4.2.1 Confidence Interval Estimates of the True Probability of Detection

The objective is to estimate the true proportion of defects of a particular type and size that can be detected by a given NDE method. The best single estimate, \bar{p} , of the true

detectable proportion is the number of flaws detected divided by the total number of flaws present:

$$\bar{p} = \frac{n}{N} \quad (4)$$

If the binomial experiment (N, n_k^*, p) is repeated an infinite number of times and if p_k is computed each time, then the average of all the p_k s will be equal to p . So \bar{p} is an unbiased estimator of the true probability of crack detection.

Since the probability is small that \bar{p} will exactly equal p on any specific replication of the experiment, an interval estimator that will contain p most of the time is considered useful. A lower one-sided confidence interval can be used to estimate a lower bound on the true probability of crack detection. The lower bound, p_1 , for n detections of N cracks is computed as follows:

$$\text{Solve } \alpha = \sum_{i=n}^N \binom{N}{i} p_1^i (1-p_1)^{N-i} \quad (5)$$

for p_1 , where

$$\alpha = 1 - G \quad (6)$$

The following interpretation can be given for a 100G percent lower binomial confidence interval. If the binomial experiment (N, n_k, p) is repeated many times (theoretically infinite), and if p_{1k} is computed each time, then 100G percent of these lower confidence intervals will be equal to or lower than p . Thus, there is 100G percent "confidence" that the lower bound, p_1 , computed for any specific binomial experiment will be less than or equal to the true probability of crack detection. The choice of G is arbitrary and depends on how sure one needs to be that the true probability of detection is in the interval from p_1 to 1, (the larger the value of G , the smaller the calculated lower bound p_1 will be).

* n_k is the number of successes in the K^{th} replication of a binomial experiment consisting of N measurements.

4.2.2 Sample Size Determination

The objective is to determine the sample size required to estimate the lower confidence limit and confidence level. This can be accomplished by utilizing equation (6). By specifying the confidence level, G , and the lower confidence limit p_1 , a set of values (which must be integers) can be computed for N and n . Each combination of N and n in this set indicates the number of inspections and the number of detections required to achieve the specified probability of detection (POD) at the stated confidence level. For example, if G and p_1 are chosen to be 0.95 and 0.9 respectively, equation (5) becomes

$$0.95 = 1 - \sum_{i=n}^N \binom{N}{i} (0.9)^i (0.1)^{N-i}. \quad (7)$$

One of the combinations of N and n is 29 and 29 respectively. This represents the smallest sample size that can be utilized to meet the minimum specified values for G and p_1 . The next smallest sample size is $N=46$. In this case n must equal at least 45 to achieve 90% probability of detection at 95% confidence level. The higher the reliability requirements, of course, the larger the sample size required.

Equation (5) can also be used to calculate the number of added NDE tests required to upgrade an existing batch of data in the hope of achieving higher reliability estimates. Equation (5) takes on the form

$$1-G = \sum_{i=n+\delta-\epsilon}^{N+\delta} \binom{N+\delta}{i} p_1^i (1-p_1)^{N+\delta-i} \quad (8)$$

where δ is the required number of additional tests and ϵ is the maximum number of additional misses (nondetections). For example, if an experiment consisting of 29 inspections and 28 detections was performed, the reliability (equation 5) is 90% probability of detection at 80% confidence level. If a 95% confidence level is desired, the additional data requirements are indicated by equation (8). Thus, $\delta = 17$ with $\epsilon = 0$ represents the minimum added sample required to upgrade the existing data.

4.3 Comparison of Alternative Statistical Procedures

Table 4-1 lists the probability of detection at the 95% confidence level for four commonly used probability analysis methods, (Binomial, Normal, Poisson, and Chi-Square). The comparison is on the basis of 30 trials with 10, 15, 20, 25, 29 and 30 detections. The Binomial gives the exact results. The Normal approximation gives confidence values greater than the Binomial for large successes (30/30), and very nearly equal to the Binomial for intermediate successes (15 or 20/30). The Poisson approximation gives values less than the Binomial method. It is a good approximation only for cases with large number of trials with small number of successes. For 30 trials, the Chi-Square method gives values less than the Binomial for 10 to 30 successes. Like the Poisson, the Chi-Square values approach those of the Binomial for less than 10 successes in 30 trials.

However, a closer approximation to the Binomial for both the Poisson and Chi-Square can be achieved by using a conditional approach. By first calculating the upper one-sided confidence limit for the probability of missing a flaw (q_p), the lower one-sided confidence limit for $P_1 = 1 - q_p$ can then be approximated when $1 - n < n$. By using this conditional approach, a new set of values is calculated and included in Table 4-1 under the conditional approach column. These new values give a much better approximation to the Binomial when the number of successes is high.

Since the Poisson and Chi-Square approximations yield almost the same values, only one set of values was calculated under the new conditional approach.

For larger or smaller number of trials, the above comparisons is not necessarily true but the comparison generally shows the importance of analyzing binomial measurements with binomial statistics.

Table 4-1 Comparison of Probability of Detection
Values Obtained by Approximation to the
Binomial Distribution

NUMBER OF SUCCESSFUL DETECTIONS IN 30 TRIALS	POINT ESTIMATE OF PROBABILITY OF DETECTION (\bar{p})	LOWER ONE SIDED CONFIDENCE LIMITS AT 95% CL				CONDITIONAL APPROACH
		BINOMIAL (Exact)	NORMAL	POISSON*	CHI-SQUARE *	POISSON AND CHI-SQUARE
10	0.333	0.193	0.192	0.181	0.181	0.181
15	0.500	0.339	0.350	0.308	0.308	0.308
20	0.667	0.501	0.525	0.441	0.442	0.435
25	0.833	0.681	0.721	0.578	0.579	0.650
29	0.967	0.851	0.913	0.691	0.691	0.842
30	1.000	0.905	1.000	0.715	0.720	0.900

*No conditional information was used in obtaining these numbers, see "Reliability Management Methods and Mathematics," Lloyd and Litow, Prentice Hall, 1962, pp. 218-219

4.4 Data Cumulation Methods

The calculated value for the lower confidence limit (probability of detection, p_1 , at some selected confidence level, CL) is influenced by the total number of measurements (sample size). In order to achieve a high POD at a high CL, such as 90% at 95% confidence level, a minimum of 29 measurements have to be made without a miss for a given flaw size. Because of the high costs involved, it is generally not economical to make 29 or more measurements for each flaw size for the entire range of flaw sizes of interest. At the same time, in the inspection of actual structural components, it is unlikely to have 29 or more measurements at any specific flaw size. As a result, size interval grouping has been used in order to obtain a sufficient number of measurements to compute a high p_1 at a high CL and to smooth over the flaw sizes that have no measurements. A cumulation plan permits the accumulation of data over a range of flaw sizes for computing a p_1 which is representative of that range.

Several cumulation procedures were considered. These procedures include (1) the range interval "RI", (2) the overlapping 60 points "OSP" and (3) the procedure developed under this contract which will be called the optimized probability method "OPM." Other procedures evaluated are reported in Reference 1. For the same set of data, the computed p_1 can be considerably different depending on which of these cumulative procedures is used. Generally, NDE reliability is demonstrated by inspecting specimens containing flaws distributed uniformly over a wide flaw size range. The smallest flaws should be virtually nondetectable and the largest flaws should be 100% detectable. First, the raw data set is arranged in order of increasing flaw size with the appropriate outcome indicated for each measurement. The various cumulative procedures are applied as follows:

(a) Range interval method. The data are separated into groups of equal flaw size increments. The probability of detection at the one sided lower confidence limit is computed for each group separately and plotted as a histogram bar. A conservative p_1 curve can be obtained by connecting the upper right hand corner of the bars. This procedure is most appropriate for computing probabilities of detection and confidence limits when large numbers of data are available so that all histogram bars represent large data samples. It is important to note that sample size (N) may vary widely between intervals.

(b) Overlapping sixty point method ($N = 60$). One begins by combining detection results for the largest sixty crack sizes. The POD is calculated for this interval and plotted at the largest flaw size within the size range spanned. The next data increment is obtained by starting at the median flaw size of the first interval and combining the data for the next smaller 60 cracks. The POD of the second set is plotted at its largest flaw size and the process is repeated until all data have been combined. Each interval overlaps its adjacent interval by 30 data points. Note that the sample size is the same for each interval, but the breadth of the interval can vary widely.

(c) Optimized Probability Method. The ordered NDE data are grouped into J (a computer input number) intervals of successively increasing size range. The POD of the largest size range is computed at some desired confidence level. The next smaller size range data are combined with the first and the POD of the second grouping is computed. This process is continued until J probabilities of detection are computed, and the largest value of POD obtained is plotted at the largest flaw size contained in the corresponding composite grouping. The largest flaw size interval is removed from consideration and this procedure is repeated starting from the next to largest flaw size grouping. The pattern is repeated until J probability of detections can be plotted. Note that if J is sufficiently large, the POD curve produced by this method will be the upper envelope of either the RI or the OSP method. The advantage to this method is that the sample size (N) is maximized, and results in the maximum possible value of p_1 for the available data. A basic assumption is that the larger the flaw, the more detectable it is.

V. RESULTS

Of the twenty sets of data collected, only seven sets were statistically analyzed. These seven sets appeared to meet the criteria stated in Section III of this report. Each of these seven sets, in turn, was subdivided into subsets and analyzed according to the NDE method and material types. Appendix D contains a computer listing of NDE data and detection reliability results that were analyzed during this program. Table 5-1 summarizes the results of the statistical analysis. There is a total of one hundred and twelve subsets and the subset number is given in the first column of Table 5-1. The second column gives data source. The third and fourth columns identify the material and defect type respectively. The fifth and sixth columns identify the specimen geometry and NDE method respectively. The seventh column lists some of the pertinent parameters, and the eighth column gives the crack length at which 90% probability of detection at 95% confidence level $POD_{90}(CL_{95})$ was first achieved. The shortest crack length that reached $POD_{90}(CL_{95})$ by either the OPM or OSP scheme was used and is herein referred to as the threshold level. In many instances, the $POD(CL_{95})$ became smaller than 90% at crack lengths above the threshold level. This is particularly true for the OSP scheme (see Appendix D). For more details on the NDE parameters and inspection procedures that were used to acquire each set or subset of data, one has to refer to the original data reference.

The first set of data analyzed is from Martin Marietta (Contract NAS 9 12276). Four subsets, one by ultrasonic surface wave, one by penetrant, one by eddy current, and one by the X-ray method, were available before the specimens were chemically etched and another four subsets were available after chemically etching the test specimens.

The second and third sets of data analyzed are from Rockwell International-Space Division (Contract NAS 9-14000) and General Dynamics, Convair Aerospace Division (Contract NAS 9-12326). This set of data includes data from Contract NAS 9-12276 with the specimens in the "after-etched" condition.

TABLE 5-1 SUMMARY OF NDE DATA STATISTICALLY ANALYZED

CAUTION: The crack lengths in the POD90(CL95) column are not intended to be used for design purposes unless the user demonstrates a similar capability

DATA SUB-SET*	DATA SOURCE	MATERIAL TYPE	DEFECT TYPE	SPECIMEN GEOMETRY	NDE METHOD	PERTINENT PARAMETERS	CRACK LENGTH POD90(CL95) cm
1	Martin Marietta NAS 9 12276	2219-T87 A1	Fatigue Cracks	Flat Plates	Ultrasonic- Surface Wave	Before Etch, and with 3 Ops; 10 MHz	.345
2					Liquid Penetrant	Same as above, Uresco P151,K410,D499C	.665
3					Eddy Current	Same as above; NDT-3; 100KHz	.274
4					X-ray	Same as above	-
5					Ultrasonic- Surface Wave	After Etch, and with 3 Ops.	.211
6					Liquid Penetrant	Same as above	.274
7					Eddy Current	Same as above	-
8					X-ray	Same as above	.665
9	Rockwell Inter. Space Div. (NAS9- 14000); Martin Marietta, and GD Convair	2219-T87	Fatigue Cracks	Flat Plates	Ultrasonic- Shear Wave (Surface Wave)	After Etch, and by Operator O	.737
10					f = 2.25 MHz	Operator P	.221
11					for RI-SD	Operator Q	.699
12					f = 10 MHz	Operator R	.699
13					for GD Convair	Operator S	.358
14					Liquid Penetrant	After Etch, and by Operator H	.282
15					P-133,D495A	Operator I	.737
16					for RI - SD	Operator J	.737
17						Operator K	.333
18						Operator L	.737
19						Operator M	.340
20						Operator N	1.36
21					Eddy Current Defectometer Model 2.154	After Etch, and by Operator T	.665
22					f = 2 MHz	Operator U	.201
23					for RI - SD	Operator V	-
24						Operator W	.333
25						Operator X	.320

*Data Set Numbers are Included on the Corresponding Computer Output in Appendix D.

TABLE 5-1 SUMMARY OF NDE DATA STATISTICALLY ANALYZED (Continued)

DATA SUB-SET	DATA SOURCE	MATERIAL TYPE	DEFECT TYPE	SPECIMEN GEOMETRY	NDE METHOD	PERTINENT PARAMETERS	CRACK LENGTH POD90 (CL95) cm
26					X-ray	After Etch and by Operator A	-
27						Operator B	-
28						Operator C	-
29						Operator D	-
30						Operator E	.737
31						Operator F	-
32						Operator G	-
33	RI-SD, Martin Marietta, &GDC	2219-T87 Al	Fatigue Cracks	Flat Plate	Ultrasonics	After Etch and Merged Results of 5 Operators	.201
34					Liquid Penetrant	After Etch and Merged Results of 7 Operators	.237
35					Eddy Current	After Etch and Merged Results of 5 Operators	.282
36	RI-B-1 Division (TFD-72-925)	Ti-6Al-4V	Fatigue Cracks	Flat Plate	Liquid Pene.	Used P5F-1 Penetrant	.183
37	(TFD-72-1005)					Used P5F-2	.170
38	(TFD-72-1515)					Used P5F-2 and D100 Developer	.178
39	(TFD-72-793)					Used P5F-2.5	.127
40	(TFD-72-767)	7075-T6511 Al	Fatigue Cracks	Flat Plates		Used P5F-2.5	.173
41	(TFD-73-532)					Used P5F-2.5, NQ-1	.203
42	(TFD-73-532)					Used P5F-2.5, D100	
43	(TFD-73-496)	PH13-8 Mo. St.	Fatigue Cracks	Flat Plates		Used P5F-2 and NQ-1 Developer	
44	(TFD-73-371)	Ti-6Al-4V	Fatigue/ Cracks Corroded	Welded Flat Plates	Ultrasonic, Shear Wave		.173
45	(TFD-73-372)	4330V St.				Simulate Welded Flaws	.211
46	(TFD-73-140)	PH17-4 St.				Simulate Flaws in Wrought St.	.218
47	(TFD-72-768)	PH17-4 St.	Fatigue Cracks	Flat Plates			-
48	RI-SD, MM, GDC, and RI-B1	2219-T87 and 7075-T6511 Al	Fatigue Cracks	Flat Plates	Liquid Penetrant	Merged Results from the Four Data Source on Al	.241

TABLE 5-1 SUMMARY OF NDE DATA STATISTICALLY ANALYZED (Continued)

DATA SUB-SET	DATA SOURCE	MATERIAL TYPE	DEFECT TYPE	SPECIMEN GEOMETRY	NDE METHOD	PERTINENT PARAMETERS	CRACK LENGTH cm
49	Lockheed GA	4330V St.	Fatigue Cracks	Cylindrical	Liquid Penetrant	Laboratory Condition	-
50	(TR-68-32)			Shell	Magniflux ZL-2, ZE-3, and ZP-4	Production Condition	-
51		7075-T6511 A1		7.62 cm in dia.		Laboratory Condition	-
52		4330V St.		0.64 cm thick	Mag. Particle	" "	-
53		4330V St.			Ultrasonic	" "	-
					Shear Wave 5 MHz	" "	-
54		7075-T6511 A1			Ultrasonic	" "	-
					Shear Wave	" "	-
55		7075-T6511 A1			X-ray	" "	-
56		4330V St.			X-ray	" "	-
57	Boeing, W.Kan.	7178-T651 A1	Fatigue Cracks	KC-135 Wings	Eddy Current	Hand Held E.C. Probe at Tear Down Insp. at Depot Level	-
						Results of Team 2 (Atypical of 3 more teams)	-
58						Results of Team 4 (A- typical)	-
59						Merged results of 5 teams	-
60	Boeing Comm.	2024-T6 A1	Forge Closed	Tandem T	Liquid Penetrant	Production Insp.	-
61	Airplane Co.	4340 M St	"	Solid Cyl., Threaded	ZL-2A and 30A;	" "	-
62	(TR-74-241)	"	"	Hollow Cyl., Filletted	ZE-4B;	" "	-
63		"	"	Hollow Cyl.,	ZP-9B	" "	-
64		"	"	Solid Cyl.	Plus Others	" "	-
65		2074-T6 A1	"	Tandem T	Liquid Penetrant	Laboratory Insp.	.178

TABLE 5-1 SUMMARY OF NDE DATA STATISTICALLY ANALYZED (Continued)

DATA SUB-SET	DATA SOURCE	MATERIAL TYPE	DEFECT TYPE	SPECIMEN GEOMETRY	NDE METHOD	PERTINENT PARAMETERS	CRACK LENGTH
66		4340 M St	Forged Closed Threaded	Solid Cyl., Threaded	ZL-2A and 30A;	Laboratory Insp.	POD90(CL95) cm .584
67		"	EDM, Slots	Hollow Cyl., Filleted	ZE-4B;	" "	.787
68		"	"	Hollow Cyl.,	ZP-9B;		-
69		"	"	Solid Cyl., Fil.	Plus Others		.229
70		"	"	" "			.406
71		2024-T6 Al	"	Tandem T	Ultrasonics	Production Insp.	.533
72		4340 M St.	"	Solid Cyl. Threaded	5 and 10 MHz		-
73		"	"	Hollow Cyl. Filleted	Shear and Surface		.330
74		"	"	Hollow Cyl.	Wave		-
75		"	"	Solid Cyl., Filleted			.178
76		"	"	" "			.356
77		"	"	Solid Cyl.	Ultrasonics	Laboratory Insp.	.356
78		"	"	" " Filleted	5 and 10 MHz		.229
79		"	"	Hollow Cyl.	Shear and Surface		.254
80		"	"	" " Filleted	Wave		.330
81		2024-T6 Al	"	Tandem T			.432
82		4340 M St.	"	Solid Cyl.	X-ray	Production Insp.	-
83			"	" " Filleted			-
84			"	Hollow "			-
85			"	" " "			-
86			"	Solid " Threaded			-
87		2024-T6 Al	"	Tandem T			-
88		4340 M St	"	Solid Cyl.	X-ray	Laboratory Insp.	-
89		4340 M St		Hollow " Filleted			-
90		"		Solid " Filleted			-
91		"		Hollow "			-

TABLE 5-1 SUMMARY OF NDE DATA STATISTICALLY ANALYZED (Continued)

DATA SUB-SET	DATA SOURCE	MATERIAL TYPE	DEFECT TYPE	SPECIMEN GEOMETRY	NDE METHOD	PERTINENT PARAMETERS	CRACK LENGTH
						POI90 (CL95)	cm
92		2024-T6 Al		Tandem T			.279
93		4340 M St.	Forge	Solid Cyl.	Mag. Particle	Production Insp.	.305
94		"	Closed	" " , Filleted			.330
95		"	EDM Slots	Hollow "			-
96		"	"	" " , Filleted			-
97		"	"	Solid " , Threaded			-
98		"	"	Solid Cyl.	Mag. Particle	Laboratory Insp.	.305
99		"	"	Hollow " , Filleted			.329
100		"	"	Solid " , Threaded			-
101		"	"	" " , Filleted			.178
102		"	"	Hollow "			.254
103		"	"	Solid Cyl.	Eddy Current	Production Insp.	.400
104		"	"	" " , Filleted	ED400 and 520		.762
105		"	"	Hollow Cyl.	at f=100 KHz		-
106		"	"	" " , Filleted			-
107		2024-T6 Al	"	Tandem T			.330
108		"	"	Tandem T	Eddy Current	Laboratory Insp.	.457
109		4340 M St.	"	Solid Cyl.	ED400 and 520		.508
110		"	"	Hollow Cyl., Fil.	at f=100 KHz		.356
111		"	"	Solid " , Filleted			.584
112		"	"	Hollow Cyl.			-

There are five subsets of data obtained with the ultrasonic method, each subset for a different inspector, three inspectors for Contract NAS 9-12276, one for NAS 9-14000, and one for NAS 9-12326. There are seven subsets of data obtained with the liquid penetrant method, each subset by a different inspector, three inspectors for NAS 9-12276, three for NAS 9-14000, and one for NAS 9-12326. There are five subsets of data obtained with the eddy current method, each subset by a different inspector, three inspectors for NAS 9-12276, one for NAS 9-14000, and one for NAS 9-12326. There are seven subsets of data obtained with the X-ray method, each subset by a different inspector: three inspectors for NAS 9-12276, three for NAS 9-14000, and one for NAS 9-12326. Subsets 33, 34 and 35 were obtained by merging the data of five ultrasonic inspectors, seven penetrant inspectors, and five eddy current inspectors. The X-ray data were not merged because the results are not worthy of further consideration.

The fourth set of data analyzed is from Rockwell International B-1 Division, B-1 NDI Demonstration Program. There were twelve subsets of data in this set. The fifth set of data analyzed is from Lockheed, Georgia, AFML Report No. TR-68-32. There are eight subsets in this data set. The sixth set of data analyzed is from Boeing Company of Wichita, Kansas. This set of data was obtained from eddy current inspection of bolt holes, after pulling off the bolts, from actual aircraft parts.

The seventh set of data analyzed is from the Boeing Commercial Airplane Company, AFML Report No. TR-74-241. There are fifty-three subsets in this set of data.

Data subset number 48 was obtained by merging the data from Martin Marietta (NAS 9-12276), Rockwell Int.-Space Division (NAS 9-14000), General Dynamics' Convair Division (NAS 9 12326), and Rockwell Int.-B-1 Division for aluminum for the liquid penetrant method.

All the data described in this report were taken from a total of nine alloys of aluminum, titanium, and steel. These alloys are described in Table 5-2. The predominant amount of data were taken with the four aluminum alloys.

Table 5-2 Alloys with Valid Data

<u>Aluminum</u>	<u>Steel</u>	<u>Titanium</u>
2219-T87	PH13-8MO	6A1-4V
7075-T6511	4330V	
2024-T6	PH17-4	
7178-T651	4340M	

VI. DISCUSSION OF RESULTS

The tabulated and graphical computer output format (Appendix D), is convenient for assessing the state-of-the-art in NDE reliability. It contains:

- (1) the binomial experiment results (N,n) in each of 32 crack size intervals (tabulated in units of Mils and plotted in both Mils and cm.);
- (2) the 50 percent lower confidence limit for each interval $POD(CL50)$
- (3) the 95 percent lower confidence limit $POD(CL95)$; and
- (4) the number of new measurements required in each interval to demonstrate a 90 percent probability of detection at a 95 percent confidence level " $POD90(CL95)$ ".

These data are useful for comparing the effects of material, inspector, and inspection parameters on NDE reliability and seeing where data deficiencies lie.

As can be seen in Figure D-1a the POD fluctuates widely throughout 32 ranges for this set of data because of the variation in the number of measurements, N , reported in each range. Twenty of the ranges contain less than 29 measurements while six ranges contained no measurements at all. The number of measurements per range can be increased by broadening the flaw size interval per range, but there is still no assurance that all of the broader ranges will contain measurements. Fluctuation in the probability of detection due to the variation in the number of measurements in a range is a shortcoming of the range interval method.

Figure D-1b shows the tabulated and graphic results obtained by using the optimized probability method (OPM) for the set of data in Figure D-1a. As can be seen, the number of measurements available for each interval is much larger than for the range scheme. The thirty-first interval lists 183 detections out of 183 measurements resulting in a POD of 98% plotted at 1.18 cm. The POD computed with the OPM increases monotonically with increasing crack length and does not fluctuate as in the range scheme. The POD at 95% CL reaches 89% for the first time at .32 cm for the OPM versus .358 cm for the range scheme.

Figure D-1c shows graphic and tabulated results using the overlapping 60 points scheme. In this scheme, the number of measurements for each POD calculation is constant (60). Fluctuation in the POD can be attributed primarily to human operator and inspection process variations. The POD at 95% CL reaches 89% for the first time at .328 cm, which is intermediate between the OPM and the RI results.

6.1 Effects of Material, Source, and Inspection Parameters

It is apparent from data subsets 1 through 8 in Table 5-1 that the sensitivity is increased for ultrasonic, liquid penetrant, and X-ray techniques after the test specimens were chemically etched. This increase is reasonable since the crack openings are enlarged. The sensitivity is decreased, however, for eddy current method after chemically etching the specimens. This effect is difficult to explain.

Data subsets 9 through 32 show that the difference in the POD90(CL95) obtained by different inspection operators within a company vary as much as those obtained by companies which use different inspection parameters and procedures. Several observations can be made with subsets 9 - 14:

(1) Operators P and S in subsets 10 and 13 can be considered to be model operators. Not only did they achieve a smaller POD90(CL95) threshold level than other operators, they were able to maintain the POD(CL95) at a relatively constant (and high) level for crack lengths above the threshold level (Figures D-10 and D-13). (2) Subsets 10 and 13 show that the sensitivity of the ultrasonic method increases or remains constant for increasing crack length, particularly for crack lengths above the threshold level. (3) Fluctuations in the POD(CL95) for crack lengths above the threshold level are primarily caused by fluctuations in operator efficiency and less likely by the sensitivity of the NDE method.

Subsets 14-20 (Figures D-14 to D-20) show more fluctuation in the POD(CL95) due to variation in operator efficiency than to types of penetrant or procedures used by the three different companies that made the measurements. There is a large variation in the threshold level of the seven operators. Three operators demonstrated threshold levels around .33 cm, another three demonstrated the level at .737 cm, and the seventh one demonstrated it at 1.35 cm. One should keep in mind that most of these POD (CL95) curves are relatively flat and the POD(CL95) is greater than 80% from .254 cm on to the longer crack length.

Like the ultrasonic and penetrant results, the eddy current results showed considerable differences in the threshold level for the five different operators. In fact Operator V did not demonstrate POD90(CL95). However, he did demonstrate POD88(CL95) at a crack length of .737 cm. Operator T demonstrated POD90(CL95) at a crack length of .665 cm. However, he reached POD88(CL95) at a crack length of .399 cm.

X-ray is not a good inspection technique for reliably detecting fatigue cracks. Data sets, 26 to 32 show that only one operator can achieve POD90(CL95). This forecasts that X-ray techniques will not be viable procedures for detecting fatigue cracks. However, this does not necessarily mean that the technique should not be used to detect other defects such as porosity.

Merging data provides a means for observing overall detection reliability trends. When the data for five ultrasonic operators were merged (subset No. 33) and calculated with the OSP scheme the POD(CL95) reached 95% at a crack length of 0.66 cm (see Figure D-33c). However, it fell below 95% at higher crack length, and it reached a minimum of 79% at a crack length of 0.810 cm. When the results of seven penetrant operators were merged (subset No. 34) and calculated with the OSP scheme, the POD(CL95) reached 92% at a crack length of 0.26 cm (see Figure D-34c), but it fell below 90% between 0.26 cm and 0.63 cm. It peaked to 95% at 0.65 cm, then fell below 90% and reached a minimum of 81% at a crack length of 1.12 cm. When the results of five eddy current operators were merged (subset No. 35) and calculated with the OSP scheme, the POD(CL95) reached 92% at a crack length of 0.32 cm (see Figure D-35c). But like the ultrasonic and penetrant results, the POD(CL95) for the eddy current fell below 90% at higher crack length and it reached a minimum of 81% at 0.88 cm.

Data subsets 36 through 47 (Figures D-36 to D-47) are from the B-1 NDI demonstration program. These data show that the POD(CL95) either increases monotonically or remains constant with increasing crack length once the threshold level is reached. In several data sets no further measurements were made once the desired threshold level was demonstrated. It is interesting that the threshold level as well as a large portion of the POD(CL95) curve does not differ greatly for several types

of penetrant applied to materials such as Ti-6Al-4V, 7075-T6511 Al, PH 13-8 Mo steel, 4330V steel, and PH 17-4 steel.

Data subset 48 represents the merged results of four data sources (RI-Space Division, Martin Marietta, General Dynamics Convair, and RI-B-1) on 2219-T87 Al by the liquid penetrant method on flat plates.

Data subsets 49 through 56 were obtained with fatigue cracks in 4330V steel and 7075-T6511 Al having a cylindrical shape (7.62 cm in diameter and .62 cm thick). Data were taken in both the laboratory and production environments. None of the curves for these 8 sets of data attained POD90(CL95), however, the penetrant results for 7075-T6511 Al did demonstrate POD87(CL95) at a crack length of 1.0 cm, POD87(CL95) at a crack length of 1.17 cm, and POD89(CL95) at 1.47 cm. The POD for ultrasonic shear wave reached a value of POD86(CL95) at a crack length of .80 cm and POD87(CL95) at a 1.27 cm.

Data subsets 57, 58, and 59 were obtained with eddy current inspection of bolt holes during tear-down inspection of KC-135 wings at the depot level. The same holes were inspected by five separate inspection teams. The inspection results from four of the five teams were about the same. Figure D-57 shows the results of team number two which is representative of the four teams. Figure D-58 shows that the detection reliability of team number four is considerably different than the other four teams. Figure D-59 shows the merged results of the five teams. None of the five teams achieved POD90(CL95).

Data subsets 60 through 112 (Figures D-60 to D-112) were obtained from the Practical Sensitivity Limits program which was conducted by Boeing Commercial Airplane Company and supported by the NDE Branch of Air Force Materials Laboratory. The inspection results were obtained in both the laboratory and production lines of several Boeing Divisions. Divisions used different NDI procedure or specification, as well as different NDI techniques. For example, ultrasonic shear and surface waves of 5 and 10 MHz were used, different liquid penetrant systems in either the Group V or VI category were used, etc. Because the results were obtained under different NDE procedures, it is difficult to make comparison between results from different data sources. Furthermore, the majority of the defects used in this program were forging cracks instead of fatigue cracks, nevertheless the length of the crack at POD90(CL95) found by each of the NDI techniques is comparable, in most cases, to those found at other companies using fatigue cracks.

6.2 Statistical Analysis Procedures

All NDE measurements are considered to be binomial and describable by binomial distribution functions and binomial statistics. Because of this consideration, lower one sided confidence limits and data deficiencies can be rigorously computed.

The only factor which reduces mathematical rigor is the crack length parameter. It is necessary to group NDE data into a size interval that will contain a population of 29 successes without a miss in order to show 95 percent confidence that the probability of detection exceeds 90 percent. If a miss is encountered, it is necessary to have a higher population (see Table 6-1) in order to demonstrate POD90(CL95).

Table 6-1

Interval Sample Size and
Successes Required to Achieve POD90(CL95)

No. of Misses	Interval Population Required, N	No. of Successes, n
0	29	29
1	46	45
2	61	59
3	76	73
4	89	85
5	103	98
6	116	110
7	129	122
8	142	134
9	154	145
10	167	157

Once an acceptable size interval has been chosen that will produce a reasonable population, there remains a problem of selecting the crack length within the range at which to plot the computed POD(CL95). For conservatism, the POD curves in this report are plotted through the maximum crack length in the interval. The crack interval is also indicated by a horizontal line connecting maximum and minimum crack sizes.

Three procedures for determining the probability of detection for the lower one-sided confidence level are compared in this report. Described earlier in Section 4.3, they were the range interval (RI) method, the optimized probability method (OPM) and the overlapping sixty point method (OSP). The optimized probability method is preferred over the RI or OSP but requires more computational time. The main claim to success for the OSP method is that it forces groupings to be large enough to provide the capability for achieving POD95 (CL95). The OPM should provide the upper envelope to both the RI and the OSP methods.

6.3 Data Deficiencies

The data described in this report represents more than 30,000 measurements, yet there are many gaps in the probability of detection for different defect types, material types, and specimen geometry by the five NDE methods (ultrasonics, liquid penetrant, eddy current, X-ray, and magnetic particle). The most data are available for fatigue cracks in flat plates of 2219-T87 aluminum which reasonably characterize the reliability of all five NDE methods. There are also several sets of data for fatigue cracks in aluminum cylinders, forging cracks in extruded aluminum (tandem T configuration), and fatigue cracks in bolt holes of actual aluminum aircraft parts. There is a notable data deficiency for steel. Most of the steel data are for fatigue and forged cracks in cylinders. There are, however, four sets of data for fatigue cracks in flat plates of steel. Only five sets of data are available for titanium and all of them were taken on flat plates.

With the exception of the B-1 NDE demonstration data most of the data exhibit a gap over some range of the crack lengths. A perfect example of this is the data from Martin Marietta, Rockwell International-Space Division, and General Dynamics-Convair Division. All these three companies made measurements using the same set of specimens which contains two gaps. As can be seen from the crack size distribution curve in Figure 6-1, there are no cracks with length between 0.47 to 0.59 cm and between 1.03 to 1.17 cm. Thus, no cracks can be detected in these two gaps and the probability of detection, regardless of which cumulative scheme is being used, is affected. A set of specimens without gaps in the crack size distribution curve is needed to study the actual probability of detection in future programs.

6.4 Application to Fracture Mechanics

The threshold crack length (the shortest crack length that reached to POD90(CL95)) that was detected by the different NDE techniques is given in Table 5-1. However, as can be seen from the curves in Appendix D, the POD (CL95) in many instances falls below 90% for some crack length longer than the threshold level. Thus the potential user is cautioned against using these threshold crack lengths in the design process. In the first place, the POD can vary from company to company even when the same inspection procedures were used because of training procedures and using different inspectors. In the second place, some of these POD curves do not have a zero or positive slope for crack length above the threshold level. The decrease in the POD above the threshold level could be a real phenomenon and might not necessarily be attributed to human factors. There are scatter reports, in the case of liquid penetrant, that indicate penetrant washes out of wide cracks before the developer is applied.

In the fracture mechanics design process, one must be assured with some probability at some confidence level that no cracks larger than the assumed size can be present in the structure. Thus, for fracture mechanics to be a viable design process, the probability of detection as a function of crack length must be monotonically increasing or at least levels off above some selected threshold crack length.

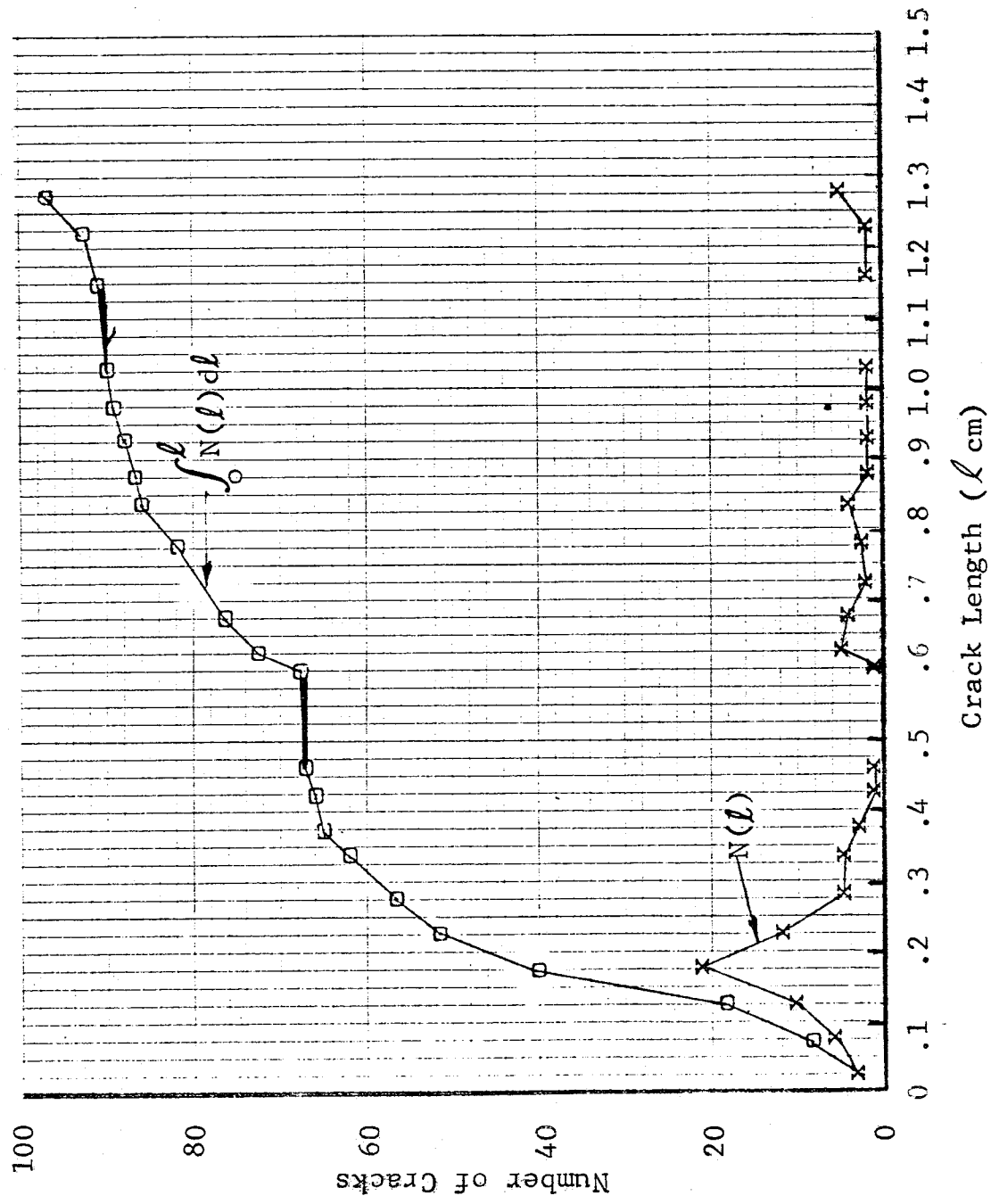


Figure 6-1 Differential and Integral Crack Distribution Function for the Martin Marietta Demonstration Program. 2219-T87.

6.5 Optimum Demonstration Program

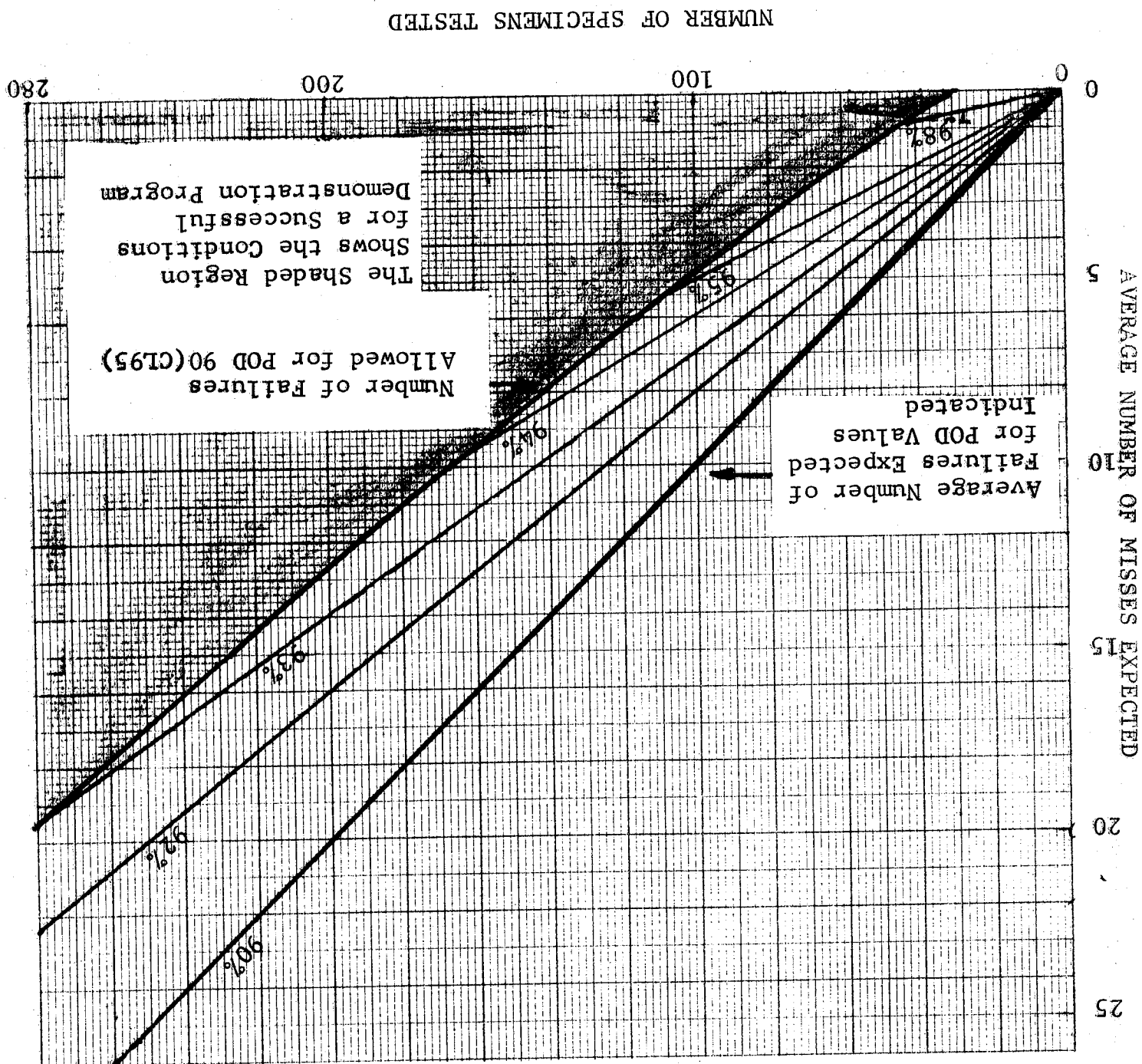
In order to determine the reliability of an NDE technique without operator influence, the optimum demonstration program will have to employ computer automation in scanning specimens and interpreting NDE signals. It should incorporate ultrasonic, eddy current and penetrant inspection into each demonstration program.

The data in this report can be used to estimate the sample size required for the optimum demonstration program. For example, if one can afford to test 100 specimens and requires a 50-50 chance of success in demonstrating POD90/CL95 then one would have to select a data set representative of this expected capability and select a crack length for his demonstration program for which the probability of detection is at least 95%. If he can afford only 45 specimens then he must choose a crack length for which the probability of detection is at least 98%. This can be seen in Figure 6-5 where number of misses corresponding to POD90(CL95) is plotted against the number of specimens tested. The shaded region is the region of success for which POD 90(CL95) has been met or exceeded. The broken lines show the number of failures expected for various values of POD (98, 95, 94, 93, 92, and 90%).

Assume that data set # 1 (Figure D-1) is for a geometry and NDE method that is most representative of those required in a demonstration program. These data demonstrate a POD(CL95) at .345 cm. Figure D-1a would lead one to believe that POD 90(CL95) might be demonstrated at about .27 cm for which 38 out of 39 cracks were detected. Figure D-1a shows that one can be 50 percent confident that the probability of detection exceeds 95% for this case if his NDE techniques are as good as those used to produce data set # 1. Figure 6-2 shows that if 110 test cracks were fabricated and tested and that less than 5 cracks were missed, then the demonstration program would be successful.

The previous example is indicative of the usefulness of these data as a means for minimizing the number of specimens required for achieving a successful demonstration program. The common practice of manufacturing a large number of crack specimens for which there is little chance to achieve POD 90(CL95) will be eliminated by this approach to designing an optimum demonstration program.

Figure 6-2 Conditions for Success in Selecting
a Sample Size that will Potentially
Demonstrate POD90(CI95)



VII. CONCLUSIONS

This program was sponsored by NASA as a service to the new fracture mechanics approach to structural design whereby system reliability may be related to the expectation that flaws larger than a specific size may exist in the structure. The program objectives were to (1) collect all available NDE reliability data, (2) examine the validity of the data, (3) select and computerize a statistical procedure for analyzing the data, and (4) generally assess the current state-of-the-art in NDE. We feel that the surface has been broken by this program but vigorous follow-on work would be very valuable to the field of structural design.

Some of the specific conclusions that can be drawn from the contents of this report and the experience gained in performing this study are:

- (1) The human factors influence stands out as dominating in influencing NDE reliability. Although a company can demonstrate a 90 percent probability of detecting a crack at a lower one sided confidence limit at the 95 percent confidence level, there is no guarantee that this is indicative of a continuing capability unless some form of automation has replaced human judgment. This then indicates a need for some type of periodic audit of capability.
- (2) Although more than 30,000 measurements have been filed in a computer library and analyzed to determine the NDE reliability of X-ray, ultrasonics, eddy current, and penetrants, there are still many gaps in the data: There are no eddy current data in the data bank for titanium nor are there much data for crack lengths near .5 or near 1.2 cm. These data deficiencies cause large uncertainties in the POD plots for these crack lengths.
- (3) Binomial statistics are recommended for analyzing NDE reliability data. This report contains a comprehensive discussion of the preferred analysis model.
- (4) The optimized probability method (OPM) of data cumulation is preferred over the range interval or the overlapping sixty point scheme for computing probability of detection. The optimum probability model which was developed during this program is discussed in this report.

(5) Data show that the X-ray technique is not viable for detecting tight fatigue cracks.

(6) In order to obtain optimum results from an NDE demonstration program, special care must be taken in the design of flaw size distribution. The cumulative distribution must always maintain a positive slope or there will be gaps without data which can have deleterious effects on the POD curves as a function of flaw sizes.

(7) The data presented in this report are offered as a guide for manufacturers who intend to perform an NDE reliability demonstration program and can identify data sets that represent their expected NDE capabilities. However, due to the human factor influence on POD, the data cannot be used as design information. Each company must develop reliability numbers for their own use.

(8) A continuing program to maintain an NDE reliability data file and to optimize the data processing procedures formulated during this program would be useful to the field of fracture mechanics. As the data base becomes larger it will begin to support parametric studies of the influence of NDE variables.

APPENDIX A

A MODEL TO GRADE THE QUALITY OF THE DATA SETS

The thoroughness of the characterization of the defect-specimen and the documentation of the inspection procedures affects the quality and the usefulness of the data sets. A designer will not have confidence in using the data unless the inspection procedures and defect dimensions are sufficiently documented so that it can be reproduced in future inspections.

The model described in this section will only relate to the quality of each set of data. It will not address the question of applicability. That is, a set of data obtained on flat

plates will not be graded on the basis of its applicability to the design of complex structures.

The model is empirical and the weighting factors assigned to the various known pertinent parameters are rather arbitrary. However, it does represent a first attempt to quantitatively evaluate the quality of a data set. Each of the pertinent parameters in this model is listed in the Input Data Format which will be discussed in the next subsection. The grade for a given set of data can be tallied in the computer by checking the entries to the columns containing these pertinent parameters. A score of one hundred (100) corresponds to a perfect set of data. A perfect set of data is one where all the pertinent parameters are documented.

The preliminary model to grade the data quality for the ultrasonic, eddy current, liquid penetrant, magnetic particle, and X-ray methods is given in Table A-1. The model is divided into two major groups. Group A is the characterization of specimens and defects and it is common to all techniques. Group B is the documentation of the inspection and is different for different NDE techniques. The first eight parameters in this last group are common to all techniques. Each technique has about eleven parameters that are considered pertinent to adequately document the inspection. Parameter A1 is the description of the specimen geometry and defect location. This is considered a key parameter and a value of 7 points is arbitrarily assigned to it. If no description about the specimen geometry and defect location is given, that data point or set of data will receive no points. Those parameters that are marked by an asterisk are considered key parameters. If any of them is not recorded, the data point or set will be considered for possible exclusion from statistical analysis.

Table A-1

THE GRADING FACTORS USED TO GRADE NDE DATA QUALITY

A.	Specimen - Defect Characterization Information		35
1.	Specimen geometry complexity and defect location	*	7
2.	Crack dimension verification	*	10
3.	Defect type	*	3
4.	Specimen surface condition	*	3
5.	Material characterization (thermo-mechanical history)		3
6.	Material inside defect	*	3
B.	Inspection Documentation		65
1.	False indication recording		4
2.	Inspector qualification level		3
3.	Knowledge of defect orientation, location, and presence by inspector	*	9
4.	Use of proof load	*	3
5.	Use of control specimens without crack		3
6.	Method of data recording		3
7.	Method of scanning specimens		3
8.	Insp. environment	*	3
9.	Number of insp. prior to this insp.		3
10.	Parameters recorded by nondestructive testing standards		
a.	Radiography		38
1)	Radiographic source	*	3
2)	Ref. standard		3

10. (Continued)

3) Detector type	*	4
4) Voltage	*	4
5) Current	*	4
6) Exposure time	*	4
7) Source/film distance	*	4
8) Angle of entry	*	3
9) Film development parameters		3
10) Radiograph density	*	3
11) Radiographic equipment type		3
b. Ultrasonics		38
1) Ultrasonic method	*	4
2) Frequency	*	4
3) Transducer type and size	*	4
4) Reference standard type and size	*	4
5) Angle of incidence (inside the material)	*	3
6) Equipment type		3
7) Gate alarm level (% of ref. signal)	*	4
8) Gain setting (% of screen saturation)	*	4
9) Type of coupling		3
10) Index interval	*	3
11) Contact or Immersion		3

10. (Continued)

c. Eddy Current		38
1) Method of Scan	*	3
2) Coil size	*	4
3) Coil arrangement and shape	*	3
4) Frequency	*	4
5) Reference type and size	*	4
6) Equipment type		3
7) Index interval	*	3
8) % of meter response (Real Part)	*	4
9) % of meter response (Imaginary Part)	*	4
10) Lift-off compensation		3
11) Signal processing		3
d. Penetrant		38
1) Penetrant type	*	4
2) Developer type	*	4
3) Classification of penetrant (group no.)		2
4) Emulsifier type	*	4
5) Pre-insp. surface cleaning and penetrant removal	*	3
6) Method of penetrant application		3
7) Dwell time	*	4
8) Development time	*	4

10. (Continued)

9) Wash time		4
10) Light type and intensity at specimen surface		3
11) Reference standard type		3
e. Magnetic Particle		38
1) Type of current used	*	4
2) Current level (Amperes)	*	4
3) Method of magnetization		4
4) Direction of magnetization	*	4
5) Magnetic flux density	*	4
6) Magnetic particle type and size	*	3
7) Magnetic particle density		3
8) Type of liquid vehicle		3
9) Method of particle application		3
10) Equipment type		3
11) Dwell time (seconds)	*	4

APPENDIX B

DATA POOLING

B.1 Data Pooling by NDE Method and Parameters

Data that meet the preliminary criterion as described in Subsection 3.1 are input to the computer for statistical analysis. Then data from several sets are pooled and analyzed if they have a common set of parameters. Data from different NDE methods are not to be pooled. For a given NDE method such as ultrasonic shear wave at 5 MHz, reliability curves will be plotted for a material type, a defect type, an environment, a specimen geometry and defect location, and either before or after some enhancement such as a proof test. Composite reliability curves can be plotted by pooling data with different parameters, such as pooling 5 and 10 MHz shear wave data, laboratory and production data, flat plate and cylindrical shell data, etc.

B.2 Statistical Pooling Criteria

The NDE data that is compiled for this contract was collected from different sources using different calibration factors, different equipment, different personnel, different environments, etc. Each set of data therefore contains unique source characteristics that preclude indiscriminate pooling for reliability calculations.

A statistical pooling criteria has been developed to safeguard against mistakes or inconsistencies in the data which would produce abnormal statistical results. The data pooling technique is based solely on the binomial distribution and is described below as a procedure which can be implemented on a computer. The procedure consists of the following four steps.

- (1) The best single estimate, \bar{p}_c , for probability of detection

$$\bar{p}_c = \frac{\sum_{k=1}^M n_k}{\sum_{k=1}^M N_k} , \quad (9)$$

where M is the number of data sets to be pooled.

- (2) The best single estimate of the true probability

$$\bar{p}_k = \frac{n_k}{N_k}, \quad (10)$$

of each of the data subsets is computed.

- (3) Consider the binomial distribution function for each data set (N_k, n_k) having a true probability of detection given by \bar{p}_c . The two-sided probability, α_2 , that (N_k, n_k) and all less likely outcomes are possible is computed from

$$\alpha_2 = 2 \sum_{i=0}^{n_k} \binom{N_k}{i} \bar{p}_c^i (1-\bar{p}_c)^{N_k-i} \quad (11)$$

$$\text{if } \frac{n_k}{N_k} < \bar{p}_c$$

or by

$$\alpha_2 = \sum_{i=n_k}^{N_k} \binom{N_k}{i} \bar{p}_c^i (1-\bar{p}_c)^{N_k-i} \quad (12)$$

$$\text{if } \frac{n_k}{N_k} > \bar{p}_c .$$

- (4) All data sets having a value of α_2 less than a reference value α' (computer input value) are removed as candidates for pooling.

The choice of α' is somewhat arbitrary and depends upon the acceptable risk. The data sets that will be rejected from pooling for a given α' value will be reviewed. If no abnormalities are found within each set of data (i.e., no mistakes in data recording, or other possible means of causing the probability of detection to be normally high or low),

a new value of α' will be tried and one that will permit the data sets to be pooled with the data base will be selected. Thus, the value for α' may be governed by operator judgment of the validity of the data.

Table B-1 is an example which contains six hypothetical binomial experiments (assuming all sets have the same measurement parameters). (For this example α' was chosen to be .05). The α_2 values for sets C, E, and F are very low. The α_2 values for sets C and E were calculated using Equation (11) and for set F was calculated using Equation (12). For set C one is only 2.22% confident that one out of eight measurements is successful. For set E one is only 0.86% confident that one out of ten measurements is successful. For set F one is only 0.11% confident that seven out of seven measurements are successful. The confidence is too low for measurements to be pooled with those of sets A, B, and D.

Upon rejecting sets C, E, and F, new α_2 values are calculated for sets A, B, and D using the \bar{p}_c (16/40). These three sets have comparable confidence limits and they will be pooled.

Table B-1
SIX SETS OF DATA FROM DIFFERENT SOURCES
(A-F) TESTED FOR POOLING

<u>Source</u>	<u>N</u> Number of <u>Measurements</u>	<u>n</u> Number of <u>Successes</u>	α_2 (<u>Alpha</u>)
A	24	9	.4085 (accepted)
B	8	3	.3612 (accepted)
C	8	1	.0222 (rejected)
D	8	4	.3572 (accepted)
E	10	1	.0086 (rejected)
F	7	7	.0011 (rejected)
TOTAL	65	25	
A	24	9	.3641 (accepted)
B	8	3	.3361 (accepted)
D	8	4	.3834 (accepted)
TOTAL	40	16	

APPENDIX C

NASA. FTN COMPUTER CODE

NASA. FTN is written in Fortran and organized with a main routine performing all executive functions. Main does no data manipulation, it simply calls other routines which manipulate the data.

The flow diagram Figure C-1 illustrates the run sequence of the program. Two inputs required for the program are the Master Data File and a Problem Input Deck. At the end of a production run, the program lists the computational results.

C-1 Master Data File

The master data file consists of a sequence of 'data sets'. Each data set grouping has a common combination of conditions under which a series of specimens were inspected. These conditions are described in two 256 word records (header records). The results of the inspection are called data points and are stored after the two header records. Each data point is 8 words long and contains: crack ID, detect code, crack length, crack depth, measured crack length, measured crack depth, surface finish and thickness. The 'data records' consists of 256 words which contain 32 data points in each. Each data set is labeled by a number which is unique to the data set. The data set number and the number of data records per data set are stored in the header records of each data set. The master data file is stored on magnetic tape in binary format, 256 words per record.

C-2 Program Flow (Ref. to Table C-1)

The first step in running the program is to read all the program options. The subroutine then reads the master data file to extract, data points for analysis. These data are stored on a local disk file for up to 10,000 data points. Each data point on this data file is described by four words, crack size, detect/no detect, crack ID, and data set number. The input options have already (either implicitly or explicitly) described a set of common conditions. Subroutine Order then rewrites the local data file in increasing crack size.

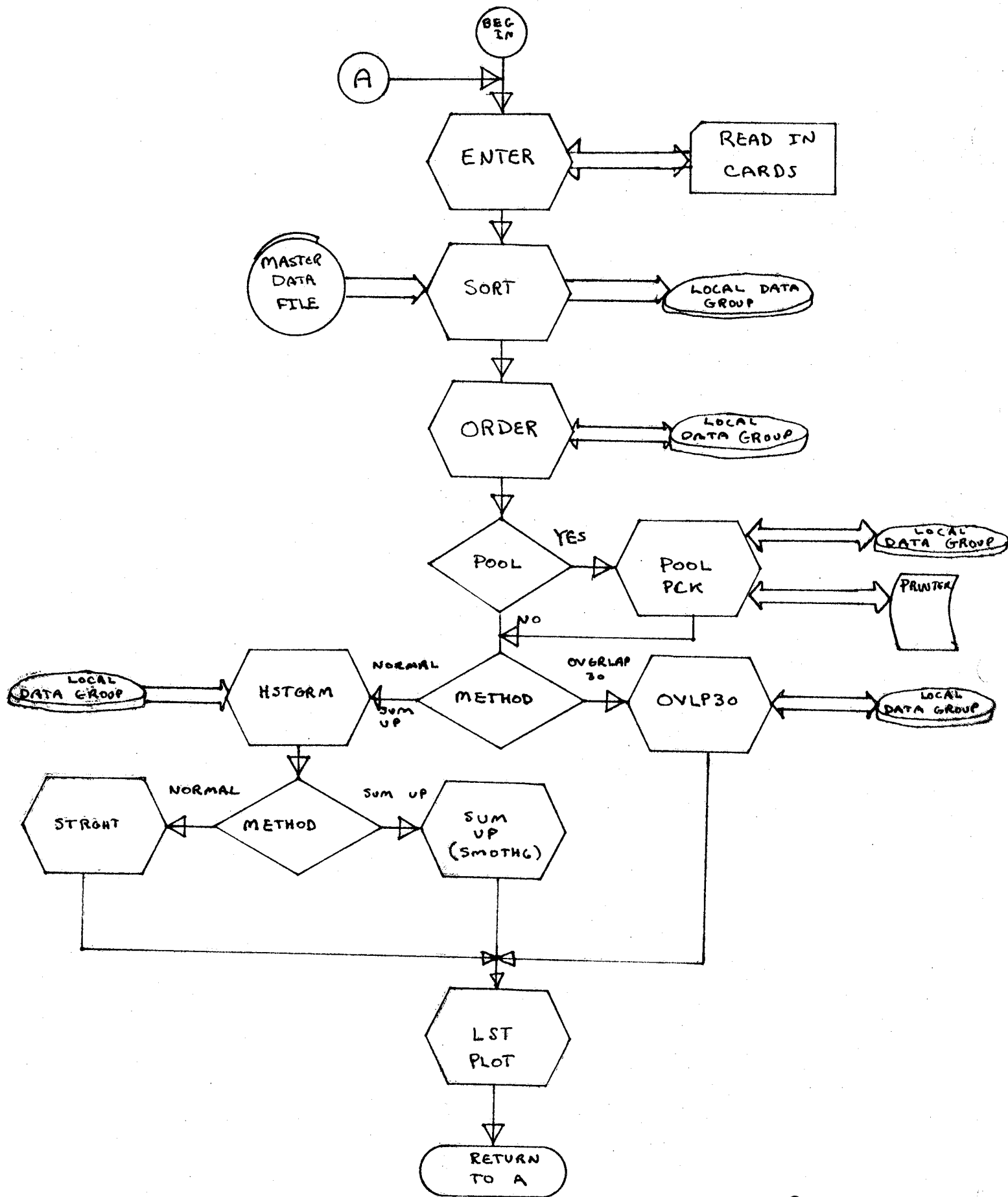


Figure C-1 Structure of Main Routine in NASA. FTN Code

C-2

Table C-1

Glossary of Programs and Subroutines
Used in NASA, FTN

NASA	-	Main program to control the program steps flow in Figure
ENTER	-	Routine to read in cards which contain the program options. The options are stored in commons for use by other routines.
SORT	-	Routine that reads the master data file, sorts out data for analysis, then writes this data on local disk file.
ORDER	-	Routine to sort the data on the local data file so that the order of the data will be by increasing crack size.
POOL	-	Routing to determine whether a particular data set belongs to the rest of the sets being considered.
POOLR	-	Routine to calculate probability of data sample belonging to a group having a known probability of detection.
RJCT	-	Routine to zero out data points of a data set that has been rejected on statistical grounds.
PCK	-	Routine to remove 'holes' in the local data file that are created by RJCT and to form a packed data file.
HSTGRM	-	Routine to sort data into 32 size interval groups.
OVLP30	-	Routine to perform an analysis of the data by using the procedure known as the "OSP" scheme.
SMOTHG	-	Routine to perform an analysis of the data by using the procedure known as the OPM.

Table C-1 (Continued)

STRGHT	- Routine to perform analysis of the data by using the procedure known as the "RI" scheme.
BIN	- Routine to calculate POD at a specific confidence limit for a binomial experiment consisting of N measurements and n successes.
DEFJC	- Routine to calculate the number of successful experiments which must be performed in order to know the lower limit probability of detection within a given confidence limit.
LST	- Routine to list the results of the analysis.
CKNRT	- Routine which performs paging of the local data file.

If pooling is desired, routine POOL can be used to calculate the probability that each data set statistically belongs to the rest of the data sets that are collected together. Any data set that gets rejected is removed from the local data file by zeroing the data points. Routine PCK takes the local data file and re-packs it so that there are no zeroed points. All data sets removed are listed on the printer. The method of analysis determines the route the program takes next. If 'overlapping 60' is chosen routing OVLP30 "OSP" takes the local data file and processes the data directly. Routing HSTGRM is used to divide the data points into 32 groups which have equal crack size intervals ranging between a minimum and maximum input crack size. All crack sizes falling below the minimum are included in the first interval and all data falling above the maximum are included in the thirty second interval. Either the routine STRGHT "RI" or the SMOTHG "OPM" analysis procedure can be selected to analyze the data. The results are then listed. The program then returns to the beginning to read more cards. If there are no more problems to be solved, the program terminates.

C-3 Sorting Option

The program has two sort options. The first option uses the data set number directly. (See Figure 4-2). The user specifies the number of data sets to be considered, then specifies the data set numbers. The second option (Figure 4-3), makes use of the header card information which includes 26 words or numerical codes for the alphanumeric data that is contained in the header records. By supplying values for these words, each header record can be compared to this 'master' input. No zero values are compared. Each time a match is made, that data set is stored on the local data file. A maximum of 5 master header records can be combined per run.

C-4 Program Limitations

The maximum crack size that can be stored and analyzed is 2.54 cm. The maximum number of data points that can be combined into a set is 1000. The maximum number of measurements that can be analyzed by the subroutine "DEFIC" which computes data deficiencies is 120.

IDSJ = NUMBER OF DATA SETS TO BE SELECTED
 JDSN = ARRAY CONTAINING THE DATA SET NUMBERS
 DSN = DATA SET NUMBER (READ FROM MASTER DATA FILE)

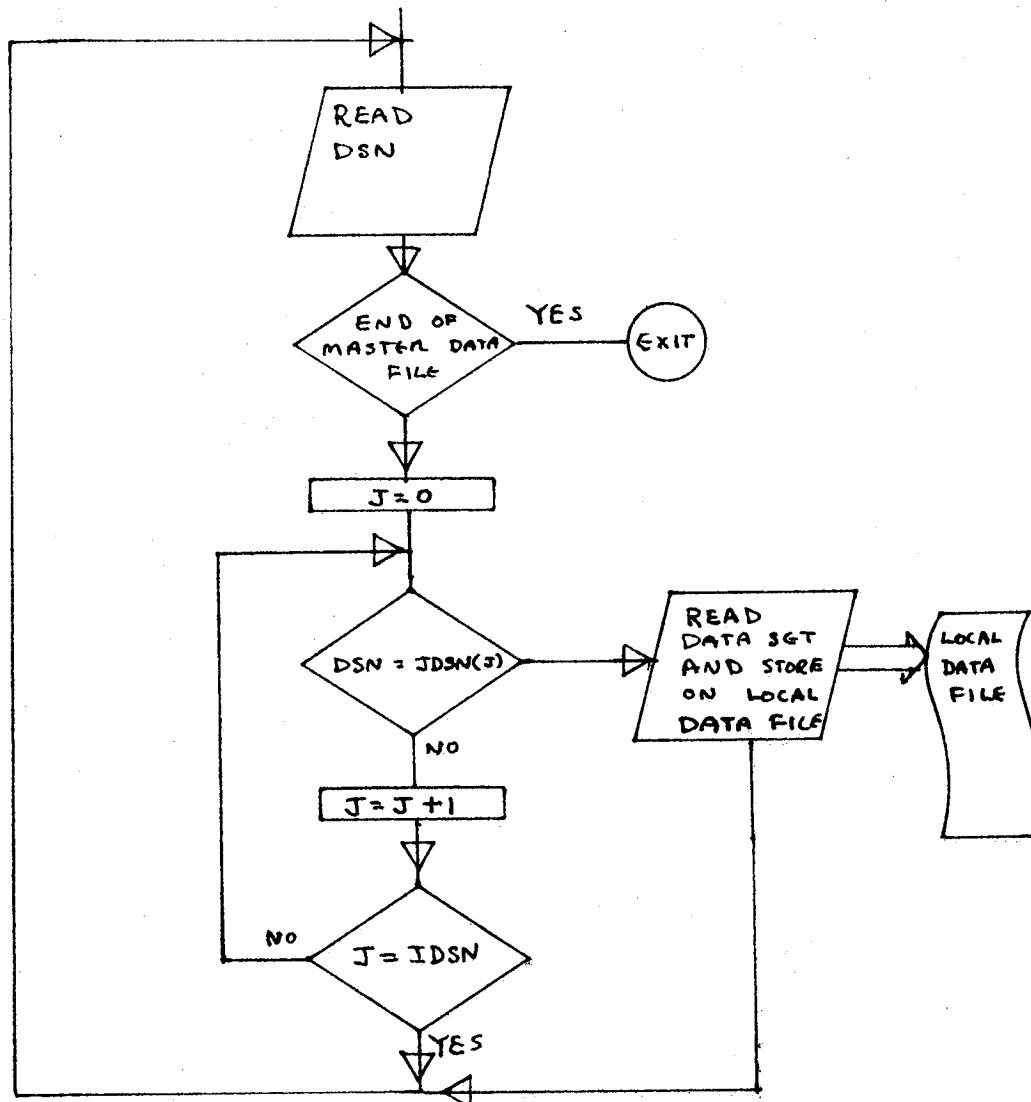


Figure C-2 Sort Subroutine Flow When Using Data Set Number Only for Sorting

C-5 Local Data File

The local data file is a direct access file which occupies a continuous block or disk space. A paging method has been incorporated to avoid executive disk I/O. The subroutine CKNXT is used for paging. At any given time, 1024 data points may be held in the core, therefore a disk access does not have to be made each time a new data point is addressed. The local data file has ten pages available for program use.

C-6 Ordering Method

A subroutine names "ORDER" reorders the local data file entries in increasing crack length then rewrites the ordered data file in place of the original unordered local data file. This ordered data is then used as input for data pooling and statistical analysis.

C-7 Lower One-Sided Confidence Limits Calculations

The binomial Equation (5) is solved by setting G equal to the confidence level desired and determining the value of p_1 which satisfies the equation. A Fortran IV program which has been made operable in a PDO 11/45 computer to perform this function is given in Figure 4-5. p_1 is the probability of detection at the lower confidence limit.

The procedure used to determine how many more measurements are required in each interval for the 95% confidence curve to reach the 90% probability of detection level is to solve Equation 8 for n and k . Figure 4-6 gives the listing of a Fortran IV program to perform this calculation.

C-6a

$ICCN = \text{NUMBER OF CONTROL CARDS (MAXIMUM OF 5)}$
 $JCCN(26, ICCN) = \text{ARRAY OF CONTROL CARD INFORMATION THAT IS INPUT}$
 $KCC(26) = \text{ARRAY OF CONTROL CARD INFORMATION FOR EACH DATA SET}$

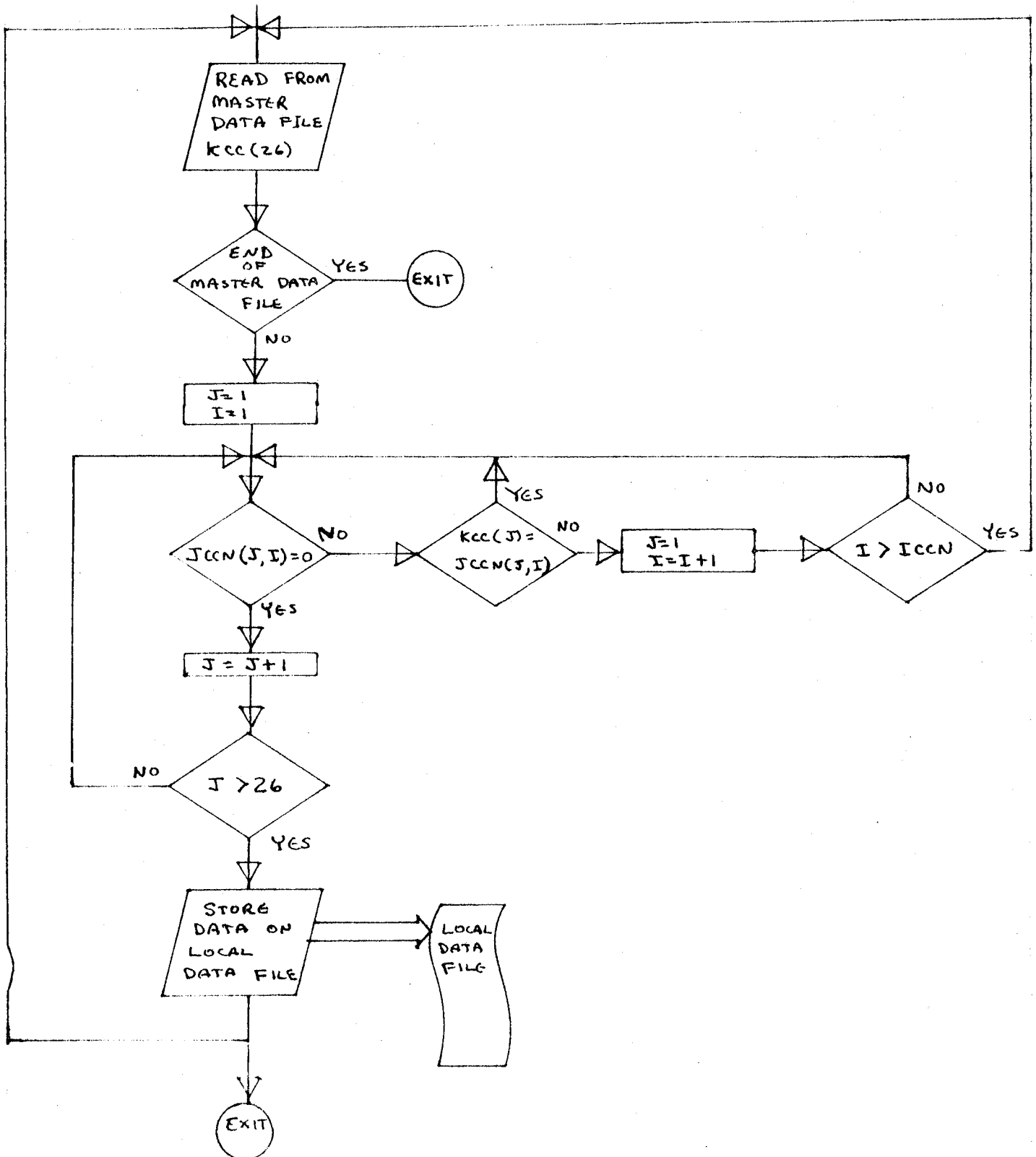


Figure C-3 Sort Subroutine Flow When Using Master Control Records to Sort on Master Data File

```

SUBROUTINE BINKAR1,AR2,AR3,AR10)
1 IF(AR2)2,2,4
2 AR10=0.0
3 RETURN
4 IF(AR2-AR1)7,5,5
5 AR10=(1.0-AR3)**(1.0/AR1)
6 RETURN
7 ATT=2.0*AR2
8 IF(ATT-AR1)9,9,12
9 AR4=AR2-1.0
10 AR5=-1.0
11 GO TO 15
12 AR4=AR1-AR2
13 AR3=1.0-AR3
14 AR5=-1.0
15 AR10=0.5
16 AR6=1.0
17 AR8=0.0
18 AR9=1.0
19 AR11=AR1
20 AR7=(AR10**AR8)*((1.0-AR10)**(AR1-AR8))
21 IF(AR8-AR4)22,27,22
22 AR8=AR8+1.0
23 AR9=AR9*AR11/AR8
24 AR11=AR11-1.0
25 AR7=AR7+AR9*(AR10**AR8)*((1.0-AR10)**(AR1-AR8))
26 GO TO 21
27 IF(AR3-AR7)28,28,30
28 AR20=AR10-AR5/(2.0**((AR6+1.0)))
29 GO TO 31
30 AR20=AR10+AR5/(2.0**((AR6+1.0)))
31 CCC=ABS(AR7-AR3)
32 IF(CCC-0.0001)36,36,33
33 AR6=AR6+1.0
34 AR10=AR20
35 GO TO 17
36 IF(ATT-AR1)6,6,37
37 AR10=1.0-AR10
38 RETURN
39 END

```

Figure C-4 Computer Code Used to Calculate Lower One-Sided Confidence Limit

C-9

```

SUBROUTINE DEFIC(AR1,AR2,FFF,AR4)
1 A=AR1-AR2+FFF
2 AR4=0.0
3 IF(A)4,4,9
4 AR4=29.0-AR1
5 IF(AR4)6,6,7
6 AR4=0.0
7 RETURN
9 X=1.0
10 AR5=0.0
11 C=1.0
12 CCC=AR1+AR4
13 AR5=0.9**CCC
14 C=(C/X)*(AR1+AR4+1.0-X)
15 DDD=AR1+AR4-X
16 AR5=AR5+(0.1**X)*C*(0.9**DDD)
17 IF(A-X)18,18,21
18 IF(0.05-AR5)19,19,7
19 AR4=AR4+1.0
   IF ( AR4 .EQ. 100. ) RETURN
20 GO TO 9
21 X=X+1.0
22 GO TO 14
23 END

```

Figure C-5 Computer Code Used to Calculate Additional Measurements Required to Achieve 90% Probability of Detection at 95% Confidence Limit

C-8 DATA INPUT FORMAT

The data are filed in mass memory by using a 'data set' concept. All the common control parameters for a group of data points are loaded together. There are 26 such control parameters. The first 14 are the same for all NDE methods, the next 12 are different for each of the five NDE methods. The results of the inspection follow the control parameters. Eight numbers are used to describe each point. (Crack ID, detect code, crack length, crack depth, measured crack length, measured crack depth, surface finish, thickness).

A typical control parameter listing is shown in Table C-1. Nine hundred eighty four flaw measurements have these parameters in common. The data in Table C-1 can be compacted for computer storage into the format shown in Table C-2. A special data set listing like that shown in Table C-1 can be prepared from the line of integers shown in Table C-2 by using the parameter key included at the end of this appendix. Four of the 984 data points for data set # 1 were entered onto each of 246 lines in the format depicted in Table C-3. Each complete data set is terminated by a 0000 entry in Columns 1 through 4 of the digital computer data sheet.

REPRODUCIBILITY OF THE
ORIGINAL PAGE IS POOR

Table C-1 Data Set Parameters
for Data Set Number 1

DATA SET NUMBER : 1

1)	5	NDE METHOD	: ULTRASONIC
2)	4	COMPANY NAME	: MARTIN MARIETTA
3)	2	PROGRAM ID	: DETECTION OF FATIGUE CRACKS
4)	1	MATERIAL	: ALUMINUM 2219-T87
5)	1	DEFECT TYPE	: FATIGUE CRK./NO CYCLE/REMOVE EDM
6)	0	OPERATOR ID	: NA
7)	7	QUALIFICATION	: QUALIFIED ACCORDING TO MIL-STD-453
8)	1	INSP. ENVIRONMENT	: PRODUCTION
9)	2	INSP. PROCEDURE	: STD. INSP. / MULTIPLE FLAW SPEC.
10)	4	DATA RECORD TYPE	: RECORD OF METER OR SCOPE DISPLAY
11)	3	MODE OF SCAN	: MECHANICAL SCAN AND INDEX
12)	3	REFERENCE STANDARD	: FLAT BOTTOM HOLE
13)	1	DEFECT MATERIAL	: AIR
14)	1	PART GEOMETRY	: FLAT PLATE

15)	1	ULTRASONIC METHOD	: SHEAR : PULSE ECHO
16)	4	FREQUENCY	: 10 MEG HZ.
17)	1	XMITER TYPE/SIZE	: FLAT FACE , .95 CM
18)	1	RECEIVER TYPE/SIZE	: FLAT FACE , .95 CM
19)	1	EQUIPMENT TYPE	: UM 715 , 10N PULSER/RECIEVER
20)	0	GAIN SET % OF SS	: NA
21)	0	ALARM SET % OF SS	: NA
22)	1	TYPE OF COUPLING	: WATER IMERSION
23)	1	ANGLE OF INCIDENCE	: 27.25 DEG.
24)	1	INDEX INTERVAL	: 318 CM (125 IN)

Table C-2 Data Set Entry for Compact Storage of
Data Set Parameters

Computer Input:

DIGITAL COMPUTER DATA SHEET

1	2	3	4	5	6	7	8	9	10	11	12	13	14	15	16	17	18	19	20	21	22	23	24	25	26	27	28	29	30	31	32	33	34	35	36	37	38	39	40	41	42	43	44	45	46	47	48	49	50	51	52
	5	4		2		1	1	0	7	1	2	4	3	3	1	1	1	4	1	1	1	0	0	1	1	1																									

Computer Output:

5 4 2 1 1 0 7 1 2 4 3 3 1 1 1 4 1 1 1 0 0 1 1 1

Table C-4 Data Key

NDI METHOD

DATA SOURCE

NDI METHOD

- 1 EDDY CURRENT
- 2 PENETRANT
- 3 MAGNETIC PARTICLE
- 4 RADIOGRAPHY
- 5 ULTRASONIC
- 6
- 7
- 8
- 9
- 10
- 11
- 12
- 13
- 14
- 15
- 16
- 17
- 18
- 19
- 20
- 21
- 22
- 23
- 24

COMPANY NAME

- 1 GENERAL DYNAMICS FW
- 2 CONVAIR/SAN DIEGO
- 3 BOEING COMMERCIAL
- 4 MARTIN MARIETTA
- 5 ROCKWELL INTER. B-1
- 6 LOCKHEED GA.
- 7 MCDONNELL DOUGLAS
- 8 AFML
- 9 TRW
- 10 GE , EVENDALE OHIO
- 11 FAIRCHILD HILLER
- 12 LOCKHEED CALIF.
- 13 ROCKWELL INTER. SPACE CENTER
- 14 BOEING WICHITA
- 15
- 16
- 17
- 18
- 19
- 20
- 21
- 22
- 23
- 24

PROGRAM ID

MATERIAL

PROGRAM ID

- 1 SENS. LIMITS OF PROD. NDE METHODS
- 2 DETECTION OF FATIGUE CRACKS
- 3 EVAL OF RELI. & SENS. OF NDE METHODS
- 4 USAF A10 SPO DEMO PROGRAM
- 5 USAF B-1 SPO DEMO PROGRAM
- 6 DETECTION OF TIGHTLY CLOSED FLAWS

7
8
9
10
11
12
13
14
15
16
17
18
19
20
21
22
23
24

MATERIAL

- 1 ALUMINUM 2219-T87
- 2 ALUMINUM 2024
- 3 4340M STEEL 270-300 KSI
- 4 TI-6AL-4V

5
6
7
8
9
10
11
12
13
14
15
16
17
18
19
20
21
22
23
24

DEFECT TYPE

OPERATOR ID

DEFECT TYPE

- 1 FATIGUE CRK./NO CYCLE/REMOVE EDM
- 2 ELOX SLOT
- 3 SAW CR
- 4 WELD DEFECT (LACK OF FUSION)
- 5 WELD DEFECT (LACK OF PENETRATION)
- 6 WELD DEFECT (POROSITY)
- 7 FORGING FLAWS WITH OXIDE IN FLAW
- 8 HYDROGEN EMBRITTLEMENT
- 9 HYDROGEN INDUCED GRINDING CRACK
- 10 FATIGUE CRACK / ADD. CYCLES / REMOVE EDM
- 11
- 12
- 13 COMPRESSED NOTCH FLAW
- 14 FATIGUE CRACKED WELDS
- 15
- 16
- 17
- 18
- 19
- 20
- 21
- 22
- 23
- 24

OPERATOR ID

- 1 A
- 2 B
- 3 C
- 4 D
- 5 E
- 6 F
- 7 G
- 8 H
- 9 I
- 10 J
- 11 K
- 12 L
- 13 M
- 14 N
- 15 O
- 16 P
- 17 Q
- 18 R
- 19 S
- 20 T
- 21 U
- 22 V
- 23 W
- 24 X

QUALIFICATION

INSP. ENVIRONMENT

QUALIFICATION

1	LEVEL 1
2	LEVEL 2
3	LEVEL 3
4	FIELD SERVICE TECHNICIAN
5	LABORATORY TECHNICIAN
6	LABORATORY ENGINEER
7	QUALIFIED ACCORDING TO MIL-STD-453
8	TECHNICALLY QUALIFIED
9	
10	CERTIFIED UNDER BOIENG A.C. 5953
11	
12	
13	
14	
15	
16	
17	
18	
19	
20	
21	
22	
23	
24	

INSP. ENVIRONMENT

1	PRODUCTION
2	LABORATORY
3	FIELD SERVICE
4	
5	
6	
7	
8	
9	
10	
11	
12	
13	
14	
15	
16	
17	
18	
19	
20	
21	
22	
23	
24	

INSP. PROCEDURE

DATA RECORD TYPE

INSP. PROCEDURE

- 1 STD. INSP. / SINGLE FLAW SPEC.
- 2 STD. INSP. / MULTIPLE FLAW SPEC.
- 3 NON STD. INSP. , SINGLE FLAW SPEC.
- 4 NON STD. INSP. , MULTIPLE FLAW SPEC.

5

6

7

8

9

- 10 MIL-STD-453 / MULTIPLE FLAW

11

12

13

14

15

16

17

18

19

20

21

22

23

24

DATA RECORD TYPE

- 1 MANUAL RECORD OF VISUAL DISPLAY
- 2 MANUAL RECORD OF METER OR SCOPE DISPLAY
- 3 MECHANICAL RECORD OF VISUAL DISPLAY
- 4 RECORD OF METER OR SCOPE DISPLAY
- 5 COMPUTER RECORD OF METER OR SCOPE DISPLA

6

7

8

9

10

11

12

13

14

15

16

17

18

19

20

21

22

23

24

MODE OF SCAN

REFERENCE STANDARD

MODE OF SCAN

- 1 MANUAL HAND SCAN
- 2 MECHANICAL SCAN , HAND INDEX
- 3 MECHANICAL SCAN AND INDEX
- 4 COMPUTER CONTROLLED SCAN
- 5
- 6
- 7
- 8
- 9
- 10
- 11
- 12
- 13
- 14
- 15
- 16
- 17
- 18
- 19
- 20
- 21
- 22
- 23
- 24

REFERENCE STANDARD

- 1 ELOX SLOT
- 2 FATIGUE CRACK
- 3 FLAT BOTTOM HOLE
- 4 FORGING FLAW
- 5 SAW CUT
- 6 SIDE DRILLED HOLE
- 7 VERTICAL DRILLED HOLE
- 8 0.039687 (1/64) FBH
- 9 0.079375 (2/64) FBH
- 10 0.119063 (3/64) FBH
- 11 0.15875 (4/64) FBH
- 12 0.198437 (5/64) FBH
- 13 REF. PANEL USED / DESCRIP. NOT KNOWN
- 14
- 15
- 16
- 17
- 18
- 19
- 20
- 21
- 22
- 23
- 24

DEFECT MATERIAL

DEFECT MATERIAL

- 1 AIR
- 2 WATER
- 3
- 4
- 5
- 6
- 7
- 8
- 9
- 10
- 11
- 12
- 13
- 14
- 15
- 16
- 17
- 18
- 19
- 20
- 21
- 22
- 23
- 24

PART GEO.

PART GEOMETRY

- 1 FLAT PLATE
- 2
- 3
- 4
- 5
- 6 WELDED BUTT JOINT WITHOUT CROWNS
- 7 INTEGRALLY STIFFENED PANEL (ISP)
- 8 WELDED BUTT JOINT WITH CROWNS
- 9 I. S. P. RIVETED TO FLAT PLATE
- 10 SOLID CYLINDER
- 11 FILLETED SOLID CYLINDER
- 12 TANDEM 'T'
- 13 HOLLOW CYLINDER
- 14 HOLLOW FILLETED CYLINDER
- 15 FLAT BAR
- 16
- 17
- 18
- 19
- 20
- 21
- 22
- 23
- 24

SPECIAL
KEY FOR EDDY CURRENT
DATA

- 1 NDE METHOD
- 2 COMPANY NAME
- 3 PROGRAM ID
- 4 MATERIAL
- 5 DEFECT TYPE
- 6 OPERATOR ID
- 7 QUALIFICATION
- 8 INSP. ENVIRONMENT
- 9 INSP. PROCEDURE
- 10 DATA RECORD TYPE
- 11 MODE OF SCAN
- 12 REFERENCE STANDARD
- 13 DEFECT MATERIAL
- 14 PART GEOMETRY

- 15 EQUIPMENT TYPE
- 16 DIAMETER OF COIL
- 17 CONF./SHAPE OF COIL
- 18 FREQUENCY
- 19 TYPE OF EC RESPONSE
- 20 LIFT-OFF COMP.
- 21 SIGNAL PROCESSING
- 22 INDEX INTERVAL

24
23
22
21
20
19
18
17
16
15
14
13
12
11
10
9
8
7
6
5
4
3
2
1

EQUIPMENT TYPE
1 NORTRON NOT-3

MAGNETEST ED-400 & ED-520
VECTOR 3 SR 150 BUDD , ULTA BRIDGE

15 EQUIPMENT TYPE

16 DIAMETER OF COIL

17 CONF./SHAPE OF COIL

18 FREQUENCY

CONF./SHAPE OF COIL

- 1 DUAL COIL , AIR CORE
- 2 SINGLE COIL HELICALLY WOUND
- 3
- 4
- 5 BOLT HOLE & SURFACE PROBE
- 6
- 7
- 8
- 9
- 10
- 11
- 12
- 13
- 14
- 15
- 16
- 17
- 18
- 19
- 20
- 21
- 22
- 23
- 24

FREQUENCY

- 1 100 KHZ
- 2 20 KHZ
- 3
- 4
- 5
- 6
- 7
- 8
- 9
- 10
- 11
- 12
- 13
- 14
- 15
- 16
- 17
- 18
- 19
- 20
- 21
- 22
- 23
- 24

19 TYPE OF EC RESPONSE

TYPE OF EC RESPONSE

1 AMPLITUDE
2 PHASE
3
4
5
6
7
8
9
10
11
12
13
14
15
16
17
18
19
20
21
22
23
24

20 LIFT-OFF COMP.

LIFT-OFF COMP.

1 NO LIFT-OFF COMPENSATION
2 LIFT-OFF COMPENSATED FOR (3MIL SHIM)
3
4
5
6
7
8
9
10
11
12
13
14
15
16
17
18
19
20
21
22
23
24

21 SIGNAL PROCESSING

SIGNAL PROCESSING
1 STRAIGHT AMPLIFICATION

2
3
4
5
6
7
8
9
10
11
12
13
14
15
16
17
18
19
20
21
22
23
24

22 INDEX INTERVAL

INDEX INTERVAL
1 3048 CM (.125 IN)
2 .0508 CM (.020 IN)

3
4
5
6
7
8
9
10
11
12
13
14
15
16
17
18
19
20
21
22
23
24

SPECIAL
KEY FOR LIQUID PENETRANT
DATA

- 1 NDE METHOD
- 2 COMPANY NAME
- 3 PROGRAM ID
- 4 MATERIAL
- 5 DEFECT TYPE
- 6 OPERATOR ID
- 7 QUALIFICATION
- 8 INSP. ENVIRONMENT
- 9 INSP. PROCEDURE
- 10 DATA RECORD TYPE
- 11 MODE OF SCAN
- 12 REFERENCE STANDARD
- 13 DEFECT MATERIAL
- 14 PART GEOMETRY

- 15 PENETRANT TYPE
- 16 DEVELOPER TYPE
- 17 CLASS OF PENETRANT
- 18 REMOVER/EMULSIFIER
- 19 APPLICATION METHOD
- 20 DWELL TIME
- 21 DEVELOPING TIME
- 22 WASH TIME
- 23 LIGHT INTENSITY
- 24 REMOVAL/PRE-CLEANING

15 PENETRANT TYPE

PENETRANT TYPE

- 1 URESCO P-151
- 2
- 3
- 4 ZL-2A , URESCO P-133 & P-134
- 5 URESCO P-149
- 6
- 7
- 8
- 9
- 10
- 11
- 12
- 13
- 14
- 15
- 16
- 17
- 18
- 19
- 20
- 21
- 22
- 23
- 24

16 DEVELOPER TYPE

DEVELOPER TYPE

- 1 URESCO D499C
- 2
- 3
- 4 MAGNAFLUX ZP-4A , -5, & -13, & URESCO 499B
- 5 URESCO D499C
- 6
- 7
- 8
- 9
- 10
- 11
- 12
- 13
- 14
- 15
- 16
- 17
- 18
- 19
- 20
- 21
- 22
- 23
- 24

18 REMOVER/EMULSIFIER

REMOVER/EMULSIFIER
 1 URESCO K410
 2
 3
 4 ZE-4A AND ZE-4B
 5
 6
 7
 8
 9
 10
 11
 12
 13
 14
 15
 16
 17
 18
 19
 20
 21
 22
 23
 24

17 CLASS OF PENETRANT

CLASS OF PENETRANT
 1 GROUP 1
 2 GROUP 2
 3 GROUP 3
 4 GROUP 4
 5 GROUP 5
 6 GROUP 6
 7 GROUP 7
 8
 9
 10
 11
 12
 13
 14
 15
 16
 17
 18
 19
 20
 21
 22
 23
 24

19 APPLICATION METHOD

APPLICATION METHOD

1 HAND BRUSH

2

3

4

5

6

7

8

9

10

11

12

13

14

15

16

17

18

19

20

21

22

23

24

20 DWELL TIME

DWELL TIME

1 30. MINUTES

2

3

4

5

6

7

8

9

10

11

12

13

14

15

16

17

18

19

20

21

22

23

24

21 DEVELOPING TIME

DEVELOPING TIME

30 MINUTES

1
2
3
4
5
6
7
8
9
10
11
12
13
14
15
16
17
18
19
20
21
22
23
24

22 WASH TIME

WASH TIME

60 MINUTES

1
2
3
4
5
6
7
8
9
10
11
12
13
14
15
16
17
18
19
20
21
22
23
24

23 LIGHT INTENSITY

LIGHT INTENSITY
1 1350 LUMENS/SQ METER
2 125 FT-CANDLES . 15 IN FROM FILTER

3
4
5
6
7
8
9
10
11
12
13
14
15
16
17
18
19
20
21
22
23
24

24 REMOVAL/PRE-CLEANING

REMOVAL/PRE-CLEANING
1 MARTIN MARIETTA (PER. NASA CR-2369)
2 CLEANED BY ALCOHOL IN ULTRASONIC CLEANER

3
4
5
6
7
8
9
10
11
12
13
14
15
16
17
18
19
20
21
22
23
24

SPECIAL
KEY FOR MAGNETIC PARTICLE
DATA

- 1 NDE METHOD
- 2 COMPANY NAME
- 3 PROGRAM ID
- 4 MATERIAL
- 5 DEFECT TYPE
- 6 OPERATOR ID
- 7 QUALIFICATION
- 8 INSP. ENVIRONMENT
- 9 INSP. PROCEDURE
- 10 DATA RECORD TYPE
- 11 MODE OF SCAN
- 12 REFERENCE STANDARD
- 13 DEFECT MATERIAL
- 14 PART GEOMETRY

- 15 EQUIPMENT
- 16 PROCEDURE
- 17 MAG. PARTICAL TYPE
- 18 SUSPENSION TYPE

15 EQUIPMENT

EQUIPMENT

- 1 TYPICAL AERO-SPACE EQUIP.
- 2 PARKER RESEARCH CO. (MOD DA-200)
- 3
- 4
- 5
- 6
- 7
- 8
- 9
- 10
- 11
- 12
- 13
- 14
- 15
- 16
- 17
- 18
- 19
- 20
- 21
- 22
- 23
- 24

16 PROCEDURE

PROCEDURE

- 1 WET CONTINUOUS FLUORESCENT PRCE.
- 2
- 3
- 4
- 5
- 6
- 7
- 8
- 9
- 10
- 11
- 12
- 13
- 14
- 15
- 16
- 17
- 18
- 19
- 20
- 21
- 22
- 23
- 24

17 MAG. PARTICAL TYPE

MAG. PARTICAL TYPE
1 MAGNAFLUX 14A
2 MAGNAFLUX 14A & 14AM
3
4
5
6
7
8
9
10
11
12
13
14
15
16
17
18
19
20
21
22
23
24

18 SUSPENSION TYPE

SUSPENSION TYPE
1 OIL & WATER BASE
2 14A IN OIL / 14AM IN AEROSOL CANS
3
4
5
6
7
8
9
10
11
12
13
14
15
16
17
18
19
20
21
22
23
24

SPECIAL
KEY FOR RADIOGRAPHY
DATA

- 1 NDE METHOD
 - 2 COMPANY NAME
 - 3 PROGRAM ID
 - 4 MATERIAL
 - 5 DEFECT TYPE
 - 6 OPERATOR ID
 - 7 QUALIFICATION
 - 8 INSP. ENVIRONMENT
 - 9 INSP. PROCEDURE
 - 10 DATA RECORD TYPE
 - 11 MODE OF SCAN
 - 12 REFERENCE STANDARD
 - 13 DEFECT MATERIAL
 - 14 PART GEOMETRY
-
- 15 RADIOGRAPHY
 - 16 EQUIPMENT TYPE
 - 17 SOURCE ENERGY
 - 18 SOURCE STRENGTH
 - 19 WINDOW MATERIAL
 - 20 TYPE OF FILM
 - 21 EXPOSURE TIME
 - 22 SOURCE TO FILM DISTA
 - 23 ANGLE OF INCIDENCE
 - 24 DENSITOMETER READING

15 RADIOGRAPHY

RADIOGRAPHY

1 X-RAY
2 NEUTRON
3
4
5
6
7
8
9
10
11
12
13
14
15
16
17
18
19
20
21
22
23
24

16 EQUIPMENT TYPE

EQUIPMENT TYPE

1
2
3
4 BALTOSPOT X-RAY
5 NORELCO X-RAY 150 KV 24MA
6
7
8
9
10
11
12
13
14
15
16
17
18
19
20
21
22
23
24

17 SOURCE ENERGY

SOURCE ENERGY	
1	30 KV FOR .1524 CM AL PANEL
2	40 KV FOR .5207 CM AL PANEL
3	45 KV FOR .3300 CM , 70 KV FOR 1.27 CM
4	
5	
6	
7	
8	
9	
10	
11	
12	
13	
14	
15	
16	
17	
18	
19	
20	
21	
22	
23	
24	

18 SOURCE STRENGTH

SOURCE STRENGTH	
1	20 MILLI-AMPS
2	3 MILLI-AMPS
3	
4	
5	
6	
7	
8	
9	
10	
11	
12	
13	
14	
15	
16	
17	
18	
19	
20	
21	
22	
23	
24	

19 WINDOW MATERIAL

WINDOW MATERIAL
BERYLLIUM

1
2
3
4
5
6
7
8
9
10
11
12
13
14
15
16
17
18
19
20
21
22
23
24

20 TYPE OF FILM

TYPE OF FILM
KODAK , TYPE M

1
2
3
4
5
6
7
8
9
10
11
12
13
14
15
16
17
18
19
20
21
22
23
24

C-2

21 EXPOSURE TIME

EXPOSURE TIME

- 1 7 MIN. FOR 1524 CM AL
- 2 15 MIN. FOR 5207 CM AL
- 3 1.5-3.0 MIN. (THICK-ENERGY DEPEND.)
- 4 1.5-2.25 MIN. (THICK-ENERGY DEPEND.)
- 5
- 6
- 7
- 8
- 9
- 10
- 11
- 12
- 13
- 14
- 15
- 16
- 17
- 18
- 19
- 20
- 21
- 22
- 23
- 24

22 SOURCE TO FILM DISTA

SOURCE TO FILM DISTA

- 1 117 CM.
- 2 122 CM.
- 3
- 4
- 5
- 6
- 7
- 8
- 9
- 10
- 11
- 12
- 13
- 14
- 15
- 16
- 17
- 18
- 19
- 20
- 21
- 22
- 23
- 24

23 ANGLE OF INCIDENCE

ANGLE OF INCIDENCE
1 0.0 DEG (NORMAL)

2
3
4
5
6
7
8
9
10
11
12
13
14
15
16
17
18
19
20
21
22
23
24

24 DENSITOMETER READING

DENSITOMETER READING
1 2.5-3.5

2
3
4
5
6
7
8
9
10
11
12
13
14
15
16
17
18
19
20
21
22
23
24

SPECIAL
KEY FOR ULTRASONICS
DATA

1 NDE METHOD
2 COMPANY NAME
3 PROGRAM ID
4 MATERIAL
5 DEFECT TYPE
6 OPERATOR ID
7 QUALIFICATION
8 INSP. ENVIRONMENT
9 INSP. PROCEDURE
10 DATA RECORD TYPE
11 MODE OF SCAN
12 REFERENCE STANDARD
13 DEFECT MATERIAL
14 PART GEOMETRY

15 ULTRASONIC METHOD
16 FREQUENCY
17 XMITTER TYPE/SIZE
18 RECEIVER TYPE/SIZE
19 EQUIPMENT TYPE
20 GAIN SET % OF SS
21 ALARM SET % OF SS
22 TYPE OF COUPLING
23 ANGLE OF INCIDENCE
24 INDEX INTERVAL

15 ULTRASONIC METHOD

ULTRASONIC METHOD

- 1 SHEAR : PULSE ECHO
- 2 SHEAR : PITCH CATCH
- 3 DELTA SCAN
- 4 COMPRESSIONAL WAVE : PULSE ECHO
- 5 COMPRESSIONAL WAVE : THROUGH TRANS.
- 6 SURFACE WAVE
- 7 SHEAR + SURFACE : PULSE ECHO
- 8 SHEAR + SURFACE + LONG. : PULSE ECHO
- 9
- 10
- 11
- 12
- 13
- 14
- 15
- 16
- 17
- 18
- 19
- 20
- 21
- 22
- 23
- 24

16 FREQUENCY

FREQUENCY

- 1 1 MEG. HERTZ
- 2 2.25 MEG HZ.
- 3 5 MEG HZ.
- 4 10 MEG HZ.
- 5 15 MEG HZ.
- 6
- 7
- 8
- 9
- 10
- 11
- 12
- 13
- 14
- 15
- 16
- 17
- 18
- 19
- 20
- 21
- 22
- 23
- 24

17 XMITTER TYPE/SIZE

XMITTER TYPE/SIZE

- 1 FLAT FACE , .95 CM
- 2 FLAT FACE , .635 CM
- 3 FLAT FACE , 1.27 CM
- 4
- 5
- 6
- 7
- 8
- 9
- 10
- 11
- 12
- 13
- 14
- 15
- 16
- 17
- 18
- 19
- 20
- 21
- 22
- 23
- 24

18 RECEIVER TYPE/SIZE

RECEIVER TYPE/SIZE

- 1 FLAT FACE , .95 CM
- 2 FLAT FACE , .635 CM
- 3 FLAT FACE , 1.27 CM
- 4
- 5
- 6
- 7
- 8
- 9
- 10
- 11
- 12
- 13
- 14
- 15
- 16
- 17
- 18
- 19
- 20
- 21
- 22
- 23
- 24

19 EQUIPMENT TYPE

EQUIPMENT TYPE

1 UM 715 , 10N PULSER/RECIEVER
2
3
4
5
6
7
8
9
10 UM 715 , USIP 11 , 424D
11
12
13
14
15
16
17
18
19
20
21
22
23
24

20 GAIN SET % OF SS

GAIN SET % OF SS

1 80 % SCREEN SATURATION
2
3
4
5
6
7
8
9
10
11
12
13
14
15
16
17
18
19
20
21
22
23
24

22 TYPE OF COUPLING

TYPE OF COUPLING
 1 WATER IMERSION
 2 OIL IMERSION
 3 WATER CONTACT
 4 OIL CONTACT

5
6
7
8
9
10
11
12
13
14
15
16
17
18
19
20
21
22
23
24

21 ALARM SET % OF SS

ALARM SET % OF SS
 1 33 % SCREEN SATURATION
 2 50 % SCREEN SATURATION

3
4
5
6
7
8
9
10
11
12
13
14
15
16
17
18
19
20
21
22
23
24

23 ANGLE OF INCIDENCE

ANGLE OF INCIDENCE

1	27.25 DEG.
2	18.00 DEG.
3	27.00-27.75 DEG.
4	32.00 DEG.
5	90.0 DEG. (NORMAL)
6	
7	
8	
9	
10	
11	
12	
13	
14	
15	
16	
17	
18	
19	
20	
21	
22	
23	
24	

24 INDEX INTERVAL

INDEX INTERVAL

1	.318 CM (.125 IN.)
2	.081 CM (.032 IN)
3	.051 CM (.020 IN)
4	.076 CM (.030 IN)
5	
6	
7	
8	
9	
10	
11	
12	
13	
14	
15	
16	
17	
18	
19	
20	
21	
22	
23	
24	

APPENDIX D

COMPUTER OUTPUT - NDE RELIABILITY DATA

The data for Figures D-1a, D-1b, and D-1c were obtained with an ultrasonic surface wave technique and at a frequency of 10 MHz. The abscissa is the surface length of a fatigue crack. The NDE technique (ultrasonics) is given on the upper left hand corner of the figures immediately after the date when the curves were plotted. Test 1, Test 2, or Test 3 is written on the same top line of the page. Test 1 refers to the range scheme where the lower one-sided confidence limit, P_1 , was calculated for equal flaw size intervals. In Figure D-1a the flaw size interval is 0.038 cm. Test 2 (Figure D-1b) refers to the use of the optimized probability method to calculate the P_1 . Test 3 (Figure D-1c) refers to the use of the overlapping sixty point scheme to calculate the p_1 . The top line of the computer output also contains the name of the company or the agency that published the report from which the data were taken. In Figure D-1 the company is Martin Marietta of Denver, Colorado. The test specimen martial type is identified in the figure caption on the bottom of the page or in Table 5-1 of Section V where the data set number can be matched with the number in parenthesis in the upper right hand side of each figure.

The first column of the tabulated results in these figures lists the range numbers. The second column gives the minimum crack length of each range and the third column gives the maximum crack length of each range.* The fourth column gives the total number of measurements or observations (N) for each size range and the fifth column gives the number of detections (n) for each size range. The probability of detection at 50% and 95% confidence level** is given in the sixth and seventh columns respectively. The last two columns list the number of new measurements that must be made with no misses and with one miss, respectively, to achieve 90% probability of detection at a 95% confidence level. The zeroes in these last two columns indicate that either no measurements need to be made or the number is too large for practical consideration.

* Tabulated data give crack lengths in mils while the graphs give both mils and cm scales. This dual labeling is offered as a convenience for the design engineer.

** Hereafter POD90(CL95) will be used to refer to a 95 percent confidence that the true probability of detection equals or exceeds 90 percent.

All the reliability curves discussed in this appendix are presented in the above format. Additional information such as flaw, type, material alloy type, contract or report identification number, and other pertinent parameters associated with the data used to generate these reliability curves and tables are included wherever possible.

(a) Range Interval Method of Data Cumulation

02-JUL-75		ULTRASONIC BY LENGTH			TEST 1, MARTIN (1)				RANGE	
RANGE	MIN LN	* MAX LN	* N	DET	50%	95%	0 MISS	1 MISS	1 MISS	
1	7	21	30	4	9	3	0	0	0	
2	25	36	40	15	30	20	0	0	0	
3	38	52	72	40	54	45	0	0	0	
4	54	67	120	98	81	74	0	0	0	
5	68	82	132	117	88	83	0	0	0	
6	83	97	87	72	82	74	0	0	0	
7	98	108	39	38	95	88	7	22	0	
8	115	126	33	31	91	82	28	43	0	
9	129	141	42	41	96	89	4	19	0	
10	146	153	18	17	90	75	23	43	0	
11	158	171	9	8	82	57	0	0	0	
12	182	184	9	8	82	57	0	0	0	
13	0	0	0	0	0	0	0	0	0	
14	0	0	0	0	0	0	0	0	0	
15	0	0	0	0	0	0	0	0	0	
16	241	247	12	11	86	66	0	0	0	
17	248	262	51	51	98	94	0	0	0	
18	268	275	9	9	92	71	0	0	0	
19	279	290	15	15	95	81	14	34	0	
20	295	306	15	15	95	81	14	34	0	
21	310	322	27	27	97	89	0	13	0	
22	323	336	30	30	97	90	0	13	0	
23	338	347	18	18	96	84	11	13	0	
24	362	362	3	3	79	36	0	0	0	
25	381	381	3	3	79	36	0	0	0	
26	393	393	3	3	79	36	0	0	0	
27	408	408	3	3	79	36	0	0	0	
28	0	0	0	0	0	0	0	0	0	
29	0	0	0	0	0	0	0	0	0	
30	0	0	0	0	0	0	0	0	0	
31	459	466	6	6	89	60	0	0	0	
32	475	979	90	89	90	94	0	0	0	

Crack Length (Mils) *

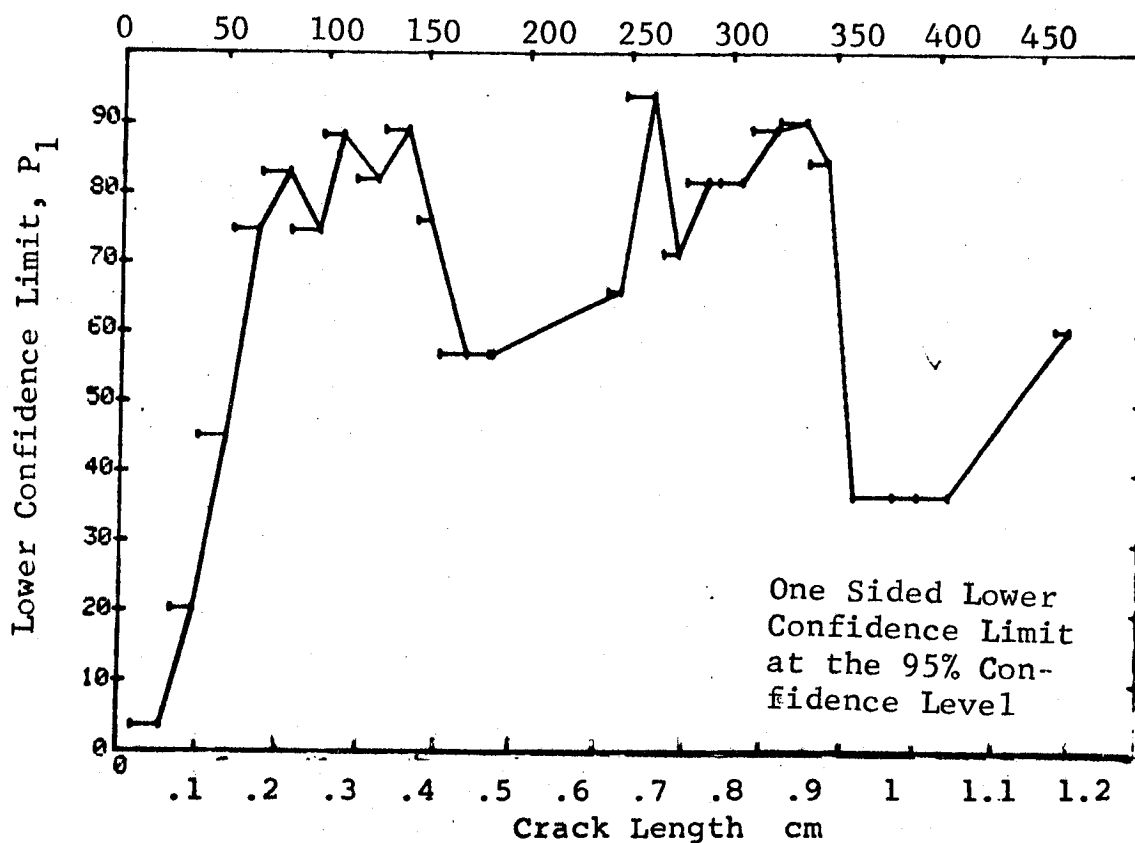


Figure D-1 Probability of Detection for 2219-T87 Al Using Ultrasonic Surface Waves. Fatigue Cracks in Flat Plates. Lab. Env.

D-8

REPRODUCIBILITY OF THE ORIGINAL PAGE IS POOR

(b) Optimum Probability Method of Data Cumulation

02-JUL-75		ULTRASONIC BY LENGTH			TEST 2 , MARTIN (1)		MCD		
RANGE	MIN	LN	MAX LN	N	DET	50%	95%	0 MISS	1 MISS
1		7*	21	39	4	0	3	0	0
2		25	36	48	15	0	20	0	0
3		38	52	72	40	0	45	0	0
4		54	67	120	98	0	74	0	0
5		68	82	132	117	0	83	0	0
6		68	97	219	189	0	81	0	0
7		98	108	39	38	0	88	7	22
8		98	126	72	69	0	89	4	17
9		98	141	114	110	0	92	0	0
10		98	153	132	127	0	92	0	0
11		98	171	141	135	0	91	0	0
12		98	184	150	143	0	91	0	0
13		0	0	0	0	0	0	0	0
14		0	0	0	0	0	0	0	0
15		0	0	0	0	0	0	0	0
16		98	247	162	154	0	91	0	0
17		248	262	51	51	0	94	0	0
18		248	275	60	60	0	95	0	0
19		248	290	75	75	0	96	0	0
20		248	306	90	90	0	96	0	0
21		248	322	117	117	0	97	0	0
22		248	336	147	147	0	97	0	0
23		248	347	165	165	0	98	0	0
24		248	362	168	168	0	98	0	0
25		248	381	171	171	0	98	0	0
26		248	393	174	174	0	98	0	0
27		248	408	177	177	0	98	0	0
28		0	0	0	0	0	0	0	0
29		0	0	0	0	0	0	0	0
30		0	0	0	0	0	0	0	0
31		248	466	183	183	0	98	0	0
32		248	979	273	272	0	98	0	0

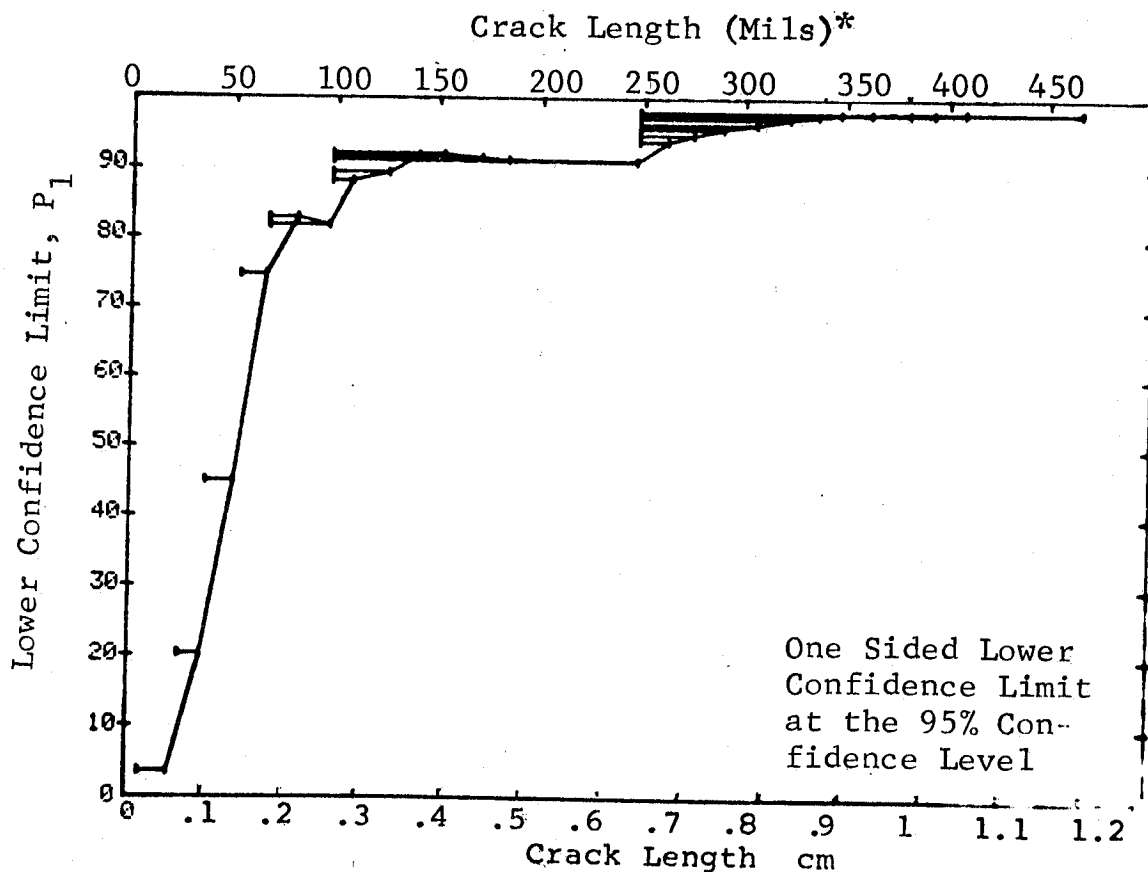


Figure D-1 (Continued)

(c) Overlapping Sixty Point Method of Data Cumulation

02-JUL-75		ULTRASONIC BY LENGTH		TEST 3		MARTIN (1)			
RANGE	MIN LN	MAX LN	N	DET	50%	95%	0 MISS	1 MISS	
1	0	0	0	0	0	0	0	0	
2	0	0	0	0	0	0	0	0	
3	0	0	0	0	0	0	0	0	
4	7	20	33	4	11	4	0	0	
5	8	30	60	10	16	9	0	0	
6	21	40	60	16	25	17	0	0	
7	31	45	60	20	32	23	0	0	
8	40	51	60	33	54	43	0	0	
9	45	58	60	42	69	58	0	0	
10	52	61	60	43	70	60	0	0	
11	58	64	60	53	87	79	0	0	
12	62	67	60	56	92	85	29	43	
13	64	70	60	53	87	79	29	43	
14	67	73	60	52	85	77	82	100	
15	70	77	60	50	82	77	82	100	
16	74	80	60	52	85	77	82	100	
17	77	83	60	56	92	85	29	43	
18	80	87	60	53	87	79	29	43	
19	84	95	60	52	85	77	82	100	
20	90	102	60	51	83	75	82	100	
21	96	115	60	52	85	77	82	100	
22	103	129	60	58	95	89	1	16	
23	117	136	60	60	98	95	0	16	
24	129	158	60	58	95	89	0	16	
25	138	248	60	55	90	83	43	100	
26	162	258	60	57	93	87	16	100	
27	249	279	60	60	98	95	0	100	
28	258	310	60	60	98	95	0	100	
29	279	326	60	60	98	95	0	100	
30	310	340	60	60	98	95	0	100	
31	326	466	60	60	98	95	0	100	
32	342	500	60	60	98	95	0	100	

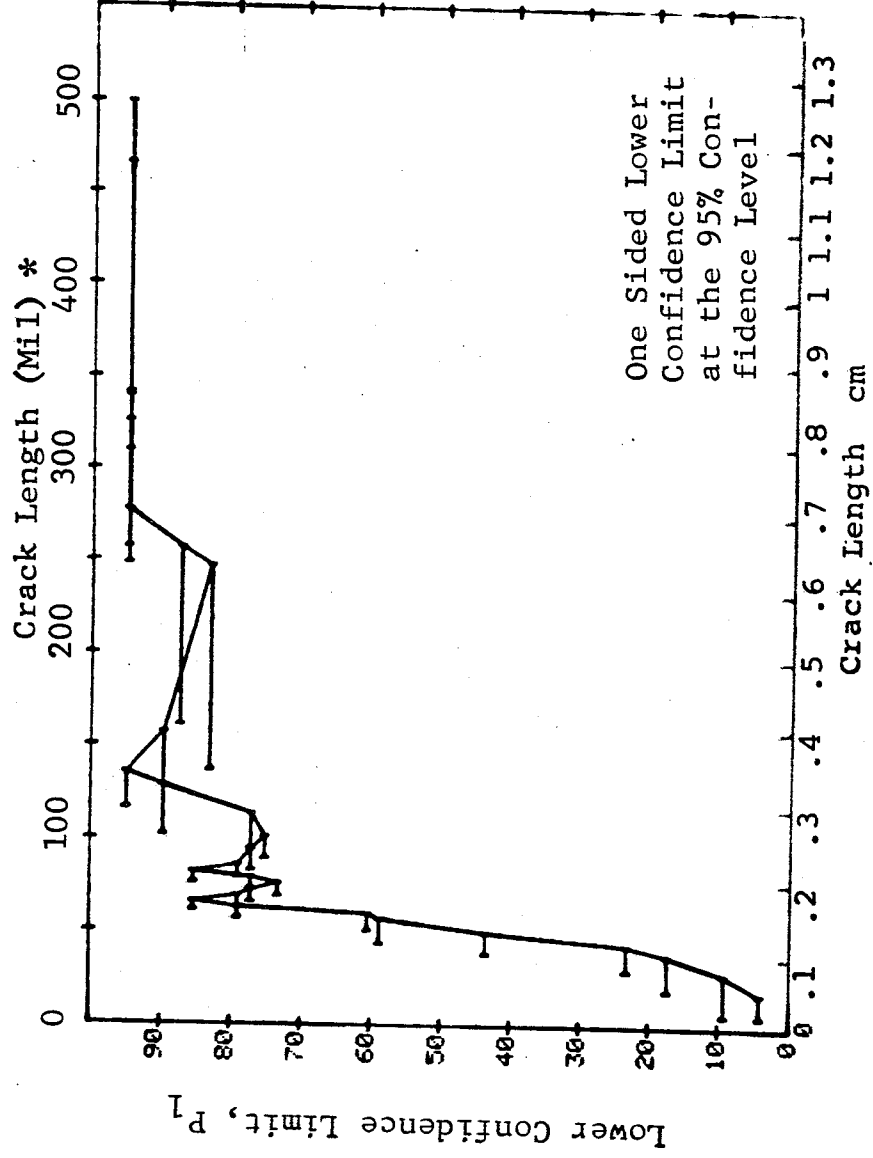


Figure D-1 (Concluded)

(a) Range Interval Method of Data Cumulation

02-JUL-75						TEST 1		PENET		MARTIN (2)		RANGE
RANGE	MIN	LN	MAX	LN	N	DET	50%	95%	MIN	MAX		
1	7*	21	39	48	13	4	26	15	0	0		
2	25	38	52	72	23	31	22	0	0	0		
3	38	52	67	120	63	52	44	0	0	0		
4	54	67	82	132	91	68	61	0	0	0		
5	68	82	97	87	60	68	59	0	0	0		
6	83	97	108	39	23	57	44	0	0	0		
7	98	108	126	33	15	43	30	0	0	0		
8	115	126	141	42	26	60	48	0	0	0		
9	129	141	153	18	11	58	39	0	0	0		
10	146	153	171	9	3	28	9	0	0	0		
11	158	171	185	9	5	50	25	0	0	0		
12	182	185	0	0	0	0	0	0	0	0		
13	0	0	0	0	0	0	0	0	0	0		
14	0	0	0	0	0	0	0	0	0	0		
15	0	0	0	0	0	0	0	0	0	0		
16	241	247	12	12	12	94	77	17	34			
17	248	262	51	50	50	96	91	0	10			
18	268	275	9	7	7	71	45	0	0	0		
19	279	290	15	13	13	82	63	0	0	0		
20	295	306	15	14	14	89	72	0	0	0		
21	310	322	27	19	19	68	52	0	0	0		
22	323	336	30	27	27	87	76	4	20			
23	338	347	18	15	15	79	62	0	0	0		
24	362	362	3	3	3	79	36	0	0	0		
25	381	381	3	3	3	79	36	0	0	0		
26	393	393	3	3	3	79	36	0	0	0		
27	408	408	3	3	3	79	36	0	0	0		
28	0	0	0	0	0	0	0	0	0	0		
29	0	0	0	0	0	0	0	0	0	0		
30	0	0	0	0	0	0	0	0	0	0		
31	459	466	6	4	4	57	27	0	0	0		
32	474	979	90	83	83	91	85	30	2			

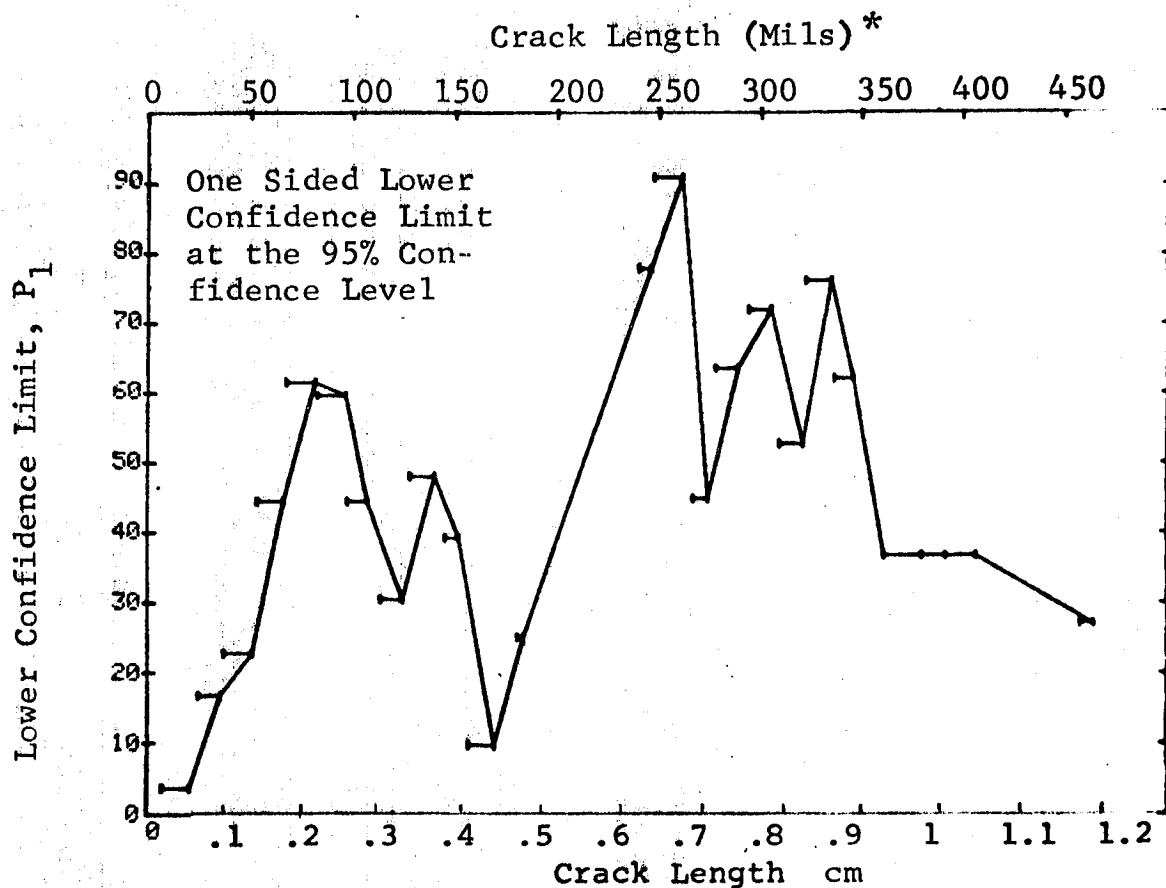


Figure D-2 Probability of Detection for 2219-T87 Al Using Liquid Penetrant. Fatigue Cracks in Flat Plates.
Lab. Env.

(b) Optimum Probability Method of Data Cumulation

02-JUL-75	PENETRANT			TEST 2, FENET, MARTIN (2)			MCD
RANGE	MIN LN	MAX LN	N	DET	50%	95%	0 MICS
1	7	21	39	4	0	3	0
2	25	36	48	13	0	16	0
3	25	52	120	36	0	23	0
4	54	67	120	63	0	44	0
5	68	82	132	91	0	61	0
6	68	97	219	151	0	63	0
7	68	108	258	174	0	62	0
8	54	126	411	252	0	57	0
9	68	141	333	215	0	60	0
10	68	153	351	226	0	59	0
11	68	171	360	229	0	59	0
12	68	185	369	234	0	59	0
13	0	0	0	0	0	0	0
14	0	0	0	0	0	0	0
15	0	0	0	0	0	0	0
16	241	247	12	12	0	77	0
17	241	262	63	62	0	92	0
18	241	275	72	69	0	89	4
19	241	290	87	82	0	88	16
20	241	306	102	96	0	88	0
21	241	322	129	115	0	83	0
22	241	336	159	142	0	84	0
23	241	347	177	157	0	84	0
24	241	362	180	160	0	84	0
25	241	381	183	163	0	84	0
26	241	393	186	166	0	84	0
27	241	408	189	169	0	84	0
28	0	0	0	0	0	0	0
29	0	0	0	0	0	0	0
30	0	0	0	0	0	0	0
31	241	466	195	173	0	84	0
32	241	979	285	256	0	86	0

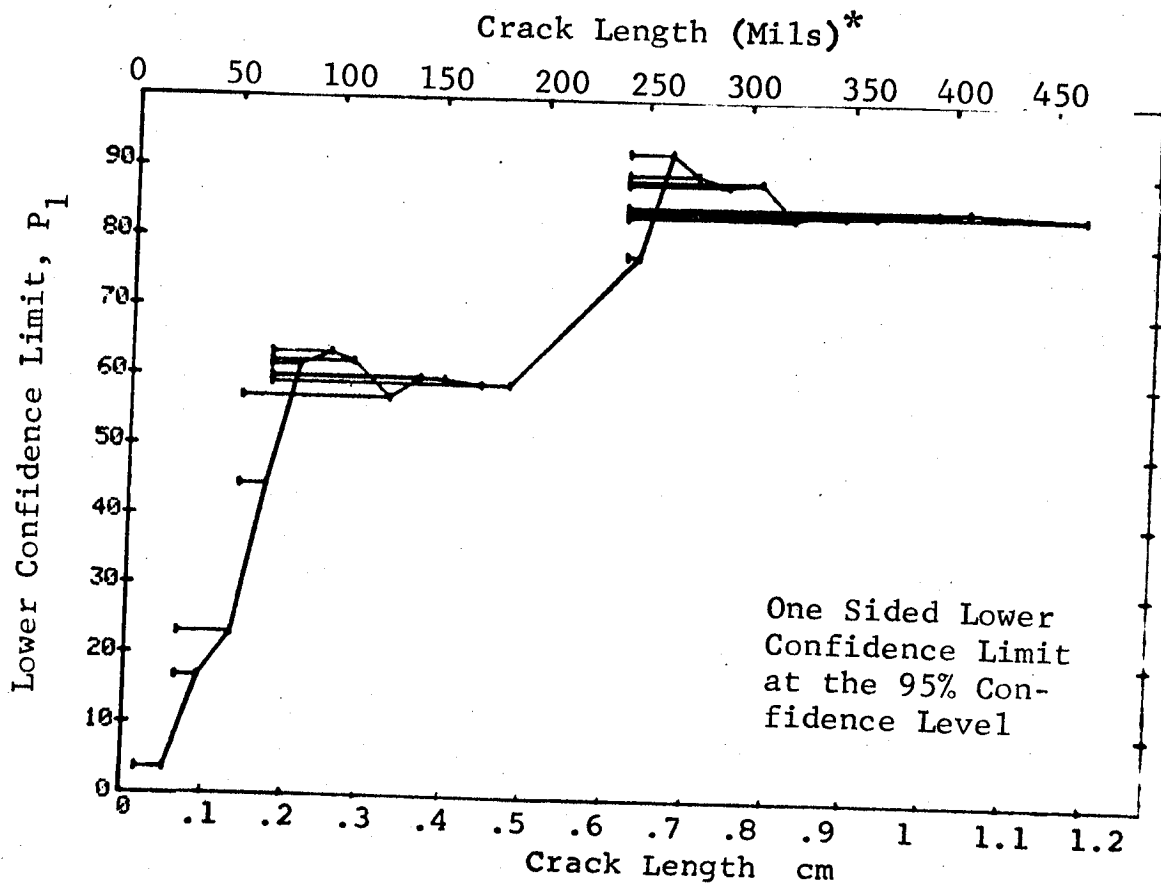


Figure D-2 (Continued)

(c) Overlapping Sixty Point Method of Data Cumulation

02-JUL-75	TEST 3	MARTIN (2)	DET	50%	95%	9	MIN	MAX
RANGE	MIN	LN	LN	LN	LN	LN	LN	LN
1	0	0	0	0	0	0	0	0
2	0	0	0	0	0	0	0	0
3	0	0	0	0	0	0	0	0
4	0	0	0	0	0	0	0	0
5	0	0	0	0	0	0	0	0
6	0	0	0	0	0	0	0	0
7	0	0	0	0	0	0	0	0
8	0	0	0	0	0	0	0	0
9	0	0	0	0	0	0	0	0
10	0	0	0	0	0	0	0	0
11	0	0	0	0	0	0	0	0
12	0	0	0	0	0	0	0	0
13	0	0	0	0	0	0	0	0
14	0	0	0	0	0	0	0	0
15	0	0	0	0	0	0	0	0
16	0	0	0	0	0	0	0	0
17	0	0	0	0	0	0	0	0
18	0	0	0	0	0	0	0	0
19	0	0	0	0	0	0	0	0
20	0	0	0	0	0	0	0	0
21	0	0	0	0	0	0	0	0
22	0	0	0	0	0	0	0	0
23	0	0	0	0	0	0	0	0
24	0	0	0	0	0	0	0	0
25	0	0	0	0	0	0	0	0
26	0	0	0	0	0	0	0	0
27	0	0	0	0	0	0	0	0
28	0	0	0	0	0	0	0	0
29	0	0	0	0	0	0	0	0
30	0	0	0	0	0	0	0	0
31	0	0	0	0	0	0	0	0
32	0	0	0	0	0	0	0	0
33	0	0	0	0	0	0	0	0
34	0	0	0	0	0	0	0	0
35	0	0	0	0	0	0	0	0
36	0	0	0	0	0	0	0	0
37	0	0	0	0	0	0	0	0
38	0	0	0	0	0	0	0	0
39	0	0	0	0	0	0	0	0
40	0	0	0	0	0	0	0	0
41	0	0	0	0	0	0	0	0
42	0	0	0	0	0	0	0	0
43	0	0	0	0	0	0	0	0
44	0	0	0	0	0	0	0	0
45	0	0	0	0	0	0	0	0
46	0	0	0	0	0	0	0	0
47	0	0	0	0	0	0	0	0
48	0	0	0	0	0	0	0	0
49	0	0	0	0	0	0	0	0
50	0	0	0	0	0	0	0	0
51	0	0	0	0	0	0	0	0
52	0	0	0	0	0	0	0	0
53	0	0	0	0	0	0	0	0

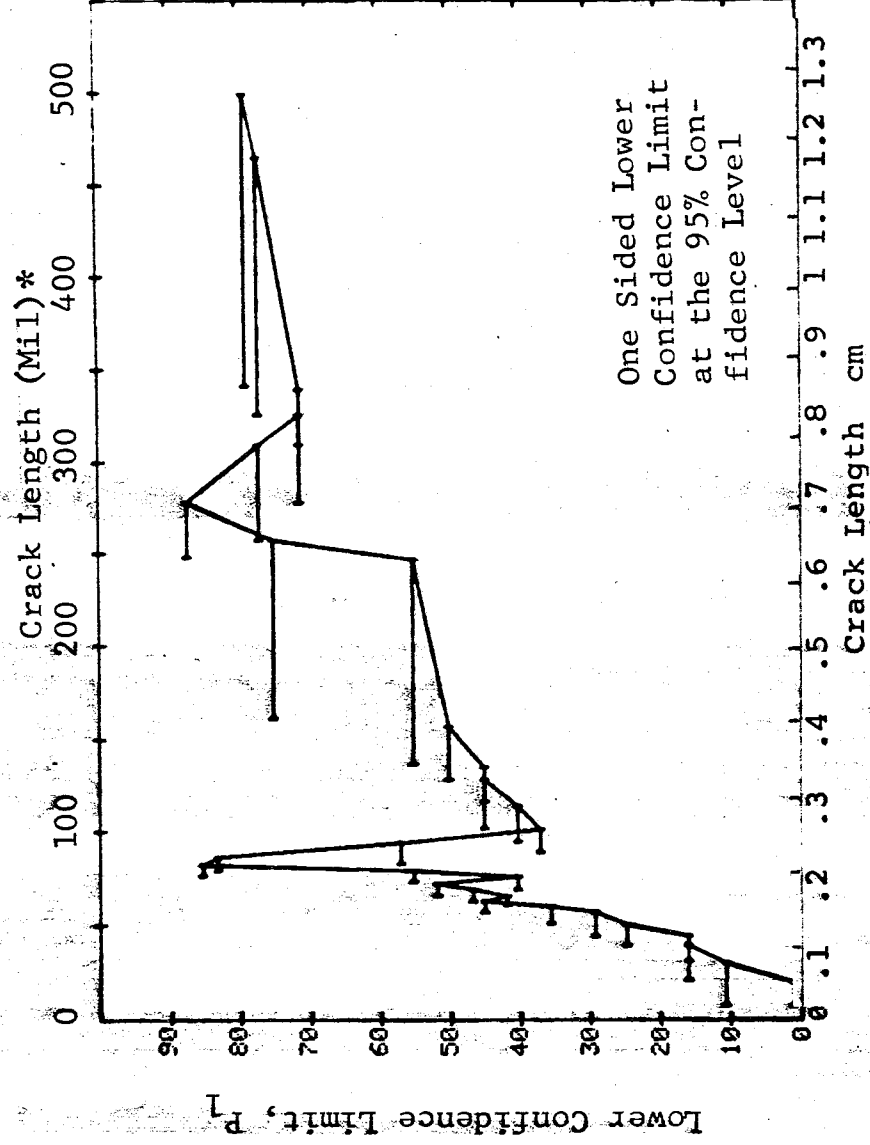


Figure D-2 (Concluded)

(a) Range Interval Method of Data Cumulation

02-JUL-75	EDDY CURRENT			TEST 1 EDDY CURRENT				(3) RANGE
RANGE	MIN	LN *	MAX LN *	N	DET	50%	95%	0 MILS
1		7	21	39	5	11	5	0
2	25		36	48	10	20	11	0
3	38		52	72	40	54	45	0
4	54		67	120	85	70	63	0
5	68		82	133	109	81	75	0
6	83		97	87	78	88	82	67
7	98		108	39	39	98	92	0
8	115		126	33	30	88	78	43
9	129		141	42	39	91	82	34
10	146		153	18	18	96	84	11
11	158		171	9	9	92	71	0
12	182		185	9	7	71	45	0
13	0		0	0	0	0	0	0
14	0		0	0	0	0	0	0
15	0		0	0	0	0	0	0
16	241		247	12	11	86	66	0
17	248		262	51	51	98	94	0
18	268		275	9	9	92	71	0
19	279		290	14	13	88	70	0
20	295		306	15	14	89	72	0
21	310		322	27	26	93	83	19
22	323		336	30	30	97	90	0
23	338		347	18	16	85	68	0
24	362		362	3	3	79	36	0
25	381		381	3	3	79	36	0
26	393		393	3	3	79	36	0
27	408		408	3	3	79	36	0
28	0		0	0	0	0	0	0
29	0		0	0	0	0	0	0
30	0		0	0	0	0	0	0
31	459		466	6	6	89	60	0
32	475		979	90	85	93	88	13

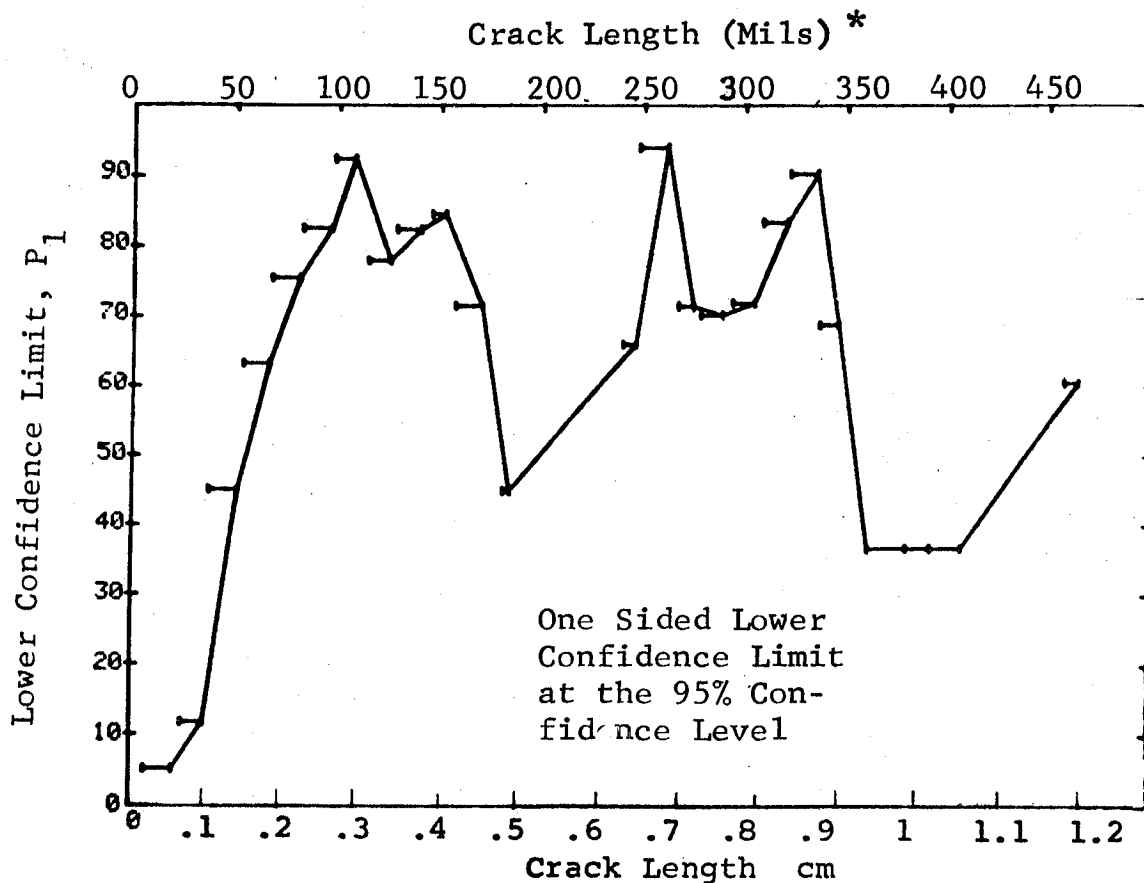


Figure D-3 Probability of Detection for 2219-T87 Al Using Eddy Current. Fatigue Cracks in Flat Plates. Lab. Env.

(b) Optimum Probability Method of Data Cumulation

07-JUL-75		EDDY CURRENT		N	TEST 2, MARTIN, (3)			MISS	MCD
RANGE	MIN LN	7*	MAX LN		DET	50%	95%		
1			21*	39	5	0	5	0	0
2	25		86	48	10	0	11	0	0
3	38		52	72	40	0	45	0	0
4	54		67	120	84	0	62	0	0
5	68		82	133	109	0	75	0	0
6	83		97	87	78	0	82	67	80
7	98		108	39	39	0	92	0	7
8	98		126	72	69	0	89	4	17
9	98		141	113	107	0	89	0	0
10	98		153	131	125	0	91	0	0
11	98		171	140	134	0	91	0	0
12	98		185	149	141	0	90	0	0
13	0		0	0	0	0	0	0	0
14	0		0	0	0	0	0	0	0
15	0		0	0	0	0	0	0	0
16	98		247	161	152	0	90	0	0
17	248		262	51	51	0	94	0	0
18	248		275	60	60	0	95	0	0
19	248		290	74	73	0	93	0	0
20	248		306	89	87	0	93	0	0
21	248		322	116	113	0	93	0	0
22	248		336	146	143	0	94	0	0
23	248		347	164	159	0	93	0	0
24	248		362	167	162	0	93	0	0
25	248		381	170	165	0	93	0	0
26	248		393	173	168	0	94	0	0
27	248		408	176	171	0	94	0	0
28	0		0	0	0	0	0	0	0
29	0		0	0	0	0	0	0	0
30	0		0	0	0	0	0	0	0
31	248		466	182	177	0	94	0	0
32	248		979	272	261	0	93	0	0

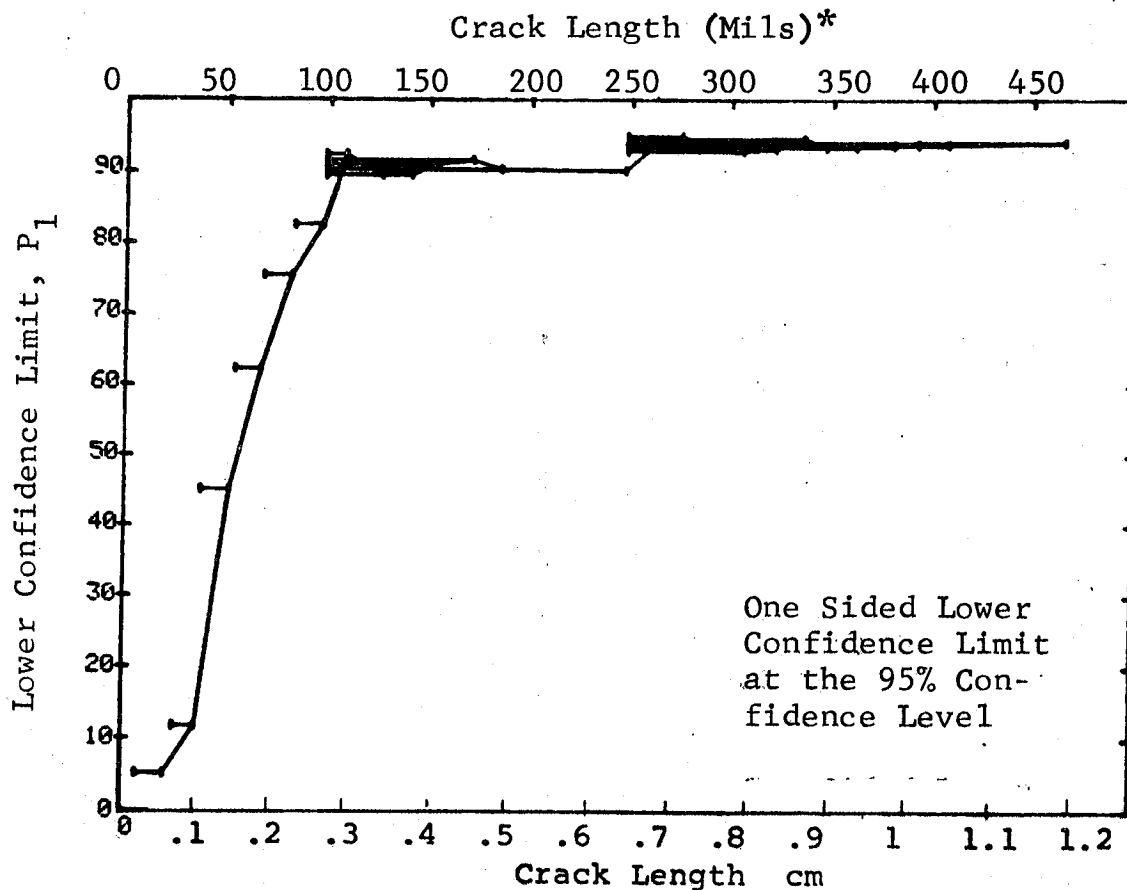


Figure D-3 (Continued)

(c) Overlapping Sixty Point Method of Data Cumulation

02-JUL-75				TEST 3 EDDY CURRENT METHOD (3)			
RANGE	MIN	LN	MAX	LN	* DET	50%	95%
1	1	0	0	0	0	0	0
2	2	0	0	0	0	0	0
3	3	0	0	0	0	0	0
4	4	7	20	0	4	11	4
5	5	8	30	33	11	17	10
6	6	21	40	60	14	22	14
7	7	31	45	60	22	35	26
8	8	40	51	60	33	54	43
9	9	45	58	60	36	59	48
10	10	52	61	60	38	62	51
11	11	58	64	60	44	72	62
12	12	62	67	60	47	77	67
13	13	64	70	60	46	75	65
14	14	67	73	60	43	70	60
15	15	70	77	60	43	70	60
16	16	74	80	60	52	85	77
17	17	77	83	60	57	93	87
18	18	80	87	60	54	88	81
19	19	83	95	60	55	90	83
20	20	87	102	60	56	92	85
21	21	95	115	60	54	88	81
22	22	102	129	60	56	92	85
23	23	115	136	60	58	95	89
24	24	129	158	60	58	95	89
25	25	136	248	60	56	92	85
26	26	158	258	60	57	93	87
27	27	248	279	60	58	98	95
28	28	258	310	60	58	95	89
29	29	279	326	60	57	93	87
30	30	310	340	60	57	93	87
31	31	326	466	60	58	95	89
32	32	342	500	60	58	95	89

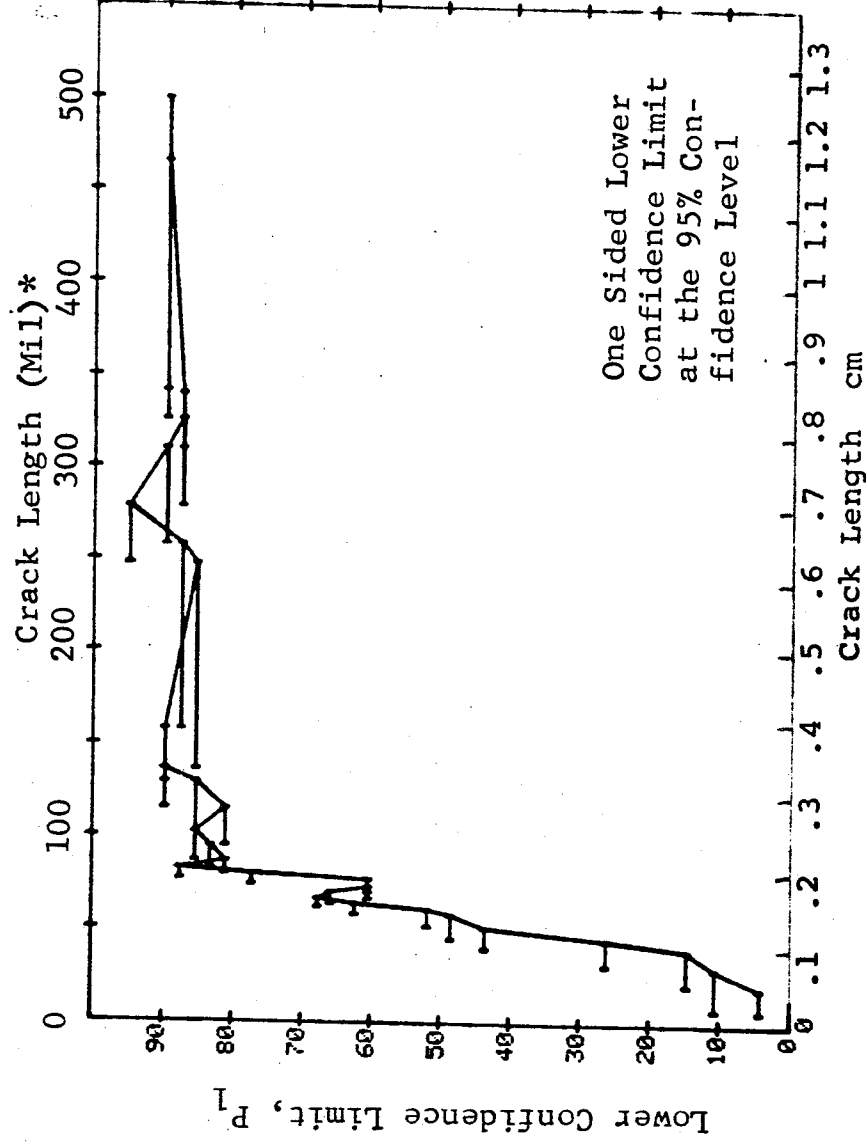


Figure D-3 (Concluded)

(a) Range Interval Method of Data Cumulation

02-JUL-75			RADIOGRAPHY		TEST 1 X-RAY		MARTIN 1.4	
RANGE	MIN LN	1.7*	MAX LN	N	DET	50%	95%	0 MILS
1	25	21	36	39	1	1	0	0
2	38	36	52	48	0	0	0	0
3	54	52	71	71	2	2	0	0
4	68	67	82	116	2	1	0	0
5	83	82	97	134	2	1	0	0
6	98	97	108	86	1	0	0	0
7	115	108	126	39	1	1	0	0
8	129	126	141	33	0	0	0	0
9	146	141	153	42	1	1	0	0
10	158	153	171	18	1	3	0	0
11	182	171	185	9	0	7	0	0
12	0	0	0	0	1	0	0	0
13	0	0	0	0	0	0	0	0
14	0	0	0	0	0	0	0	0
15	0	0	0	0	0	0	0	0
16	241	247	262	12	0	0	0	0
17	248	262	275	51	4	7	2	0
18	268	275	290	9	0	0	0	0
19	279	290	306	16	0	0	0	0
20	295	306	322	14	0	4	0	0
21	310	322	336	27	1	6	1	0
22	323	336	347	30	1	2	0	0
23	338	347	362	18	0	0	0	0
24	362	362	381	3	0	0	0	0
25	381	381	393	3	0	0	0	0
26	393	393	408	3	0	0	0	0
27	408	408	0	0	0	0	0	0
28	0	0	0	0	0	0	0	0
29	0	0	0	0	0	0	0	0
30	0	0	0	0	0	0	0	0
31	459	466	475	6	1	10	0	0
32	475	979	979	94	71	74	67	0

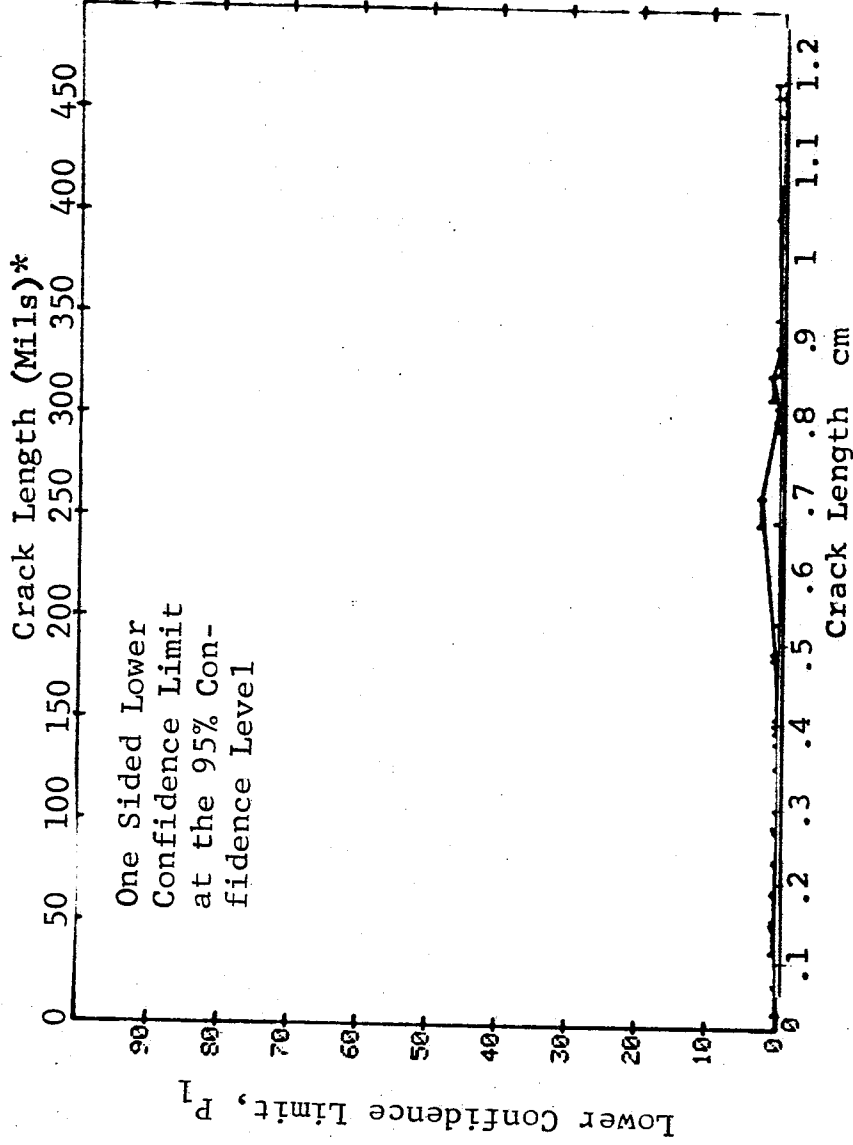


Figure D-4 Probability of Detection for 2219-T87 Al Using X-ray. Fatigue Cracks in Flat Plates. Lab. Env.

(b) Optimum Probability Method of Data Cumulation

02-JUL-75				TEST 2, X-RAY, MARTIN 4				
RANGE	MIN LN	* MAX LN *	N	DET	50%	95%	0 MISS	1 00
1	7	21	39	1	0	0	0	0
2	7	36	87	1	0	0	0	0
3	7	52	158	3	0	0	0	0
4	38	67	187	4	0	0	0	0
5	38	82	321	6	0	0	0	0
6	38	97	407	7	0	0	0	0
7	38	108	446	8	0	0	0	0
8	38	126	479	8	0	0	0	0
9	38	141	521	9	0	0	0	0
10	38	153	539	10	0	1	0	0
11	38	171	548	10	0	0	0	0
12	38	185	557	11	0	1	0	0
13	0	0	0	0	0	0	0	0
14	0	0	0	0	0	0	0	0
15	0	0	0	0	0	0	0	0
16	38	247	569	11	0	1	0	0
17	182	262	72	5	0	0	0	0
18	182	275	81	5	0	0	0	0
19	146	290	124	6	0	0	0	0
20	146	306	138	7	0	0	0	0
21	182	322	138	8	0	0	0	0
22	182	336	168	9	0	0	0	0
23	146	347	213	10	0	0	0	0
24	146	362	216	10	0	0	0	0
25	146	381	219	10	0	0	0	0
26	146	393	222	10	0	0	0	0
27	146	408	225	10	0	0	0	0
28	0	0	0	0	0	0	0	0
29	0	0	0	0	0	0	0	0
30	0	0	0	0	0	0	0	0
31	146	466	231	11	0	0	0	0
32	475	979	94	71	0	0	0	0

Crack Length (Mils) *

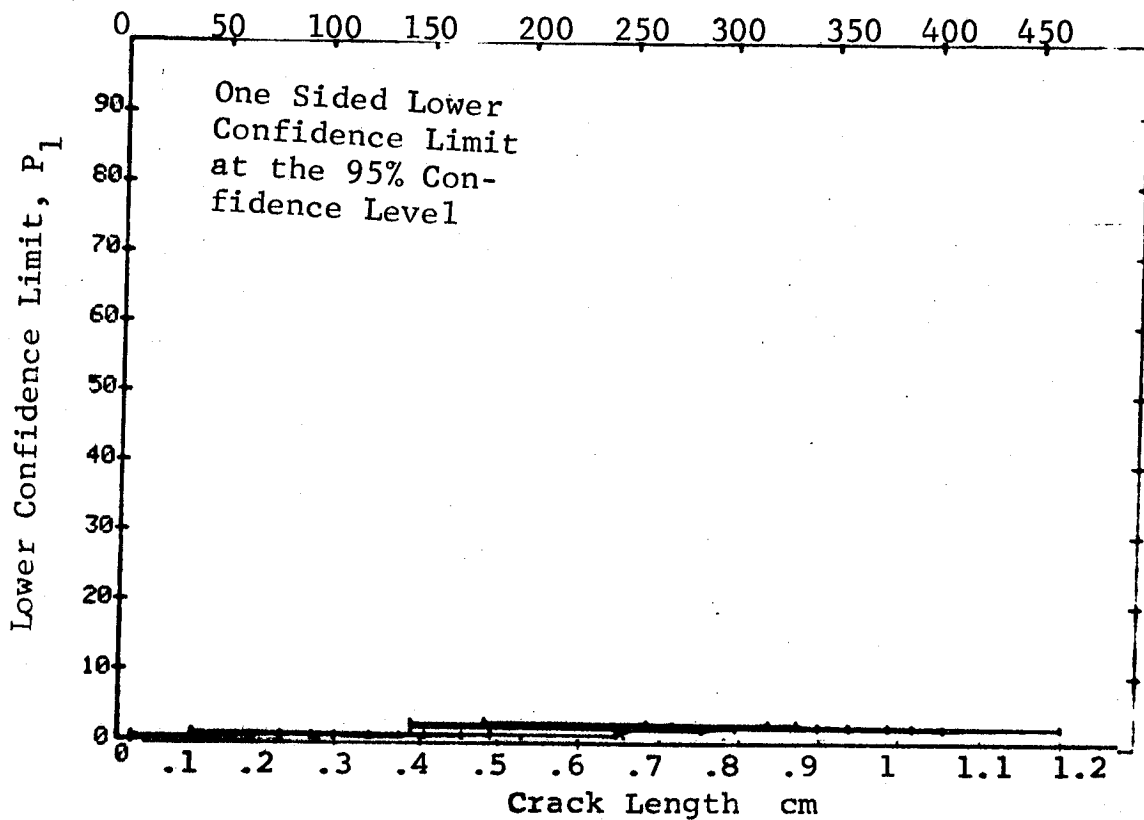


Figure D-4 (Continued)

(a) Range Interval Method of Data Cumulation

03-JUL-75		ULTRASONIC BY LENGTH			TEST 1, MARTIN 150			RANGE	
RANGE	MIN LN	* MAX LN	N	DET	50%	95%	0 MISS	1 MISS	
1	7	21*	39	12	29	18	0	0	
2	25	36	48	35	71	60	0	0	
3	38	52	72	58	79	71	0	0	
4	54	67	120	101	83	77	0	0	
5	68	82	132	119	89	84	0	0	
6	83	97	87	76	86	79	92	100	
7	98	108	39	33	83	71	0	0	
8	115	126	33	27	79	67	0	0	
9	129	141	42	37	86	76	61	74	
10	146	153	18	16	85	68	0	0	
11	158	171	9	7	71	45	0	0	
12	182	185	9	9	92	71	0	0	
13	0	0	0	0	0	0	0	0	
14	0	0	0	0	0	0	0	0	
15	0	0	0	0	0	0	0	0	
16	241	247	12	11	86	66	0	0	
17	248	262	51	51	98	94	0	0	
18	268	275	9	9	92	71	0	0	
19	279	290	15	14	89	72	0	0	
20	295	306	15	15	95	81	14	31	
21	310	322	27	25	90	78	34	42	
22	323	336	29	28	94	84	17	32	
23	338	347	18	16	85	68	0	0	
24	362	362	3	3	79	36	0	0	
25	381	381	3	3	79	36	0	0	
26	393	393	3	3	79	36	0	0	
27	408	408	3	3	79	36	0	0	
28	0	0	0	0	0	0	0	0	
29	0	0	0	0	0	0	0	0	
30	0	0	0	0	0	0	0	0	
31	459	466	6	6	89	60	0	0	
32	475	979	90	83	91	85	30	50	

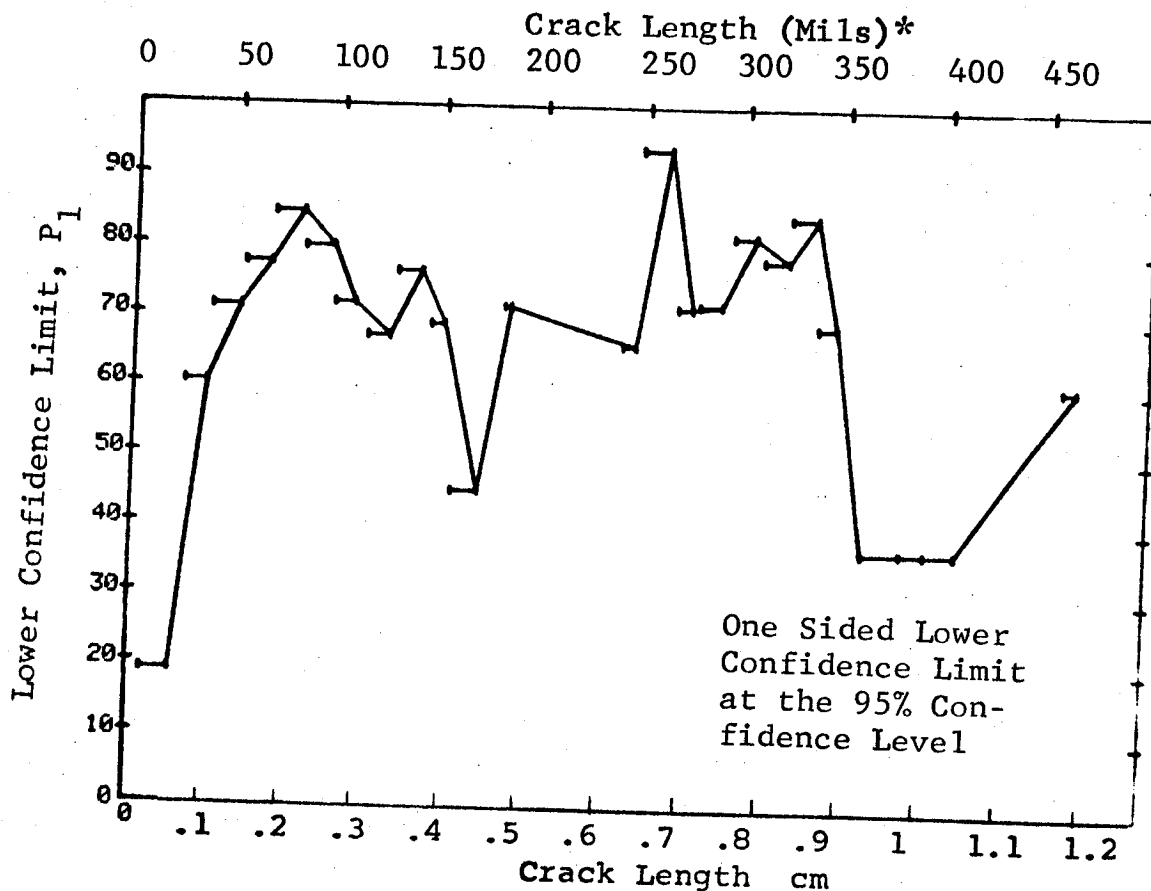


Figure D-5. Probability of Detection for 2219-T87 Al Using Ultrasonic Surface Waves. Etched Fatigue Cracks in Flat Plates. Lab. Env.

(b) Optimum Probability Method of Data Cumulation

03-JUL-75		ULTRASONIC BY LENGTH			TEST 2, MARTIN (5)			MCD	
RANGE	MIN LN	* MAX LN	* N	DET	50%	95%	0 MISS	1 MISS	
1	7	21	39	12	0	18	0	0	
2	25	36	48	35	0	60	0	0	
3	38	52	72	58	0	71	0	0	
4	38	67	192	159	0	77	0	0	
5	68	82	132	119	0	84	0	0	
6	68	97	219	195	0	84	0	0	
7	68	108	258	228	0	84	0	0	
8	68	126	291	255	0	83	0	0	
9	68	141	333	292	0	84	0	0	
10	68	153	351	308	0	84	0	0	
11	68	171	360	315	0	84	0	0	
12	68	185	369	324	0	84	0	0	
13	0	0	0	0	0	0	0	0	
14	0	0	0	0	0	0	0	0	
15	0	0	0	0	0	0	0	0	
16	68	247	381	335	0	84	0	0	
17	248	262	51	51	0	94	0	0	
18	248	275	60	60	0	95	0	0	
19	248	290	75	74	0	93	0	0	
20	248	306	90	89	0	94	0	0	
21	248	322	117	114	0	93	0	0	
22	248	336	146	142	0	93	0	0	
23	182	347	185	178	0	93	0	0	
24	182	362	188	181	0	93	0	0	
25	182	381	191	184	0	93	0	0	
26	182	393	194	187	0	93	0	0	
27	182	408	197	190	0	93	0	0	
28	0	0	0	0	0	0	0	0	
29	0	0	0	0	0	0	0	0	
30	0	0	0	0	0	0	0	0	
31	182	466	203	196	0	93	0	0	
32	182	979	293	279	0	92	0	0	

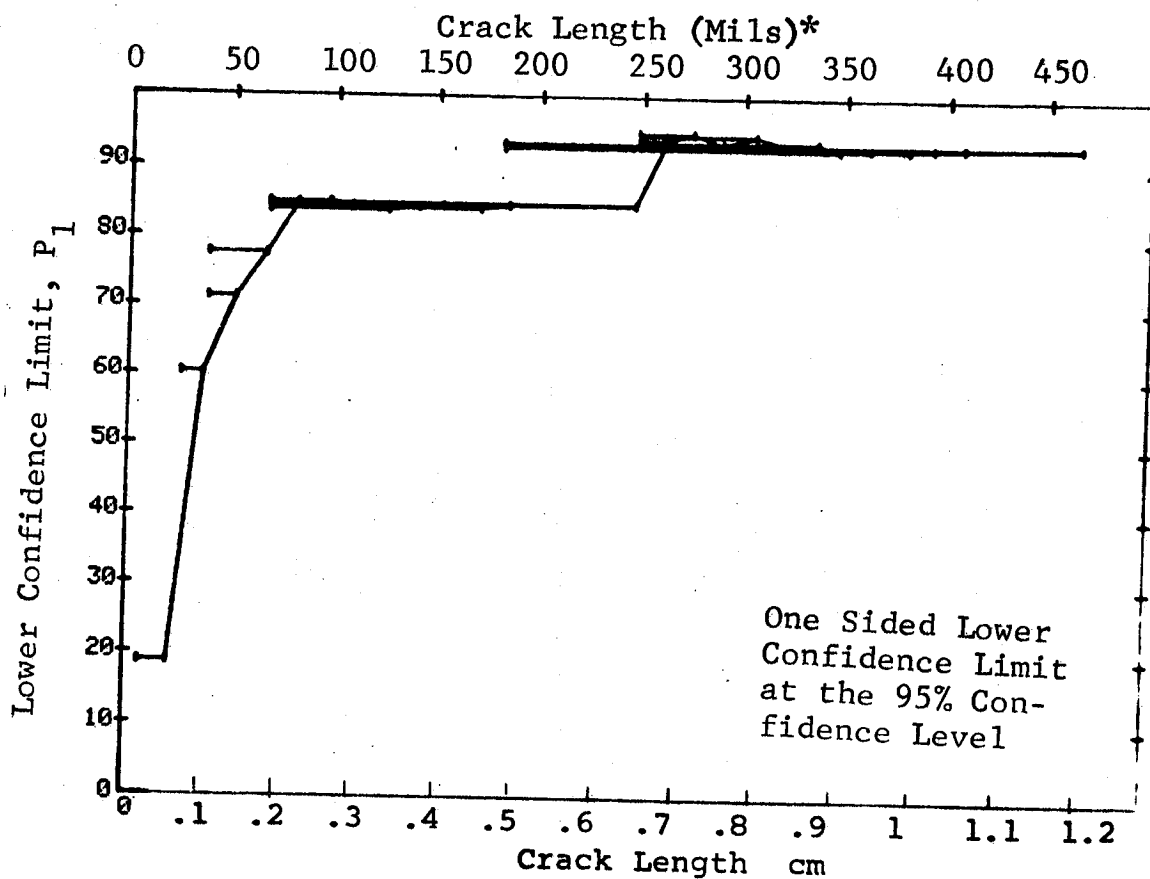


Figure D-5 (Continued)

(c) Overlapping Sixty Point Method of Data Cumulation

03-JUL-75			ULTRASONIC BY LENGTH			TEST 3, MARTIN 50				
RANGE	MIN LN	MAX LN	N	DET	50%	95%	0 MISS	1 MISS		
1	0	0	0	0	0	0	0	0		
2	0	0	0	0	0	0	0	0		
3	0	0	0	0	0	0	0	0		
4	7	20	32	8	23	13	0	0		
5	7	30	60	29	47	37	0	0		
6	20	40	60	42	69	58	0	0		
7	30	45	60	43	70	60	0	0		
8	40	51	60	48	79	69	0	0		
9	45	58	60	47	77	67	0	0		
10	51	61	60	49	80	71	0	0		
11	58	64	60	57	93	87	16	29		
12	61	67	60	53	87	79	69	82		
13	64	70	60	51	83	75	94	100		
14	67	73	60	53	87	79	69	82		
15	70	77	60	50	82	73	0	0		
16	73	80	60	53	87	79	69	82		
17	77	83	60	59	97	92	0	1		
18	80	87	60	55	90	83	43	56		
19	83	95	60	53	87	79	69	82		
20	87	102	60	51	83	75	94	100		
21	95	115	60	47	77	67	0	0		
22	102	129	60	51	83	75	94	100		
23	115	136	60	53	87	79	69	82		
24	129	158	60	53	87	79	69	82		
25	136	248	60	54	88	81	56	69		
26	158	258	60	57	93	87	16	17		
27	248	279	60	60	98	95	0	0		
28	258	310	60	59	97	92	0	0		
29	279	326	60	57	93	87	16	17		
30	310	340	60	56	92	85	16	17		
31	326	466	60	57	93	87	16	17		
32	342	500	60	56	92	85	16	17		

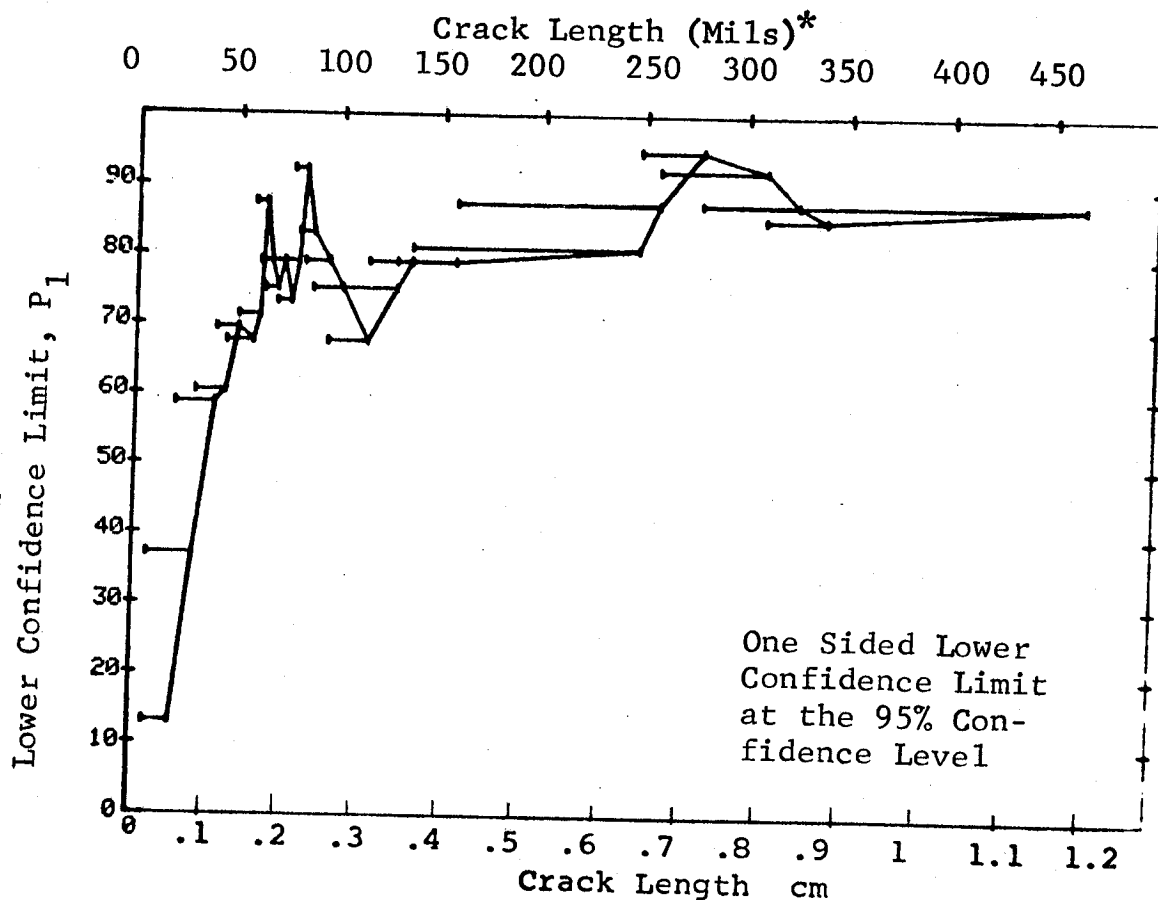


Figure D-5 (Concluded)

(a) Range Interval Method of Data Cumulation

02-JUL-75			PENETRANT		N	TEST 1		PENET	MMP 7114		RANGE
RANGE	MIN	LN	7 *	MAX		DET	50%		6	MIL	
1					39	10	24	95	0	0	0
2	25		21 *		48	31	51	14	0	0	0
3	38		36		72	57	78	69	0	0	0
4	54		52		119	98	81	75	0	0	0
5	68		67		132	113	85	79	0	0	0
6	83		82		87	79	90	84	55	0	0
7	98		97		39	39	98	92	0	0	0
8	115		108		33	27	79	67	0	0	0
9	129		126		42	41	96	89	4	0	0
10	146		141		18	16	85	68	0	0	0
11	158		153		9	9	92	71	0	0	0
12	182		171		9	9	92	71	0	0	0
13			185		0	0	0	0	0	0	0
14			0		0	0	0	0	0	0	0
15			0		0	0	0	0	0	0	0
16			0		0	0	0	0	0	0	0
17	241		247		12	11	86	66	0	0	0
18	249		252		51	51	98	94	0	0	0
19	268		275		9	9	92	71	0	0	0
20	279		290		15	15	95	81	14	0	0
21	295		306		15	15	95	81	14	0	0
22	310		322		27	25	90	78	34	0	0
23	323		336		30	30	97	90	0	0	0
24	338		347		18	16	85	68	0	0	0
25	362		362		3	3	79	36	0	0	0
26	381		381		3	3	79	36	0	0	0
27	393		393		3	2	50	13	0	0	0
28	408		408		3	3	79	36	0	0	0
29			0		0	0	0	0	0	0	0
30			0		0	0	0	0	0	0	0
31	459		466		6	6	89	60	0	0	0
32	475		979		91	91	99	96	0	0	0

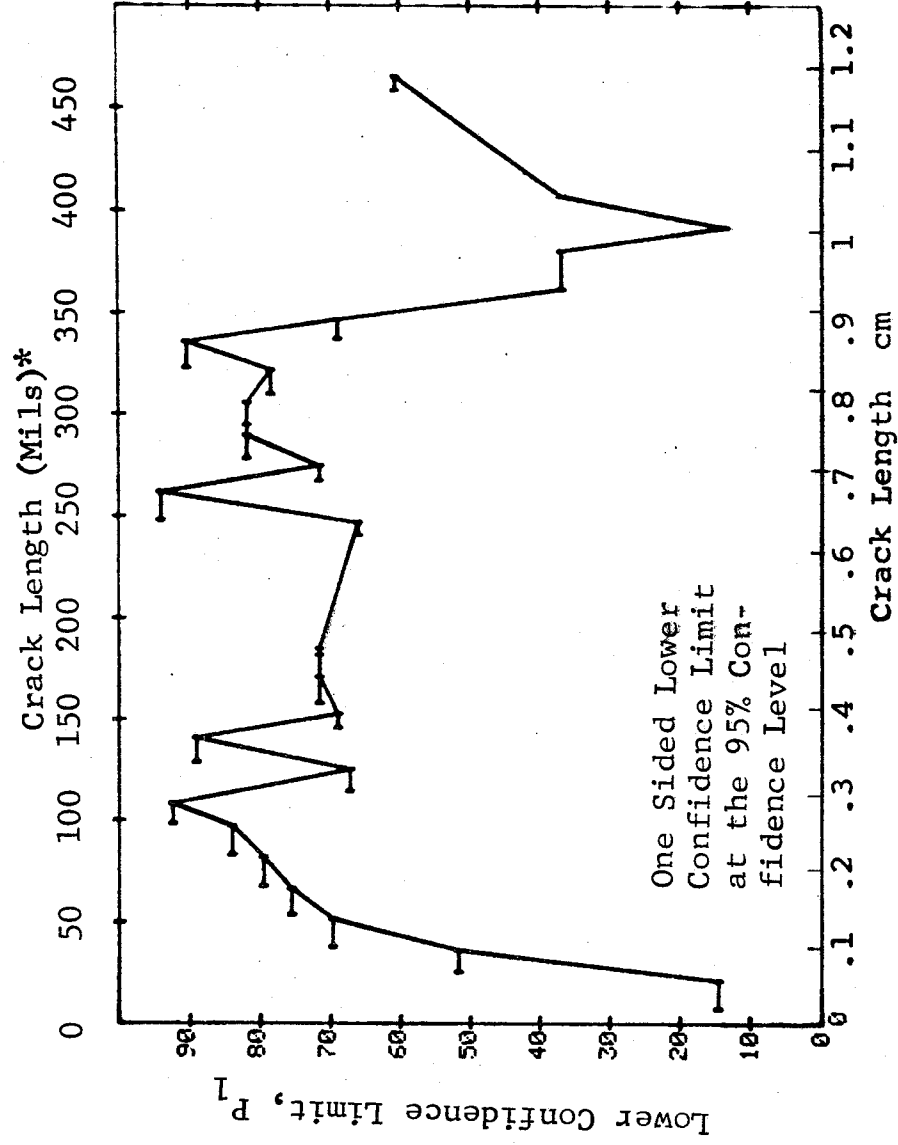


Figure D-6 Probability of Detection for 2219-T87 Al Using Liquid Penetrant. Etched Fatigue Cracks in Flat Plates. Lab. Env.

(b) Optimum Probability Method of Data Cumulation

02-JUL-75		PENETRANT			TEST 2, PENET			MAP 1111-6		MCD
RANGE	MIN LN	* MAX LN	*	N	DET	50%	95%	0 MILES	1 MILE	
1	7	21		39	10	0	14	0	0	
2	25	36		48	31	0	51	0	0	
3	38	52		72	57	0	69	0	0	
4	38	67		191	155	0	75	0	0	
5	54	82		251	211	0	79	0	0	
6	83	97		87	79	0	84	55	67	
7	98	108		39	39	0	92	0	0	
8	83	126		159	145	0	86	0	0	
9	129	141		42	41	0	89	4	19	
10	83	153		219	202	0	88	0	0	
11	129	171		69	66	0	89	7	20	
12	129	185		78	75	0	90	0	11	
13	0	0		0	0	0	0	0	0	
14	0	0		0	0	0	0	0	0	
15	0	0		0	0	0	0	0	0	
16	129	247		90	86	0	90	0	13	
17	248	262		51	51	0	94	0	0	
18	248	275		60	60	0	95	0	0	
19	248	290		75	75	0	96	0	0	
20	248	306		90	90	0	96	0	0	
21	158	322		147	144	0	94	0	0	
22	248	336		147	145	0	95	0	0	
23	158	347		195	190	0	94	0	0	
24	158	362		198	193	0	94	0	0	
25	158	381		201	196	0	94	0	0	
26	158	393		204	198	0	94	0	0	
27	158	408		207	201	0	94	0	0	
28	0	0		0	0	0	0	0	0	
29	0	0		0	0	0	0	0	0	
30	0	0		0	0	0	0	0	0	
31	158	466		213	207	0	94	0	0	
32	408	979		100	100	0	97	0	0	

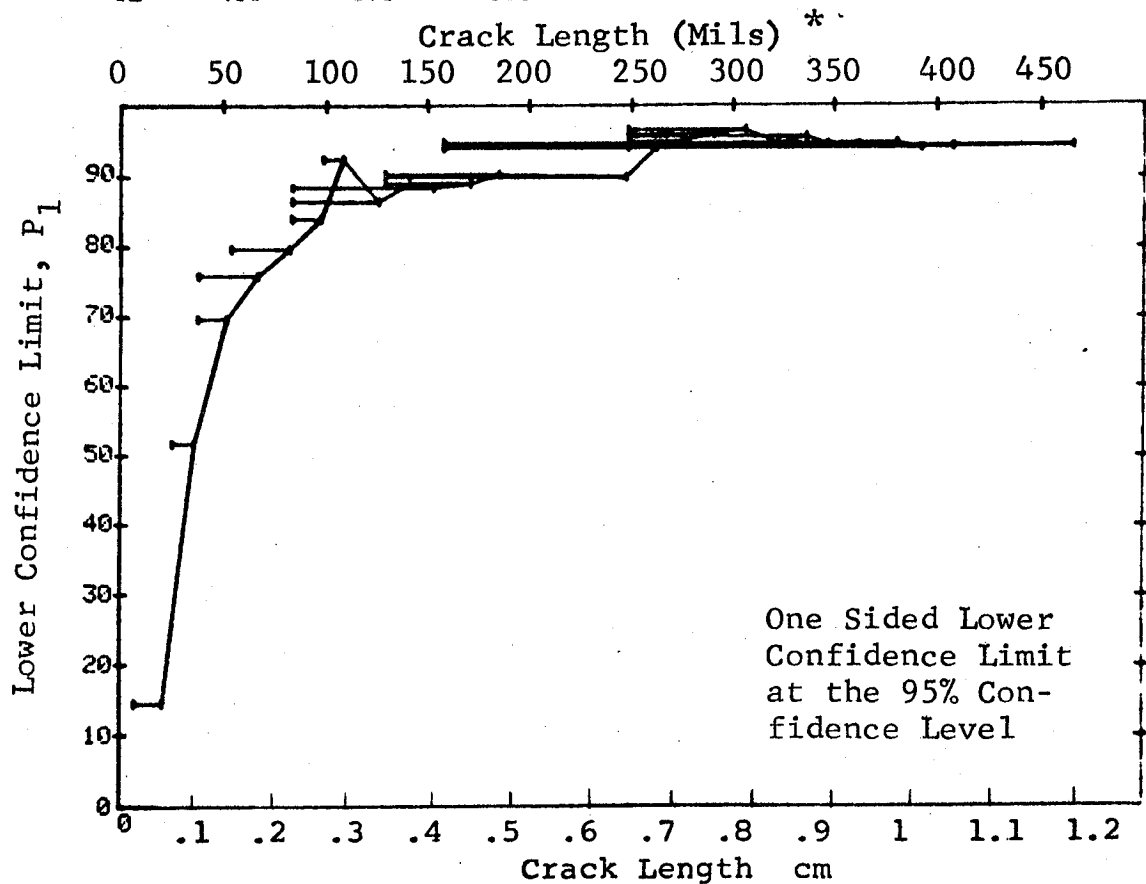


Figure D-6 (Continued)

(c) Overlapping Sixty Point Method of Data Cumulation

02-JUL-75				TEST 3, PENET. MFTTH(6)			
RANGE	MIN	LN	MAX	DET	50%	95%	0 MFC
1	0	0	0	0	0	0	0
2	0	0	0	0	0	0	0
3	0	0	0	0	0	0	0
4	0	0	0	0	0	0	0
5	0	0	0	0	0	0	0
6	0	0	0	0	0	0	0
7	0	0	0	0	0	0	0
8	0	0	0	0	0	0	0
9	0	0	0	0	0	0	0
10	0	0	0	0	0	0	0
11	0	0	0	0	0	0	0
12	0	0	0	0	0	0	0
13	0	0	0	0	0	0	0
14	0	0	0	0	0	0	0
15	0	0	0	0	0	0	0
16	0	0	0	0	0	0	0
17	0	0	0	0	0	0	0
18	0	0	0	0	0	0	0
19	0	0	0	0	0	0	0
20	0	0	0	0	0	0	0
21	0	0	0	0	0	0	0
22	0	0	0	0	0	0	0
23	0	0	0	0	0	0	0
24	0	0	0	0	0	0	0
25	0	0	0	0	0	0	0
26	0	0	0	0	0	0	0
27	0	0	0	0	0	0	0
28	0	0	0	0	0	0	0
29	0	0	0	0	0	0	0
30	0	0	0	0	0	0	0
31	0	0	0	0	0	0	0
32	0	0	0	0	0	0	0

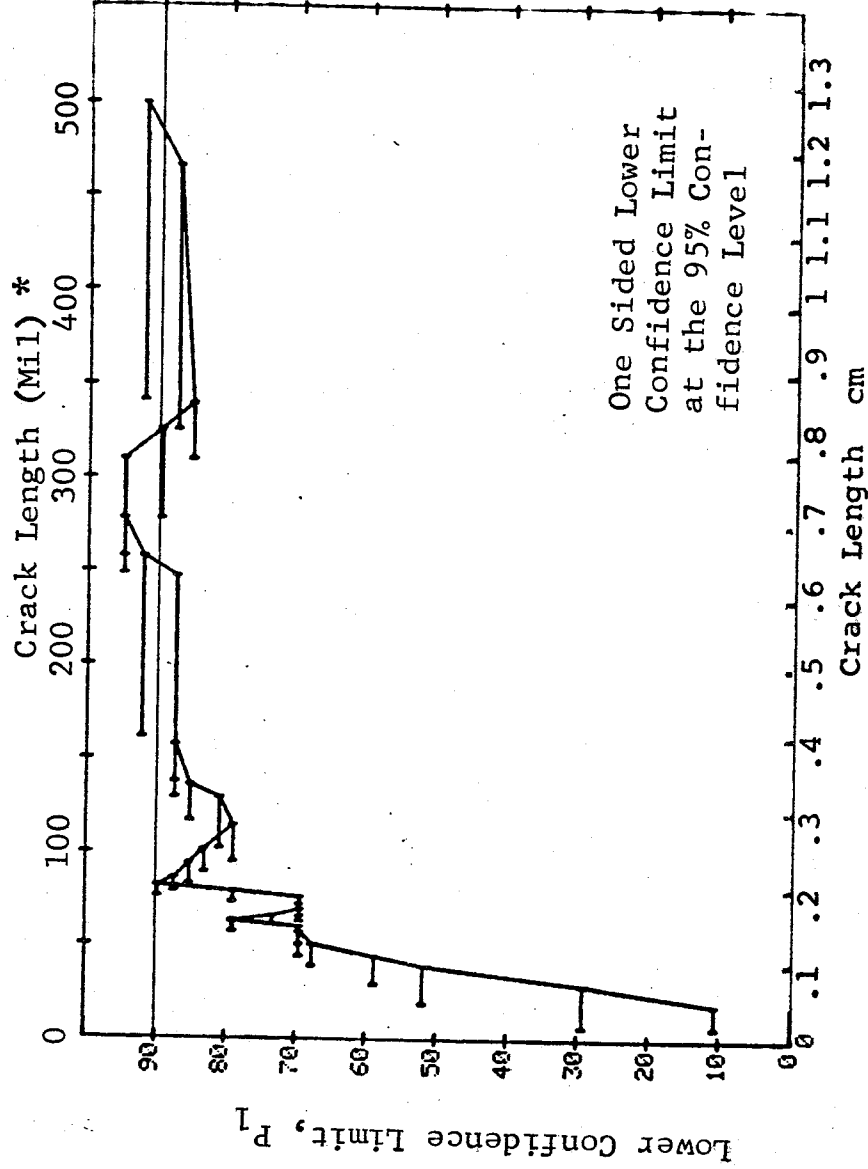


Figure D-6 (Concluded)

(a) Range Interval Method of Data Cumulation

22-JUL-75	EDDY CURRENT SEC II			TEST 1		MARTIN (7)			
RANGE	MIN	LN	* MAX LN	N	DET	50%	95%	0 MISS	1 MISS
1	7	31*	39	6	14	6	0	0	0
2	25	36	48	6	11	5	0	0	0
3	38	52	72	17	23	15	0	0	0
4	54	67	121	62	50	43	0	0	0
5	68	82	131	80	60	53	0	0	0
6	83	97	87	69	78	70	0	0	0
7	98	108	39	31	77	66	0	0	0
8	115	126	34	30	86	75	55	59	59
9	129	141	42	38	88	79	47	61	61
10	146	153	18	16	85	68	0	0	0
11	158	171	9	9	92	71	0	0	0
12	182	185	9	7	71	45	0	0	0
13	0	0	0	0	0	0	0	0	0
14	0	0	0	0	0	0	0	0	0
15	0	0	0	0	0	0	0	0	0
16	241	247	12	11	86	66	0	0	0
17	248	262	51	47	90	82	38	50	50
18	268	275	9	9	92	71	0	0	0
19	279	290	15	14	89	72	0	0	0
20	295	306	15	13	82	63	0	0	0
21	310	322	27	26	93	83	19	24	24
22	323	336	30	29	94	85	15	21	21
23	338	347	18	15	79	62	0	0	0
24	362	362	3	3	79	36	0	0	0
25	381	381	3	3	79	36	0	0	0
26	393	393	3	3	79	36	0	0	0
27	408	408	3	2	50	13	0	0	0
28	0	0	0	0	0	0	0	0	0
29	0	0	0	0	0	0	0	0	0
30	0	0	0	0	0	0	0	0	0
31	459	466	6	6	89	60	0	0	0
32	475	979	90	86	94	90	0	13	13

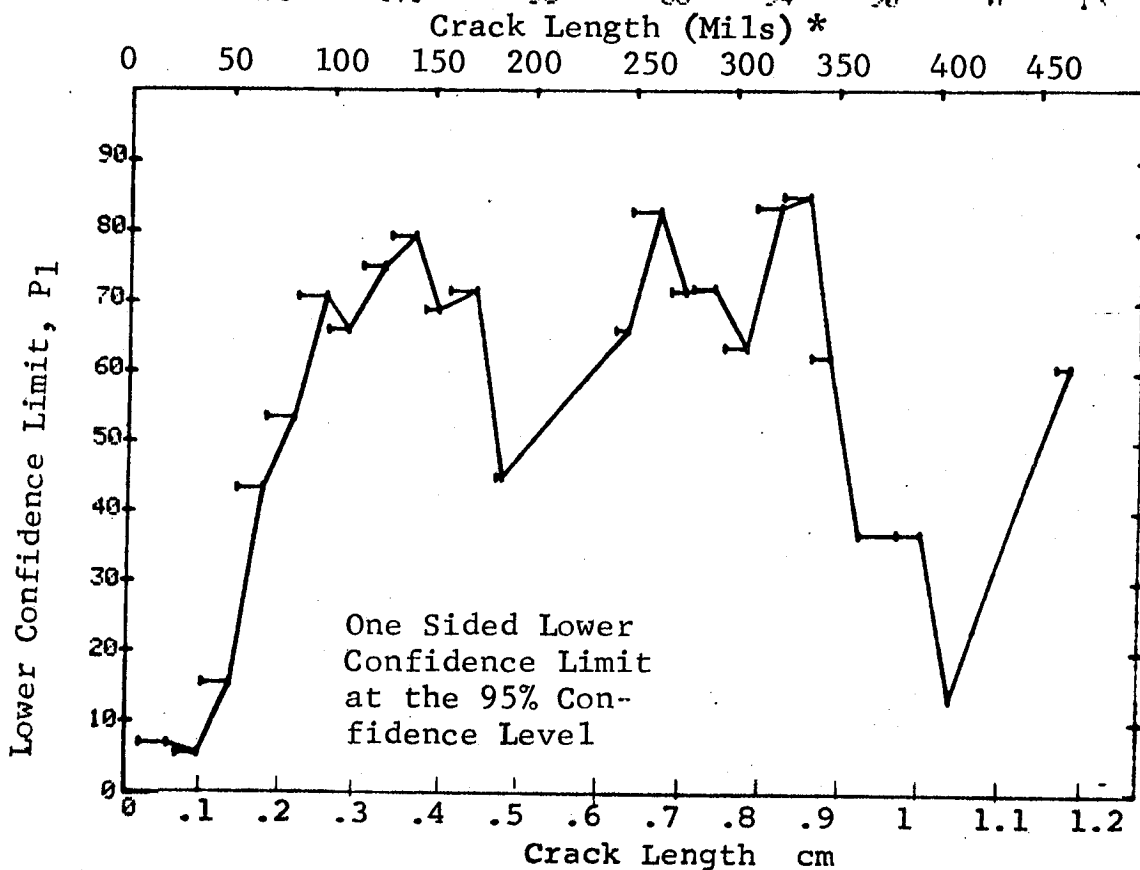


Figure D-7 Probability of Detection for 2219-T87 Al Using Eddy Current. Etched Fatigue Cracks in Flat Plates. Lab. Env.

(b) Optimum Probability Method of Data Cumulation

22-JUL-75	EDDY CURRENT	SED II	TEST 2	MARTIN (7)		
RANGE	MIN LN	* MAX LN *	DEF	50%	95%	0 MISS 1 MISS
1	7	21	39	6	6	0
2	7	36	107	12	6	0
3	38	52	72	17	0	0
4	54	67	121	52	15	0
5	68	82	131	80	43	0
6	83	97	87	69	53	0
7	83	108	126	100	70	0
8	83	126	160	130	72	0
9	115	141	76	68	75	0
10	115	153	94	84	81	65
11	115	171	103	93	82	73
12	115	185	112	100	84	0
13	0	0	0	0	83	0
14	0	0	0	0	0	0
15	0	0	0	0	0	0
16	115	247	124	111	0	0
17	115	262	175	158	83	0
18	129	275	150	137	85	0
19	129	290	165	151	86	0
20	129	306	180	164	87	0
21	241	322	129	120	86	0
22	241	336	159	149	88	0
23	241	347	177	164	87	0
24	241	362	180	167	88	0
25	241	381	183	170	88	0
26	241	393	186	173	88	0
27	241	408	189	175	89	0
28	0	0	0	0	88	0
29	0	0	0	0	0	0
30	0	0	0	0	0	0
31	241	466	195	181	89	0
32	310	979	183	173	90	0

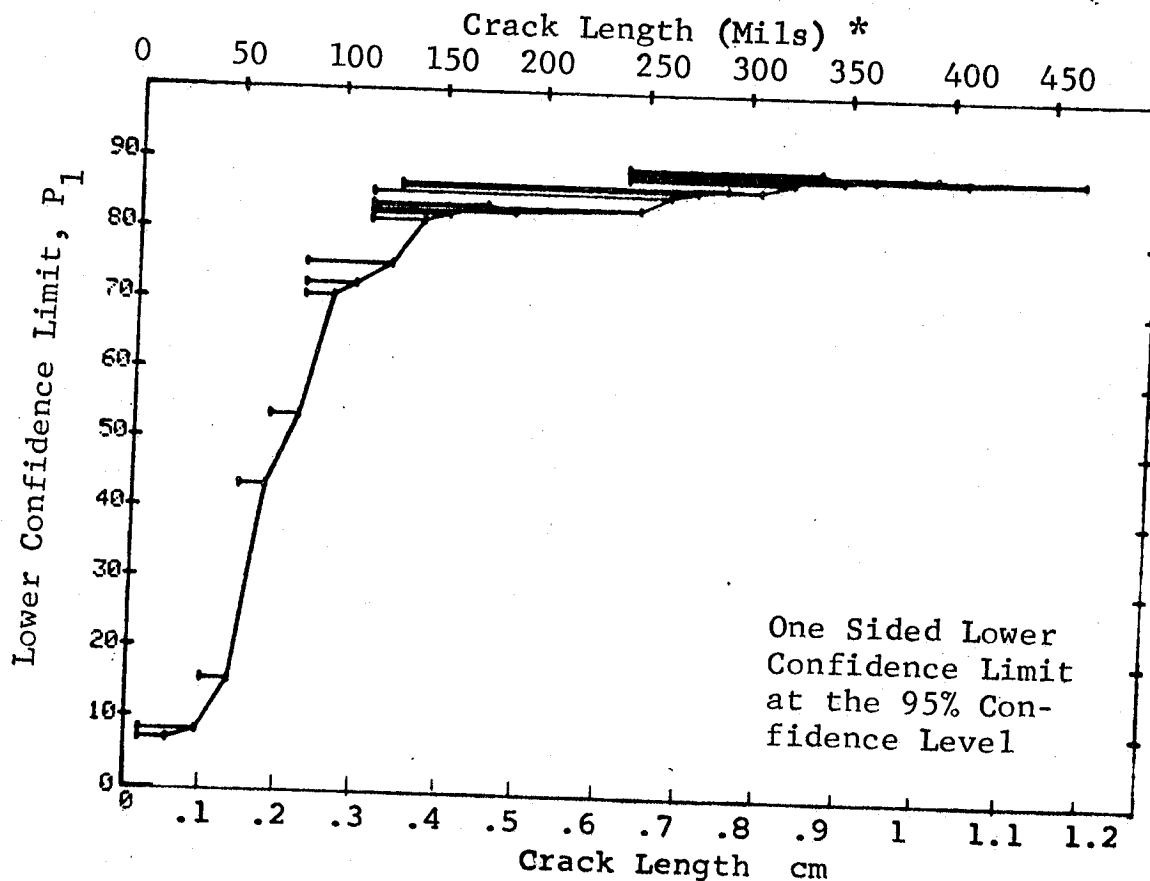


Figure D-7 (Continued)

(c) Overlapping Sixty Point Method of Data Cumulation

22-JUL-75	EDDY	CURRENT	SED	II	TEST	3	MARTIN	(7)	MISS	MISS
RANGE	MIN	LN	MAX	LN	DET	50%	95%	0	MISS	MISS
1	0	0	0	0	0	0	0	0	0	0
2	0	0	0	0	0	0	0	0	0	0
3	0	0	0	0	0	0	0	0	0	0
4	0	0	0	0	0	0	0	0	0	0
5	0	0	0	0	0	0	0	0	0	0
6	0	0	0	0	0	0	0	0	0	0
7	0	0	0	0	0	0	0	0	0	0
8	0	0	0	0	0	0	0	0	0	0
9	0	0	0	0	0	0	0	0	0	0
10	45	58	61	60	19	30	14	0	0	0
11	58	62	67	60	26	42	32	0	0	0
12	64	67	70	60	35	57	46	0	0	0
13	67	70	74	60	37	44	37	0	0	0
14	70	74	77	60	30	49	38	0	0	0
15	74	77	80	60	32	52	41	0	0	0
16	77	80	84	60	37	52	50	0	0	0
17	80	84	90	60	49	60	50	0	0	0
18	84	90	96	60	50	62	50	0	0	0
19	84	90	96	60	46	75	65	0	0	0
20	96	103	115	60	46	75	65	0	0	0
21	96	103	115	60	52	85	77	0	0	0
22	103	117	129	60	55	90	83	0	0	0
23	117	129	136	60	55	90	83	0	0	0
24	129	136	158	60	54	88	81	0	0	0
25	136	158	248	60	54	88	81	0	0	0
26	162	258	279	60	57	93	87	0	0	0
27	249	310	326	60	56	92	85	0	0	0
28	258	310	340	60	56	92	85	0	0	0
29	279	340	466	60	55	93	87	0	0	0
30	310	340	466	60	55	93	87	0	0	0
31	326	466	500	60	57	93	87	0	0	0
32	342	500		60	57	93	87	0	0	0

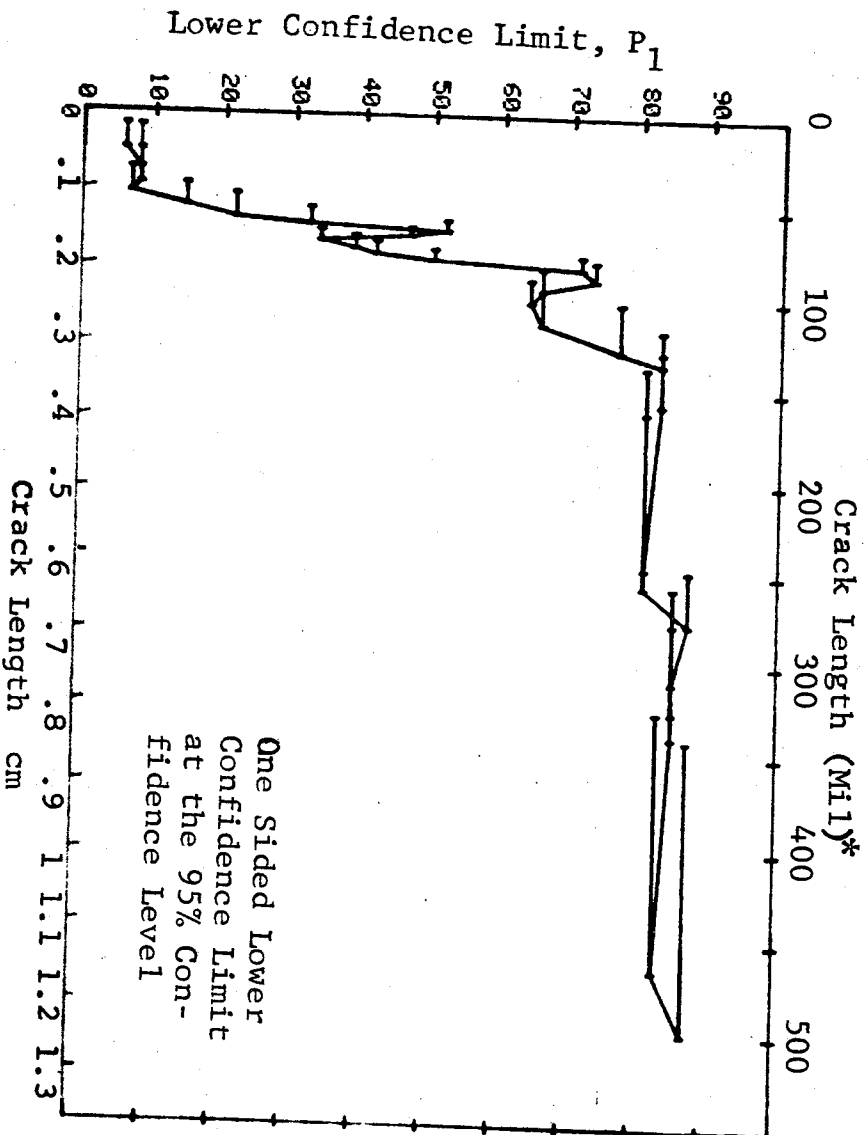


Figure D-7 (Concluded)

(a) Range Interval Method of Data Cumulation

02-JUL-75		RADIOGRAPHY		N	TEST 1		X-RAY		MARTIN	
RANGE	MIN LN	* MAX LN	*		DFT	50%	95%	0 MISS	0 MISS	0 MISS
1	21	21	*	39	1	1	0	0	0	0
2	23	36		49	8	15	8	0	0	0
3	38	52		72	18	24	16	0	0	0
4	54	67		120	41	33	27	0	0	0
5	68	82		131	60	45	38	0	0	0
6	83	97		87	54	61	52	0	0	0
7	98	108		39	15	37	25	0	0	0
8	115	126		33	7	20	10	0	0	0
9	129	141		42	11	25	15	0	0	0
10	146	153		18	11	58	39	0	0	0
11	158	171		9	6	60	34	0	0	0
12	182	185		9	3	28	9	0	0	0
13	0	0		0	0	0	0	0	0	0
14	0	0		0	0	0	0	0	0	0
15	0	0		0	0	0	0	0	0	0
16	241	247		12	12	94	77	17	34	0
17	248	262		51	50	96	91	0	10	0
18	268	275		9	9	92	71	0	0	0
19	279	290		15	13	82	63	0	0	0
20	295	306		15	12	76	56	0	0	0
21	310	322		27	13	46	31	0	0	0
22	323	336		30	23	74	60	0	0	0
23	338	347		18	15	79	62	0	0	0
24	362	362		3	1	20	1	0	0	0
25	381	381		3	2	50	13	0	0	0
26	393	393		3	3	79	36	0	0	0
27	408	408		3	3	79	36	0	0	0
28	0	0		0	0	0	0	0	0	0
29	0	0		0	0	0	0	0	0	0
30	0	0		0	0	0	0	0	0	0
31	459	466		6	6	89	60	0	0	0
32	475	979		90	88	97	93	0	0	0

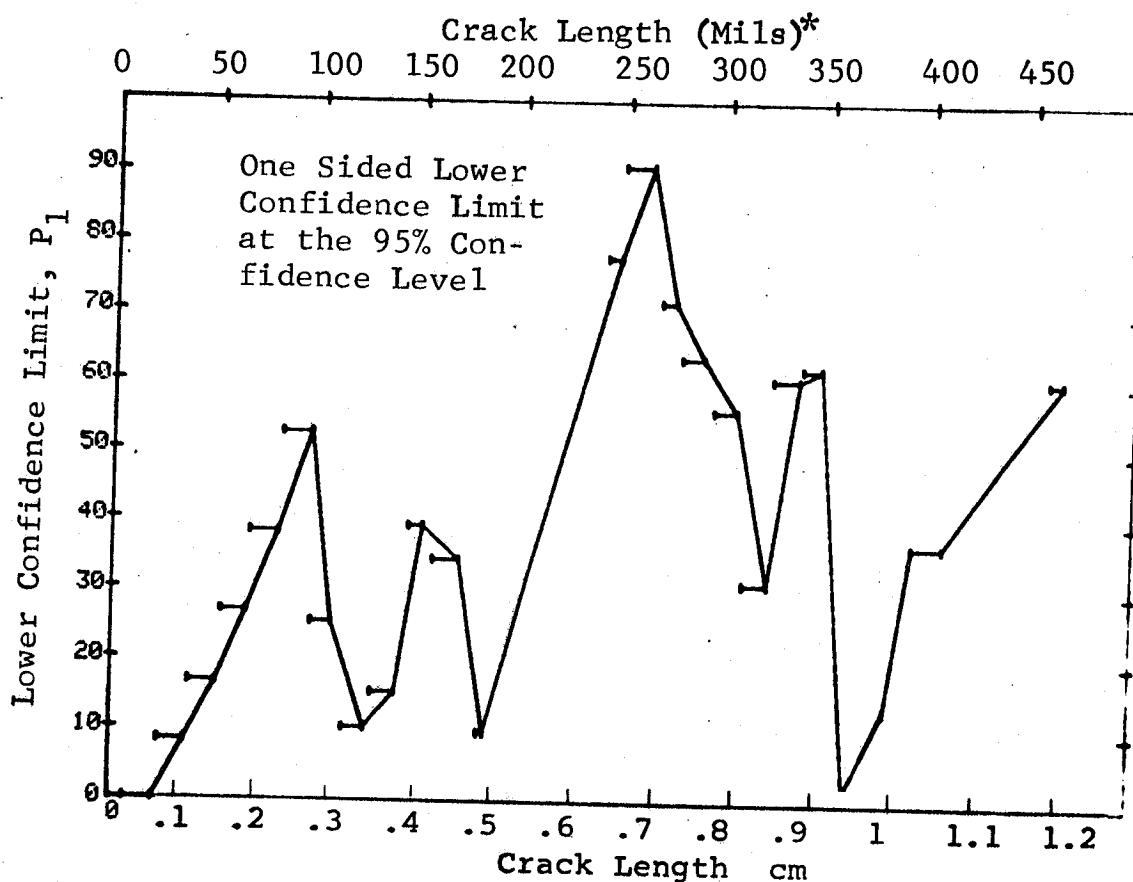


Figure D-8 Probability of Detection for 2219-T87 Al Using X-ray. Etched Fatigue Cracks in Flat Plates. Lab. Env. D-24

(b) Optimum Probability Method of Data Cumulation

02-JUL-75				TEST 2, X-RAY, MARTIN (8)			
RANGE	MIN LN	* MAX LN	N	DET	50%	95%	0 MILS
1	7	21*	39	1	0	0	0
2	23	36	49	0	0	0	0
3	38	52	72	18	0	16	0
4	54	67	120	41	0	27	0
5	68	82	131	60	0	38	0
6	83	97	87	54	0	52	0
7	83	108	126	69	0	47	0
8	68	126	290	136	0	41	0
9	68	141	332	147	0	39	0
10	68	153	350	158	0	40	0
11	146	171	27	17	0	45	0
12	68	185	368	167	0	41	0
13	0	0	0	0	0	0	0
14	0	0	0	0	0	0	0
15	0	0	0	0	0	0	0
16	241	247	12	12	0	77	0
17	241	262	63	62	0	92	0
18	241	275	72	71	0	93	0
19	241	290	87	84	0	91	0
20	241	306	102	96	0	88	0
21	241	322	129	109	0	78	0
22	241	336	159	132	0	77	0
23	241	347	177	147	0	77	0
24	241	362	180	148	0	76	0
25	241	381	183	150	0	76	0
26	241	393	186	153	0	77	0
27	241	408	189	156	0	77	0
28	0	0	0	0	0	0	0
29	0	0	0	0	0	0	0
30	0	0	0	0	0	0	0
31	241	466	195	162	0	78	0
32	393	479	102	100	0	78	0

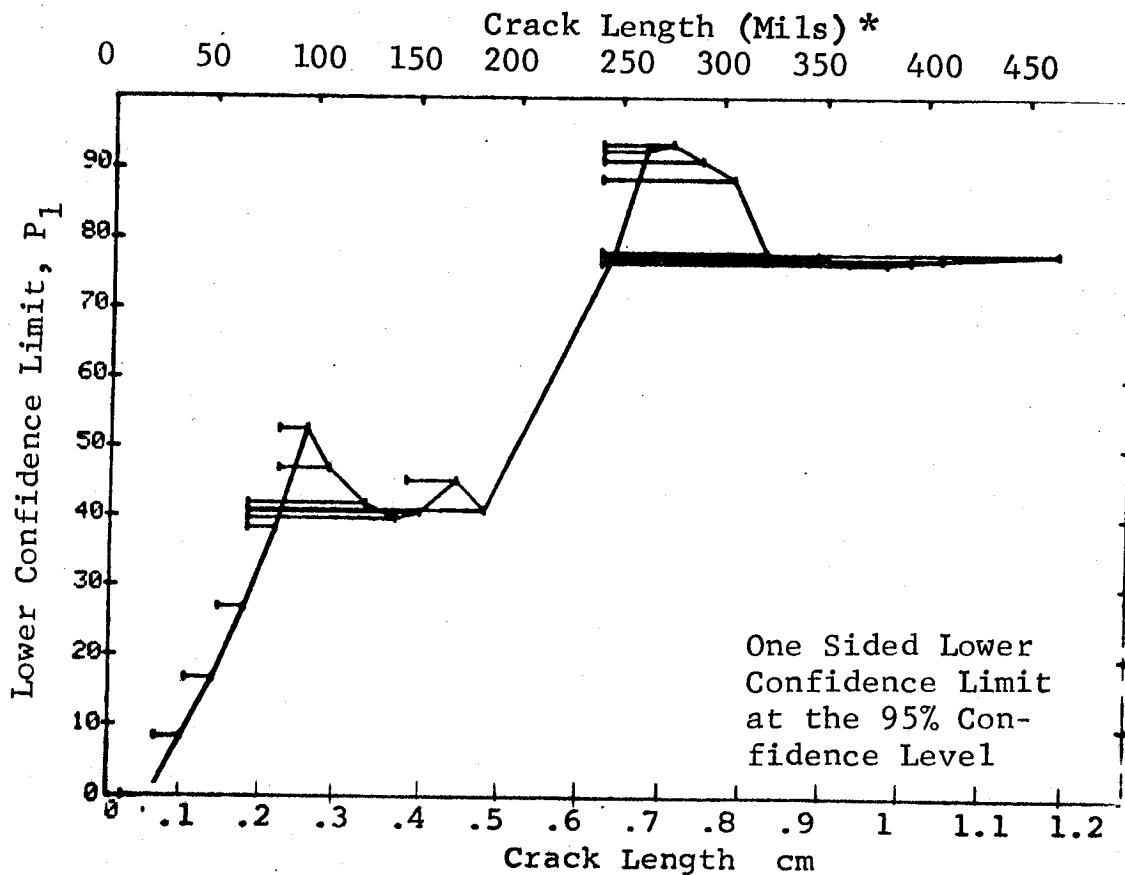


Figure D-8 (Continued)

(c) Overlapping Sixty Point Method of Data Cumulation

02-JUL-75				TEST 3, X-RAY, MARTIN (8)				
RANGE	MIN LN	MAX LN *	N	DET	50%	95%	0 MID	1 MID
1	0	0	0	0	0	0	0	0
2	0	0	0	0	0	0	0	0
3	0	0	0	0	0	0	0	0
4	7	20	32	0	0	0	0	0
5	7	30	60	7	11	5	0	0
6	20	40	60	10	16	9	0	0
7	30	45	60	8	12	6	0	0
8	40	50	60	13	20	13	0	0
9	45	58	60	16	25	17	0	0
10	51	61	60	21	34	24	0	0
11	58	64	60	26	42	32	0	0
12	61	67	60	19	30	21	0	0
13	64	70	60	23	37	27	0	0
14	67	73	60	28	45	35	0	0
15	70	77	60	18	29	20	0	0
16	73	80	60	25	40	30	0	0
17	77	83	60	41	67	57	0	0
18	80	87	60	45	74	64	0	0
19	83	95	60	37	60	50	0	0
20	87	102	60	27	44	33	0	0
21	95	115	60	21	34	24	0	0
22	102	129	60	18	29	20	0	0
23	115	136	60	16	25	17	0	0
24	129	158	60	21	34	24	0	0
25	136	248	60	36	59	48	0	0
26	158	258	60	51	83	75	94	181
27	248	279	60	59	97	92	0	1
28	258	310	60	55	90	83	43	56
29	279	326	60	40	65	50	0	0
30	310	340	60	36	59	48	0	0
31	326	466	60	48	79	69	0	0
32	340	500	60	55	90	83	40	50

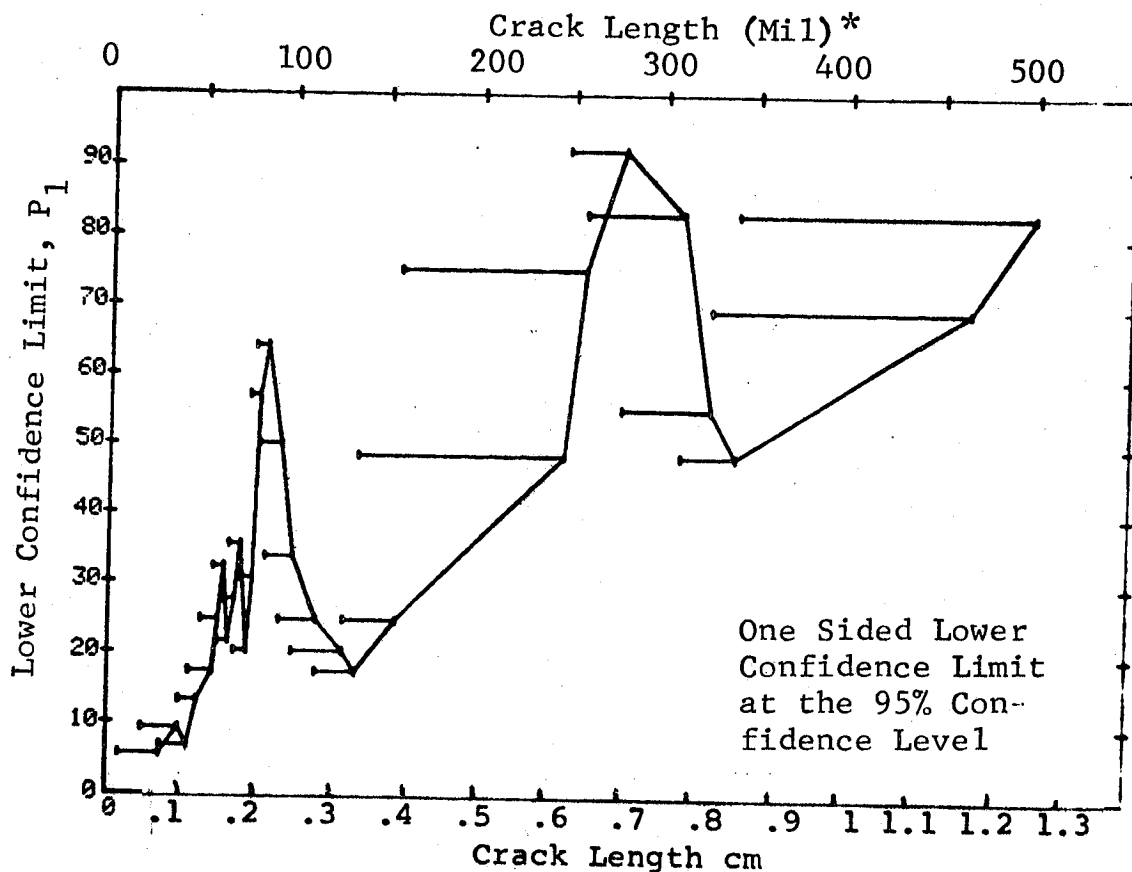


Figure D-8 (Concluded)

(a) Range Interval Method of Data Cumulation

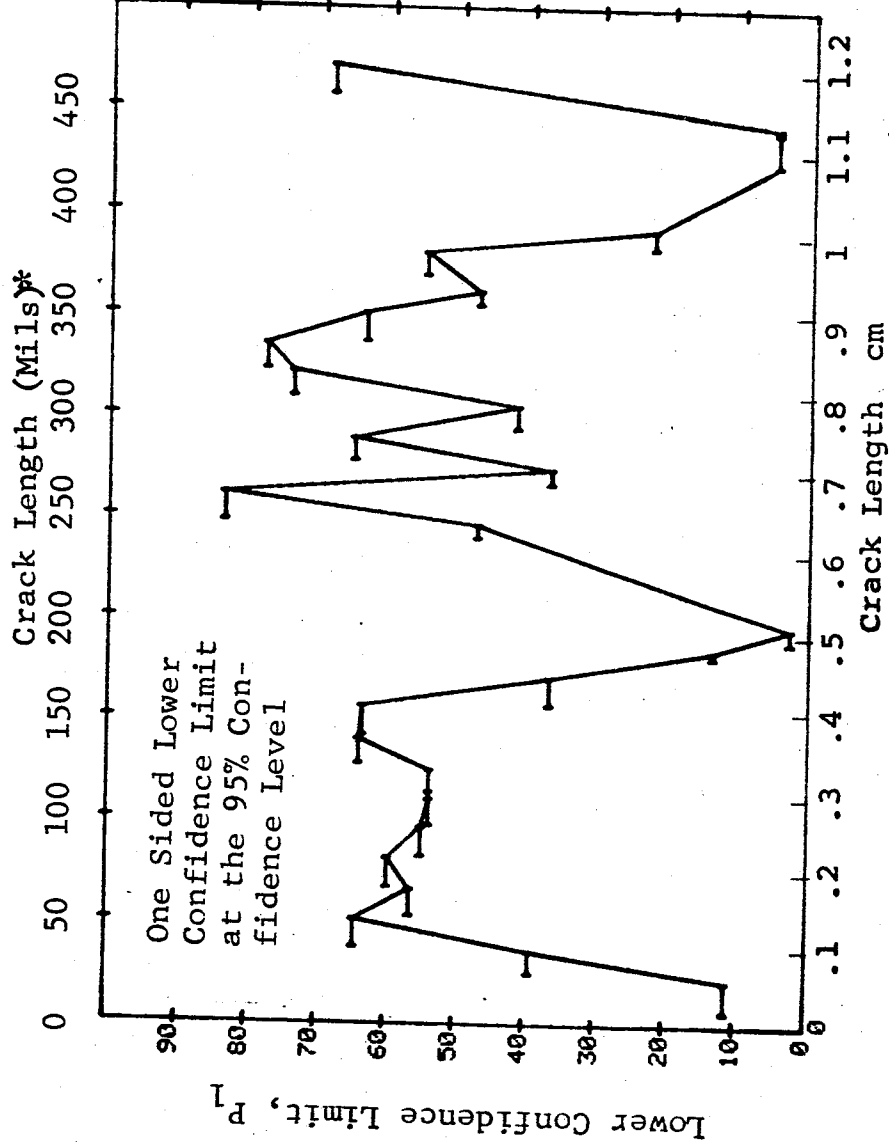
[illegible]

Figure D-9 Probability of Detection for 2219-T87 Al Using Ultrasonic Shear Wave. Etched-Fatigue Cracks in Flat Plates Measured by Operator O. Lab. Env.

D-27

(b) Optimum Probability Method of Data Cumulation

03-JUL-75		ULTRASONIC		N	TEST 2		ROCKWELL SC, 101		(9)
RANGE	MIN LN	MIN LN	MIN LN		DET	50%	95%	0 MISS	
1	7*	32*	13	4	0	11	0	0	
2	25	36	18	11	0	39	0	0	
3	38	52	23	19	0	64	0	0	
4	38	67	69	51	0	63	0	0	
5	38	82	122	89	0	65	0	0	
6	38	97	161	116	0	65	0	0	
7	38	111	178	129	0	66	0	0	
8	38	126	195	142	0	67	0	0	
9	38	141	214	158	0	68	0	0	
10	129	157	34	29	0	71	0	0	
11	129	171	37	32	0	73	0	0	
12	129	185	40	34	0	72	0	0	
13	98	197	76	61	0	71	0	0	
14	0	0	0	0	0	0	0	0	
15	0	0	0	0	0	0	0	0	
16	129	247	46	39	0	73	0	0	
17	241	262	21	21	0	86	0	25	
18	241	275	24	24	0	88	0	22	
19	241	290	31	31	0	90	0	15	
20	241	306	37	36	0	87	0	24	
21	241	322	47	46	0	90	0	14	
22	241	336	59	58	0	92	0	12	
23	241	352	70	68	0	91	0	6	
24	241	362	74	72	0	91	0	2	
25	241	381	79	77	0	92	0	0	
26	241	393	81	79	0	92	0	0	
27	241	408	82	79	0	90	0	0	
28	241	426	83	80	0	90	0	0	
29	241	442	84	81	0	91	0	0	
30	241	444	85	82	0	91	0	0	
31	241	472	93	90	0	91	0	0	
32	241	979	152	147	0	93	0	0	

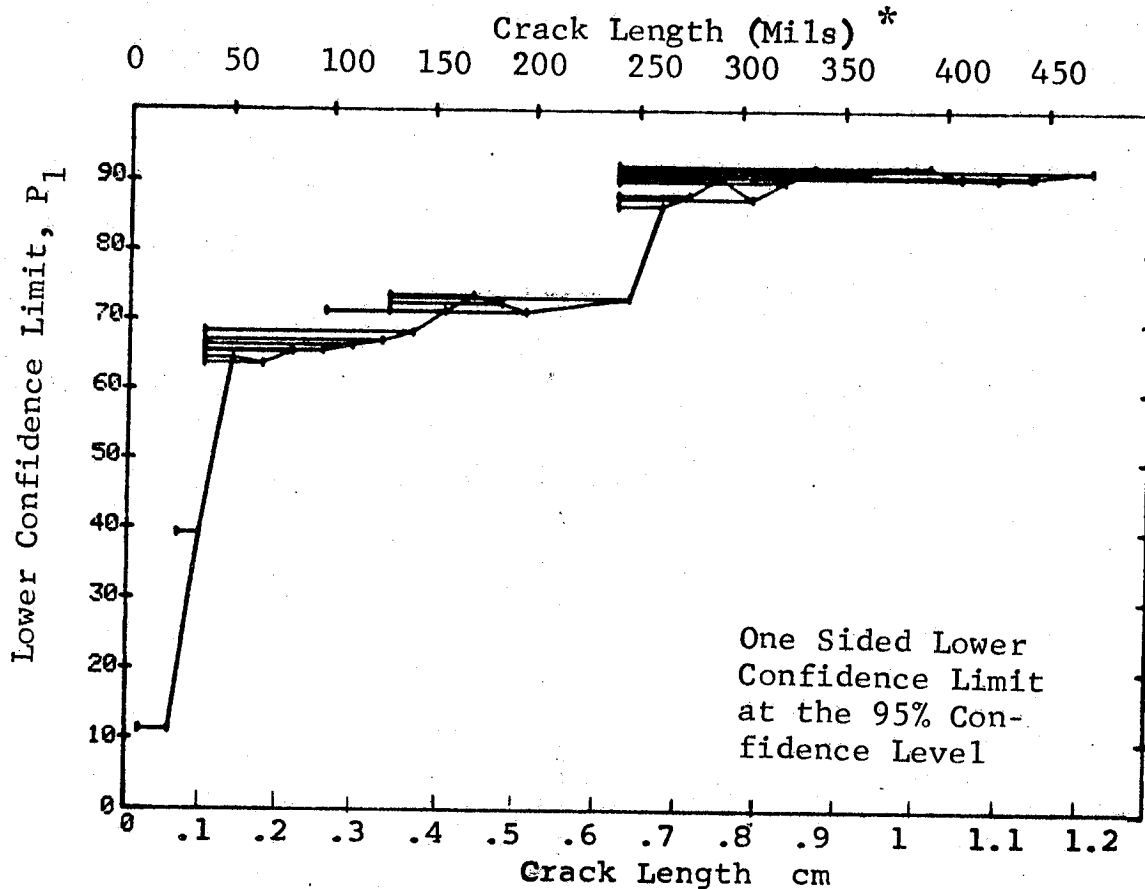


Figure D-9 (Continued)

(c) Overlapping Sixty Point Method of Data Cumulation

03-JUL-75		ULTRASONIC		N	TEST 3 : ROCKWELL SC. 101 (9)				
RANGE	MIN LN	MAX LN			DET	50%	95%	0 MISS	1 MISS
1	0	* 0 *		0	0	0	0	0	0
2	0	0		0	0	0	0	0	0
3	0	0		0	0	0	0	0	0
4	0	0		0	0	0	0	0	0
5	0	0		0	0	0	0	0	0
6	0	0		0	0	0	0	0	0
7	0	0		0	0	0	0	0	0
8	0	0		0	0	0	0	0	0
9	0	0		0	0	0	0	0	0
10	0	0		0	0	0	0	0	0
11	0	0		0	0	0	0	0	0
12	0	0		0	0	0	0	0	0
13	0	0		0	0	0	0	0	0
14	0	0		0	0	0	0	0	0
15	0	0		0	0	0	0	0	0
16	0	0		0	0	0	0	0	0
17	0	0		0	0	0	0	0	0
18	0	0		0	0	0	0	0	0
19	0	0		0	0	0	0	0	0
20	0	0		0	0	0	0	0	0
21	7	49	52	33	62	51	0	0	0
22	31	63	60	44	72	62	0	0	0
23	51	70	60	40	65	55	0	0	0
24	64	79	60	44	72	62	0	0	0
25	70	87	60	44	72	62	0	0	0
26	79	105	60	40	65	55	0	0	0
27	88	131	60	45	74	64	0	0	0
28	105	162	60	50	82	73	0	0	0
29	132	275	60	54	88	81	56	69	
30	171	330	60	57	93	87	16	29	
31	279	442	60	57	93	87	16	29	
32	331	500	60	56	92	85	29	43	

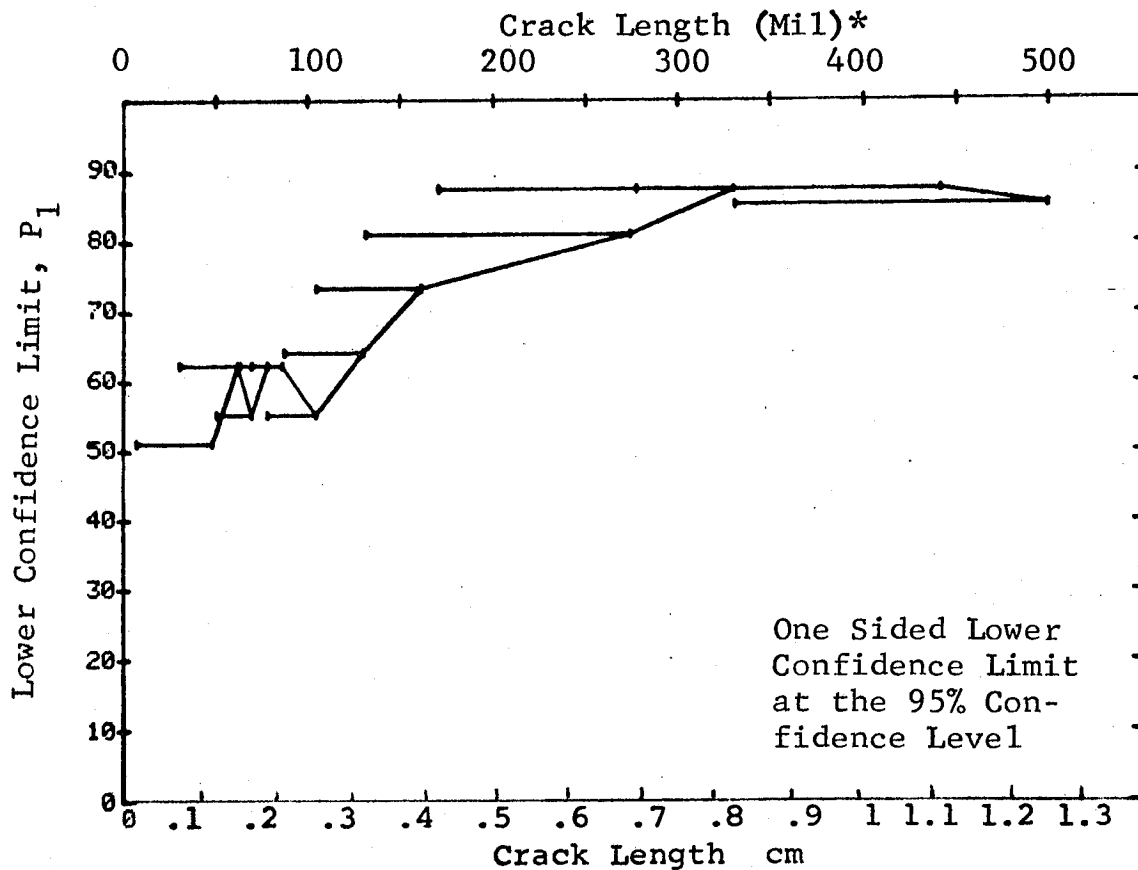


Figure D-9 (Concluded)

(a) Range Interval Method of Data Cumulation

03-JUL-75 ULTRASONIC				TEST 1, ROCKWELL C, 100' (10)				
RANGE	MIN LN	* MAX LN *	N	DET	50%	95%	0 MISS	1 MISS
1	7	22	13	4	27	11	0	0
2	25	36	18	15	73	62	0	0
3	38	52	23	19	79	64	0	0
4	54	67	46	39	83	73	0	0
5	68	82	53	51	94	88	0	23
6	83	97	39	39	98	92	0	7
7	98	111	17	16	90	75	29	44
8	115	126	17	17	96	83	12	29
9	129	141	19	19	96	85	10	27
10	143	157	15	15	95	81	14	31
11	158	171	3	3	79	36	0	0
12	182	185	3	3	79	36	0	0
13	190	197	2	2	70	22	0	0
14	207	207	1	1	50	5	0	0
15	0	0	0	0	0	0	0	0
16	241	247	4	4	84	47	0	0
17	248	262	17	17	96	83	12	29
18	268	275	3	3	79	36	0	0
19	279	290	6	6	89	60	0	0
20	295	306	6	6	89	60	0	0
21	310	322	10	10	93	74	0	0
22	323	336	12	12	94	77	17	34
23	338	352	11	11	93	76	18	35
24	356	362	4	4	84	47	0	0
25	370	381	5	5	87	54	0	0
26	384	393	2	2	70	22	0	0
27	408	408	1	1	50	5	0	0
28	426	426	1	1	50	5	0	0
29	442	442	1	1	50	5	0	0
30	444	450	2	2	70	22	0	0
31	458	472	7	7	90	65	0	0
32	474	979	59	59	98	95	0	0

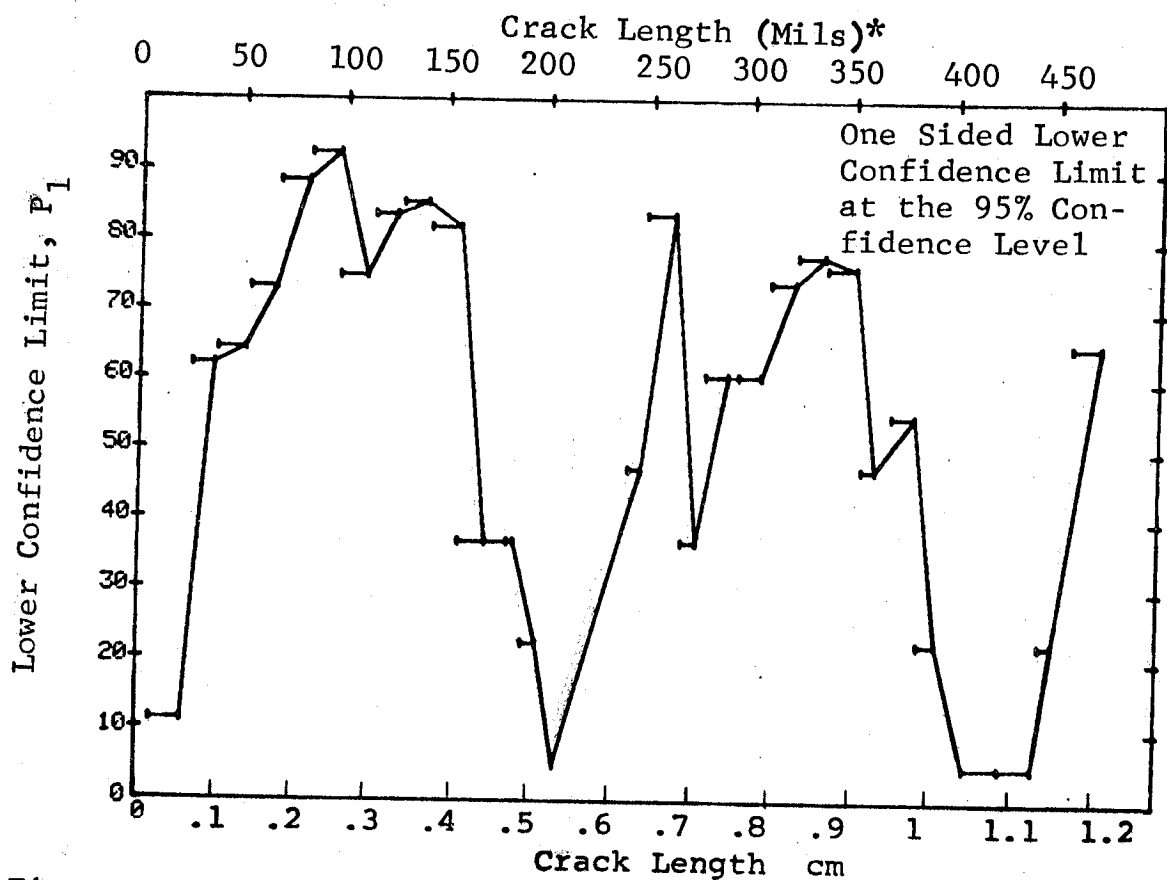


Figure D-10 Probability of Detection for 2219-T87 Al Using Ultrasonic Shear Wave. Etched-Fatigue Cracks in Flat Plates Measured by Operator P. Lab. Env.

(b) Optimum Probability Method of Data Cumulation

03-JUL-75 RANGE	MIN	LN	LN *	ULTRASONIC MAX LN	N	TEST 2, FOOTWELL SC		P		(10)
						DET	50%	95%	MISS	
1	25	68	97	111	109	4	0	11	0	0
2	25	68	97	126	126	15	0	63	0	0
3	25	68	97	141	92	34	0	70	0	0
4	25	68	97	157	107	73	0	88	0	0
5	68	97	97	171	110	51	0	93	8	23
6	68	97	97	185	113	90	0	93	0	0
7	68	97	97	197	115	106	0	93	0	0
8	68	97	97	207	116	123	0	93	0	0
9	83	83	83	247	120	136	0	94	0	0
10	83	83	83	262	137	91	0	95	0	0
11	83	83	83	275	140	106	0	95	0	0
12	83	83	83	290	145	109	0	95	0	0
13	83	83	83	306	146	112	0	95	0	0
14	83	83	83	322	146	114	0	95	0	0
15	83	83	83	336	146	115	0	95	0	0
16	83	83	83	352	146	115	0	95	0	0
17	83	83	83	381	146	119	0	96	0	0
18	83	83	83	393	146	136	0	96	0	0
19	83	83	83	408	146	139	0	96	0	0
20	115	115	115	426	146	145	0	96	0	0
21	115	115	115	442	146	96	0	96	0	0
22	115	115	115	450	146	106	0	97	0	0
23	115	115	115	472	146	118	0	97	0	0
24	115	115	115	979	146	129	0	97	0	0
25	115	115	115		146	133	0	97	0	0
26	115	115	115		146	138	0	97	0	0
27	115	115	115		146	140	0	97	0	0
28	115	115	115		146	141	0	97	0	0
29	115	115	115		146	142	0	97	0	0
30	115	115	115		146	143	0	97	0	0
31	115	115	115		146	145	0	98	0	0
32	115	115	115		211	152	0	98	0	0
					211	211	0	98	0	0

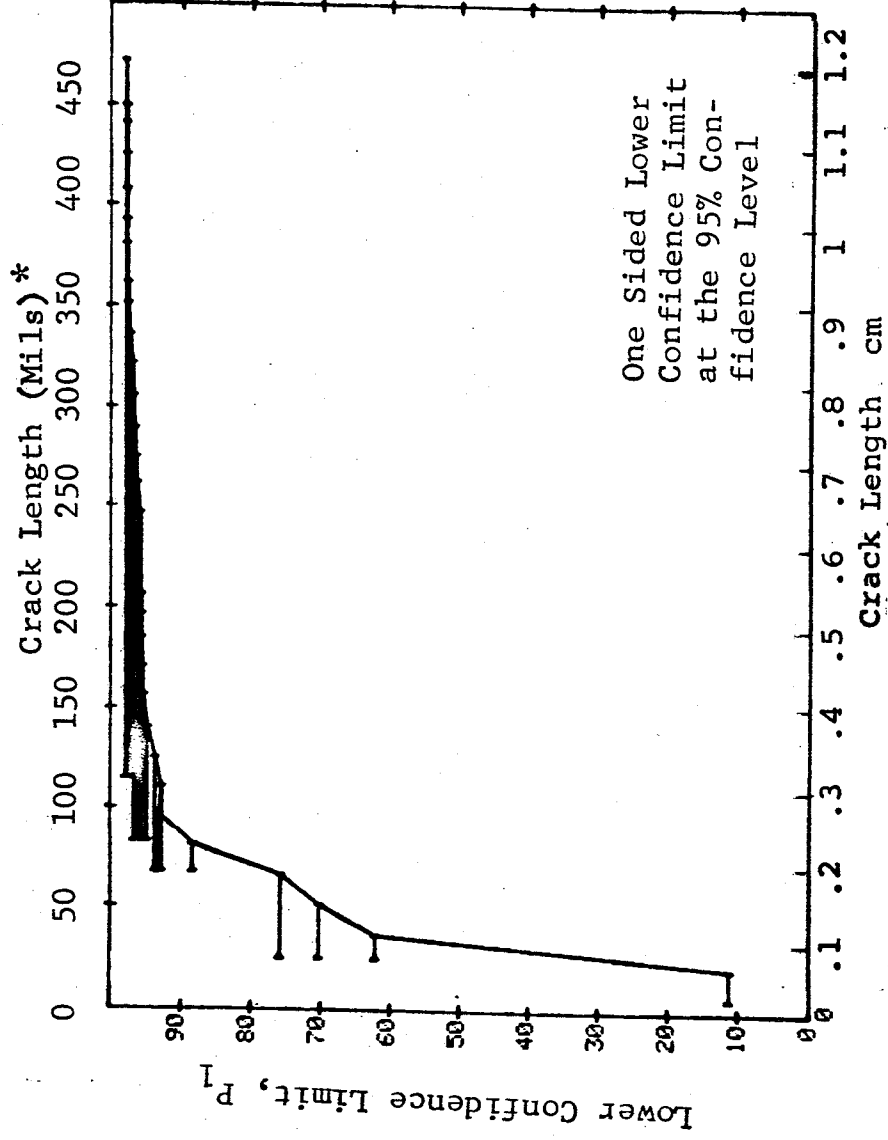


Figure D-10 (Continued)

for

(c) Overlapping Sixty Point Method of Data Cumulation

03-JUL-75		ULTRASONIC			TEST 3, ROCKWELL SC, P (10)					
RANGE	MIN LN	* MAX LN	*	N	DET	50%	95%	0 MISS	1 MISS	
1	0	0		0	0	0	0	0	0	
2	0	0		0	0	0	0	0	0	
3	0	0		0	0	0	0	0	0	
4	0	0		0	0	0	0	0	0	
5	0	0		0	0	0	0	0	0	
6	0	0		0	0	0	0	0	0	
7	0	0		0	0	0	0	0	0	
8	0	0		0	0	0	0	0	0	
9	0	0		0	0	0	0	0	0	
10	0	0		0	0	0	0	0	0	
11	0	0		0	0	0	0	0	0	
12	0	0		0	0	0	0	0	0	
13	0	0		0	0	0	0	0	0	
14	0	0		0	0	0	0	0	0	
15	0	0		0	0	0	0	0	0	
16	0	0		0	0	0	0	0	0	
17	0	0		0	0	0	0	0	0	
18	0	0		0	0	0	0	0	0	
19	0	0		0	0	0	0	0	0	
20	0	0		0	0	0	0	0	0	
21	7	49		52	36	68	57	0	0	
22	31	63		60	51	83	75	94	100	
23	51	70		60	52	85	77	82	94	
24	64	79		60	55	90	83	43	56	
25	70	87		60	59	97	92	0	1	
26	79	105		60	60	98	95	0	0	
27	88	131		60	59	97	92	0	1	
28	105	162		60	59	97	92	0	1	
29	132	269		60	60	98	95	0	0	
30	171	330		60	60	98	95	0	0	
31	275	442		60	60	98	95	0	0	
32	331	500		60	60	98	95	0	0	

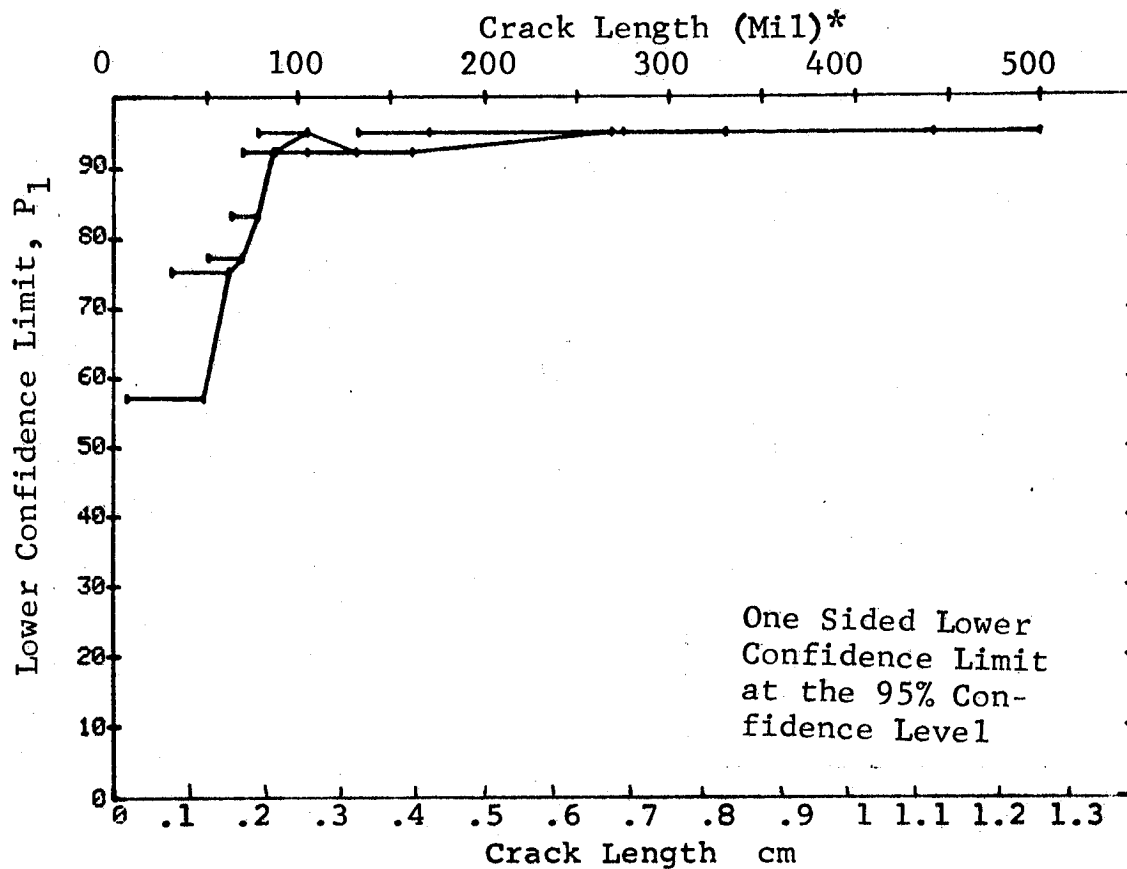


Figure D-10 (Concluded)

(b) Optimum Probability Method of Data Cumulation

03-JUL-75		ULTRASONIC		N	TEST 1 - ROCKWELL SC		SC		(11)
RANGE	MIN LN	MAX LN			DFT	50%	95%	0 MISS	
1		* 22 *	13	3	20	6	0	0	0
2	25	16	18	3	47	29	0	0	0
3	38	52	24	18	72	56	0	0	0
4	54	67	46	37	79	68	0	0	0
5	68	82	53	46	85	76	76	89	0
6	83	97	39	31	77	66	0	0	0
7	98	111	17	13	73	53	0	0	0
8	115	126	17	16	90	75	29	44	0
9	129	141	19	14	70	52	0	0	0
10	143	157	15	10	63	42	0	0	0
11	158	171	3	2	50	13	0	0	0
12	182	185	3	3	79	36	0	0	0
13	190	197	2	2	70	22	0	0	0
14	0	0	0	0	0	0	0	0	0
15	0	0	0	0	0	0	0	0	0
16	241	247	4	4	84	47	0	0	0
17	248	262	17	17	96	83	12	29	0
18	268	275	3	3	79	36	0	0	0
19	279	290	7	7	90	65	0	0	0
20	295	306	6	6	89	60	0	0	0
21	310	322	10	10	93	74	0	0	0
22	323	336	12	12	94	77	17	34	0
23	338	352	11	10	85	63	0	0	0
24	356	362	4	4	84	47	0	0	0
25	370	381	5	4	68	34	0	0	0
26	384	393	2	2	70	22	0	0	0
27	408	408	1	1	50	5	0	0	0
28	426	426	1	1	50	5	0	0	0
29	442	442	1	1	50	5	0	0	0
30	444	444	1	1	50	5	0	0	0
31	458	472	7	7	90	65	0	0	0
32	474	979	59	55	92	85	30	44	0

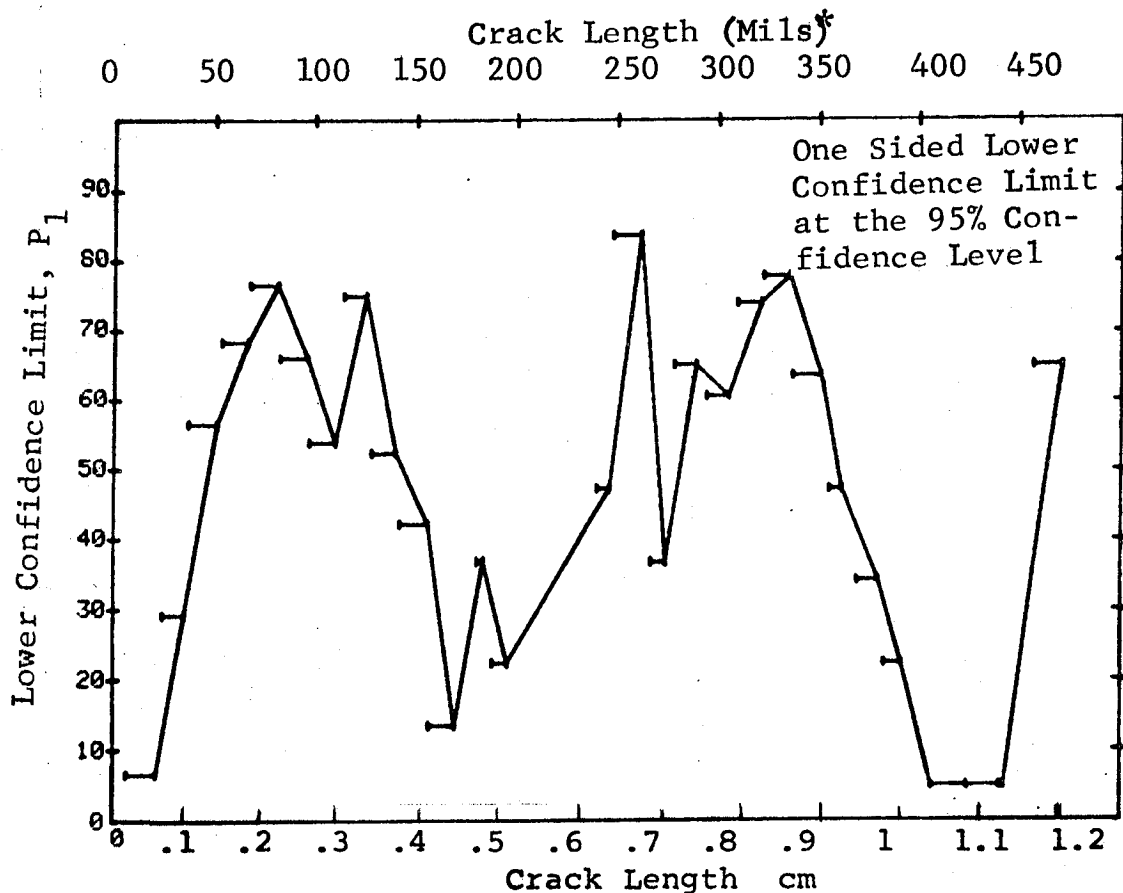


Figure D-11 Probability of Detection for 2219-T87 Al Using Ultrasonic Shear Waves. Etched Fatigue Cracks in Flat Plates Measured by Operator Q. Lab. Env.

(b) Optimum Probability Method of Data Cumulation

03-JUL-75			ULTRASONIC			TEST 2, ROCKWELL SC, '0' (11)				
RANGE	MIN LN	MAX LN	MIN LN	MAX LN	N	DET	50%	95%	0 MISS	1 MISS
1	7	22	*	*	13	3	0	6	0	0
2	25	36			18	9	0	29	0	0
3	38	52			24	18	0	56	0	0
4	38	67			70	55	0	68	0	0
5	68	82			53	46	0	76	0	0
6	54	97			138	114	0	76	0	0
7	54	111			155	127	0	76	0	0
8	68	126			126	106	0	77	0	0
9	54	141			191	157	0	77	0	0
10	54	157			206	167	0	76	0	0
11	54	171			209	169	0	75	0	0
12	54	185			212	172	0	76	0	0
13	54	197			214	174	0	76	0	0
14	0	0			0	0	0	0	0	0
15	0	0			0	0	0	0	0	0
16	54	247			218	178	0	76	0	0
17	182	262			26	26	0	89	3	20
18	182	275			29	29	0	90	0	17
19	182	290			36	36	0	92	0	10
20	182	306			42	42	0	93	0	4
21	182	322			52	52	0	94	0	0
22	182	336			64	64	0	95	0	0
23	182	352			75	74	0	93	0	0
24	182	362			79	78	0	94	0	0
25	182	381			84	82	0	92	0	0
26	182	393			86	84	0	92	0	0
27	182	408			87	85	0	92	0	0
28	182	426			88	86	0	93	0	0
29	182	442			89	87	0	93	0	0
30	182	444			90	88	0	93	0	0
31	182	472			97	95	0	93	0	0
32	182	979			156	150	0	92	0	0

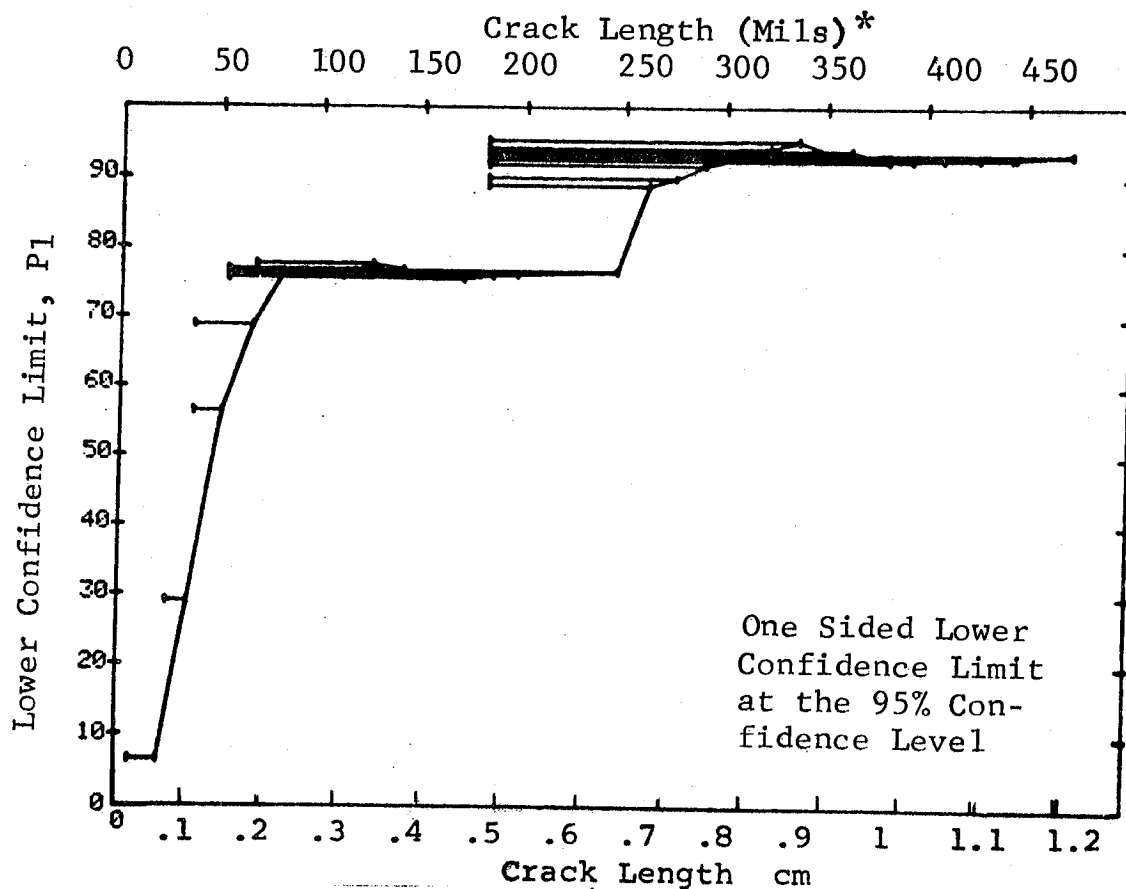


Figure D-11 (Continued)

(c) Overlapping Sixty Point Method of Data Cumulation

03-JUL-75		ULTRASONIC			N	TEST 3, ROCKWELL SC, '0' (11)				
RANGE	MIN LN	* MAX LN	* MAX LN			DET	50%	95%	0 MISS	1 MISS
1	0	0	0		0	0	0	0	0	0
2	0	0	0		0	0	0	0	0	0
3	0	0	0		0	0	0	0	0	0
4	0	0	0		0	0	0	0	0	0
5	0	0	0		0	0	0	0	0	0
6	0	0	0		0	0	0	0	0	0
7	0	0	0		0	0	0	0	0	0
8	0	0	0		0	0	0	0	0	0
9	0	0	0		0	0	0	0	0	0
10	0	0	0		0	0	0	0	0	0
11	0	0	0		0	0	0	0	0	0
12	0	0	0		0	0	0	0	0	0
13	0	0	0		0	0	0	0	0	0
14	0	0	0		0	0	0	0	0	0
15	0	0	0		0	0	0	0	0	0
16	0	0	0		0	0	0	0	0	0
17	0	0	0		0	0	0	0	0	0
18	0	0	0		0	0	0	0	0	0
19	0	0	0		0	0	0	0	0	0
20	0	0	0		0	0	0	0	0	0
21	7	49		52	27	50	39	0	0	0
22	31	63		60	46	75	65	0	0	0
23	49	69		60	50	82	73	0	0	0
24	63	79		60	50	82	73	0	0	0
25	70	87		60	51	83	75	94	100	0
26	79	104		60	49	80	71	0	0	0
27	87	131		60	49	80	71	0	0	0
28	105	158		60	47	77	67	0	0	0
29	131	269		60	50	82	73	0	0	0
30	162	329		60	59	97	92	0	1	1
31	275	426		60	58	95	89	1	16	16
32	330	500		60	57	93	87	16	29	29

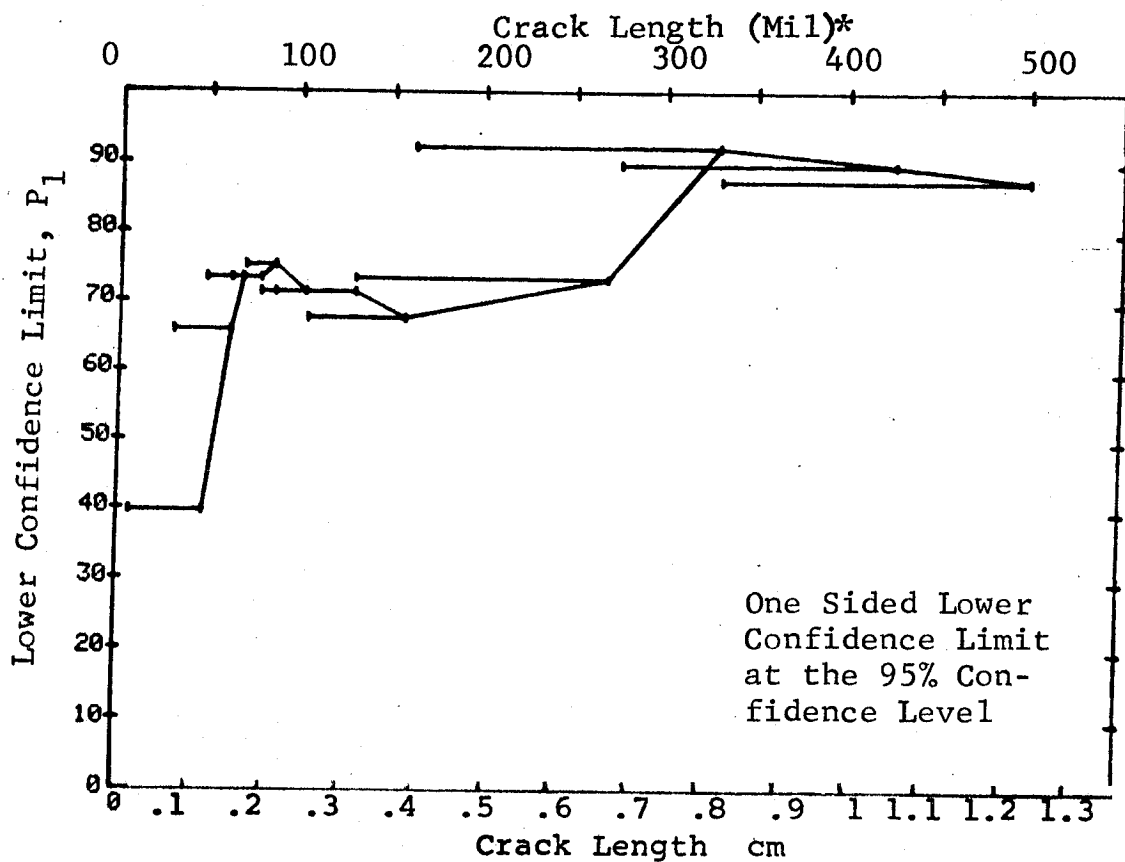


Figure D-11 (Concluded)

(a) Range Interval Method of Data Cumulation

24-JUL-75	ULTRASONIC	TEST 1, (12)	ROCKWELL SC	R-15
RANGE	MIN LN	DET	50% MISS	1 MISS
1	25	13	42	0
2	59	18	69	0
3	54	22	79	0
4	68	47	88	56
5	83	37	93	63
6	98	15	84	22
7	111	16	90	0
8	129	18	91	29
9	143	12	76	27
10	158	3	50	0
11	182	2	79	0
12	190	0	70	0
13	0	0	0	0
14	0	0	0	0
15	241	4	84	0
16	248	17	96	47
17	268	3	79	83
18	279	7	90	36
19	295	6	89	65
20	310	8	74	60
21	323	12	94	49
22	338	11	67	77
23	356	4	84	47
24	370	4	68	34
25	384	2	70	0
26	408	1	50	0
27	426	1	50	0
28	442	1	50	0
29	444	1	50	0
30	472	8	91	0
31	458	55	92	68
32	474	59	85	44

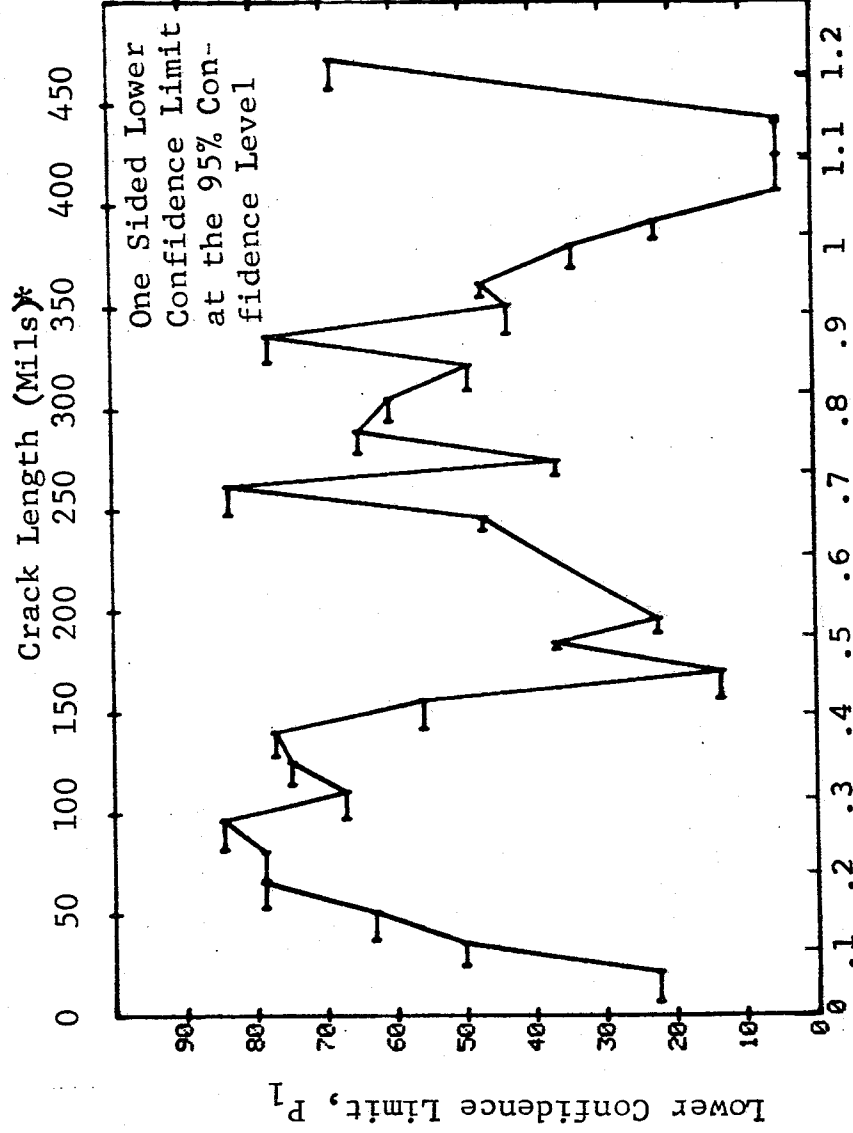


Figure D-12 Probability of Detection for 2219-T87 Al Using Ultrasonic Shear Waves. Etched Fatigue Cracks in Flat Plates Measured by Operator R. Lab. Env. D-36

(b) Optimum Probability Method of Data Cumulation

24-JUL-75			ULTRASONIC		TEST 2, (12)		ROCKWELL SC R		MISS		MISS	
RANGE	MIN	LN	7*	MAX	LN	DET	50%	95%	0	MISS	1	MISS
1	25	13	22*	36	13	6	0	22	0	0	0	0
2	25	18	36	52	18	13	0	50	0	0	0	0
3	54	40	52	67	40	31	0	64	0	0	0	0
4	54	47	82	97	47	42	0	78	0	0	0	0
5	54	100	97	111	100	89	0	82	79	91	0	0
6	54	139	126	141	139	126	0	85	0	0	0	0
7	83	156	111	126	156	141	0	85	30	43	0	0
8	83	73	141	126	73	68	0	86	24	37	0	0
9	83	92	141	126	92	86	0	87	0	0	0	0
10	68	160	157	141	160	145	0	85	0	0	0	0
11	54	210	171	157	210	189	0	85	0	0	0	0
12	54	213	185	171	213	192	0	85	0	0	0	0
13	68	168	197	185	168	152	0	85	0	0	0	0
14	0	0	0	0	0	0	0	0	0	0	0	0
15	0	0	0	0	0	0	0	0	0	0	0	0
16	54	219	247	0	219	198	0	86	0	0	0	0
17	182	262	262	247	262	198	0	89	3	20	0	0
18	182	275	275	262	275	26	0	90	0	17	0	0
19	182	290	290	275	290	29	0	92	0	10	4	0
20	182	306	306	290	306	36	0	93	0	24	0	0
21	182	322	322	306	322	42	0	88	0	12	0	0
22	182	336	336	322	336	50	0	90	0	0	0	0
23	83	352	352	336	352	62	0	87	0	0	0	0
24	83	362	362	352	362	170	0	88	0	0	0	0
25	83	381	381	362	381	174	0	87	0	0	0	0
26	83	393	393	381	393	178	0	87	0	0	0	0
27	83	408	408	393	408	180	0	87	0	0	0	0
28	83	426	426	408	426	181	0	87	0	0	0	0
29	68	442	442	426	442	182	0	87	0	0	0	0
30	83	444	444	426	444	230	0	87	0	0	0	0
31	83	472	472	444	472	184	0	88	0	0	0	0
32	182	979	979	472	979	192	0	88	0	0	0	0
						147	0	89	0	0	0	0

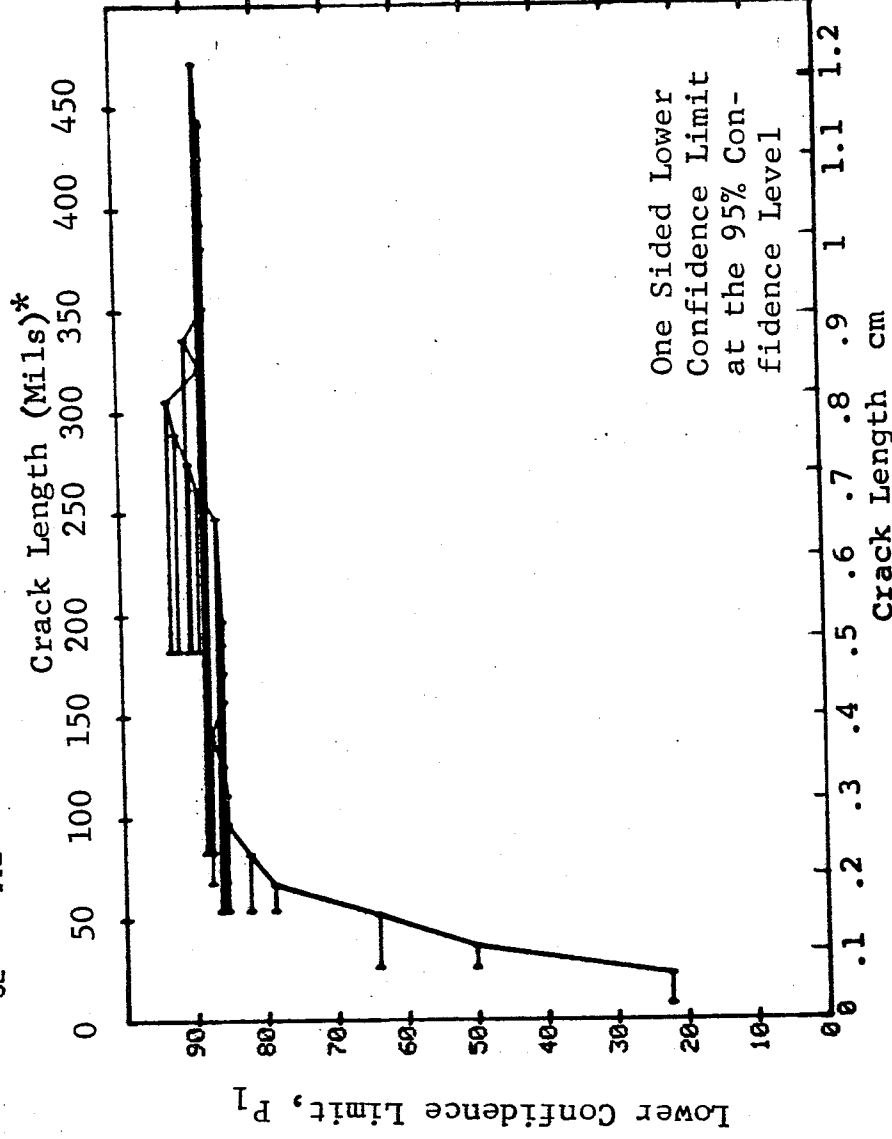


Figure D-12 (Continued)

(c) Overlapping Sixty Point Method of Data Cumulation

24-JUL-75		ULTRASONIC		N	TEST 3. (12)		ROCKWELL SC		R
RANGE	MIN LN	* MAX LN	*		DET	50%	95%	0 MISS	
1	0	0	*	0	0	0	0	0	0
2	0	0		0	0	0	0	0	0
3	0	0		0	0	0	0	0	0
4	0	0		0	0	0	0	0	0
5	0	0		0	0	0	0	0	0
6	0	0		0	0	0	0	0	0
7	0	0		0	0	0	0	0	0
8	0	0		0	0	0	0	0	0
9	0	0		0	0	0	0	0	0
10	0	0		0	0	0	0	0	0
11	0	0		0	0	0	0	0	0
12	0	0		0	0	0	0	0	0
13	0	0		0	0	0	0	0	0
14	0	0		0	0	0	0	0	0
15	0	0		0	0	0	0	0	0
16	0	0		0	0	0	0	0	0
17	0	0		0	0	0	0	0	0
18	0	0		0	0	0	0	0	0
19	0	0		0	0	0	0	0	0
20	0	0		0	0	0	0	0	0
21	7	51		52	36	68	57	0	0
22	31	63		60	49	80	71	0	0
23	52	70		60	51	83	75	94	100
24	64	79		60	53	87	79	69	82
25	70	87		60	57	93	87	16	29
26	79	105		60	56	92	85	29	43
27	88	131		60	56	92	85	29	43
28	105	162		60	54	88	81	56	69
29	132	275		60	55	90	83	43	56
30	171	330		60	58	95	89	1	16
31	279	442		60	54	88	81	56	69
32	331	500		60	54	88	81	56	69

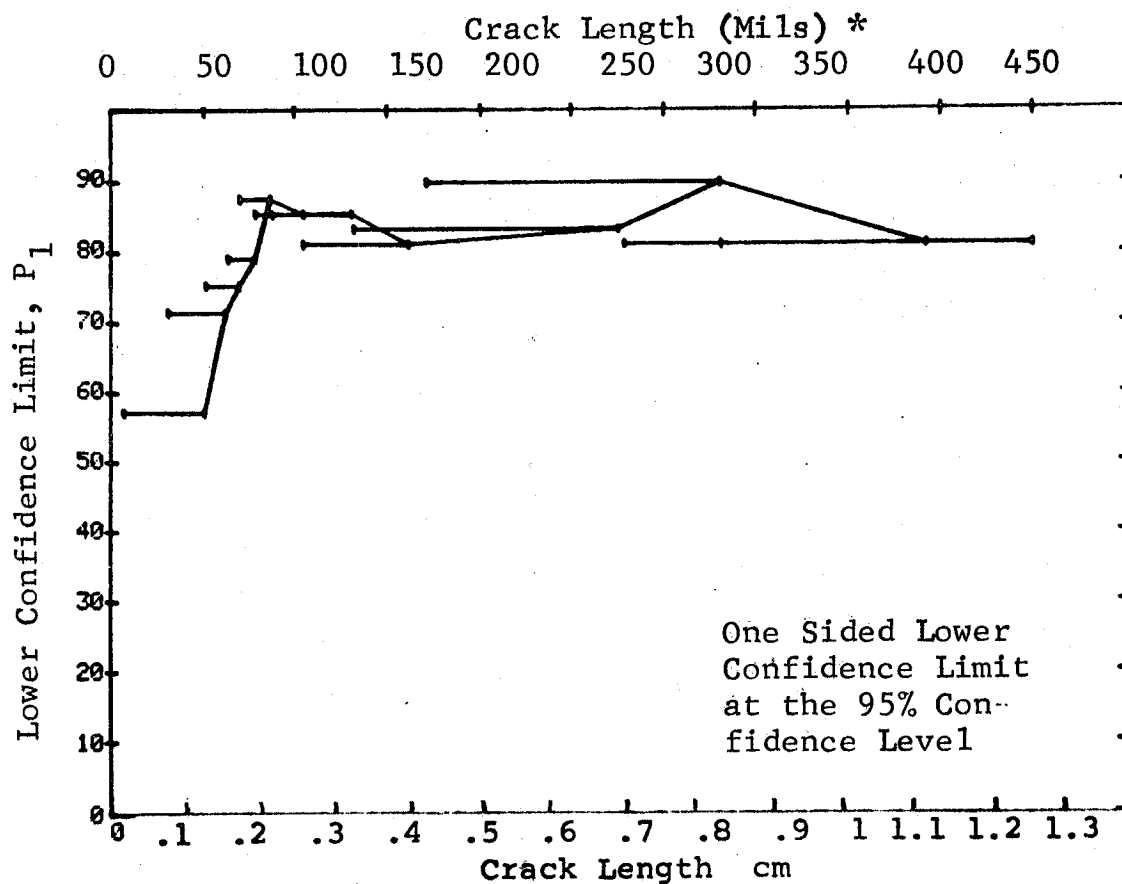


Figure D-12 (Concluded)

(a) Range Interval Method of Data Cumulation

24-JUL-75	ULTRASONIC		TEST 1, (13)		ROCKWELL		s	
RANGE	MIN LN	MAX LN	N	DET	50%	95%	0 MISS	1 MISS
1	7	22	13	4	27	11	0	0
2	25	36	18	13	69	50	0	0
3	38	52	23	17	71	54	0	0
4	54	67	46	38	81	70	0	0
5	68	82	53	50	93	86	23	36
6	83	97	39	36	90	81	37	50
7	98	111	17	17	96	83	12	29
8	115	126	17	16	90	75	29	44
9	129	141	19	18	91	77	27	42
10	143	157	15	14	89	72	0	0
11	158	171	3	3	79	36	0	0
12	182	185	3	3	79	36	0	0
13	190	197	2	2	70	22	0	0
14	0	0	0	0	0	0	0	0
15	0	0	0	0	0	0	0	0
16	241	247	4	3	61	24	0	0
17	248	262	17	17	96	83	12	29
18	268	275	3	3	79	36	0	0
19	279	290	7	6	77	47	0	0
20	295	306	6	6	89	60	0	0
21	310	322	10	10	93	74	0	0
22	323	336	12	10	78	56	0	0
23	338	352	11	10	85	63	0	0
24	356	362	4	4	84	47	0	0
25	370	381	5	4	68	34	0	0
26	384	393	2	2	70	22	0	0
27	408	408	1	1	50	5	0	0
28	426	426	1	1	50	5	0	0
29	442	442	1	1	50	5	0	0
30	444	444	1	1	50	5	0	0
31	458	472	8	8	91	68	0	0
32	474	979	59	59	98	95	0	0

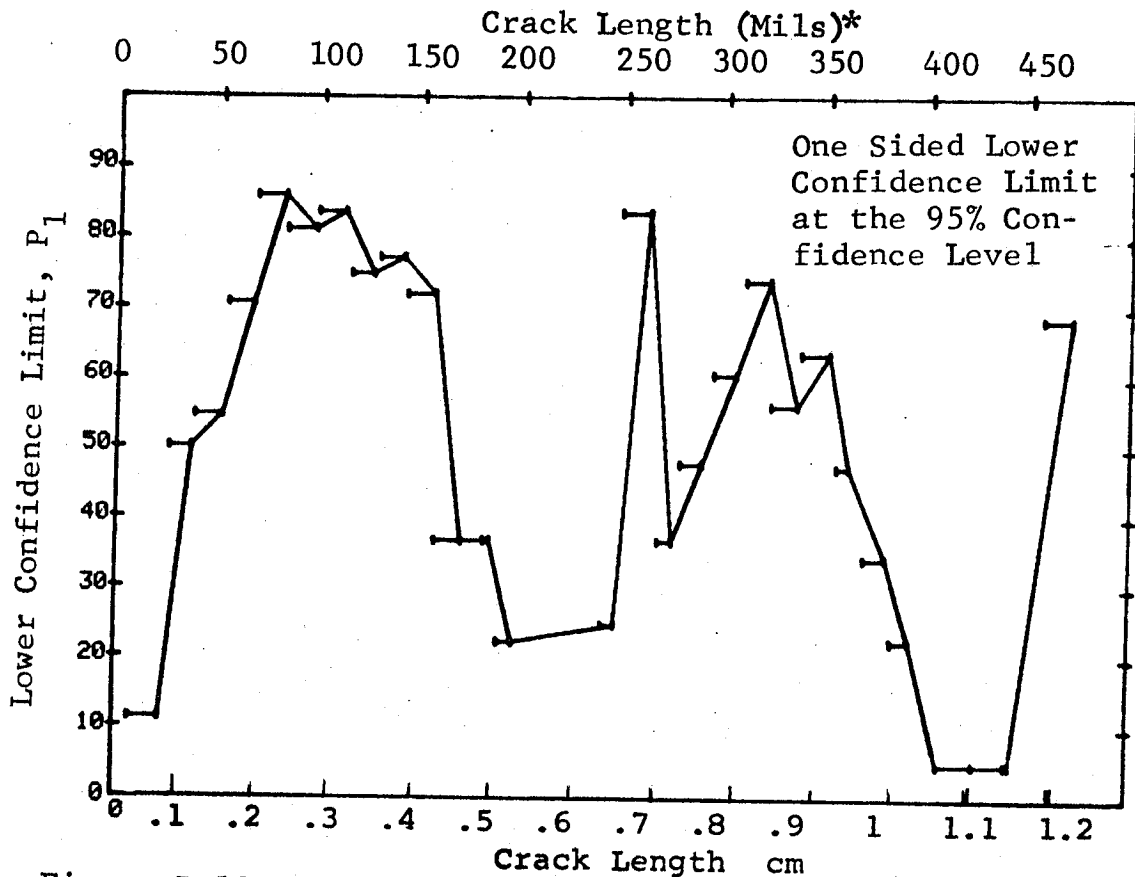


Figure D-13 Probability of Detection for 2219-T87 Al Using Ultrasonic Shear Waves. Etched Fatigue Cracks in Flat Plates Measured by Operator S. Lab. Env. D-39

(b) Optimum Probability Method of Data Cumulation

24-JUL-75		ULTRASONIC		N	TEST 2. (13)		ROCKWELL SC		S
RANGE	MIN LN	MAX LN	*		DET	50%	95%	0 MISS	
1	7	22	*	13	4	0	11	0	0
2	25	36		18	13	0	50	0	0
3	25	52		41	30	0	59	0	0
4	54	67		46	38	0	70	0	0
5	68	82		53	50	0	86	23	36
6	68	97		92	86	0	87	24	37
7	68	111		109	103	0	89	0	0
8	68	126		126	119	0	89	0	0
9	68	141		145	137	0	90	0	0
10	68	157		160	151	0	90	0	0
11	68	171		163	154	0	90	0	0
12	68	185		166	157	0	90	0	0
13	68	197		168	159	0	90	0	0
14	0	0		0	0	0	0	0	0
15	0	0		0	0	0	0	0	0
16	68	247		172	162	0	90	0	0
17	68	262		189	179	0	91	0	0
18	68	275		192	182	0	91	0	0
19	68	290		199	188	0	91	0	0
20	68	306		205	194	0	91	0	0
21	68	322		215	204	0	91	0	0
22	68	336		227	214	0	91	0	0
23	68	352		238	224	0	90	0	0
24	68	362		242	228	0	91	0	0
25	68	381		247	232	0	90	0	0
26	68	393		249	234	0	90	0	0
27	68	408		250	235	0	90	0	0
28	68	426		251	236	0	90	0	0
29	68	442		252	237	0	90	0	0
30	68	444		253	238	0	91	0	0
31	68	472		261	246	0	91	0	0
32	384	979		73	73	0	95	0	0

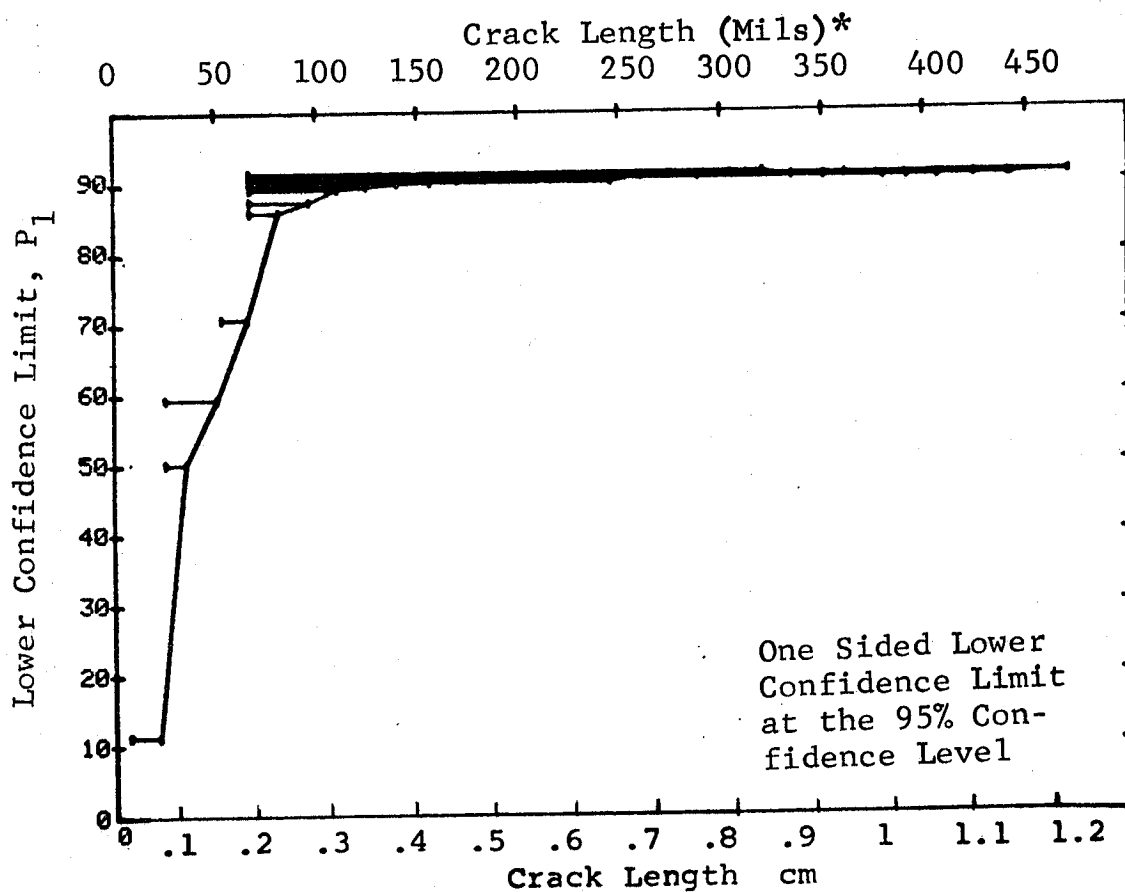


Figure D-13 (Continued)

(c) Overlapping Sixty Point Method of Data Cumulation

24-JUL-75		ULTRASONIC		TEST 3, (13)		ROCKWELL SC		s	
RANGE	MIN	LN	MAX	LN	DET	50%	95%	0 MISS	1 MISS
1		0	*	0	*	0	0	0	0
2		0		0		0	0	0	0
3		0		0		0	0	0	0
4		0		0		0	0	0	0
5		0		0		0	0	0	0
6		0		0		0	0	0	0
7		0		0		0	0	0	0
8		0		0		0	0	0	0
9		0		0		0	0	0	0
10		0		0		0	0	0	0
11		0		0		0	0	0	0
12		0		0		0	0	0	0
13		0		0		0	0	0	0
14		0		0		0	0	0	0
15		0		0		0	0	0	0
16		0		0		0	0	0	0
17		0		0		0	0	0	0
18		0		0		0	0	0	0
19		0		0		0	0	0	0
20		0		0		0	0	0	0
21		7		49		32	60	49	0
22		31		63		46	75	65	0
23		51		70		51	83	75	94
24		64		79		54	88	81	56
25		70		87		57	93	87	16
26		79		105		57	93	87	16
27		88		131		56	92	85	29
28		105		162		57	93	87	16
29		132		275		58	95	89	1
30		171		330		58	95	89	1
31		279		442		55	90	83	43
32		331		503		56	92	85	29

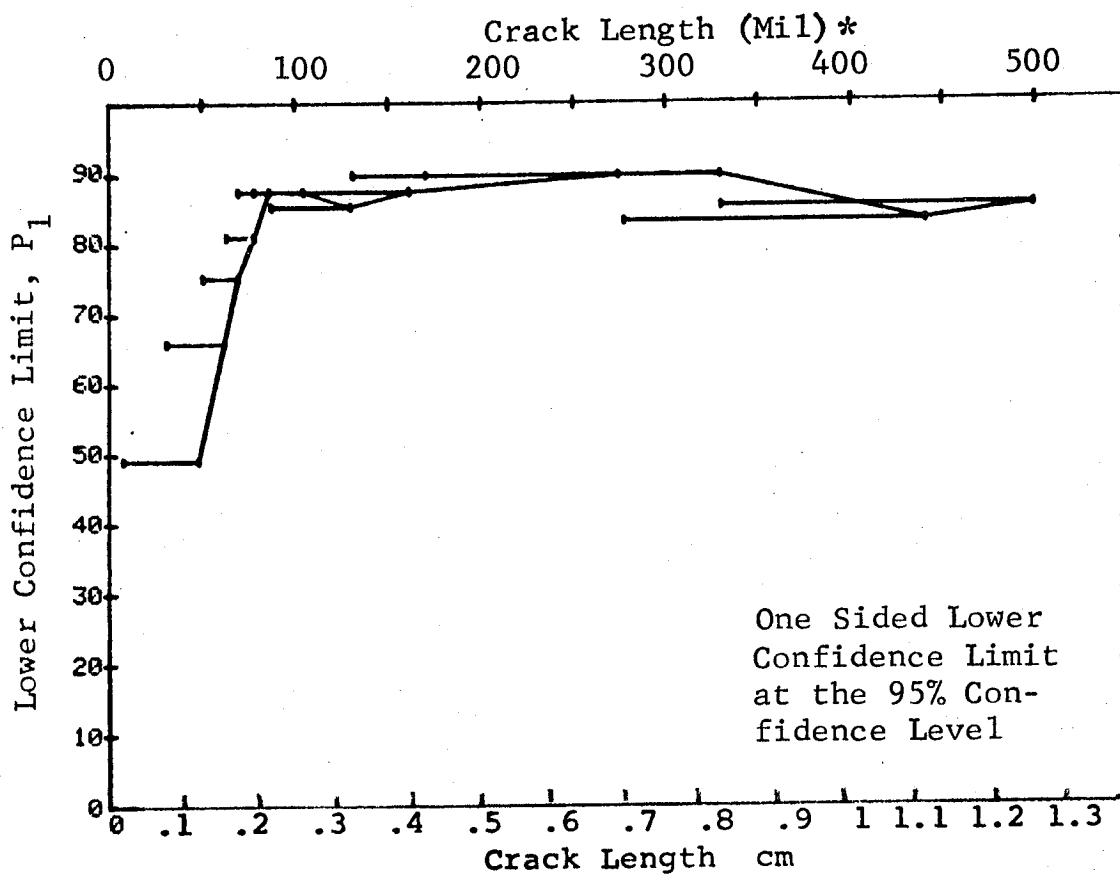


Figure D-13 (Concluded)

(a) Range Interval Method of Data Cumulation

24-JUL-75	TEST 1, (14)	ROCKWELL SC	H
RANGE MIN LN	DET	95%	MISS
1	4	11	0
2	9	29	0
3	21	75	53
4	39	73	0
5	47	78	73
6	37	83	23
7	17	83	22
8	15	96	0
9	18	84	42
10	14	89	0
11	3	79	0
12	3	70	0
13	2	22	0
14	0	0	0
15	0	0	0
16	4	84	0
17	17	96	39
18	3	79	0
19	7	90	0
20	6	89	0
21	10	93	0
22	11	86	0
23	11	93	35
24	4	84	0
25	4	68	0
26	2	70	0
27	1	50	0
28	1	50	0
29	1	50	0
30	1	50	0
31	8	91	0
32	59	98	0

24-JUL-75	PENETRANT	N
RANGE MIN LN	MAX LN *	
1	7	13
2	25	18
3	38	23
4	54	46
5	67	53
6	82	38
7	97	17
8	111	17
9	126	19
10	141	15
11	157	3
12	171	2
13	182	0
14	197	0
15	0	0
16	0	0
17	241	4
18	262	17
19	275	3
20	290	7
21	306	6
22	322	10
23	336	12
24	352	11
25	362	4
26	381	5
27	393	2
28	408	1
29	426	1
30	442	1
31	444	1
32	458	8

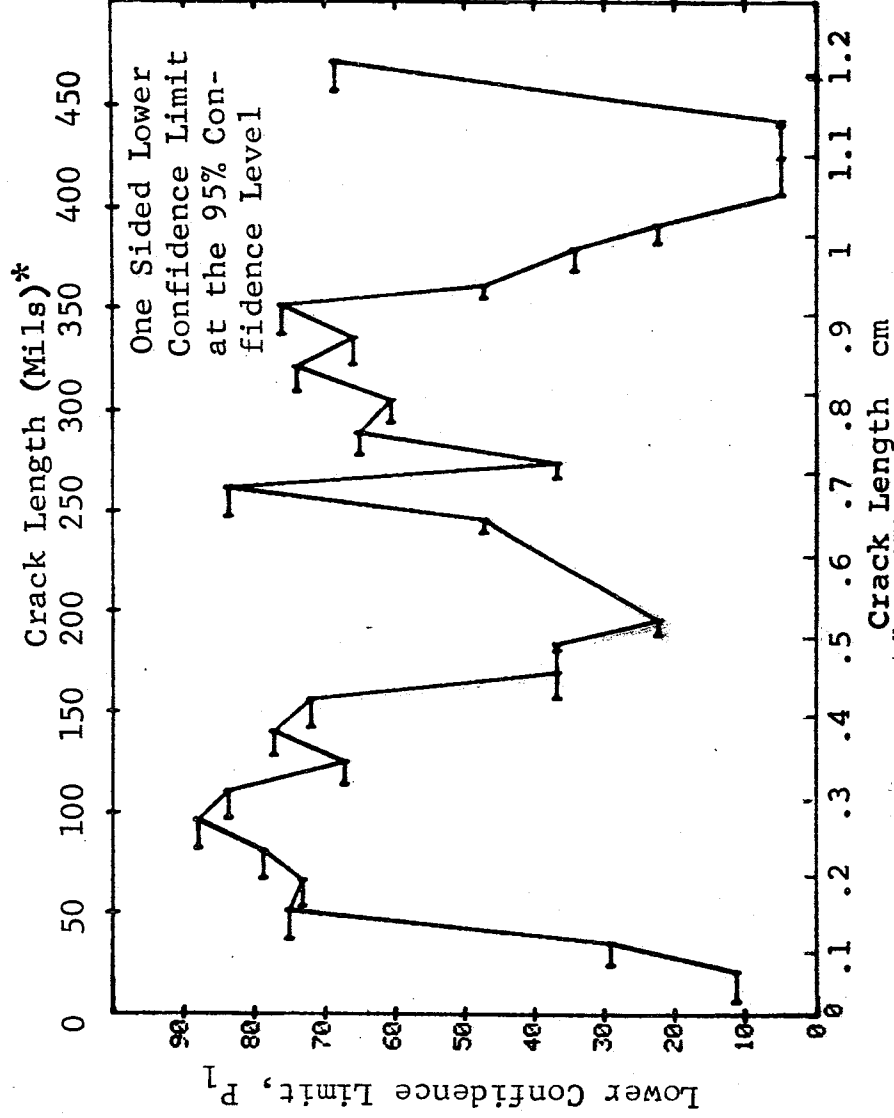


Figure D-14 Probability of Detection for 2219-T87 Al Using Liquid Penetrant. Etched Fatigue Cracks in Flat Plates Measured by Operator H. Lab. Env.

(b) Optimum Probability Method of Data Cumulation

24-JUL-75			PENETRANT		N	TEST 2, (14)		ROCKWELL C		H
RANGE	MIN	LN	MAX	LN		DET	50%	95%	0 MISS	
1		7 *	22 *		13	4	0	11	0	0
2	25		36		18	9	0	29	0	0
3	38		52		23	21	0	75	0	0
4	38		67		69	60	0	78	0	0
5	38		82		122	107	0	81	0	0
6	83		97		38	37	0	88	8	23
7	83		111		55	54	0	91	0	6
8	83		126		72	69	0	89	4	17
9	83		141		91	87	0	90	0	12
10	83		157		106	101	0	90	0	0
11	83		171		109	104	0	90	0	0
12	83		185		112	107	0	90	0	0
13	83		197		114	109	0	90	0	0
14	0		0		0	0	0	0	0	0
15	0		0		0	0	0	0	0	0
16	83		247		118	113	0	91	0	0
17	83		262		135	130	0	92	0	0
18	83		275		138	133	0	92	0	0
19	83		290		145	140	0	92	0	0
20	158		306		45	45	0	93	0	1
21	158		322		55	55	0	94	0	0
22	83		336		173	167	0	93	0	0
23	158		352		78	77	0	94	0	0
24	158		362		82	81	0	94	0	0
25	83		381		193	186	0	93	0	0
26	83		393		195	188	0	93	0	0
27	83		408		196	189	0	93	0	0
28	83		426		197	190	0	93	0	0
29	83		442		198	191	0	93	0	0
30	83		444		199	192	0	93	0	0
31	158		472		101	99	0	93	0	0
32	158		979		160	158	0	96	0	0

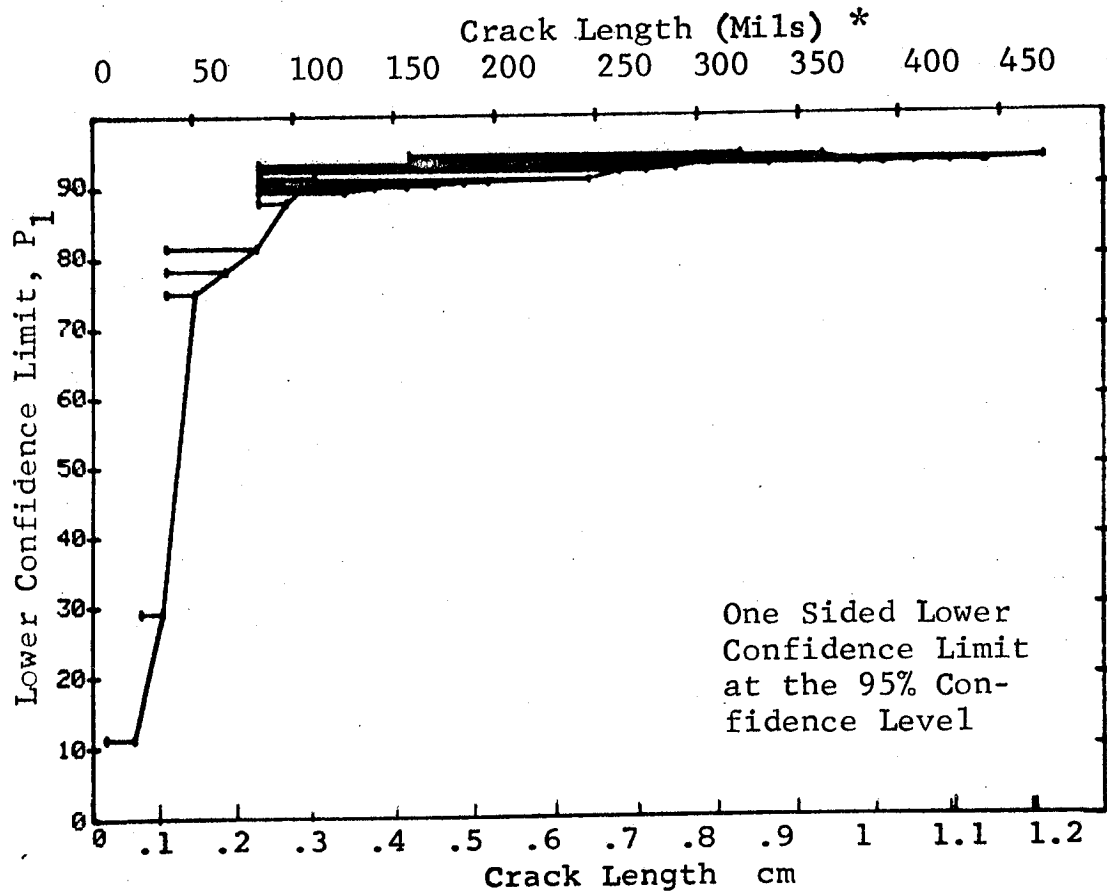


Figure D-14 (Continued)

(c) Overlapping Sixty Point Method of Data Cumulation

24-JUL-75	PENETRANT		TEST 3, (14)		ROCKWELL C		H
RANGE	MIN LN	MAX LN	DET	50%	95%	0 MIN	MISS
1	0 *	0 *	0	0	0	0	0
2	0	0	0	0	0	0	0
3	0	0	0	0	0	0	0
4	0	0	0	0	0	0	0
5	0	0	0	0	0	0	0
6	0	0	0	0	0	0	0
7	0	0	0	0	0	0	0
8	0	0	0	0	0	0	0
9	0	0	0	0	0	0	0
10	0	0	0	0	0	0	0
11	0	0	0	0	0	0	0
12	0	0	0	0	0	0	0
13	0	0	0	0	0	0	0
14	0	0	0	0	0	0	0
15	0	0	0	0	0	0	0
16	0	0	0	0	0	0	0
17	0	0	0	0	0	0	0
18	0	0	0	0	0	0	0
19	0	0	0	0	0	0	0
20	0	0	0	0	0	0	0
21	7	49	31	59	43	0	0
22	30	63	50	82	73	0	0
23	49	69	50	82	73	0	0
24	63	79	54	89	81	56	69
25	70	87	56	92	85	29	43
26	79	105	56	95	85	1	16
27	87	131	58	95	89	29	43
28	105	162	56	92	85	1	16
29	132	275	58	95	89	1	16
30	171	330	59	97	92	0	1
31	279	442	58	95	89	1	16
32	331	500	55	97	92	0	1
			55	97	92	0	1

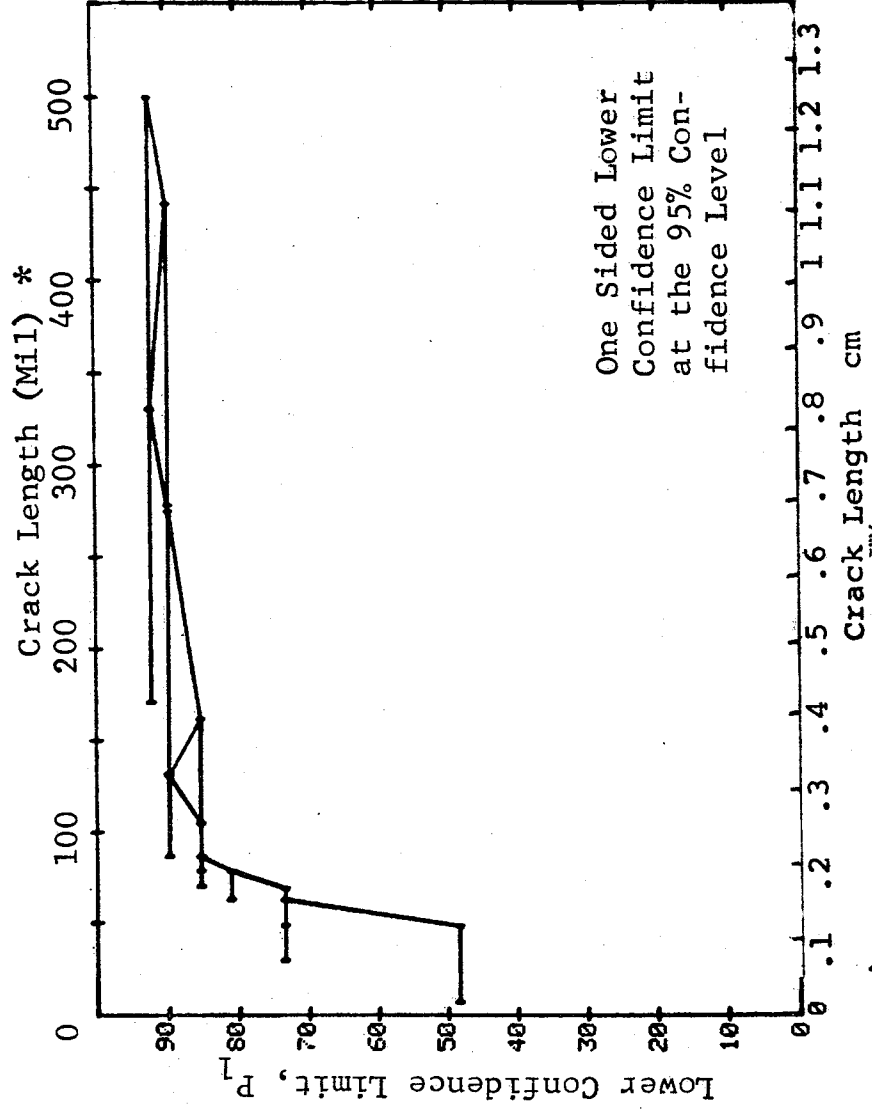


Figure D-14 (Concluded)

REPRODUCIBILITY OF THE
ORIGINAL PAGE IS POOR

(a) Range Interval Method of Data Cumulation

24-JUL-75	RANGE	MIN	LN	PENETRANT	MAX	LN	*
1	25	7	13	0	0	0	0
2	38	25	18	17	17	17	17
3	54	32	23	32	32	32	32
4	68	44	46	44	44	44	44
5	83	68	53	68	68	68	68
6	98	83	39	88	88	88	88
7	115	98	17	111	111	111	111
8	129	115	17	126	126	126	126
9	143	129	19	141	141	141	141
10	158	143	15	171	171	171	171
11	182	158	3	185	185	185	185
12	190	182	3	197	197	197	197
13	0	190	0	0	0	0	0
14	0	0	0	0	0	0	0
15	241	0	4	247	247	247	247
16	248	241	17	262	262	262	262
17	268	248	3	275	275	275	275
18	279	268	7	290	290	290	290
19	295	279	6	306	306	306	306
20	310	295	10	322	322	322	322
21	323	310	12	336	336	336	336
22	338	323	11	352	352	352	352
23	356	338	4	362	362	362	362
24	370	356	5	381	381	381	381
25	384	370	2	393	393	393	393
26	408	384	1	408	408	408	408
27	426	408	1	426	426	426	426
28	442	426	1	442	442	442	442
29	444	442	1	444	444	444	444
30	458	444	1	472	472	472	472
31	474	458	6	979	979	979	979
32		474	59				

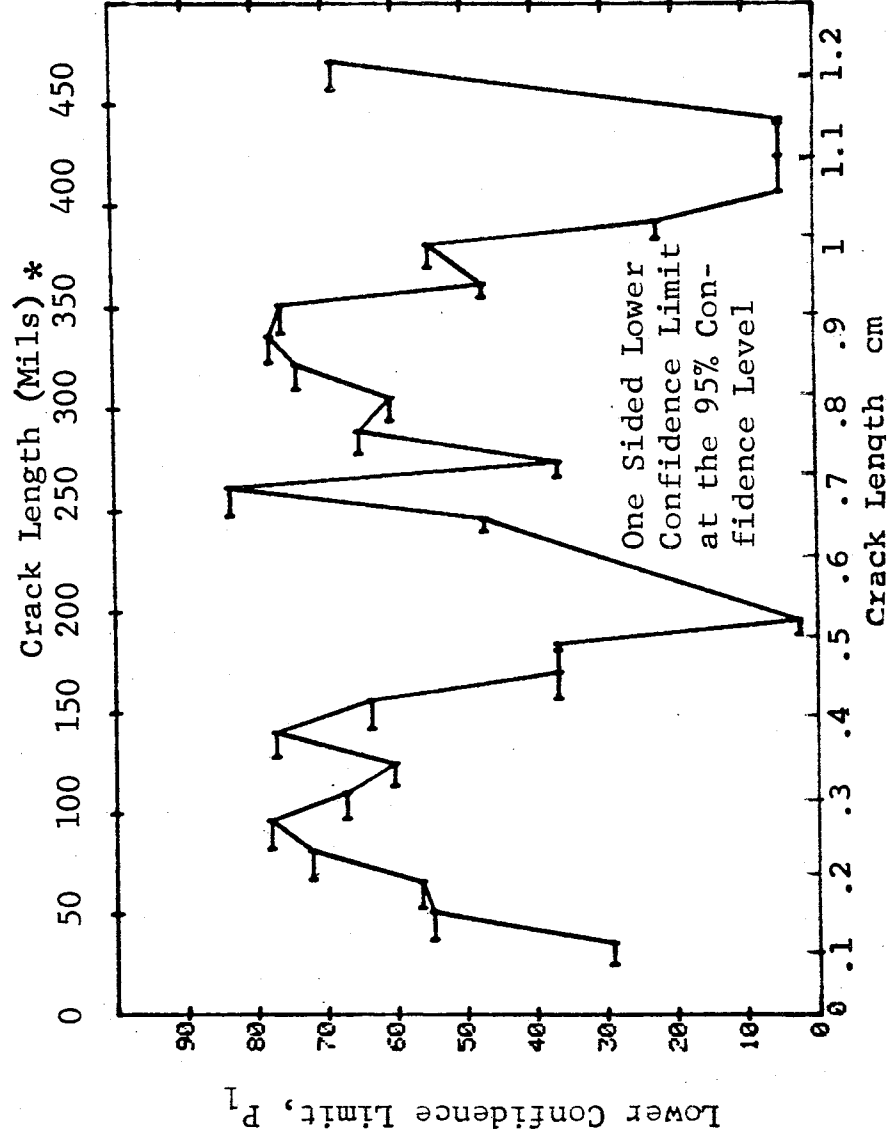


Figure D-15 Probability of Detection for 2219-T87 Al Using Liquid Penetrant. Etched Fatigue Cracks in Flat Plates Measured by Operator I. Lab. Env.

(b) Optimum Probability Method of Data Cumulation

24-JUL-75			PENETRANT		TEST 2, (19)		POCFWELL 50		1, MILS	
RANGE	MIN	LN	MAX	LN	DET	50%	95%	0	0	0
1	2	25	22	7	0	0	0	0	0	0
2	3	38	75	13	0	0	0	0	0	0
3	4	38	52	18	17	0	29	0	0	0
4	5	68	67	23	49	0	54	0	0	0
5	6	68	82	69	44	0	60	0	0	0
6	7	68	97	53	79	0	72	0	0	0
7	8	83	111	92	50	0	73	0	0	0
8	9	68	126	56	108	0	79	0	0	0
9	10	83	141	126	82	0	79	0	0	0
10	11	83	157	92	95	0	82	75	87	0
11	12	83	171	107	98	0	82	0	0	0
12	13	83	185	110	101	0	82	0	0	0
13	14	83	197	113	102	0	82	0	0	0
14	15	0	0	115	0	0	0	0	0	0
15	16	0	0	0	0	0	0	0	0	0
16	17	83	247	119	106	0	83	0	0	0
17	18	241	262	21	21	0	83	0	0	0
18	19	241	275	24	24	0	83	0	0	0
19	20	241	290	31	31	0	90	0	25	0
20	21	241	306	37	37	0	90	0	22	0
21	22	241	322	47	47	0	92	0	15	0
22	23	241	336	59	59	0	93	0	0	0
23	24	241	352	70	70	0	95	0	0	0
24	25	241	362	74	74	0	95	0	0	0
25	26	241	381	79	79	0	96	0	0	0
26	27	241	393	81	81	0	96	0	0	0
27	28	241	408	82	82	0	96	0	0	0
28	29	241	426	83	83	0	96	0	0	0
29	30	241	442	84	84	0	96	0	0	0
30	31	241	444	85	85	0	96	0	0	0
31	32	241	472	93	93	0	96	0	0	0
32		241	979	152	151	0	96	0	0	0

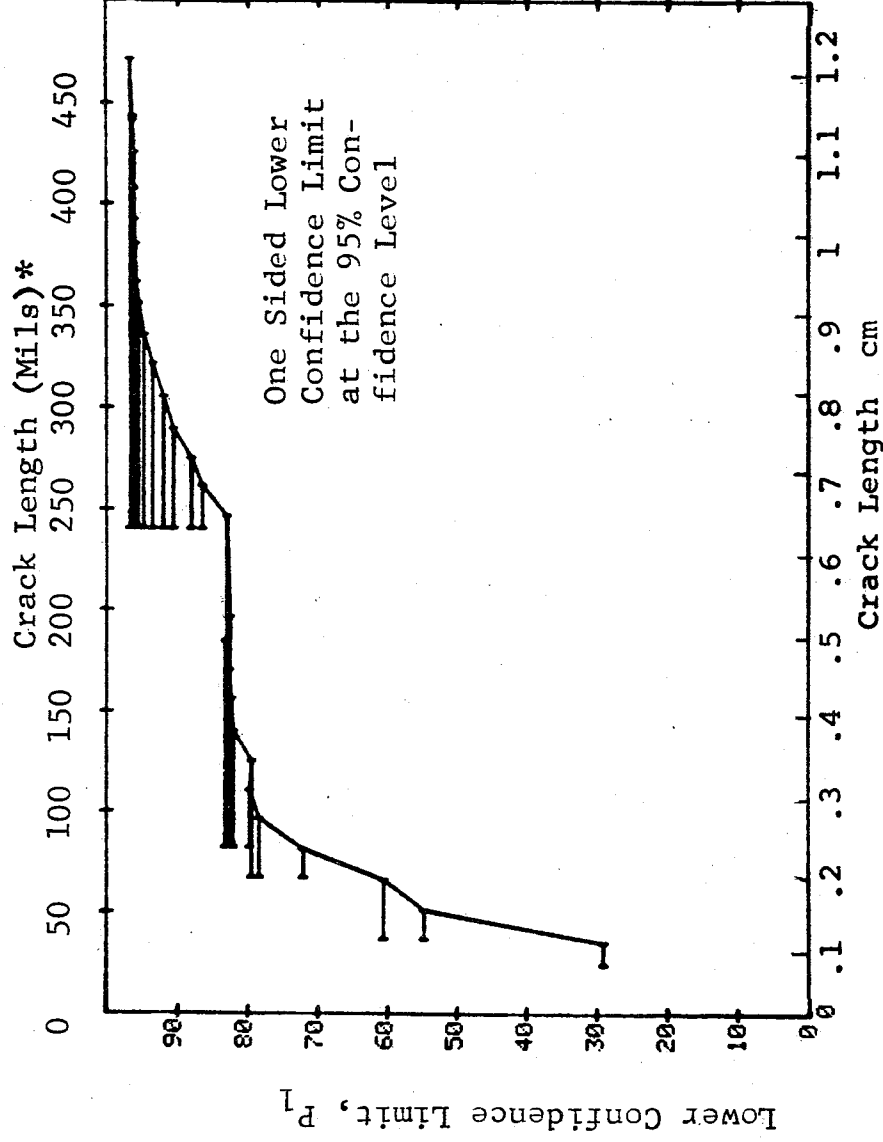


Figure D-15 (Continued)

(c) Overlapping Sixty Point Method of Data Cumulation

24-JUL-75	PENETRANT		TEST 3, (15)		BOCKWELL 541	
RANGE	MIN LN	MAX LN	DET	50%	95%	0 MIN
1	0	0	0	0	0	0
2	0	0	0	0	0	0
3	0	0	0	0	0	0
4	0	0	0	0	0	0
5	0	0	0	0	0	0
6	0	0	0	0	0	0
7	0	0	0	0	0	0
8	0	0	0	0	0	0
9	0	0	0	0	0	0
10	0	0	0	0	0	0
11	0	0	0	0	0	0
12	0	0	0	0	0	0
13	0	0	0	0	0	0
14	0	0	0	0	0	0
15	0	0	0	0	0	0
16	0	0	0	0	0	0
17	0	0	0	0	0	0
18	0	0	0	0	0	0
19	0	0	0	0	0	0
20	0	0	0	0	0	0
21	7	49	0	0	0	0
22	31	63	25	47	36	69
23	51	70	42	69	58	58
24	64	79	43	70	60	65
25	70	87	46	75	65	73
26	79	105	50	82	79	79
27	88	131	53	87	81	69
28	105	162	54	88	85	69
29	132	275	55	92	92	43
30	171	330	59	97	92	1
31	279	442	59	98	92	0
32	331	500	59	97	92	0

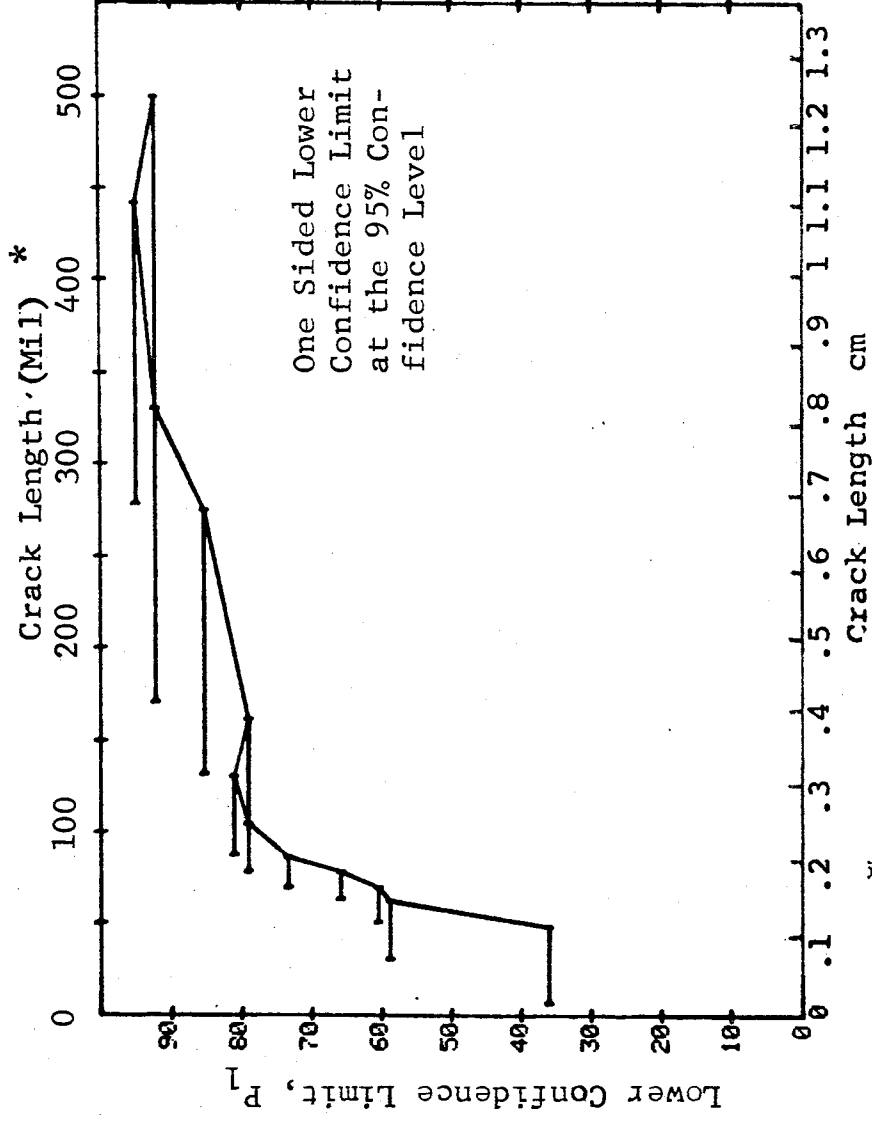


Figure D-15 (Concluded)

(a) Range Interval Method of Data Cumulation

24-JUL-75	PENETRANT		TEST 1, (16)		POINTWELL 50 J	
RANGE	MIN LN	*MAX LN *	DET	50%	95%	99%
1	7	23	3	20	6	0
2	23	38	6	30	15	0
3	38	54	9	37	22	0
4	54	68	29	61	43	0
5	68	83	36	66	55	0
6	83	98	30	75	63	0
7	98	111	16	84	75	44
8	111	126	15	86	67	0
9	126	141	17	86	70	0
10	141	157	13	82	63	0
11	157	171	3	79	36	0
12	171	185	3	79	36	0
13	185	197	1	29	0	0
14	197	0	0	0	0	0
15	0	0	0	0	0	0
16	0	247	0	84	42	0
17	247	262	4	86	83	29
18	262	275	7	79	36	0
19	275	290	6	89	60	0
20	290	306	9	83	60	0
21	306	322	12	84	60	34
22	322	336	10	85	77	0
23	336	352	4	84	47	0
24	352	362	5	87	54	0
25	362	381	2	70	22	0
26	381	393	1	50	5	0
27	393	408	1	50	5	0
28	408	426	1	50	5	0
29	426	442	1	50	5	0
30	442	444	1	50	5	0
31	444	458	3	91	68	0
32	458	474	59	97	92	1

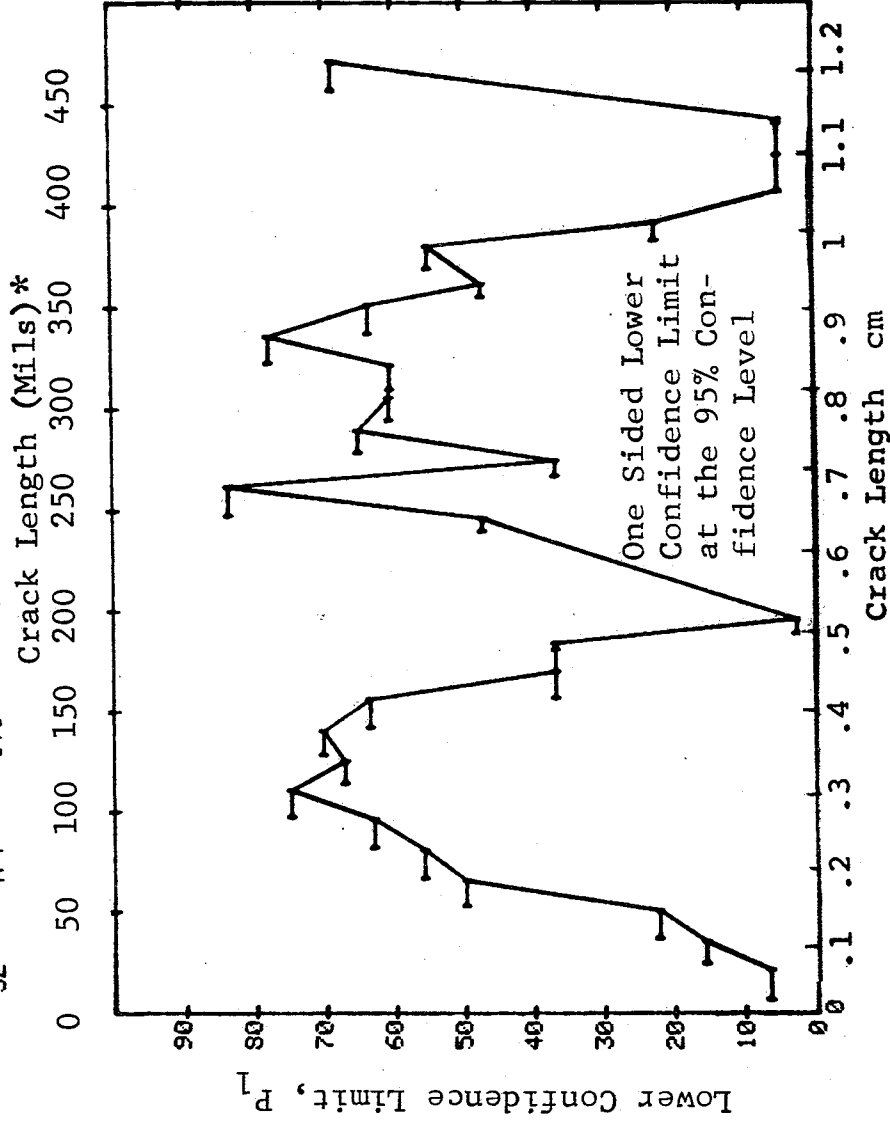


Figure D-16 Probability of Detection for 2219-T87 Al Using Liquid Penetrant. Etched Fatigue Cracks in Flat Plates Measured by Operator J D-48 Lab. Env.

(b) Optimum Probability Method of Data Cumulation

24-JUL-75		PENETRANT		N	TEST 2, (16)		ROCKWELL		J
RANGE	MIN LN	* MAX LN			DET	50%	95%	0 MIL	
1	7	22*	13	3	0	0	0	0	0
2	7	16	81	9	0	0	16	0	0
3	25	52	41	15	0	0	24	0	0
4	54	67	46	29	0	0	49	0	0
5	54	82	99	65	0	0	57	0	0
6	83	97	39	30	0	0	63	0	0
7	98	111	17	16	0	0	75	0	0
8	98	126	34	31	0	0	78	0	0
9	98	141	53	48	0	0	81	50	10
10	98	157	68	61	0	0	81	61	11
11	98	171	71	64	0	0	82	58	11
12	98	185	74	67	0	0	82	55	11
13	98	197	76	68	0	0	81	66	11
14	0	0	0	0	0	0	0	0	0
15	0	0	0	0	0	0	0	0	0
16	98	247	80	72	0	0	82	62	14
17	241	262	21	21	0	0	86	3	25
18	241	275	24	24	0	0	88	5	20
19	241	290	31	31	0	0	90	0	15
20	241	306	37	37	0	0	92	0	9
21	241	322	47	46	0	0	90	0	14
22	241	336	59	58	0	0	92	0	2
23	241	352	70	68	0	0	91	0	6
24	241	362	74	72	0	0	91	0	2
25	241	381	79	77	0	0	92	0	0
26	241	393	81	79	0	0	92	0	0
27	241	408	82	80	0	0	92	0	0
28	241	426	83	81	0	0	92	0	0
29	241	442	84	82	0	0	92	0	0
30	241	444	85	83	0	0	92	0	0
31	241	472	93	91	0	0	93	0	0
32	241	979	153	150	0	0	95	0	0

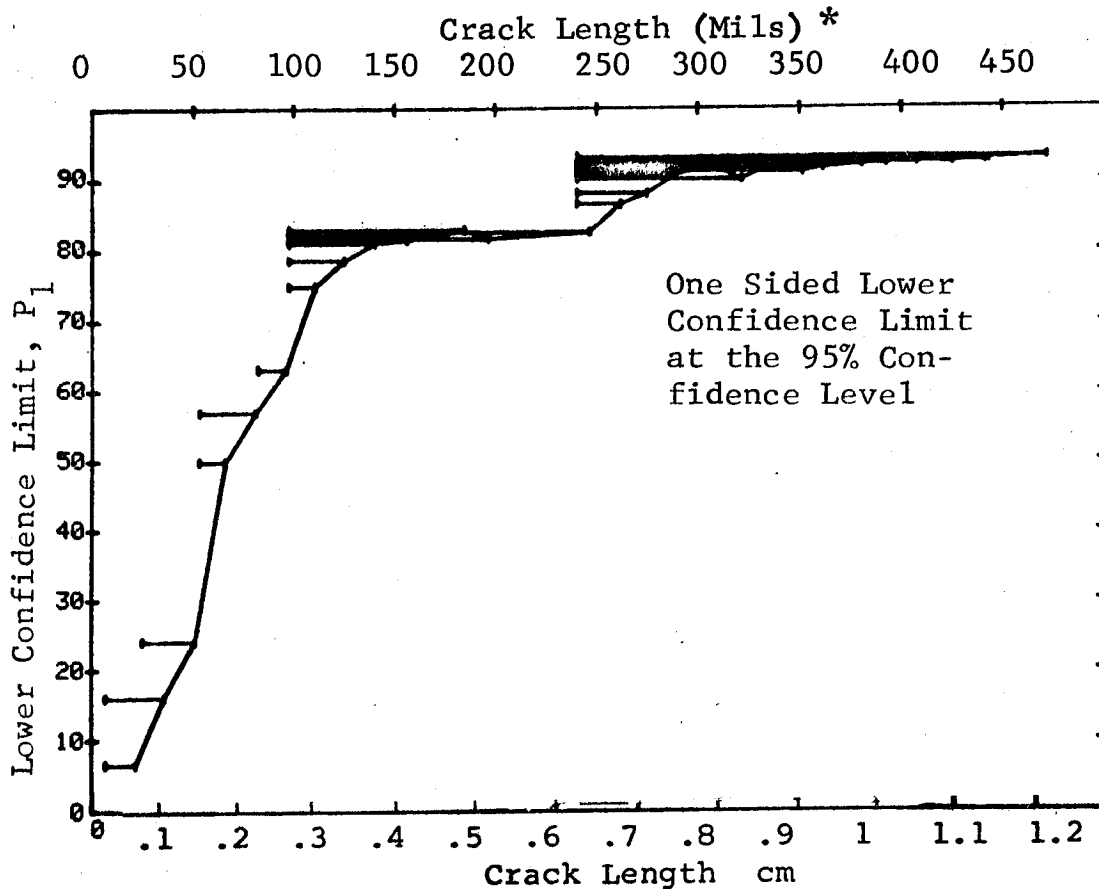


Figure D-18 (Continued)

(c) Overlapping Sixty Point Method of Data Cumulation

24-JUL-75			PENETRANT			N	TEST 3, (16)			ROCKWELL SC J		
RANGE	MIN	LN	* MAX	LN	*		DET	50%	95%	0 MISS	1 MISS	
1	0	0	0	0		0	0	0	0	0	0	
2	0	0	0	0		0	0	0	0	0	0	
3	0	0	0	0		0	0	0	0	0	0	
4	0	0	0	0		0	0	0	0	0	0	
5	0	0	0	0		0	0	0	0	0	0	
6	0	0	0	0		0	0	0	0	0	0	
7	0	0	0	0		0	0	0	0	0	0	
8	0	0	0	0		0	0	0	0	0	0	
9	0	0	0	0		0	0	0	0	0	0	
10	0	0	0	0		0	0	0	0	0	0	
11	0	0	0	0		0	0	0	0	0	0	
12	0	0	0	0		0	0	0	0	0	0	
13	0	0	0	0		0	0	0	0	0	0	
14	0	0	0	0		0	0	0	0	0	0	
15	0	0	0	0		0	0	0	0	0	0	
16	0	0	0	0		0	0	0	0	0	0	
17	0	0	0	0		0	0	0	0	0	0	
18	0	0	0	0		0	0	0	0	0	0	
19	0	0	0	0		0	0	0	0	0	0	
20	0	0	0	0		0	0	0	0	0	0	
21	7		49			52	16	29	20	0	0	
22	31		63			60	29	47	37	0	0	
23	51		70			60	37	60	50	0	0	
24	64		79			60	42	69	58	0	0	
25	70		87			60	40	65	55	0	0	
26	79		105			60	45	74	64	0	0	
27	88		131			60	57	93	87	16	29	
28	105		162			60	54	88	81	56	69	
29	132		275			60	55	90	83	43	56	
30	171		330			60	58	95	89	1	16	
31	279		442			60	58	95	89	1	16	
32	331		500			60	58	95	89	1	16	

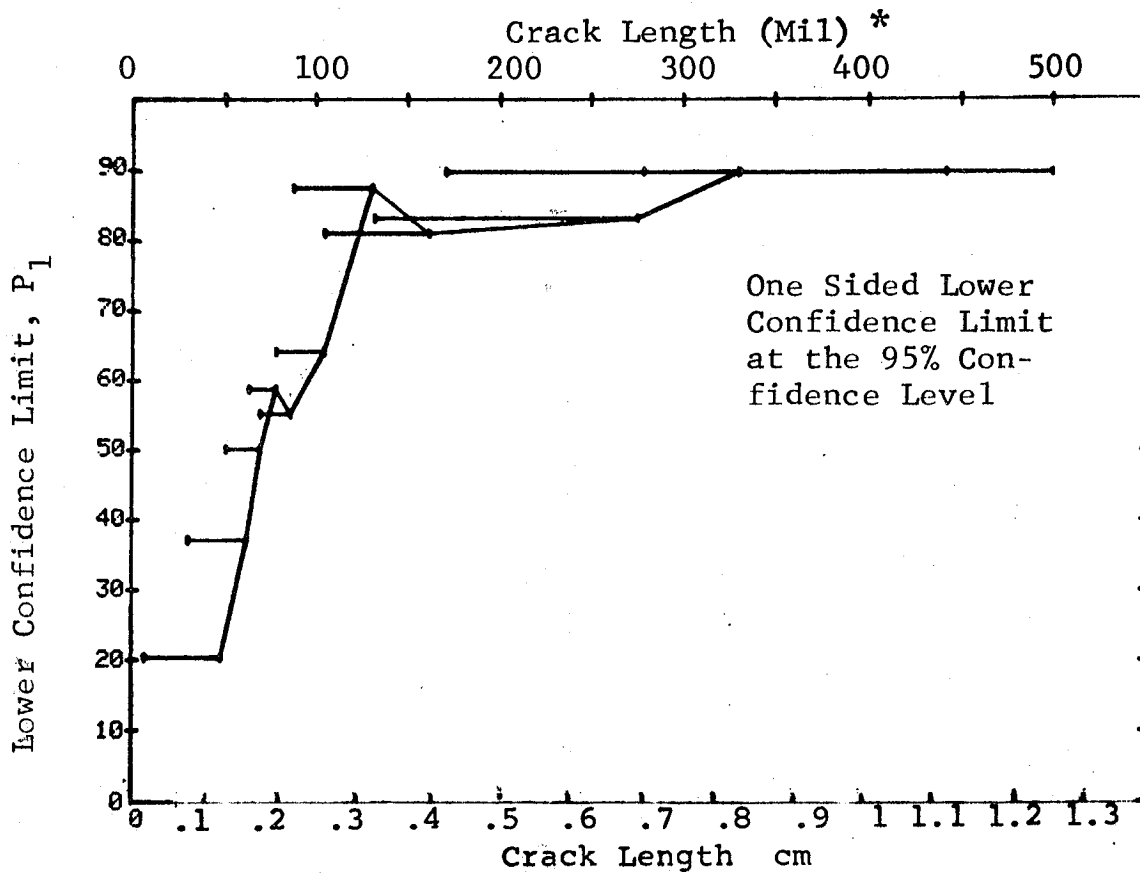


Figure D-16 (Concluded)

(a) Range Interval Method of Data Cumulation

24-JUL-75	PENETRANT		TEST 1, (17)		ROCKWELL SC		K	
RANGE	MIN LN	MAX LN	DET	50%	0	0	0	0
1	25	36	3	20	6	0	0	0
2	38	52	9	47	29	0	0	0
3	54	67	16	67	50	0	0	0
4	68	82	37	79	58	0	0	0
5	83	97	46	84	74	0	0	0
6	98	111	37	93	84	22	37	29
7	115	126	17	96	83	12	22	24
8	129	141	16	90	75	28	44	27
9	143	157	19	96	81	10	27	21
10	158	171	15	95	81	14	27	21
11	182	195	3	79	36	0	0	0
12	190	197	3	79	36	0	0	0
13	0	0	2	70	2	0	0	0
14	0	0	0	0	0	0	0	0
15	0	0	0	0	0	0	0	0
16	241	247	0	84	47	0	0	0
17	248	262	4	96	85	12	29	29
18	268	275	17	79	36	0	0	0
19	279	290	3	90	65	0	0	0
20	295	306	6	89	60	0	0	0
21	310	322	10	93	74	17	34	34
22	323	336	12	94	77	18	35	35
23	338	352	11	93	76	0	0	0
24	356	362	4	84	47	0	0	0
25	370	381	5	87	54	0	0	0
26	384	393	2	70	22	0	0	0
27	408	408	1	50	5	0	0	0
28	426	426	1	50	5	0	0	0
29	442	442	1	50	5	0	0	0
30	444	444	1	50	5	0	0	0
31	458	472	8	91	68	0	0	0
32	474	479	59	98	95	0	0	0

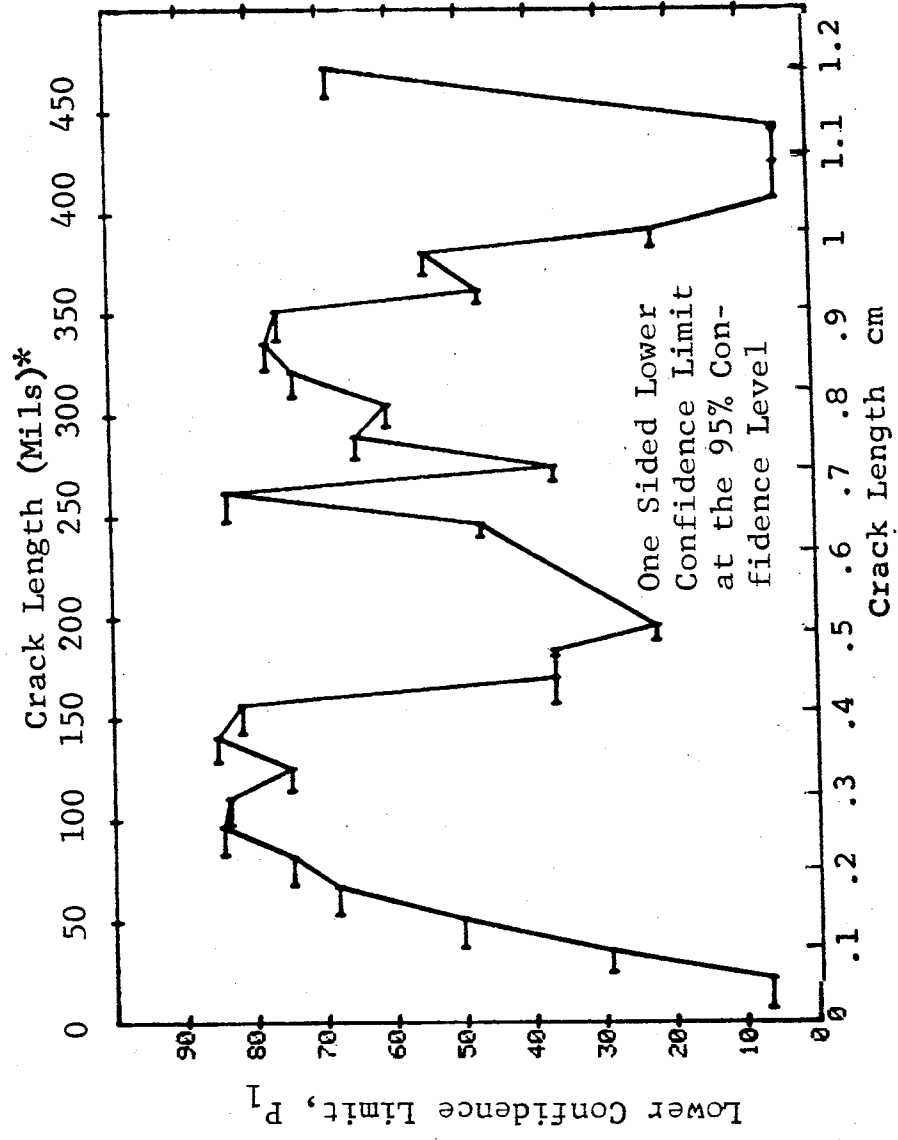


Figure D-17 Probability of Detection for 2219-T8/ Al Using Liquid Penetrant. Etched Fatigue Cracks in Flat Plates Measured by Operator K Lab. Env.

(b) Optimum Probability Method of Data Cumulation

24-JUL-75 RANGE	MIN	LN	7	MAX	LN	*	N	TEST 2, DET	50%	(17) 95%	ROCKWELL 0 MISS	50 K 1 MISS
1	1	25	38	32	35	13	18	3	0	6	0	0
2	2	38	54	52	52	18	23	9	0	29	0	0
3	3	54	54	67	67	23	46	16	0	50	0	0
4	4	54	83	82	82	46	100	37	0	68	0	0
5	5	83	83	97	97	100	39	83	0	75	0	0
6	6	83	83	111	111	39	56	37	0	84	22	37
7	7	83	83	126	126	56	73	54	0	89	3	30
8	8	83	83	141	141	73	92	70	0	89	3	16
9	9	98	98	157	157	92	68	89	0	91	0	0
10	10	98	98	171	171	68	73	67	0	93	0	0
11	11	98	98	185	185	73	71	70	0	93	0	0
12	12	98	98	197	197	71	74	73	0	93	0	0
13	13	0	0	0	0	74	76	75	0	93	0	0
14	14	0	0	0	0	76	0	0	0	0	0	0
15	15	0	0	0	0	0	0	0	0	0	0	0
16	16	98	98	247	247	0	80	0	0	0	0	0
17	17	129	129	262	262	80	63	79	0	94	0	0
18	18	129	129	275	275	63	66	63	0	95	0	0
19	19	129	129	290	290	66	73	66	0	95	0	0
20	20	129	129	306	306	73	79	73	0	95	0	0
21	21	129	129	322	322	79	89	79	0	96	0	0
22	22	129	129	336	336	89	101	89	0	97	0	0
23	23	129	129	352	352	101	112	101	0	97	0	0
24	24	129	129	362	362	112	116	112	0	97	0	0
25	25	129	129	381	381	116	121	116	0	97	0	0
26	26	129	129	393	393	121	123	121	0	97	0	0
27	27	129	129	408	408	123	124	123	0	97	0	0
28	28	129	129	426	426	124	125	124	0	97	0	0
29	29	129	129	442	442	125	126	125	0	97	0	0
30	30	129	129	444	444	126	127	126	0	97	0	0
31	31	129	129	472	472	127	135	127	0	97	0	0
32	32	129	129	979	979	135	194	135	0	97	0	0
		129	129			194		194		98		0

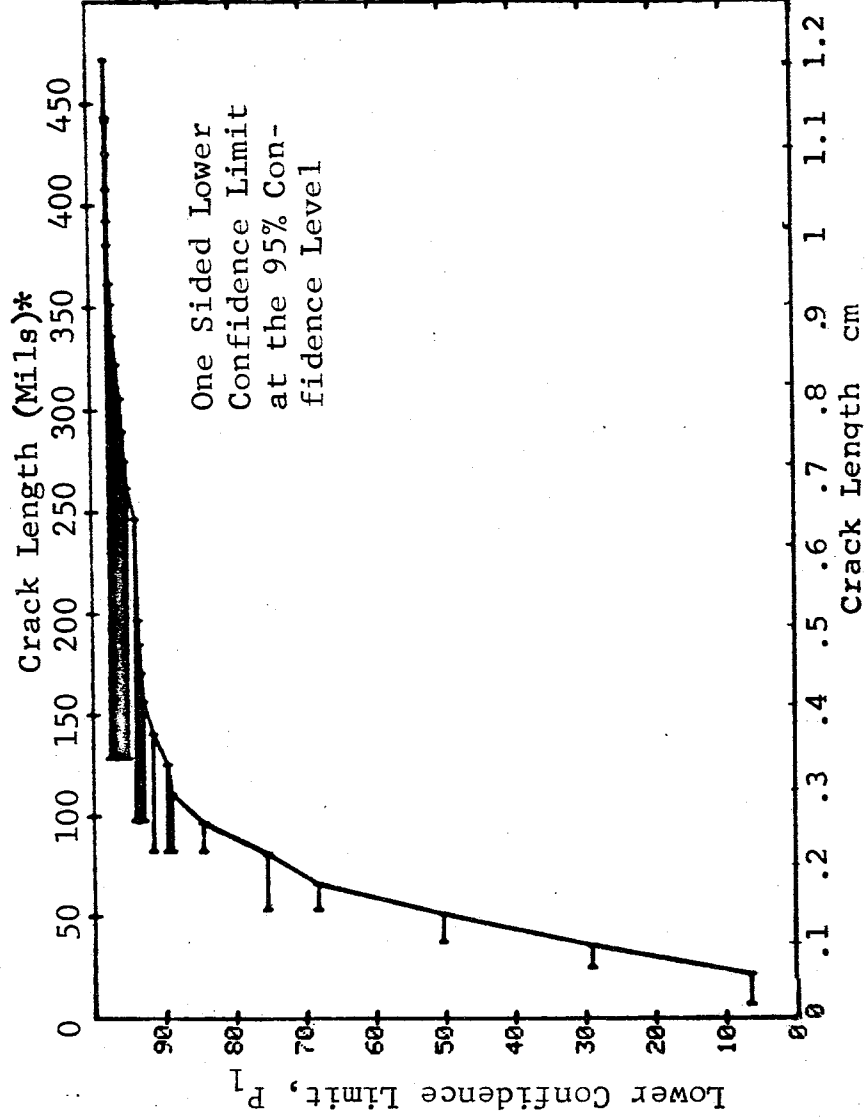


Figure D-17 (Continued) for A1 for Opera

(c) Overlapping Sixty Point Method of Data Cumulation

24-UL-75 RANGE	MIN LN	PENETRANT MAX LN	N	TEST 3, (17) DET	50%	95%	ROCKWELL C	MISS	K
1	0	0	0	0	0	0	0	0	0
2	0	0	0	0	0	0	0	0	0
3	0	0	0	0	0	0	0	0	0
4	0	0	0	0	0	0	0	0	0
5	0	0	0	0	0	0	0	0	0
6	0	0	0	0	0	0	0	0	0
7	0	0	0	0	0	0	0	0	0
8	0	0	0	0	0	0	0	0	0
9	0	0	0	0	0	0	0	0	0
10	0	0	0	0	0	0	0	0	0
11	0	0	0	0	0	0	0	0	0
12	0	0	0	0	0	0	0	0	0
13	0	0	0	0	0	0	0	0	0
14	0	0	0	0	0	0	0	0	0
15	0	0	0	0	0	0	0	0	0
16	0	0	0	0	0	0	0	0	0
17	0	0	0	0	0	0	0	0	0
18	0	0	0	0	0	0	0	0	0
19	0	0	0	0	0	0	0	0	0
20	0	0	0	0	0	0	0	0	0
21	7	51	0	27	50	78	0	0	0
22	32	64	53	45	74	64	0	0	0
23	52	70	60	47	77	67	0	0	0
24	64	79	60	51	83	75	0	0	0
25	70	87	60	54	88	81	94	56	100
26	79	105	60	56	92	85	29	43	69
27	88	131	60	59	97	92	0	1	1
28	105	162	60	59	97	92	0	0	0
29	132	275	60	60	98	95	0	0	0
30	171	330	60	60	98	95	0	0	0
31	279	442	60	60	98	95	0	0	0
32	331	500	60	60	98	95	0	0	0

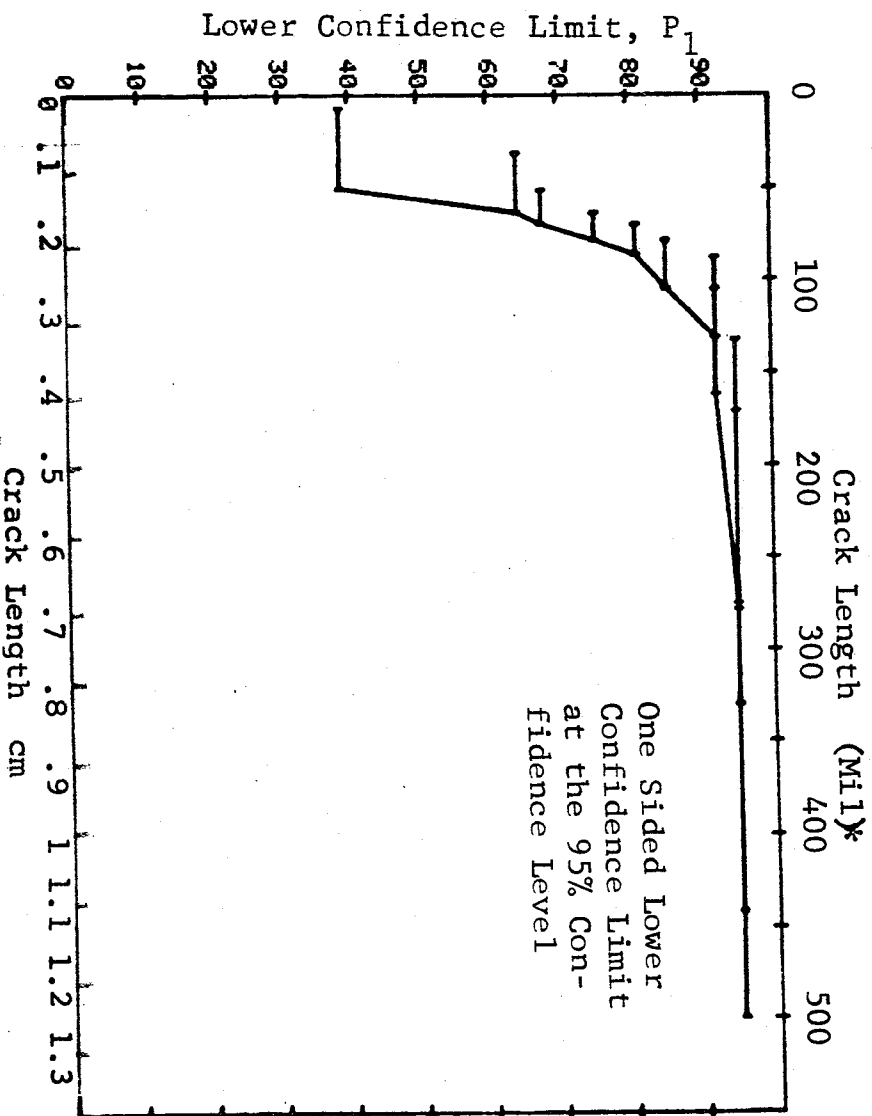


Figure D-17 (Concluded)

(a) Range Interval Method of Data Cumulation

24-JUL-75		PENETRANT		TEST 1, (18)		ROCKWELL SC	
RANGE	MIN LN *	MAX LN	DET	50%	95%	MISS	L
1	25	32	3	20	6	0	0
2	38	36	13	69	50	0	0
3	54	52	15	62	45	0	0
4	68	67	34	72	61	0	0
5	83	82	46	85	76	76	89
6	98	97	34	85	74	0	0
7	111	111	15	84	67	0	0
8	115	126	15	84	67	0	0
9	129	141	15	75	58	0	0
10	143	157	11	69	48	0	0
11	158	171	3	79	36	0	0
12	182	185	3	79	36	0	0
13	190	197	1	29	2	0	0
14	0	0	0	0	0	0	0
15	0	0	0	0	0	0	0
16	241	247	4	84	47	12	29
17	248	262	17	96	83	0	0
18	268	275	3	79	65	0	0
19	279	290	7	90	41	0	0
20	295	306	5	73	74	0	0
21	310	322	10	93	66	0	0
22	323	336	11	86	34	0	0
23	338	352	11	77	47	0	0
24	356	362	4	84	47	0	0
25	370	381	2	31	7	0	0
26	384	393	1	29	2	0	0
27	408	408	1	50	5	0	0
28	426	426	1	50	0	0	0
29	442	442	0	0	0	0	0
30	444	444	1	50	0	0	0
31	458	472	1	67	40	0	0
32	474	979	54	90	83	44	57

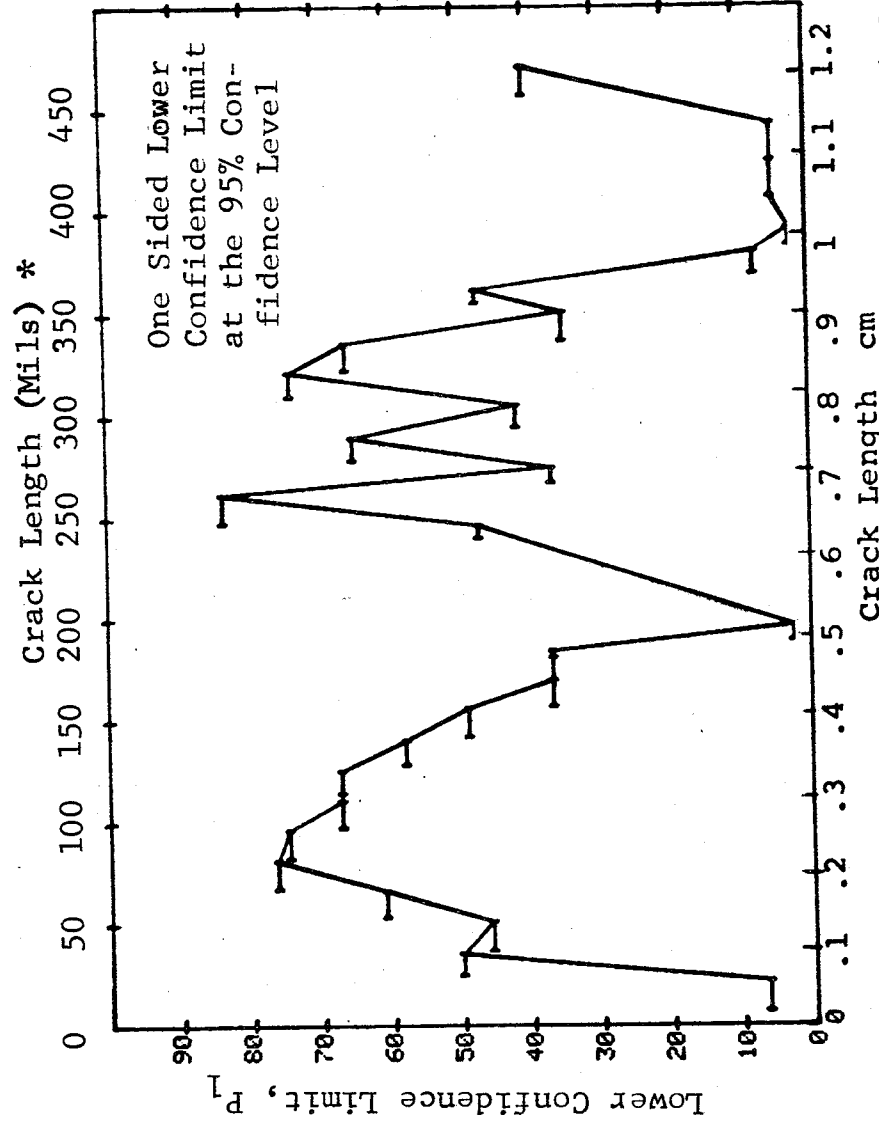


Figure D-18 Probability of Detection for 2219-T87 Al Using Liquid Penetrant. Etched Fatigue Cracks in Flat Plates Measured by Operator L. Lab. Env.

(b) Optimum Probability Method of Data Cumulation

24-JUL-75 RANGE	MIN LN	PENETRANT MAX LN *	N	TEST 27 (18) DET	50%	95%	POCKWELL MISS	L MISS
1	25	22 *	13	3	0	6	0	0
2	25	26	18	13	0	50	0	0
3	25	32	41	28	0	54	0	0
4	25	67	87	62	0	76	0	0
5	68	82	53	46	0	79	0	0
6	68	97	92	80	0	79	0	0
7	68	111	109	95	0	80	0	0
8	68	126	126	110	0	81	0	0
9	68	141	145	125	0	80	0	0
10	68	157	160	136	0	79	0	0
11	68	171	163	139	0	79	0	0
12	68	185	166	142	0	80	0	0
13	68	197	168	143	0	79	0	0
14	0	0	0	0	0	0	0	0
15	0	0	0	0	0	0	0	0
16	68	247	172	147	0	80	0	0
17	241	262	21	21	0	86	3	25
18	241	275	24	24	0	88	5	23
19	241	290	31	31	0	90	0	15
20	241	306	37	36	0	97	0	24
21	241	322	47	46	0	90	0	14
22	241	336	59	57	0	99	2	12
23	241	352	70	64	0	83	46	59
24	241	362	74	68	0	82	42	55
25	68	381	247	213	0	81	0	0
26	68	393	249	214	0	81	0	0
27	68	408	250	215	0	81	0	0
28	68	426	251	216	0	81	0	0
29	68	442	252	216	0	81	0	0
30	68	444	253	217	0	81	0	0
31	68	472	261	223	0	81	0	0
32	159	979	164	141	0	83	0	0

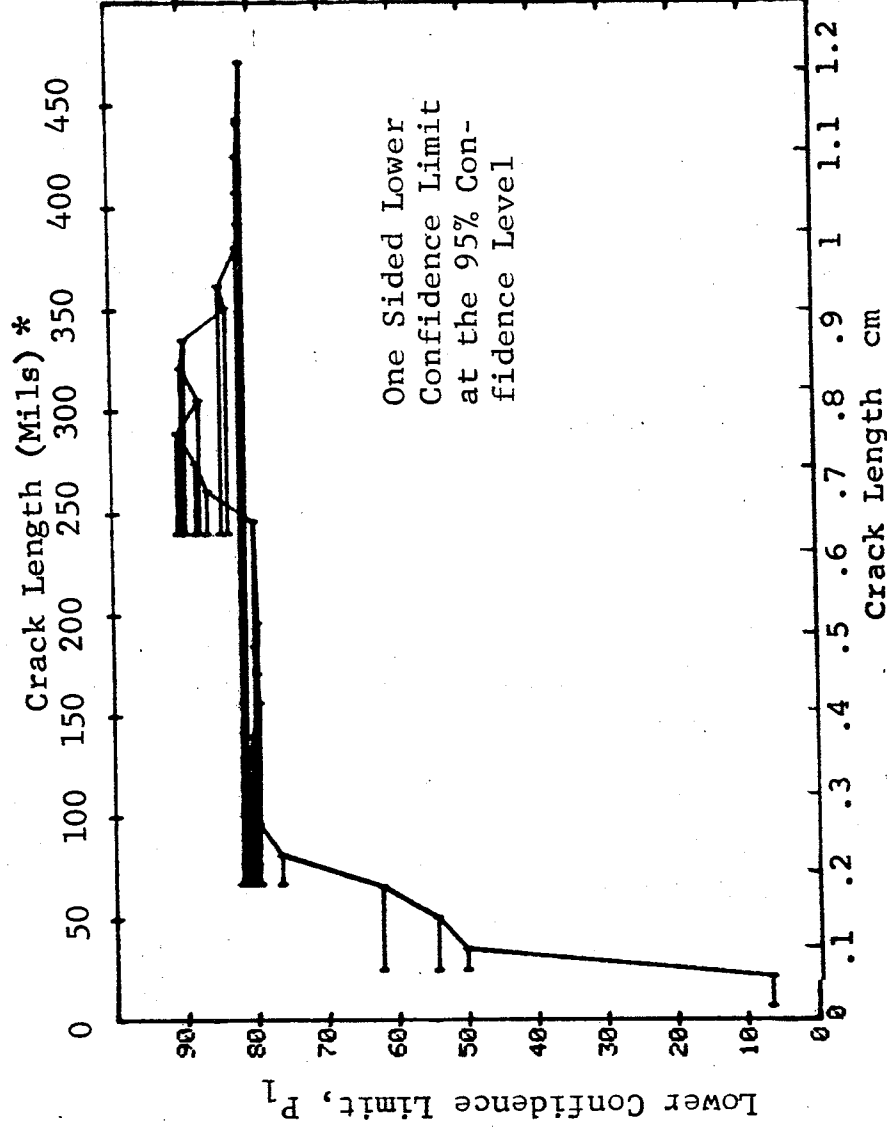


Figure D-18 (Continued)

(c) Overlapping Sixty Point Method of Data Cumulation

24-JUL-75		PENETRANT		N	TEST 3, (18)		ROCKWELL 90 L		
RANGE	MIN LN	MAX LN	*		DET	50%	95%	0 MISS	1 MISS
1	0	0	*	0	0	0	0	0	0
2	0	0		0	0	0	0	0	0
3	0	0		0	0	0	0	0	0
4	0	0		0	0	0	0	0	0
5	0	0		0	0	0	0	0	0
6	0	0		0	0	0	0	0	0
7	0	0		0	0	0	0	0	0
8	0	0		0	0	0	0	0	0
9	0	0		0	0	0	0	0	0
10	0	0		0	0	0	0	0	0
11	0	0		0	0	0	0	0	0
12	0	0		0	0	0	0	0	0
13	0	0		0	0	0	0	0	0
14	0	0		0	0	0	0	0	0
15	0	0		0	0	0	0	0	0
16	0	0		0	0	0	0	0	0
17	0	0		0	0	0	0	0	0
18	0	0		0	0	0	0	0	0
19	0	0		0	0	0	0	0	0
20	0	0		0	0	0	0	0	0
21	7	49		52	30	56	45	0	0
22	31	63		60	44	72	62	0	0
23	51	70		60	43	70	60	0	0
24	64	79		60	47	77	67	0	0
25	70	87		60	55	90	83	43	56
26	79	105		60	53	87	79	69	82
27	88	131		60	52	85	77	82	94
28	105	162		60	49	80	71	0	0
29	132	275		60	52	85	77	0	94
30	171	330		60	58	95	89	1	16
31	279	442		60	49	80	71	0	0
32	331	500		60	46	75	65	0	0

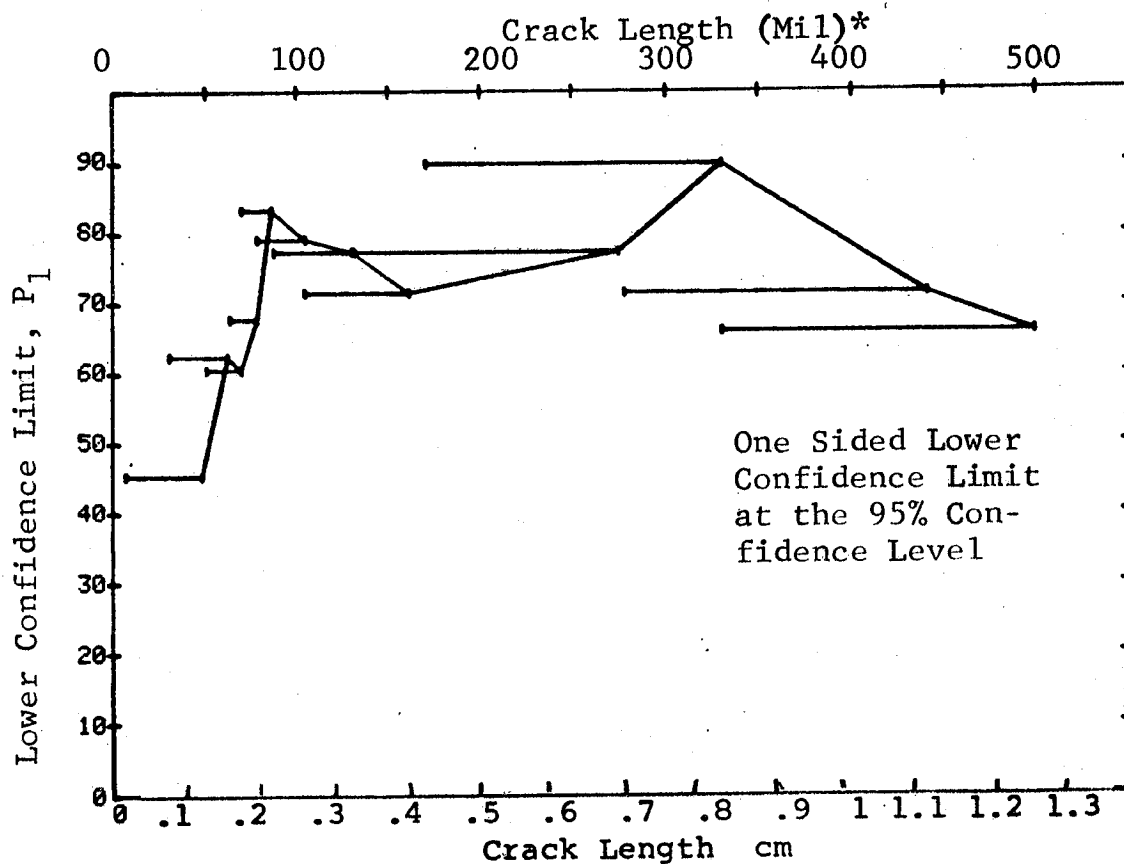


Figure D-18 (Concluded)

REPRODUCIBILITY OF THE
ORIGINAL PAGE IS POOR

(a) Range Interval Method of Data Cumulation

18-SEP-75	RANGE	MIN	LN *	LN *	MAX	LN *	PENETRANT
1	1	10	41	103	134	162	197
2	2	10	42	103	134	162	197
3	3	10	42	103	134	162	197
4	4	10	42	103	134	162	197
5	5	10	42	103	134	162	197
6	6	10	42	103	134	162	197
7	7	10	42	103	134	162	197
8	8	10	42	103	134	162	197
9	9	10	42	103	134	162	197
10	10	10	42	103	134	162	197
11	11	10	42	103	134	162	197
12	12	10	42	103	134	162	197
13	13	10	42	103	134	162	197
14	14	10	42	103	134	162	197
15	15	10	42	103	134	162	197
16	16	10	42	103	134	162	197
17	17	10	42	103	134	162	197
18	18	10	42	103	134	162	197
19	19	10	42	103	134	162	197
20	20	10	42	103	134	162	197
21	21	10	42	103	134	162	197
22	22	10	42	103	134	162	197
23	23	10	42	103	134	162	197
24	24	10	42	103	134	162	197
25	25	10	42	103	134	162	197
26	26	10	42	103	134	162	197
27	27	10	42	103	134	162	197
28	28	10	42	103	134	162	197
29	29	10	42	103	134	162	197
30	30	10	42	103	134	162	197
31	31	10	42	103	134	162	197
32	32	10	42	103	134	162	197

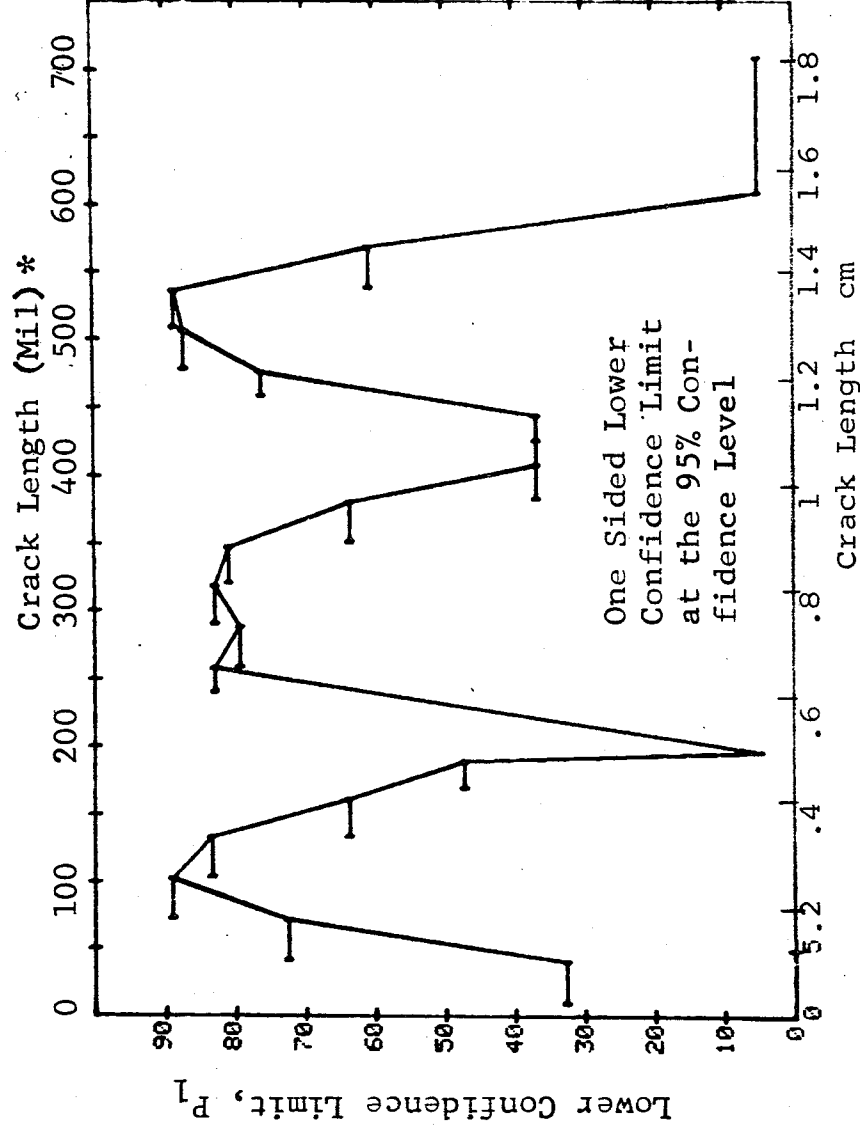


Figure D-19 Probability of Detection for 2219-T87 A1 Using Liquid Penetrant. Etched Fatigue Cracks in Flat Plates Measured by Operator M. Lab. Env.

(b) Optimum Probability Method of Data Cumulation

18-SEP-75	PENETRANT			P-2, (19)		M	95% MISE	
RANGE	MIN	LN	MAX LN	N	DET	50%	95%	0 MISE
1	10	*	41	36	17	0	32	0
2	42		72	60	65	0	72	0
3	73		103	82	78	0	89	0
4	73		134	118	112	0	90	0
5	73		162	144	133	0	87	0
6	73		190	148	137	0	87	0
7	73		197	149	138	0	88	0
8	73		258	165	154	0	89	0
9	171		288	34	34	0	91	12
10	171		318	50	50	0	94	0
11	171		347	73	72	0	93	0
12	171		381	84	82	0	92	0
13	171		408	87	85	0	92	0
14	171		444	90	88	0	93	0
15	171		475	101	99	0	93	0
16	171		506	123	121	0	94	0
17	171		535	148	146	0	95	0
18	171		568	154	152	0	95	0
19	0		0	0	0	0	0	0
20	171		610	155	153	0	95	0
21	0		0	0	0	0	0	0
22	0		0	0	0	0	0	0
23	171		710	156	154	0	96	0
24	0		0	0	0	0	0	0
25	0		0	0	0	0	0	0
26	0		0	0	0	0	0	0
27	0		0	0	0	0	0	0
28	0		0	0	0	0	0	0
29	0		0	0	0	0	0	0
30	0		0	0	0	0	0	0
31	0		0	0	0	0	0	0
32	171		979	157	155	0	96	0

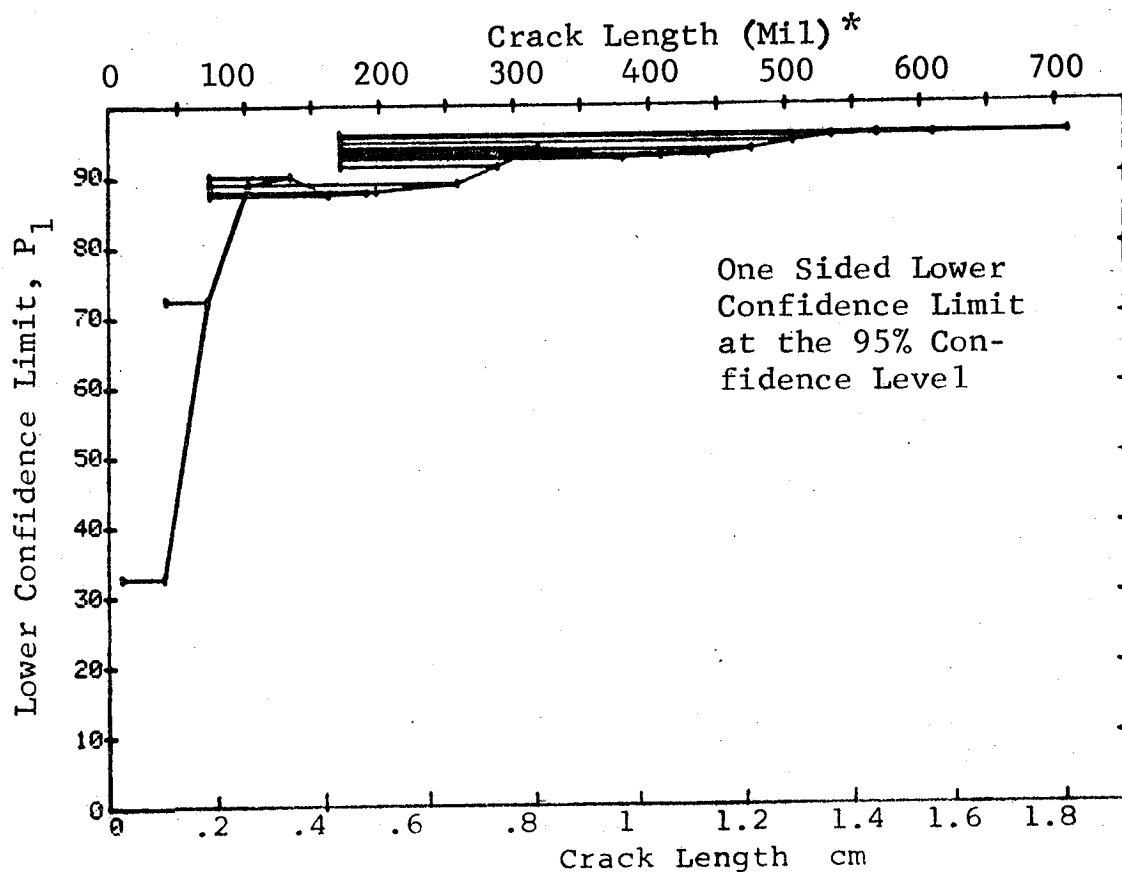


Figure D-19 (Continued) for Δ^1

REPRODUCIBILITY OF THE ORIGINAL PAGE IS POOR

(c) Overlapping Sixty Point Method of Data Cumulation

18-SEP-75	PENETRANT		P-7 (19)	M		
RANGE MIN	LN	MAX LH	DET	50%	95%	0.01
1	0 *	0 *	0	0	0	0
2	0	0	0	0	0	0
3	0	0	0	0	0	0
4	0	0	0	0	0	0
5	0	0	0	0	0	0
6	0	0	0	0	0	0
7	0	0	0	0	0	0
8	0	0	0	0	0	0
9	0	0	0	0	0	0
10	0	0	0	0	0	0
11	0	0	0	0	0	0
12	0	0	0	0	0	0
13	0	0	0	0	0	0
14	0	0	0	0	0	0
15	0	0	0	0	0	0
16	0	0	0	0	0	0
17	0	0	0	0	0	0
18	0	0	0	0	0	0
19	0	0	0	0	0	0
20	10	52	30	56	45	0
21	32	64	46	75	65	0
22	54	70	49	80	71	0
23	64	80	52	85	77	0
24	71	89	55	90	83	0
25	80	106	58	95	88	0
26	89	134	58	95	89	1
27	106	182	58	87	79	1
28	134	283	55	90	83	45
29	183	333	60	98	93	1
30	287	458	60	95	89	1
31	374	506	60	95	89	1
32	459	550	60	98	93	1

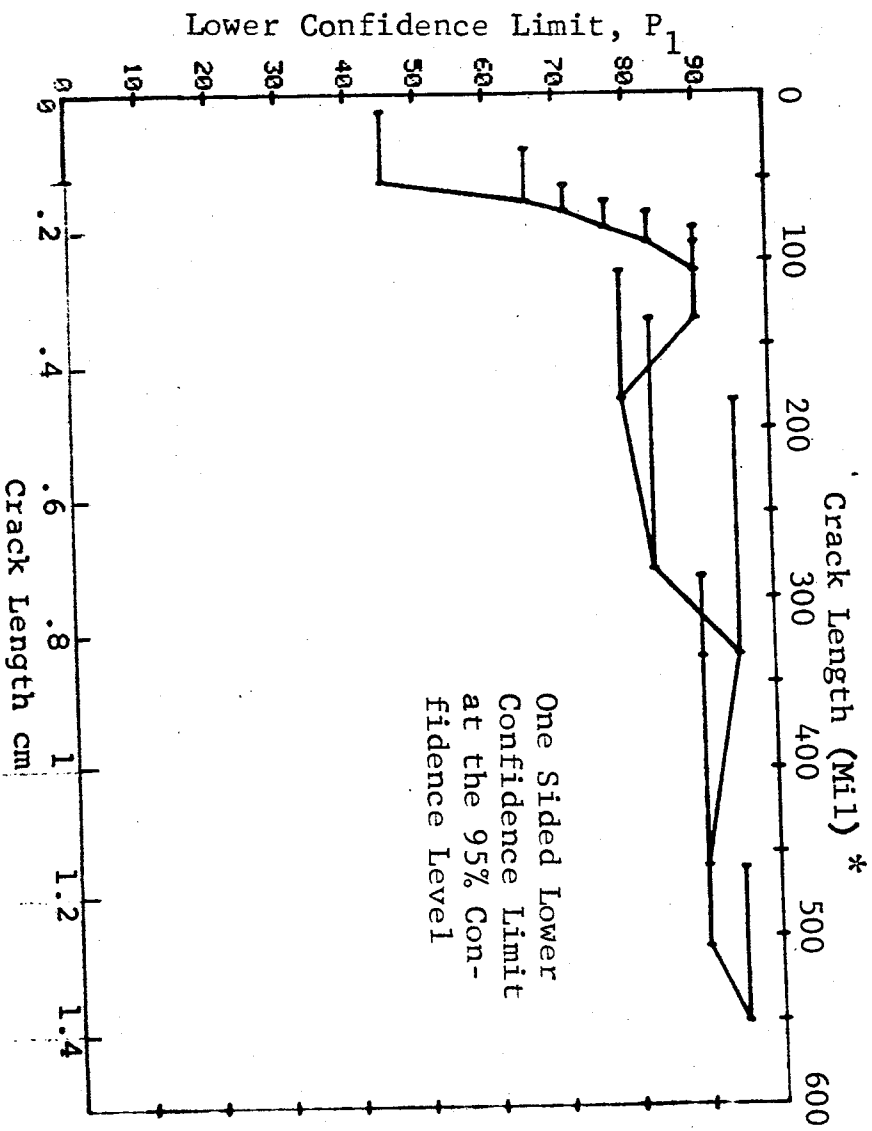


Figure D-19 (Concluded)

(a) Range Interval Method of Data Cumulation

18-SEP-75	PENETRANT		P-1, (20) N		50%	95%	0 Mils	1 Mil
RANGE	MIN LN	MAX LN *	N	DET				
1	10	41	37	12	31	19	0	0
2	42	2	80	60	74	65	0	0
3	73	103	82	72	87	80	25	27
4	104	134	36	32	87	76	57	0
5	135	162	26	20	74	59	0	0
6	171	190	5	5	87	54	0	0
7	197	197	1	1	50	5	0	0
8	241	258	16	15	89	73	0	0
9	259	288	13	13	94	79	16	33
10	290	318	16	15	89	73	0	0
11	321	347	23	20	84	69	0	0
12	352	381	11	10	85	63	0	0
13	384	408	3	3	79	36	0	0
14	426	444	3	3	79	36	0	0
15	458	475	11	11	93	76	18	35
16	478	506	22	21	92	80	24	32
17	508	535	25	25	97	88	4	21
18	538	568	6	6	89	60	0	0
19	0	0	0	0	0	0	0	0
20	610	610	1	1	50	5	0	0
21	0	0	0	0	0	0	0	0
22	0	0	0	0	0	0	0	0
23	710	710	1	1	50	5	0	0
24	0	0	0	0	0	0	0	0
25	0	0	0	0	0	0	0	0
26	0	0	0	0	0	0	0	0
27	0	0	0	0	0	0	0	0
28	0	0	0	0	0	0	0	0
29	0	0	0	0	0	0	0	0
30	0	0	0	0	0	0	0	0
31	0	0	0	0	0	0	0	0
32	979	979	1	1	50	5	0	0

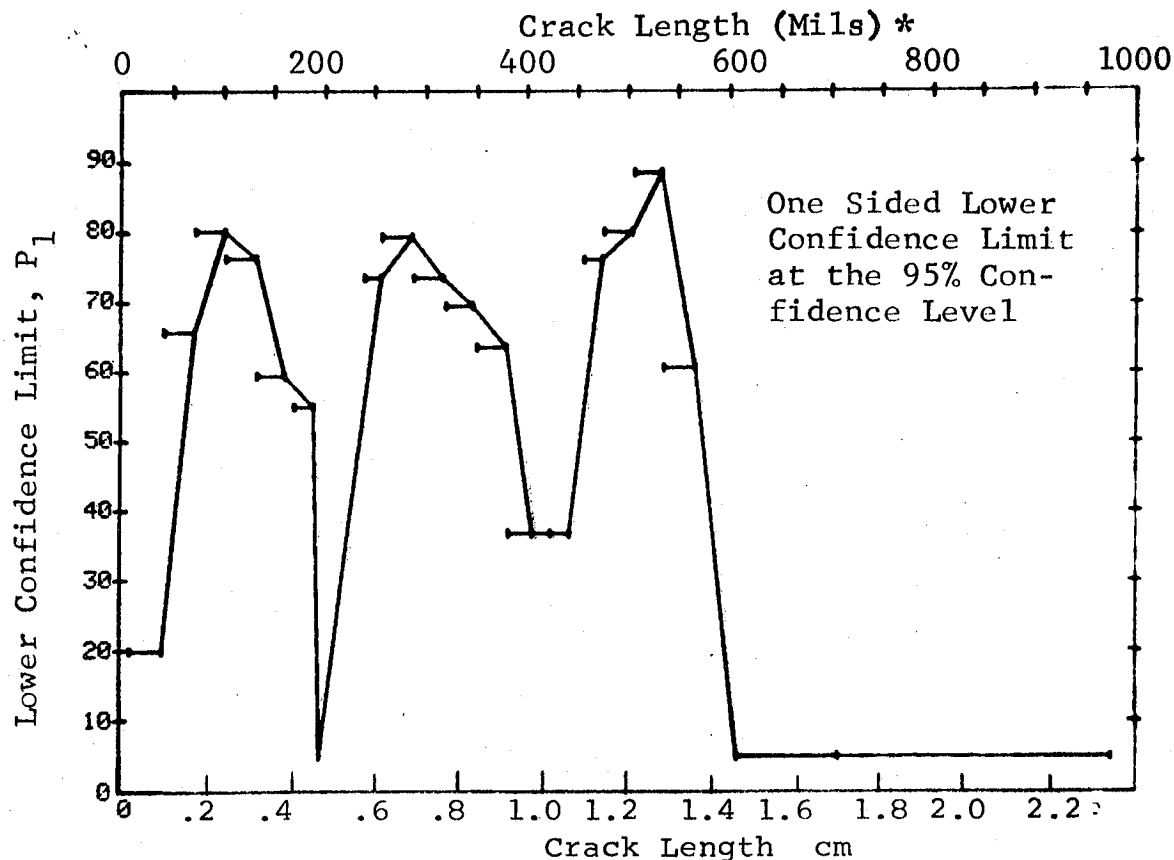


Figure D-20 Probability of Detection for 2219-T87 Al Using Liquid Penetrant. Etched Fatigue Cracks in Flat Plates Measured by Operator N. Lab. Env.

(b) Optimum Probability Method of Data Cumulation

18-SEP-75	PENETRANT		P-2, (20) N		95%		0 MISS	
RANGE	MIN	LN	MAX LN	H	DET	50%	95%	0 MISS
1	10	*	41	*	37	12	0	19
2	42		72		60	0	0	65
3	73		103		82	0	0	80
4	73		134	118	104	0	0	82
5	73		162	144	124	0	0	80
6	73		190	149	129	0	0	81
7	73		197	150	130	0	0	81
8	73		258	166	145	0	0	82
9	171		288	35	34	0	0	87
10	171		318	51	49	0	0	88
11	171		347	74	69	0	0	86
12	171		381	85	79	0	0	86
13	171		408	88	82	0	0	86
14	171		444	91	85	0	0	87
15	171		475	102	96	0	0	88
16	171		506	124	117	0	0	89
17	384		535	64	63	0	0	92
18	384		568	70	69	0	0	93
19	0		0	0	0	0	0	0
20	384		610	71	70	0	0	93
21	0		0	0	0	0	0	0
22	0		0	0	0	0	0	0
23	384		710	72	71	0	0	93
24	0		0	0	0	0	0	0
25	0		0	0	0	0	0	0
26	0		0	0	0	0	0	0
27	0		0	0	0	0	0	0
28	0		0	0	0	0	0	0
29	0		0	0	0	0	0	0
30	0		0	0	0	0	0	0
31	0		0	0	0	0	0	0
32	384		979	73	72	0	0	93

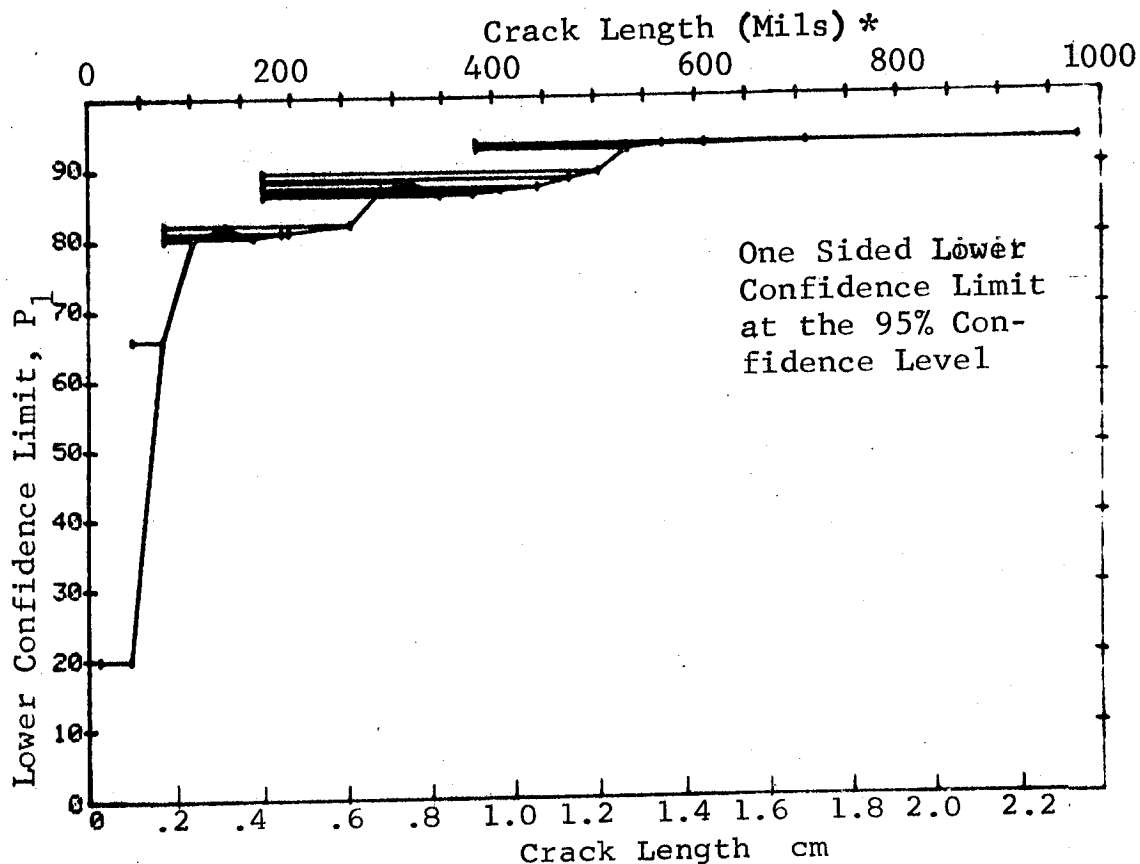


Figure D-20 (Continued)

(c) Overlapping Sixty Point Method of Data Cumulation

18-SEP-75	PENETRANT			N	P-3,	(20)	N	95%	0 MID	1 MID
RANGE	MIN	LN	* MAX LN *		DET	50%				
1		0	0	0	0	0	0	0	0	0
2		0	0	0	0	0	0	0	0	0
3		0	0	0	0	0	0	0	0	0
4		0	0	0	0	0	0	0	0	0
5		0	0	0	0	0	0	0	0	0
6		0	0	0	0	0	0	0	0	0
7		0	0	0	0	0	0	0	0	0
8		0	0	0	0	0	0	0	0	0
9		0	0	0	0	0	0	0	0	0
10		0	0	0	0	0	0	0	0	0
11		0	0	0	0	0	0	0	0	0
12		0	0	0	0	0	0	0	0	0
13		0	0	0	0	0	0	0	0	0
14		0	0	0	0	0	0	0	0	0
15		0	0	0	0	0	0	0	0	0
16		0	0	0	0	0	0	0	0	0
17		0	0	0	0	0	0	0	0	0
18		0	0	0	0	0	0	0	0	0
19		0	0	0	0	0	0	0	0	0
20	10		54	54	26	47	36	0	0	0
21	33		64	60	44	72	62	0	0	0
22	55		71	60	45	74	64	0	0	0
23	64		80	60	45	74	64	0	0	0
24	71		89	60	50	82	73	0	0	0
25	80		106	60	55	90	83	43	0	0
26	90		134	60	54	88	81	56	0	0
27	108		183	60	50	82	73	66	0	0
28	134		283	60	53	87	79	66	0	0
29	185		333	60	57	93	87	45	0	0
30	287		458	60	55	90	83	45	0	0
31	334		506	60	56	92	85	45	0	0
32	459		550	60	59	97	92	45	0	0

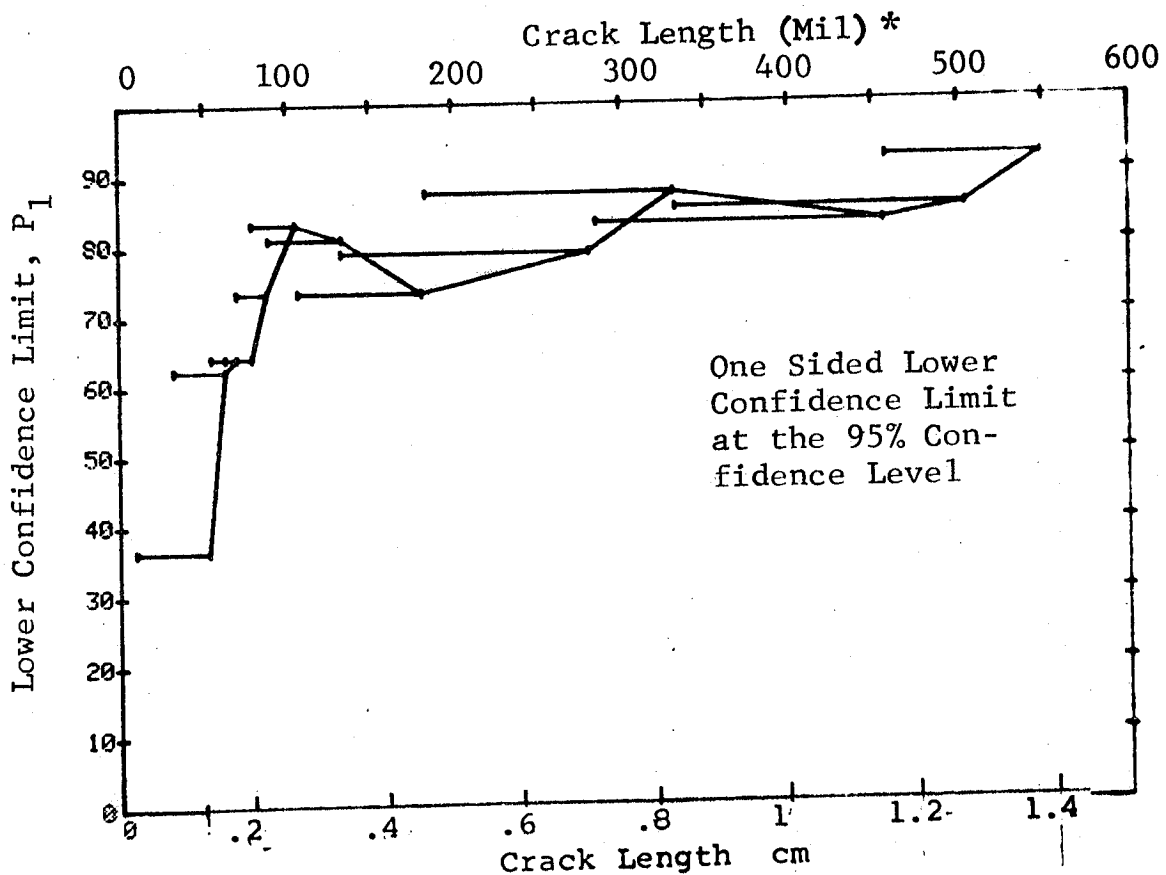


Figure D-20 (Concluded)

REPRODUCIBILITY OF THE ORIGINAL PAGE IS POOR

(a) Range Interval Method of Data Cumulation

24-JUL-75 EDDY CURRENT				TEST 1. (21) T					
RANGE	MIN	LN	N	DET	50%	95%	0 MISS	1 MISS	
1		7	13	1	5	0	0	0	
2	25	36	18	2	9	2	0	0	
3	38	51	23	3	11	3	0	0	
4	54	67	46	30	64	52	0	0	
5	68	82	53	36	66	55	0	0	
6	83	97	38	36	93	84	23	38	
7	98	111	18	16	85	68	0	0	
8	115	126	17	16	90	75	29	44	
9	129	141	19	17	86	70	0	0	
10	143	157	15	15	95	81	14	31	
11	158	171	3	3	79	36	0	0	
12	182	185	3	3	79	36	0	0	
13	190	197	2	2	70	22	0	0	
14	0	0	0	0	0	0	0	0	
15	232	232	1	1	50	5	0	0	
16	241	247	3	3	79	36	0	0	
17	248	262	17	17	96	83	12	29	
18	268	275	3	3	79	36	0	0	
19	279	290	7	7	90	65	0	0	
20	295	304	6	6	89	60	0	0	
21	310	322	10	10	93	74	0	0	
22	323	336	12	12	94	77	17	34	
23	338	352	11	11	93	76	18	35	
24	356	362	4	4	84	47	0	0	
25	370	381	5	5	87	54	0	0	
26	384	393	2	2	70	22	0	0	
27	408	408	1	1	50	5	0	0	
28	426	426	1	1	50	5	0	0	
29	442	442	1	1	50	5	0	0	
30	444	444	1	1	50	5	0	0	
31	458	472	8	8	91	68	0	0	
32	474	979	59	59	98	95	0	0	

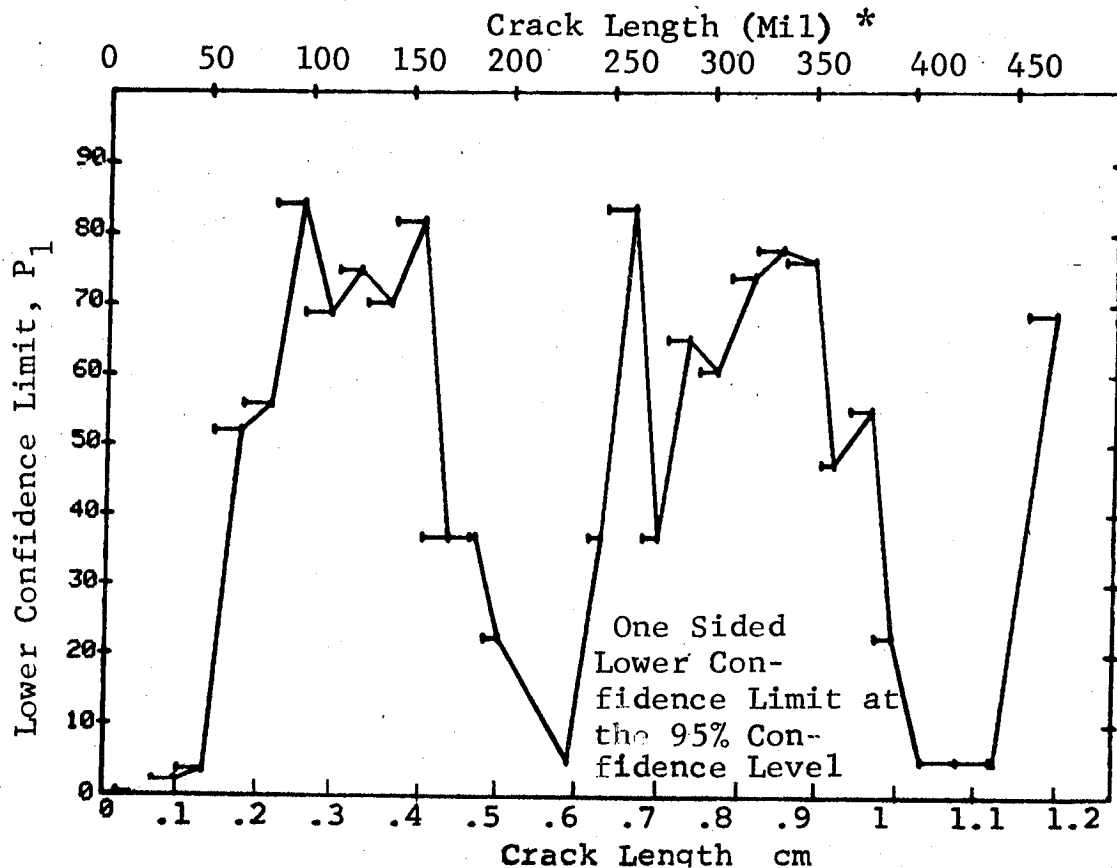


Figure D-21 Probability of Detection for 2219-T87 Al Using Eddy Current. Etched Fatigue Cracks in Flat Plates Measured by Operator T. Lab. Env.

24-JUL-75	TEST 2, (21)	ROCKWELL SC T
RANGE	DET	50%
1	1	0
2	3	0
3	6	2
4	30	4
5	66	52
6	36	58
7	52	84
8	68	84
9	85	86
10	100	88
11	103	88
12	106	88
13	108	88
14	0	0
15	109	88
16	27	89
17	44	93
18	47	93
19	54	94
20	60	95
21	70	95
22	82	96
23	93	96
24	97	97
25	102	97
26	104	97
27	105	97
28	106	97
29	107	97
30	108	97
31	116	97
32	117	98



(c) Overlapping Sixty Point Method of Data Cumulation

24-JUL-75			EDDY CURRENT			N	TEST 3		(21)		ROCKWELL SC		T
RANGE	MIN	LN	MAX	LN	*		DET	50%	95%	0 MISS	1 MISS		
1		0	0	0	*	0	0	0	0	0	0	0	
2		0	0	0		0	0	0	0	0	0	0	
3		0	0	0		0	0	0	0	0	0	0	
4		0	0	0		0	0	0	0	0	0	0	
5		0	0	0		0	0	0	0	0	0	0	
6		0	0	0		0	0	0	0	0	0	0	
7		0	0	0		0	0	0	0	0	0	0	
8		0	0	0		0	0	0	0	0	0	0	
9		0	0	0		0	0	0	0	0	0	0	
10		0	0	0		0	0	0	0	0	0	0	
11		0	0	0		0	0	0	0	0	0	0	
12		0	0	0		0	0	0	0	0	0	0	
13		0	0	0		0	0	0	0	0	0	0	
14		0	0	0		0	0	0	0	0	0	0	
15		0	0	0		0	0	0	0	0	0	0	
16		0	0	0		0	0	0	0	0	0	0	
17		0	0	0		0	0	0	0	0	0	0	
18		0	0	0		0	0	0	0	0	0	0	
19		0	0	0		0	0	0	0	0	0	0	
20		0	0	0		0	0	0	0	0	0	0	
21	7		49			52	5	8	3	0	0	0	
22	31		63			60	23	37	27	0	0	0	
23	49		70			60	36	59	48	0	0	0	
24	64		79			60	37	60	50	0	0	0	
25	70		87			60	50	82	73	0	0	0	
26	79		105			60	55	90	83	43	56	0	
27	88		131			60	53	87	79	69	82	0	
28	105		162			60	57	93	87	16	29	0	
29	132		275			60	60	98	95	0	0	0	
30	171		330			60	60	98	95	0	0	0	
31	279		442			60	60	98	95	0	0	0	
32	331		500			60	60	98	95	0	0	0	

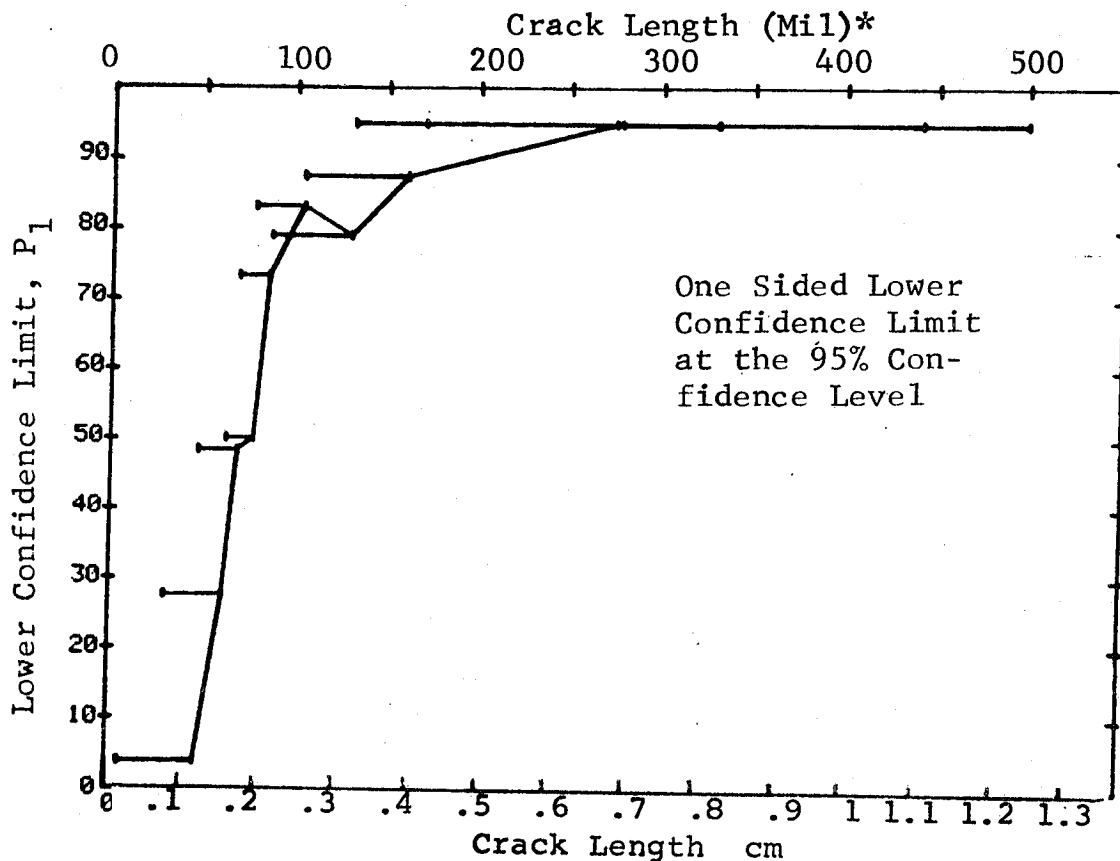


Figure D-21 (Concluded)

(a) Range Interval Method of Data Cumulation

03-JUL-75		EDDY CURRENT		N	TEST 1 - ROCKWELL SC, 'U'				(22)
RANGE	MIN LN	* MAX LN	*		DET	50%	95%	0 MISS	
1	7	22	*	13	3	20	6	0	0
2	25	26		18	6	30	15	0	0
3	38	52		25	13	50	34	0	0
4	54	67		48	42	86	76	68	81
5	68	82		50	50	98	94	0	0
6	83	97		39	35	88	78	50	64
7	98	111		17	16	90	75	29	44
8	115	126		18	18	96	84	11	28
9	129	141		18	18	96	84	11	28
10	143	157		15	15	95	81	14	31
11	158	171		3	3	79	36	0	0
12	182	185		3	3	79	36	0	0
13	190	197		2	2	70	22	0	0
14	0	0		0	0	0	0	0	0
15	0	0		0	0	0	0	0	0
16	241	247		4	4	84	47	0	0
17	248	262		16	16	95	82	13	30
18	268	275		3	3	79	36	0	0
19	279	290		7	7	90	66	0	0
20	295	306		6	6	89	60	0	0
21	310	322		10	10	93	74	0	0
22	323	336		12	12	94	77	17	34
23	338	352		11	11	93	76	18	35
24	356	362		4	4	84	47	0	0
25	370	381		5	5	87	54	0	0
26	384	393		2	2	70	22	0	0
27	408	408		1	1	50	5	0	0
28	426	426		1	1	50	5	0	0
29	442	442		1	1	50	5	0	0
30	444	444		1	1	50	5	0	0
31	458	472		8	8	91	68	0	0
32	474	979		59	59	98	95	0	0

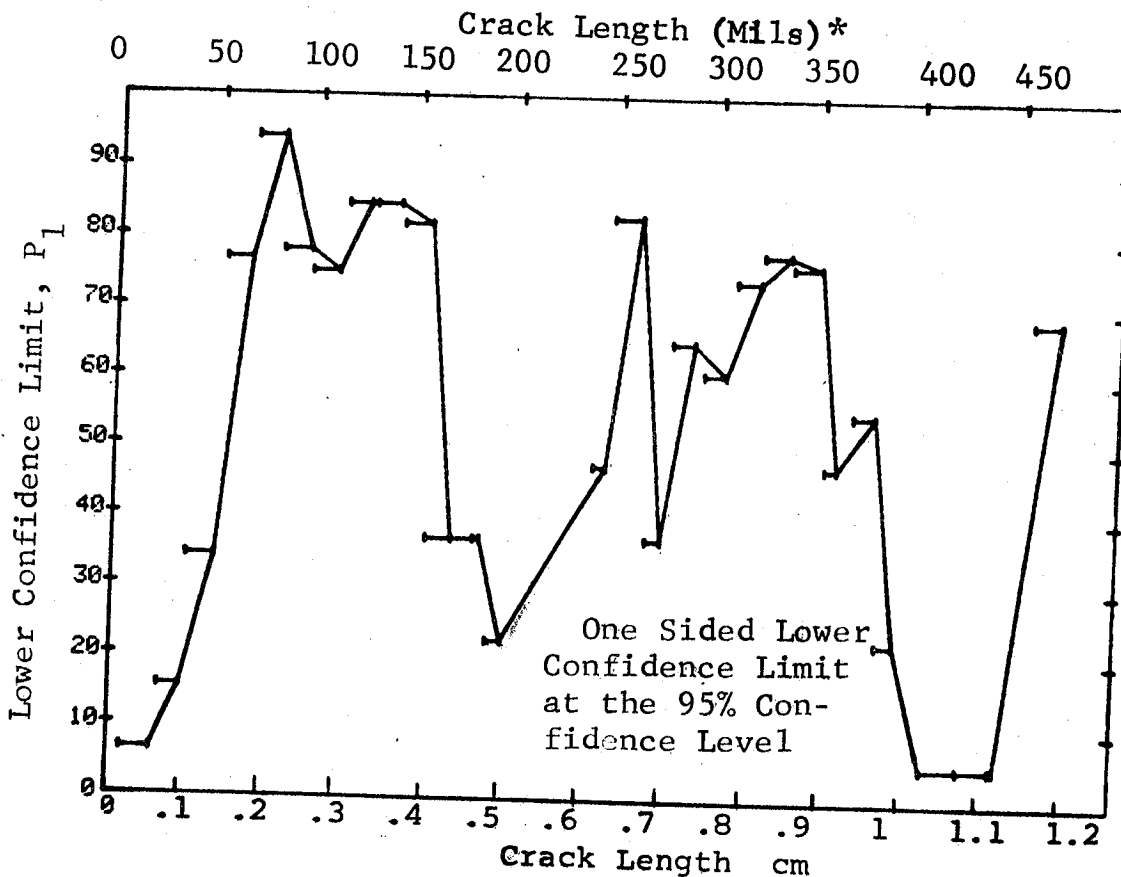


Figure D-22 Probability of Detection for 2219-T87 Al Using Eddy Current. Etched Fatigue Cracks in Flat Plates Measured by Operator U. Lab. Env.

(b) Optimum Probability Method of Data Cumulation

03-JUL-75 EDDY CURRENT				TEST 2, ROCKWELL SC, 'U'				
RANGE	MIN LN	MAX LN	N	DET	50%	95%	0 MISS	(22) 1 MISS
1	7	22	13	3	0	6	0	0
2	7	36	31	9	0	16	0	0
3	38	52	25	13	0	34	0	0
4	54	67	48	42	0	76	0	0
5	68	82	50	50	0	94	0	0
6	68	97	89	85	0	90	0	14
7	68	111	106	101	0	90	0	0
8	68	126	124	119	0	91	0	0
9	68	141	142	137	0	92	0	0
10	115	157	51	51	0	94	0	0
11	115	171	54	54	0	94	0	0
12	115	185	57	57	0	94	0	0
13	115	197	59	59	0	95	0	0
14	0	0	0	0	0	0	0	0
15	0	0	0	0	0	0	0	0
16	115	247	63	63	0	95	0	0
17	115	262	79	79	0	96	0	0
18	115	275	82	82	0	96	0	0
19	115	290	89	89	0	96	0	0
20	115	306	95	95	0	96	0	0
21	115	322	105	105	0	97	0	0
22	115	336	117	117	0	97	0	0
23	115	352	128	128	0	97	0	0
24	115	362	132	132	0	97	0	0
25	115	381	137	137	0	97	0	0
26	115	393	139	139	0	97	0	0
27	115	408	140	140	0	97	0	0
28	115	426	141	141	0	97	0	0
29	115	442	142	142	0	97	0	0
30	115	444	143	143	0	97	0	0
31	115	472	151	151	0	98	0	0
32	115	979	210	210	0	98	0	0

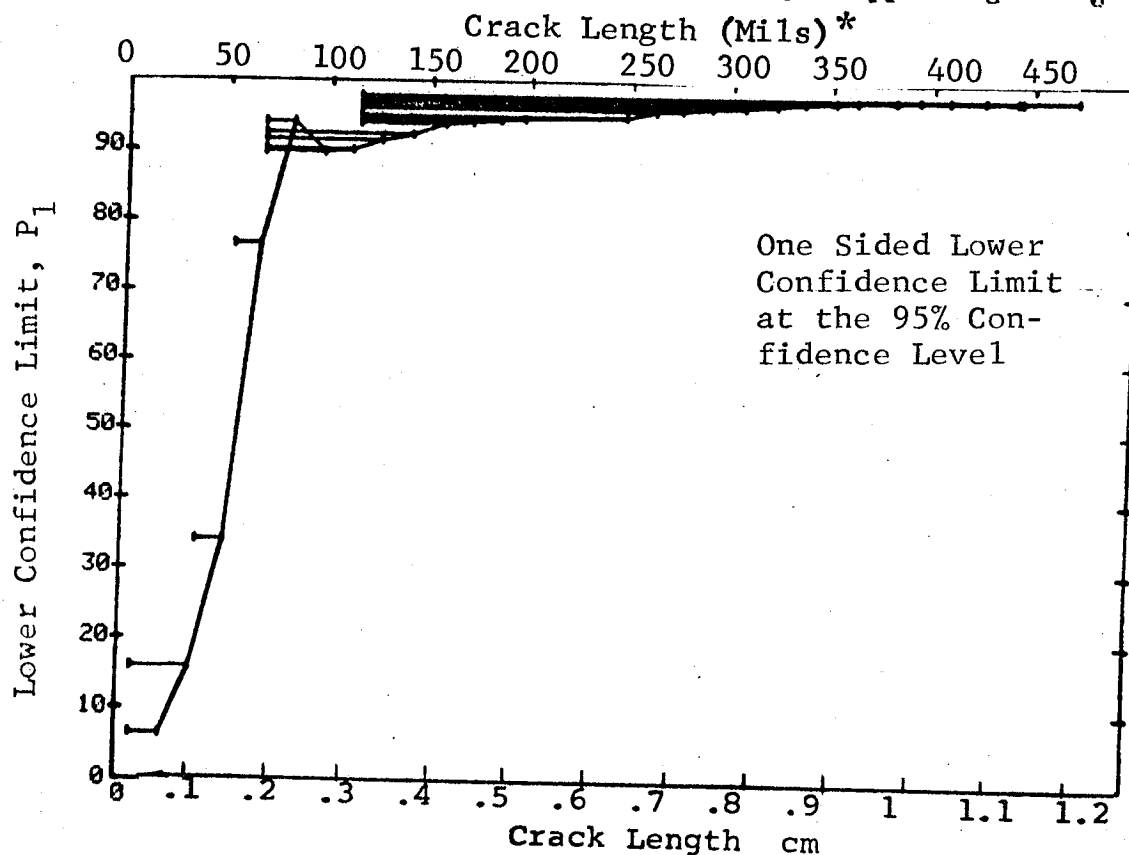


Figure D-22 (Continued)

(c) Overlapping Sixty Point Method of Data Cumulation

03-JUL-75			EDDY CURRENT		TEST 3 PORTWELL SC, 'U'			(22)	
RANGE	MIN	LN	MAX	LN *	DET	50%	95%	MISS	MISS
1	0	0	0	0	0	0	0	0	0
2	0	0	0	0	0	0	0	0	0
3	0	0	0	0	0	0	0	0	0
4	0	0	0	0	0	0	0	0	0
5	0	0	0	0	0	0	0	0	0
6	0	0	0	0	0	0	0	0	0
7	0	0	0	0	0	0	0	0	0
8	0	0	0	0	0	0	0	0	0
9	0	0	0	0	0	0	0	0	0
10	0	0	0	0	0	0	0	0	0
11	0	0	0	0	0	0	0	0	0
12	0	0	0	0	0	0	0	0	0
13	0	0	0	0	0	0	0	0	0
14	0	0	0	0	0	0	0	0	0
15	0	0	0	0	0	0	0	0	0
16	0	0	0	0	0	0	0	0	0
17	0	0	0	0	0	0	0	0	0
18	0	0	0	0	0	0	0	0	0
19	0	0	0	0	0	0	0	0	0
20	0	0	0	0	0	0	0	0	0
21	7	31	49	63	20	37	51	82	94
22	31	49	63	79	38	62	77	0	1
23	49	63	79	87	52	85	92	0	1
24	63	79	87	104	59	97	99	43	56
25	79	87	104	131	55	90	92	29	43
26	87	104	131	158	56	92	95	0	0
27	104	131	158	175	60	96	98	0	0
28	131	158	175	200	60	98	98	0	0
29	158	175	200	225	60	98	98	0	0
30	175	200	225	250	60	98	98	0	0
31	200	225	250	275	60	98	98	0	0
32	225	250	275	300	60	98	98	0	0

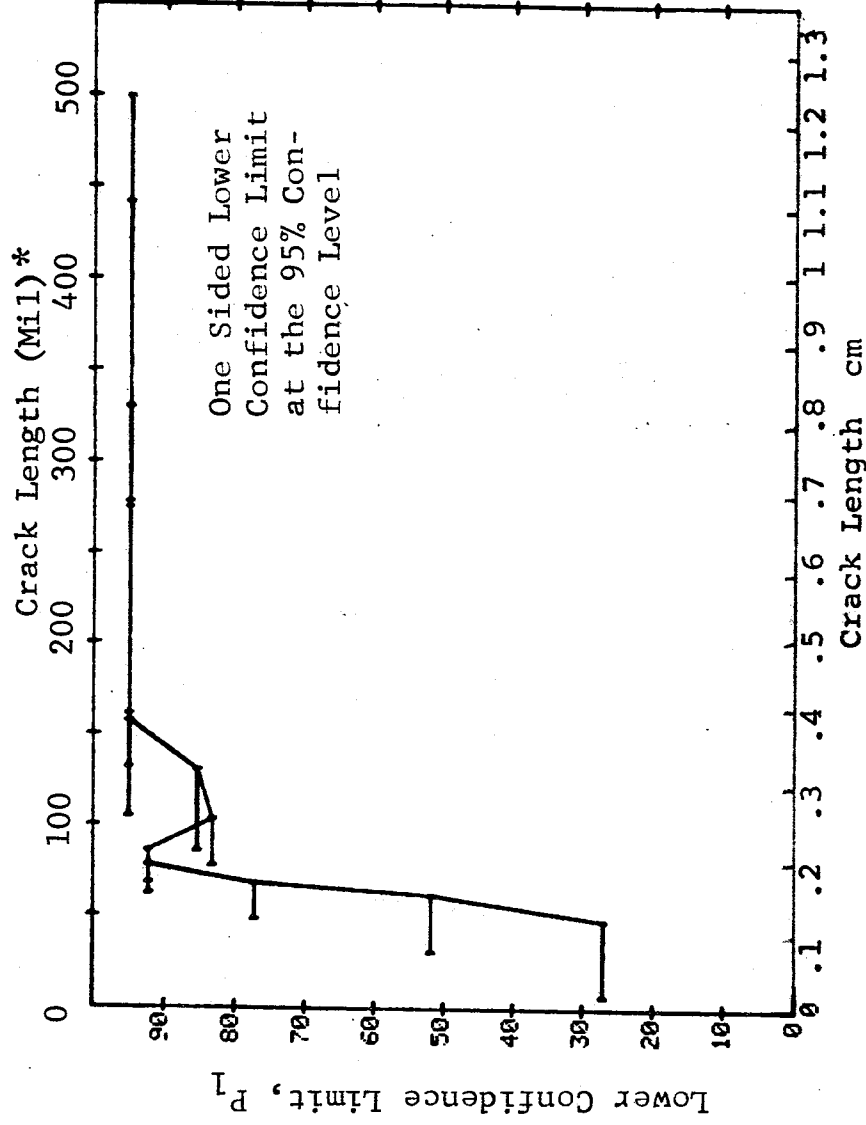


Figure D-22 (Continued)

(a) Range Interval Method of Data Cumulation

03-JUL-75 EDDY CURRENT				TEST 1, ROCKWELL SC. 'U' (23)				
RANGE	MIN LN	* MAX LN	N	DET	50%	95%	0 MISS	1 MISS
1	7	22	13	1	5	0	0	0
2	25	36	18	2	9	2	0	0
3	38	52	23	10	41	25	0	0
4	54	67	47	26	54	42	0	0
5	68	82	53	44	81	72	0	0
6	83	97	38	34	87	77	51	65
7	98	111	17	16	90	75	29	44
8	115	126	17	16	90	75	29	44
9	129	141	19	16	81	64	0	0
10	143	157	15	12	76	56	0	0
11	158	171	3	3	79	36	0	0
12	182	185	3	1	20	1	0	0
13	190	197	2	2	70	22	0	0
14	0	0	0	0	0	0	0	0
15	0	0	0	0	0	0	0	0
16	241	247	4	3	61	24	0	0
17	248	262	16	16	95	82	13	30
18	268	275	3	3	79	36	0	0
19	279	290	6	6	89	60	0	0
20	295	306	7	5	63	34	0	0
21	310	322	10	9	83	60	0	0
22	323	336	12	12	94	77	17	34
23	338	352	11	9	76	52	0	0
24	356	362	4	4	84	47	0	0
25	370	381	5	4	68	34	0	0
26	384	393	2	2	70	22	0	0
27	408	408	1	1	50	5	0	0
28	426	426	1	1	50	5	0	0
29	435	442	3	2	50	13	0	0
30	444	444	1	1	50	5	0	0
31	458	472	8	8	91	68	0	0
32	474	979	57	52	90	92	40	59

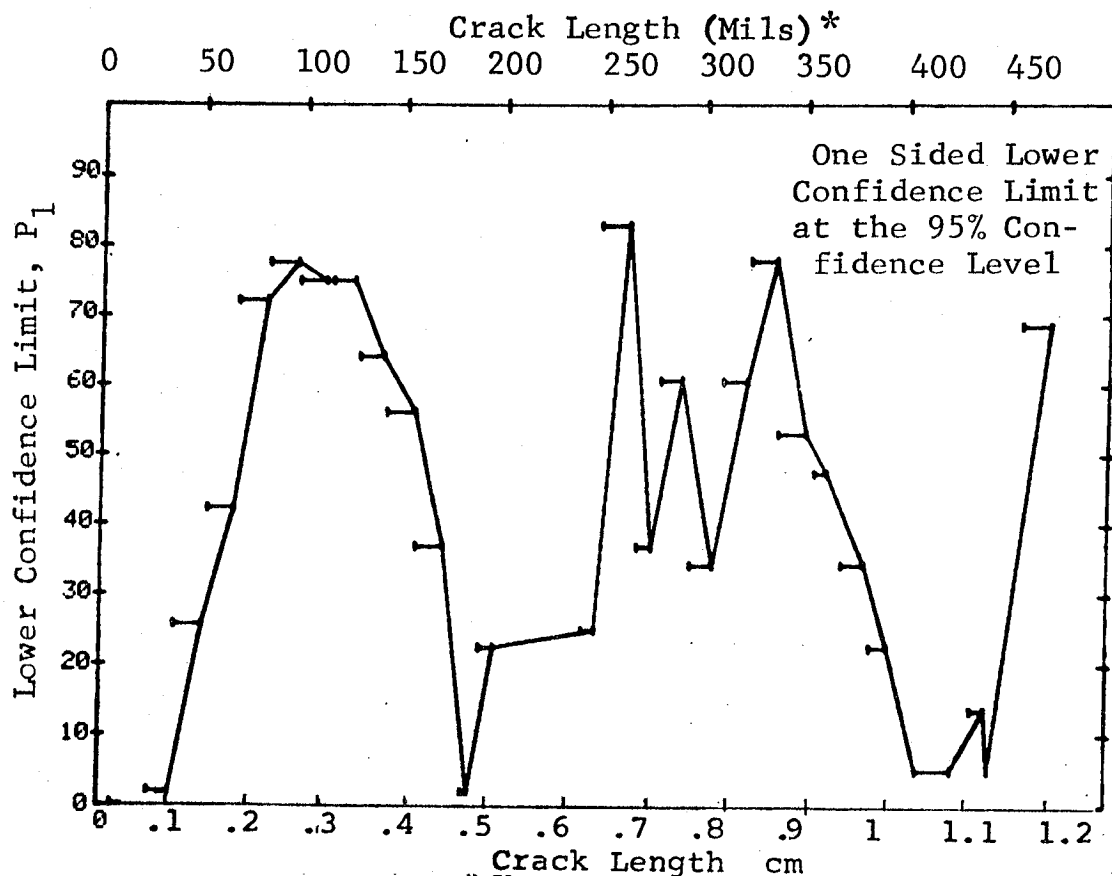


Figure D-23 Probability of Detection for 2219-T87 Al Using Eddy Current. Etched Fatigue Cracks in Flat Plates Measured by Operator V. Lab. Env.

(b) Optimum Probability Method of Data Cumulation

03-JUL-75 EDDY CURRENT				TEST 2, ROCKWELL SC, 'U' (23)				
RANGE	MIN LN	MAX LN	N	DET	50%	95%	0 MISS	1 MISS
1	7 *	32 *	13	1	0	0	0	0
2	7	36	31	3	0	0	0	0
3	38	52	23	10	0	25	0	0
4	54	67	47	26	0	42	0	0
5	68	82	53	44	0	72	0	0
6	68	97	91	78	0	78	0	0
7	83	111	55	50	0	81	48	61
8	83	126	72	66	0	84	44	57
9	83	141	91	82	0	83	63	76
10	83	157	106	94	0	82	0	0
11	83	171	109	97	0	82	0	0
12	83	185	112	98	0	81	0	0
13	83	197	114	100	0	81	0	0
14	0	0	0	0	0	0	0	0
15	0	0	0	0	0	0	0	0
16	83	247	118	103	0	81	0	0
17	83	262	134	119	0	83	0	0
18	248	275	19	19	0	85	10	27
19	248	290	25	25	0	88	4	21
20	83	306	150	133	0	83	0	0
21	83	322	160	142	0	83	0	0
22	248	336	54	51	0	86	22	35
23	248	352	65	60	0	84	38	51
24	248	362	69	64	0	85	34	47
25	83	381	192	171	0	84	0	0
26	248	393	76	70	0	85	40	53
27	248	408	77	71	0	85	39	52
28	248	426	78	72	0	85	38	51
29	248	442	81	74	0	84	43	61
30	83	444	200	178	0	84	0	0
31	248	472	90	83	0	85	39	52
32	248	979	147	135	0	87	0	0

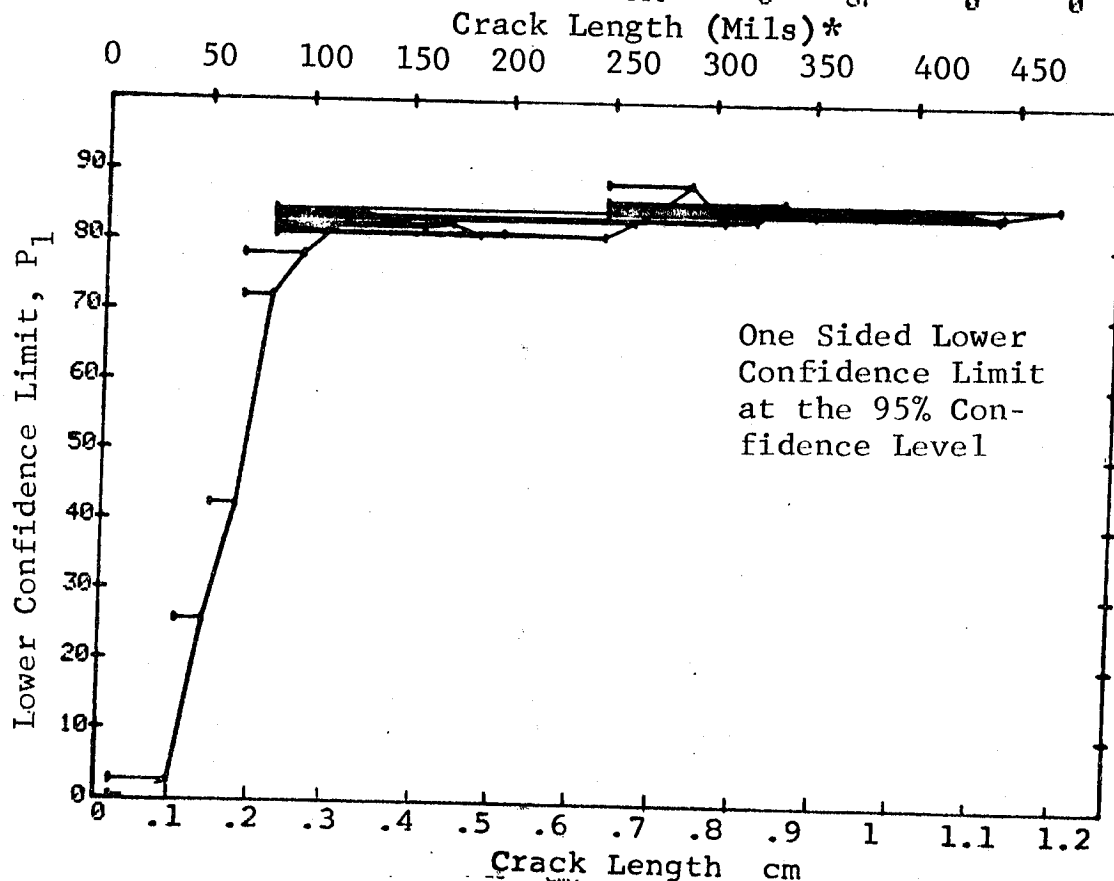


Figure D-23 (Continued)

REPRODUCIBILITY OF THE
ORIGINAL PAGE IS POOR

(c) Overlapping Sixty Point Method of Data Cumulation

03-JUL-75			EDDY CURRENT		TEST 3, ROCKWELL SC. 'U'		(23)	
RANGE	MIN	LN	MAX	LN	DET	50%	95%	MISS
1	0	0	0	0	0	0	0	0
2	0	0	0	0	0	0	0	0
3	0	0	0	0	0	0	0	0
4	0	0	0	0	0	0	0	0
5	0	0	0	0	0	0	0	0
6	0	0	0	0	0	0	0	0
7	0	0	0	0	0	0	0	0
8	0	0	0	0	0	0	0	0
9	0	0	0	0	0	0	0	0
10	0	0	0	0	0	0	0	0
11	0	0	0	0	0	0	0	0
12	0	0	0	0	0	0	0	0
13	0	0	0	0	0	0	0	0
14	0	0	0	0	0	0	0	0
15	0	0	0	0	0	0	0	0
16	0	0	0	0	0	0	0	0
17	0	0	0	0	0	0	0	0
18	0	0	0	0	0	0	0	0
19	0	0	0	0	0	0	0	0
20	0	0	0	0	0	0	0	0
21	7	32	51	53	12	21	13	0
22	32	52	63	60	26	42	32	0
23	52	64	70	60	35	59	48	0
24	64	70	79	60	43	70	60	0
25	70	79	87	60	52	85	77	0
26	79	88	105	60	56	92	85	82
27	88	106	132	60	54	88	81	43
28	106	134	171	60	52	85	77	69
29	134	182	279	60	53	87	79	82
30	182	283	331	60	54	88	81	69
31	283	333	442	60	53	87	79	82
32	333		500	60	54	88	81	69

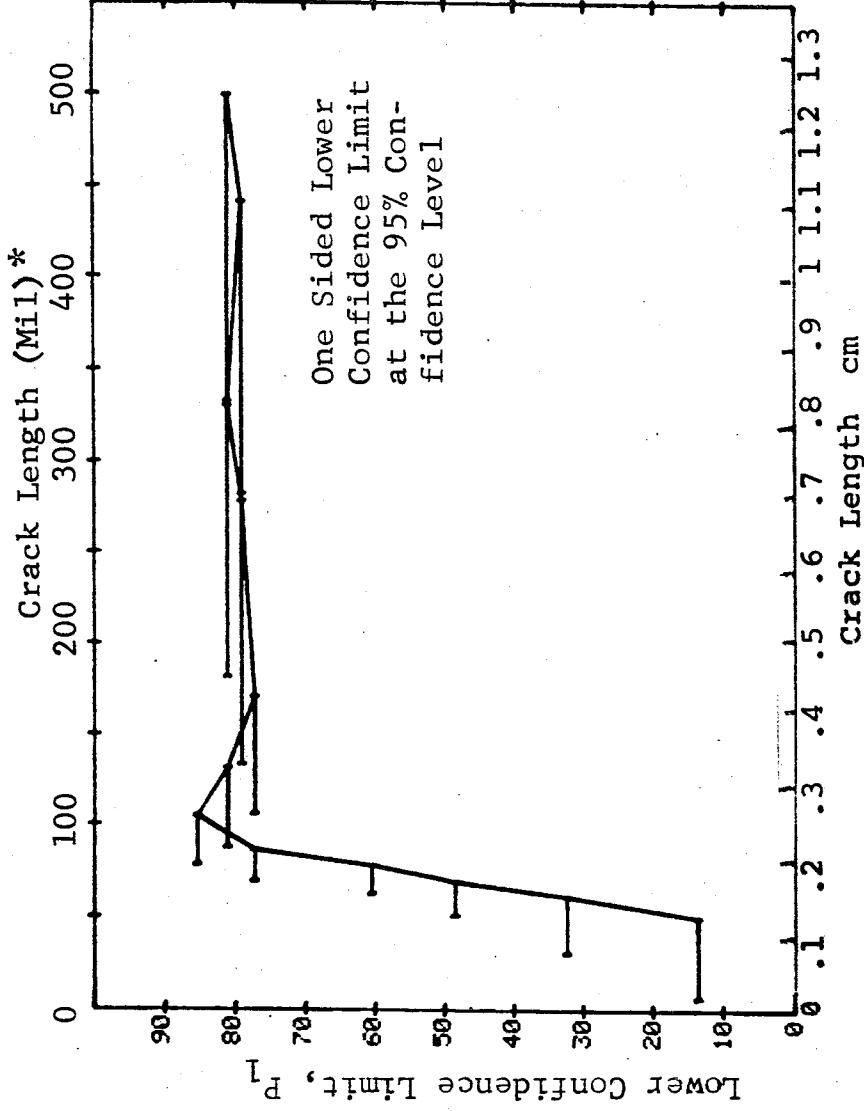


Figure D-23 (Concluded)

(a) Range Interval Method of Data Cumulation

03-JUL-75 EDDY CURRENT				TEST 1, ROCKWELL SC, 'W' (24)				
RANGE	MIN LN	MAX LN	N	DET	50%	95%	0 MISS	1 MISS
1	7	22	13	2	12	2	0	0
2	25	66	18	6	30	15	0	0
3	38	52	22	8	34	19	0	0
4	54	67	46	10	20	12	0	0
5	68	82	53	47	87	78	63	76
6	83	97	39	37	93	84	22	37
7	98	111	17	17	96	83	12	29
8	115	126	17	16	90	75	29	44
9	129	141	19	17	86	70	0	0
10	143	157	15	12	76	56	0	0
11	158	171	3	3	79	36	0	0
12	182	185	3	3	79	36	0	0
13	190	197	2	2	70	22	0	0
14	0	0	0	0	0	0	0	0
15	0	0	0	0	0	0	0	0
16	241	247	4	4	84	47	0	0
17	248	262	17	17	96	83	12	29
18	268	275	3	3	79	36	0	0
19	279	290	7	6	77	47	0	0
20	295	306	6	6	89	60	0	0
21	310	322	10	10	93	74	0	0
22	323	336	12	11	86	66	0	0
23	338	352	11	9	76	52	0	0
24	356	362	4	4	84	47	0	0
25	370	381	5	4	68	34	0	0
26	384	393	2	2	70	22	0	0
27	408	408	1	1	50	5	0	0
28	426	426	1	1	50	5	0	0
29	442	442	1	0	0	0	0	0
30	444	444	1	1	50	5	0	0
31	458	472	8	7	79	52	0	0
32	474	979	58	53	90	82	45	58

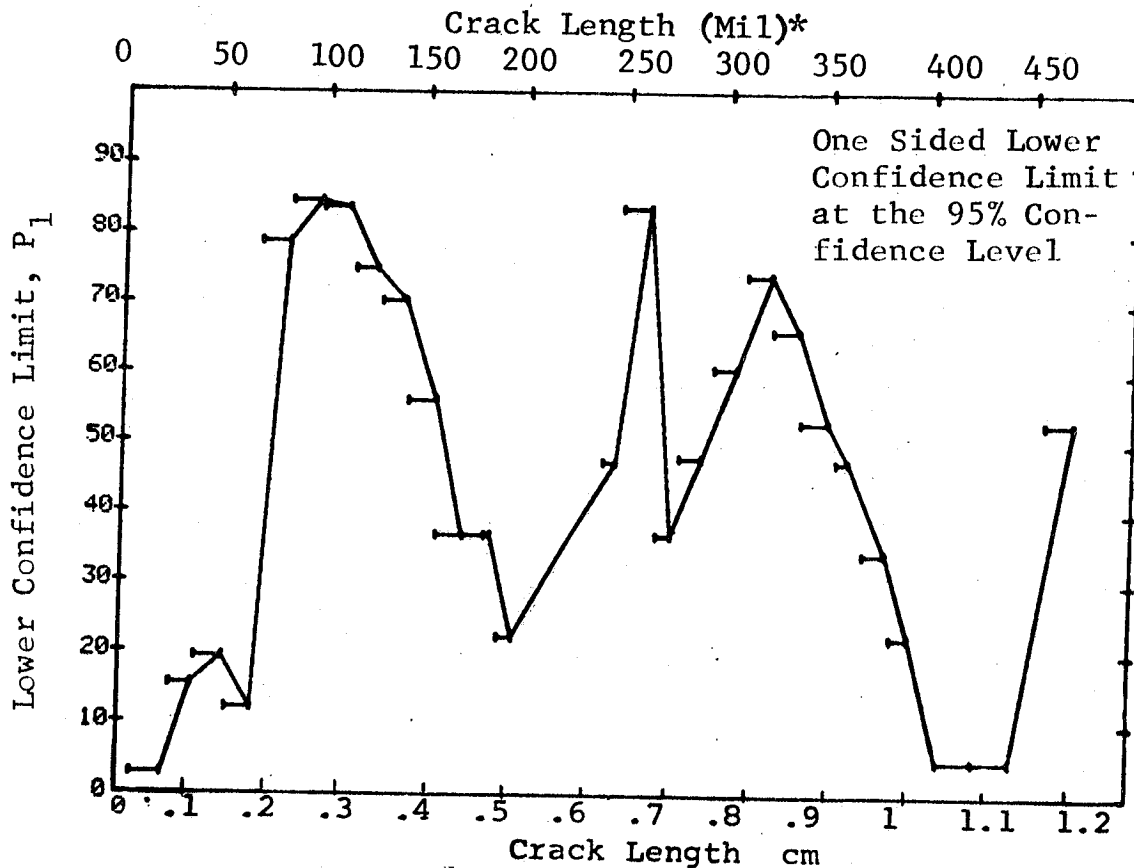


Figure D-24 Probability of Detection for 2219-T87 Al Using Eddy Current. Etched Fatigue Cracks in Flat Plates Measured by Operator W. Lab. Env.

(b) Optimum Probability Method of Data Cumulation

03-JUL-75 EDDY CURRENT				TEST 2, ROCKWELL SC. 'W' (24)				
RANGE	MIN LN	MAX LN	N	DET	50%	95%	0 MISS	1 MISS
1	7*	23*	13	2	0	2	0	0
2	25	36	18	6	0	15	0	0
3	25	52	40	14	0	22	0	0
4	25	67	86	24	0	20	0	0
5	68	82	53	47	0	78	0	0
6	68	97	92	84	0	84	50	62
7	83	111	56	54	0	89	5	20
8	83	126	73	70	0	89	3	16
9	83	141	92	87	0	88	11	24
10	83	157	107	99	0	86	0	0
11	83	171	110	102	0	87	0	0
12	83	185	113	105	0	87	0	0
13	83	197	115	107	0	87	0	0
14	0	0	0	0	0	0	0	0
15	0	0	0	0	0	0	0	0
16	83	247	119	111	0	88	0	0
17	158	262	29	29	0	90	0	17
18	158	275	32	32	0	91	0	14
19	83	290	146	137	0	89	0	0
20	158	306	45	44	0	89	1	16
21	158	322	55	54	0	91	0	6
22	158	336	67	65	0	90	0	0
23	83	352	185	173	0	89	0	0
24	83	362	189	177	0	89	0	0
25	83	381	194	181	0	89	0	0
26	83	393	196	183	0	89	0	0
27	83	408	197	184	0	89	0	0
28	83	426	198	185	0	89	0	0
29	68	442	252	232	0	88	0	0
30	83	444	200	186	0	89	0	0
31	83	472	208	193	0	89	0	0
32	83	979	266	246	0	89	0	0

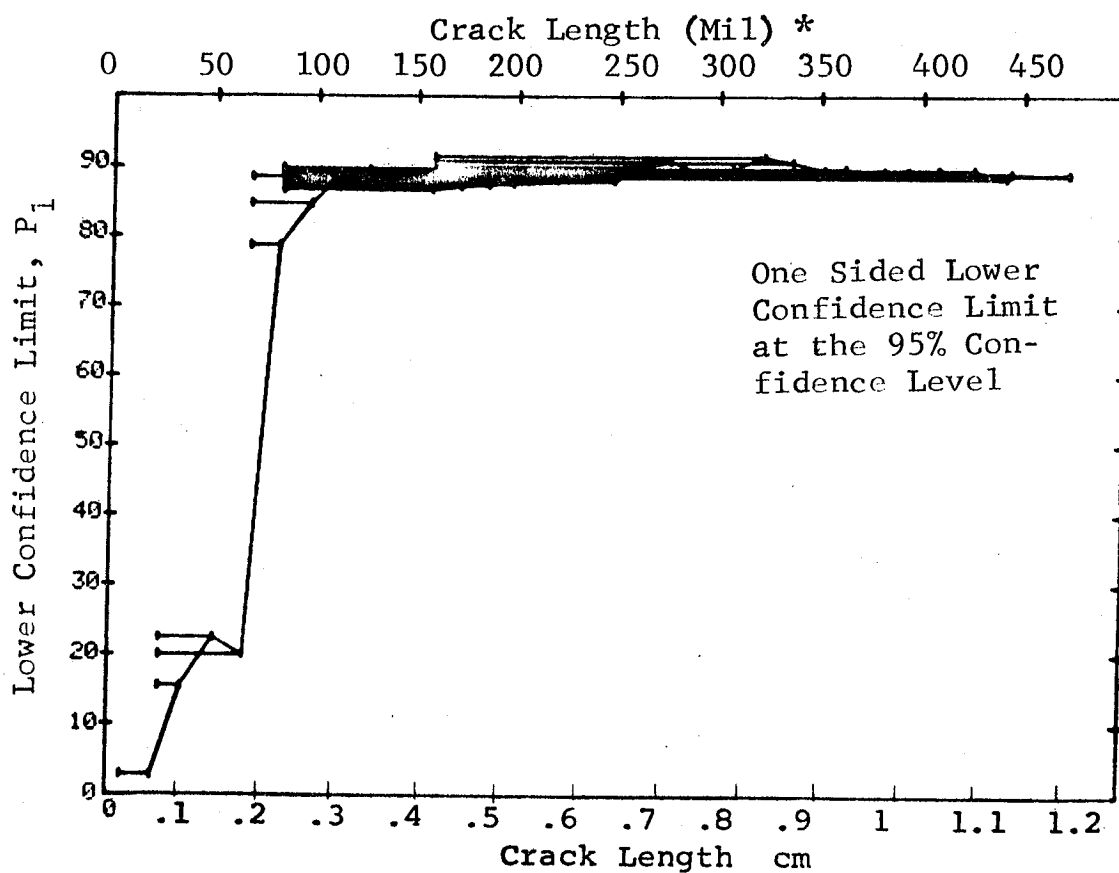


Figure D-24 (Continued)

for

(c) Overlapping Sixty Point Method of Data Cumulation

03-JUL-75		EDDY CURRENT		N	TEST 3, ROCKWELL SC, 'W' (24)				
RANGE	MIN LN	* MAX LN	*		DET	50%	95%	0 MISS	1 MISS
1	0	0	*	0	0	0	0	0	0
2	0	0	*	0	0	0	0	0	0
3	0	0	*	0	0	0	0	0	0
4	0	0	*	0	0	0	0	0	0
5	0	0	*	0	0	0	0	0	0
6	0	0	*	0	0	0	0	0	0
7	0	0	*	0	0	0	0	0	0
8	0	0	*	0	0	0	0	0	0
9	0	0	*	0	0	0	0	0	0
10	0	0	*	0	0	0	0	0	0
11	0	0	*	0	0	0	0	0	0
12	0	0	*	0	0	0	0	0	0
13	0	0	*	0	0	0	0	0	0
14	0	0	*	0	0	0	0	0	0
15	0	0	*	0	0	0	0	0	0
16	0	0	*	0	0	0	0	0	0
17	0	0	*	0	0	0	0	0	0
18	0	0	*	0	0	0	0	0	0
19	0	0	*	0	0	0	0	0	0
20	0	0	*	0	0	0	0	0	0
21	7	49	*	51	16	30	20	0	0
22	30	63	*	60	16	25	17	0	0
23	51	70	*	60	19	30	21	0	0
24	64	79	*	60	43	70	60	0	0
25	70	87	*	60	55	90	83	43	56
26	79	105	*	60	57	93	87	16	29
27	87	131	*	60	59	97	92	0	1
28	106	162	*	60	54	88	81	56	69
29	132	275	*	60	55	90	83	43	56
30	171	330	*	60	59	97	92	0	1
31	279	442	*	60	54	88	81	56	69
32	331	500	*	60	52	85	77	82	94

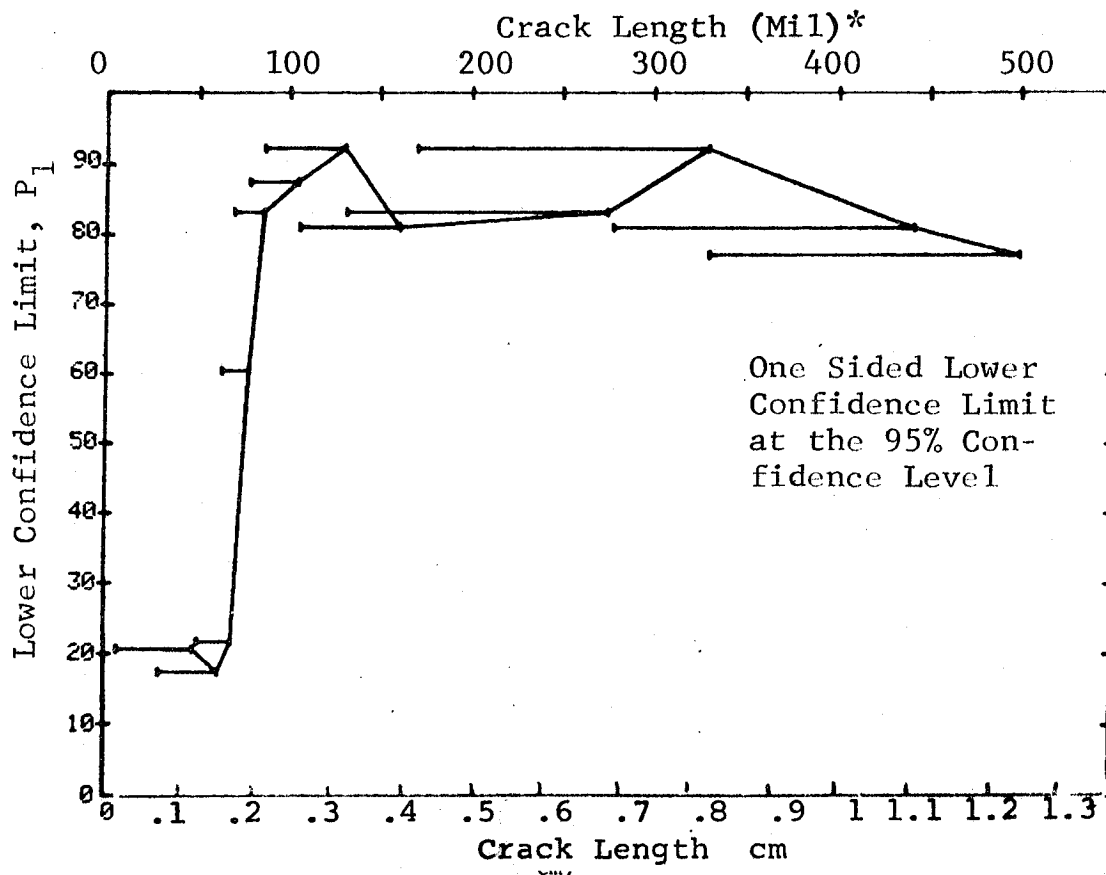


Figure D-24 (Concluded)

(a) Range Interval Method of Data Cumulation

03-JUL-75		EDDY CURRENT		TEST 1, FULLWELL SC. (25)	
RANGE	MIN LN	MAX LN	DET	50%	95%
1	25	30	1	5	0
2	38	52	7	14	0
3	54	67	0	32	0
4	68	82	31	64	0
5	87	97	36	90	0
6	98	111	17	96	0
7	115	126	17	96	0
8	129	141	17	87	0
9	143	157	17	83	0
10	156	171	13	79	0
11	182	185	13	79	0
12	190	197	3	70	0
13	0	0	2	0	0
14	0	0	0	0	0
15	0	0	0	0	0
16	241	247	4	0	0
17	248	261	4	84	0
18	268	275	16	95	0
19	279	290	7	79	0
20	295	306	6	69	0
21	310	322	10	93	0
22	323	336	10	94	0
23	338	352	12	85	0
24	356	362	11	63	0
25	370	381	4	34	0
26	384	393	2	84	0
27	408	408	1	70	0
28	426	426	1	50	0
29	442	442	1	50	0
30	444	444	1	50	0
31	458	472	8	91	0
32	474	979	58	97	92

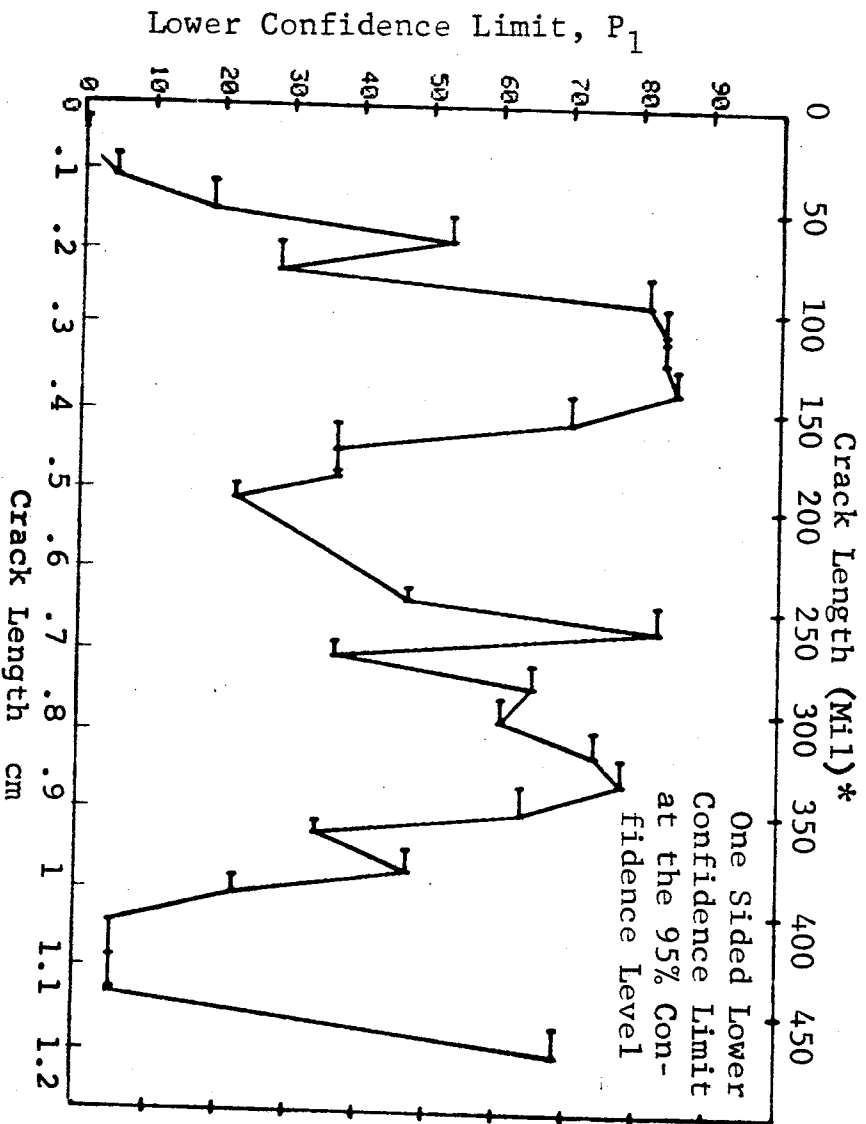


Figure D-25 Probability of Detection for 2219-T87 Al Using Eddy Current. Etched Fatigue Cracks in Flat Plates Measured by Operator X. Lab. Env.

(b) Optimum Probability Method of Data Cumulation

03-JUL-75 EDDY CURRENT				TEST 2, ROCKWELL SC, 'X' (25)				
RANGE	MIN LN	MAX LN	N	DET	50%	95%	0 MISS	1 MISS
1	7	* 22 *	13	1	0	0	0	0
2	25	36	18	3	0	4	0	0
3	38	52	23	8	0	18	0	0
4	54	67	47	31	0	52	0	0
5	54	82	100	52	0	43	0	0
6	83	97	39	36	0	81	37	50
7	83	111	56	53	0	86	20	33
8	98	126	34	34	0	91	0	12
9	98	141	53	53	0	94	0	0
10	98	157	67	66	0	93	0	0
11	98	171	70	69	0	93	0	0
12	98	185	73	72	0	93	0	0
13	98	197	75	74	0	93	0	0
14	0	0	0	0	0	0	0	0
15	0	0	0	0	0	0	0	0
16	98	247	79	78	0	94	0	0
17	98	261	95	94	0	95	0	0
18	98	275	98	97	0	95	0	0
19	98	290	105	104	0	95	0	0
20	98	306	111	110	0	95	0	0
21	98	322	121	120	0	96	0	0
22	98	336	133	132	0	96	0	0
23	98	352	144	142	0	95	0	0
24	98	362	149	146	0	94	0	0
25	98	381	153	150	0	95	0	0
26	98	393	155	152	0	95	0	0
27	98	408	156	153	0	95	0	0
28	98	426	157	154	0	95	0	0
29	98	442	158	155	0	95	0	0
30	98	444	159	156	0	95	0	0
31	98	472	167	164	0	95	0	0
32	98	979	226	222	0	95	0	0

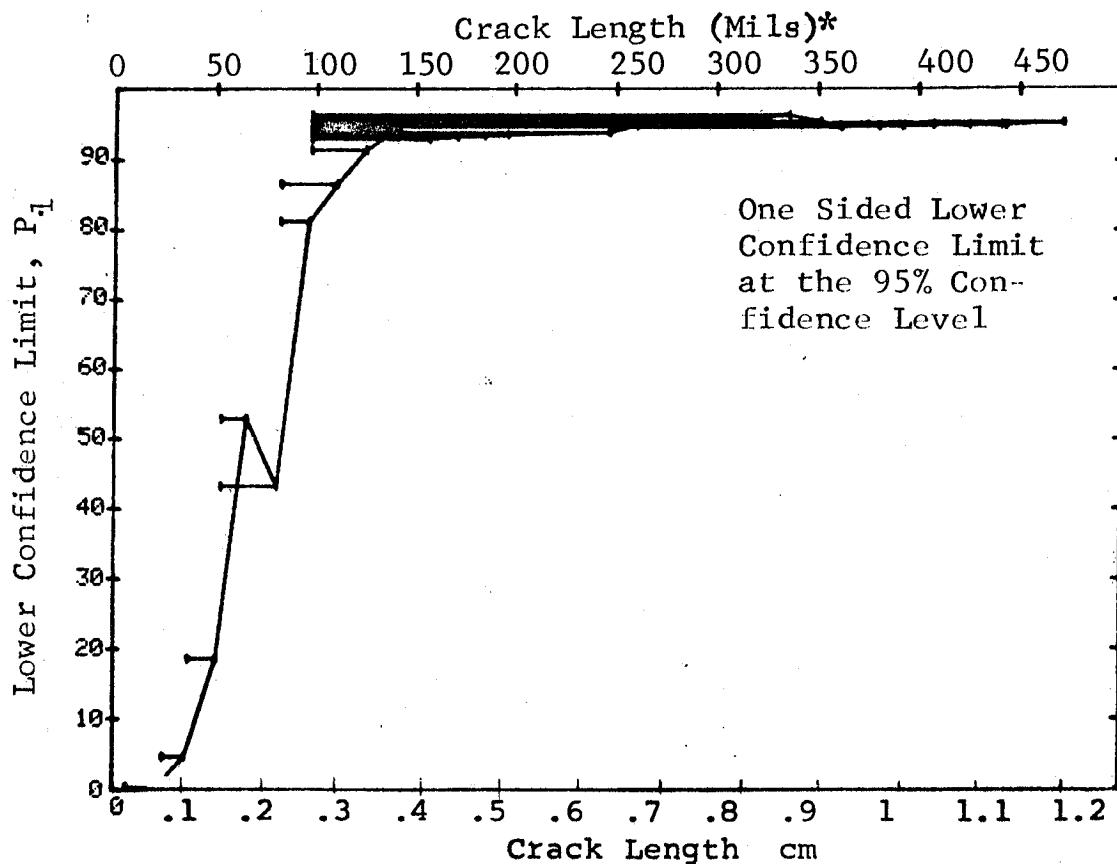


Figure D-25 (Continued)

(c) Overlapping Sixty Point Method of Data Cumulation

03-JUL-75		EDDY CURRENT		N	TEST 3. ROCKWELL SC. 'X' (25)				
RANGE	MIN LN	* MAX LN	* LN		DET	50%	95%	0 MISS	1 MISS
1	0	0	0	0	0	0	0	0	0
2	0	0	0	0	0	0	0	0	0
3	0	0	0	0	0	0	0	0	0
4	0	0	0	0	0	0	0	0	0
5	0	0	0	0	0	0	0	0	0
6	0	0	0	0	0	0	0	0	0
7	0	0	0	0	0	0	0	0	0
8	0	0	0	0	0	0	0	0	0
9	0	0	0	0	0	0	0	0	0
10	0	0	0	0	0	0	0	0	0
11	0	0	0	0	0	0	0	0	0
12	0	0	0	0	0	0	0	0	0
13	0	0	0	0	0	0	0	0	0
14	0	0	0	0	0	0	0	0	0
15	0	0	0	0	0	0	0	0	0
16	0	0	0	0	0	0	0	0	0
17	0	0	0	0	0	0	0	0	0
18	0	0	0	0	0	0	0	0	0
19	0	0	0	0	0	0	0	0	0
20	0	0	0	0	0	0	0	0	0
21	7	49	51	10	18	11	0	0	0
22	30	63	60	25	40	30	0	0	0
23	49	69	60	35	57	46	0	0	0
24	63	79	60	29	47	37	0	0	0
25	69	86	60	33	54	43	0	0	0
26	79	103	60	51	83	75	94	100	0
27	87	129	60	60	98	95	0	0	0
28	104	158	60	59	97	92	0	1	0
29	131	275	60	59	97	92	0	1	0
30	162	330	60	60	98	95	0	0	0
31	279	442	60	58	95	89	1	16	0
32	331	500	60	57	93	87	16	29	0

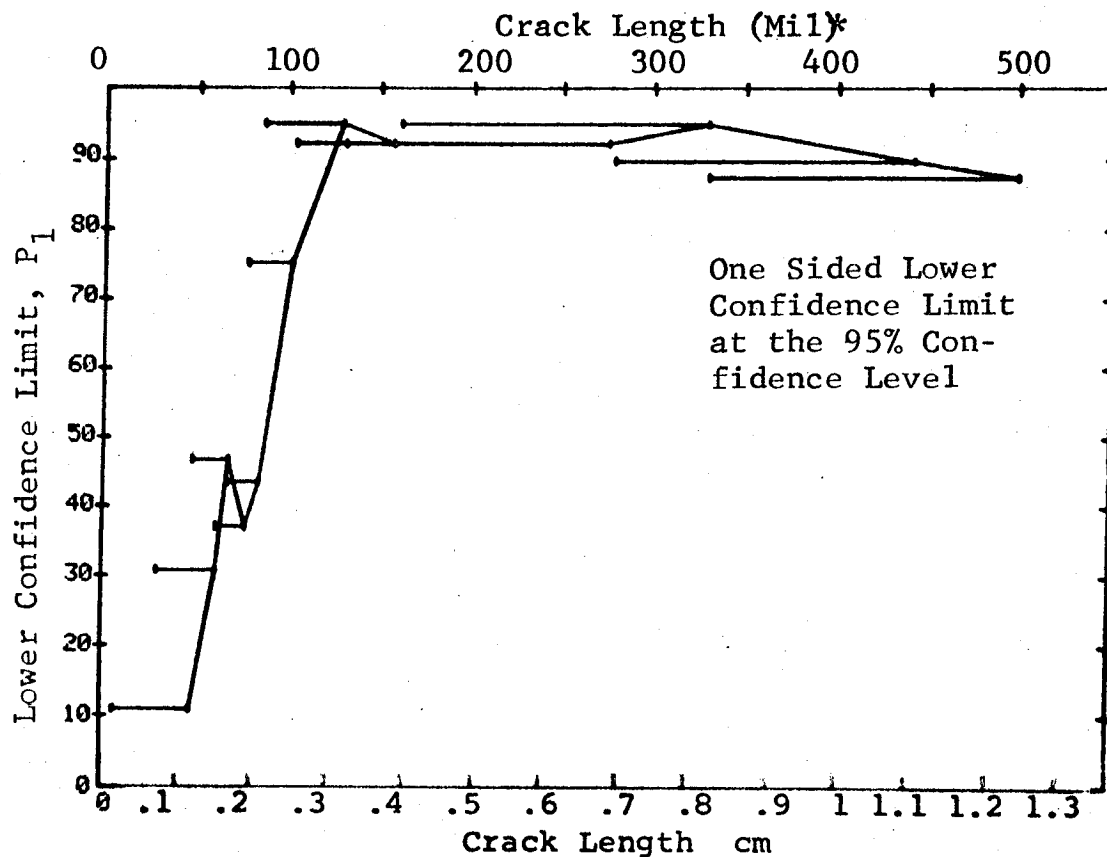


Figure D-25 (Concluded)

(a) Range Interval Method of Data Cumulation

03-JUL-75			RADIOGRAPHY		TEST 1, ROCKWELL SCALING (26)	
RANGE	MIN	LN	MAX	LN	DET	50%
1	7	25	32	13	0	0
2	25	38	52	18	9	0
3	38	54	67	23	11	0
4	54	68	82	46	14	0
5	68	83	97	53	21	0
6	83	98	111	39	18	0
7	98	115	126	17	16	0
8	115	129	141	17	0	0
9	129	143	157	19	0	0
10	143	158	171	15	0	0
11	158	182	185	3	0	0
12	182	190	197	3	0	0
13	190	0	0	2	0	0
14	0	0	0	2	0	0
15	0	0	0	0	1	0
16	241	247	247	0	0	0
17	248	262	262	4	0	0
18	268	275	275	17	84	47
19	279	290	290	3	90	75
20	295	306	306	7	34	36
21	310	322	322	6	26	4
22	323	336	336	10	45	26
23	338	352	352	12	29	12
24	356	362	362	11	93	24
25	370	381	381	4	61	34
26	384	393	393	5	87	54
27	408	408	408	2	70	22
28	426	426	426	1	0	0
29	442	442	442	1	0	0
30	444	444	444	1	50	0
31	458	472	472	1	50	0
32	474	979	979	8	91	68
				59	83	83
					54	44

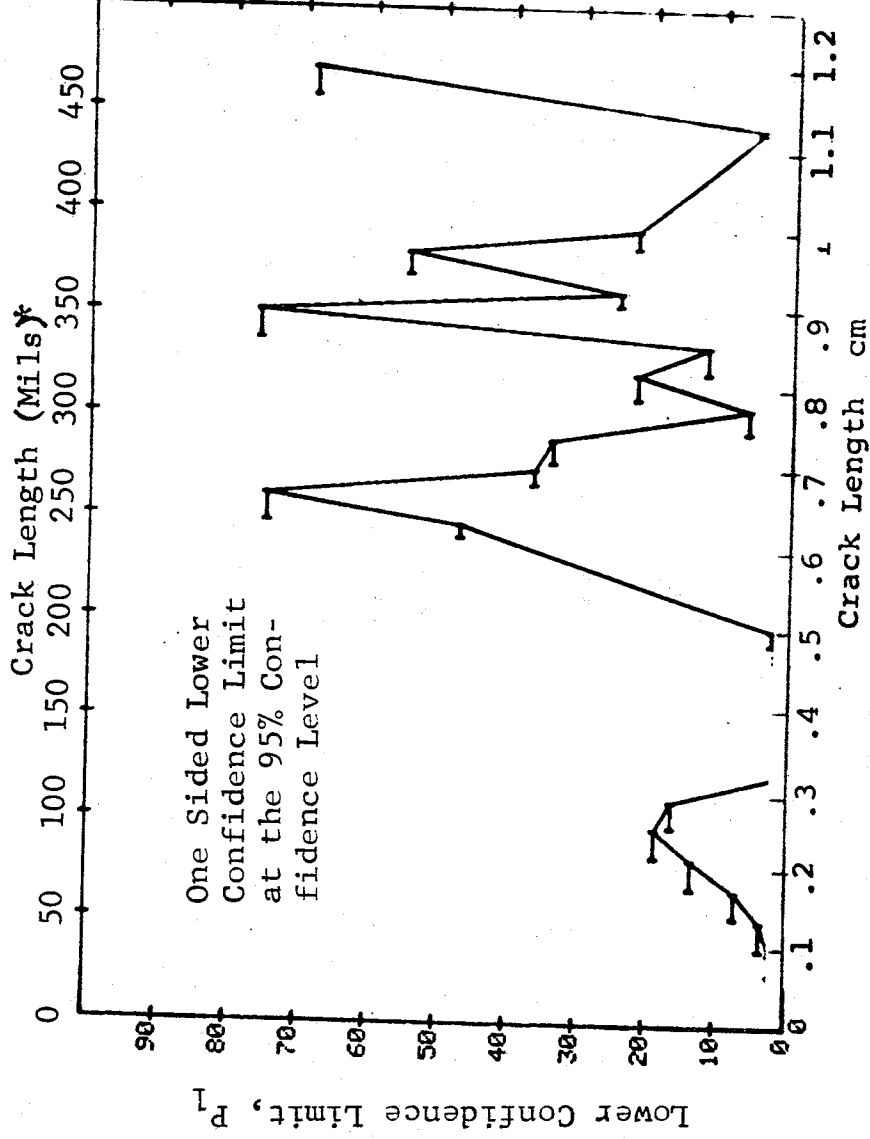


Figure D-26 Probability of Detection for 2219-T87 A1 Using X-ray. Etched Fatigue Cracks in Flat Plates Measured by Operator A. Lab. Env.

(b) Optimum Probability Method of Data Cumulation

03-JUL-75		RADIOGRAPHY		N	TEST 2, ROCKWELL SC.			(26)	
RANGE	MIN LN	* MAX LN *			DET	50%	95%	0 MISS	1 MISS
1	7	22	13	0	0	0	0	0	0
2	25	36	18	2	0	2	0	0	0
3	25	52	41	5	0	4	0	0	0
4	25	67	87	12	0	8	0	0	0
5	68	82	53	12	0	13	0	0	0
6	83	97	39	12	0	18	0	0	0
7	83	111	56	18	0	21	0	0	0
8	68	126	126	31	0	18	0	0	0
9	68	141	145	32	0	16	0	0	0
10	68	157	160	33	0	15	0	0	0
11	68	171	163	33	0	15	0	0	0
12	68	185	166	34	0	15	0	0	0
13	68	197	168	35	0	15	0	0	0
14	0	0	0	0	0	0	0	0	0
15	0	0	0	0	0	0	0	0	0
16	241	247	4	0	0	0	0	0	0
17	241	262	21	4	0	47	0	0	0
18	241	275	24	20	0	79	0	0	0
19	241	290	31	23	0	81	22	0	0
20	241	306	37	28	0	76	0	0	0
21	241	322	47	30	0	67	0	0	0
22	241	336	59	35	0	61	0	0	0
23	338	352	11	39	0	54	0	0	0
24	338	362	15	11	0	76	0	0	0
25	338	381	20	14	0	72	0	0	0
26	338	393	22	19	0	78	0	0	0
27	338	408	23	21	0	80	24	0	0
28	338	426	24	21	0	75	0	0	0
29	338	442	25	21	0	70	0	0	0
30	338	444	26	22	0	71	0	0	0
31	338	472	34	23	0	72	0	0	0
32	442	979	69	31	0	78	0	0	0
				64	0	85	34	0	0

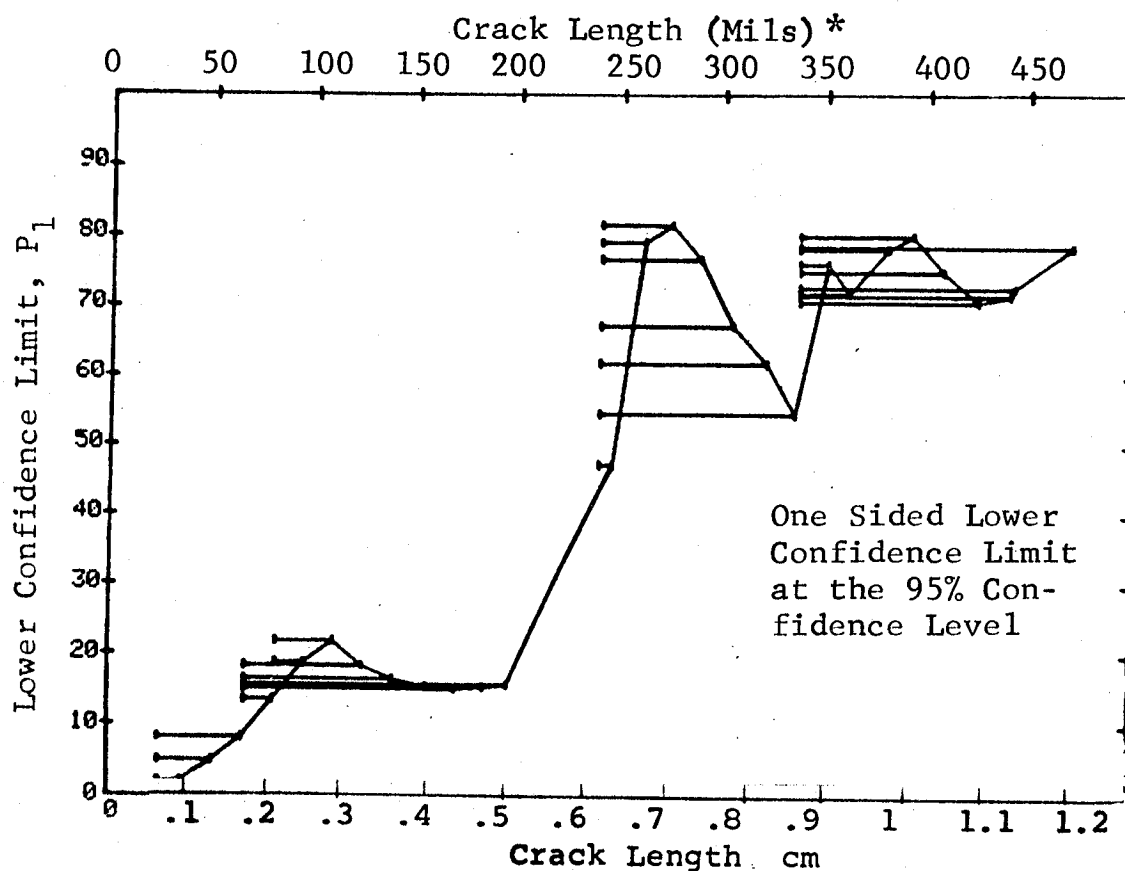


Figure D-26 (Continued)

(c) Overlapping Sixty Point Method of Data Cumulation

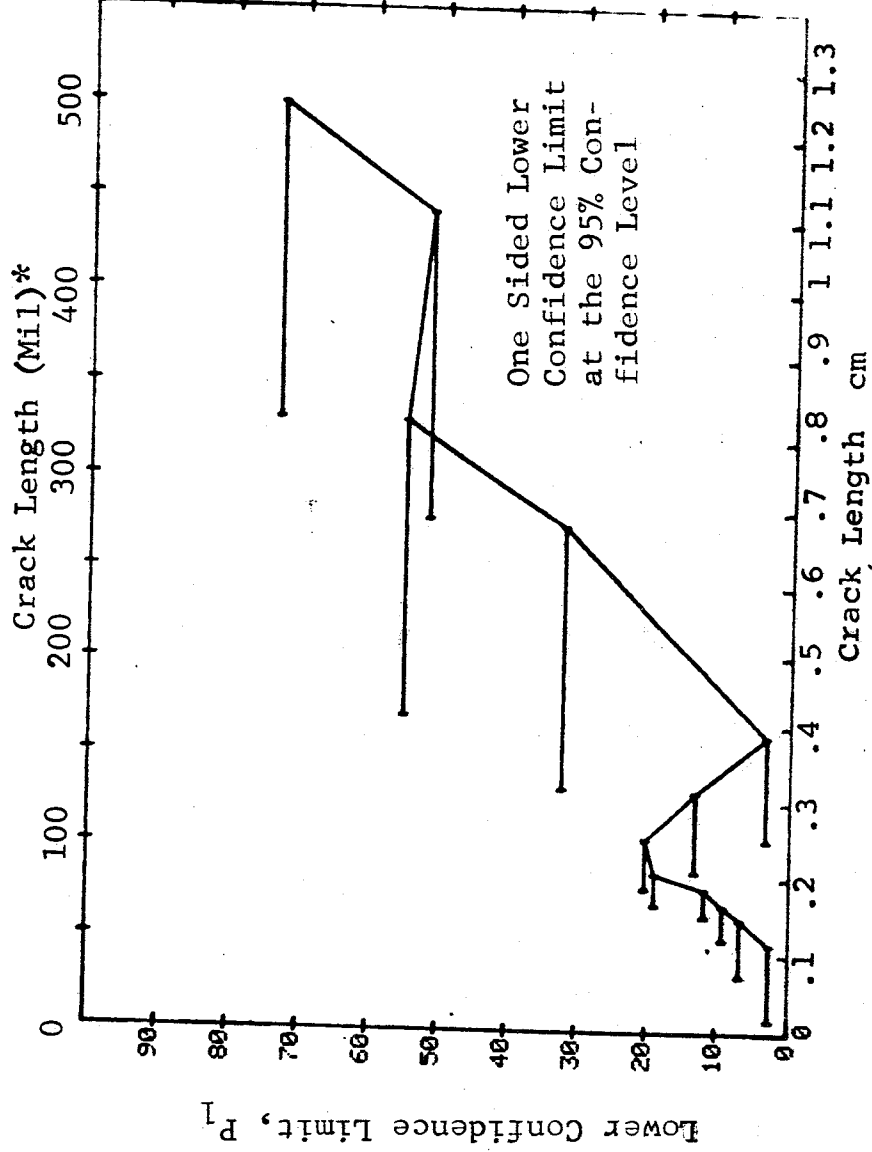
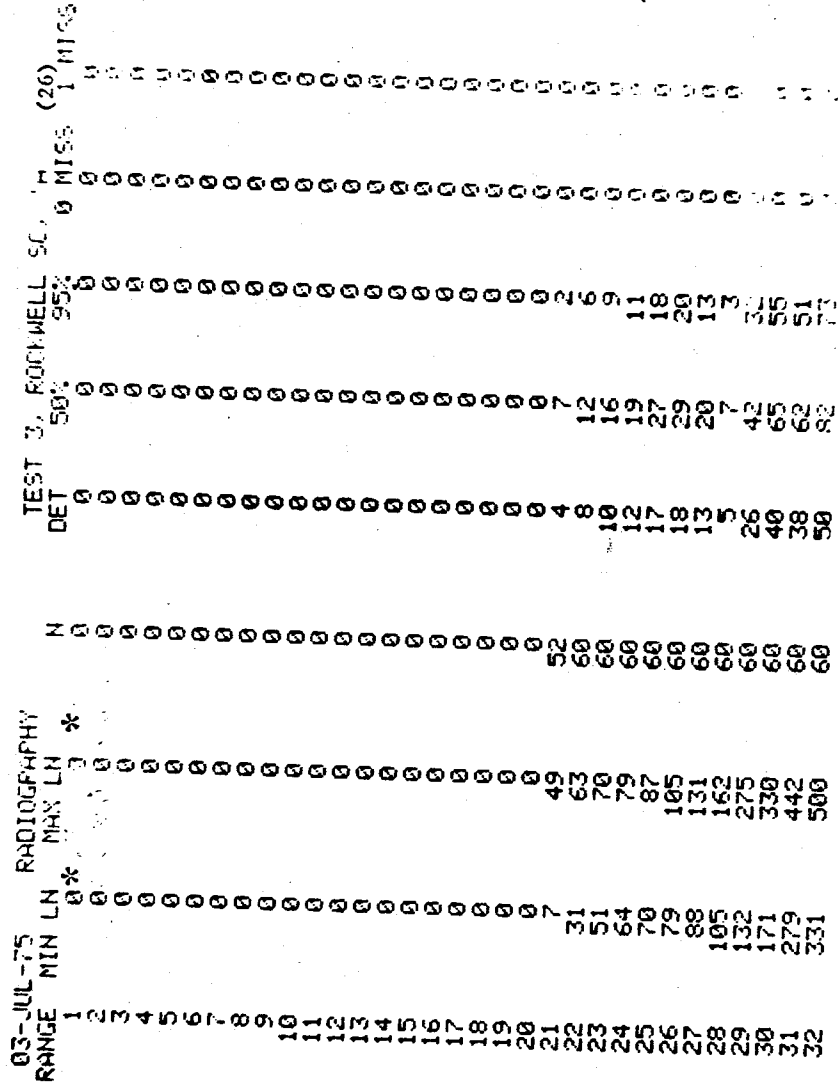


Figure D-26 (Concluded)

(a) Range Interval Method of Data Cumulation

03-JUL-75			RADIOGRAPHY		TEST 1, ROCKWELL SC. L. (27)	
RANGE	MIN LN	MAX LN	* *	N	DET	50% 95% 0 MISS 1 MISS
1	7	25	22	13	1	5 0 0 0
2	25	38	36	18	1	3 0 0 0
3	38	54	52	23	1	2 0 0 0
4	54	68	67	46	5	2 0 0 0
5	68	93	82	53	9	10 4 9 0
6	93	97	97	37	8	16 9 0 0
7	98	111	111	17	2	20 2 0 0
8	115	126	126	17	0	9 0 0 0
9	129	141	141	19	0	0 0 0 0
10	143	157	157	15	1	4 0 0 0
11	158	171	171	3	0	0 0 0 0
12	182	185	185	3	0	0 0 0 0
13	190	197	197	2	0	0 0 0 0
14	0	0	0	0	0	0 0 0 0
15	0	0	0	0	0	0 0 0 0
16	241	247	247	4	4	84 47 0 0
17	248	262	262	17	16	90 73 29 44
18	268	275	275	3	3	79 35 0 0
19	279	290	290	7	6	47 41 0 0
20	295	306	306	6	2	26 15 0 0
21	310	322	322	10	4	35 21 0 0
22	323	336	336	12	3	21 17 0 0
23	338	352	352	11	10	85 63 0 0
24	356	362	362	4	3	61 24 0 0
25	370	381	381	5	5	87 54 0 0
26	384	393	393	2	1	29 25 0 0
27	408	408	408	1	1	50 0 0 0
28	426	426	426	1	0	0 0 0 0
29	442	442	442	1	1	50 55 0 0
30	444	444	444	1	1	50 68 0 0
31	458	472	472	8	8	91 83 0 0
32	474	979	979	59	54	90 44 0 0

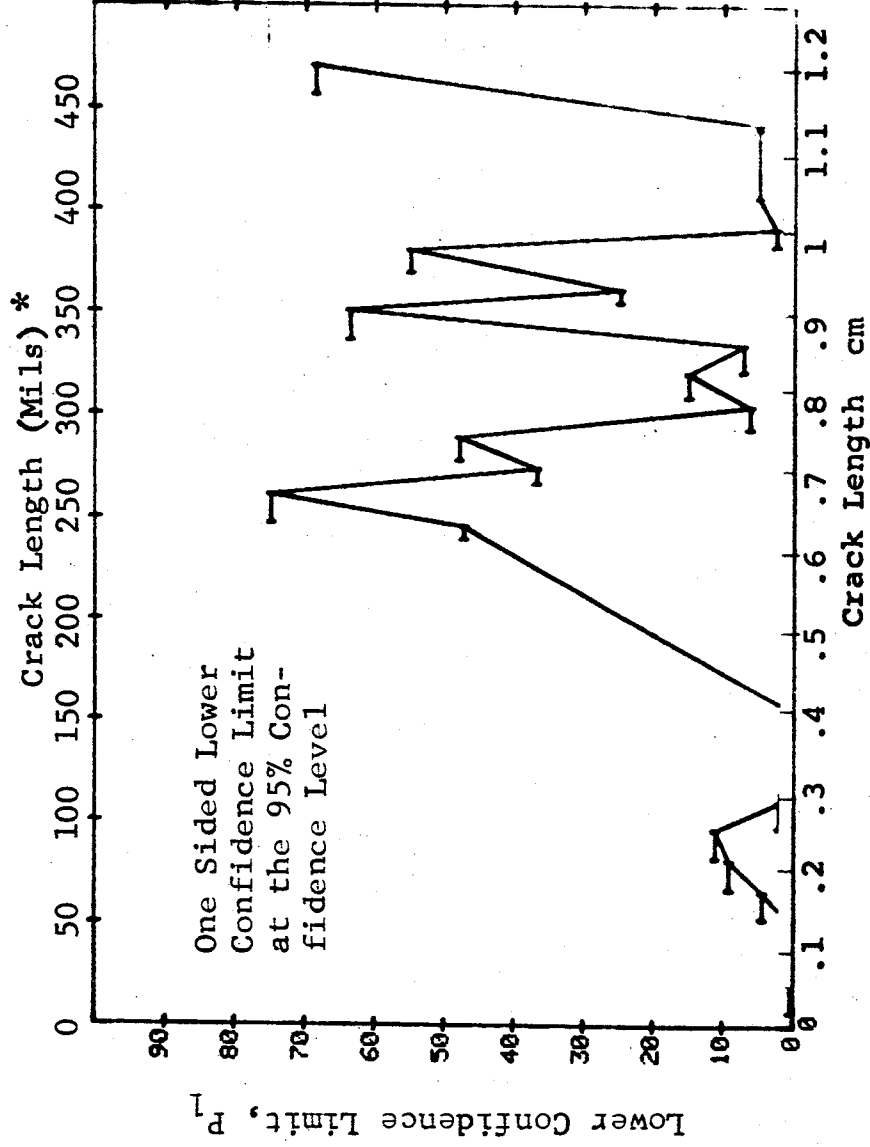


Figure D-27 Probability of Detection for 2219-T87 Al Using X-ray. Etched Fatigue Cracks in Flat Plates Measured by Operator B. Lab. Env.

(b) Optimum Probability Method of Data Cumulation

03-JUL-75 RADIOGRAPHY				TEST 2, ROOMWELL SC. '0' (27)			
RANGE	MIN	LN	* *	DET	SUC.	MISS	MISS
1	1	7	22	1	0	0	0
2	2	7	36	2	0	0	0
3	3	7	67	3	1	0	0
4	4	54	67	4	1	0	0
5	54	68	82	5	4	0	0
6	68	68	97	6	9	0	0
7	68	111	97	7	12	0	0
8	68	126	111	8	11	0	0
9	54	141	126	9	10	0	0
10	54	157	141	10	8	0	0
11	68	171	157	11	8	0	0
12	54	185	171	12	8	0	0
13	54	197	185	13	8	0	0
14	0	0	197	14	0	0	0
15	0	0	0	15	0	0	0
16	241	241	0	16	0	0	0
17	241	241	247	17	0	0	0
18	241	241	262	18	47	0	0
19	241	241	275	19	79	0	0
20	241	241	290	20	81	22	36
21	241	241	306	21	81	30	45
22	241	241	322	22	70	0	0
23	338	338	336	23	61	0	0
24	338	338	352	24	52	0	0
25	338	338	362	25	63	0	0
26	338	338	381	26	63	0	0
27	338	338	393	27	71	0	0
28	338	338	408	28	68	0	0
29	338	338	426	29	69	0	0
30	338	338	442	30	65	0	0
31	338	338	444	31	68	0	0
32	442	442	472	32	75	0	0
			979	33	85	34	47
				34			

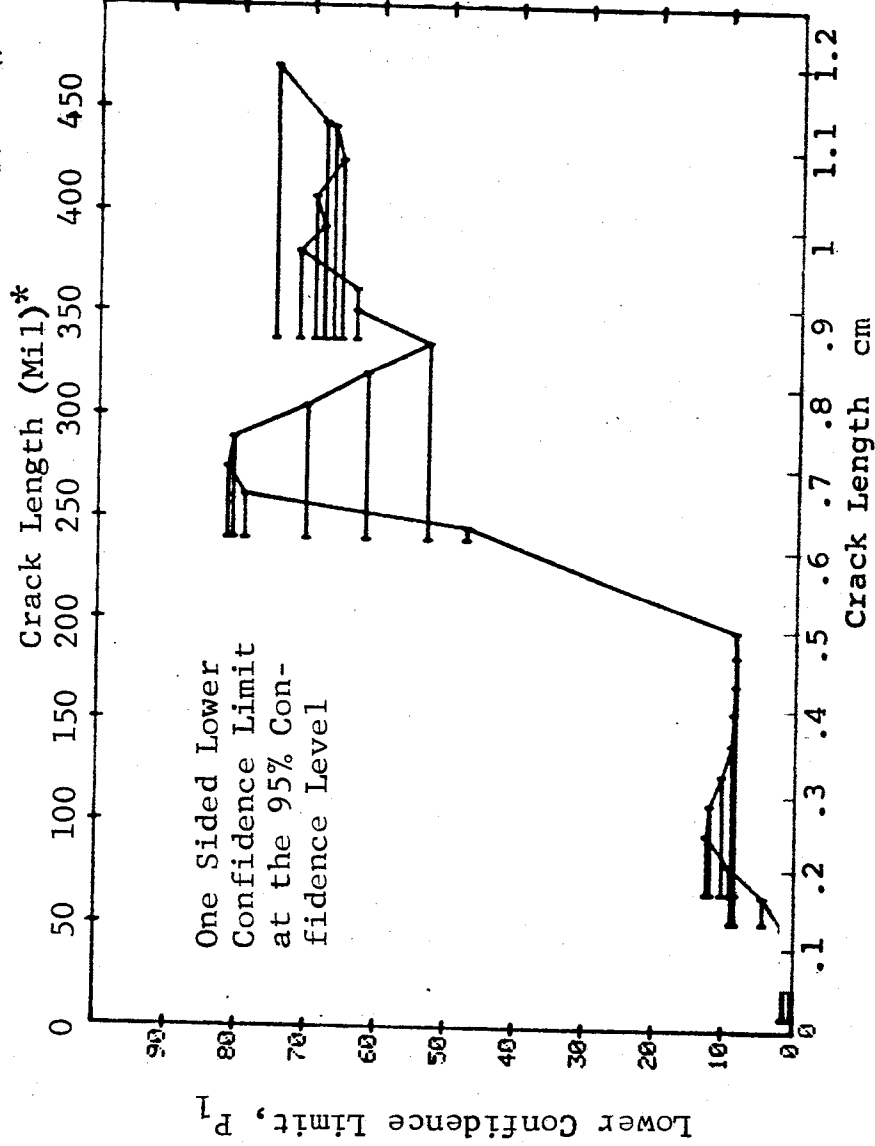


Figure D-27 (Continued)

(c) Overlapping Sixty Point Method of Data Cumulation

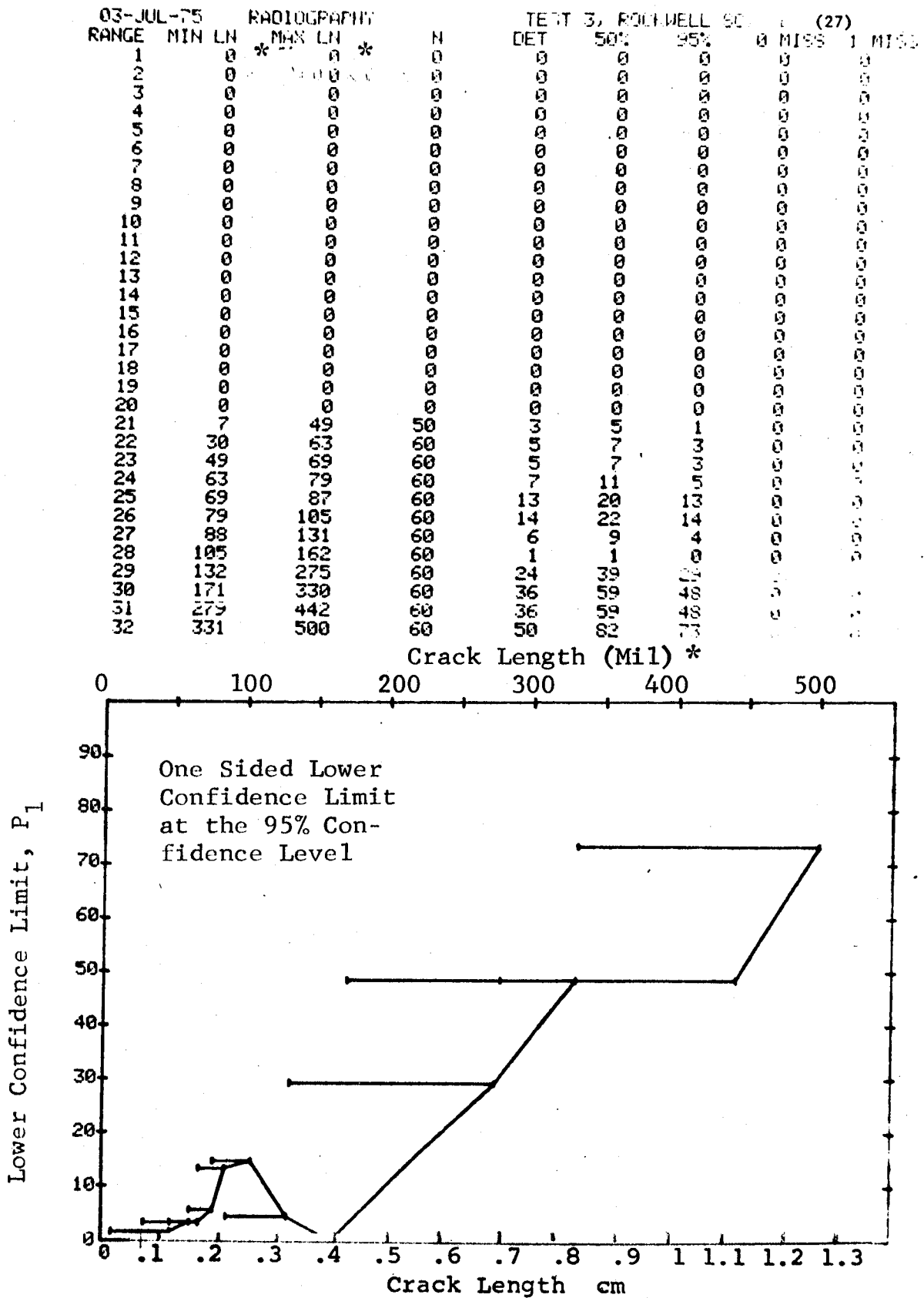


Figure D-27 (Concluded)

(a) Range Interval Method of Data Cumulation

23-JUL-75			RADIOGRAPHY		TEST 1, DEN=20, ROCKWELL C, 1 MI (28)	
RANGE	MIN	LN	MAX	LN	DET	50C
1	1	7	22	*	0	0
2	25	38	55	*	0	0
3	38	54	67	*	0	0
4	54	68	82	*	0	0
5	68	83	97	*	1	0
6	83	98	111	*	1	0
7	98	115	126	*	3	0
8	115	129	141	*	6	0
9	129	143	157	*	15	0
10	143	158	171	*	3	0
11	158	182	185	*	4	0
12	182	190	197	*	0	0
13	190	0	0	*	0	0
14	0	0	0	*	0	0
15	0	0	0	*	0	0
16	241	247	262	*	0	0
17	248	268	275	*	61	24
18	268	279	290	*	84	61
19	279	295	306	*	50	13
20	295	310	322	*	50	22
21	310	323	336	*	10	0
22	323	338	352	*	16	0
23	338	356	362	*	76	0
24	356	370	381	*	61	52
25	370	384	393	*	68	24
26	384	408	426	*	70	22
27	408	426	442	*	0	0
28	426	442	444	*	0	0
29	442	458	472	*	0	0
30	458	474	479	*	50	0
31	474	0	0	*	79	5
32	0	0	0	*	30	51
					48	71
					59	0

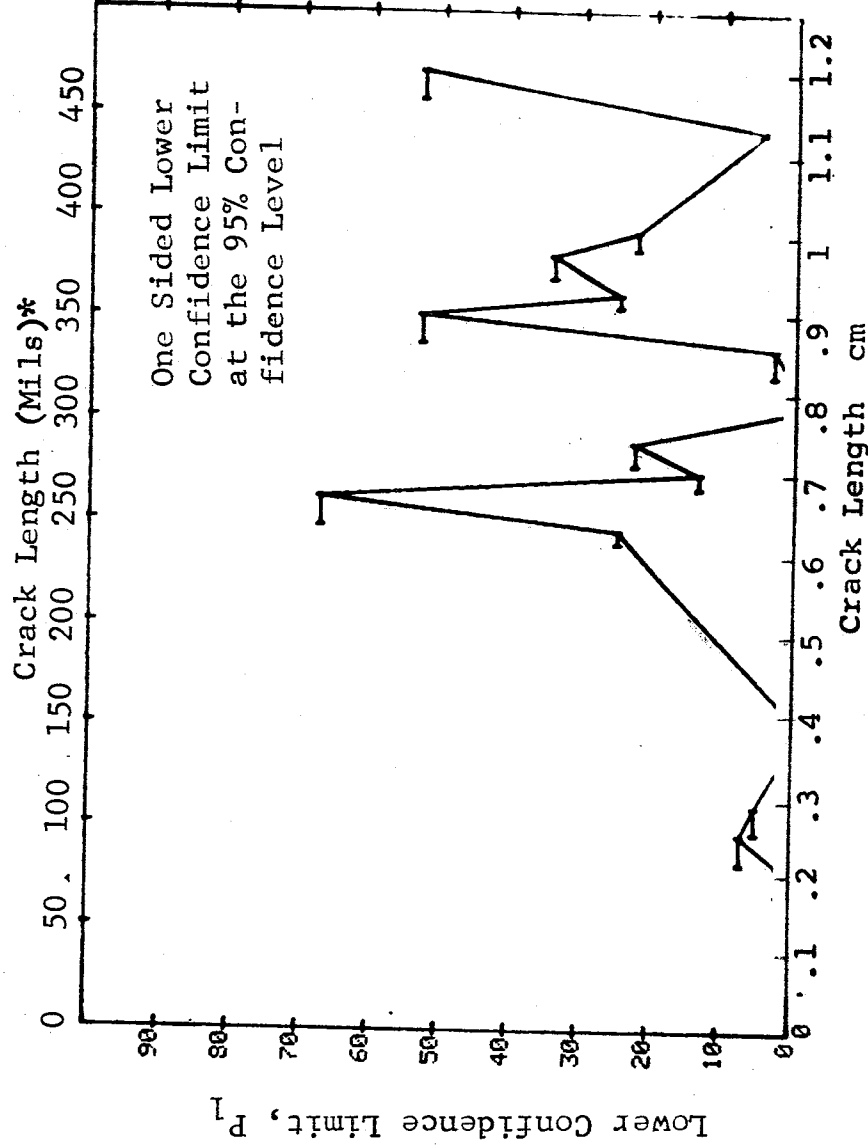


Figure D-28 Probability of Detection for 2219-T87 Al Using X-ray. Etched Fatigue Cracks in Flat Plates Measured by Operator C. Lab. Env. D-84

(b) Optimum Probability Method of Data Cumulation

23-JUL-75			RADIOGRAPHY			TEST 2, DSH=20, ROCKWELL 30, c (28)				
RANGE	MIN	LN	MAX	LN	N	DET	50%	95%	0 MISS	1 MISS
1		7 *	22 *		13	0	0	0	0	0
2	25		36		13	0	0	0	0	0
3	38		52		23	1	0	0	0	0
4	38		67		69	2	0	0	0	0
5	38		82		122	5	0	1	0	0
6	83		97		39	6	0	6	0	0
7	83		111		56	9	0	8	0	0
8	83		126		73	9	0	6	0	0
9	83		141		92	10	0	6	0	0
10	83		157		107	11	0	5	0	0
11	83		171		110	11	0	5	0	0
12	83		185		113	11	0	5	0	0
13	83		197		115	11	0	5	0	0
14	0		0		0	0	0	0	0	0
15	0		0		0	0	0	0	0	0
16	241		247		4	3	0	24	0	0
17	248		262		17	15	0	67	0	0
18	241		275		24	20	0	65	0	0
19	241		290		31	24	0	61	0	0
20	241		306		37	25	0	52	0	0
21	241		322		47	26	0	42	0	0
22	241		336		59	28	0	36	0	0
23	338		352		11	9	0	52	0	0
24	338		362		15	12	0	56	0	0
25	338		381		20	16	0	59	0	0
26	338		393		22	18	0	63	0	0
27	338		408		23	18	0	59	0	0
28	338		426		24	18	0	56	0	0
29	338		442		25	19	0	52	0	0
30	338		444		26	20	0	52	0	0
31	338		472		34	27	0	64	0	0
32	442		979		69	57	0	73	0	0

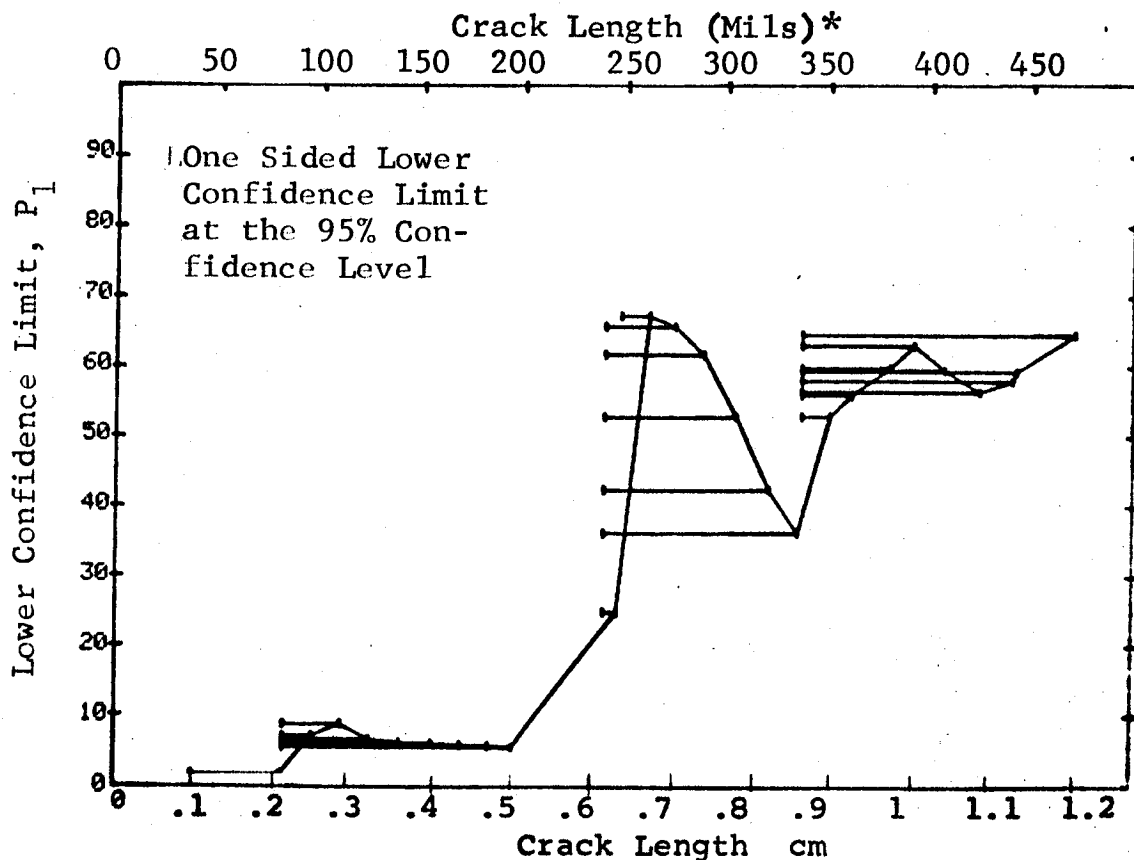


Figure D-28 (Continued)

(c) Overlapping Sixty Point Method of Data Cumulation

23-JUL-75		RADIOGRAPHY		N	TEST 3, DSH=20, ROCKWELL SC. (28) c				
RANGE	MIN LN	* MAX LN	* LN		DET	50%	95%	0 MISS	1 MISS
1	0	*	0	0	0	0	0	0	0
2	0		0	0	0	0	0	0	0
3	0		0	0	0	0	0	0	0
4	0		0	0	0	0	0	0	0
5	0		0	0	0	0	0	0	0
6	0		0	0	0	0	0	0	0
7	0		0	0	0	0	0	0	0
8	0		0	0	0	0	0	0	0
9	0		0	0	0	0	0	0	0
10	0		0	0	0	0	0	0	0
11	0		0	0	0	0	0	0	0
12	0		0	0	0	0	0	0	0
13	0		0	0	0	0	0	0	0
14	0		0	0	0	0	0	0	0
15	0		0	0	0	0	0	0	0
16	0		0	0	0	0	0	0	0
17	0		0	0	0	0	0	0	0
18	0		0	0	0	0	0	0	0
19	0		0	0	0	0	0	0	0
20	0		0	0	0	0	0	0	0
21	7	49	52	1	1	1	0	0	0
22	31	63	60	2	2	2	0	0	0
23	51	70	60	1	1	1	0	0	0
24	64	79	60	1	1	1	0	0	0
25	70	87	60	9	14	8	0	0	0
26	79	105	60	10	16	9	0	0	0
27	88	131	60	4	6	2	0	0	0
28	105	162	60	3	4	1	0	0	0
29	132	275	60	21	34	24	0	0	0
30	171	330	60	27	44	33	0	0	0
31	279	442	60	27	44	33	0	0	0
32	331	500	60	43	70	60	0	0	0

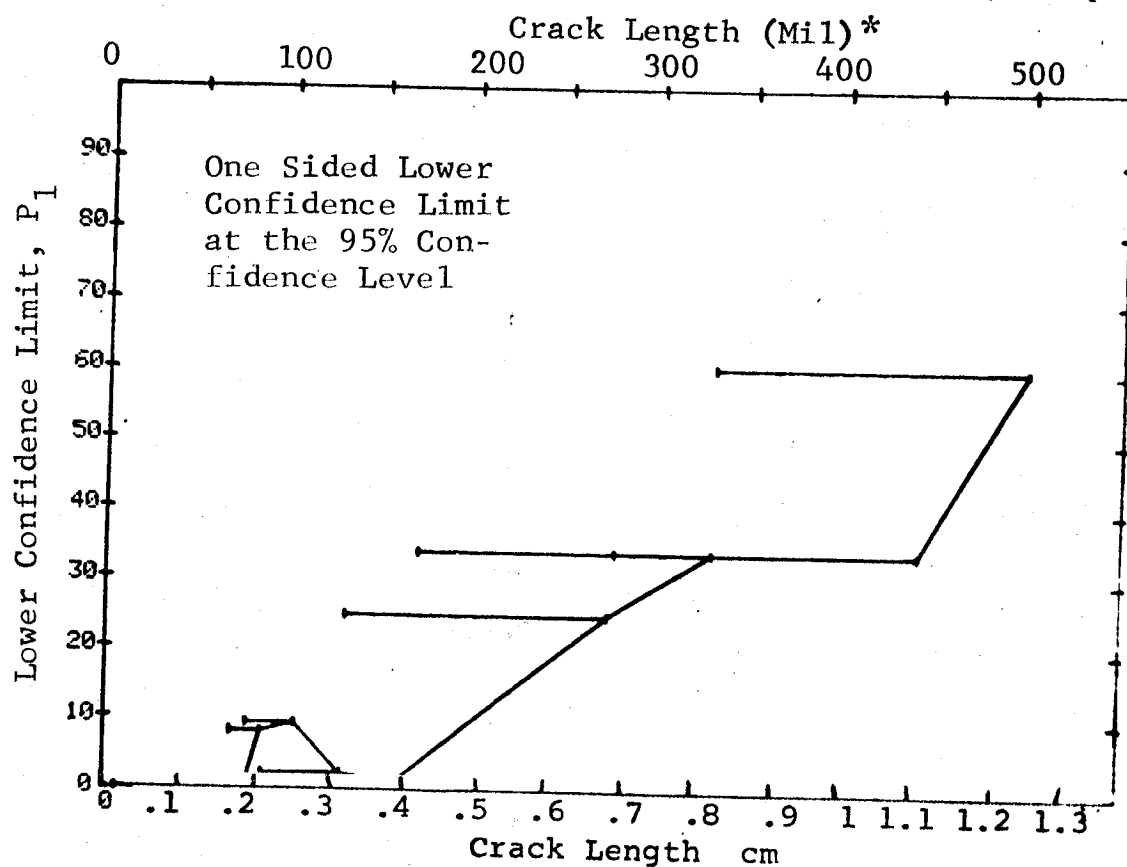


Figure D-28 (Concluded)

(a) Range Interval Method of Data Cumulation

23-JUL-75 RADIOGRAPHY				TEST 1, DSN=21, ROCKWELL SC. D (29)				
RANGE	MIN LN	* MAX LN *	N	DET	50%	95%	0 MISS	1 MISS
1	7	32	13	1	5	0	0	0
2	25	36	18	2	9	2	0	0
3	38	52	23	2	7	1	0	0
4	54	67	46	7	14	7	0	0
5	68	82	53	9	16	9	0	0
6	83	97	39	16	39	27	0	0
7	98	111	17	6	32	16	0	0
8	115	126	17	1	3	0	0	0
9	129	141	19	3	13	4	0	0
10	143	157	15	2	10	2	0	0
11	158	171	3	0	0	0	0	0
12	182	185	3	0	0	0	0	0
13	190	197	2	1	29	2	0	0
14	0	0	0	0	0	0	0	0
15	0	0	0	0	0	0	0	0
16	241	247	4	3	61	24	0	0
17	248	262	17	16	90	75	29	44
18	268	275	3	3	79	36	0	0
19	279	290	7	3	36	12	0	0
20	295	306	6	1	10	0	0	0
21	310	322	10	3	25	8	0	0
22	323	336	12	4	29	12	0	0
23	338	352	11	8	67	43	0	0
24	356	362	4	3	61	24	0	0
25	370	381	5	5	87	54	0	0
26	384	393	2	2	70	22	0	0
27	408	408	1	0	0	0	0	0
28	426	426	1	0	0	0	0	0
29	442	442	1	1	50	5	0	0
30	444	444	1	1	50	5	0	0
31	456	472	8	8	91	68	0	0
32	474	979	59	58	97	92	0	0

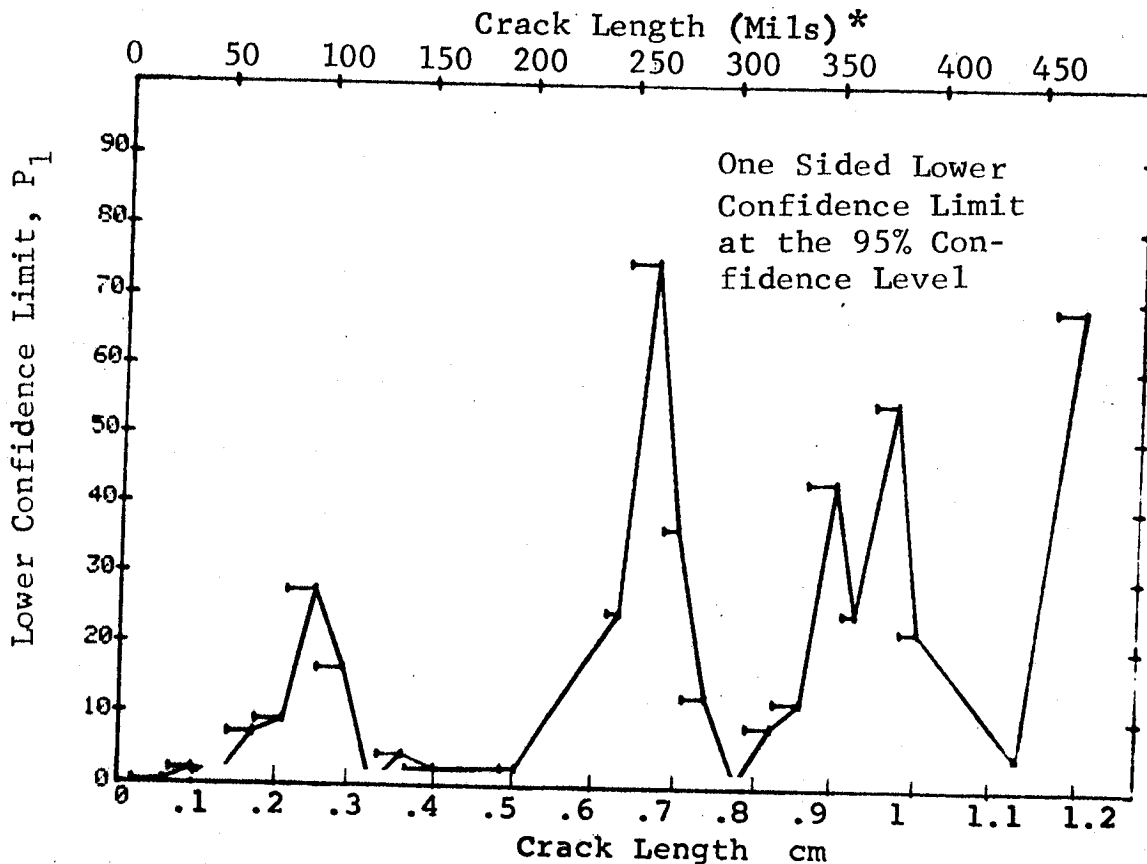


Figure D-29 Probability of Detection for 2219-T87 Al Using X-ray. Etched Fatigue Cracks in Flat Plates Measured by Operator D. Lab. Env.

(b) Optimum Probability Method of Data Cumulation

23-JUL-75		RADIOGRAPHY			TEST 2, DSN=21, ROCKWELL C, D (29)					
RANGE	MIN LN	* MAX LN	* N	DET	50%	95%	0 MISS	1 MISS		
1	7	22	13	1	0	0	0	0		
2	7	36	21	3	0	2	0	0		
3	7	52	54	5	0	3	0	0		
4	54	67	46	7	0	7	0	0		
5	54	82	99	16	0	10	0	0		
6	83	97	39	16	0	27	0	0		
7	83	111	56	22	0	28	0	0		
8	83	126	73	23	0	22	0	0		
9	83	141	92	26	0	20	0	0		
10	83	157	107	28	0	19	0	0		
11	83	171	110	28	0	18	0	0		
12	83	185	113	28	0	18	0	0		
13	83	197	115	29	0	18	0	0		
14	0	0	0	0	0	0	0	0		
15	0	0	0	0	0	0	0	0		
16	190	247	6	4	0	27	0	0		
17	248	262	17	16	0	75	0	0		
18	248	275	20	19	0	78	0	0		
19	241	290	31	25	0	65	0	0		
20	241	306	37	26	0	55	0	0		
21	241	322	47	29	0	48	0	0		
22	241	336	59	33	0	44	0	0		
23	241	352	70	41	0	48	0	0		
24	241	362	74	44	0	44	0	0		
25	338	381	20	16	0	59	0	0		
26	370	393	7	7	0	65	0	0		
27	338	408	23	18	0	59	0	0		
28	338	426	24	18	0	56	0	0		
29	338	442	25	19	0	56	0	0		
30	338	444	26	20	0	50	0	0		
31	442	472	10	10	0	74	0	0		
32	442	479	69	68	0	93	0	0		

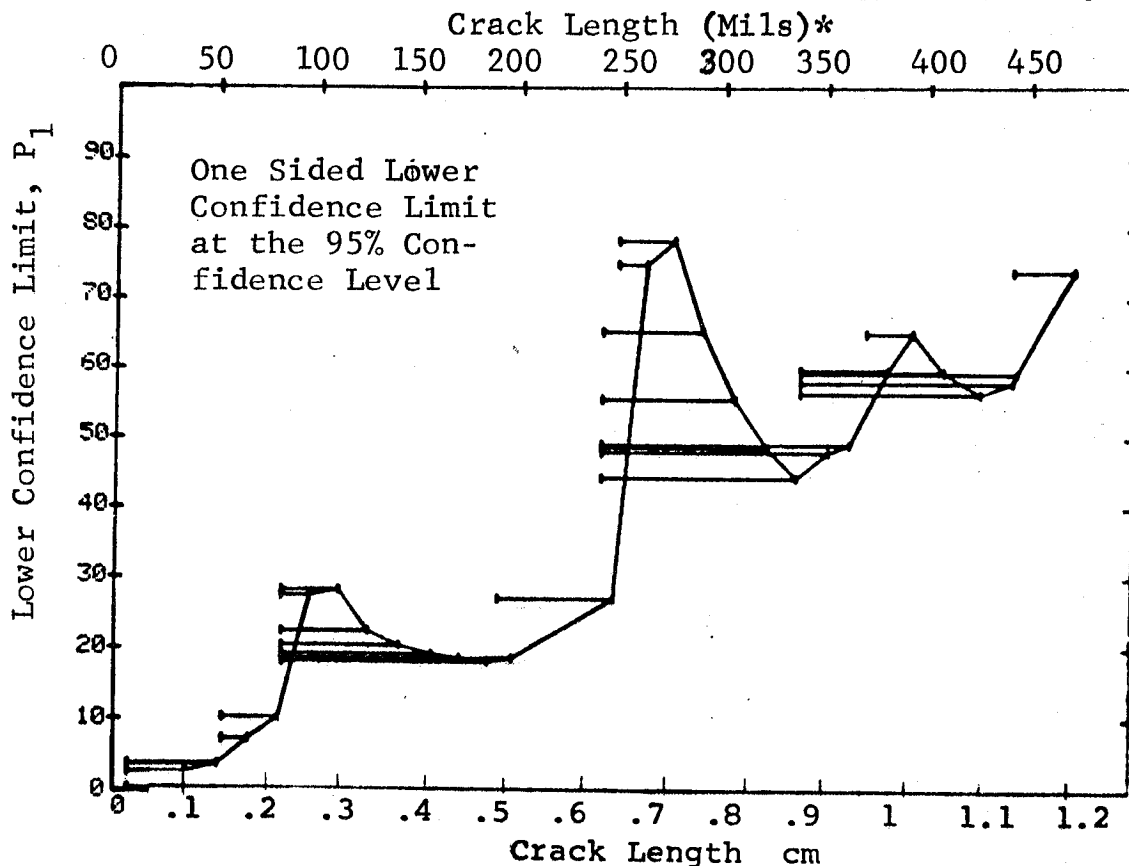


Figure D-29 (Continued)

(c) Overlapping Sixty Point Method of Data Cumulation

23-JUL-75	RADIOGRAPHY	TEST	3. DSN#21, ROCKWELL SC	D (29)
RANGE MIN LN	MAX LN *	DET	50% 95% 0 MISS 1 MISS	
1	0	0	0	0
2	0	0	0	0
3	0	0	0	0
4	0	0	0	0
5	0	0	0	0
6	0	0	0	0
7	0	0	0	0
8	0	0	0	0
9	0	0	0	0
10	0	0	0	0
11	0	0	0	0
12	0	0	0	0
13	0	0	0	0
14	0	0	0	0
15	0	0	0	0
16	0	0	0	0
17	0	0	0	0
18	0	0	0	0
19	0	0	0	0
20	0	0	0	0
21	7	4	7	0
22	31	10	16	0
23	51	9	14	0
24	64	7	11	0
25	70	16	35	0
26	79	24	29	0
27	88	15	16	0
28	105	7	11	0
29	132	28	45	0
30	171	32	52	0
31	279	30	49	0
32	331	51	83	0
			94	100

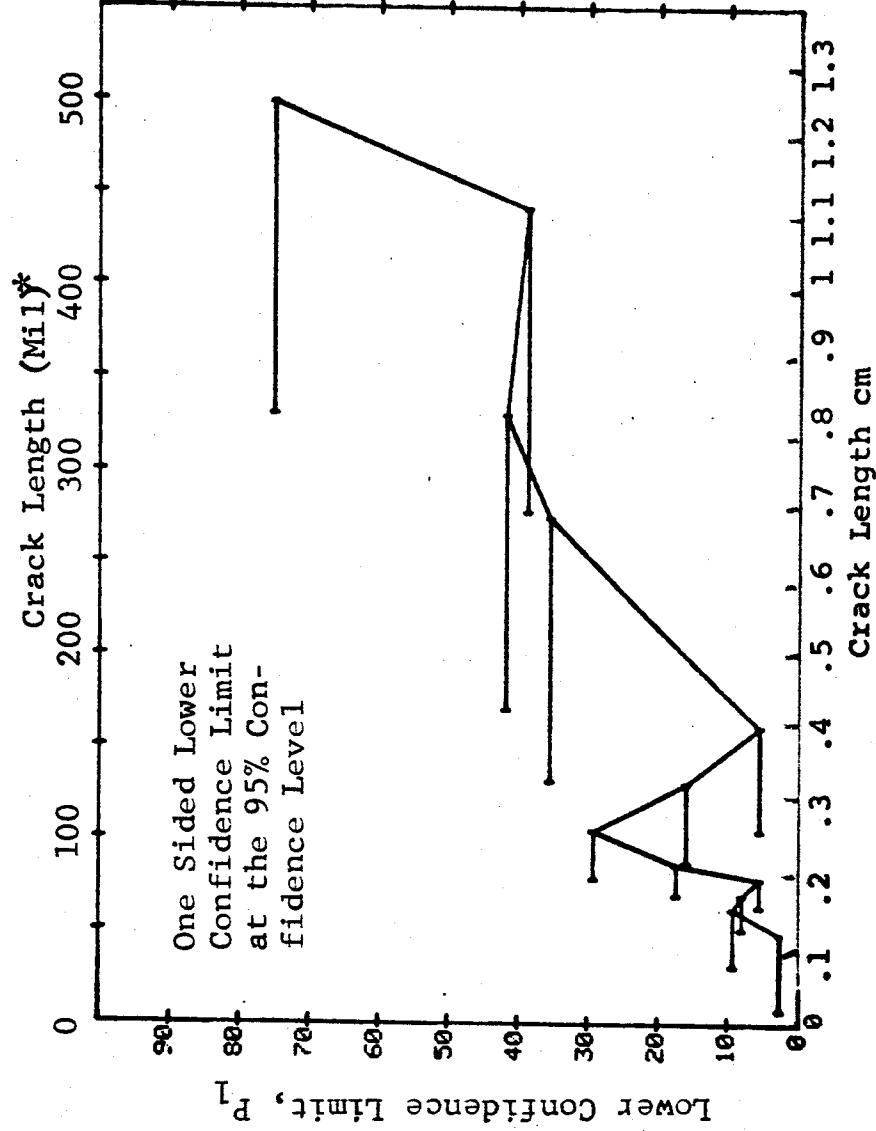


Figure D-29 (Concluded)

(a) Range Interval Method of Data Cumulation

23-JUL-75	RANGE MIN	LN	RADIOGRAPHY	TEST 1	DET	50%	95%	(30)	E	MISS	MISS
1	1	20	18*	0	0	0	0	0	0	0	0
2	2	30	28	3	3	23	7	0	0	0	0
3	3	41	40	1	1	4	7	0	0	0	0
4	4	52	51	4	4	18	7	0	0	0	0
5	5	63	62	8	8	29	16	0	0	0	0
6	6	74	73	13	13	29	16	0	0	0	0
7	7	85	84	15	15	38	26	0	0	0	0
8	8	96	95	12	12	44	29	0	0	0	0
9	9	108	106	6	6	29	14	0	0	0	0
10	10	118	117	1	1	8	0	0	0	0	0
11	11	129	126	1	1	12	0	0	0	0	0
12	12	140	138	2	2	10	0	0	0	0	0
13	13	151	150	2	2	12	0	0	0	0	0
14	14	162	158	1	1	10	0	0	0	0	0
15	15	171	171	1	1	29	0	0	0	0	0
16	16	182	183	1	1	29	0	0	0	0	0
17	17	185	190	1	1	29	0	0	0	0	0
18	18	197	197	1	1	50	0	0	0	0	0
19	19	0	0	0	0	0	0	0	0	0	0
20	20	0	0	0	0	0	0	0	0	0	0
21	21	0	0	0	0	0	0	0	0	0	0
22	22	241	249	0	0	0	0	0	0	0	0
23	23	250	260	0	0	0	0	0	0	0	0
24	24	261	269	7	7	90	65	0	18	0	0
25	25	275	279	11	11	93	76	0	0	0	0
26	26	283	290	5	5	87	54	0	0	0	0
27	27	295	304	5	5	79	56	0	0	0	0
28	28	306	313	4	4	87	54	0	0	0	0
29	29	317	326	5	5	68	54	0	0	0	0
30	30	328	336	3	3	63	54	0	0	0	0
31	31	338	347	4	4	32	19	0	0	0	0
32	32	352	362	6	6	44	34	0	0	0	0
				3	3	61	24	0	0	0	0

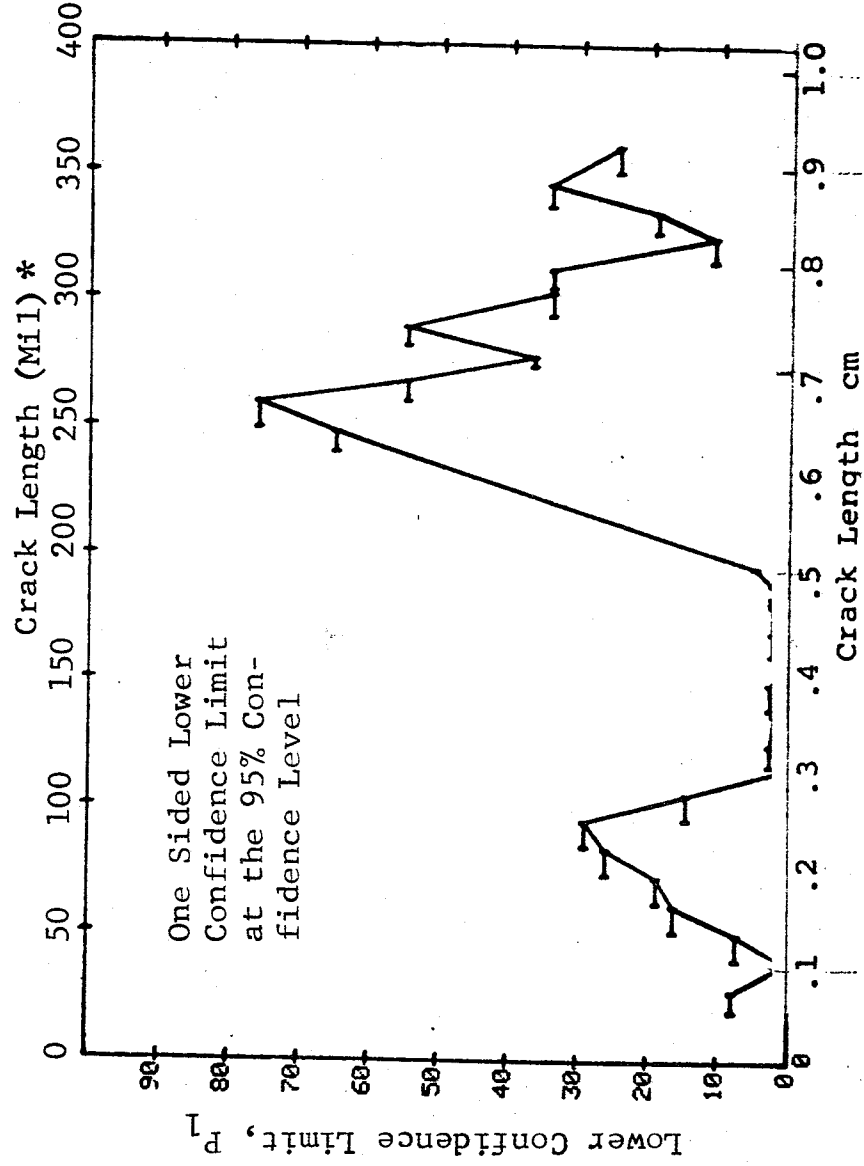


Figure D-30 Probability of Detection for 2219-T87 Al Using X-ray. Etched Fatigue Cracks in Flat Plates Measured by Operator E. Lab. Env. D-90

3

(b) Overlapping Sixty Point Method of Data Cumulation

23-JUL-75		RADIOGRAPHY		N	TEST 2, 1		(30). ROCKWELL SC		E
RANGE	MIN LN	* MAX LN *			DET	50%	95%	0 MISS	
1	7	18	8	0	0	0	0	0	0
2	20	28	11	3	0	7	0	0	0
3	20	40	26	4	0	5	0	0	0
4	20	51	45	8	0	9	0	0	0
5	52	62	26	3	0	16	0	0	0
6	52	73	69	21	0	21	0	0	0
7	74	84	38	15	0	26	0	0	0
8	74	95	64	27	0	31	0	0	0
9	74	106	83	33	0	30	0	0	0
10	74	117	91	34	0	28	0	0	0
11	63	126	147	49	0	26	0	0	0
12	52	138	189	59	0	25	0	0	0
13	52	150	202	61	0	24	0	0	0
14	52	158	208	62	0	24	0	0	0
15	52	171	210	63	0	24	0	0	0
16	52	183	212	64	0	25	0	0	0
17	52	190	214	65	0	25	0	0	0
18	63	197	189	58	0	25	0	0	0
19	0	0	0	0	0	0	0	0	0
20	0	0	0	0	0	0	0	0	0
21	0	0	0	0	0	0	0	0	0
22	197	249	8	8	0	68	0	0	0
23	197	260	19	19	0	85	10	27	0
24	197	269	24	24	0	88	5	22	0
25	197	279	27	27	0	89	2	19	0
26	197	290	32	32	0	91	0	14	0
27	197	304	37	36	0	87	9	24	0
28	197	313	44	41	0	83	32	45	0
29	197	326	52	44	0	73	0	0	0
30	197	336	60	48	0	69	0	0	0
31	197	347	69	54	0	68	0	0	0
32	197	362	73	57	0	68	0	0	0

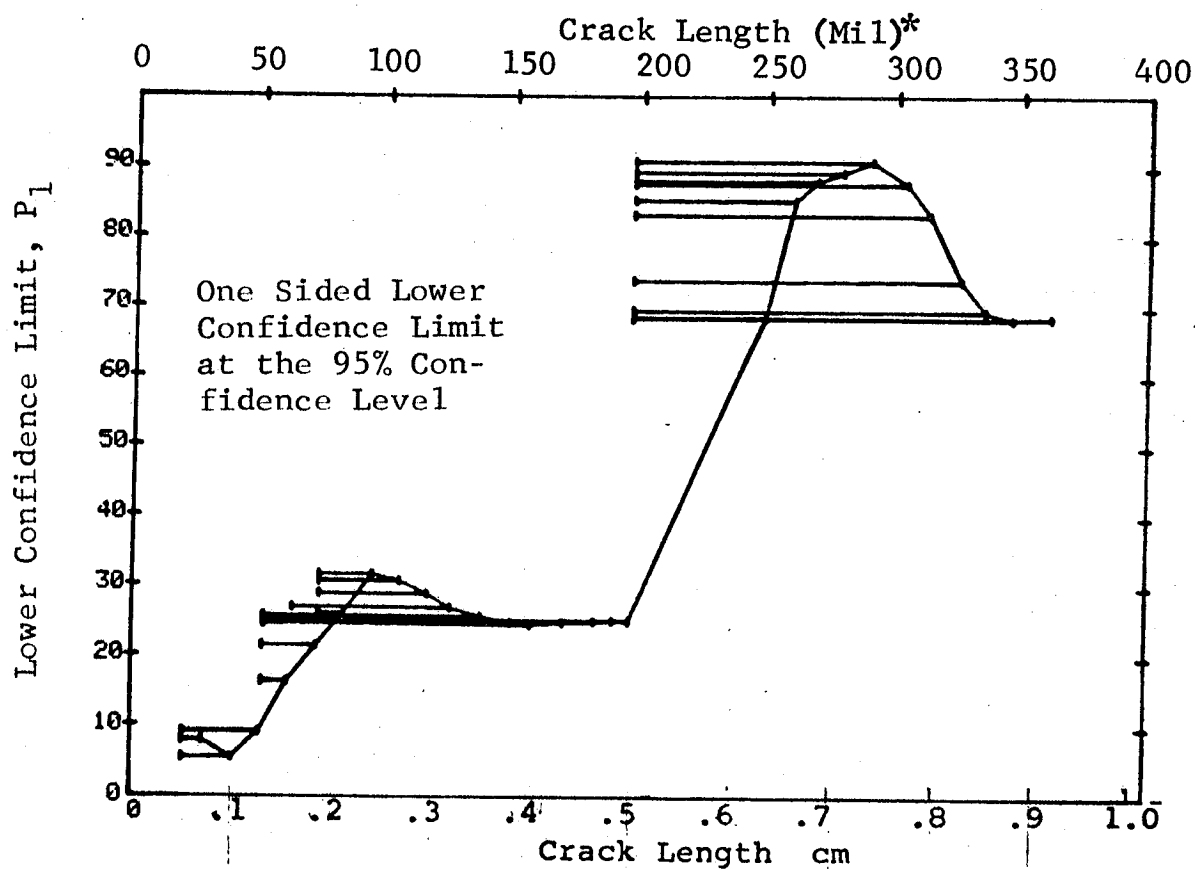


Figure D-30 (Continued)

(c) Overlapping Sixty Point Method of Data Cumulation

23-JUL-75		RADIOGRAPHY		N	TEST 3. (30)		ROCKWELL SC E		
RANGE	MIN LN	* MAX LN	*		DET	50%	95%	0 MISS	1 MISS
1	0	0	*	0	0	0	0	0	0
2	0	0		0	0	0	0	0	0
3	0	0		0	0	0	0	0	0
4	0	0		0	0	0	0	0	0
5	0	0		0	0	0	0	0	0
6	0	0		0	0	0	0	0	0
7	0	0		0	0	0	0	0	0
8	0	0		0	0	0	0	0	0
9	0	0		0	0	0	0	0	0
10	0	0		0	0	0	0	0	0
11	0	0		0	0	0	0	0	0
12	0	0		0	0	0	0	0	0
13	0	0		0	0	0	0	0	0
14	0	0		0	0	0	0	0	0
15	0	0		0	0	0	0	0	0
16	0	0		0	0	0	0	0	0
17	0	0		0	0	0	0	0	0
18	0	0		0	0	0	0	0	0
19	0	0		0	0	0	0	0	0
20	0	0		0	0	0	0	0	0
21	0	0		0	0	0	0	0	0
22	7	44		40	5	11	5	0	0
23	21	60		60	12	19	11	0	0
24	45	67		60	17	27	18	0	0
25	61	76		60	19	30	21	0	0
26	68	84		60	22	35	26	0	0
27	76	97		60	25	40	30	0	0
28	85	123		60	20	32	23	0	0
29	97	144		60	12	19	11	0	0
30	124	257		60	22	35	26	0	0
31	145	313		60	45	74	64	0	0
32	257	362		60	44	72	62	0	0

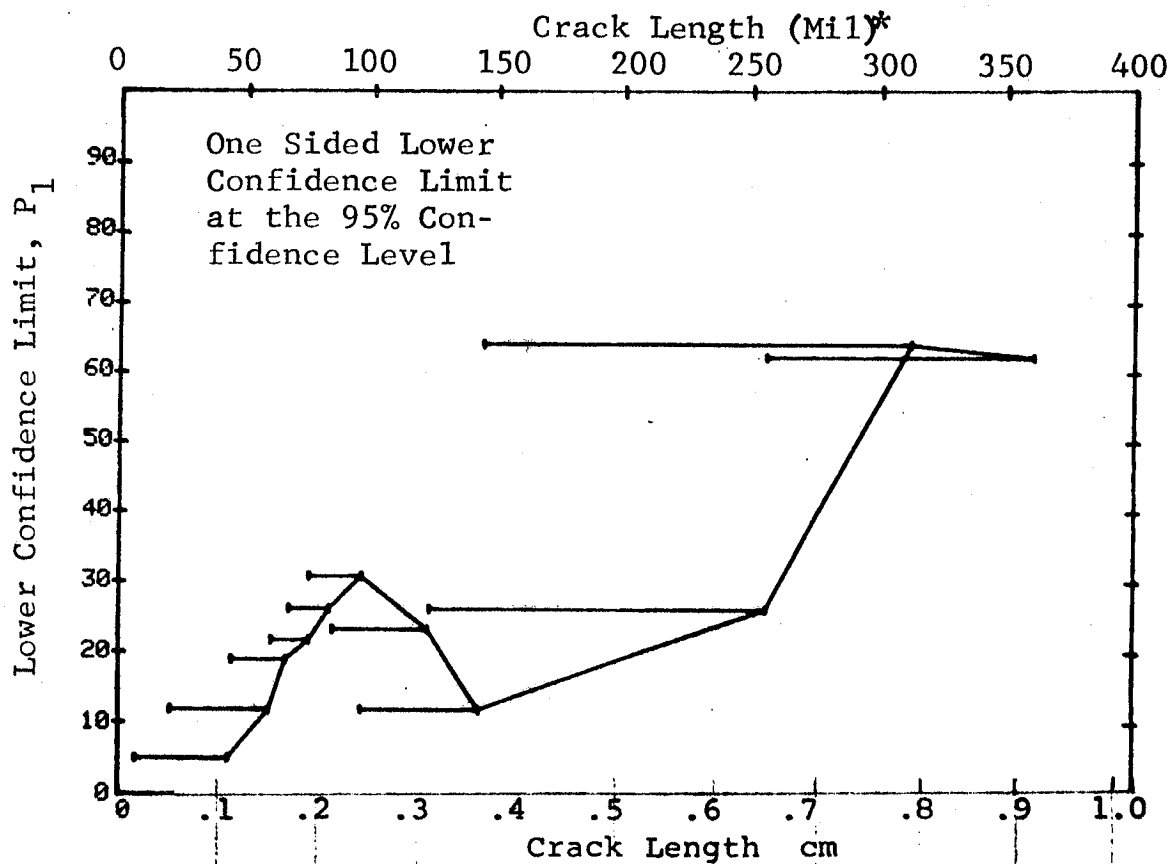


Figure D-30 (Concluded)

(a) Range Interval Method of Data Cumulation

23-JUL-75 RADIOGRAPHY				TEST 1, (31)				F	
RANGE	MIN LN	* MAX LN	N	DET	50%	95%	0 MISS	1 MISS	
1	7	22	13	2	12	2	0	0	
2	25	36	18	3	14	4	0	0	
3	38	52	23	7	28	15	0	0	
4	54	67	46	13	27	17	0	0	
5	68	82	53	23	42	31	0	0	
6	83	97	39	18	44	32	0	0	
7	98	111	17	5	26	12	0	0	
8	115	126	16	4	22	9	0	0	
9	129	141	20	5	22	10	0	0	
10	143	157	15	0	50	29	0	0	
11	158	171	3	2	50	13	0	0	
12	182	185	3	2	50	13	0	0	
13	190	197	2	1	29	0	0	0	
14	0	0	0	0	0	0	0	0	
15	0	0	0	0	0	0	0	0	
16	241	247	4	4	84	47	0	0	
17	248	262	17	16	90	75	29	44	
18	268	275	3	3	79	36	0	0	
19	279	290	7	6	77	47	0	0	
20	295	306	6	5	73	41	0	0	
21	310	322	10	4	35	15	0	0	
22	323	336	12	9	70	47	0	0	
23	338	352	11	9	76	52	0	0	
24	356	362	4	2	38	9	0	0	
25	370	381	5	4	68	34	0	0	
26	384	393	2	2	70	22	0	0	
27	408	408	1	1	50	5	0	0	
28	426	426	1	0	0	0	0	0	
29	442	442	1	1	50	5	0	0	
30	444	444	1	0	0	0	0	0	
31	458	472	8	5	67	40	0	0	
32	474	979	59	51	85	76	83	95	

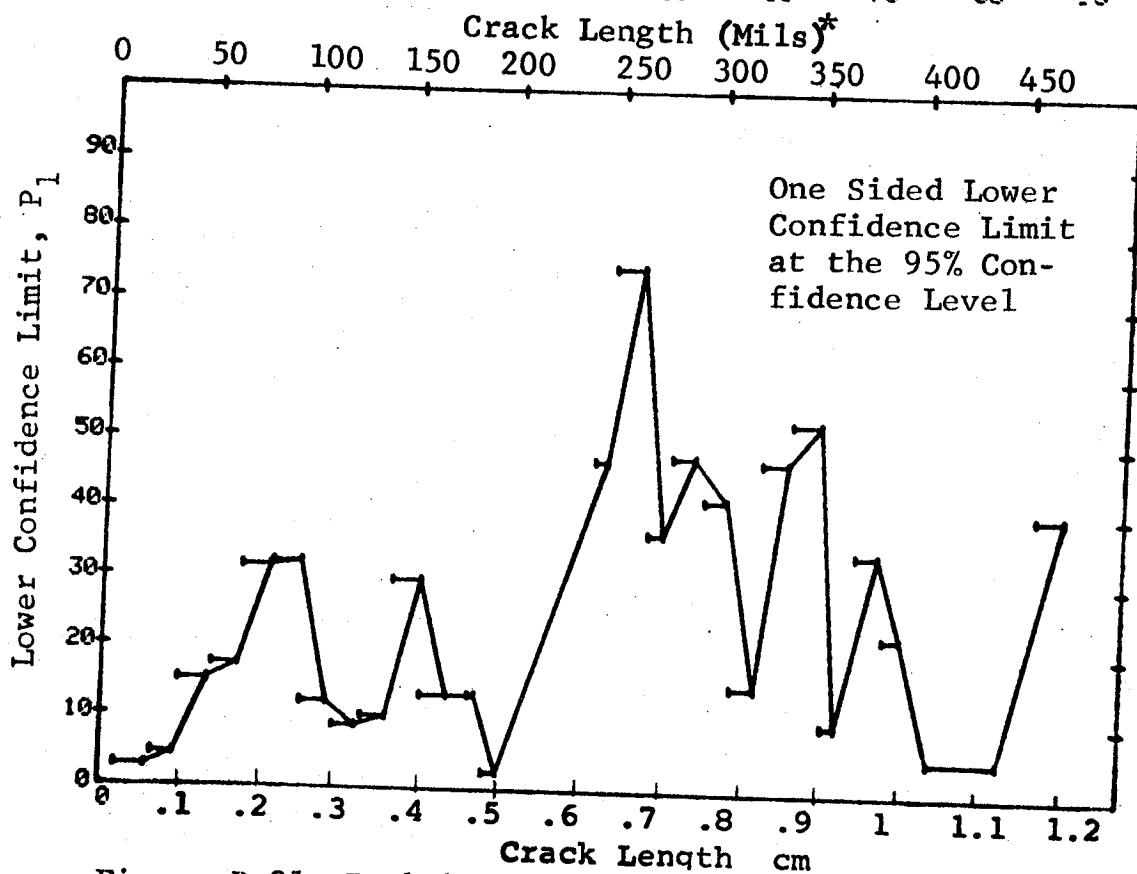


Figure D-31 Probability of Detection for 2219-T87 Al Using X-ray. Etched Fatigue Cracks in Flat Plates Measured by Operator F. Lab. Env.

(b) Optimum Probability Method of Data Cumulation

23-JUL-75				RADIOGRAPHY		TEST 2, (31)		ROCKWELL SC		P	
RANGE	MIN	LN	MAX	LN	N	DET	50%	95%	0 MISS	1 MISS	1 MISS
1	7	7	7	22 *	13	2	0	2	0	0	0
2	7	7	86	52	31	5	0	6	0	0	0
3	38	38	67	82	23	7	0	15	0	0	0
4	38	38	67	82	69	20	0	20	0	0	0
5	68	68	97	111	53	23	0	31	0	0	0
6	68	68	97	111	92	41	0	35	0	0	0
7	68	68	126	141	109	46	0	34	0	0	0
8	68	68	126	141	125	50	0	32	0	0	0
9	68	68	157	171	145	55	0	31	0	0	0
10	143	143	185	197	160	63	0	32	0	0	0
11	143	143	185	197	18	10	0	34	0	0	0
12	143	143	185	197	21	12	0	37	0	0	0
13	143	143	185	197	23	13	0	37	0	0	0
14	0	0	0	0	0	0	0	0	0	0	0
15	0	0	0	0	0	0	0	0	0	0	0
16	241	241	262	275	4	4	0	47	0	0	0
17	241	241	262	275	21	20	0	79	0	0	0
18	241	241	290	306	24	23	0	81	22	37	37
19	241	241	306	322	31	29	0	81	30	45	45
20	241	241	306	322	37	34	0	80	39	52	52
21	241	241	336	352	47	38	0	69	0	0	0
22	241	241	352	362	59	47	0	70	0	0	0
23	241	241	362	381	70	56	0	69	0	0	0
24	241	241	381	393	74	58	0	70	0	0	0
25	241	241	408	426	79	62	0	69	0	0	0
26	241	241	426	442	81	64	0	70	0	0	0
27	241	241	442	472	82	65	0	70	0	0	0
28	241	241	442	472	83	65	0	69	0	0	0
29	241	241	442	472	84	66	0	69	0	0	0
30	241	241	472	479	85	66	0	68	0	0	0
31	241	241	472	479	85	72	0	69	0	0	0
32	474	474	479	479	59	51	0	76	0	0	0

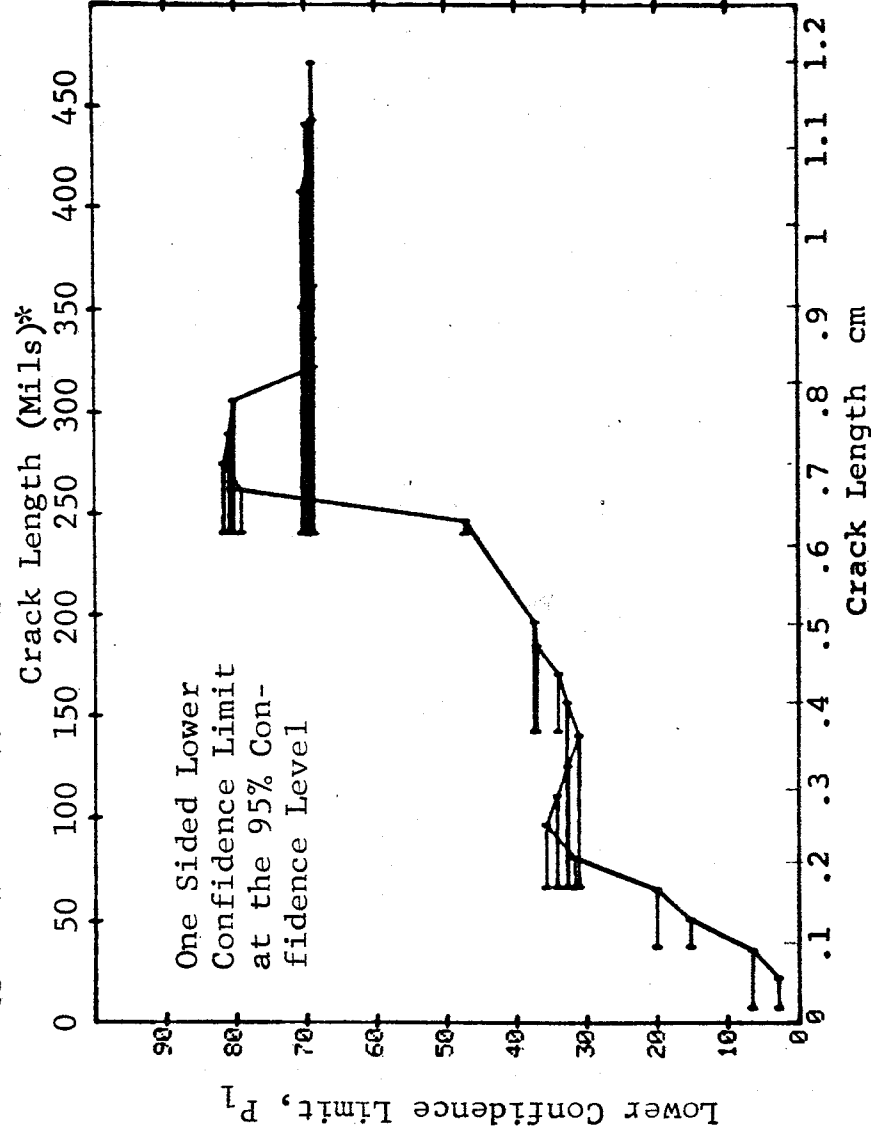


Figure D-31 (Continued)

D-94

REPRODUCIBILITY OF THE
ORIGINAL PAGE IS POOR

(c) Overlapping Sixty Point Method of Data Cumulation

23-JUL-75			RADIOGRAPHY		TEST 3A (31)		ROCKWELL SC F	
RANGE	MIN	LN	MAX	LN *	DET	50%	95%	MISS
1	1	0	0	0	0	0	0	0
2	1	0	0	0	0	0	0	0
3	1	0	0	0	0	0	0	0
4	1	0	0	0	0	0	0	0
5	1	0	0	0	0	0	0	0
6	1	0	0	0	0	0	0	0
7	1	0	0	0	0	0	0	0
8	1	0	0	0	0	0	0	0
9	1	0	0	0	0	0	0	0
10	1	0	0	0	0	0	0	0
11	1	0	0	0	0	0	0	0
12	1	0	0	0	0	0	0	0
13	1	0	0	0	0	0	0	0
14	1	0	0	0	0	0	0	0
15	1	0	0	0	0	0	0	0
16	1	0	0	0	0	0	0	0
17	1	0	0	0	0	0	0	0
18	1	0	0	0	0	0	0	0
19	1	0	0	0	0	0	0	0
20	1	0	0	0	0	0	0	0
21	7	0	49	0	0	0	0	0
22	31	52	63	52	11	0	0	0
23	51	60	70	60	16	0	0	0
24	64	60	79	60	19	0	0	0
25	79	60	87	60	21	0	0	0
26	79	60	105	60	29	0	0	0
27	88	60	131	60	26	0	0	0
28	105	60	162	60	19	0	0	0
29	132	60	275	60	38	0	0	0
30	171	60	330	60	47	0	0	0
31	279	60	442	60	43	0	0	0
32	331	60	500	60	47	0	0	0

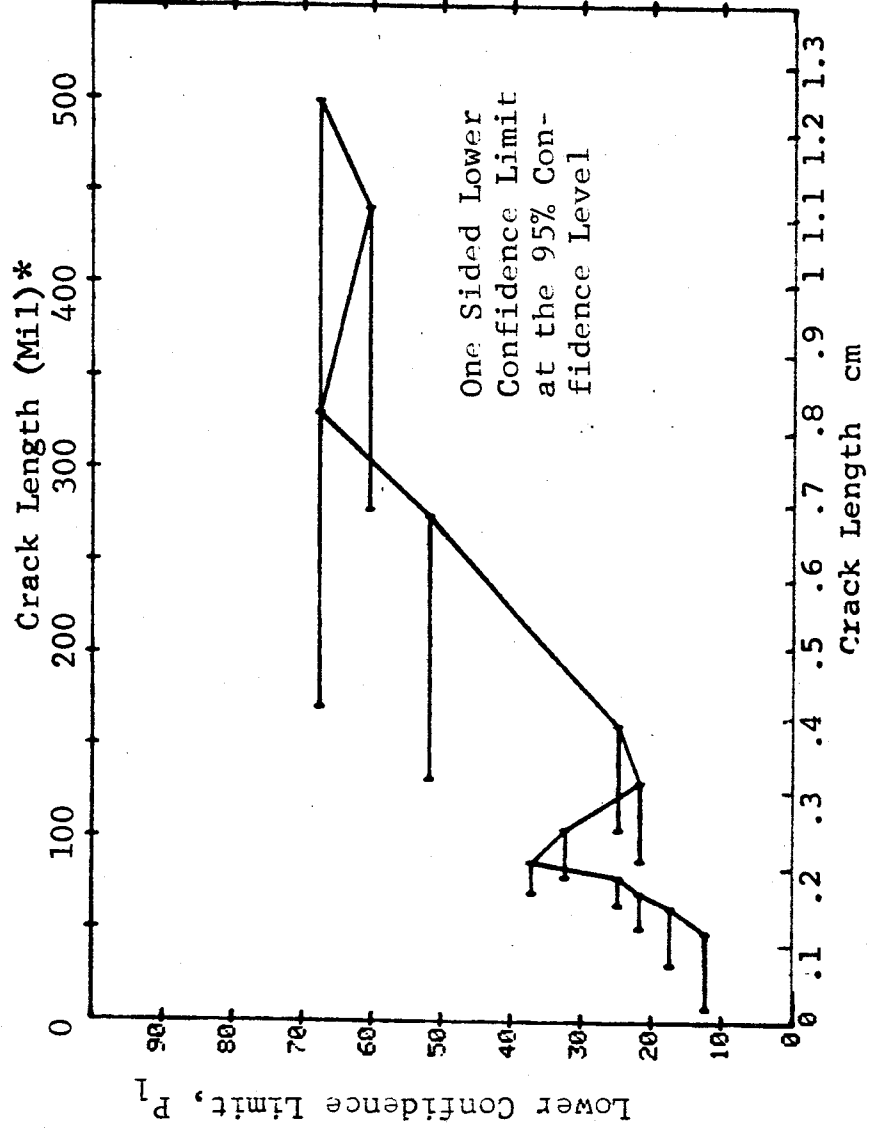


Figure D-31 (Concluded)

(a) Range Interval Method of Data Cumulation

18-SEP-75	RADIOGRAPHY		P-1,		G	
RANGE	MIN	LN	DET	50%	95%	0 MILS
1	10	41 *	5	12	5	0
2	42	72	24	29	21	0
3	73	103	40	47	38	0
4	104	134	6	16	29	0
5	135	162	12	44	24	0
6	171	185	13	61	24	0
7	197	197	1	50	5	0
8	241	258	16	95	82	13
9	259	288	12	87	68	0
10	290	318	11	74	55	0
11	321	347	15	65	43	0
12	352	391	8	79	36	0
13	384	408	3	0	0	0
14	426	444	0	0	0	0
15	458	475	7	58	0	0
16	478	506	17	74	58	0
17	508	535	21	81	66	0
18	538	568	6	89	60	0
19	610	610	0	0	0	0
20	610	610	1	50	5	0
21	710	710	0	0	0	0
22	710	710	0	0	0	0
23	710	710	1	50	5	0
24	0	0	0	0	0	0
25	0	0	0	0	0	0
26	0	0	0	0	0	0
27	0	0	0	0	0	0
28	0	0	0	0	0	0
29	0	0	0	0	0	0
30	0	0	0	0	0	0
31	0	0	0	0	0	0
32	979	979	1	50	5	0

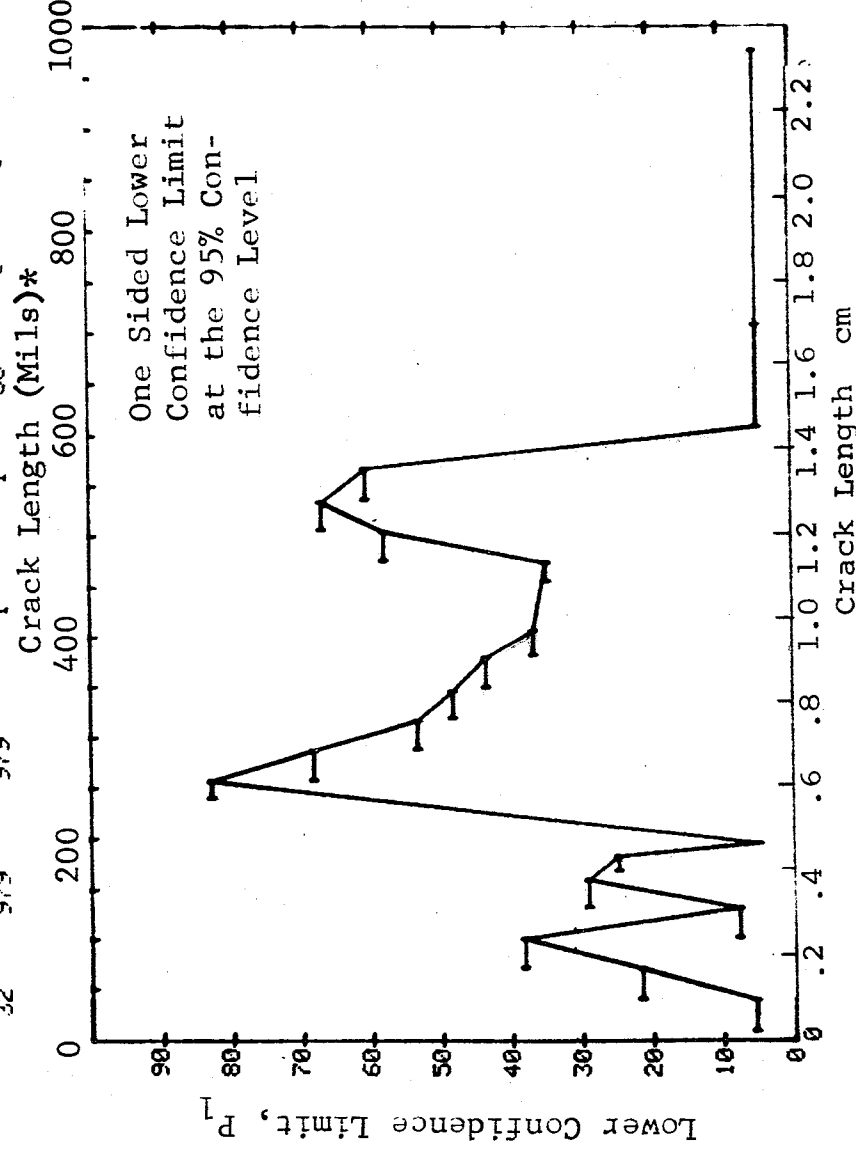


Figure D-32 Probability of Detection for 2219-T87 Al Using X-ray. Etched Fatigue Cracks in Flat Plates Measured by Operator G. Lab. Env. D-96

(b) Optimum Probability Method of Data Cumulation

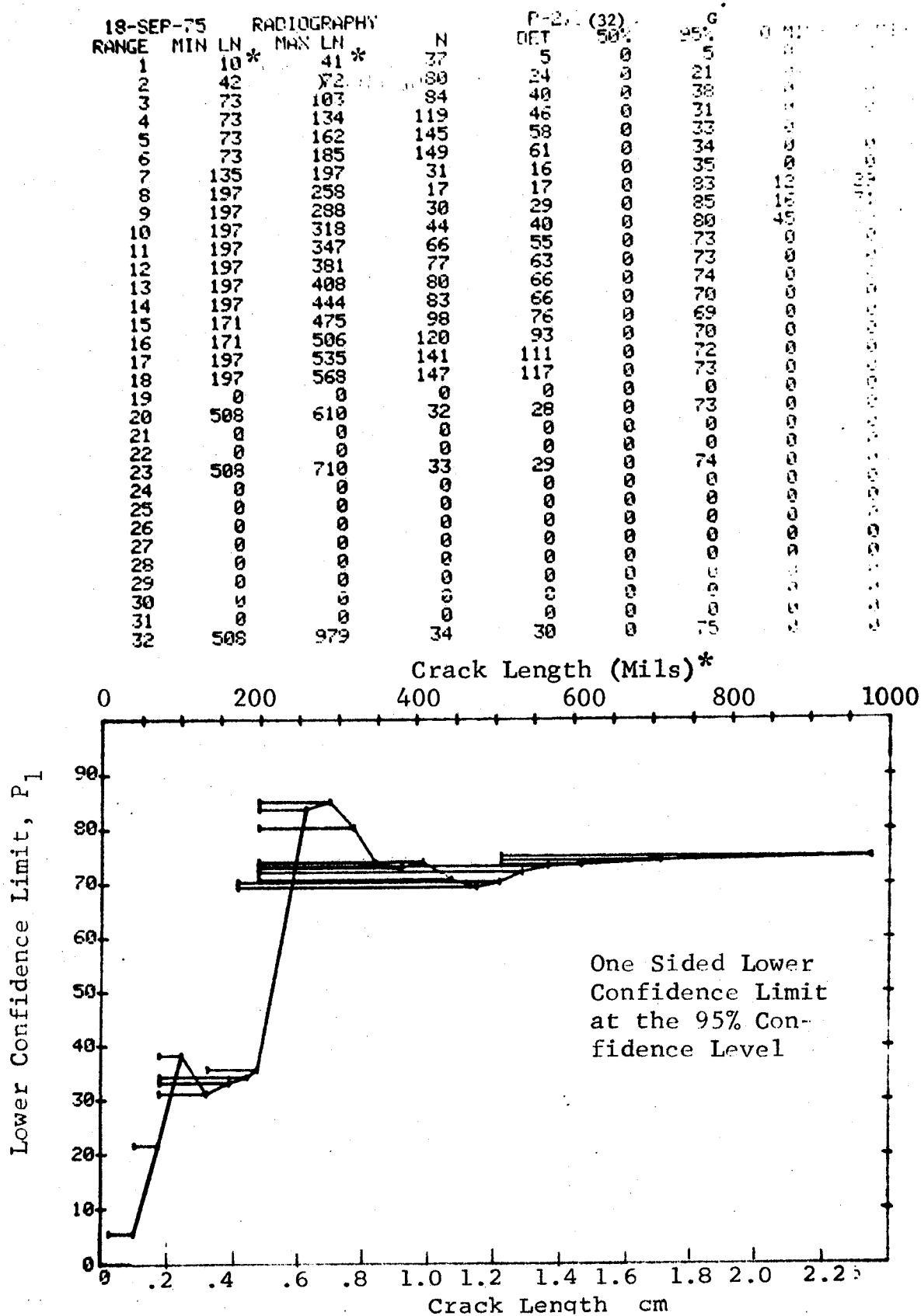


Figure D-32 (Continued)

(c) Overlapping Sixty Point Method of Data Cumulation

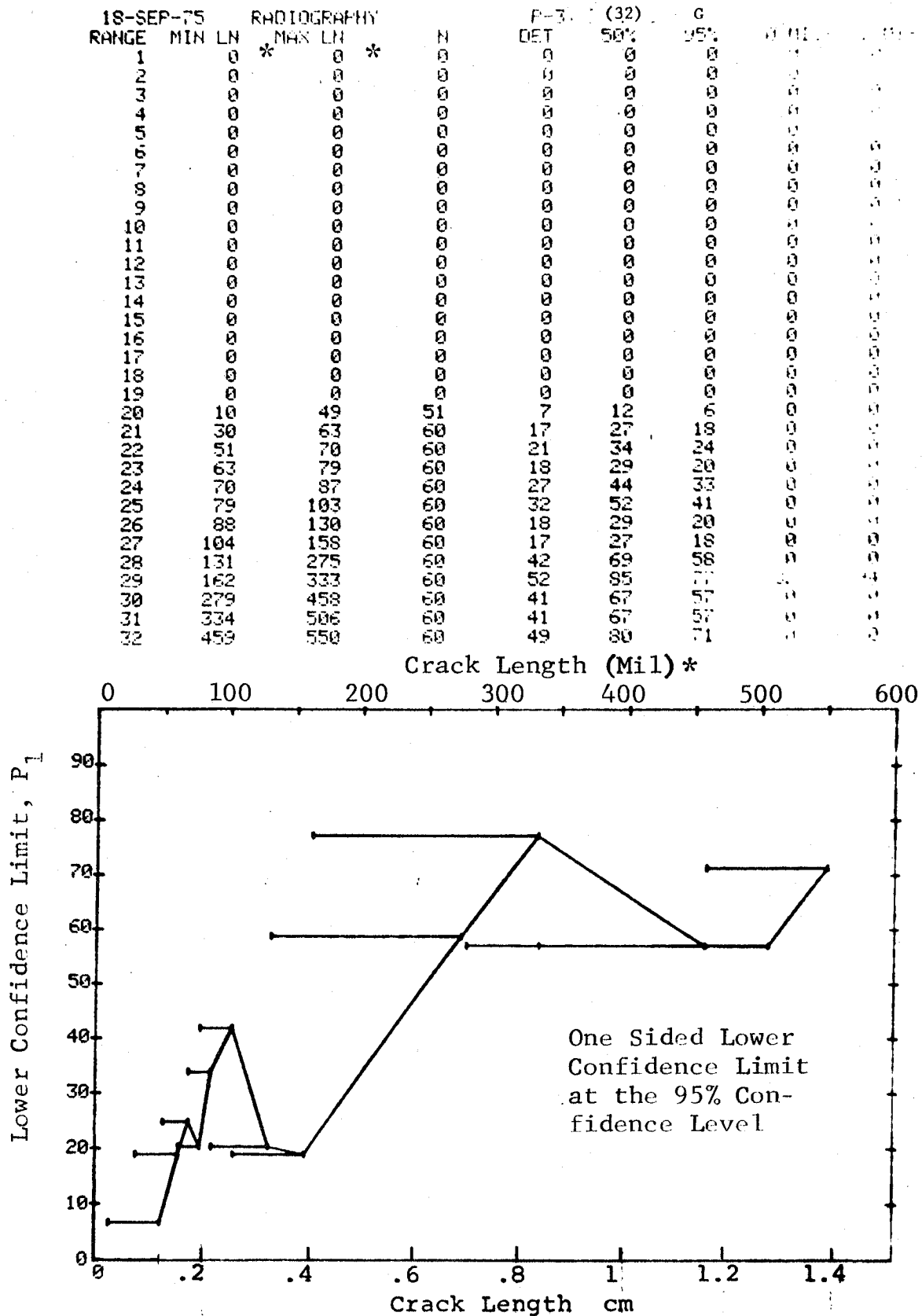


Figure D-32 (Concluded)

(a) Range Interval Method of Data Cumulation

24-JUL-75				ULTRASONIC				TEST 1, MERGE, ROCKWELL SC (33)					
RANGE	MIN	LN	*	MAX	LN	*	N	DET	50%	95%	0 MISS	1 MISS	
1		7		22			65	21	31	22	0	0	
2	29			36			90	61	67	58	0	0	
3	38			52			115	91	78	71	0	0	
4	54			67			231	188	81	76	0	0	
5	68			82			265	232	87	83	0	0	
6	83			97			195	170	86	82	0	0	
7	98			111			85	74	86	79	94	100	
8	115			126			85	78	91	85	44	57	
9	129			141			95	85	88	82	72	94	
10	143			157			75	64	84	76	100	100	
11	158			171			15	13	82	63	0	0	
12	182			185			15	14	89	72	0	0	
13	190			197			10	9	83	60	0	0	
14	207			207			1	1	50	5	0	0	
15	0			0			0	0	0	0	0	0	
16	241			247			20	19	91	78	26	41	
17	248			262			85	85	99	96	0	0	
18	268			275			15	15	95	81	14	31	
19	279			290			34	33	95	86	12	27	
20	295			306			30	29	94	85	16	31	
21	310			322			50	48	94	87	11	26	
22	323			336			60	58	95	89	1	16	
23	338			352			55	49	87	79	61	74	
24	356			362			20	20	96	86	9	26	
25	370			381			25	22	85	71	0	0	
26	384			393			10	10	93	74	0	0	
27	408			408			5	4	68	34	0	0	
28	426			426			5	5	87	54	0	0	
29	442			442			5	5	87	54	0	0	
30	444			450			6	6	89	60	0	0	
31	456			472			38	38	98	92	0	8	
32	474			979			295	285	96	94	0	0	

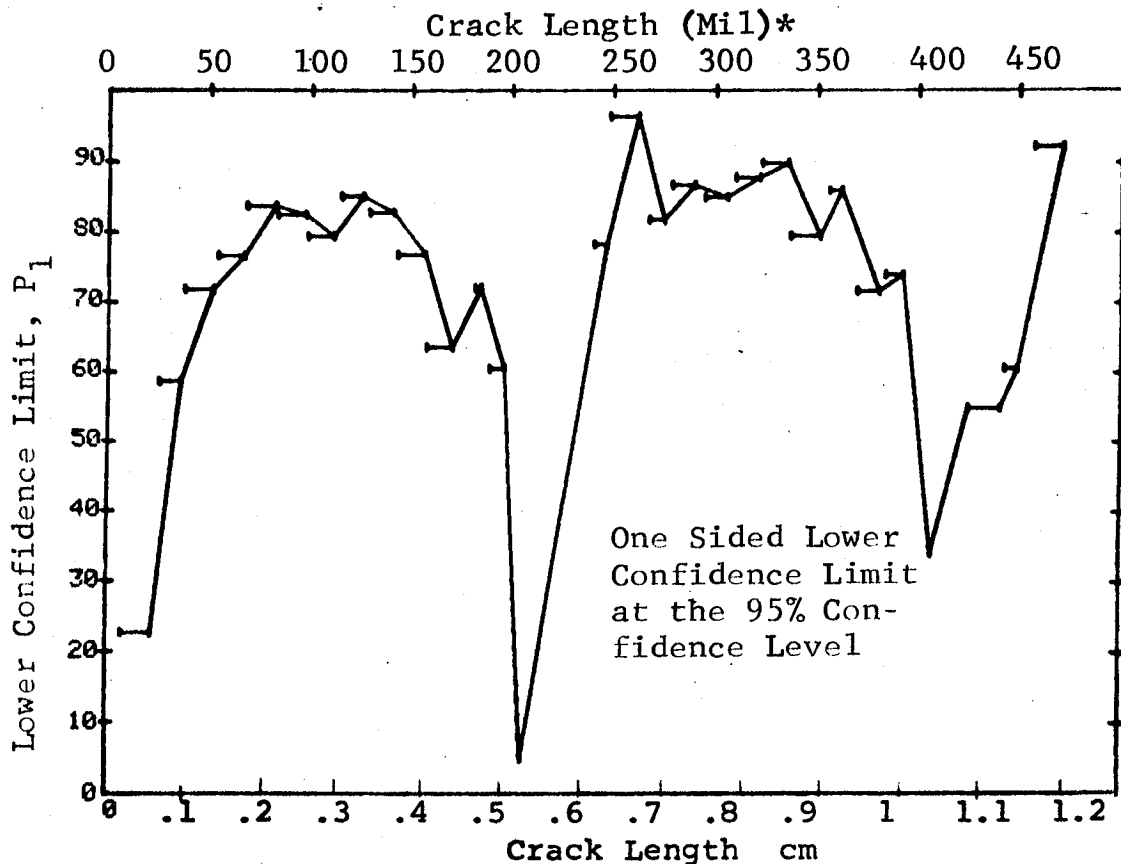


Figure D-33 Probability of Detection for 2219-T87 Al Using Ultrasonics. Etched Fatigue Cracks in Flat Plates Merged for 5 Operators. Lab. Env. D-99

(b) Optimum Probability Method of Data Cumulation

24-JUL-75			ULTRASONIC			TEST 2, MERGE, ROCKWELL SC (33)				
RANGE	MIN LN		* MAX LN *		N	DET	50%	95%	0 MISS	1 MISS
1	7		22		65	21	0	22	0	0
2	25		36x		90	61	0	58	0	0
3	38		52		115	91	0	71	0	0
4	54		67		231	188	0	76	0	0
5	68		82		265	232	0	83	0	0
6	68		97		460	402	0	84	0	0
7	68		111		545	476	0	84	0	0
8	68		126		630	554	0	85	0	0
9	115		141		180	163	0	86	0	0
10	68		157		800	703	0	85	0	0
11	68		171		815	716	0	85	0	0
12	68		185		830	730	0	85	0	0
13	68		197		840	739	0	85	0	0
14	68		207		841	740	0	85	0	0
15	0		0		0	0	0	0	0	0
16	115		247		316	283	0	86	0	0
17	248		262		85	85	0	96	0	0
18	248		275		100	100	0	97	0	0
19	248		290		134	133	0	96	0	0
20	248		306		164	162	0	96	0	0
21	248		322		214	210	0	95	0	0
22	248		336		274	268	0	95	0	0
23	207		352		350	337	0	94	0	0
24	248		362		349	337	0	94	0	0
25	207		381		395	379	0	93	0	0
26	207		393		405	389	0	94	0	0
27	207		408		410	393	0	93	0	0
28	207		426		415	398	0	93	0	0
29	207		442		420	403	0	93	0	0
30	207		450		426	409	0	94	0	0
31	426		472		54	54	0	94	0	0
32	426		979		349	339	0	95	0	0

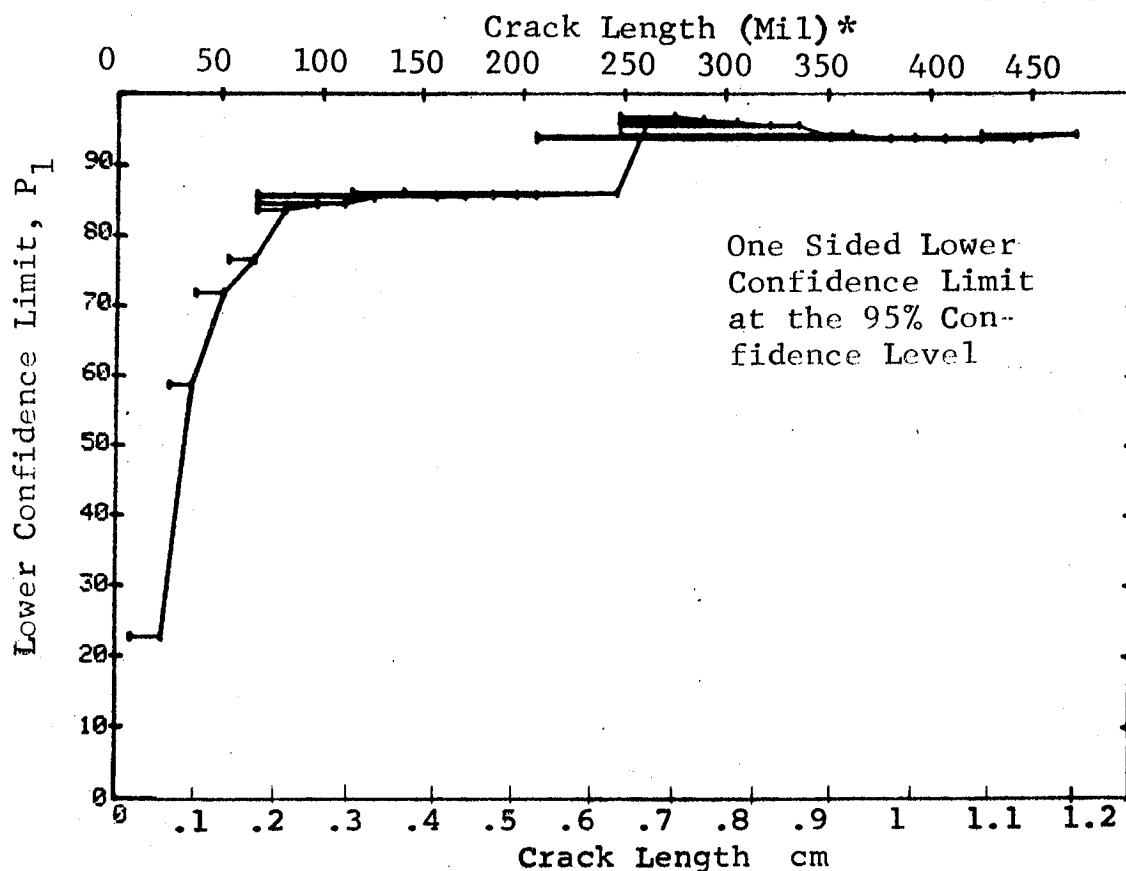


Figure D-33 (Continued)

(c) Overlapping Sixty Point Method of Data Cumulation

24-JUL-75		ULTRASONIC		TEST 3. MERGE, ROCKWELL SC (33)															
RANGE	NIN	LN *	MAX LN *	N	DET	50%	95%	0 MISS	1 MISS	50%	95%	0 MISS	1 MISS	50%	95%	0 MISS	1 MISS		
1	1	95	100	60	51	83	75	94	100	83	75	94	100	83	75	94	100		
2	2	97	105	60	52	85	77	82	94	85	77	82	94	85	77	82	94		
3	3	100	109	60	54	88	81	56	69	88	81	56	69	88	81	56	69		
4	4	105	118	60	55	90	83	43	56	90	83	43	56	90	83	43	56		
5	5	109	123	60	55	90	83	43	56	90	83	43	56	90	83	43	56		
6	6	118	126	60	54	88	81	56	69	88	81	56	69	88	81	56	69		
7	7	123	131	60	53	87	79	69	82	87	79	69	82	87	79	69	82		
8	8	126	135	60	54	88	81	56	69	88	81	56	69	88	81	56	69		
9	9	131	140	60	51	83	75	94	100	83	75	94	100	83	75	94	100		
10	10	135	144	60	50	82	73	0	0	82	73	0	0	82	73	0	0		
11	11	140	151	60	53	87	79	69	82	87	79	69	82	87	79	69	82		
12	12	144	162	60	56	92	85	29	43	92	85	29	43	92	85	29	43		
13	13	151	197	60	57	93	87	16	16	93	87	16	16	93	87	16	16		
14	14	162	249	60	58	95	89	0	0	95	89	0	0	95	89	0	0		
15	15	197	257	60	60	98	95	0	0	98	95	0	0	98	95	0	0		
16	16	249	260	60	59	97	92	0	0	97	92	0	0	97	92	0	0		
17	17	257	275	60	58	95	89	0	0	95	89	0	0	95	89	0	0		
18	18	260	290	60	59	97	92	0	0	97	92	0	0	97	92	0	0		
19	19	275	304	60	58	95	89	0	0	95	89	0	0	95	89	0	0		
20	20	290	313	60	57	93	87	16	16	93	87	16	16	93	87	16	16		
21	21	304	323	60	59	97	92	0	0	97	92	0	0	97	92	0	0		
22	22	313	330	60	57	93	87	16	16	93	87	16	16	93	87	16	16		
23	23	323	338	60	53	87	79	69	82	87	79	69	82	87	79	69	82		
24	24	330	342	60	55	90	83	43	56	90	83	43	56	90	83	43	56		
25	25	338	362	60	56	92	85	29	43	92	85	29	43	92	85	29	43		
26	26	342	372	60	56	92	85	29	43	92	85	29	43	92	85	29	43		
27	27	362	442	60	59	97	92	0	0	97	92	0	0	97	92	0	0		
28	28	372	466	60	59	97	92	0	0	97	92	0	0	97	92	0	0		
29	29	442	475	60	59	97	92	0	0	97	92	0	0	97	92	0	0		
30	30	466	484	60	58	95	89	0	0	95	89	0	0	95	89	0	0		
31	31	478	495	60	58	95	89	0	0	95	89	0	0	95	89	0	0		
32	32	489	500	60	56	92	85	29	43	92	85	29	43	92	85	29	43		

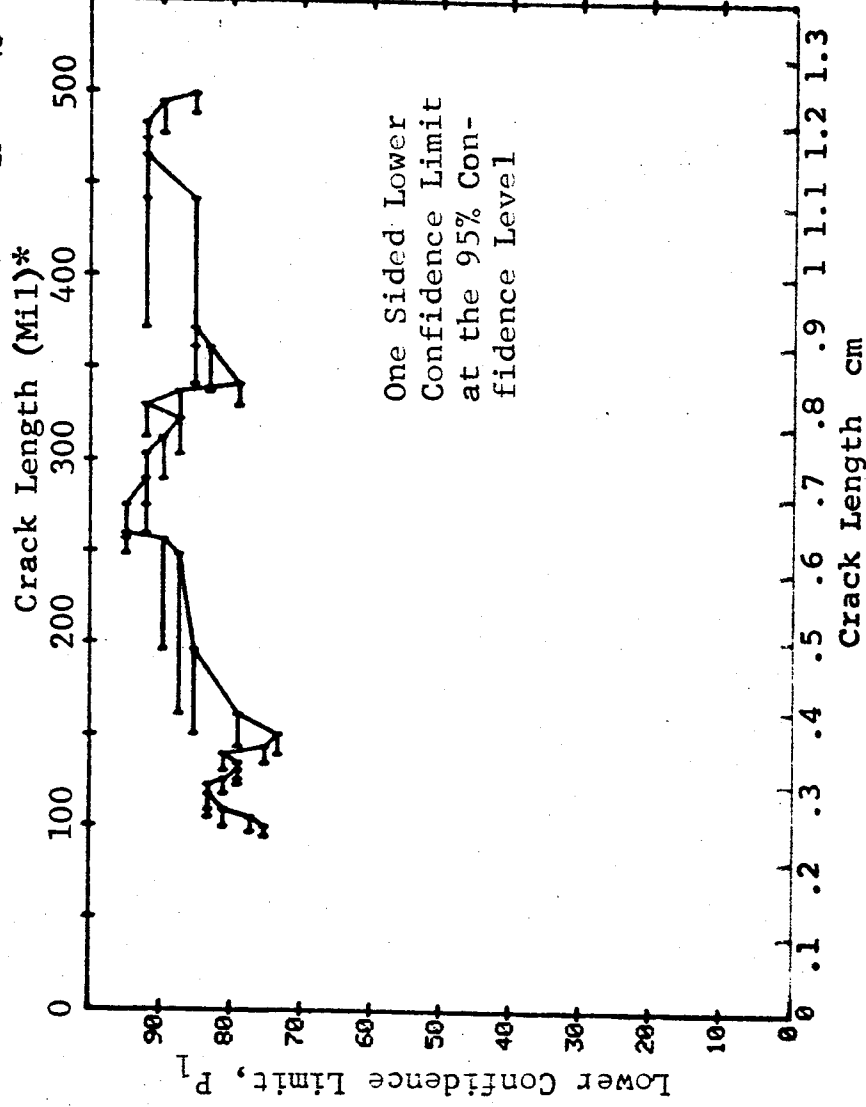


Figure D-33 (Continued)

(c) Overlapping Sixty Point Method of Data Cumulation

24-JUL-75 ULTRASONIC						TEST 3, MERGE, ROCKWELLSC (33)				
RANGE	MIN	LN	MAX	LN	N	DET	50%	95%	0 MISS	1 MISS
1		55 *	60 *		60	46	75	65	0	0
2		58	62		60	53	87	79	69	82
3		60	63		60	52	85	77	82	94
4		62	64		60	49	80	71	0	0
5		63	66		60	48	79	69	0	0
6		65	67		60	51	83	75	94	100
7		66	69		60	52	85	77	82	94
8		67	69		60	47	77	67	0	0
9		69	72		60	48	79	69	0	0
10		70	74		60	55	90	83	43	56
11		72	76		60	52	85	77	82	94
12		75	77		60	50	82	73	0	0
13		76	79		60	56	92	85	29	43
14		78	80		60	57	93	87	16	29
15		79	82		60	54	88	81	56	69
16		80	84		60	53	87	79	69	82
17		83	85		60	51	83	75	94	100
18		84	87		60	52	85	77	82	94
19		86	90		60	51	83	75	94	100
20		87	94		60	52	85	77	82	94
21		91	96		60	55	90	83	43	56
22		95	98		60	51	83	75	94	100
23		97	104		60	51	83	75	94	100
24	100		108		60	54	88	81	56	69
25	105		117		60	55	90	83	43	56
26	109		123		60	54	88	81	56	69
27	118		125		60	55	90	83	43	56
28	123		131		60	53	87	79	69	82
29	126		135		60	52	85	77	82	94
30	131		140		60	54	88	81	56	69
31	135		144		60	51	83	75	94	100
32	140		150		60	50	82	73	0	0

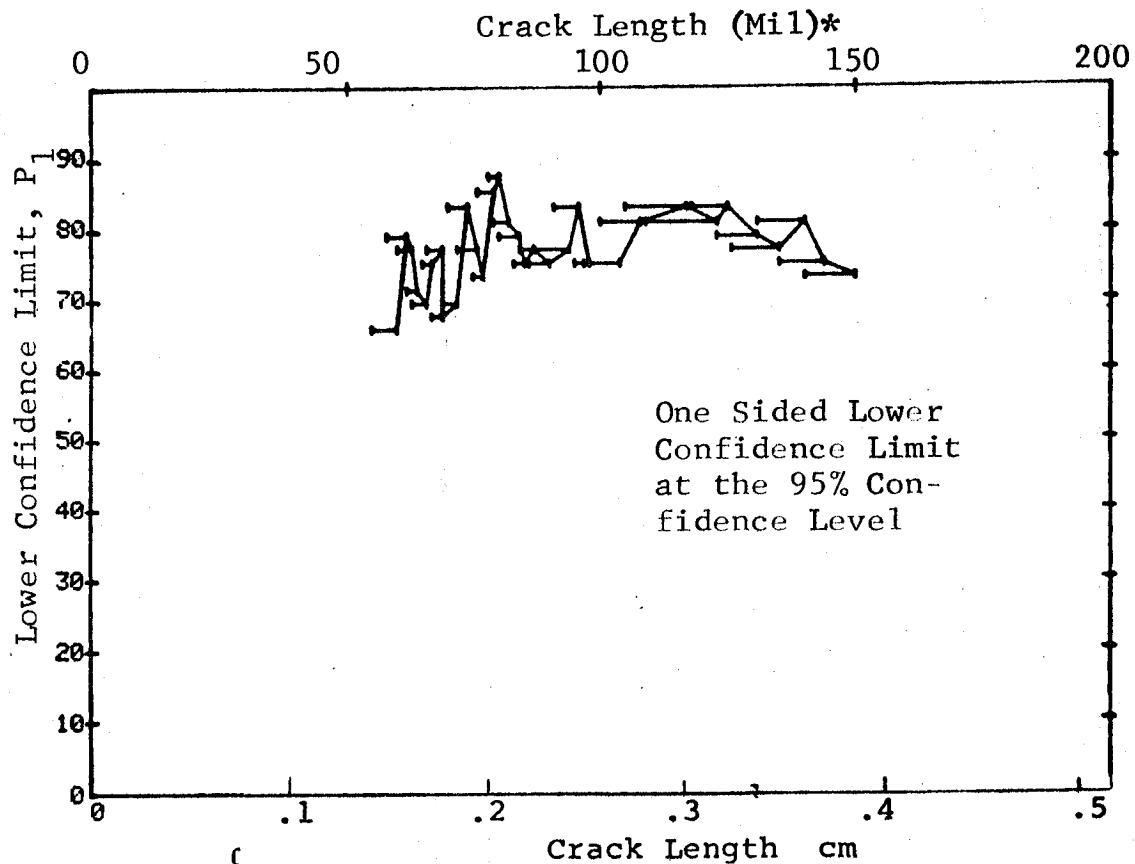


Figure D-33 (Continued)

(c) Overlapping Sixty Point Method of Data Cumulation

24-JUL-75				ULTRASONIC		TEST 3, MERGE, ROCKWELL SC (33)						
RANGE	MIN	LN	*	MAX	LN	*	N	DET	50%	95%	0 MISS	1 MISS
1		7	*	21	*		51	11	20	12	0	0
2	15			26			50	26	42	32	0	0
3	21			31			60	41	67	57	0	0
4	26			35			60	40	65	55	0	0
5	31			41			60	39	64	53	0	0
6	35			45			60	42	69	58	0	0
7	41			47			60	52	85	77	82	94
8	45			51			60	51	83	75	94	100
9	47			55			60	44	72	62	0	0
10	51			58			60	45	74	64	0	0
11	55			60			60	49	80	71	0	0
12	59			62			60	52	85	77	82	94
13	61			63			60	52	85	77	82	94
14	62			65			60	49	80	71	0	0
15	64			66			60	46	75	65	0	0
16	65			67			60	50	82	73	0	0
17	67			69			60	53	87	79	69	82
18	68			70			60	49	80	71	0	0
19	69			72			60	49	80	71	0	0
20	70			75			60	54	88	81	56	69
21	73			76			60	50	82	73	0	0
22	75			78			60	51	83	75	94	100
23	76			79			60	58	95	89	1	16
24	78			80			60	56	92	85	29	43
25	79			83			60	54	88	81	56	69
26	81			84			60	51	83	75	94	100
27	83			86			60	51	83	75	94	100
28	85			87			60	55	90	83	43	56
29	86			91			60	51	83	75	94	100
30	88			95			60	51	83	75	94	100
31	91			97			60	53	87	79	69	82
32	95			100			60	51	83	75	94	100

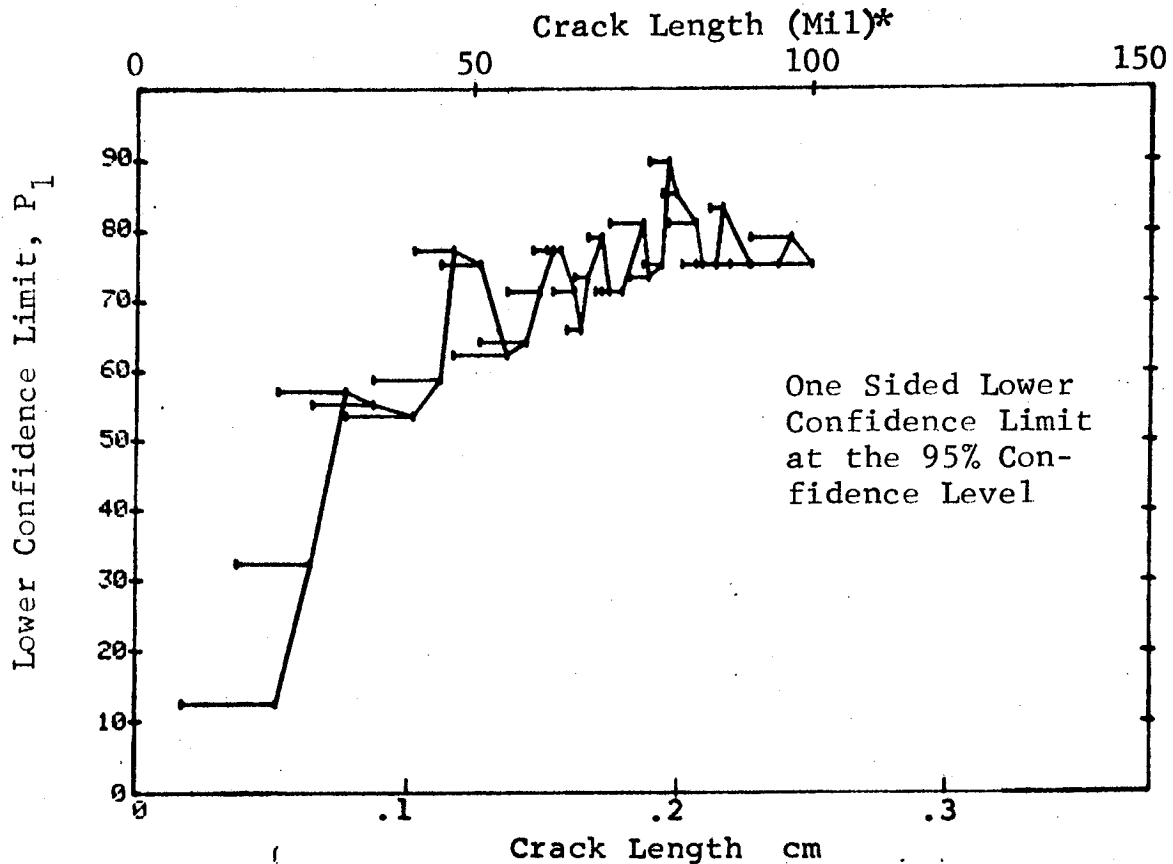


Figure D-33 (Concluded)

REPRODUCIBILITY OF THE
ORIGINAL PAGE IS POOR

(a) Range Interval Method of Data Cumulation

22-JUL-75 PENETRANT				MERGE PENETRANT ROCKWELL C (34)				
RANGE	MIN LN	MAX LN	N	DET	50%	95%	0 MISS	1 MISS
1	7	22	65	13	19	12	0	0
2	25	38	115	46	50	41	0	0
3	38	52	115	78	67	59	0	0
4	54	67	230	171	74	69	0	0
5	68	82	266	219	82	78	0	0
6	83	97	193	172	88	84	0	0
7	98	111	85	80	93	88	18	31
8	115	126	85	75	87	80	82	94
9	129	141	95	87	90	85	47	59
10	143	157	75	66	87	79	79	92
11	158	171	15	15	95	81	14	31
12	182	185	15	15	95	81	14	31
13	190	197	10	7	64	39	0	0
14	0	0	0	0	0	0	0	0
15	0	0	0	0	0	0	0	0
16	241	247	20	20	96	86	9	25
17	248	262	85	85	99	96	0	0
18	268	275	15	15	95	81	14	31
19	279	290	35	35	98	91	0	0
20	295	306	30	29	94	85	15	31
21	310	322	50	49	96	90	0	0
22	323	336	60	58	95	89	1	1
23	338	352	55	50	89	81	48	81
24	356	362	20	20	95	86	9	25
25	370	381	25	21	81	66	0	0
26	384	393	10	9	83	60	0	0
27	408	408	5	5	87	54	0	0
28	426	426	5	5	87	54	0	0
29	442	442	5	4	80	54	0	0
30	444	444	5	5	87	54	0	0
31	458	472	40	38	93	85	21	36
32	474	5009	297	290	97	95	0	0

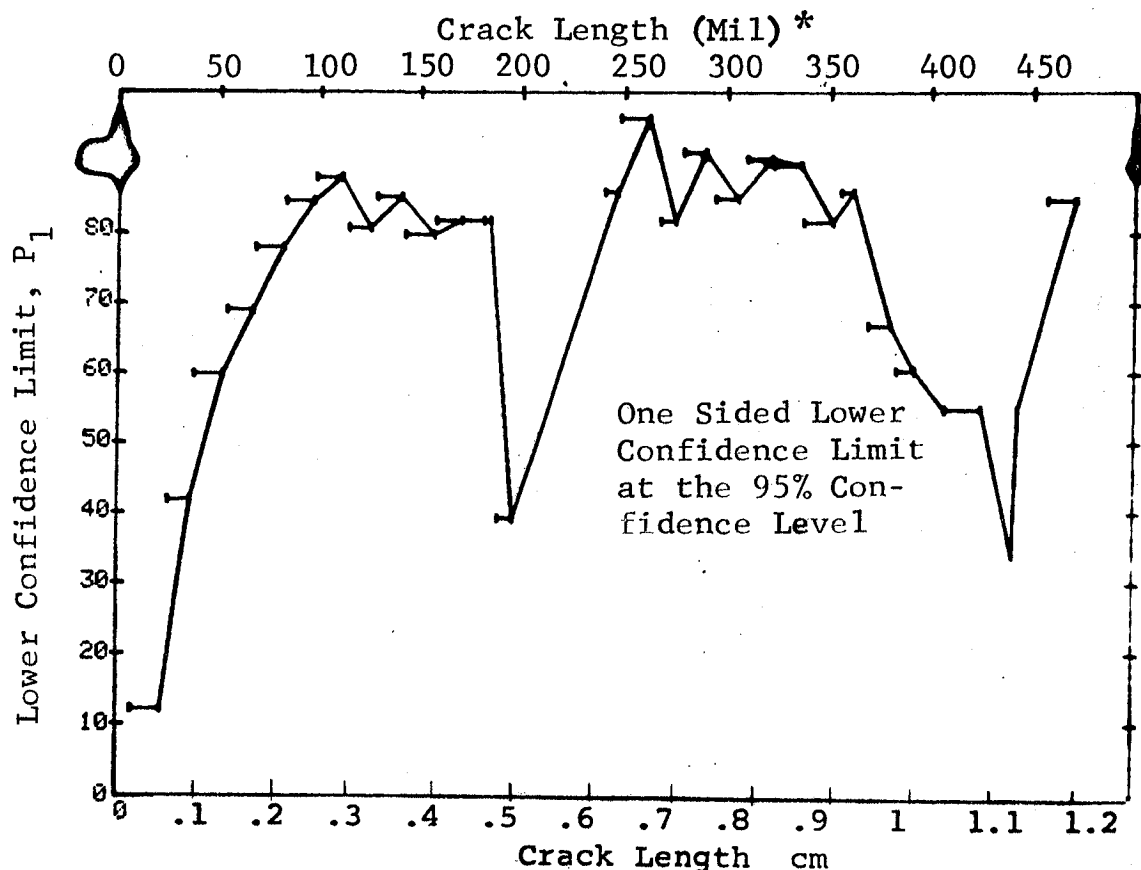


Figure D-34 Probability of Detection for 2219-T87 A1 Using Liquid Penetrant. Etched Fatigue Cracks in Lab. Env. Flat Plates Merged for 7 Operators. D-104

(b) Optimum Probability Method of Data Cumulation

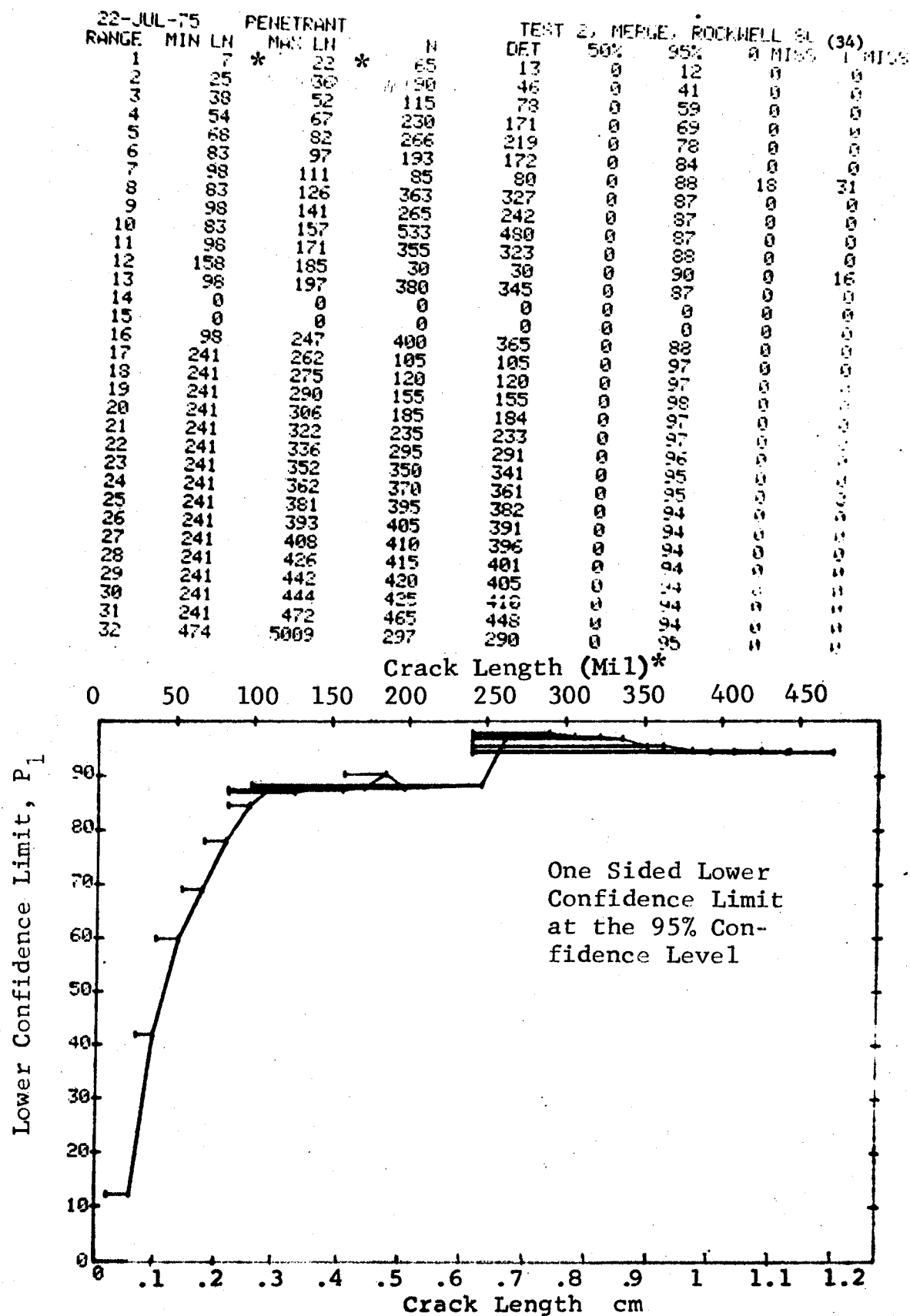


Figure D-34 (Continued)

(c) Overlapping Sixty Point Method of Data Cumulation

22-JUL-75		PENETRANT		TEST 3, MERGE, ROCKWELL C (34)					
RANGE	MIN LN	* MAX LN *	N	DET	50%	95%	0 MIL	1 MIL	
1	95	100	60	59	97	92	0	1	
2	97	105	60	57	93	87	16		
3	101	109	60	55	90	83	43		
4	105	118	60	55	90	83	43		
5	111	123	60	53	87	79	69		
6	119	126	60	53	87	79	69		
7	124	131	60	56	92	85	29		
8	129	135	60	54	88	81	56		
9	132	140	60	53	87	79	69		
10	136	144	60	54	88	81	56		
11	141	151	60	52	85	77	82		
12	145	162	60	55	90	83	43		
13	153	197	60	56	92	85	29		
14	171	249	60	57	93	87	16		
15	241	257	60	60	98	95	0		
16	249	260	60	60	98	95	0		
17	257	275	60	60	98	95	0		
18	261	290	60	60	98	95	0		
19	279	304	60	59	97	92	0		
20	290	313	60	58	95	89	1		
21	306	323	60	59	97	92	0		
22	317	330	60	59	97	92	0		
23	326	338	60	57	93	87	16		
24	331	342	60	55	90	83	43		
25	340	362	60	56	92	85	29		
26	345	372	60	55	90	83	43		
27	362	442	60	54	88	81	56		
28	381	466	60	58	95	89	1		
29	444	475	60	57	93	87	16		
30	466	484	60	57	93	87	16		
31	478	495	60	59	97	92	0		
32	489	500	60	57	93	87	16		

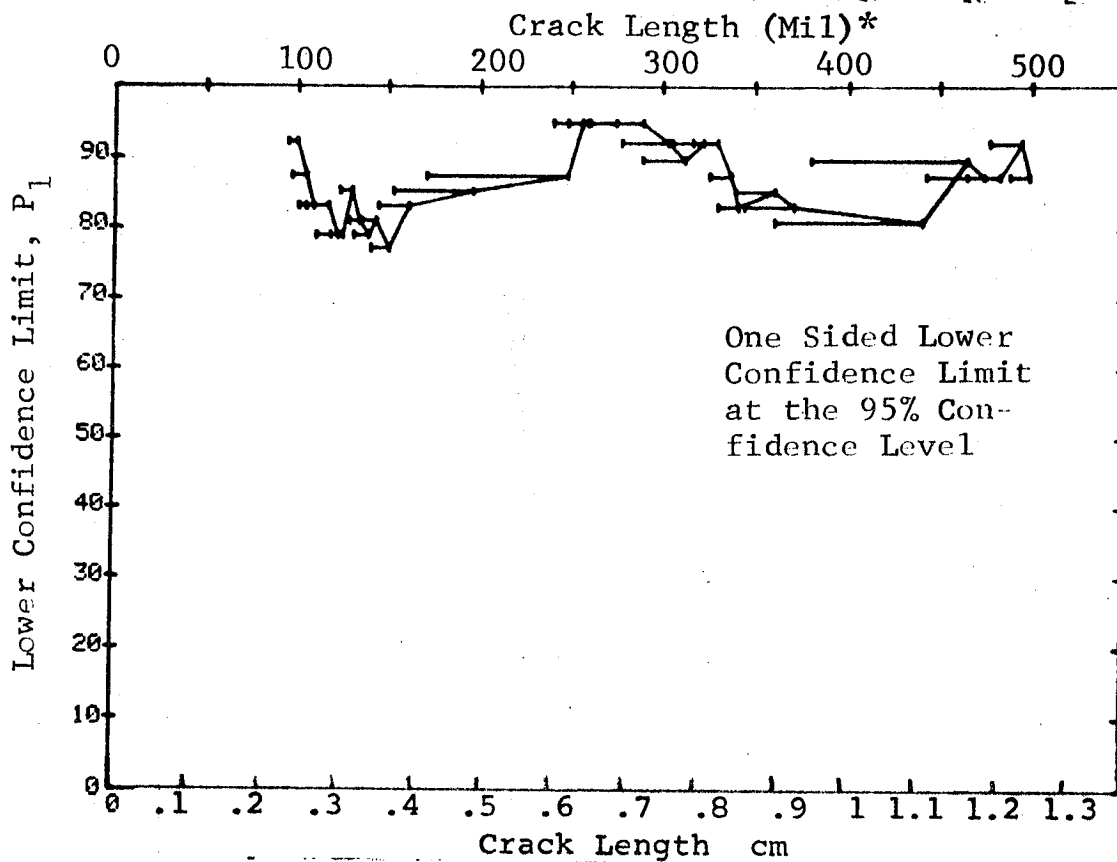


Figure D-34 (Continued)

(c) Overlapping Sixty Point Method of Data Cumulation

22-JUL-75			PENETRANT		TEST 3, MERGE, ROCKWELL SC (34)		DFT		50%		0 MISC		1 MISC	
RANGE	MIN	LN	MAX	LN *	N									
1	1	62*	65*		60		45	74	952	0	0	0	0	0
2	2	64	67		60		44	72	64	0	0	0	0	0
3	3	65	68		60		46	75	65	0	0	0	0	0
4	4	67	69		60		45	75	65	0	0	0	0	0
5	5	68	70		60		39	64	53	0	0	0	0	0
6	6	69	73		60		43	70	60	0	0	0	0	0
7	7	70	75		60		55	90	83	43	56	29	43	56
8	8	73	77		60		57	93	87	16	29	43	56	29
9	9	75	78		60		56	92	85	56	0	0	0	0
10	10	77	80		60		54	88	81	0	0	0	0	0
11	11	78	81		60		47	77	67	0	0	0	0	0
12	12	80	83		60		46	75	65	0	0	0	0	0
13	13	81	85		60		47	77	67	0	0	0	0	0
14	14	83	86		60		55	90	83	43	56	29	43	56
15	15	85	89		60		56	92	85	16	29	43	56	29
16	16	86	92		60		57	93	87	0	0	0	0	0
17	17	89	95		60		58	95	89	0	0	0	0	0
18	18	92	97		60		59	97	92	0	0	0	0	0
19	19	95	102		60		56	92	85	0	0	0	0	0
20	20	98	106		60		55	90	83	0	0	0	0	0
21	21	103	115		60		55	90	83	0	0	0	0	0
22	22	106	119		60		55	90	83	0	0	0	0	0
23	23	116	124		60		52	85	80	0	0	0	0	0
24	24	121	129		60		54	88	81	0	0	0	0	0
25	25	124	134		60		56	92	85	0	0	0	0	0
26	26	129	136		60		53	87	80	0	0	0	0	0
27	27	134	143		60		53	87	80	0	0	0	0	0
28	28	137	146		60		55	90	83	0	0	0	0	0
29	29	143	153		60		53	87	80	0	0	0	0	0
30	30	149	162		60		55	90	83	0	0	0	0	0
31	31	153	162		60		56	92	85	0	0	0	0	0
32	32	183	242		60		57	93	87	0	0	0	0	0

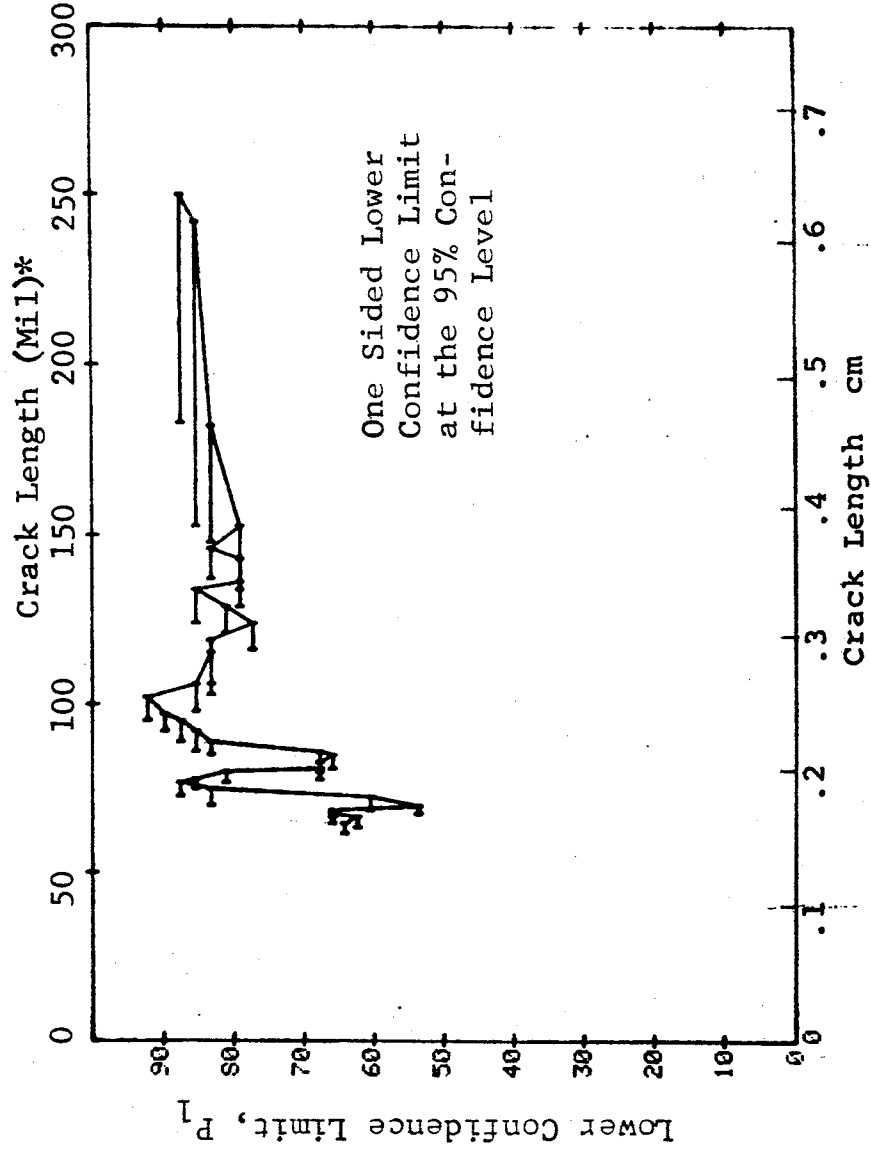


Figure D-34 (Concluded)

(a) Range Interval Method of Data Cumulation

24-JUL-75				EDDY CURRENT		TEST 1, MERGE, ROCKWELL SC (35)	
RANGE	MIN	LN	7 *	MAX	LN	DET	50% 95% MISS
1	1	25	22	36	11	3	0 0 0
2	2	38	52	52	20	19	6 0 0
3	3	54	67	116	35	42	14 0 0
4	4	68	82	234	-49	139	28 0 0
5	5	83	97	262	75	198	-49 0 0
6	6	98	111	193	91	178	70 0 0
7	7	115	126	86	94	82	88 0 0
8	8	129	141	86	95	83	91 3 0
9	9	143	157	94	91	87	85 0 0
10	10	158	171	74	89	67	82 48 0
11	11	182	185	15	95	65	55 68 0
12	12	190	197	15	82	63	14 31 0
13	13	0	0	10	93	74	0 0 0
14	14	232	232	0	0	0	0 0 0
15	15	241	247	1	50	0	0 0 0
16	16	248	262	19	91	18	27 42 0
17	17	268	275	82	99	82	77 0 0
18	18	279	290	15	95	99	95 31 0
19	19	306	306	34	95	33	81 32 0
20	20	322	322	31	91	29	12 45 0
21	21	333	336	50	96	49	30 11 0
22	22	356	352	60	97	59	81 1 0
23	23	370	362	55	89	92	90 61 0
24	24	384	381	21	92	22	48 40 0
25	25	408	393	24	89	10	37 52 0
26	26	426	408	10	93	10	74 0 0
27	27	442	426	5	87	5	54 0 0
28	28	444	442	5	63	5	54 0 0
29	29	458	444	5	87	5	54 0 0
30	30	472	472	5	95	39	58 0 0
31	31	474	479	40	96	281	93 21 0
32	32			292			

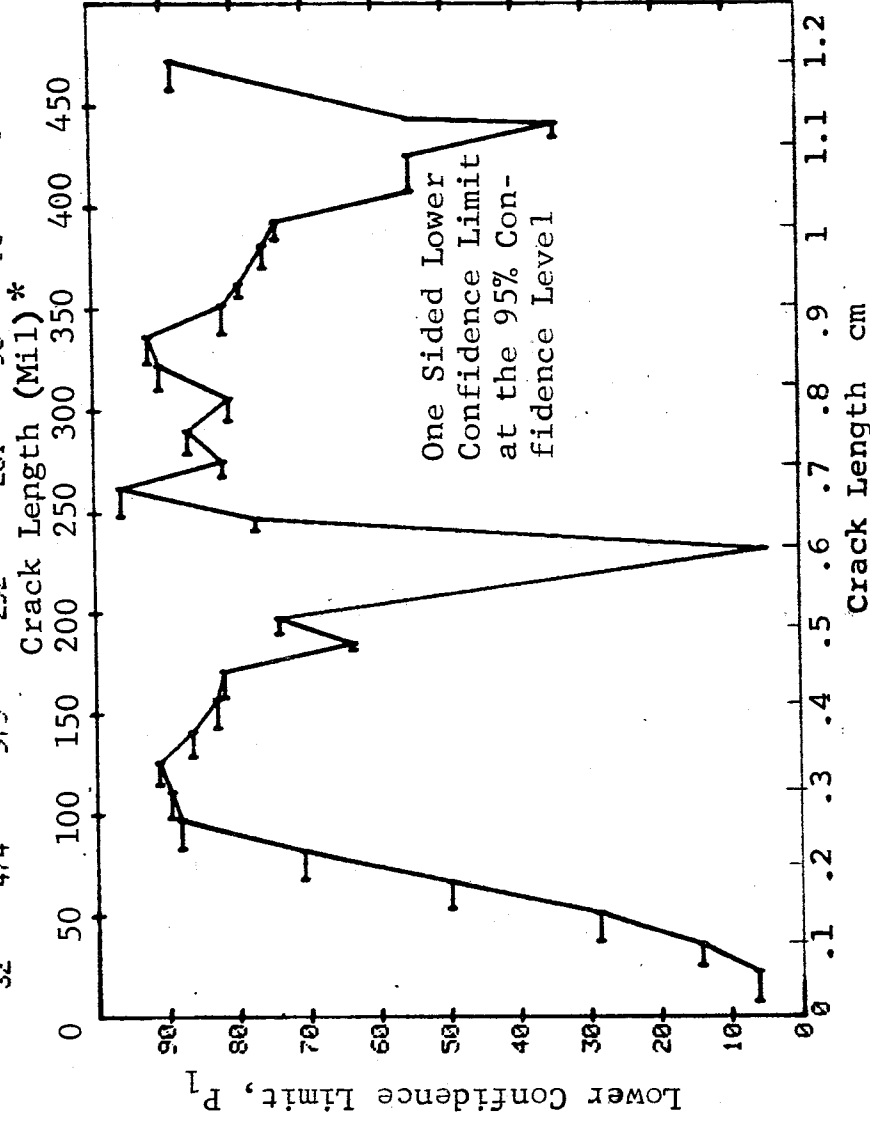


Figure D-35 Probability of Detection for 2219-T87 Al Using Eddy Current. Etched Fatigue Cracks in Flat Plates Merged for 5 Operators. D-108 Lab. Env.

(b) Optimum Probability Method of Data Cumulation

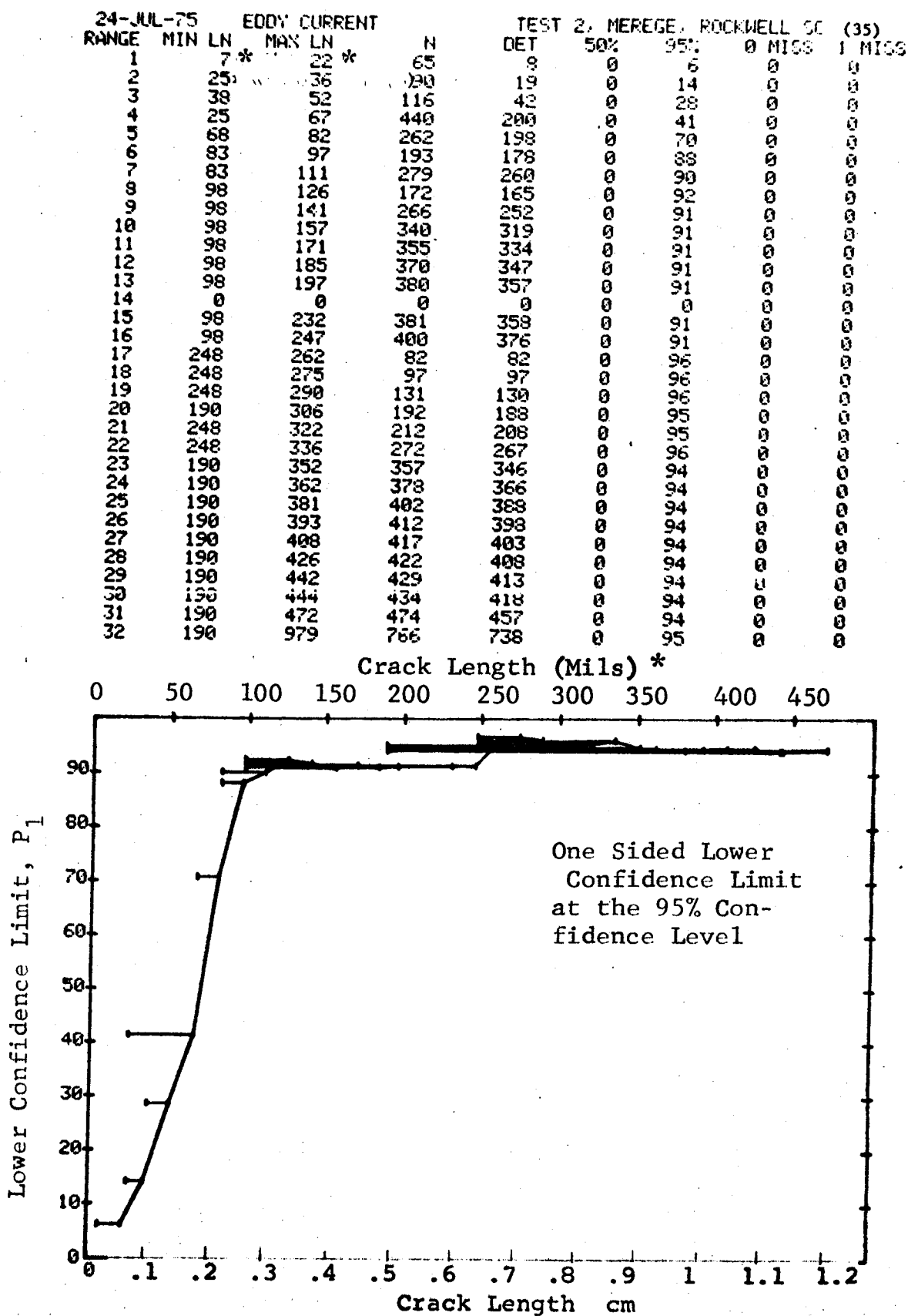


Figure D-35 (Continued)

(c) Overlapping Sixty Point Method of Data Cumulation

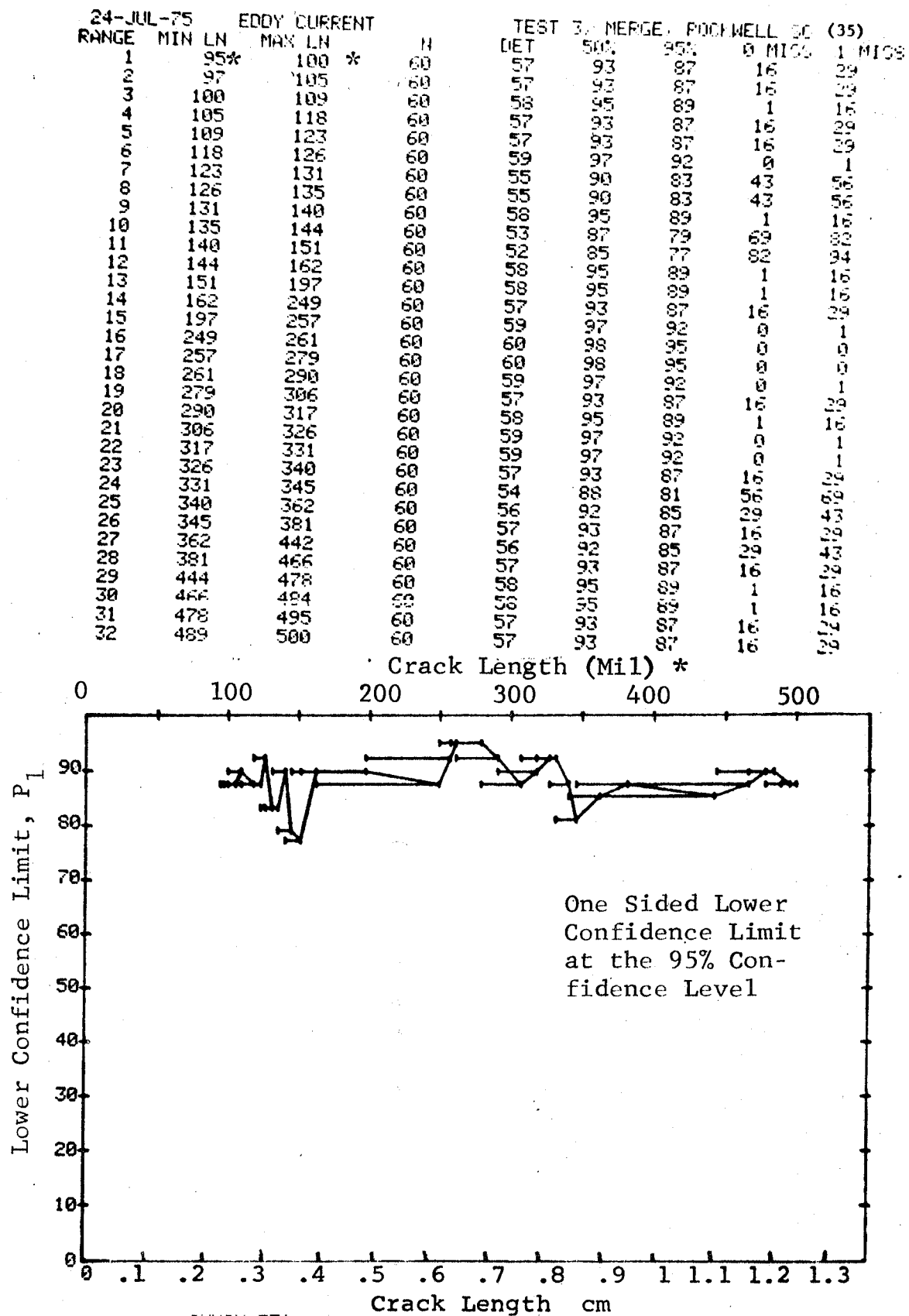


Figure D-35 (Continued)

(c) Overlapping Sixty Point Method of Data Cumulation

24-JUL-75 EDDY CURRENT				TEST 3, MERGED, ROCKWELL SC (35)				
RANGE	MIN	LN	MAX LN	N	DET	50%	95%	0 MISS
1	7	*	21	51	5	9	3	0
2	15		26	60	10	16	9	0
3	21		31	60	12	19	11	0
4	26		35	60	12	19	11	0
5	31		40	60	18	29	20	0
6	35		45	60	19	30	21	0
7	41		47	60	18	29	20	0
8	45		49	60	21	34	24	0
9	47		55	60	27	44	33	0
10	49		58	60	25	40	30	0
11	55		60	60	29	47	37	0
12	58		62	60	33	54	43	0
13	60		63	60	38	62	51	0
14	62		65	60	44	72	62	0
15	63		66	60	37	60	50	0
16	65		67	60	37	60	50	0
17	66		69	60	41	67	57	0
18	67		70	60	39	64	53	0
19	69		72	60	37	60	50	0
20	70		75	60	42	69	58	0
21	72		76	60	44	72	62	0
22	75		78	60	44	72	62	0
23	76		79	60	52	85	77	82
24	78		80	60	57	93	87	16
25	79		83	60	51	83	75	94
26	80		84	60	48	79	69	0
27	83		86	60	55	90	83	43
28	84		87	60	58	95	89	1
29	86		91	60	54	88	81	55
30	87		95	60	55	90	83	43
31	91		97	60	57	93	87	16
32	95		100	60	57	93	87	16

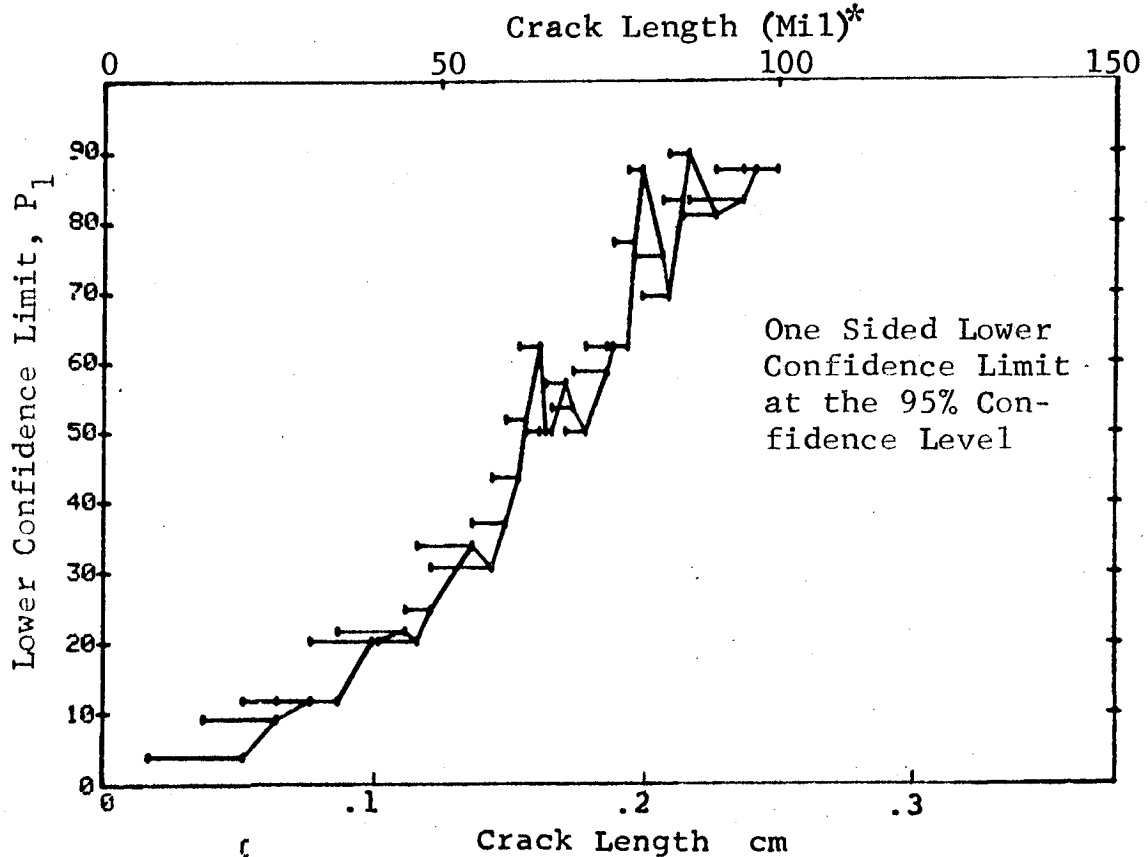


Figure D-35 (Concluded)

(a) Range Interval Method of Data Cumulation

29-JUL-75	PENETRANT		TEST 1		(36) ROCKWELL B-1				
RANGE	MIN	LN *	MAX	LN	DET	50% 70	95% 22	MISS 0	MISS 1
1	0	31	0	0	2	0	0	0	0
2	0	0	0	0	0	0	0	0	0
3	47	47	47	0	3	79	36	0	0
4	54	55	55	0	8	91	68	0	0
5	62	62	62	0	4	84	47	0	0
6	67	72	72	0	14	95	80	15	32
7	75	80	80	0	23	97	87	6	23
8	0	0	0	0	0	0	0	0	0
9	91	92	92	0	14	95	80	15	32
10	0	0	0	0	0	0	0	0	0
11	105	105	105	0	4	84	47	0	0
12	113	114	114	0	14	95	80	15	32
13	0	0	0	0	0	0	0	0	0
14	124	124	124	0	5	87	54	0	0
15	130	133	133	0	8	91	68	0	0
16	0	0	0	0	0	0	0	0	0
17	0	0	0	0	0	0	0	0	0
18	0	0	0	0	0	0	0	0	0
19	0	0	0	0	0	0	0	0	0
20	0	0	0	0	0	0	0	0	0
21	184	184	184	0	7	90	65	0	0
22	0	0	0	0	0	0	0	0	0
23	0	0	0	0	0	0	0	0	0
24	205	205	205	0	4	84	47	0	0
25	0	0	0	0	0	0	0	0	0
26	218	218	218	0	11	93	76	18	35
27	0	0	0	0	0	0	0	0	0
28	0	0	0	0	0	0	0	0	0
29	0	0	0	0	0	0	0	0	0
30	245	245	245	0	7	90	65	0	0
31	250	250	250	0	1	50	5	0	0
32	0	0	0	0	0	0	0	0	0

Crack Length (Mil) *	
1	0
2	0
3	0
4	0
5	0
6	0
7	0
8	0
9	0
10	0
11	0
12	0
13	0
14	0
15	0
16	0
17	0
18	0
19	0
20	0
21	0
22	0
23	0
24	0
25	0
26	0
27	0
28	0
29	0
30	0
31	0
32	0

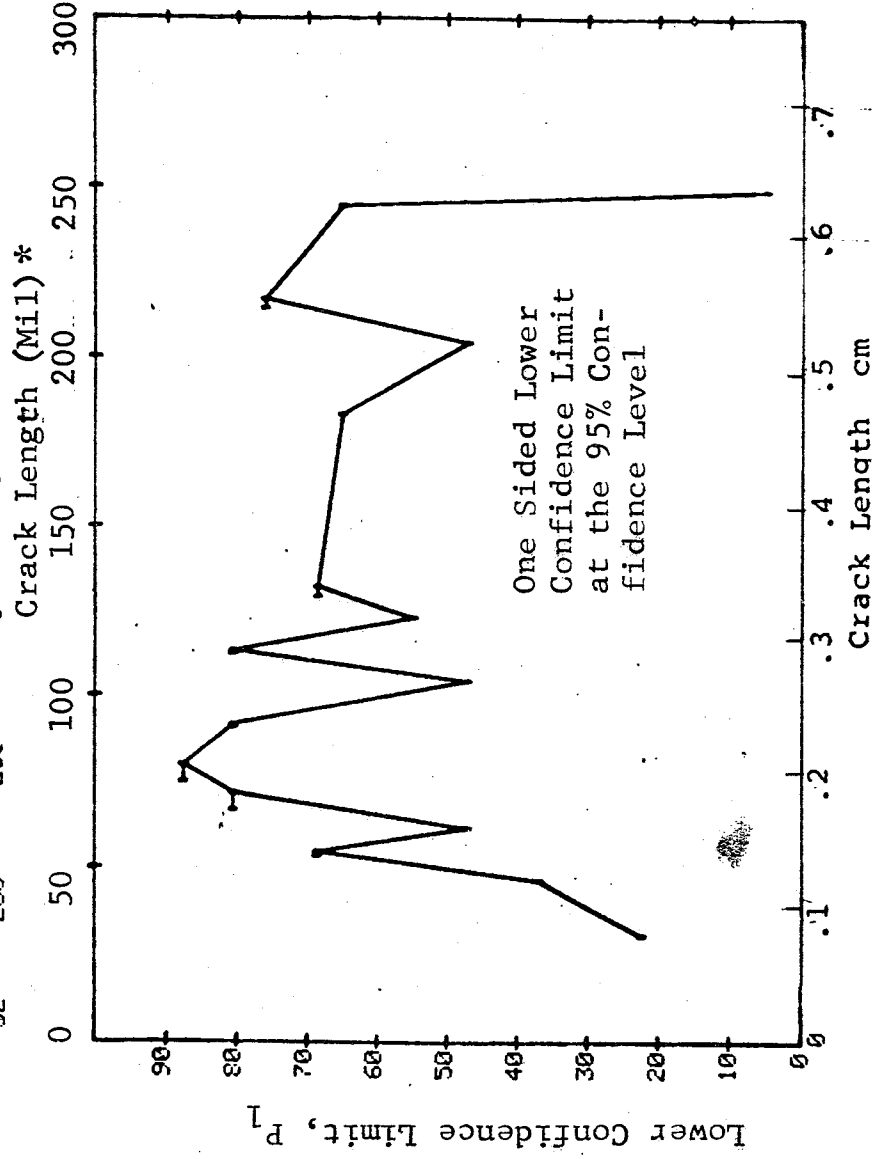


Figure D-36 Probability of Detection for Ti-6Al-4V Using Liquid Penetrant. Fatigue Cracks in Flat Plates.
Prod. Env.

(b) Optimum Probability Method of Data Cumulation

29-JUL-75			PENETRANT		TEST 2 (36)		ROCKWELL E-1	
RANGE	MIN	LN	* LN	MAX LN	DET	50%	95%	MISS
1	31	0	31	0	2	0	22	0
2	31	0	0	0	0	0	0	0
3	31	0	47	0	5	0	0	0
4	31	55	55	0	13	0	54	0
5	31	62	62	0	17	0	79	0
6	31	72	72	0	31	0	83	29
7	31	80	80	0	54	0	90	15
8	31	0	0	0	0	0	94	0
9	31	0	92	0	0	0	0	0
10	31	0	0	0	68	0	95	0
11	31	105	105	0	0	0	0	0
12	31	114	114	0	72	0	95	0
13	31	0	0	0	86	0	96	0
14	31	124	124	0	0	0	0	0
15	31	133	133	0	91	0	96	0
16	31	0	0	0	99	0	97	0
17	31	0	0	0	0	0	0	0
18	31	0	0	0	0	0	0	0
19	31	0	0	0	0	0	0	0
20	31	0	0	0	0	0	0	0
21	31	0	0	0	0	0	0	0
22	31	184	184	0	106	0	97	0
23	31	0	0	0	0	0	0	0
24	31	0	0	0	0	0	0	0
25	31	205	205	0	110	0	97	0
26	31	0	0	0	0	0	0	0
27	31	218	218	0	121	0	97	0
28	31	0	0	0	0	0	0	0
29	31	0	0	0	0	0	0	0
30	31	0	0	0	0	0	0	0
31	31	245	245	0	128	0	97	0
32	31	250	250	0	129	0	97	0

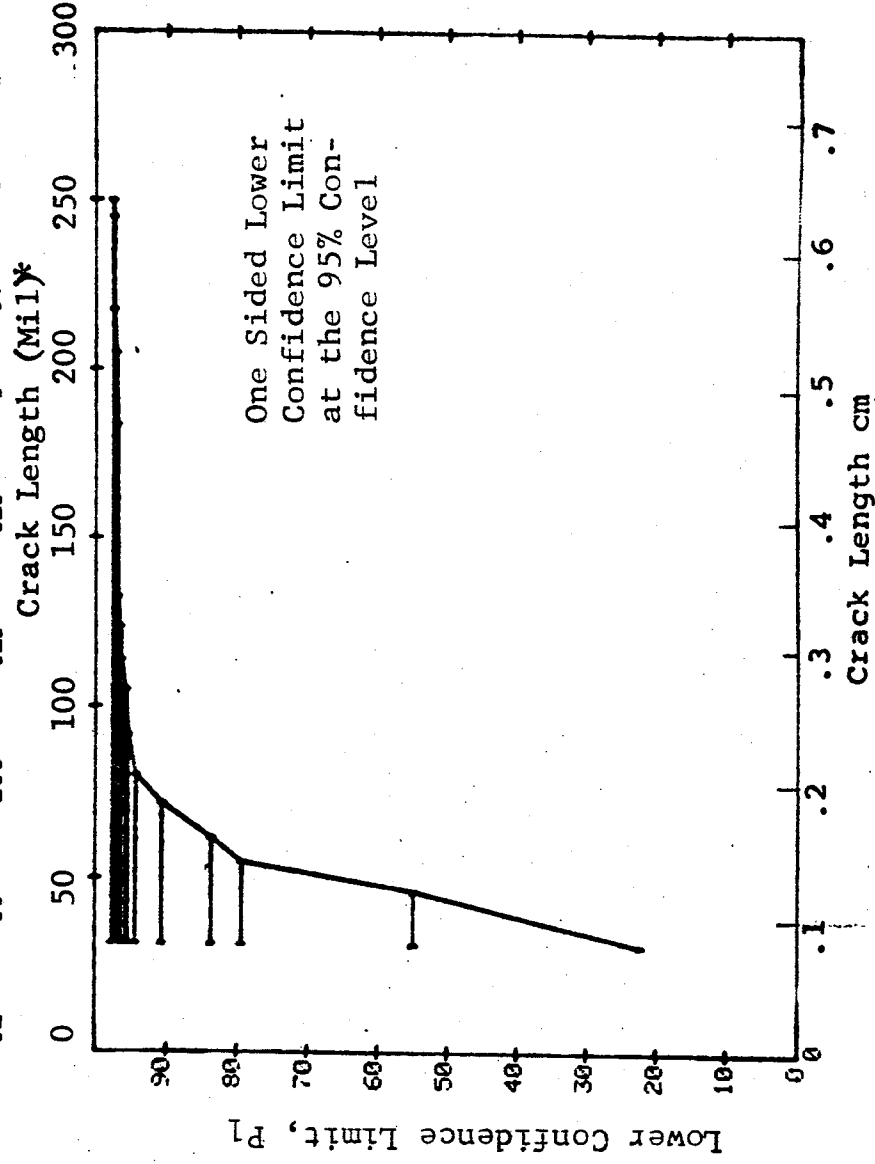


Figure D-36 (Continued)

(c) Overlapping Sixty Point Method of Data Cumulation

29-JUL-75	PENETRANT	TEST 3	(36) ROCKWELL B-1	1 MISS
RANGE MIN LN *	MAX LN *	DET	50%	95%
1	0	0	0	0
2	0	0	0	0
3	0	0	0	0
4	0	0	0	0
5	0	0	0	0
6	0	0	0	0
7	0	0	0	0
8	0	0	0	0
9	0	0	0	0
10	0	0	0	0
11	0	0	0	0
12	0	0	0	0
13	0	0	0	0
14	0	0	0	0
15	0	0	0	0
16	0	0	0	0
17	0	0	0	0
18	0	0	0	0
19	0	0	0	0
20	0	0	0	0
21	0	0	0	0
22	0	0	0	0
23	0	0	0	0
24	0	0	0	0
25	0	0	0	0
26	0	0	0	0
27	0	0	0	0
28	0	0	0	0
29	31	39	98	92
30	55	60	98	95
31	78	60	98	95
32	105	60	98	95

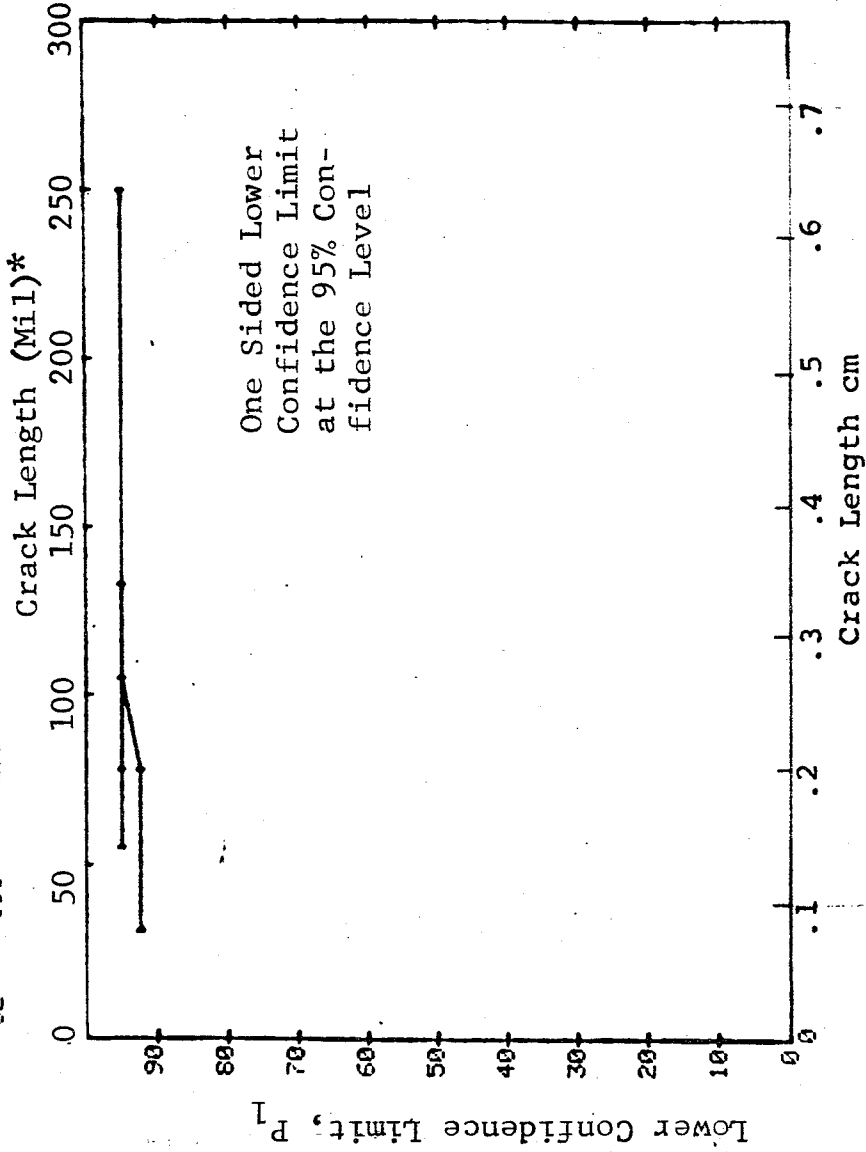


Figure D-36 (Concluded)

(a) Range Interval Method of Data Cumulation

29-JUL-75		PENETRANT		TEST 1. (37)		ROCKWELL B-1				
RANGE	MIN	LN	MAX LN	N	DET	50%	95%	0 MISS	1 MISS	
1		31*	31	*	4	3	61	24	0	0
2		0	0		0	0	0	0	0	0
3		47	47		9	9	92	71	0	0
4		54	55	18	18	96	84	11	29	0
5		0	0		0	0	0	0	0	0
6		62	67	20	20	96	86	9	26	0
7		70	70	10	10	92	74	0	0	0
8		78	78	8	8	91	63	0	0	0
9		80	80	7	7	90	65	0	0	0
10		91	91	8	8	91	68	0	0	0
11		92	92	8	8	91	68	0	0	0
12		0	0		0	0	0	0	0	0
13		0	0		0	0	0	0	0	0
14		113	114	13	13	94	79	16	33	0
15		0	0		0	0	0	0	0	0
16		124	124	7	7	90	63	0	0	0
17		130	133	11	11	93	76	18	35	0
18		0	0		0	0	0	0	0	0
19		0	0		0	0	0	0	0	0
20		0	0		0	0	0	0	0	0
21		0	0		0	0	0	0	0	0
22		0	0		0	0	0	0	0	0
23		0	0		0	0	0	0	0	0
24		0	0		0	0	0	0	0	0
25		0	0		0	0	0	0	0	0
26		184	184	8	8	91	68	0	0	0
27		0	0		0	0	0	0	0	0
28		0	0		0	0	0	0	0	0
29		205	205	5	5	87	54	0	0	0
30		0	0		0	0	0	0	0	0
31		215	215	5	5	87	54	0	0	0
32		218	245	12	12	94	77	17	34	0

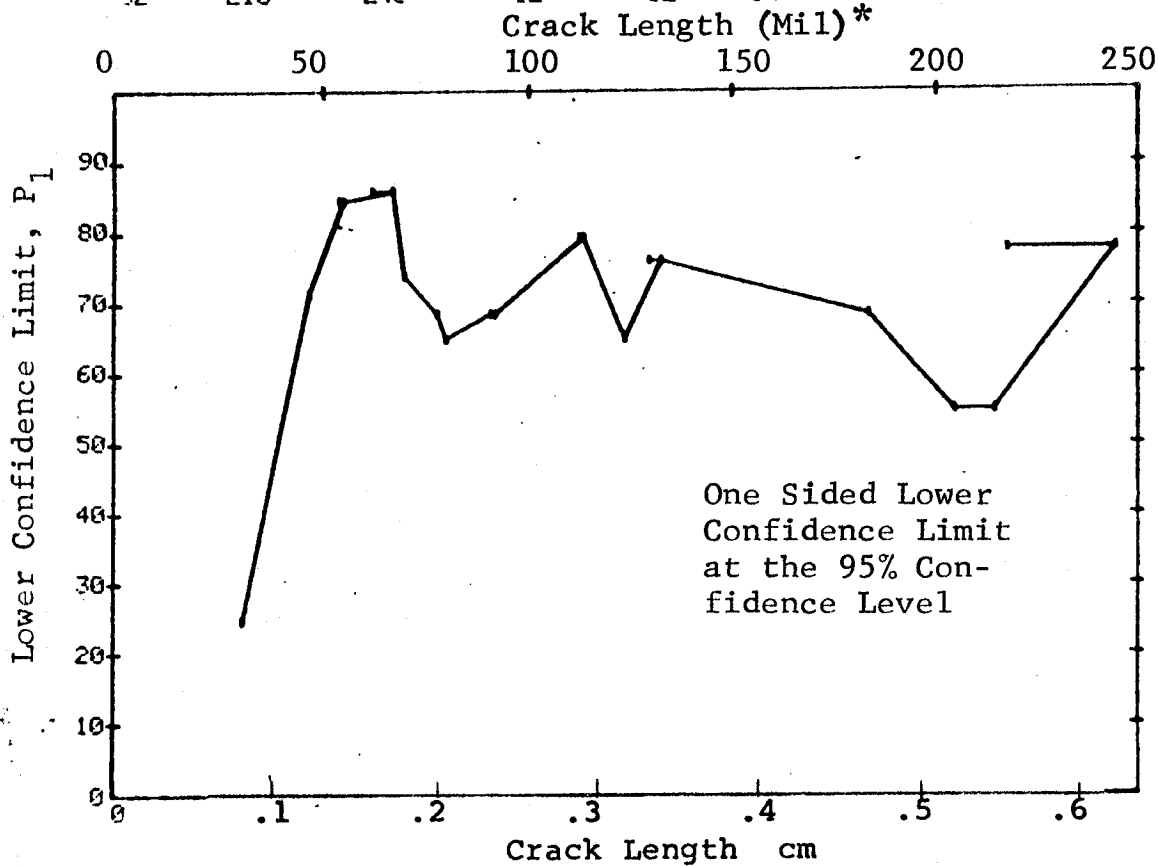


Figure D-37 Probability of Detection for Ti-6Al-4V Using Liquid Penetrant. Fatigue Cracks in Flat Plates.
Prod. Env.

(b) Optimum Probability Method of Data Cumulation

29-JUL-75		PENETRANT			TEST 2, (37)		ROCKWELL I 2-1		
RANGE	MIN	LN	MAX LN	N	DET	50%	95%	0 MISS	1 MISS
1		31*	31*	4	3	0	24	0	0
2		0	0	0	0	0	0	0	0
3		47	47	9	9	0	71	0	0
4		47	55	27	27	0	89	2	19
5		0	0	0	0	0	0	0	0
6		47	67	47	47	0	93	0	0
7		47	70	57	57	0	94	0	0
8		47	78	65	65	0	95	0	0
9		47	80	72	72	0	95	0	0
10		47	91	80	80	0	96	0	0
11		47	92	88	88	0	96	0	0
12		0	0	0	0	0	0	0	0
13		0	0	0	0	0	0	0	0
14		47	114	101	101	0	97	0	0
15		0	0	0	0	0	0	0	0
16		47	124	108	108	0	97	0	0
17		47	133	119	119	0	97	0	0
18		0	0	0	0	0	0	0	0
19		0	0	0	0	0	0	0	0
20		0	0	0	0	0	0	0	0
21		0	0	0	0	0	0	0	0
22		0	0	0	0	0	0	0	0
23		0	0	0	0	0	0	0	0
24		0	0	0	0	0	0	0	0
25		0	0	0	0	0	0	0	0
26		47	184	127	127	0	97	0	0
27		0	0	0	0	0	0	0	0
28		0	0	0	0	0	0	0	0
29		47	205	132	132	0	97	0	0
30		0	0	0	0	0	0	0	0
31		47	215	137	137	0	97	0	0
32		47	245	149	149	0	98	0	0

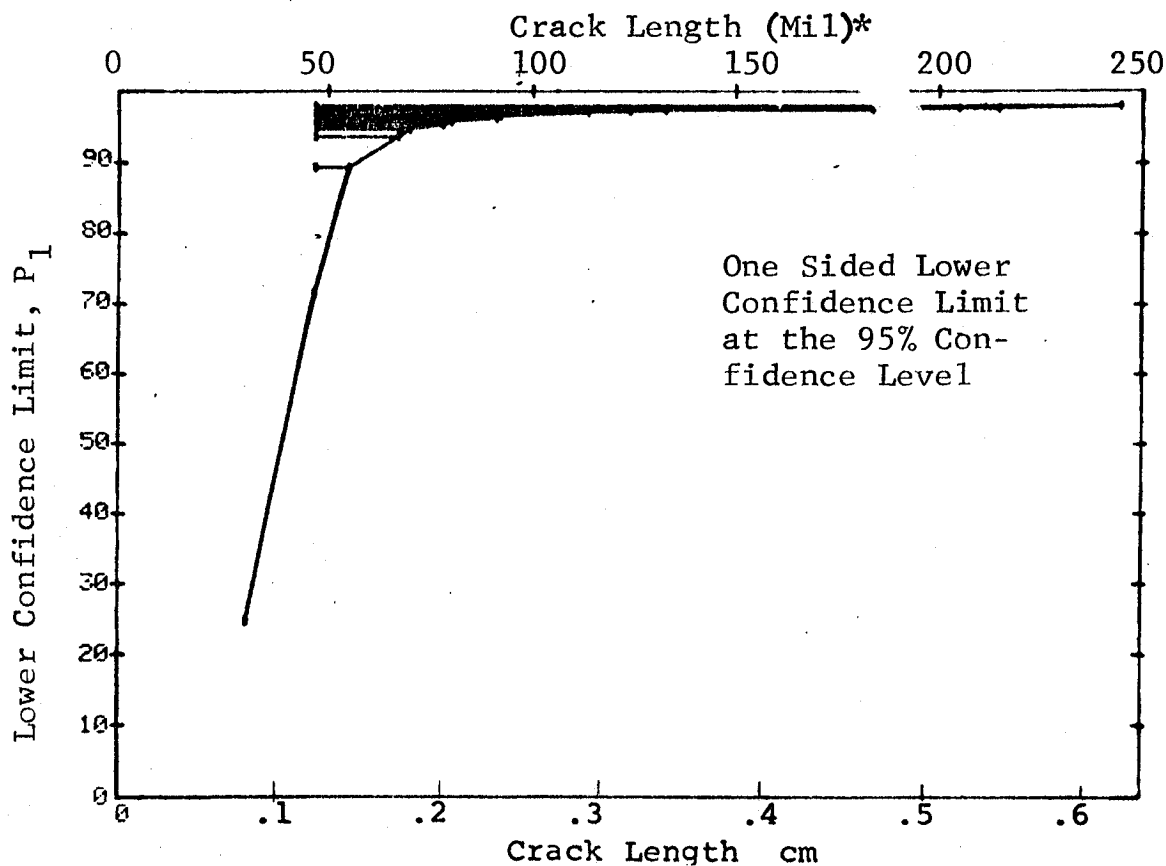


Figure D-37 (Continued)

(c) Overlapping Sixty Point Method of Data Cumulation

29-JUL-75	PENETRANT			TEST 3 (37)			ROCKWELL I D-1		
RANGE	MIN LN	* MAX LN	*	DET	50%	95%	0 MISS	1 MISS	
1	0	0	*	0	0	0	0	0	0
2	0	0		0	0	0	0	0	0
3	0	0		0	0	0	0	0	0
4	0	0		0	0	0	0	0	0
5	0	0		0	0	0	0	0	0
6	0	0		0	0	0	0	0	0
7	0	0		0	0	0	0	0	0
8	0	0		0	0	0	0	0	0
9	0	0		0	0	0	0	0	0
10	0	0		0	0	0	0	0	0
11	0	0		0	0	0	0	0	0
12	0	0		0	0	0	0	0	0
13	0	0		0	0	0	0	0	0
14	0	0		0	0	0	0	0	0
15	0	0		0	0	0	0	0	0
16	0	0		0	0	0	0	0	0
17	0	0		0	0	0	0	0	0
18	0	0		0	0	0	0	0	0
19	0	0		0	0	0	0	0	0
20	0	0		0	0	0	0	0	0
21	0	0		0	0	0	0	0	0
22	0	0		0	0	0	0	0	0
23	0	0		0	0	0	0	0	0
24	0	0		0	0	0	0	0	0
25	0	0		0	0	0	0	0	0
26	0	0		0	0	0	0	0	0
27	0	0		0	0	0	0	0	0
28	31	62		32	94	86	13	28	0
29	31	78		59	97	92	0	1	0
30	62	113		60	98	95	0	0	0
31	78	133		60	98	95	0	0	0
32	113	245		60	98	95	0	0	0

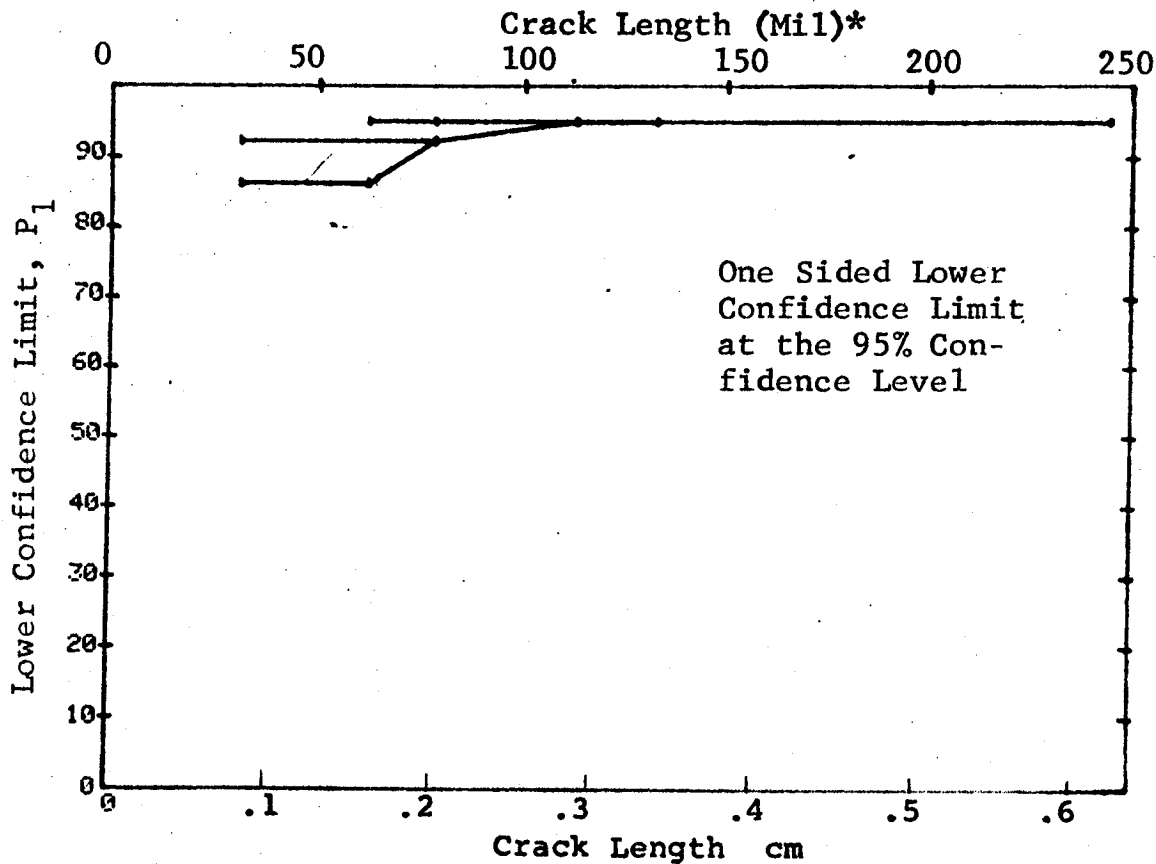


Figure D-37 (Concluded)

(a) Range Interval Method of Data Cumulation

09-OCT-75		PENETRANT		N	TEST 1		(38)	0 MISS	1 MISS
RANGE	MIN LN	MAX LN	47 *		DET	50%			
1	0	0	0	4	4	34	47	0	0
2	0	0	0	0	0	0	0	0	0
3	0	0	0	0	0	0	0	0	0
4	0	0	0	0	0	0	0	0	0
5	0	0	0	0	0	0	0	0	0
6	0	0	0	0	0	0	0	0	0
7	0	0	0	0	0	0	0	0	0
8	0	0	0	0	0	0	0	0	0
9	0	0	0	0	0	0	0	0	0
10	0	0	0	0	0	0	0	0	0
11	0	0	0	0	0	0	0	0	0
12	0	0	0	0	0	0	0	0	0
13	0	0	0	0	0	0	0	0	0
14	0	0	0	0	0	0	0	0	0
15	0	0	0	0	0	0	0	0	0
16	0	0	0	0	0	0	0	0	0
17	0	0	0	0	0	0	0	0	0
18	0	0	0	0	0	0	0	0	0
19	0	0	0	0	0	0	0	0	0
20	0	0	0	0	0	0	0	0	0
21	0	0	0	0	0	0	0	0	0
22	0	0	0	0	0	0	0	0	0
23	0	0	0	0	0	0	0	0	0
24	0	0	0	0	0	0	0	0	0
25	0	0	0	0	0	0	0	0	0
26	0	0	0	0	0	0	0	0	0
27	0	0	0	0	0	0	0	0	0
28	0	0	0	0	0	0	0	0	0
29	0	0	0	0	0	0	0	0	0
30	0	0	0	0	0	0	0	0	0
31	0	0	0	0	0	0	0	0	0
32	54	70		26	26	97	89	3	20

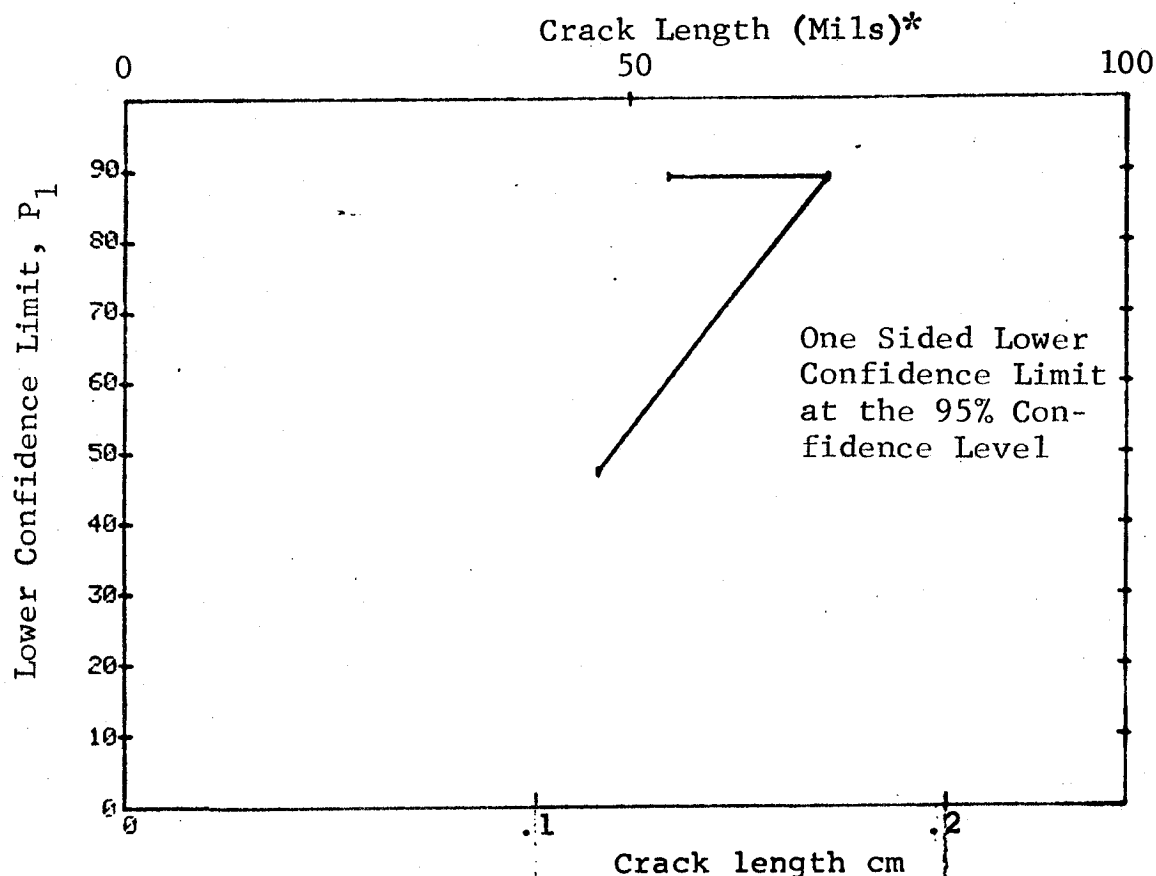


Figure D-38 Probability of Detection for Ti-6Al-4V Using Liquid Penetrant. Fatigue Cracks in Flat Plates.
Prod. Env. D-118

(b) Optimum Probability Method of Data Cumulation

09-OCT-75		PENETRANT		TEST 2		(38)		MISS		MISS	
RANGE	MIN	LN	47*	MAX	LN	47*	DET	50%	95%	0	1
1	0	0	0	0	0	0	4	0	0	0	0
2	0	0	0	0	0	0	0	0	0	0	0
3	0	0	0	0	0	0	0	0	0	0	0
4	0	0	0	0	0	0	0	0	0	0	0
5	0	0	0	0	0	0	0	0	0	0	0
6	0	0	0	0	0	0	0	0	0	0	0
7	0	0	0	0	0	0	0	0	0	0	0
8	0	0	0	0	0	0	0	0	0	0	0
9	0	0	0	0	0	0	0	0	0	0	0
10	0	0	0	0	0	0	0	0	0	0	0
11	0	0	0	0	0	0	0	0	0	0	0
12	0	0	0	0	0	0	0	0	0	0	0
13	0	0	0	0	0	0	0	0	0	0	0
14	0	0	0	0	0	0	0	0	0	0	0
15	0	0	0	0	0	0	0	0	0	0	0
16	0	0	0	0	0	0	0	0	0	0	0
17	0	0	0	0	0	0	0	0	0	0	0
18	0	0	0	0	0	0	0	0	0	0	0
19	0	0	0	0	0	0	0	0	0	0	0
20	0	0	0	0	0	0	0	0	0	0	0
21	0	0	0	0	0	0	0	0	0	0	0
22	0	0	0	0	0	0	0	0	0	0	0
23	0	0	0	0	0	0	0	0	0	0	0
24	0	0	0	0	0	0	0	0	0	0	0
25	0	0	0	0	0	0	0	0	0	0	0
26	0	0	0	0	0	0	0	0	0	0	0
27	0	0	0	0	0	0	0	0	0	0	0
28	0	0	0	0	0	0	0	0	0	0	0
29	0	0	0	0	0	0	0	0	0	0	0
30	0	0	0	0	0	0	0	0	0	0	0
31	0	0	0	0	0	0	0	0	0	0	0
32	0	0	0	0	0	0	0	0	0	0	16

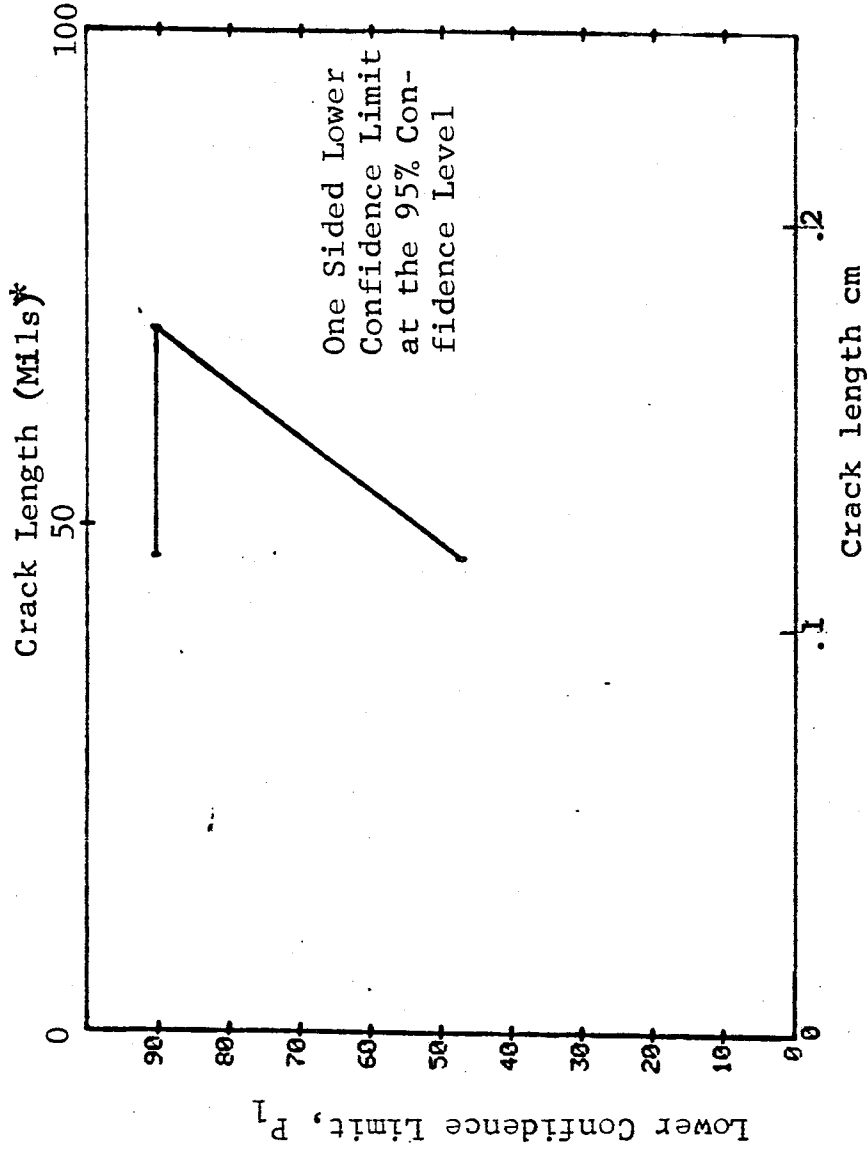
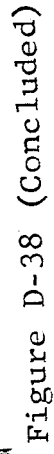


Figure D-38 (Continued)

[illegible]

(a) Range Interval Method of Data Cumulation

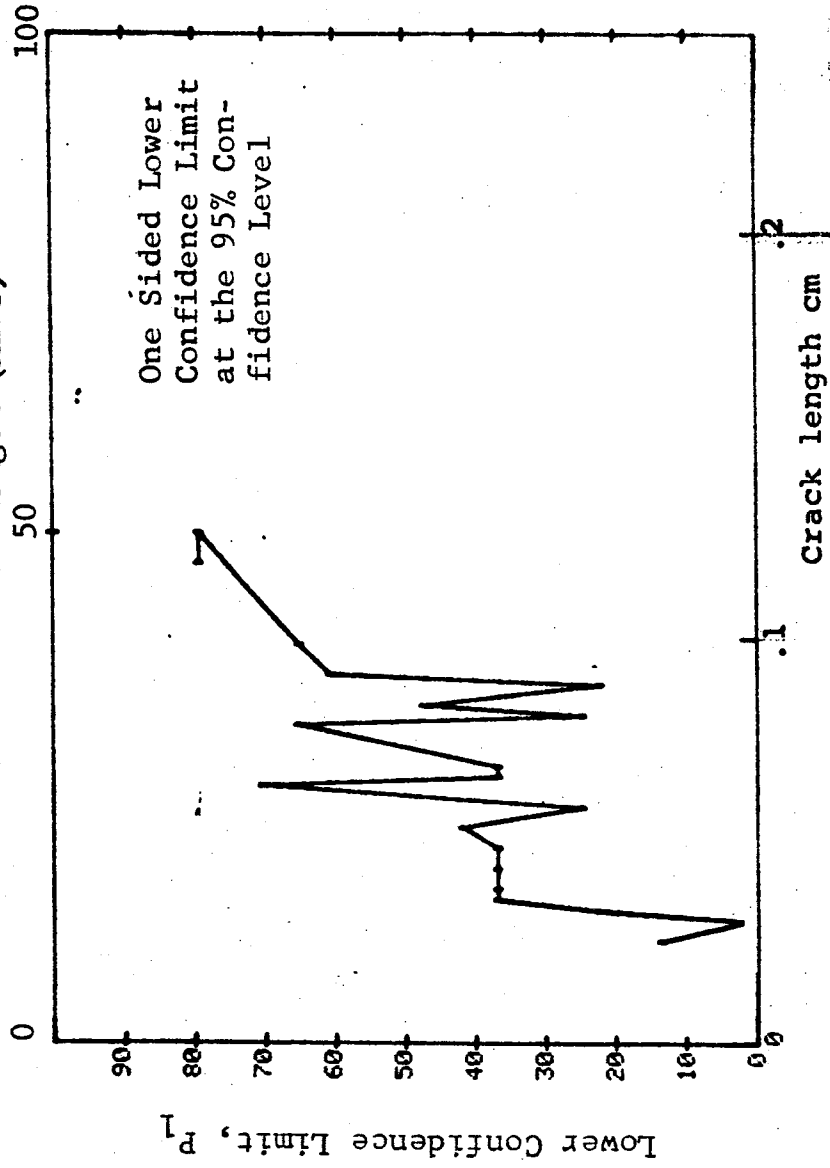
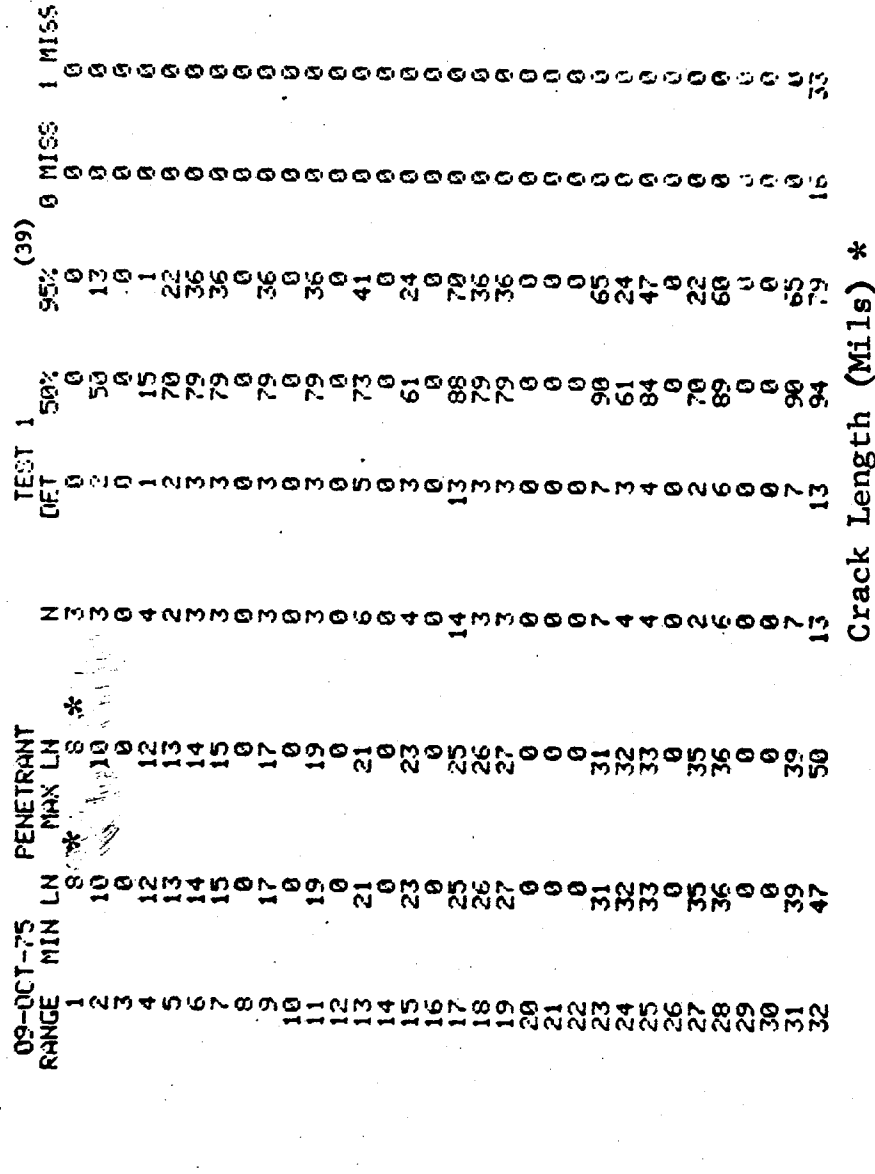


Figure D-39 Probability of Detection for Ti-6Al-4V Using Liquid Penetrant. Fatigue Cracks in Flat Plates. Prod. Env.

(b) Optimum Probability Method of Data Cumulation

09-OCT-75		PENETRANT		N	TEST 2		(39)		
RANGE	MIN	LN	MAX LN		DET	50%	95%	0 MISS	1 MISS
1		8*	8*	3	0	0	0	0	0
2		10	10	3	2	0	13	0	0
3		0	0	0	0	0	0	0	0
4		10	12	7	3	0	12	0	0
5		10	13	9	5	0	25	0	0
6		13	14	5	5	0	54	0	0
7		13	15	8	8	0	68	0	0
8		0	0	0	0	0	0	0	0
9		13	17	11	11	0	76	0	0
10		0	0	0	0	0	0	0	0
11		13	19	14	14	0	80	15	32
12		0	0	0	0	0	0	0	0
13		13	21	20	19	0	78	0	0
14		0	0	0	0	0	0	0	0
15		13	23	24	22	0	75	0	0
16		0	0	0	0	0	0	0	0
17		13	25	38	35	0	80	38	51
18		13	26	41	38	0	82	35	48
19		13	27	44	41	0	83	32	45
20		0	0	0	0	0	0	0	0
21		0	0	0	0	0	0	0	0
22		0	0	0	0	0	0	0	0
23		13	31	51	48	0	85	25	38
24		13	32	55	51	0	84	34	48
25		13	33	59	55	0	85	30	44
26		0	0	0	0	0	0	0	0
27		13	35	61	57	0	85	28	42
28		13	36	67	63	0	86	22	36
29		0	0	0	0	0	0	0	0
30		0	0	0	0	0	0	0	0
31		13	39	74	70	0	88	15	24
32		33	50	32	32	0	91	0	14

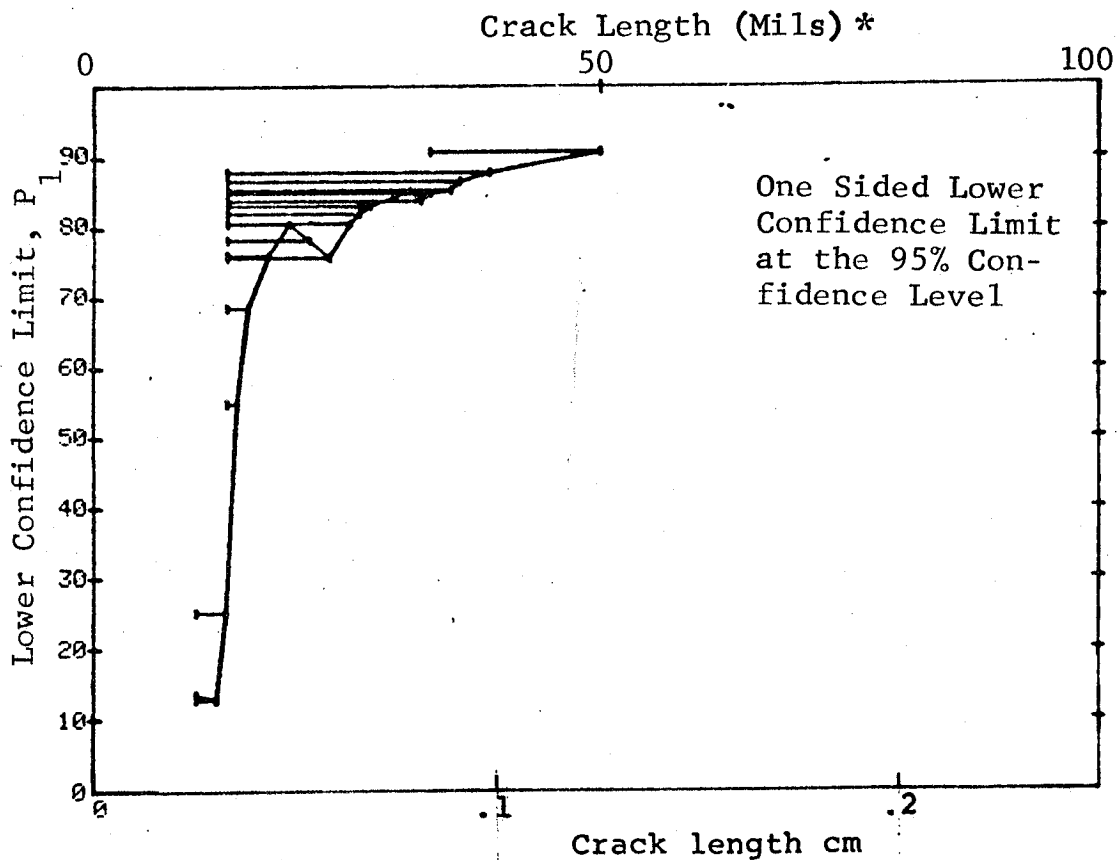


Figure D-39 (Continued)

(c) Overlapping Sixty Point Method of Data Cumulation

09-OCT-75	PENETRANT		TEST 3		(39)	MISS		MISS
RANGE	MIN	LN	MAX	LN	DET	50%	95%	1 MISS
1	0	0	0	0	0	0	0	0
2	0	0	0	0	0	0	0	0
3	0	0	0	0	0	0	0	0
4	0	0	0	0	0	0	0	0
5	0	0	0	0	0	0	0	0
6	0	0	0	0	0	0	0	0
7	0	0	0	0	0	0	0	0
8	0	0	0	0	0	0	0	0
9	0	0	0	0	0	0	0	0
10	0	0	0	0	0	0	0	0
11	0	0	0	0	0	0	0	0
12	0	0	0	0	0	0	0	0
13	0	0	0	0	0	0	0	0
14	0	0	0	0	0	0	0	0
15	0	0	0	0	0	0	0	0
16	0	0	0	0	0	0	0	0
17	0	0	0	0	0	0	0	0
18	0	0	0	0	0	0	0	0
19	0	0	0	0	0	0	0	0
20	0	0	0	0	0	0	0	0
21	0	0	0	0	0	0	0	0
22	0	0	0	0	0	0	0	0
23	0	0	0	0	0	0	0	0
24	0	0	0	0	0	0	0	0
25	0	0	0	0	0	0	0	0
26	0	0	0	0	0	0	0	0
27	0	0	0	0	0	0	0	0
28	0	0	0	0	0	0	0	0
29	0	0	0	0	0	0	0	0
30	8	12	25	0	0	0	0	0
31	12	33	50	37	28	74	61	0
32	25	50		60	53	87	79	0
				60	58	95	89	16

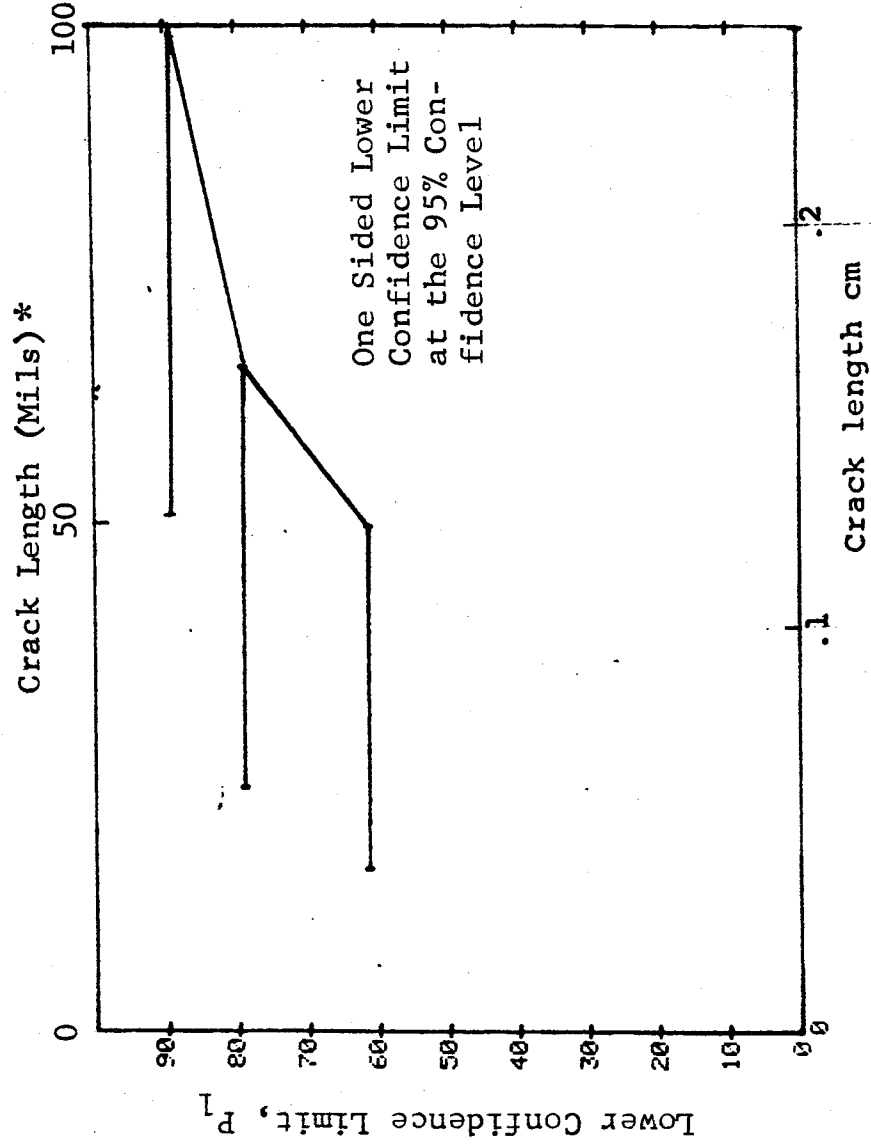


Figure D-39 (Concluded)

(a) Range Interval Method of Data Cumulation

09-OCT-75	PENETRANT		TEST 1		95%	(40)	1 MISS
RANGE	MIN	LN	MAX	LN	DET	MISS	
1	37	*	37	*	5	0	0
2	44	*	44	*	7	0	0
3	51	*	51	*	7	0	0
4	60	*	60	*	7	0	0
5	68	*	68	*	0	0	0
6	76	*	76	*	0	0	0
7	85	*	85	*	7	0	0
8	91	*	91	*	3	0	0
9	93	*	93	*	0	0	0
10	101	*	101	*	2	17	34
11	105	*	105	*	12	17	34
12	110	*	110	*	7	0	0
13	113	*	113	*	12	0	0
14	115	*	115	*	7	0	0
15	125	*	125	*	5	0	0
16	135	*	135	*	4	0	0
17	147	*	147	*	0	0	0
18	153	*	153	*	10	0	0
19	162	*	162	*	0	0	0
20	164	*	164	*	4	0	0
21	176	*	176	*	0	0	0
22	189	*	189	*	2	0	0
23	194	*	194	*	0	0	0
24	194	*	194	*	12	0	34
25	194	*	194	*	3	0	0
26	194	*	194	*	4	0	0
27	194	*	194	*	0	0	0
28	194	*	194	*	0	0	0
29	194	*	194	*	3	0	0
30	194	*	194	*	0	0	0
31	194	*	194	*	0	0	0
32	194	*	194	*	5	0	0

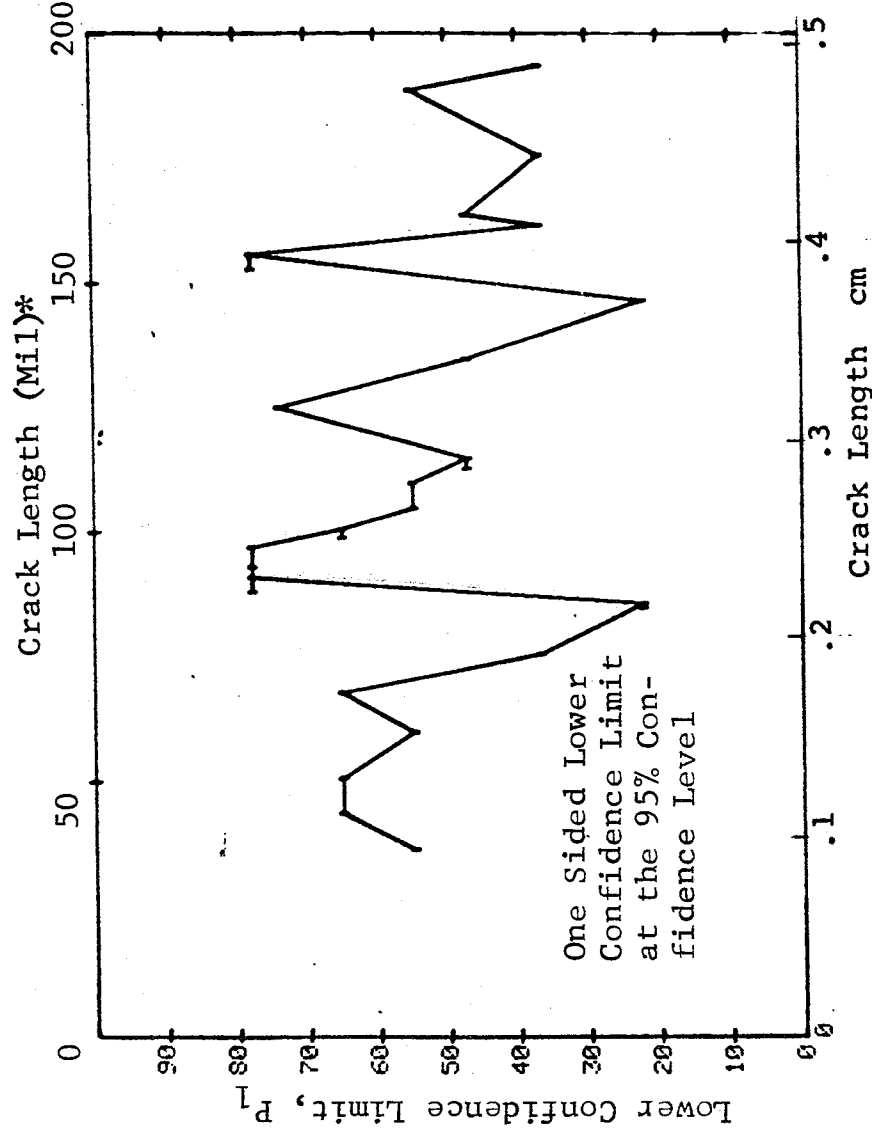


Figure D-40 Probability of Detection for 7075-T6511 Al Using Liquid Penetrant. Fatigue Cracks in Flat Plates.
Prod. Env. D-124

(b) Optimum Probability Method of Data Cumulation

09-OCT-75 RANGE	MIN	PENETRANT		N	TEST 2		(40)		0 MISS	1 MISS
		LN *	MAX LN *		DET	50%	95%	54		
1	1	37	37	5	5	0	0	54	0	0
2	2	37	44	12	12	0	0	77	0	0
3	3	37	51	19	19	0	0	85	10	27
4	4	0	0	0	24	0	0	0	0	0
5	5	37	60	24	0	0	0	88	5	22
6	6	0	0	0	0	0	0	0	0	0
7	7	37	68	31	31	0	0	90	0	15
8	8	37	76	34	34	0	0	91	0	12
9	9	0	0	0	36	0	0	0	0	0
10	10	37	86	36	36	0	0	92	0	10
11	11	37	91	48	48	0	0	93	0	0
12	12	37	97	60	60	0	0	95	0	0
13	13	37	101	67	67	0	0	95	0	0
14	14	37	105	72	72	0	0	95	0	0
15	15	37	110	77	77	0	0	96	0	0
16	16	37	115	81	81	0	0	96	0	0
17	17	0	0	0	0	0	0	0	0	0
18	18	37	125	91	91	0	0	96	0	0
19	19	0	0	0	0	0	0	0	0	0
20	20	37	135	95	95	0	0	96	0	0
21	21	0	0	0	0	0	0	0	0	0
22	22	37	147	97	97	0	0	96	0	0
23	23	0	0	0	0	0	0	0	0	0
24	24	37	156	109	109	0	0	97	0	0
25	25	37	162	112	112	0	0	97	0	0
26	26	37	164	116	116	0	0	97	0	0
27	27	0	0	0	0	0	0	0	0	0
28	28	37	176	119	119	0	0	97	0	0
29	29	0	0	0	0	0	0	0	0	0
30	30	0	0	0	0	0	0	0	0	0
31	31	37	189	124	124	0	0	97	0	0
32	32	37	194	127	127	0	0	97	0	0

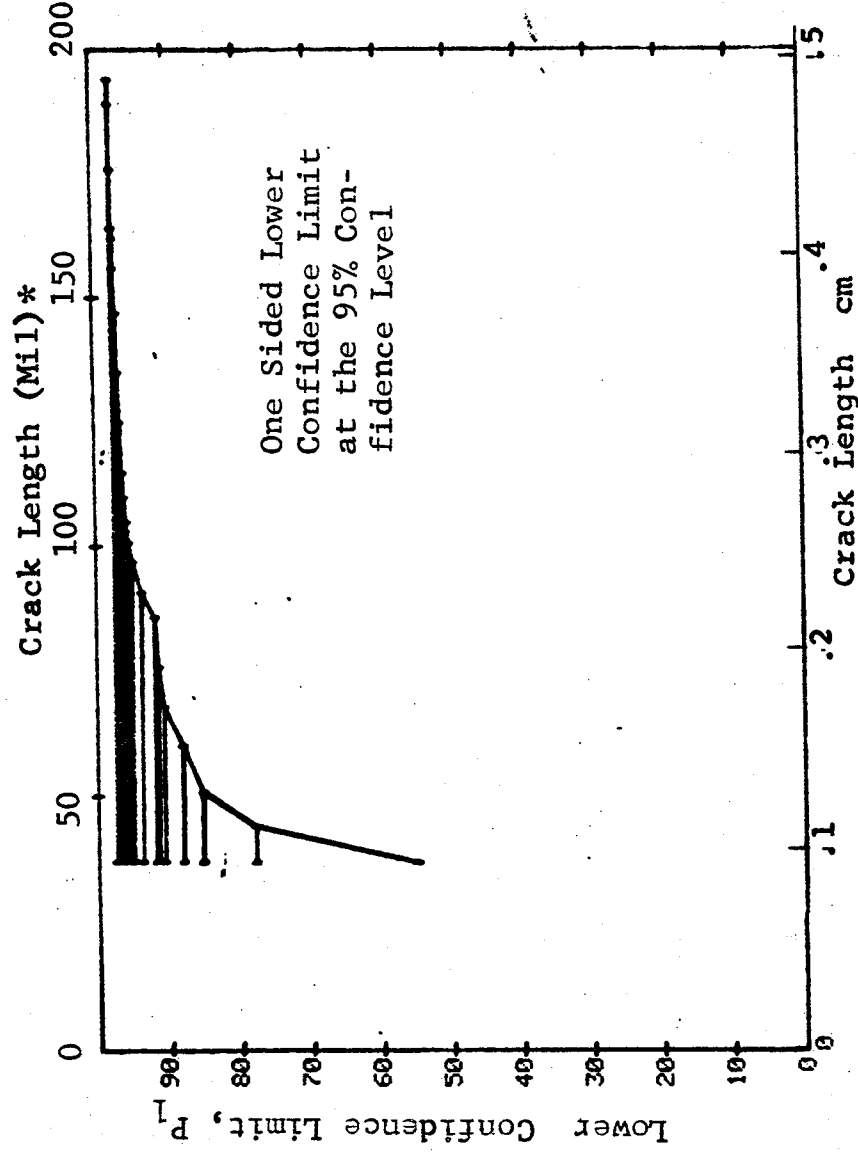


Figure D-40 (Continued)

(c) Overlapping Sixty Point Method of Data Cumulation

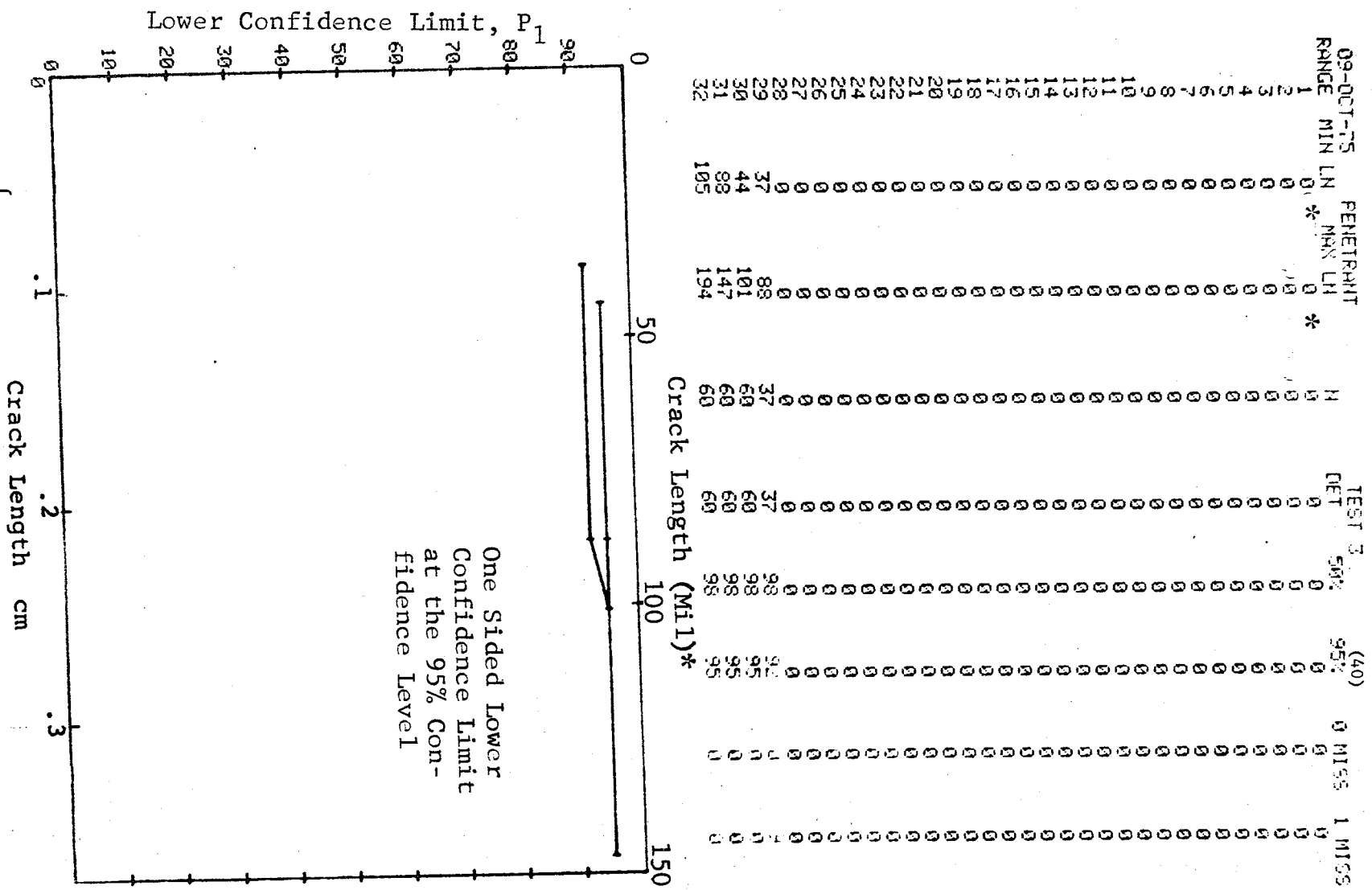


Figure D-40 (Concluded)

(a) Range Interval Method of Data Cumulation

09-OCT-75	RANGE	MIN	LN	MAX	LN	PENETRANT	H	DET	TEST 1	50%	95%	(41)	MISS	1 MISS
1			44	*	0		10	10	50%	93	74	0	0	0
2			0		0		0	0	0	0	0	0	0	0
3			0		0		0	0	0	0	0	0	0	0
4			0		0		0	0	0	0	0	0	0	0
5			0		0		0	0	0	0	0	0	0	0
6			0		0		0	0	0	0	0	0	0	0
7			0		0		0	0	0	0	0	0	0	0
8			0		0		0	0	0	0	0	0	0	0
9			0		0		0	0	0	0	0	0	0	0
10			0		0		0	0	0	0	0	0	0	0
11			0		0		0	0	0	0	0	0	0	0
12			0		0		0	0	0	0	0	0	0	0
13			0		0		0	0	0	0	0	0	0	0
14			0		0		0	0	0	0	0	0	0	0
15			0		0		0	0	0	0	0	0	0	0
16			0		0		0	0	0	0	0	0	0	0
17			0		0		0	0	0	0	0	0	0	0
18			0		0		0	0	0	0	0	0	0	0
19			0		0		0	0	0	0	0	0	0	0
20			0		0		0	0	0	0	0	0	0	0
21			0		0		0	0	0	0	0	0	0	0
22			0		0		0	0	0	0	0	0	0	0
23			0		0		0	0	0	0	0	0	0	0
24			0		0		0	0	0	0	0	0	0	0
25			0		0		0	0	0	0	0	0	0	0
26			0		0		0	0	0	0	0	0	0	0
27			0		0		0	0	0	0	0	0	0	0
28			0		0		0	0	0	0	0	0	0	0
29			0		0		0	0	0	0	0	0	0	0
30			0		0		0	0	0	0	0	0	0	0
31			0		0		0	0	0	0	0	0	0	0
32			0		0		0	0	0	0	0	0	0	0

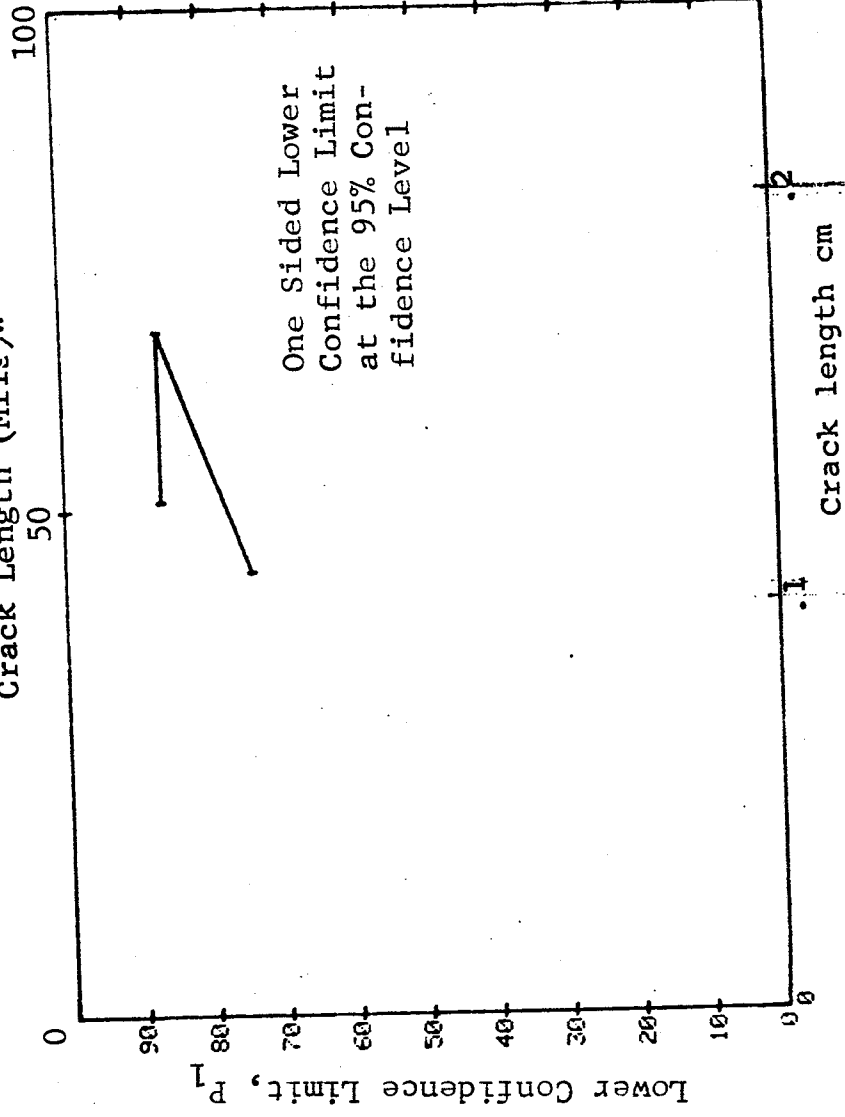


Figure D-41 Probability of Detection for 7075-T6511 Al Using Liquid Penetrant. Fatigue Cracks in Flat Plates.

Prod. Env. D-127

(b) Optimum Probability Method of Data Cumulation

09-OCT-75 RANGE	NIN	LN	44*	PENETRANT MAX LN	44*	H	TEST 2 DET	50%	(41) 95%	0 MISS	1 MISS
1	1	0	0	0	0	10	10	0	74	0	0
2	2	0	0	0	0	0	0	0	0	0	0
3	3	0	0	0	0	0	0	0	0	0	0
4	4	0	0	0	0	0	0	0	0	0	0
5	5	0	0	0	0	0	0	0	0	0	0
6	6	0	0	0	0	0	0	0	0	0	0
7	7	0	0	0	0	0	0	0	0	0	0
8	8	0	0	0	0	0	0	0	0	0	0
9	9	0	0	0	0	0	0	0	0	0	0
10	10	0	0	0	0	0	0	0	0	0	0
11	11	0	0	0	0	0	0	0	0	0	0
12	12	0	0	0	0	0	0	0	0	0	0
13	13	0	0	0	0	0	0	0	0	0	0
14	14	0	0	0	0	0	0	0	0	0	0
15	15	0	0	0	0	0	0	0	0	0	0
16	16	0	0	0	0	0	0	0	0	0	0
17	17	0	0	0	0	0	0	0	0	0	0
18	18	0	0	0	0	0	0	0	0	0	0
19	19	0	0	0	0	0	0	0	0	0	0
20	20	0	0	0	0	0	0	0	0	0	0
21	21	0	0	0	0	0	0	0	0	0	0
22	22	0	0	0	0	0	0	0	0	0	0
23	23	0	0	0	0	0	0	0	0	0	0
24	24	0	0	0	0	0	0	0	0	0	0
25	25	0	0	0	0	0	0	0	0	0	0
26	26	0	0	0	0	0	0	0	0	0	0
27	27	0	0	0	0	0	0	0	0	0	0
28	28	0	0	0	0	0	0	0	0	0	0
29	29	0	0	0	0	0	0	0	0	0	0
30	30	0	0	0	0	0	0	0	0	0	0
31	31	0	0	0	0	0	0	0	0	0	0
32	44	68	31	31	0	0	0	0	0	0	15

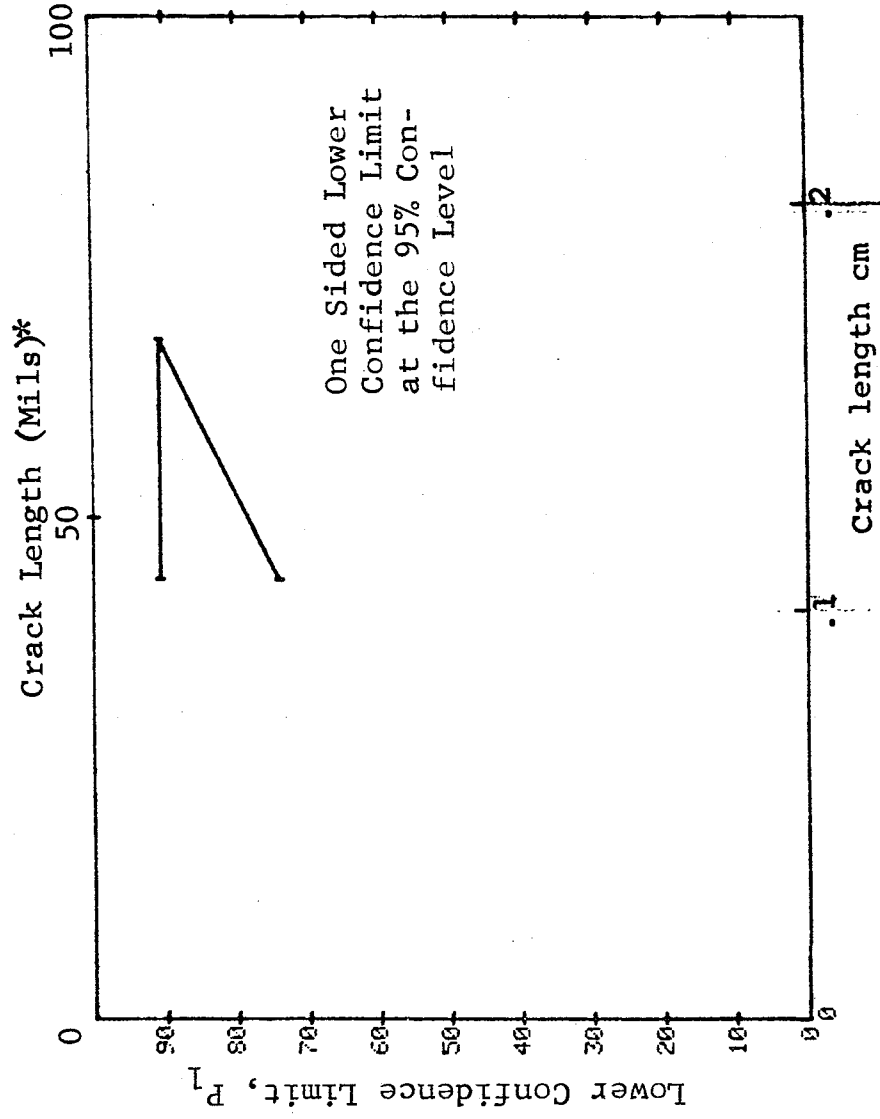


Figure D-41 (Continued)

(c) Overlapping Sixty Point Method of Data Cumulation

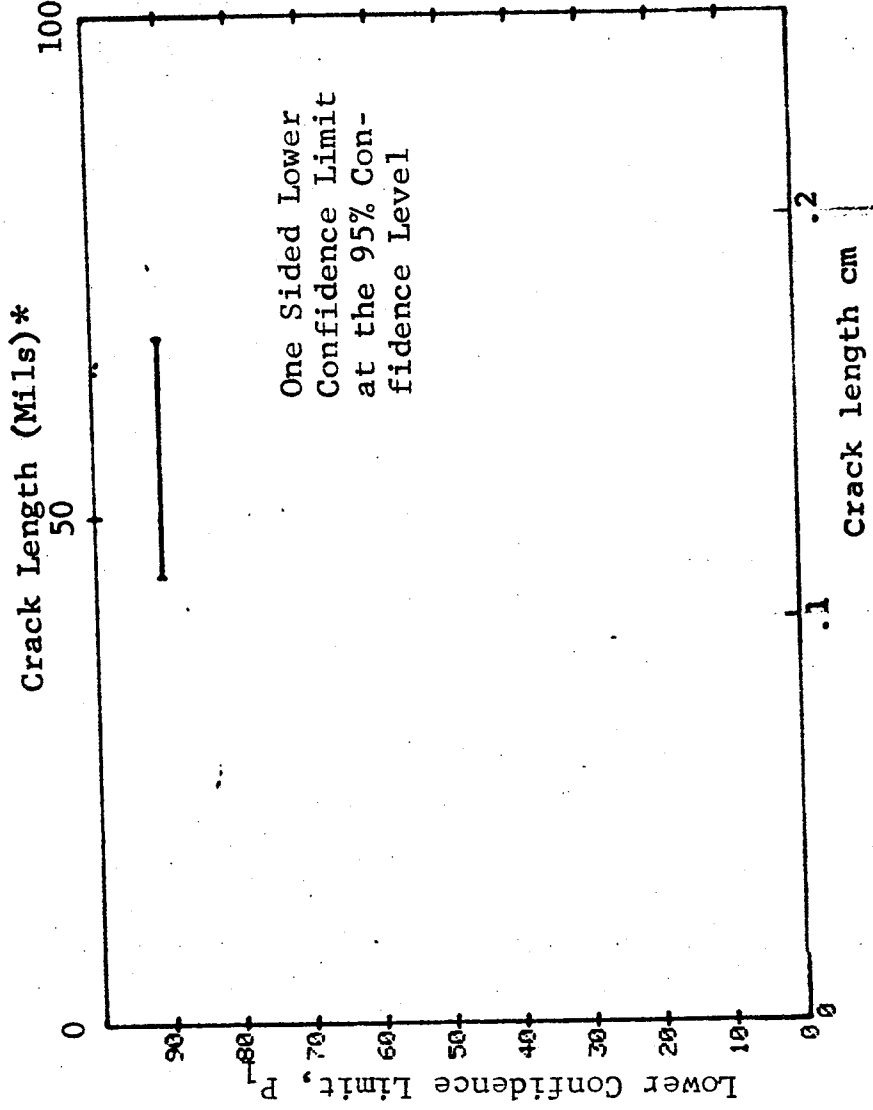
[illegible]

Figure D-41 (Continued)

(a) Range Interval Method of Data Cumulation

09-OCT-75		PENETRANT		TEST 1		(42)		95%		MISS		MISS	
RANGE	MIN LN	44 *	MAX LN	44 *	DET	50%	93	74	0	MISS	0	MISS	1
1	2	3	4	5	6	7	8	9	10	11	12	13	14
15	16	17	18	19	20	21	22	23	24	25	26	27	28
29	30	31	32	51	68	21	21	96	86	3	35		

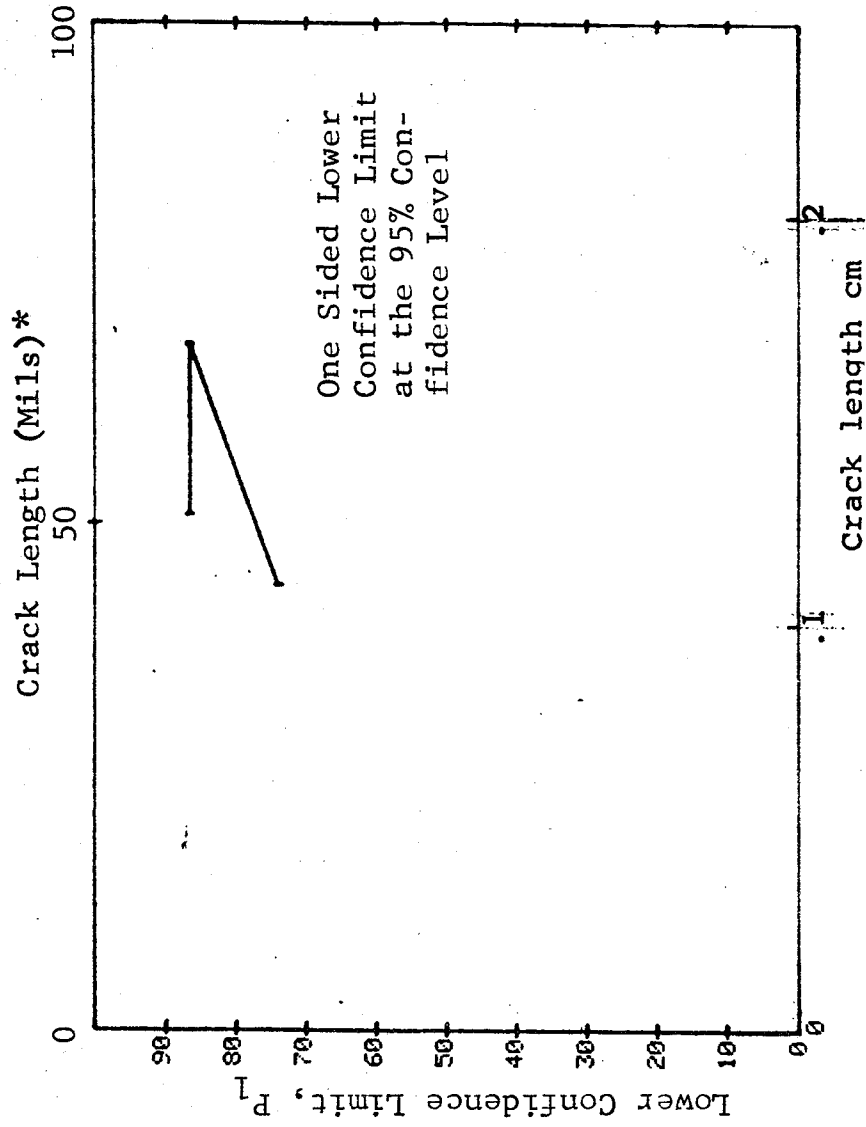


Figure D-42 Probability of Detection for 7075-T6511 Al Using Liquid Penetrant. Fatigue Cracks in Flat Plates.

(b) Optimum Probability Method of Data Cumulation

09-OCT-75		PENETRANT		TEST 2		(42)		MISS		MISS	
RANGE	MIN	LN	MAX LN	DET	50%	95%	N	0	MISS	1	MISS
1	0	44*	0	10	0	74	10	0	0	0	0
2	0	0	0	0	0	0	0	0	0	0	0
3	0	0	0	0	0	0	0	0	0	0	0
4	0	0	0	0	0	0	0	0	0	0	0
5	0	0	0	0	0	0	0	0	0	0	0
6	0	0	0	0	0	0	0	0	0	0	0
7	0	0	0	0	0	0	0	0	0	0	0
8	0	0	0	0	0	0	0	0	0	0	0
9	0	0	0	0	0	0	0	0	0	0	0
10	0	0	0	0	0	0	0	0	0	0	0
11	0	0	0	0	0	0	0	0	0	0	0
12	0	0	0	0	0	0	0	0	0	0	0
13	0	0	0	0	0	0	0	0	0	0	0
14	0	0	0	0	0	0	0	0	0	0	0
15	0	0	0	0	0	0	0	0	0	0	0
16	0	0	0	0	0	0	0	0	0	0	0
17	0	0	0	0	0	0	0	0	0	0	0
18	0	0	0	0	0	0	0	0	0	0	0
19	0	0	0	0	0	0	0	0	0	0	0
20	0	0	0	0	0	0	0	0	0	0	0
21	0	0	0	0	0	0	0	0	0	0	0
22	0	0	0	0	0	0	0	0	0	0	0
23	0	0	0	0	0	0	0	0	0	0	0
24	0	0	0	0	0	0	0	0	0	0	0
25	0	0	0	0	0	0	0	0	0	0	0
26	0	0	0	0	0	0	0	0	0	0	0
27	0	0	0	0	0	0	0	0	0	0	0
28	0	0	0	0	0	0	0	0	0	0	0
29	0	0	0	0	0	0	0	0	0	0	0
30	0	0	0	0	0	0	0	0	0	0	0
31	0	0	0	0	0	0	0	0	0	0	0
32	0	0	0	0	0	0	0	0	0	0	15
		44	68	31	0	98	31	0	0	0	0

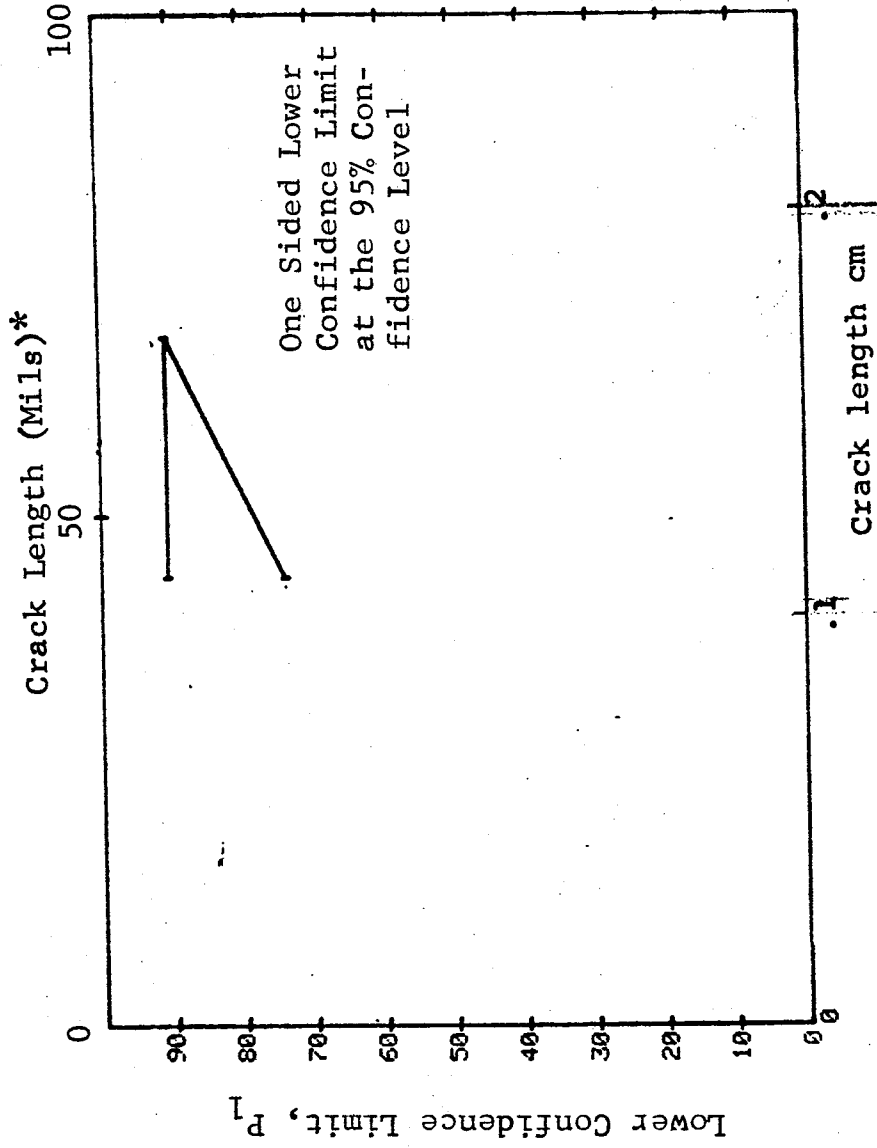


Figure D-42 (Continued)

(c) Overlapping Sixty Point Method of Data Cumulation

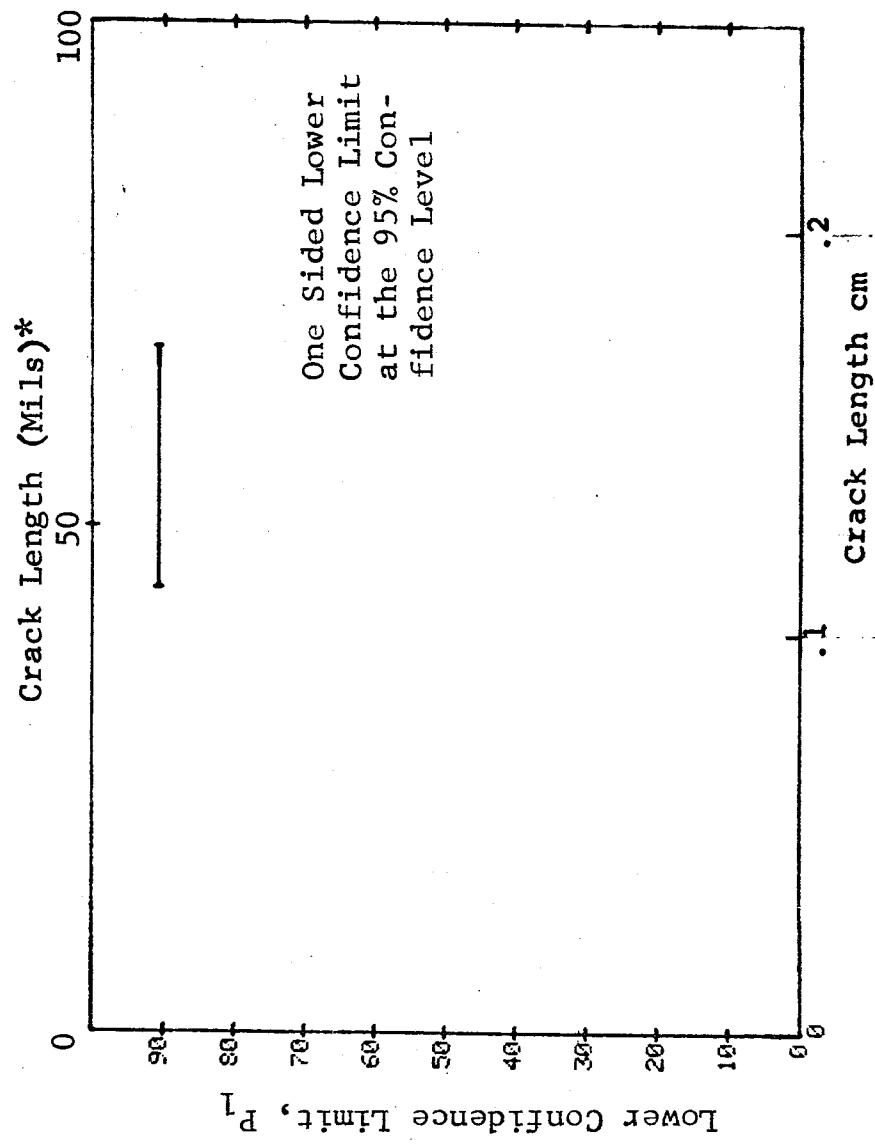
[illegible]

Figure D-42 (Concluded)

(a) Range Interval Method of Data Cumulation

09-OCT-75 RANGE	MIN	LN	* LN	* MAX	PENETRANT	N	TEST 1 DFT	50%	95%	(43)	0 MISS	1 MISS
1	1	19	0	19	0	3	0	0	0	0	0	0
2	2	0	0	0	0	0	0	0	0	0	0	0
3	3	0	0	0	0	0	0	0	0	0	0	0
4	4	0	0	0	0	0	0	0	0	0	0	0
5	5	0	0	0	0	0	0	0	0	0	0	0
6	6	0	0	0	0	0	0	0	0	0	0	0
7	7	0	0	0	0	0	0	0	0	0	0	0
8	8	0	0	0	0	0	0	0	0	0	0	0
9	9	0	0	0	0	0	0	0	0	0	0	0
10	10	0	0	0	0	0	0	0	0	0	0	0
11	11	0	0	0	0	0	0	0	0	0	0	0
12	12	0	0	0	0	0	0	0	0	0	0	0
13	13	0	0	0	0	0	0	0	0	0	0	0
14	14	0	0	0	0	0	0	0	0	0	0	0
15	15	0	0	0	0	0	0	0	0	0	0	0
16	16	0	0	0	0	0	0	0	0	0	0	0
17	17	0	0	0	0	0	0	0	0	0	0	0
18	18	0	0	0	0	0	0	0	0	0	0	0
19	19	0	0	0	0	0	0	0	0	0	0	0
20	20	39	0	39	0	5	5	87	54	0	0	0
21	21	0	0	0	0	0	0	0	0	0	0	0
22	22	0	0	0	0	0	0	0	0	0	0	0
23	23	0	0	0	0	0	0	0	0	0	0	0
24	24	0	0	0	0	0	0	0	0	0	0	0
25	25	0	0	0	0	0	0	0	0	0	0	0
26	26	0	0	0	0	0	0	0	0	0	0	0
27	27	0	0	0	0	0	0	0	0	0	0	0
28	28	0	0	0	0	0	0	0	0	0	0	0
29	29	0	0	0	0	0	0	0	0	0	0	0
30	30	49	0	49	0	7	7	90	65	0	0	0
31	31	0	0	0	0	0	0	97	88	0	0	0
32	32	60	0	80	0	24	24	0	0	0	0	0

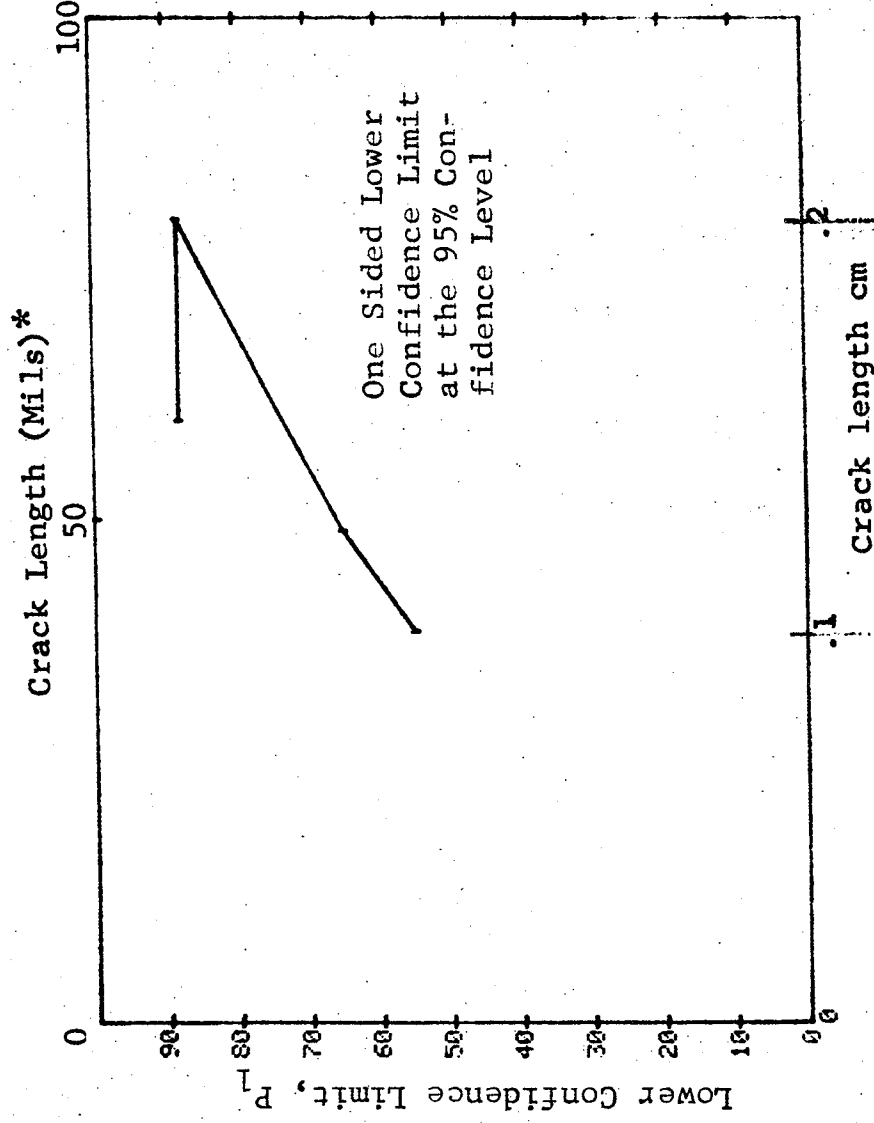


Figure D-43 Probability of Detection for PH13-8 Mo. St. Using Liquid Penetrant. Fatigue Cracks in Flat Plates. Prod. Env. D-133

(b) Optimum Probability Method of Data Cumulation

09-OCT-75	PENETRANT		TEST		(43)	0 MISS		1 MISS
RANGE MIN LN	LN	MAX LN	N	DET	50%	95%	0 MISS	1 MISS
1	19 *	19 *	3	0	0	0	0	0
2	0	0	0	0	0	0	0	0
3	0	0	0	0	0	0	0	0
4	0	0	0	0	0	0	0	0
5	0	0	0	0	0	0	0	0
6	0	0	0	0	0	0	0	0
7	0	0	0	0	0	0	0	0
8	0	0	0	0	0	0	0	0
9	0	0	0	0	0	0	0	0
10	0	0	0	0	0	0	0	0
11	0	0	0	0	0	0	0	0
12	0	0	0	0	0	0	0	0
13	0	0	0	0	0	0	0	0
14	0	0	0	0	0	0	0	0
15	0	0	0	0	0	0	0	0
16	0	0	0	0	0	0	0	0
17	0	0	0	0	0	0	0	0
18	0	0	0	0	0	0	0	0
19	0	0	0	0	0	0	0	0
20	39	39	5	5	0	54	0	0
21	0	0	0	0	0	0	0	0
22	0	0	0	0	0	0	0	0
23	0	0	0	0	0	0	0	0
24	0	0	0	0	0	0	0	0
25	0	0	0	0	0	0	0	0
26	0	0	0	0	0	0	0	0
27	0	0	0	0	0	0	0	0
28	0	0	0	0	0	0	0	0
29	0	0	0	0	0	0	0	0
30	39	49	12	12	0	77	0	0
31	0	0	0	0	0	0	0	0
32	39	80	35	36	0	92	0	10

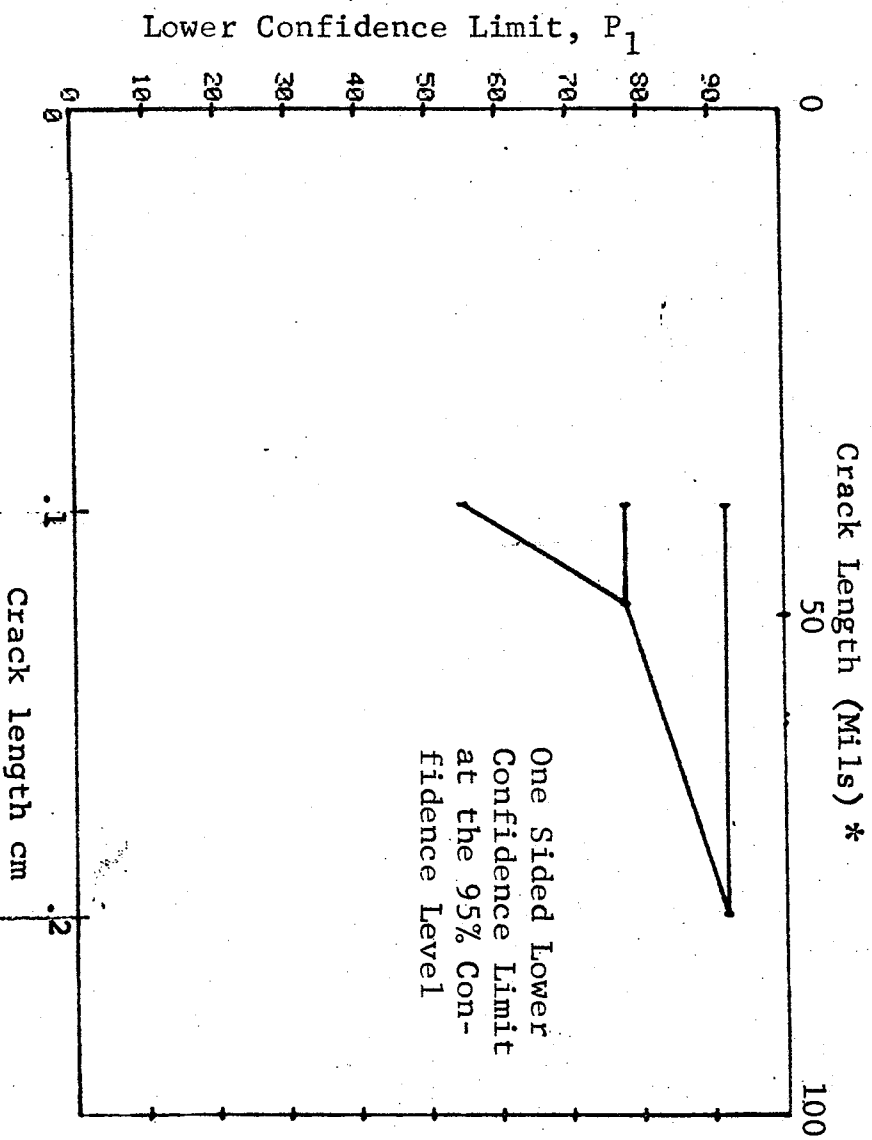
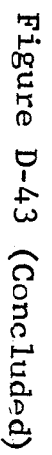


Figure D-43 (Continued)

	09-OCT-75	PENETRANT	TEST 3	(43)
RANGE MIN LN	MAX LN	DET	50%	95%
1	*	0	0	0
2	0	0	0	0
3	0	0	0	0
4	0	0	0	0
5	0	0	0	0
6	0	0	0	0
7	0	0	0	0
8	0	0	0	0
9	0	0	0	0
10	0	0	0	0
11	0	0	0	0
12	0	0	0	0
13	0	0	0	0
14	0	0	0	0
15	0	0	0	0
16	0	0	0	0
17	0	0	0	0
18	0	0	0	0
19	0	0	0	0
20	0	0	0	0
21	0	0	0	0
22	0	0	0	0
23	0	0	0	0
24	0	0	0	0
25	0	0	0	0
26	0	0	0	0
27	0	0	0	0
28	0	0	0	0
29	0	0	0	0
30	0	0	0	0
31	0	0	0	0
32	0	0	0	0



(a) Range Interval Method of Data Cumulation

09-OCT-75		ULTRASONIC		N	TEST 1		(44)	
RANGE	MIN	LN	* MAX LN *		DET	50%	95%	0 MISS
1		48	52	29	28	94	84	17
2		0	0	0	0	0	0	0
3		60	62	16	16	95	82	13
4		68	68	9	9	92	71	0
5		0	0	0	0	0	0	0
6		75	75	6	6	89	60	0
7		0	0	0	0	0	0	0
8		0	0	0	0	0	0	0
9		90	90	11	11	93	76	18
10		95	98	20	20	96	86	9
11	102	102	102	4	4	84	47	0
12	0	0	0	0	0	0	0	0
13	110	110	110	7	7	90	65	0
14	0	0	0	0	0	0	0	0
15	0	0	0	0	0	0	0	0
16	0	0	0	0	0	0	0	0
17	0	0	0	0	0	0	0	0
18	0	0	0	0	0	0	0	0
19	142	142	142	5	5	87	54	0
20	145	148	148	7	7	90	65	0
21	0	0	0	0	0	0	0	0
22	155	158	158	8	8	91	68	0
23	160	160	160	4	4	84	47	0
24	165	165	165	4	4	84	47	0
25	0	0	0	0	0	0	0	0
26	0	0	0	0	0	0	0	0
27	0	0	0	0	0	0	0	0
28	0	0	0	0	0	0	0	0
29	0	0	0	0	0	0	0	0
30	195	195	195	3	3	79	36	0
31	0	0	0	0	0	0	0	0
32	218	218	218	4	4	84	47	0

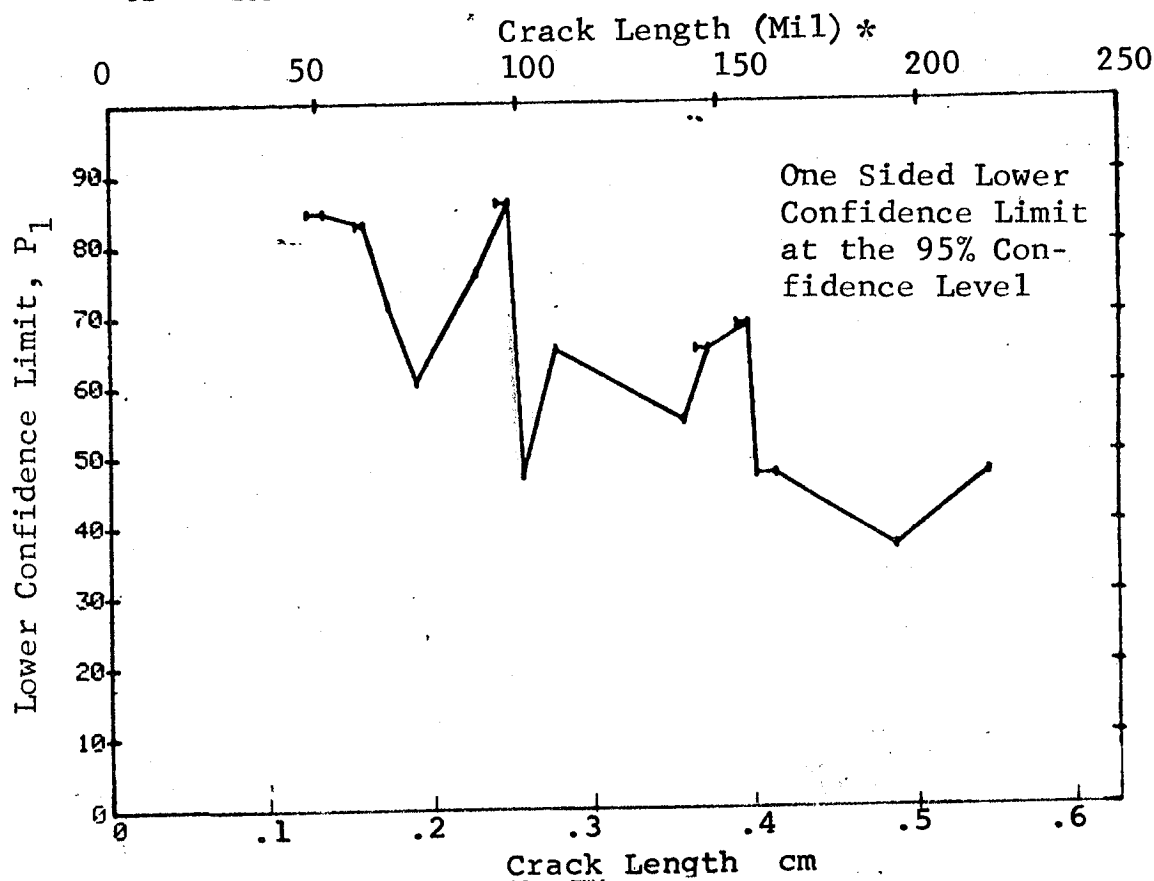


Figure D-44 Probability of Detection for Ti-6Al-4V Using Ultrasonic Shear Wave. Fatigue Cracks in Welded Flat Corroded Plates. Prod. Env.

(b) Optimum Probability Method of Data Cumulation

09-OCT-75 RANGE	MIN	ULTRASONIC		N	TEST 2 DET	50%	95%	(44)		1 MISS	32
		LN	MAX LN					0 MISS	1 MISS		
1	48 *	0	52 *	29	28	0	84	17	0	0	0
2	48	0	0	0	0	0	0	0	0	0	0
3	48	0	62	45	44	0	89	1	1	16	0
4	48	0	68	54	53	0	91	0	0	0	0
5	48	0	75	60	59	0	92	0	0	0	0
6	0	0	0	0	0	0	0	0	0	1	0
7	0	0	0	0	0	0	0	0	0	0	0
8	0	0	0	0	0	0	0	0	0	0	0
9	48	0	90	71	70	0	93	0	0	0	0
10	60	0	98	62	62	0	93	0	0	0	0
11	60	0	102	66	66	0	95	0	0	0	0
12	0	0	0	0	0	0	0	0	0	0	0
13	60	0	110	73	73	0	95	0	0	0	0
14	0	0	0	0	0	0	0	0	0	0	0
15	0	0	0	0	0	0	0	0	0	0	0
16	0	0	0	0	0	0	0	0	0	0	0
17	0	0	0	0	0	0	0	0	0	0	0
18	0	0	0	0	0	0	0	0	0	0	0
19	60	0	142	78	78	0	96	0	0	0	0
20	60	0	148	85	85	0	96	0	0	0	0
21	0	0	0	0	0	0	0	0	0	0	0
22	60	0	158	93	93	0	96	0	0	0	0
23	60	0	160	97	97	0	96	0	0	0	0
24	60	0	165	101	101	0	97	0	0	0	0
25	0	0	0	0	0	0	0	0	0	0	0
26	0	0	0	0	0	0	0	0	0	0	0
27	0	0	0	0	0	0	0	0	0	0	0
28	0	0	0	0	0	0	0	0	0	0	0
29	0	0	0	0	0	0	0	0	0	0	0
30	60	0	195	104	104	0	97	0	0	0	0
31	0	0	0	0	0	0	0	0	0	0	0
32	60	0	218	108	108	0	97	0	0	0	0

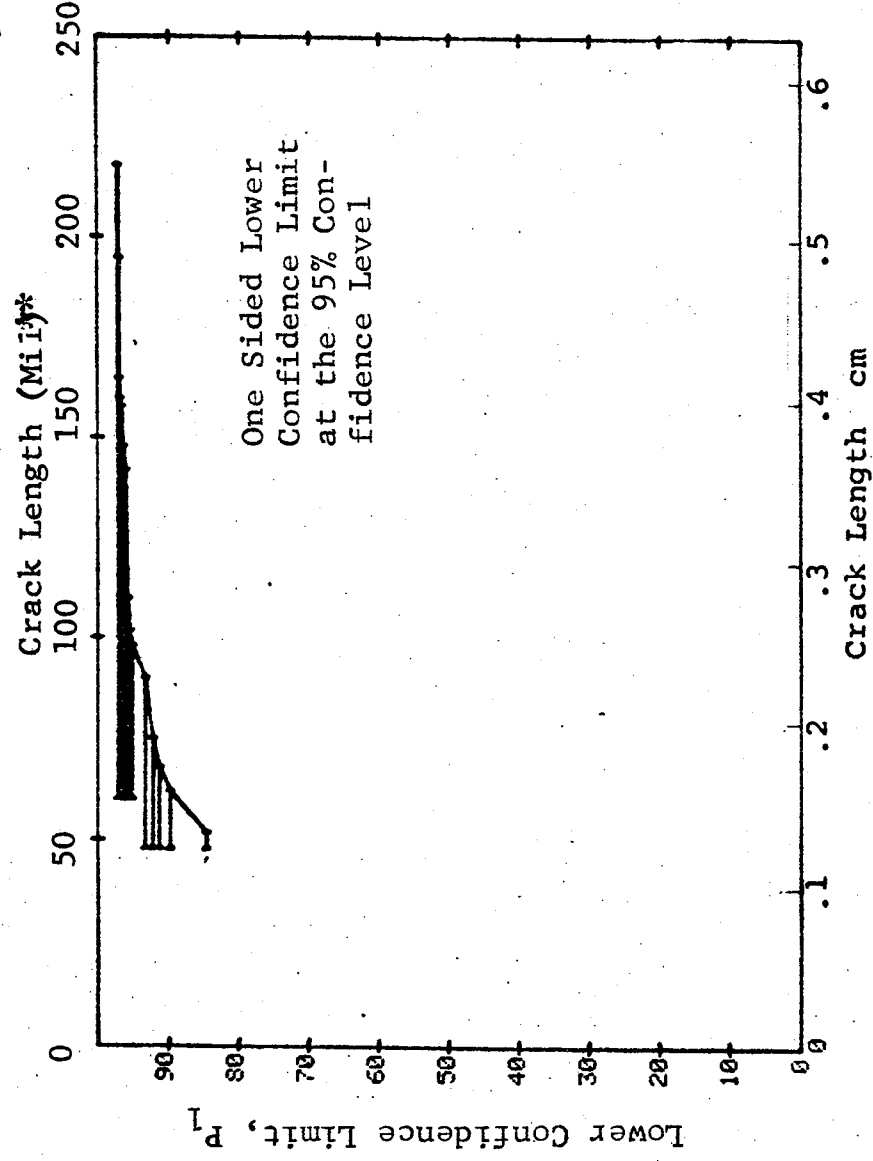


Figure D-44 (Continued)

(c) Overlapping Sixty Point Method of Data Cumulation

09-OCT-75		ULTRASONIC		TEST 3			(44)			
RANGE	MIN	LN	MAX	LN	N	DET	50%	95%	0 MISS	1 MISS
1		0 *		0 *	0	0	0	0	0	0
2		0		0	0	0	0	0	0	0
3		0		0	0	0	0	0	0	0
4		0		0	0	0	0	0	0	0
5		0		0	0	0	0	0	0	0
6		0		0	0	0	0	0	0	0
7		0		0	0	0	0	0	0	0
8		0		0	0	0	0	0	0	0
9		0		0	0	0	0	0	0	0
10		0		0	0	0	0	0	0	0
11		0		0	0	0	0	0	0	0
12		0		0	0	0	0	0	0	0
13		0		0	0	0	0	0	0	0
14		0		0	0	0	0	0	0	0
15		0		0	0	0	0	0	0	0
16		0		0	0	0	0	0	0	0
17		0		0	0	0	0	0	0	0
18		0		0	0	0	0	0	0	0
19		0		0	0	0	0	0	0	0
20		0		0	0	0	0	0	0	0
21		0		0	0	0	0	0	0	0
22		0		0	0	0	0	0	0	0
23		0		0	0	0	0	0	0	0
24		0		0	0	0	0	0	0	0
25		0		0	0	0	0	0	0	0
26		0		0	0	0	0	0	0	0
27		0		0	0	0	0	0	0	0
28		0		0	0	0	0	0	0	0
29	48		68		47	46	95	95	0	14
30	50		95		60	60	98	95	0	0
31	68		142		60	60	98	95	0	0
32	95		218		60	60	98	95	0	0

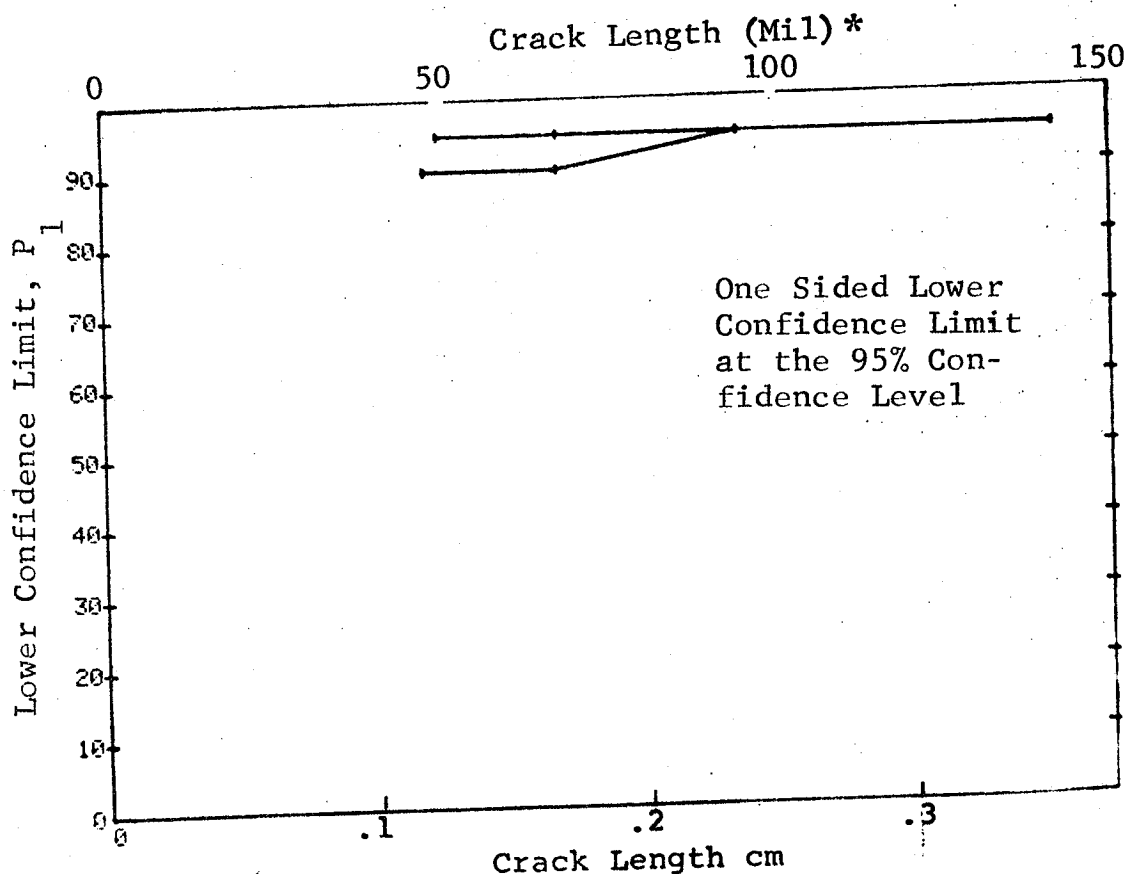


Figure D-44 (Concluded)

(a) Range Interval Method of Data Cumulation

09-OCT-75	ULTRASONIC	TEST 1	95%	MISS	MISS
RANGE	LN	DET			
1	58 *	4	32	0	0
2	64 *	5	31	0	0
3	72 *	9	54	0	0
4	76	13	71	0	0
5	83	10	79	16	33
6	86	11	74	0	0
7	90	14	53	0	0
8	95	15	21	14	31
9	99	14	80	15	32
10	106	8	68	0	0
11	109	11	76	18	35
12	117	8	68	0	0
13	119	3	36	0	0
14	126	4	47	0	0
15	0	0	0	0	0
16	0	0	0	0	0
17	0	0	0	0	0
18	0	0	0	0	0
19	0	0	0	0	0
20	0	0	0	0	0
21	161	4	47	0	0
22	0	0	0	0	0
23	0	0	0	0	0
24	0	0	0	0	0
25	0	0	0	0	0
26	184	5	54	0	0
27	0	0	0	0	0
28	0	0	0	0	0
29	199	0	73	0	0
30	204	11	47	0	0
31	0	4	0	0	0
32	216	6	60	0	0

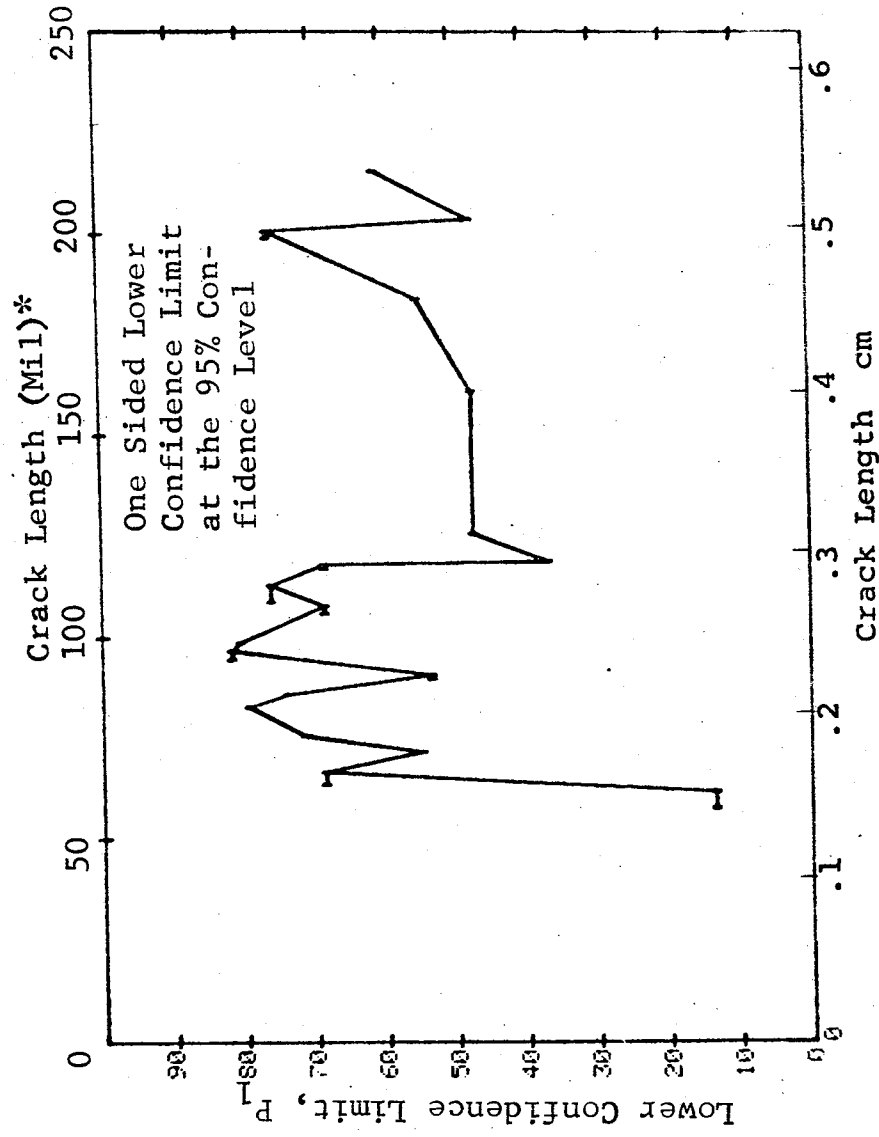


Figure D-45 Probability of Detection for 4330V Steel Using Ultrasonic Shear Wave. Simulated Weld Flaws Prod. Env.

(b) Optimum Probability Method of Data Cumulation

09-OCT-75	ULTRASONIC			N	TEST 2			(45)	MISS	1 MISS
RANGE	MIN	LN	* MAX LN *		DET	50%	95%			
1	58	*	62 *	11	4	0	13	0	0	0
2	64		63	8	8	0	68	0	0	0
3	64		72	13	13	0	72	0	0	0
4	64		76	22	22	0	87	7	24	0
5	64		83	35	35	0	91	0	11	0
6	64		86	45	45	0	93	0	1	0
7	64		91	59	56	0	87	17	30	0
8	64		97	74	71	0	89	2	15	0
9	64		99	88	85	0	91	0	1	0
10	95		108	37	37	0	92	0	9	0
11	95		113	48	48	0	93	0	0	0
12	95		118	56	56	0	94	0	0	0
13	95		119	59	59	0	95	0	0	0
14	95		126	63	63	0	95	0	0	0
15	0		0	0	0	0	0	0	0	0
16	0		0	0	0	0	0	0	0	0
17	0		0	0	0	0	0	0	0	0
18	0		0	0	0	0	0	0	0	0
19	0		0	0	0	0	0	0	0	0
20	0		0	0	0	0	0	0	0	0
21	95		161	67	67	0	95	0	0	0
22	0		0	0	0	0	0	0	0	0
23	0		0	0	0	0	0	0	0	0
24	0		0	0	0	0	0	0	0	0
25	0		0	0	0	0	0	0	0	0
26	95		184	72	72	0	95	0	0	0
27	0		0	0	0	0	0	0	0	0
28	0		0	0	0	0	0	0	0	0
29	95		201	83	83	0	96	0	0	0
30	95		204	87	87	0	96	0	0	0
31	0		0	0	0	0	0	0	0	0
32	95		216	93	93	0	96	0	0	0

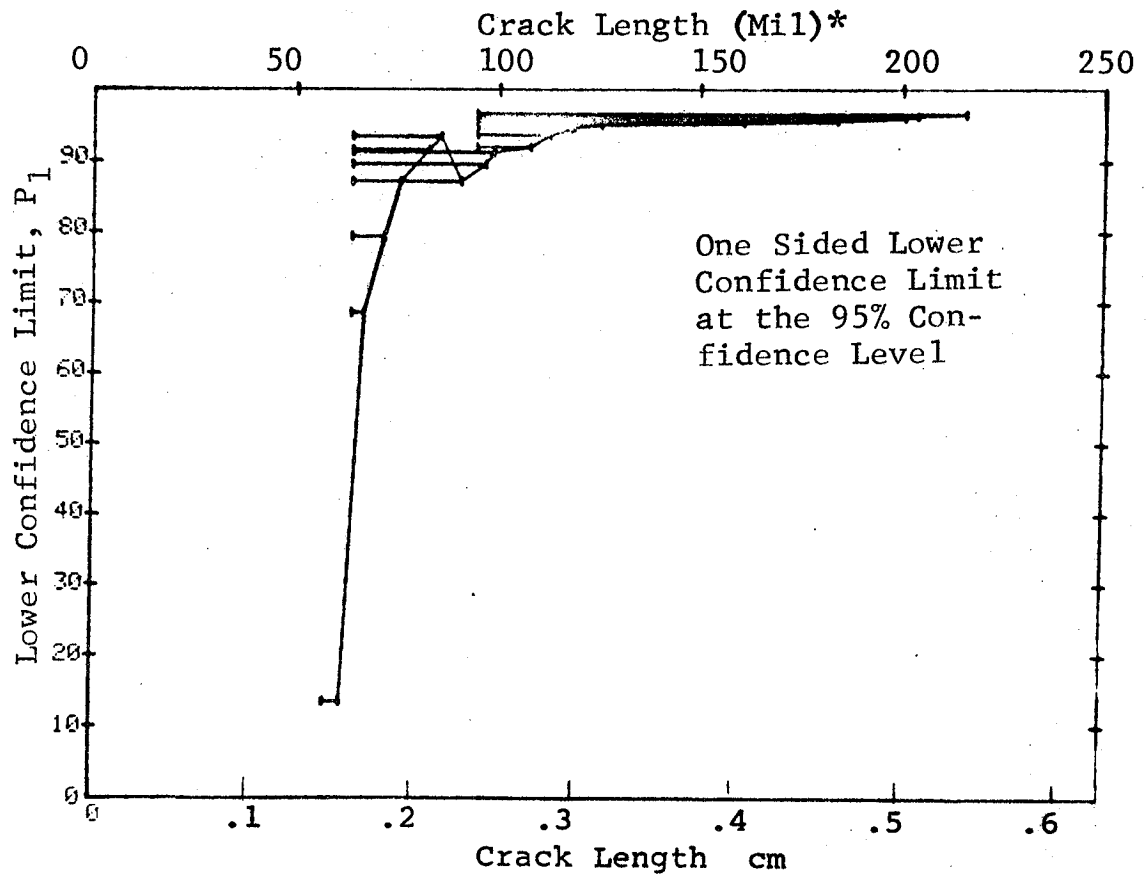


Figure D-45 (Continued)

(c) Overlapping Sixty Point Method of Data Cumulation

09-OCT-75		ULTRASONIC		TEST 3		(45)			
RANGE	MIN LN	* MAX LN	N	DET	50%	95%	0 MISS	1 MISS	
1	0	0*	0	0	0	0	0	0	
2	0	0	0	0	0	0	0	0	
3	0	0	0	0	0	0	0	0	
4	0	0	0	0	0	0	0	0	
5	0	0	0	0	0	0	0	0	
6	0	0	0	0	0	0	0	0	
7	0	0	0	0	0	0	0	0	
8	0	0	0	0	0	0	0	0	
9	0	0	0	0	0	0	0	0	
10	0	0	0	0	0	0	0	0	
11	0	0	0	0	0	0	0	0	
12	0	0	0	0	0	0	0	0	
13	0	0	0	0	0	0	0	0	
14	0	0	0	0	0	0	0	0	
15	0	0	0	0	0	0	0	0	
16	0	0	0	0	0	0	0	0	
17	0	0	0	0	0	0	0	0	
18	0	0	0	0	0	0	0	0	
19	0	0	0	0	0	0	0	0	
20	0	0	0	0	0	0	0	0	
21	0	0	0	0	0	0	0	0	
22	0	0	0	0	0	0	0	0	
23	0	0	0	0	0	0	0	0	
24	0	0	0	0	0	0	0	0	
25	0	0	0	0	0	0	0	0	
26	0	0	0	0	0	0	0	0	
27	0	0	0	0	0	0	0	0	
28	58	83	43	36	82	71	0	0	
29	64	95	60	57	93	87	10	10	
30	83	106	60	57	93	87	15	15	
31	95	126	60	60	98	95	0	0	
32	108	216	60	60	98	95	0	0	

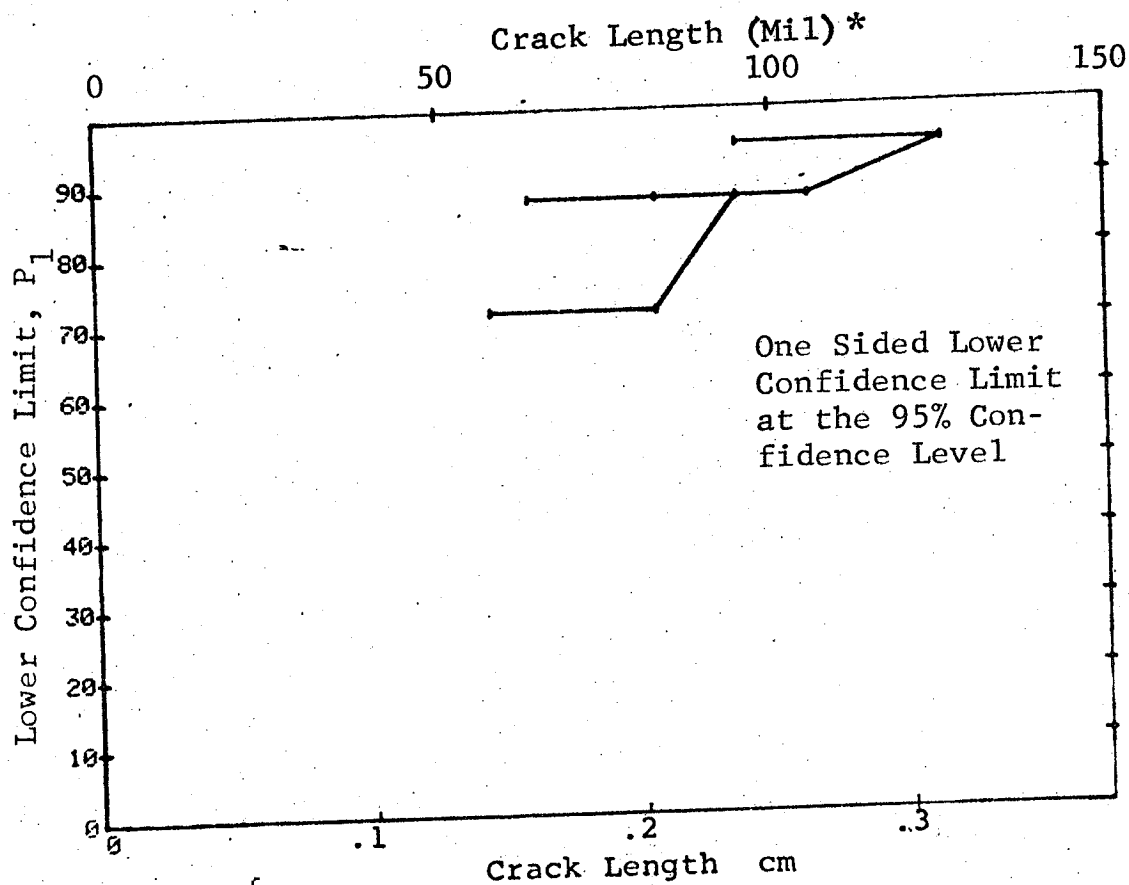


Figure D-45 Concluded)

(a) Range Interval Method of Data Cumulation

09-OCT-75				ULTRASONIC		TEST 1		(46)		95% MISS		1 MISS	
RANGE	MIN	LN	SS *	MAX	LH *	DET	50%	95%	50%	95%	50%	95%	
1	58	54	58 *	58	58 *	4	84	47	84	47	0	0	
2	72	72	72 *	72	72 *	3	91	68	91	68	0	0	
3	76	76	76 *	76	76 *	5	87	54	87	54	0	0	
4	83	83	83 *	83	83 *	4	84	47	84	47	0	0	
5	86	86	86 *	86	86 *	4	84	47	84	47	0	0	
6	91	91	91 *	91	91 *	4	84	47	84	47	0	0	
7	95	95	95 *	95	95 *	4	84	47	84	47	0	0	
8	99	99	99 *	99	99 *	3	79	36	79	36	0	0	
9	106	106	106 *	106	106 *	12	94	77	94	77	17	34	
10	109	109	109 *	109	109 *	4	84	47	84	47	0	0	
11	117	117	117 *	117	117 *	8	91	68	91	68	0	0	
12	126	126	126 *	126	126 *	11	93	76	93	76	18	35	
13	0	0	0 *	0	0 *	8	91	68	91	68	0	0	
14	126	126	126 *	126	126 *	0	0	0	0	0	0	0	
15	0	0	0 *	0	0 *	4	84	47	84	47	0	0	
16	0	0	0 *	0	0 *	0	0	0	0	0	0	0	
17	0	0	0 *	0	0 *	0	0	0	0	0	0	0	
18	0	0	0 *	0	0 *	0	0	0	0	0	0	0	
19	0	0	0 *	0	0 *	0	0	0	0	0	0	0	
20	0	0	0 *	0	0 *	0	0	0	0	0	0	0	
21	161	161	161 *	161	161 *	0	0	0	0	0	0	0	
22	0	0	0 *	0	0 *	3	79	36	79	36	0	0	
23	0	0	0 *	0	0 *	0	0	0	0	0	0	0	
24	0	0	0 *	0	0 *	0	0	0	0	0	0	0	
25	0	0	0 *	0	0 *	0	0	0	0	0	0	0	
26	184	184	184 *	184	184 *	0	0	0	0	0	0	0	
27	0	0	0 *	0	0 *	4	84	47	84	47	0	0	
28	0	0	0 *	0	0 *	0	0	0	0	0	0	0	
29	193	193	193 *	193	193 *	0	0	0	0	0	0	0	
30	204	204	204 *	204	204 *	8	91	68	91	68	0	0	
31	0	0	0 *	0	0 *	3	79	36	79	36	0	0	
32	215	215	215 *	215	215 *	0	0	0	0	0	0	0	

Crack Length (Mil) *

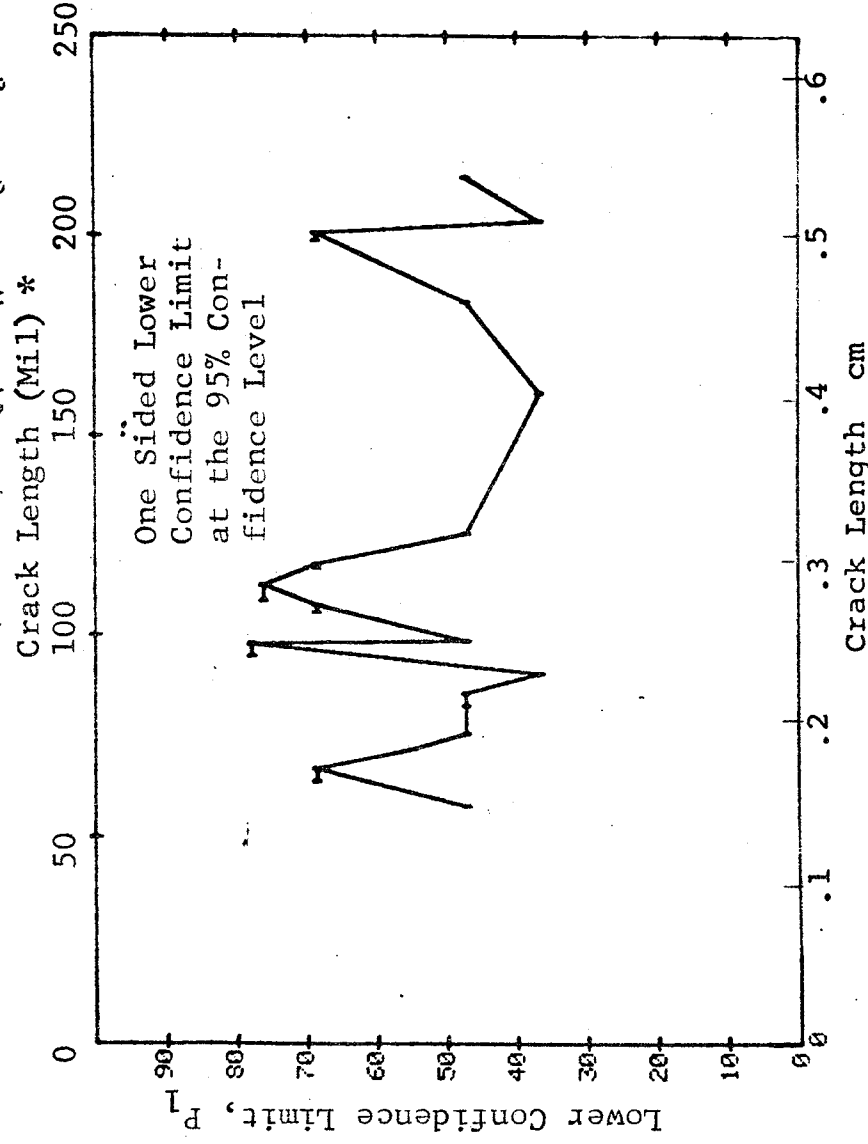


Figure D-46 Probability of Detection for PH17-4 Steel Using Ultrasonic Shear Wave. Simulated Flaws in Wrought Steel. Prod. Env.

(b) Optimum Probability Method of Data Cumulation

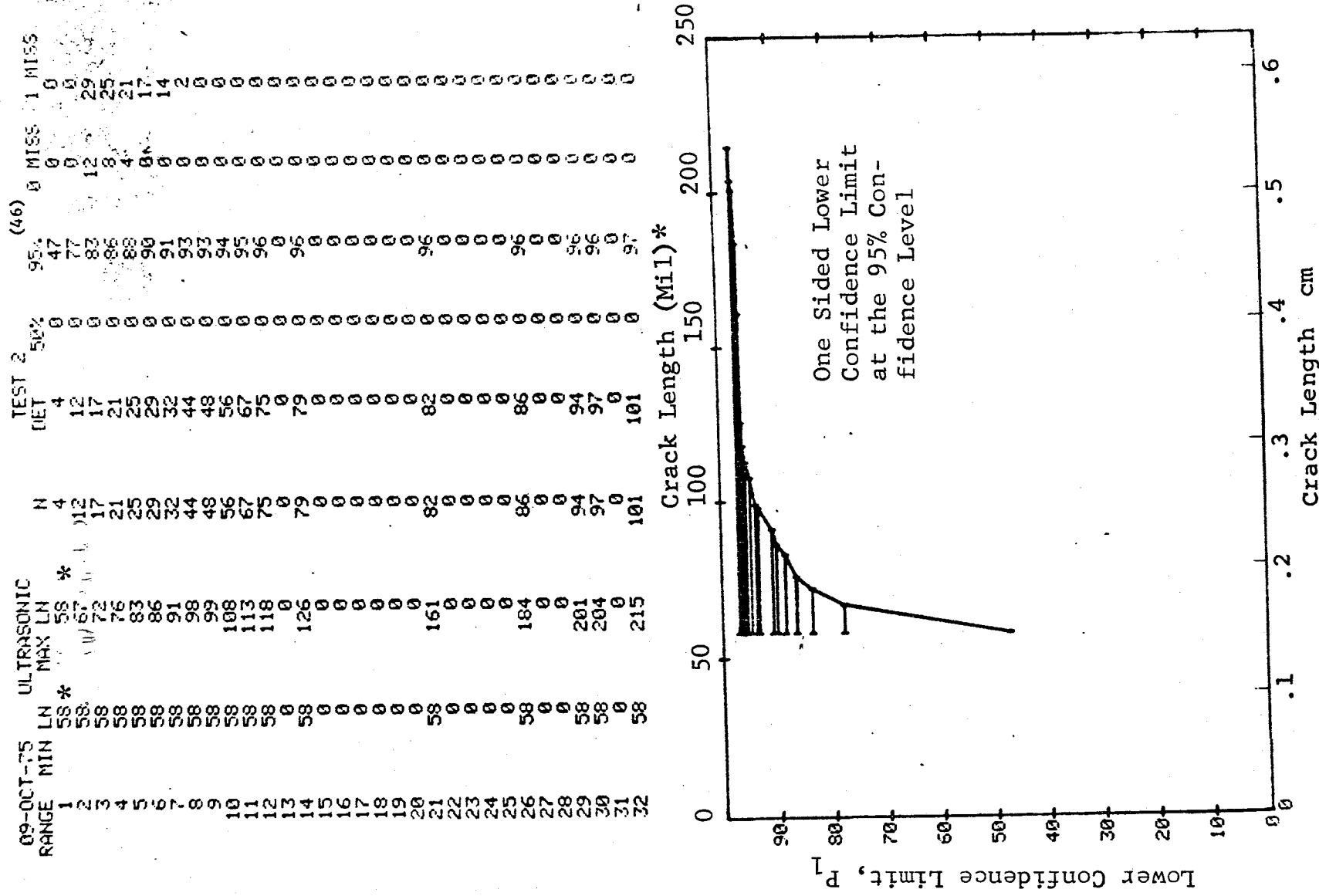


Figure D-46 (Continued)

(c) Overlapping Sixty Point Method of Data Cumulation

09-OCT-75			ULTRASONIC			TEST 3			(46)		
RANGE	MIN	LN	* MAX	LN *	N	DET	50%	95%	0 MISS	1 MISS	
1	0	0	0	0	0	0	0	0	0	0	
2	0	0	0	0	0	0	0	0	0	0	
3	0	0	0	0	0	0	0	0	0	0	
4	0	0	0	0	0	0	0	0	0	0	
5	0	0	0	0	0	0	0	0	0	0	
6	0	0	0	0	0	0	0	0	0	0	
7	0	0	0	0	0	0	0	0	0	0	
8	0	0	0	0	0	0	0	0	0	0	
9	0	0	0	0	0	0	0	0	0	0	
10	0	0	0	0	0	0	0	0	0	0	
11	0	0	0	0	0	0	0	0	0	0	
12	0	0	0	0	0	0	0	0	0	0	
13	0	0	0	0	0	0	0	0	0	0	
14	0	0	0	0	0	0	0	0	0	0	
15	0	0	0	0	0	0	0	0	0	0	
16	0	0	0	0	0	0	0	0	0	0	
17	0	0	0	0	0	0	0	0	0	0	
18	0	0	0	0	0	0	0	0	0	0	
19	0	0	0	0	0	0	0	0	0	0	
20	0	0	0	0	0	0	0	0	0	0	
21	0	0	0	0	0	0	0	0	0	0	
22	0	0	0	0	0	0	0	0	0	0	
23	0	0	0	0	0	0	0	0	0	0	
24	0	0	0	0	0	0	0	0	0	0	
25	0	0	0	0	0	0	0	0	0	0	
26	0	0	0	0	0	0	0	0	0	0	
27	0	0	0	0	0	0	0	0	0	0	
28	0	0	0	0	0	0	0	0	0	0	
29	0	0	0	0	0	0	0	0	0	0	
30	58	98	41	41	98	92	0	5	0	0	
31	67	117	60	60	98	95	0	0	0	0	
32	98	215	60	60	98	95	0	0	0	0	

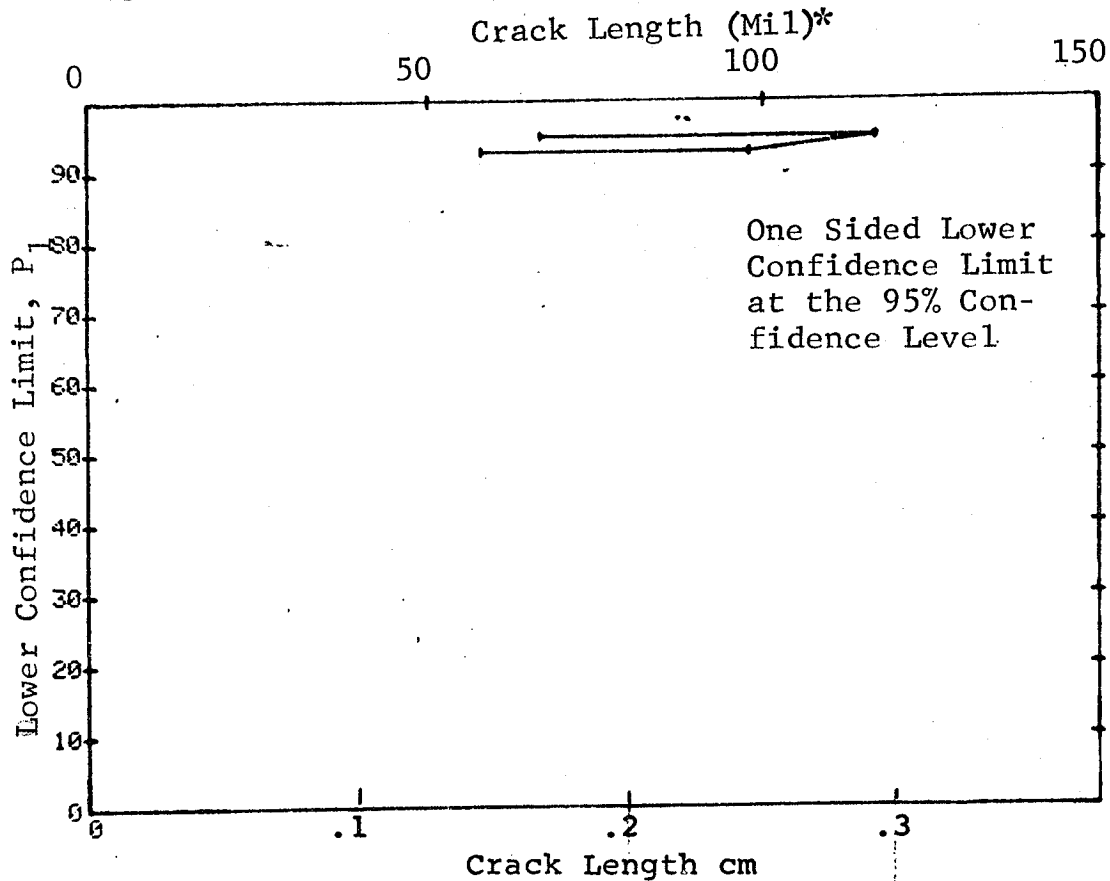


Figure D-46 (Concluded)

(a) Range Interval Method of Data Cumulation

09-OCT-75				MAGNETIC PARTICLE		TEST 1		(47)		
RANGE	MIN	LN	* MAX	LN	N	DET	50%	95%	0 MISS	1 MISS
1		32		32	3	2	50	13	0	0
2		41		143	11	11	93	76	18	35
3		0		0	0	0	0	0	0	0
4		0		0	0	0	0	0	0	0
5		0		0	0	0	0	0	0	0
6		65		65	3	3	79	36	0	0
7		70		72	14	13	88	70	0	0
8		77		80	4	4	84	47	0	0
9		0		0	0	0	0	0	0	0
10		88		91	16	16	95	82	13	30
11		93		95	7	7	90	65	0	0
12		100		100	4	4	84	47	0	0
13		0		0	0	0	0	0	0	0
14		0		0	0	0	0	0	0	0
15		117		118	11	11	93	76	18	35
16		0		0	0	0	0	0	0	0
17		132		132	5	5	87	54	0	0
18		0		0	0	0	0	0	0	0
19		141		143	9	9	92	71	0	0
20		147		149	13	13	94	79	16	33
21		0		0	0	0	0	0	0	0
22		0		0	0	0	0	0	0	0
23		170		170	6	6	89	60	0	0
24		0		0	0	0	0	0	0	0
25		181		181	6	6	89	60	0	0
26		184		184	9	9	92	71	0	0
27		0		0	0	0	0	0	0	0
28		0		0	0	0	0	0	0	0
29		0		0	0	0	0	0	0	0
30		0		0	0	0	0	0	0	0
31		0		0	0	0	0	0	0	0
32		226		226	5	5	87	54	0	0

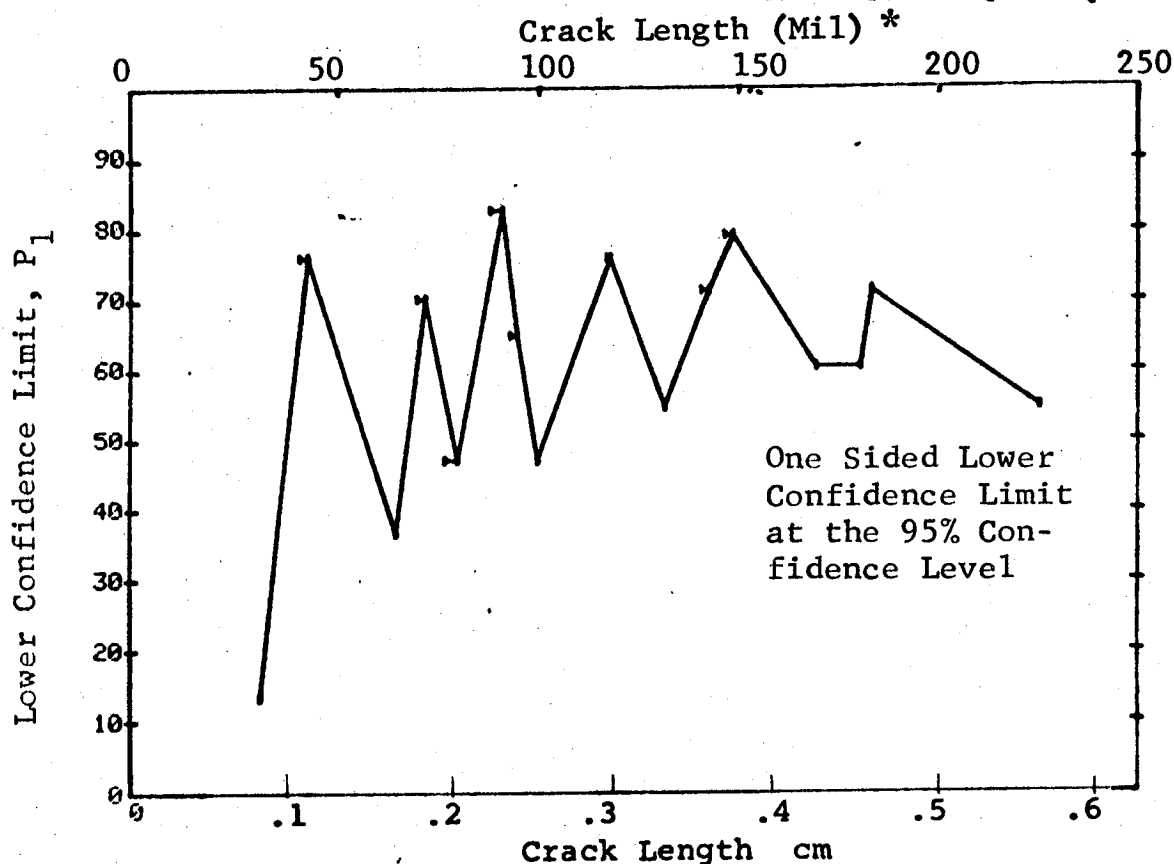


Figure D-47 Probability of Detection for PH17-4 Steel Using Ultrasonic Shear Wave. Fatigue Cracks in Flat Plates. Prod. Env.

(b) Optimum Probability Method of Data Cumulation

09-OCT-75		MAGNETIC PARTICLE			TEST 2		(47)		
RANGE	MIN	LN	MAX	LN	N	DET	50%	95%	0 MISS
1		32	*	32	*	3	2	0	13
2		41		43		11	0	76	0
3		0		0		0	0	0	0
4		0		0		0	0	0	0
5		0		0		0	0	0	0
6		41		65		14	0	80	15
7		41		72		28	0	84	18
8		41		80		32	0	86	14
9		0		0		0	0	0	0
10		41		91		48	0	90	0
11		41		95		55	0	91	0
12		41		100		59	0	92	0
13		0		0		0	0	0	0
14		0		0		0	0	0	0
15		41		118		70	0	93	0
16		0		0		0	0	0	0
17		77		132		47	0	93	0
18		0		0		0	0	0	0
19		77		143		56	0	94	0
20		77		149		69	0	95	0
21		0		0		0	0	0	0
22		0		0		0	0	0	0
23		77		170		75	0	96	0
24		0		0		0	0	0	0
25		77		181		81	0	96	0
26		77		184		90	0	96	0
27		0		0		0	0	0	0
28		0		0		0	0	0	0
29		0		0		0	0	0	0
30		0		0		0	0	0	0
31		0		0		0	0	0	0
32		77		226		95	0	96	0

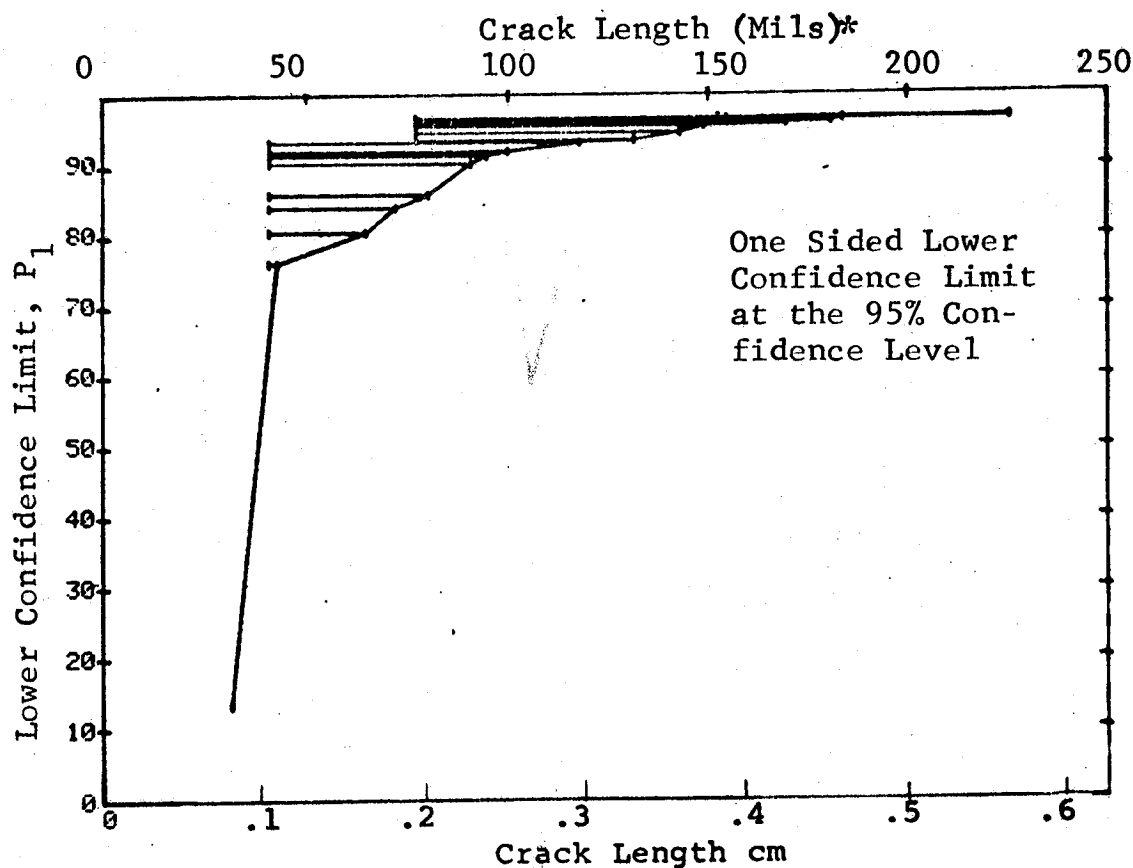


Figure D-47 (Continued)

(c) Overlapping Sixty Point Method of Data Cumulation

09-OCT-75			MAGNETIC PARTICLE		TEST 3			(47)		
RANGE	MIN	LN	MAX	LN	N	DET	50%	95%	0 MISS	1 MISS
1		0*		0*	0	0	0	0	0	0
2		0		0	0	0	0	0	0	0
3		0		0	0	0	0	0	0	0
4		0		0	0	0	0	0	0	0
5		0		0	0	0	0	0	0	0
6		0		0	0	0	0	0	0	0
7		0		0	0	0	0	0	0	0
8		0		0	0	0	0	0	0	0
9		0		0	0	0	0	0	0	0
10		0		0	0	0	0	0	0	0
11		0		0	0	0	0	0	0	0
12		0		0	0	0	0	0	0	0
13		0		0	0	0	0	0	0	0
14		0		0	0	0	0	0	0	0
15		0		0	0	0	0	0	0	0
16		0		0	0	0	0	0	0	0
17		0		0	0	0	0	0	0	0
18		0		0	0	0	0	0	0	0
19		0		0	0	0	0	0	0	0
20		0		0	0	0	0	0	0	0
21		0		0	0	0	0	0	0	0
22		0		0	0	0	0	0	0	0
23		0		0	0	0	0	0	0	0
24		0		0	0	0	0	0	0	0
25		0		0	0	0	0	0	0	0
26		0		0	0	0	0	0	0	0
27		0		0	0	0	0	0	0	0
28		0		0	0	0	0	0	0	0
29	32		88		36	34	92	83	28	40
30	41		117		60	59	97	92	0	1
31	88		149		60	60	98	95	0	0
32	117		226		60	60	98	95	0	0

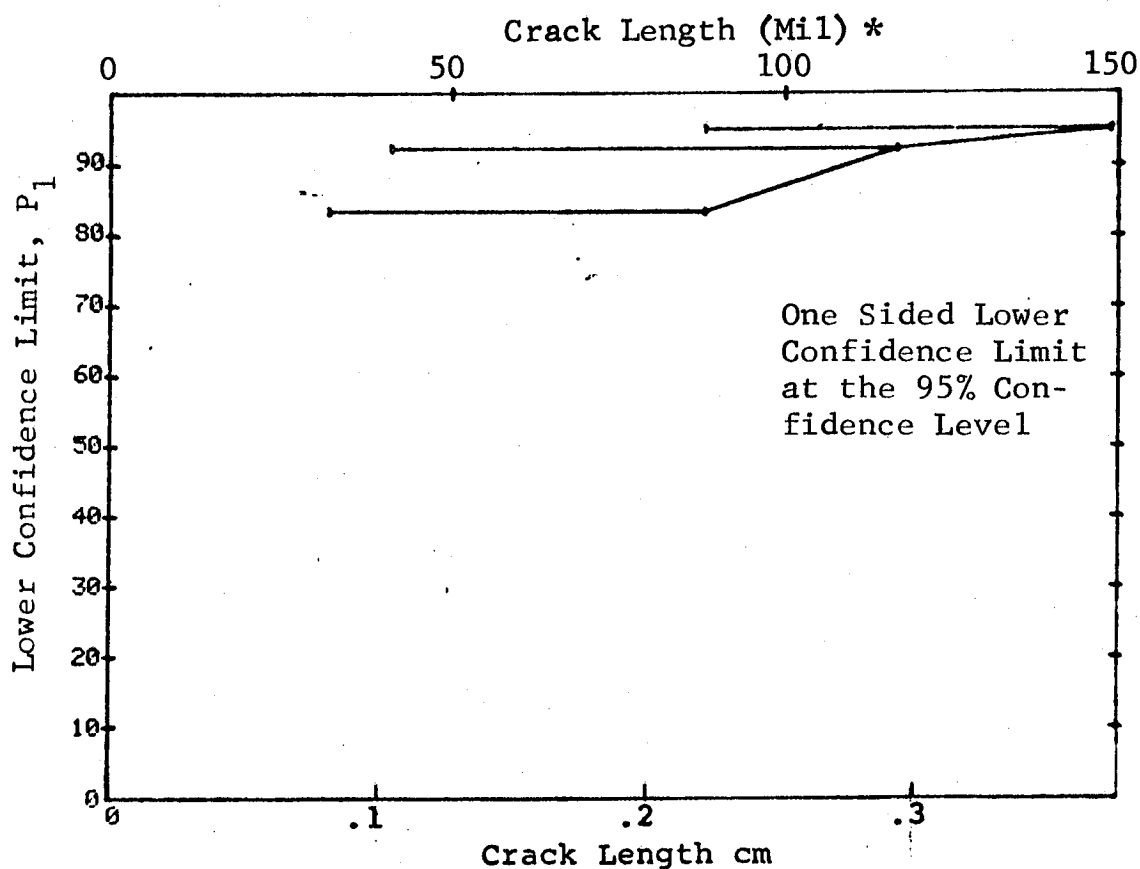


Figure D-47 (Concluded)

(a) Range Interval Method of Data Cumulation

10-OCT-75	PENETRANT	TEST 1 (MERGE ALL ALUMINUM) (48)	MISS
RANGE	MIN LH	MAX LH	MISS
1	1	38 *	0
2	40	100	0
3	70	131	0
4	101	162	0
5	132	190	0
6	164	197	0
7	194	241	0
8	241	253	0
9	256	283	0
10	287	317	0
11	318	347	0
12	352	372	0
13	381	408	0
14	426	426	0
15	442	472	0
16	474	503	0
17	504	534	0
18	535	559	0
19	568	568	0
20	610	610	0
21	0	0	0
22	0	0	0
23	710	710	0
24	0	0	0
25	0	0	0
26	0	0	0
27	0	0	0
28	0	0	0
29	0	0	0
30	0	0	0
31	0	0	0
32	979	979	0

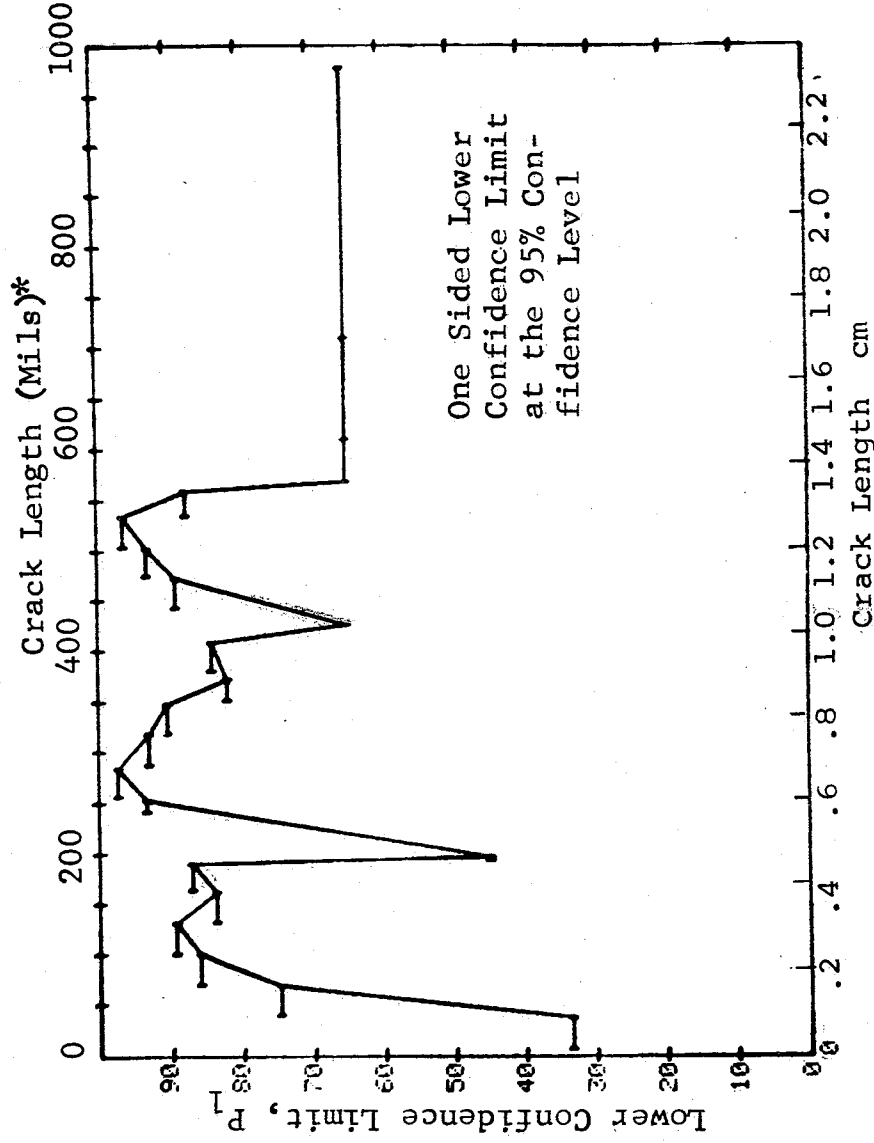


Figure D-48 Probability of Detection for Aluminum Using Liquid Penetrant Fatigue Cracks in Flat Plates.

(b) Optimum Probability Method of Data Cumulation

10-OCT-75 RANGE	MIN LN	PENETRANT MAX LN	N	DET	TEST 2 (MERGE ALL ALUMINUM) (48)	
					50%	95%
1	40	38	226	88	0	0 MISS
2	40	38	441	490	33	0
3	70	69	627	554	74	0
4	101	100	281	260	86	0
5	101	131	512	463	89	0
6	101	162	559	508	88	0
7	101	190	568	515	88	0
8	241	253	70	69	93	0
9	256	283	119	119	97	0
10	241	317	301	297	96	0
11	241	347	476	462	95	0
12	241	372	546	535	94	0
13	241	408	574	552	94	0
14	241	426	581	559	94	0
15	241	472	651	626	94	0
16	241	503	805	775	94	0
17	504	534	182	180	96	0
18	504	559	231	227	96	0
19	504	568	238	234	96	0
20	504	610	245	241	96	0
21	0	0	0	0	0	0
22	0	0	0	0	0	0
23	504	710	252	248	96	0
24	0	0	0	0	0	0
25	0	0	0	0	0	0
26	0	0	0	0	0	0
27	0	0	0	0	0	0
28	0	0	0	0	0	0
29	0	0	0	0	0	0
30	0	0	0	0	0	0
31	0	0	0	0	0	0
32	504	979	259	255	96	0

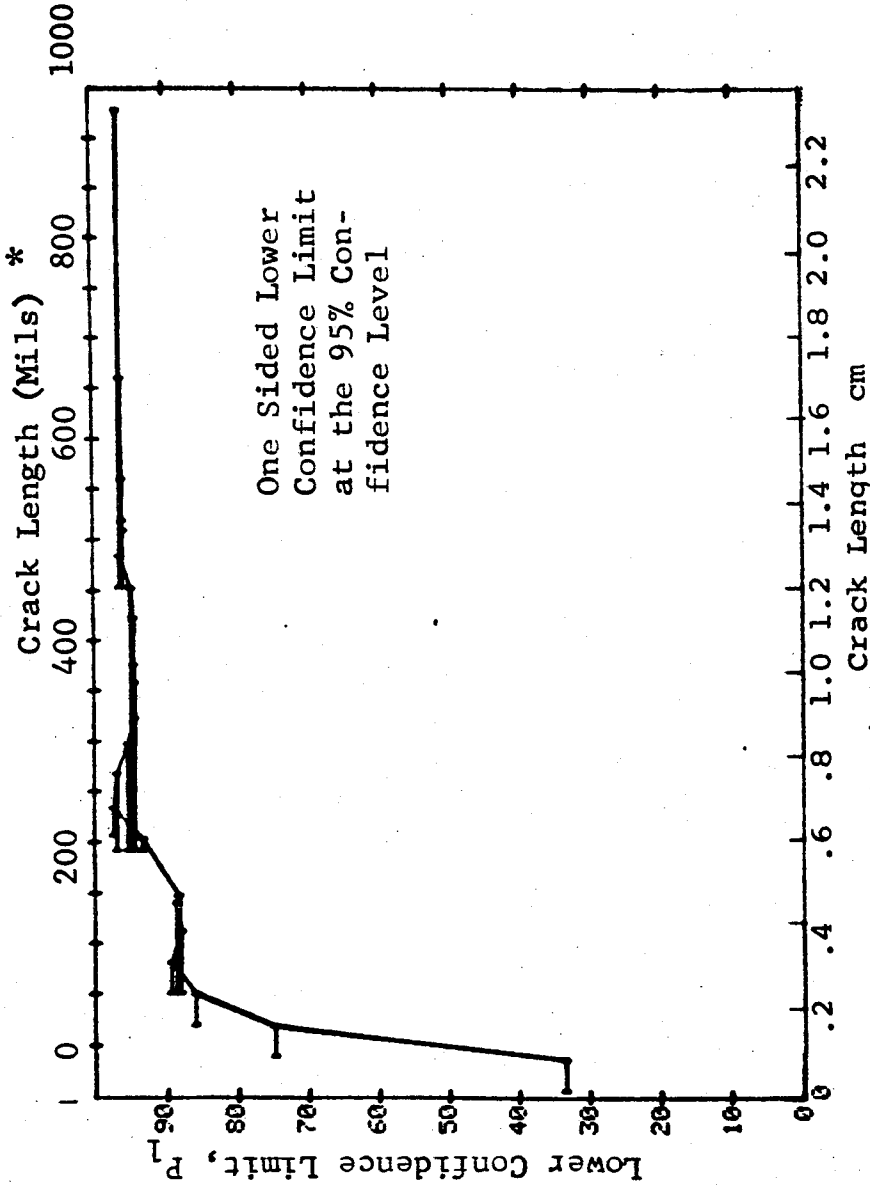


Figure D-48 (Continued)

(c) Overlapping Sixty Point Method of Data Cumulation

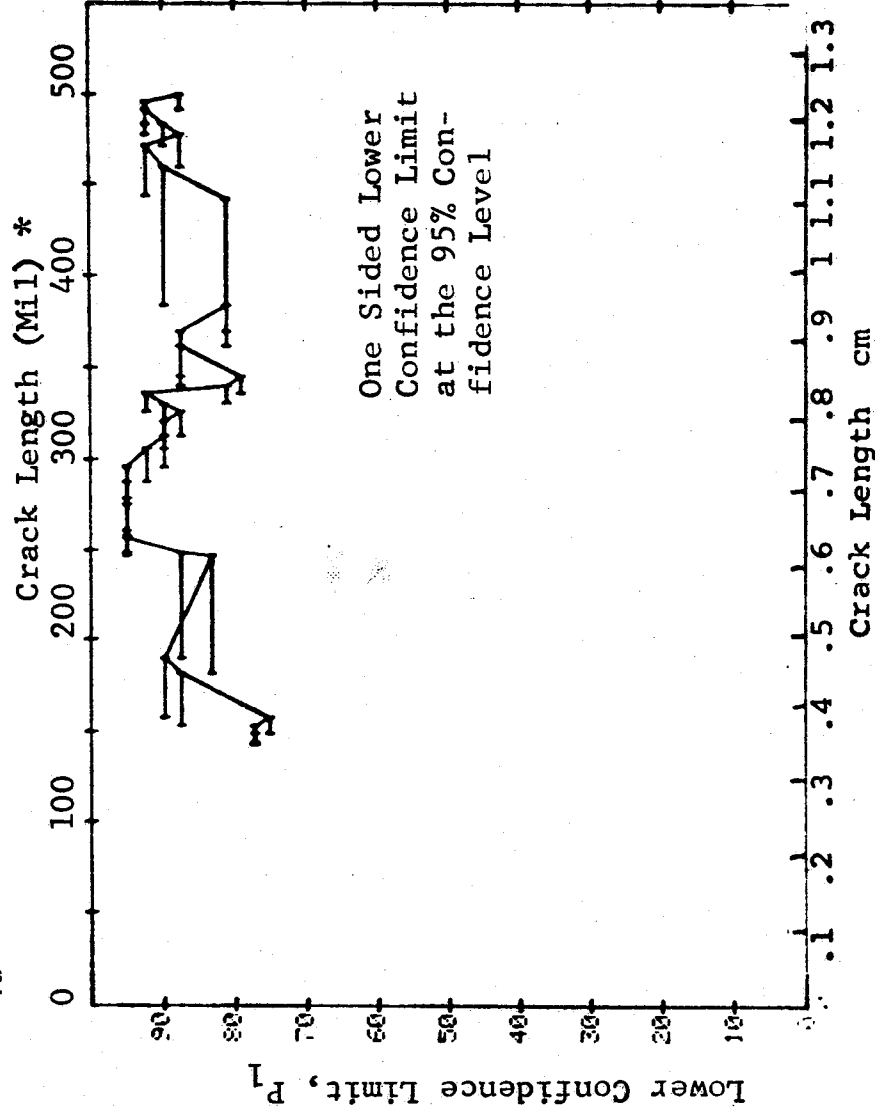
[illegible]

Figure D-48 (Continued)

REPRODUCIBILITY OF THE
ORIGINAL PAGE IS POOR

(c) Overlapping Sixty Point Method of Data Cumulation

15-OCT-75	RANGE	MIN	LN	PERCENT	HEIGHT	MAX LN	LN	W	NET	10-17	(MERGE ALL ALUMINUM)	(48)	MISS
	1		7.9	*		7.9	60	54	88	31	56	59	59
	2		7.9	*		8.0	60	54	88	31	56	59	59
	3		8.0			8.0	60	47	77	67	56	59	59
	4		8.2			8.2	60	47	80	71	0	0	0
	5		8.3			8.3	60	47	77	67	0	0	0
	6		8.5			8.5	60	47	77	67	0	0	0
	7		8.5			8.5	60	55	90	83	43	56	56
	8		8.6			8.6	60	55	90	83	43	56	56
	9		8.8			8.8	60	55	90	83	43	56	56
	10		9.0			9.0	60	57	93	87	16	61	61
	11		9.2			9.2	60	57	93	87	0	1	1
	12		9.3			9.3	60	59	97	92	0	1	1
	13		9.6			9.6	60	59	97	92	16	33	33
	14		9.7			9.7	60	57	93	87	16	33	33
	15		9.9			9.9	60	60	99	95	0	43	43
	16		9.7			10.2	60	60	99	95	0	43	43
	17		9.9			10.5	60	56	92	82	0	1	1
	18		10.3			10.8	60	59	97	92	43	56	56
	19		10.5			11.5	60	55	90	83	43	56	56
	20		10.9			11.8	60	52	85	75	82	100	100
	21		11.5			12.2	60	51	83	79	94	100	100
	22		11.8			12.4	60	51	87	87	94	100	100
	23		12.2			12.5	60	53	93	87	16	33	33
	24		12.4			12.9	60	57	93	87	16	33	33
	25		12.6			13.4	60	57	93	87	16	33	33
	26		12.9			13.5	60	54	88	81	56	94	94
	27		13.4			13.8	60	54	88	81	56	94	94
	28		13.6			14.3	60	54	88	81	56	94	94
	29		13.8			14.5	60	51	83	75	77	100	100
	30		14.3			15.0	60	51	83	75	77	100	100
	31		14.5			15.3	60	53	85	77	77	100	100
	32		15.0			15.8	60	53	85	77	77	100	100

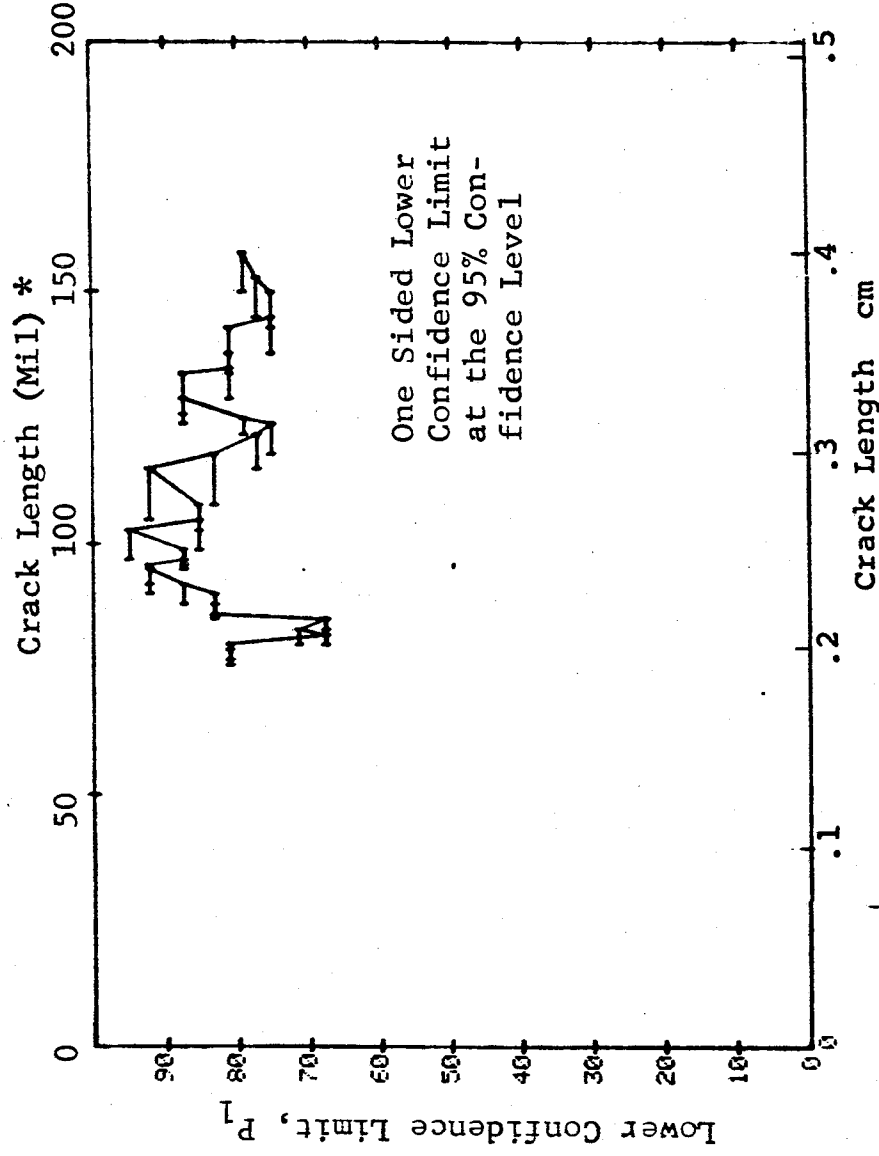
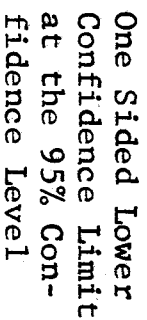


Figure D-48 (Continued)

15-OCT-75	PEREGRINE	TEST 5	(MERGE ALL ALUMINUM)	(48)	IN 50
RANGE MIN	LN	TH	500	300	0 0100
1	30	34	53	29	0
2	32	34	50	45	0
3	35	43	74	64	0
4	40	43	70	60	0
5	41	47	77	67	0
6	44	52	85	77	34
7	45	46	70	65	0
8	47	43	70	73	0
9	49	45	82	64	0
10	51	46	74	57	0
11	54	41	67	58	0
12	56	42	69	71	0
13	58	49	83	75	94
14	60	47	77	67	0
15	61	50	82	63	0
16	62	48	72	62	0
17	63	44	67	57	0
18	64	41	67	69	0
19	65	48	73	79	16
20	66	46	79	87	21
21	67	57	87	89	0
22	68	53	87	80	0
23	68	45	70	60	0
24	69	45	65	60	0
25	71	43	70	60	0
26	72	52	87	79	0
27	74	55	87	89	0
28	76	55	90	85	0
29	76	55	90	85	0
30	78	54	88	81	0
31	79	54	88	81	0
32	80	54	88	81	0
33	80	54	88	81	0
34	80	54	88	81	0
35	80	54	88	81	0
36	80	54	88	81	0
37	80	54	88	81	0
38	80	54	88	81	0
39	80	54	88	81	0
40	80	54	88	81	0
41	80	54	88	81	0
42	80	54	88	81	0
43	80	54	88	81	0
44	80	54	88	81	0
45	80	54	88	81	0
46	80	54	88	81	0
47	80	54	88	81	0
48	80	54	88	81	0
49	80	54	88	81	0
50	80	54	88	81	0
51	80	54	88	81	0
52	80	54	88	81	0
53	80	54	88	81	0
54	80	54	88	81	0
55	80	54	88	81	0
56	80	54	88	81	0
57	80	54	88	81	0
58	80	54	88	81	0
59	80	54	88	81	0
60	80	54	88	81	0
61	80	54	88	81	0
62	80	54	88	81	0
63	80	54	88	81	0
64	80	54	88	81	0
65	80	54	88	81	0
66	80	54	88	81	0
67	80	54	88	81	0
68	80	54	88	81	0
69	80	54	88	81	0
70	80	54	88	81	0
71	80	54	88	81	0
72	80	54	88	81	0
73	80	54	88	81	0
74	8				



D-152

(a) Range Interval Method of Data Cumulation

10-OCT-75	PERMEANT	TEST 1	(49)	0 MISS	1 MISS
RANGE	MIN LN	MAX LN	DET	50%	95%
1	100	70 *	0	0	0
2	120	70 *	0	0	0
3	130	70 *	0	0	0
4	150	70 *	0	0	0
5	157	70 *	0	0	0
6	170	70 *	0	0	0
7	184	70 *	0	0	0
8	200	70 *	0	0	0
9	212	70 *	0	0	0
10	236	70 *	0	0	0
11	262	70 *	0	0	0
12	288	70 *	0	0	0
13	314	70 *	0	0	0
14	337	70 *	0	0	0
15	368	70 *	0	0	0
16	394	70 *	0	0	0
17	420	70 *	0	0	0
18	446	70 *	0	0	0
19	472	70 *	0	0	0
20	499	70 *	0	0	0
21	526	70 *	0	0	0
22	105	70 *	0	0	0
23	120	70 *	0	0	0
24	130	70 *	0	0	0
25	150	70 *	0	0	0
26	157	70 *	0	0	0
27	170	70 *	0	0	0
28	184	70 *	0	0	0
29	200	70 *	0	0	0
30	212	70 *	0	0	0
31	236	70 *	0	0	0
32	262	70 *	0	0	0
	288	70 *	0	0	0
	314	70 *	0	0	0
	337	70 *	0	0	0
	368	70 *	0	0	0
	394	70 *	0	0	0
	420	70 *	0	0	0
	446	70 *	0	0	0
	472	70 *	0	0	0
	499	70 *	0	0	0
	526	70 *	0	0	0
	105	70 *	0	0	0
	120	70 *	0	0	0
	130	70 *	0	0	0
	150	70 *	0	0	0
	157	70 *	0	0	0
	170	70 *	0	0	0
	184	70 *	0	0	0
	200	70 *	0	0	0
	212	70 *	0	0	0
	236	70 *	0	0	0
	262	70 *	0	0	0
	288	70 *	0	0	0
	314	70 *	0	0	0
	337	70 *	0	0	0
	368	70 *	0	0	0
	394	70 *	0	0	0
	420	70 *	0	0	0
	446	70 *	0	0	0
	472	70 *	0	0	0
	499	70 *	0	0	0
	526	70 *	0	0	0

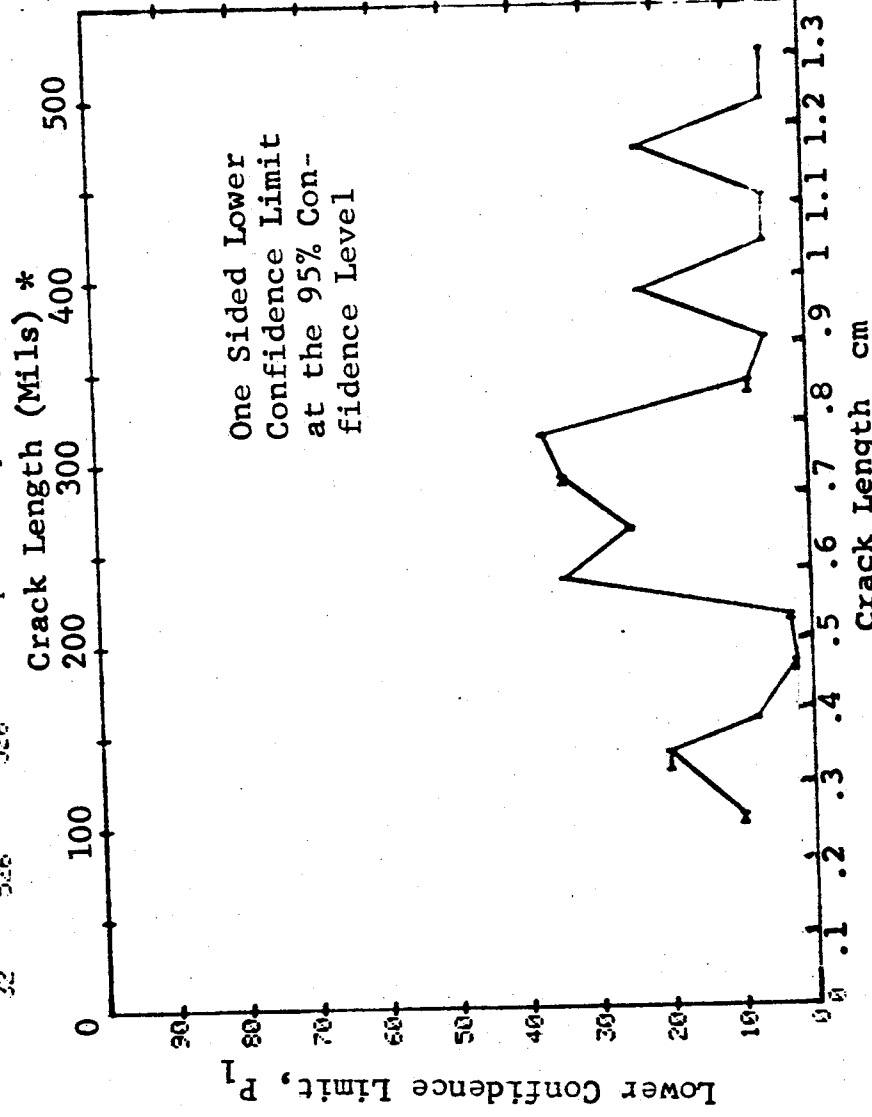


Figure D-49 Probability of Detection for 4330V Steel Using Liquid Penetrant. Fatigue Cracks in Cylindrical Shell Specimens. Lab. Env.

(b) Optimum Probability Method of Data Cumulation

10-OCT-75 RANGE	PENETRANT		TEST 2 (49) DET	50%	35%	0 MISS	1 MISS
	MIN	LN 70 *					
1	100	0	0	0	0	0	0
2	100	0	0	0	0	0	0
3	100	0	0	0	0	0	0
4	100	105	0	0	0	0	0
5	100	120	0	0	0	0	0
6	100	140	0	0	0	0	0
7	100	150	0	0	0	0	0
8	100	158	0	0	21	0	0
9	100	170	0	0	18	0	0
10	100	190	0	0	21	0	0
11	100	200	0	0	20	0	0
12	100	215	0	0	20	0	0
13	212	236	0	0	34	0	0
14	236	0	0	0	0	0	0
15	236	264	0	0	0	0	0
16	236	0	0	0	43	0	0
17	236	292	0	0	0	0	0
18	236	0	0	0	51	0	0
19	236	315	0	0	0	0	0
20	236	0	0	0	58	0	0
21	236	344	0	0	0	0	0
22	236	0	0	0	52	0	0
23	236	368	0	0	0	0	0
24	236	0	0	0	53	0	0
25	236	394	0	0	0	0	0
26	236	420	0	0	56	0	0
27	236	0	0	0	58	0	0
28	236	446	0	0	0	0	0
29	236	0	0	0	59	0	0
30	368	473	0	0	0	0	0
31	368	0	0	0	60	0	0
32	368	499	0	0	60	0	0
		526	0	0	71	0	0

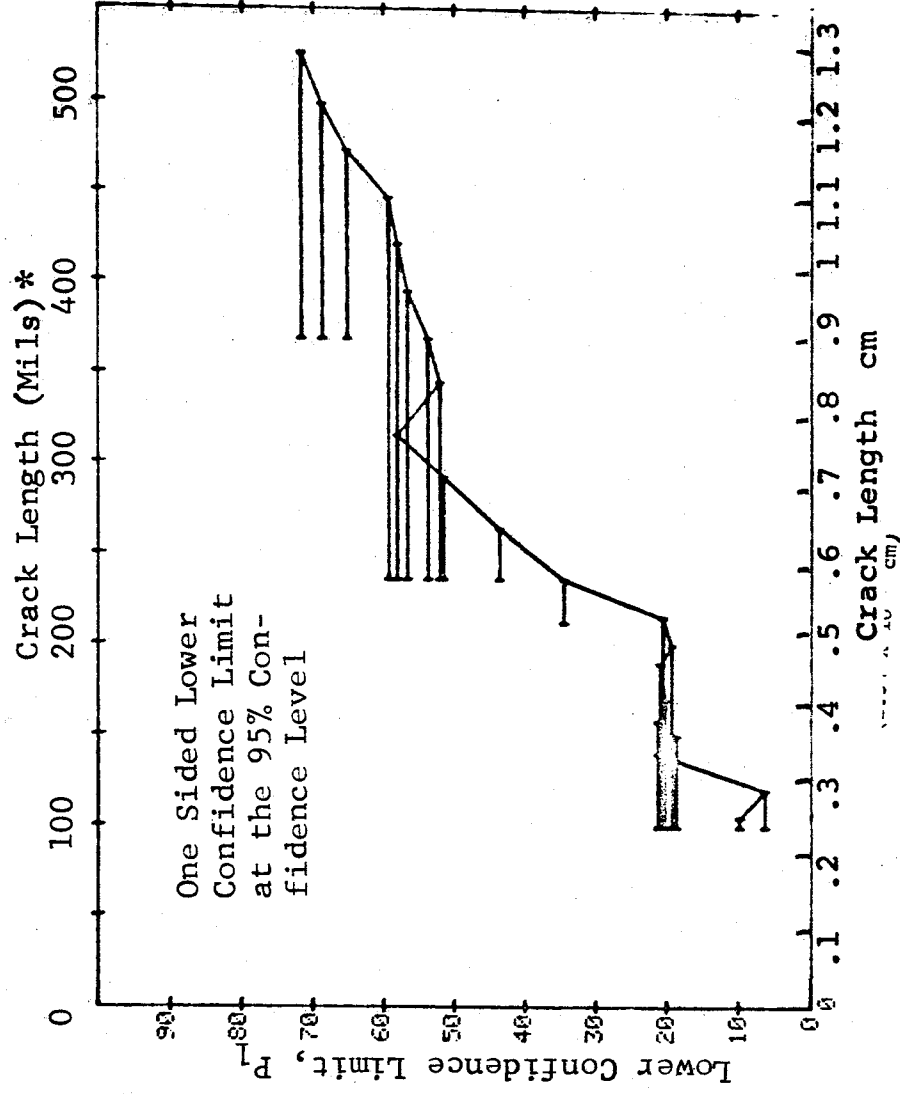


Figure D-49 (Continued)

(c) Overlapping Sixty Point Method of Data Cumulation

10-OCT-75			PENETRANT		TEST 3 (49)		0 MISS		1 MISS	
PAGE	MIN	LN	MIN	LN	DET	50%	95%			
1	0*	0*	0	0	0	0	0	0	0	0
2	0	0	0	0	0	0	0	0	0	0
3	0	0	0	0	0	0	0	0	0	0
4	0	0	0	0	0	0	0	0	0	0
5	0	0	0	0	0	0	0	0	0	0
6	0	0	0	0	0	0	0	0	0	0
7	0	0	0	0	0	0	0	0	0	0
8	0	0	0	0	0	0	0	0	0	0
9	0	0	0	0	0	0	0	0	0	0
10	0	0	0	0	0	0	0	0	0	0
11	0	0	0	0	0	0	0	0	0	0
12	0	0	0	0	0	0	0	0	0	0
13	0	0	0	0	0	0	0	0	0	0
14	0	0	0	0	0	0	0	0	0	0
15	0	0	0	0	0	0	0	0	0	0
16	0	0	0	0	0	0	0	0	0	0
17	0	0	0	0	0	0	0	0	0	0
18	0	0	0	0	0	0	0	0	0	0
19	0	0	0	0	0	0	0	0	0	0
20	0	0	0	0	0	0	0	0	0	0
21	0	0	0	0	0	0	0	0	0	0
22	0	0	0	0	0	0	0	0	0	0
23	0	0	0	0	0	0	0	0	0	0
24	0	0	0	0	0	0	0	0	0	0
25	0	0	0	0	0	0	0	0	0	0
26	0	0	0	0	0	0	0	0	0	0
27	0	0	0	0	0	0	0	0	0	0
28	0	0	0	0	0	0	0	0	0	0
29	0	0	0	0	0	0	0	0	0	0
30	0	0	0	0	0	0	0	0	0	0
31	70	236	0	0	12	33	21	0	0	0
32	128	499	0	0	34	55	45	0	0	0

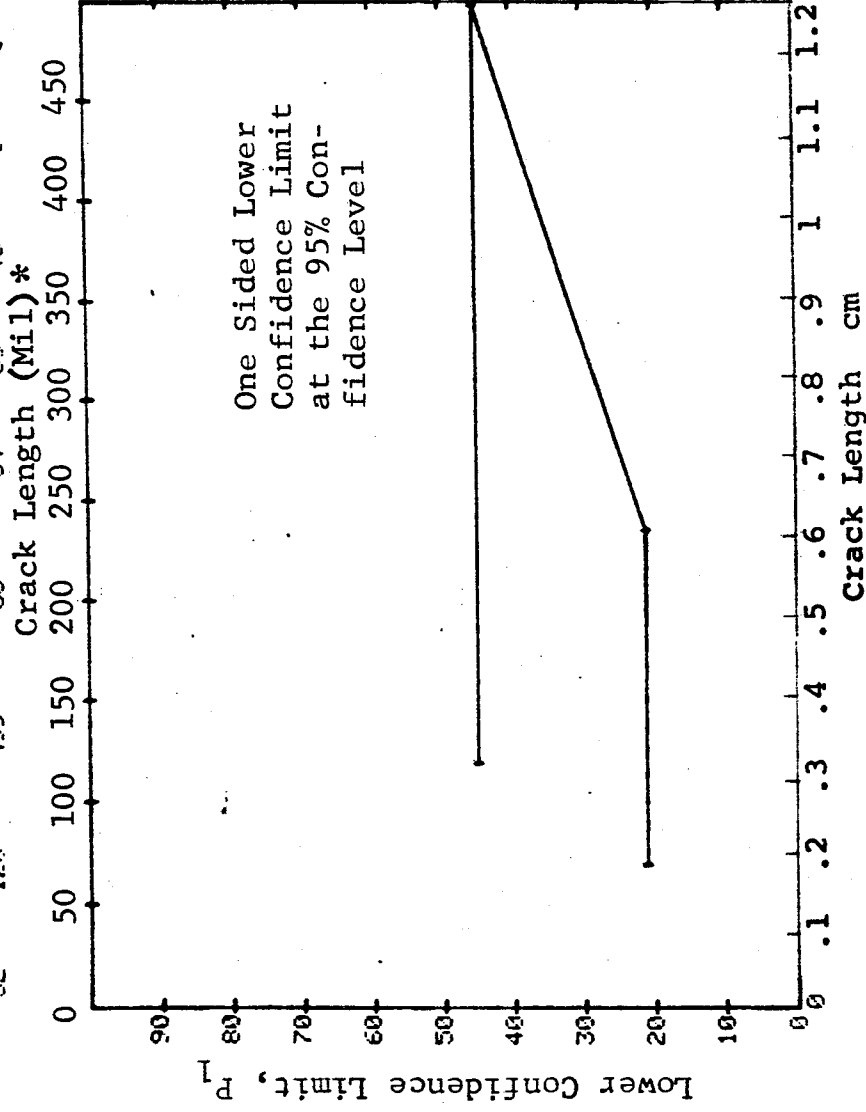


Figure D-49 (Concluded)

(a) Range Interval Method of Data Cumulation

10-OCT-75		PENETRANT		N	TEST 1 (50)			0 MISS	1 MISS
RANGE	MIN	LN 70*	MAX LN 70*		DET	50%	95%		
1		0	0	1	1	50	5	0	0
2		0	0	0	0	0	0	0	0
3	100	105	120	4	0	0	0	0	0
4	120	120	140	2	0	0	0	0	0
5	130	140	150	11	1	6	0	0	0
6	150	150	158	2	0	0	0	0	0
7	157	158	170	5	1	12	1	0	0
8	170	170	190	1	1	50	5	0	0
9	184	190	200	3	0	0	0	0	0
10	200	200	215	2	0	0	0	0	0
11	212	215	236	2	0	0	0	0	0
12	236	236	264	7	1	9	0	0	0
13	0	0	0	0	0	0	0	0	0
14	262	264	292	4	1	15	1	0	0
15	0	0	0	0	0	0	0	0	0
16	288	292	315	5	0	0	0	0	0
17	0	0	0	0	0	0	0	0	0
18	314	315	344	3	1	20	1	0	0
19	0	0	0	0	0	0	0	0	0
20	337	344	368	5	1	12	1	0	0
21	0	0	0	0	0	0	0	0	0
22	368	368	394	1	0	0	0	0	0
23	0	0	0	0	0	0	0	0	0
24	394	394	420	2	1	29	2	0	0
25	420	420	446	1	0	0	0	0	0
26	0	0	0	0	0	0	0	0	0
27	446	446	473	1	0	0	0	0	0
28	0	0	0	0	0	0	0	0	0
29	472	473	499	2	0	0	0	0	0
30	0	0	0	0	0	0	0	0	0
31	499	499	526	1	1	50	5	0	0
32	526	526		1	0	0	0	0	0

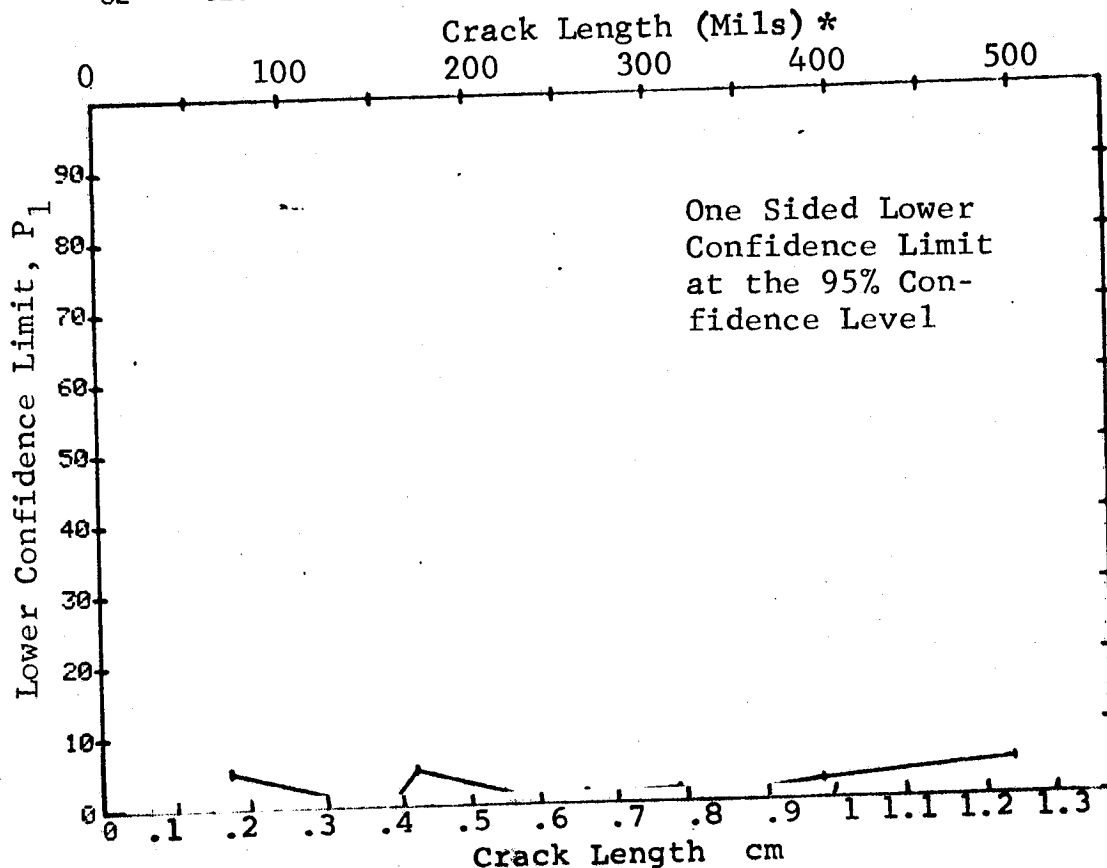


Figure D-50 Probability of Detection for 4330V Steel Using Magniflux ZL-2. Fatigue Cracks in Cylindrical Shell Specimens. Prod. Env.

(b) Optimum Probability Method of Data Cumulation

10-OCT-75		PENETRANT		N	TEST 2 (50		95%	0 MISS	1 MISS
RANGE	MIN	LN	MAX LN *		DET	50%			
1	70	70	70 *	1	1	0	5	0	0
2	0	0	0	0	0	0	0	0	0
3	70	105	105	5	1	0	1	0	0
4	70	120	120	7	1	0	0	0	0
5	70	140	140	18	2	0	2	0	0
6	70	150	150	20	2	0	1	0	0
7	70	158	158	25	3	0	3	0	0
8	157	170	170	6	2	0	6	0	0
9	70	190	190	29	4	0	4	0	0
10	70	200	200	31	4	0	4	0	0
11	70	215	215	33	4	0	4	0	0
12	70	236	236	40	5	0	5	0	0
13	0	0	0	0	0	0	0	0	0
14	70	264	264	44	6	0	6	0	0
15	0	0	0	0	0	0	0	0	0
16	70	292	292	49	6	0	5	0	0
17	0	0	0	0	0	0	0	0	0
18	70	315	315	52	7	0	6	0	0
19	0	0	0	0	0	0	0	0	0
20	157	344	344	37	6	0	7	0	0
21	0	0	0	0	0	0	0	0	0
22	157	368	368	38	6	0	7	0	0
23	0	0	0	0	0	0	0	0	0
24	157	394	394	40	7	0	8	0	0
25	157	420	420	41	7	0	8	0	0
26	0	0	0	0	0	0	0	0	0
27	157	446	446	42	7	0	8	0	0
28	0	0	0	0	0	0	0	0	0
29	157	473	473	44	7	0	9	0	0
30	0	0	0	0	0	0	0	0	0
31	157	499	499	45	8	0	9	0	0
32	157	526	526	46	8	0	9	0	0

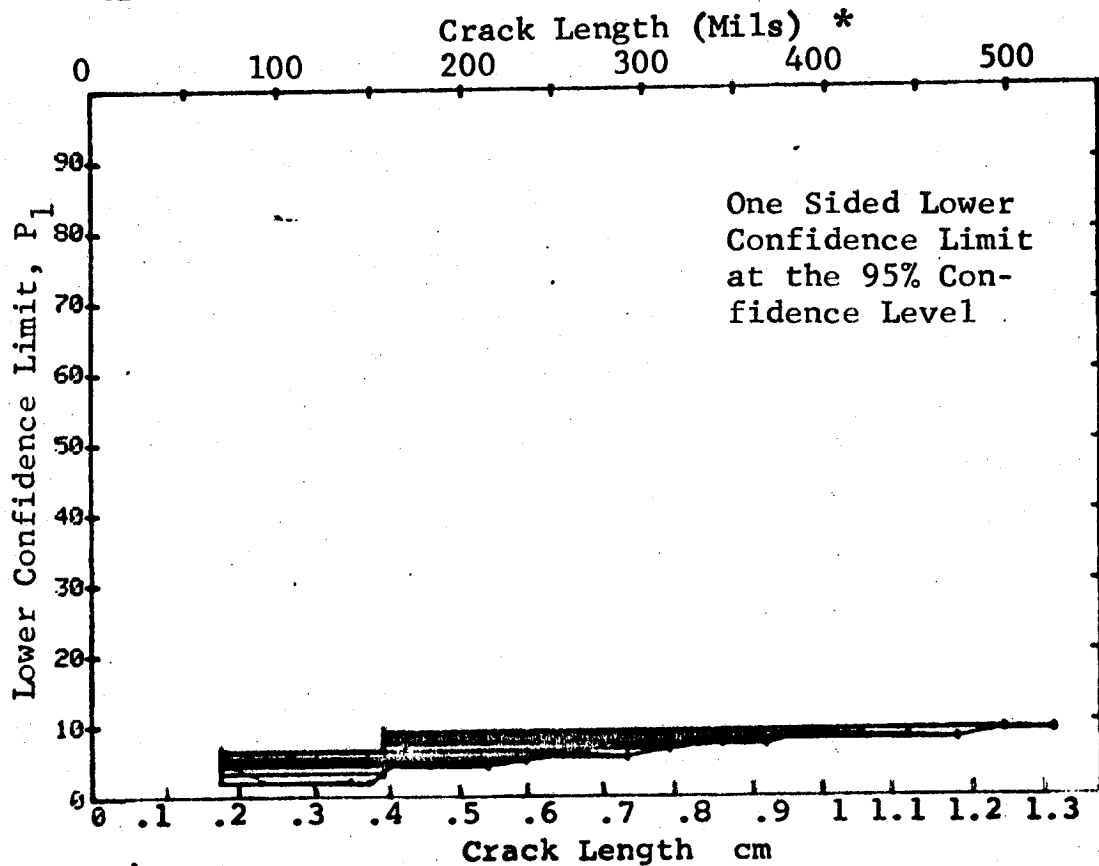


Figure D-50 (Continued)

(c) Overlapping Sixty Point Method of Data Cumulation

10-OCT-75		PENETRANT		TEST 3 (50)					
RANGE	MIN LN	MAX LN	N	DET	50%	95%	0 MISS	1 MISS	
1	0	0	0	0	0	0	0	0	
2	0	0	0	0	0	0	0	0	
3	0	0	0	0	0	0	0	0	
4	0	0	0	0	0	0	0	0	
5	0	0	0	0	0	0	0	0	
6	0	0	0	0	0	0	0	0	
7	0	0	0	0	0	0	0	0	
8	0	0	0	0	0	0	0	0	
9	0	0	0	0	0	0	0	0	
10	0	0	0	0	0	0	0	0	
11	0	0	0	0	0	0	0	0	
12	0	0	0	0	0	0	0	0	
13	0	0	0	0	0	0	0	0	
14	0	0	0	0	0	0	0	0	
15	0	0	0	0	0	0	0	0	
16	0	0	0	0	0	0	0	0	
17	0	0	0	0	0	0	0	0	
18	0	0	0	0	0	0	0	0	
19	0	0	0	0	0	0	0	0	
20	0	0	0	0	0	0	0	0	
21	0	0	0	0	0	0	0	0	
22	0	0	0	0	0	0	0	0	
23	0	0	0	0	0	0	0	0	
24	0	0	0	0	0	0	0	0	
25	0	0	0	0	0	0	0	0	
26	0	0	0	0	0	0	0	0	
27	0	0	0	0	0	0	0	0	
28	0	0	0	0	0	0	0	0	
29	0	0	0	0	0	0	0	0	
30	0	0	0	0	0	0	0	0	
31	70	236	35	4	10	4	0	0	
32	120	499	60	9	14	8	0	0	

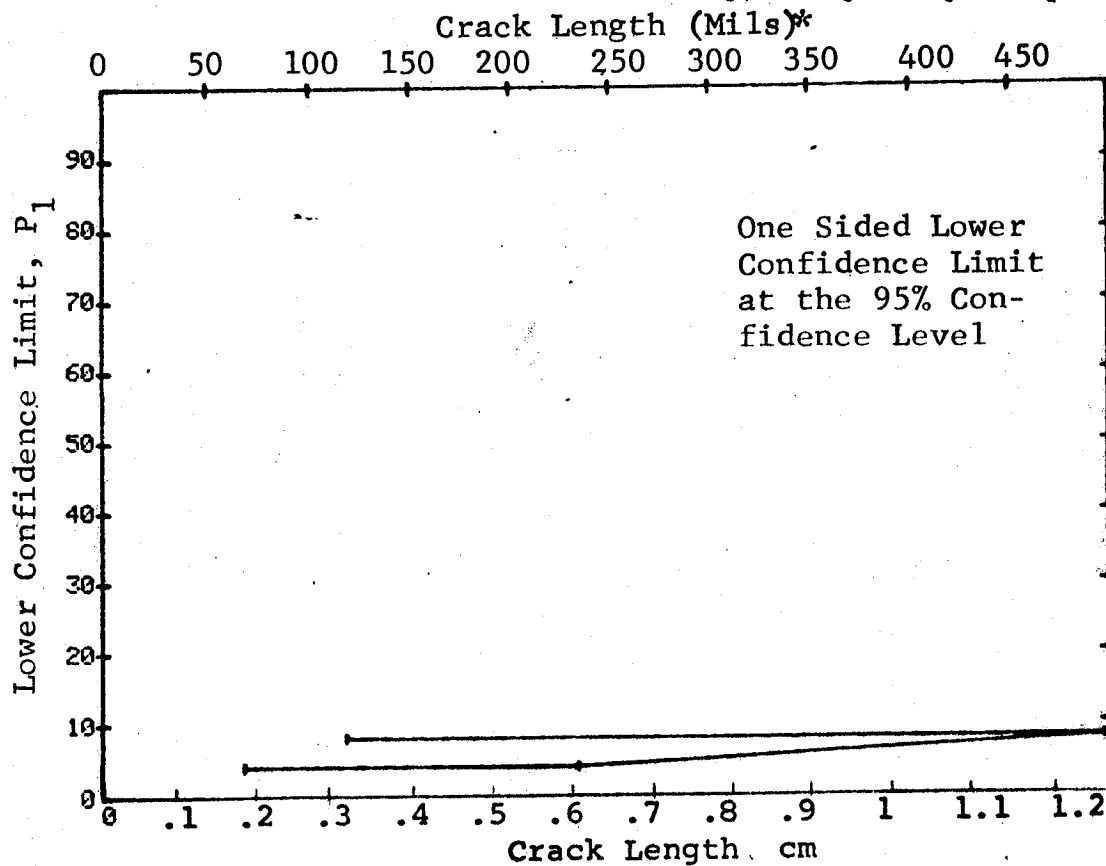


Figure D-50 (Concluded)

(a) Range Interval Method of Data Cumulation

10-OCT-75		PENETRANT		N	TEST 1		(51)	0 MISS	1 MISS
RANGE	MIN	LN	MAX LN		DET	50%	95%		
1	52*	53	*	4	0	0	0	0	0
2	70	81		6	1	10	0	0	0
3	91	92		3	1	20	1	0	0
4	105	109		6	3	28	9	0	0
5	130	137		15	4	23	9	0	0
6	0	0		0	0	0	0	0	0
7	157	162		12	2	13	3	0	0
8	183	188		6	3	42	15	0	0
9	190	196		3	2	50	13	0	0
10	210	212		2	2	70	22	0	0
11	236	239		2	1	29	2	0	0
12	242	248		3	3	79	36	0	0
13	262	267		2	2	70	22	0	0
14	289	290		2	2	70	22	0	0
15	0	0		0	0	0	0	0	0
16	314	321		3	3	79	36	0	0
17	327	341		3	3	79	36	0	0
18	344	358		3	3	79	36	0	0
19	362	362		1	1	50	5	0	0
20	382	389		2	2	70	22	0	0
21	0	0		0	0	0	0	0	0
22	422	423		2	2	70	22	0	0
23	428	431		2	2	70	22	0	0
24	0	0		0	0	0	0	0	0
25	461	461		1	1	50	5	0	0
26	0	0		0	0	0	0	0	0
27	498	498		1	1	50	5	0	0
28	0	0		0	0	0	0	0	0
29	0	0		0	0	0	0	0	0
30	0	0		0	0	0	0	0	0
31	576	577		2	2	70	22	0	0
32	604	604		1	1	50	5	0	0

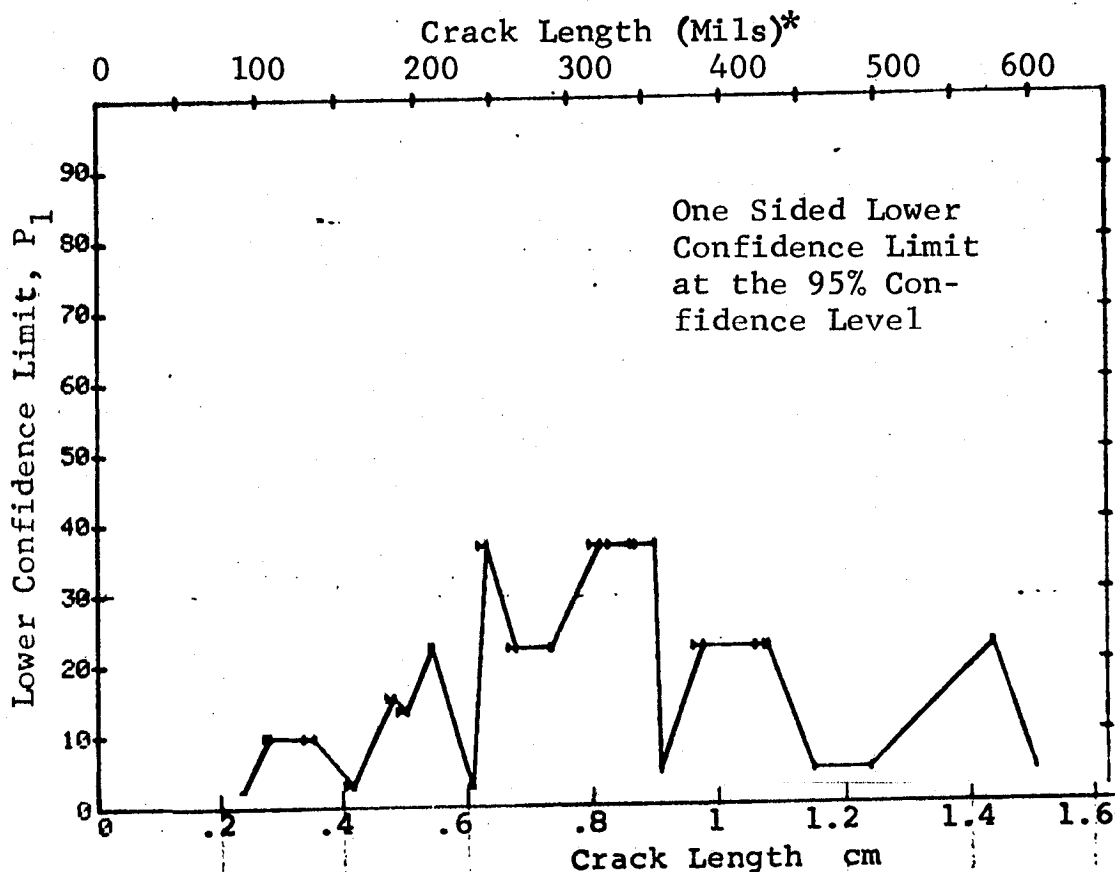


Figure D-51 Probability of Detection for 7075-T6511 Al Using Magniflux ZL-2. Fatigue Cracks in Cylindrical Shell Specimens. Lab. Env.

(b) Optimum Probability Method of Data Cumulation

10-OCT-75		PENETRANT		N	TEST 2 (51)			0 MISS	1 MISS
RANGE	NIN	LN	MAX LN		DET	50%	95%		
1	52*	53*		4	0	0	0	0	0
2	70	70		6	1	0	0	0	0
3	70	92		9	2	0	4	0	0
4	91	109		12	4	0	12	0	0
5	91	137		27	8	0	15	0	0
6	0	0		0	0	0	0	0	0
7	91	162		39	10	0	14	0	0
8	91	188		45	13	0	18	0	0
9	183	196		9	5	0	25	0	0
10	183	212		11	7	0	34	0	0
11	183	239		13	8	0	35	0	0
12	190	248		10	8	0	49	0	0
13	210	267		9	8	0	57	0	0
14	242	290		7	7	0	65	0	0
15	0	0		0	0	0	0	0	0
16	242	321		10	10	0	74	0	0
17	242	341		13	13	0	79	0	0
18	242	358		16	16	0	82	13	30
19	242	362		17	17	0	83	12	29
20	242	389		19	19	0	85	10	27
21	0	0		0	0	0	0	0	0
22	242	423		21	21	0	86	8	25
23	242	431		23	23	0	87	6	23
24	0	0		0	0	0	0	0	0
25	242	461		24	24	0	88	5	22
26	0	0		0	0	0	0	0	0
27	242	498		25	25	0	88	4	21
28	0	0		0	0	0	0	0	0
29	0	0		0	0	0	0	0	0
30	0	0		0	0	0	0	0	0
31	242	577		27	27	0	89	2	19
32	242	604		28	28	0	89	1	18

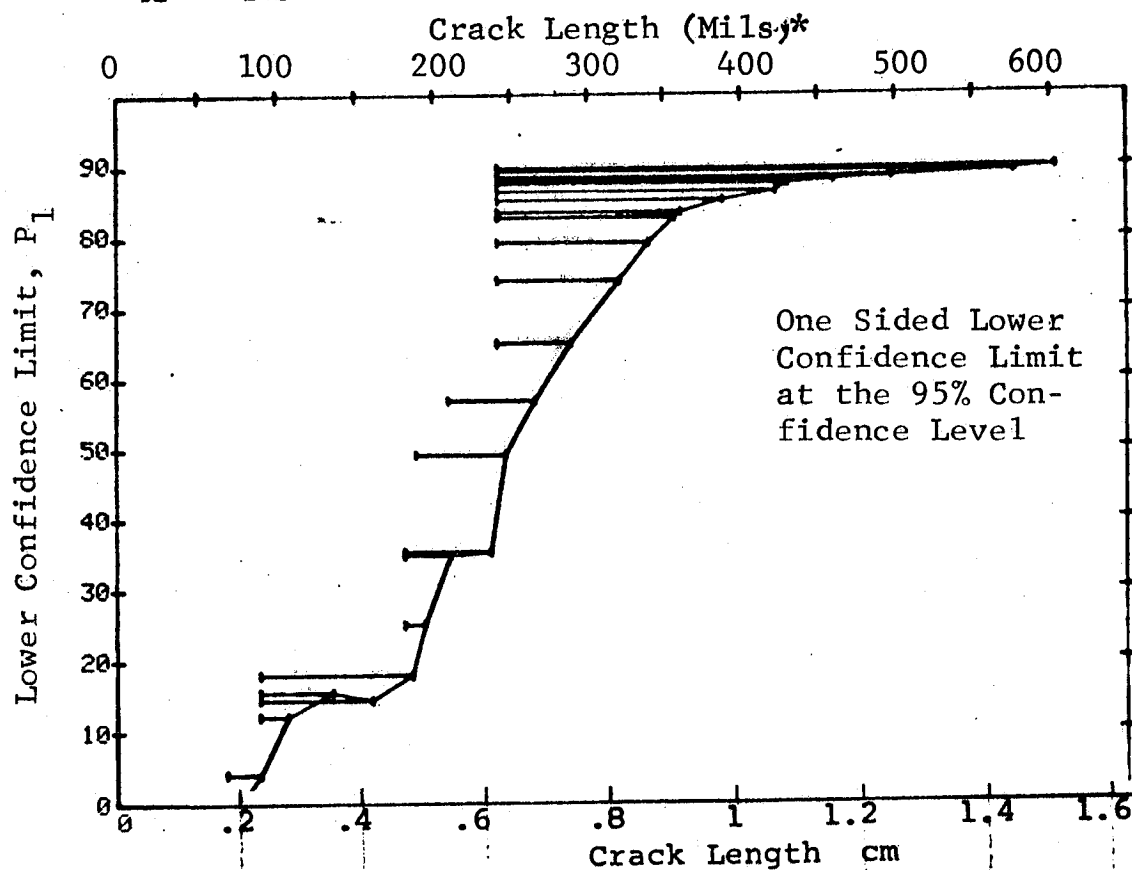
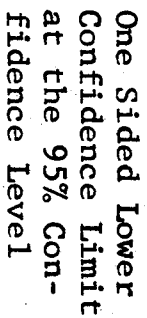


Figure D-51 (Continued)

10-07-75	RANGE	MIN	LN	PENETRANT	MAX	LN	OF	TEST 3 (51)	DET	SEC	95%	MISS	MISS
10	0	0	0	0	0	0	0	0	0	0	0	0	0
11	0	0	0	0	0	0	0	0	0	0	0	0	0
12	0	0	0	0	0	0	0	0	0	0	0	0	0
13	0	0	0	0	0	0	0	0	0	0	0	0	0
14	0	0	0	0	0	0	0	0	0	0	0	0	0
15	0	0	0	0	0	0	0	0	0	0	0	0	0
16	0	0	0	0	0	0	0	0	0	0	0	0	0
17	0	0	0	0	0	0	0	0	0	0	0	0	0
18	0	0	0	0	0	0	0	0	0	0	0	0	0
19	0	0	0	0	0	0	0	0	0	0	0	0	0
20	0	0	0	0	0	0	0	0	0	0	0	0	0
21	0	0	0	0	0	0	0	0	0	0	0	0	0
22	0	0	0	0	0	0	0	0	0	0	0	0	0
23	0	0	0	0	0	0	0	0	0	0	0	0	0
24	0	0	0	0	0	0	0	0	0	0	0	0	0
25	0	0	0	0	0	0	0	0	0	0	0	0	0
26	0	0	0	0	0	0	0	0	0	0	0	0	0
27	0	0	0	0	0	0	0	0	0	0	0	0	0
28	0	0	0	0	0	0	0	0	0	0	0	0	0
29	0	0	0	0	0	0	0	0	0	0	0	0	0
30	0	0	0	0	0	0	0	0	0	0	0	0	0
31	52	190	498	57	60	15	39	25	64	19	0	0	0
32	132			60		39				57	0	0	0



D-161

(a) Range Interval Method of Data Cumulation

10-OCT-75 RANGE	MIN	LN	MAGNETIC PARTICLE MAX LN	TEST 1 (52) DET	50:	95:	0 MISS	1 MISS
1	0:	0:	0:	0	0	0	0	0
2	100	100	105	0	0	0	0	0
3	120	120	120	0	50	13	0	0
4	130	130	131	2	70	22	0	0
5	0	0	0	2	31	7	0	0
6	0	0	0	2	0	0	0	0
7	150	150	157	0	20	0	0	0
8	170	170	170	1	50	1	0	0
9	184	184	184	1	50	5	0	0
10	200	200	200	0	0	0	0	0
11	0	0	0	0	0	0	0	0
12	0	0	0	0	0	0	0	0
13	236	236	237	0	61	24	0	0
14	0	0	0	3	0	0	0	0
15	262	262	264	0	79	35	0	0
16	0	0	0	3	0	0	0	0
17	283	283	283	0	50	5	0	0
18	292	292	292	1	50	5	0	0
19	314	314	314	1	50	5	0	0
20	0	0	0	0	0	0	0	0
21	0	0	0	0	0	0	0	0
22	0	0	0	0	0	0	0	0
23	0	0	0	0	0	0	0	0
24	0	0	0	0	0	0	0	0
25	394	394	394	0	50	5	0	0
26	0	0	0	1	0	0	0	0
27	0	0	0	0	0	0	0	0
28	0	0	0	0	0	0	0	0
29	0	0	0	0	0	0	0	0
30	0	0	0	0	0	0	0	0
31	0	0	0	0	0	0	0	0
32	499	499	499	1	50	5	0	0

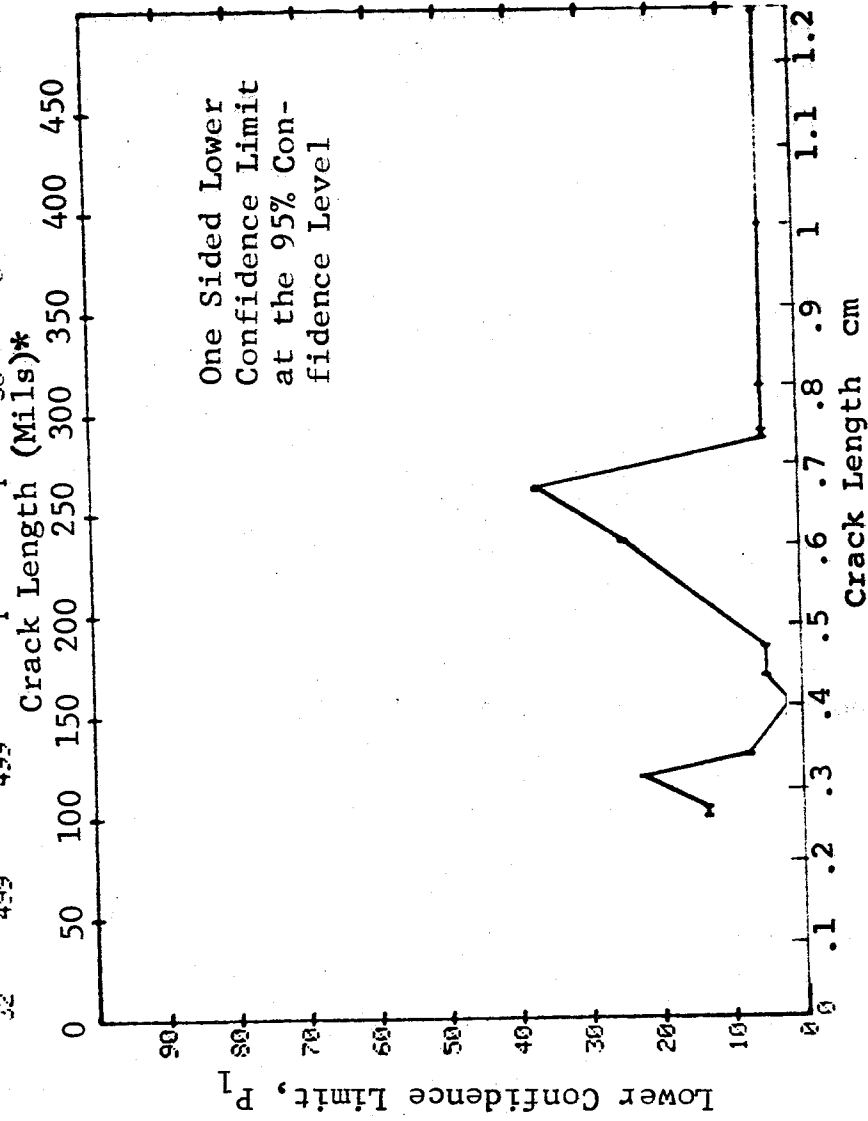


Figure D-52 Probability of Detection for 4330V Steel Using Magnetical Particle. Fatigue Cracks in Cylindrical Shell Specimens. Lab. Env.

(b) Overlapping Sixty Point Method of Data Cumulation

10-OCT-75		MAGNETIC PARTICLE		TEST 2 (52)		0 MISS		1 MISS	
RANGE	MIN LN	70*	MAX LN	DET	50%	95%			
1	100	0	70*	0	0	0	0	0	0
2	100	0	105	0	0	0	0	0	0
3	100	0	120	2	0	13	0	0	0
4	100	0	131	4	0	34	0	0	0
5	100	0	131	6	0	30	0	0	0
6	100	0	157	0	0	0	0	0	0
7	100	0	170	7	0	28	0	0	0
8	100	0	184	8	0	32	0	0	0
9	100	0	200	9	0	35	0	0	0
10	100	0	200	9	0	31	0	0	0
11	100	0	237	0	0	0	0	0	0
12	100	0	237	12	0	0	0	0	0
13	100	0	264	0	0	37	0	0	0
14	100	0	264	6	0	47	0	0	0
15	236	0	288	0	0	0	0	0	0
16	236	0	292	7	0	52	0	0	0
17	236	0	314	8	0	57	0	0	0
18	262	0	394	6	0	60	0	0	0
19	262	0	394	0	0	0	0	0	0
20	262	0	394	0	0	0	0	0	0
21	262	0	394	0	0	0	0	0	0
22	262	0	394	0	0	0	0	0	0
23	262	0	394	0	0	0	0	0	0
24	262	0	394	0	0	0	0	0	0
25	262	0	394	7	0	65	0	0	0
26	262	0	394	0	0	0	0	0	0
27	262	0	394	0	0	0	0	0	0
28	262	0	394	0	0	0	0	0	0
29	262	0	394	0	0	0	0	0	0
30	262	0	394	0	0	0	0	0	0
31	262	0	394	0	0	0	0	0	0
32	262	0	394	8	0	68	0	0	0

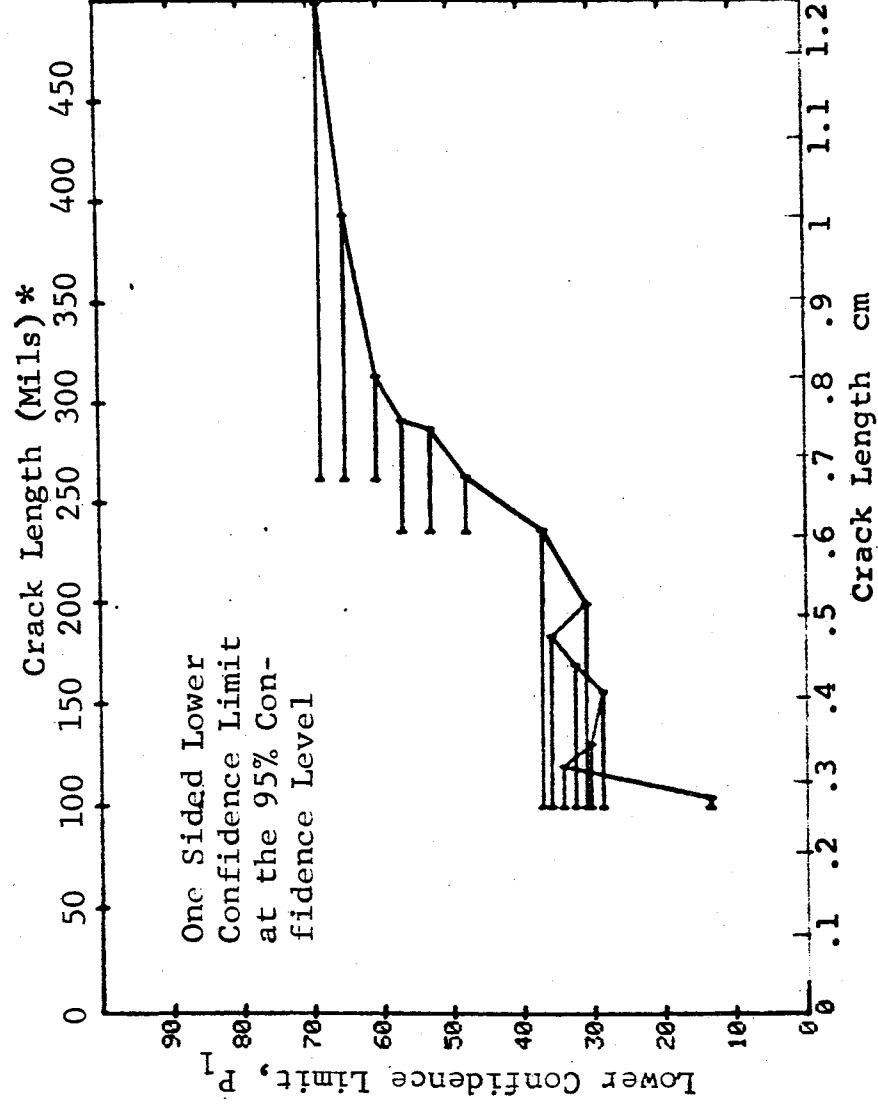


Figure D-52 (Continued)

(c) Overlapping Sixty Point Method of Data Cumulation

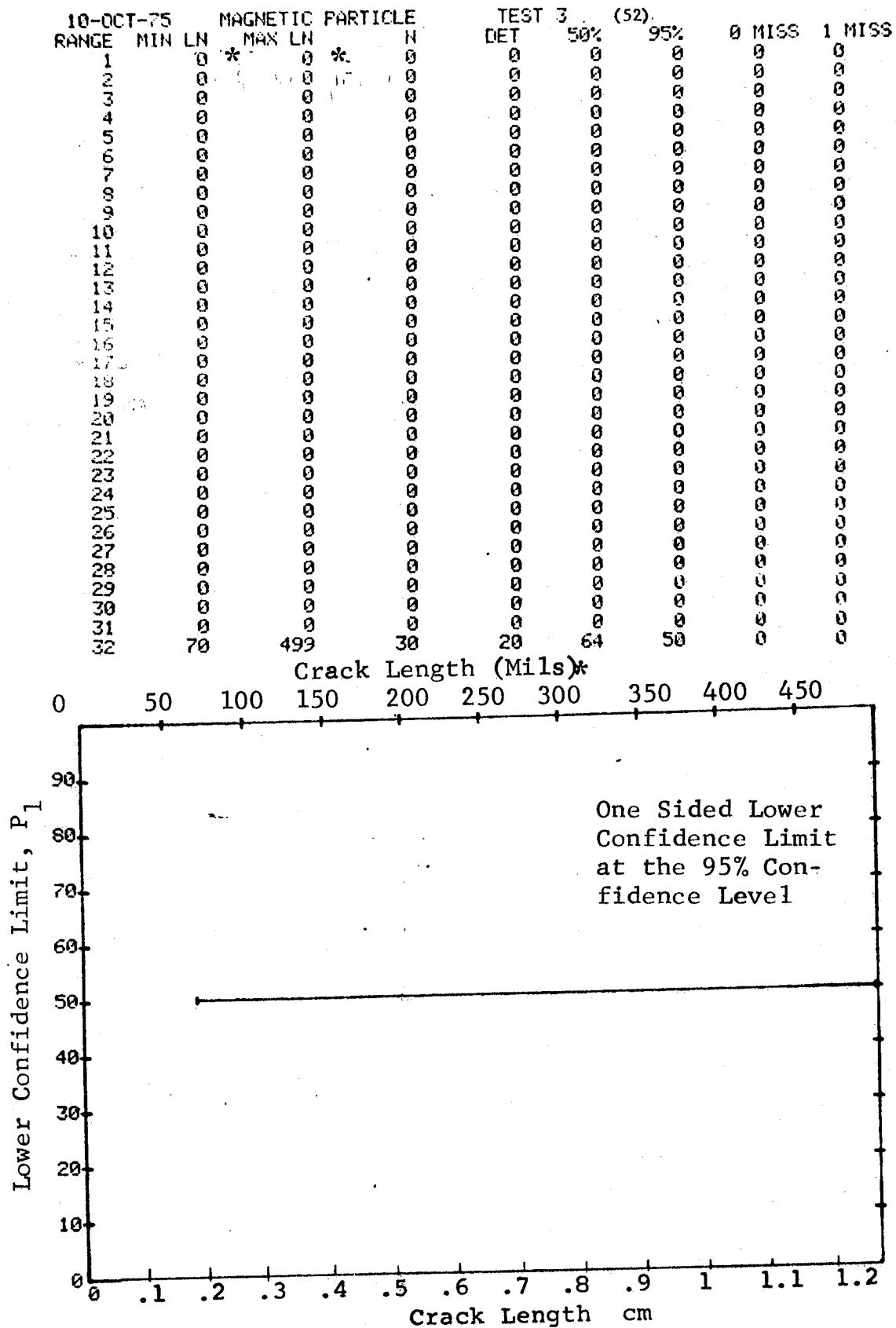


Figure D-52 (Concluded)

(a) Range Interval Method of Data Cumulation

10-OCT-75		ULTRASONIC		TEST 1 (53)		95%		0 MISS		1 MISS	
RANGE	MIN	LN	MAX LN	DET	50%						
1	70*	70*	70*	1	50	5	0	0	0	0	0
2	70*	70*	70*	0	0	0	0	0	0	0	0
3	100	105	105	2	38	0	0	0	0	0	0
4	120	120	120	1	29	2	0	0	0	0	0
5	130	140	140	2	74	49	0	0	0	0	0
6	150	150	150	0	70	22	0	0	0	0	0
7	157	158	158	5	87	54	0	0	0	0	0
8	170	170	170	1	50	5	0	0	0	0	0
9	184	190	190	1	79	36	0	0	0	0	0
10	200	200	200	3	29	2	0	0	0	0	0
11	212	215	215	1	70	22	0	0	0	0	0
12	236	236	236	2	90	65	0	0	0	0	0
13	0	0	0	7	0	0	0	0	0	0	0
14	262	264	264	0	84	47	0	0	0	0	0
15	0	0	0	4	0	0	0	0	0	0	0
16	288	292	292	0	87	54	0	0	0	0	0
17	0	0	0	5	0	0	0	0	0	0	0
18	314	315	315	0	79	36	0	0	0	0	0
19	0	0	0	3	0	0	0	0	0	0	0
20	337	344	344	0	68	34	0	0	0	0	0
21	0	0	0	4	0	0	0	0	0	0	0
22	368	368	368	0	50	5	0	0	0	0	0
23	0	0	0	1	0	0	0	0	0	0	0
24	394	394	394	0	70	22	0	0	0	0	0
25	420	420	420	2	50	5	0	0	0	0	0
26	0	0	0	1	0	0	0	0	0	0	0
27	0	0	0	0	0	0	0	0	0	0	0
28	460	460	460	0	50	5	0	0	0	0	0
29	472	473	473	1	70	22	0	0	0	0	0
30	0	0	0	0	0	0	0	0	0	0	0
31	499	499	499	2	50	5	0	0	0	0	0
32	526	526	526	0	50	5	0	0	0	0	0

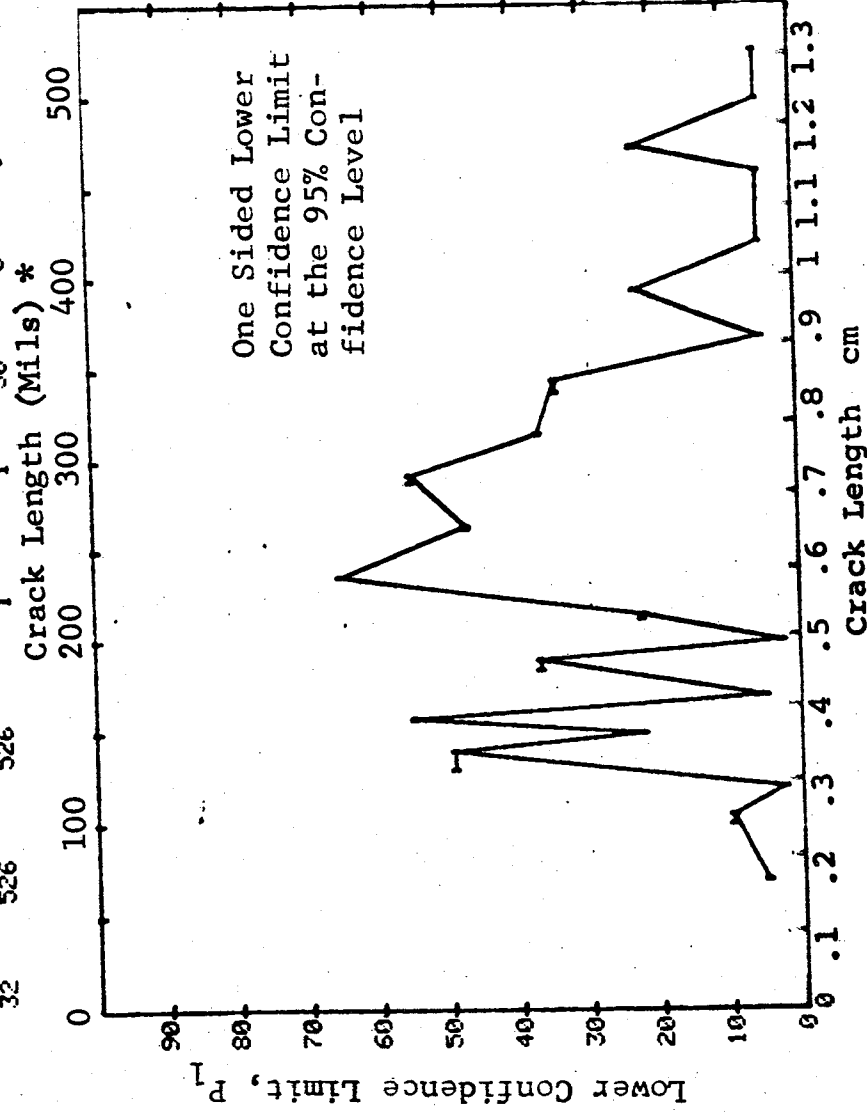


Figure D-53 Probability of Detection for 4330V Steel Using Ultrasonic Shear Wave. Fatigue Cracks in Cylindrical Shell Specimens. Lab. Env.

(b) Optimum Probability Method of Data Cumulation

10-OCT-75		ULTRASONIC		N	TEST 2 (53)		0 MISS	1 MISS
RANGE	MIN LN	* MAX LN *		DET	50%	95%		
1	70	70	1	1	0	5	0	0
2	0	0	0	0	0	0	0	0
3	70	105	5	3	0	18	0	0
4	70	120	7	4	0	22	0	0
5	130	140	10	6	0	49	0	0
6	130	150	12	10	0	56	0	0
7	130	158	17	15	0	67	0	0
8	130	170	18	16	0	68	0	0
9	150	190	11	11	0	76	0	0
10	130	200	23	20	0	69	0	0
11	150	215	15	14	0	72	0	0
12	150	236	22	21	0	80	24	39
13	0	0	0	0	0	0	0	0
14	150	264	26	25	0	83	20	35
15	0	0	0	0	0	0	0	0
16	150	292	31	30	0	85	15	30
17	0	0	0	0	0	0	0	0
18	150	315	34	33	0	86	12	27
19	0	0	0	0	0	0	0	0
20	150	344	39	37	0	84	22	37
21	0	0	0	0	0	0	0	0
22	150	368	40	38	0	85	21	36
23	0	0	0	0	0	0	0	0
24	150	394	42	40	0	85	19	34
25	150	420	43	41	0	86	18	33
26	0	0	0	0	0	0	0	0
27	0	0	0	0	0	0	0	0
28	150	460	44	42	0	86	17	32
29	150	473	46	44	0	86	15	30
30	0	0	0	0	0	0	0	0
31	150	499	47	45	0	87	14	29
32	150	526	48	46	0	87	13	28

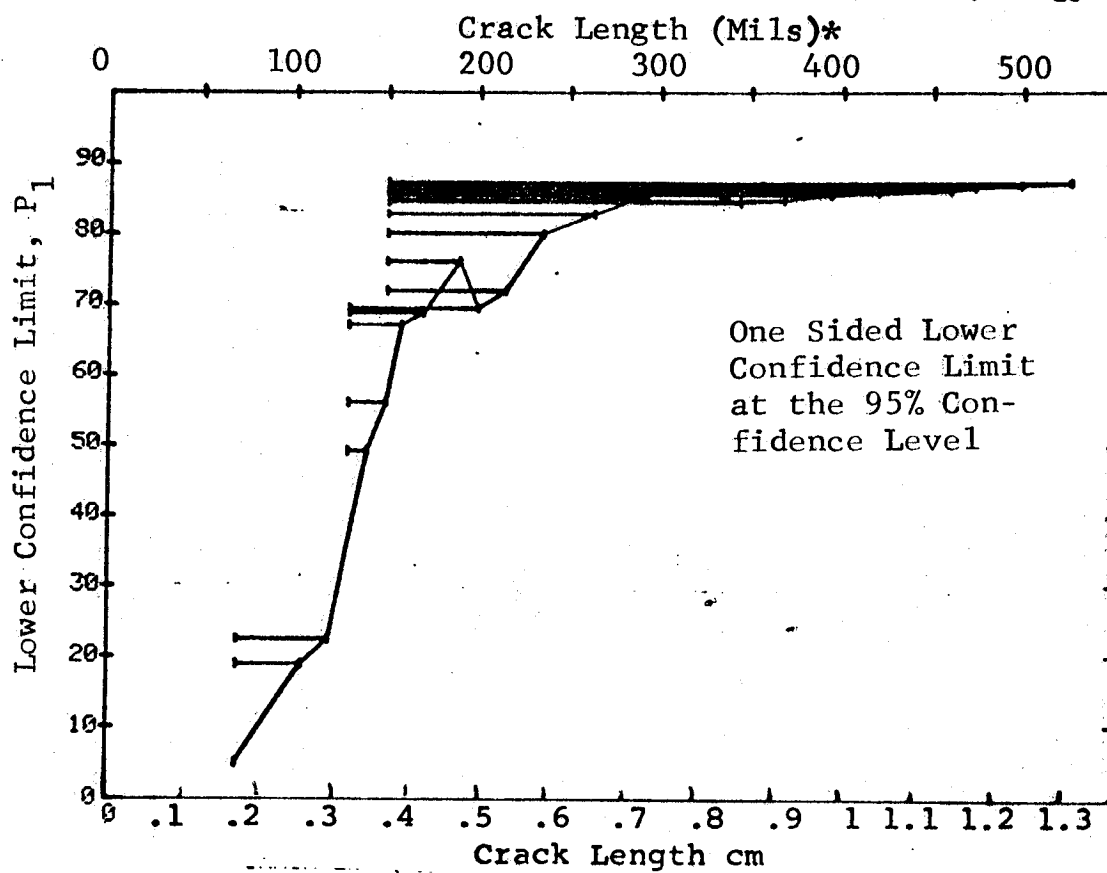


Figure D-53 (Continued)

(c) Overlapping Sixty Point Method of Data Cumulation

10-OCT-75		ULTRASONIC		N	TEST 3 (53)			0 MISS	1 MISS
RANGE	MIN	LN	MAX LN		DET	50%	95%		
1		0*	0*	0	0	0	0	0	0
2		0	0	0	0	0	0	0	0
3		0	0	0	0	0	0	0	0
4		0	0	0	0	0	0	0	0
5		0	0	0	0	0	0	0	0
6		0	0	0	0	0	0	0	0
7		0	0	0	0	0	0	0	0
8		0	0	0	0	0	0	0	0
9		0	0	0	0	0	0	0	0
10		0	0	0	0	0	0	0	0
11		0	0	0	0	0	0	0	0
12		0	0	0	0	0	0	0	0
13		0	0	0	0	0	0	0	0
14		0	0	0	0	0	0	0	0
15		0	0	0	0	0	0	0	0
16		0	0	0	0	0	0	0	0
17		0	0	0	0	0	0	0	0
18		0	0	0	0	0	0	0	0
19		0	0	0	0	0	0	0	0
20		0	0	0	0	0	0	0	0
21		0	0	0	0	0	0	0	0
22		0	0	0	0	0	0	0	0
23		0	0	0	0	0	0	0	0
24		0	0	0	0	0	0	0	0
25		0	0	0	0	0	0	0	0
26		0	0	0	0	0	0	0	0
27		0	0	0	0	0	0	0	0
28		0	0	0	0	0	0	0	0
29		0	0	0	0	0	0	0	0
30		0	0	0	0	0	0	0	0
31	70		236	34	28	80	68	43	56
32	105		499	60	55	90	83		

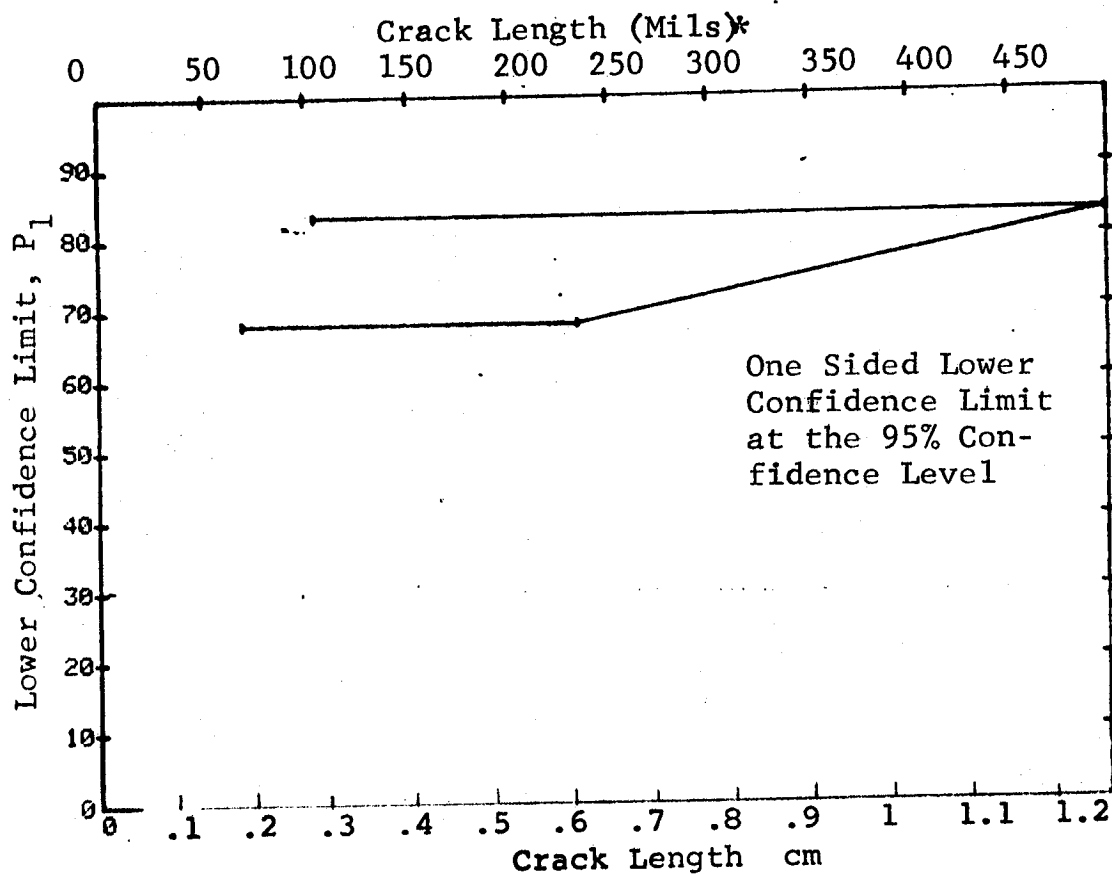


Figure D-53 (Concluded)

(a) Range Interval Method of Data Cumulation

10-OCT-75		ULTRASONIC		TEST 1 (54)					
RANGE	MIN LN	MAX LN	N	DET	50%	95%	0 MISS	1 MISS	
1	52 *	53 *	4	1	15	1	0	0	
2	70	81	6	2	26	6	0	0	
3	91	92	3	3	79	36	0	0	
4	105	109	9	6	60	34	0	0	
5	130	137	15	9	56	35	0	0	
6	0	0	0	0	0	0	0	0	
7	157	162	12	6	45	24	0	0	
8	183	188	6	4	57	27	0	0	
9	190	196	3	1	20	1	0	0	
10	210	212	2	2	70	22	0	0	
11	234	236	2	2	70	22	0	0	
12	242	248	3	3	79	36	0	0	
13	262	267	2	2	70	22	0	0	
14	290	290	2	2	70	22	0	0	
15	0	0	0	0	0	0	0	0	
16	314	322	3	3	79	36	0	0	
17	327	330	2	2	70	22	0	0	
18	342	358	4	3	61	24	0	0	
19	362	362	1	0	0	0	0	0	
20	382	389	2	2	70	22	0	0	
21	0	0	0	0	0	0	0	0	
22	422	423	2	2	70	22	0	0	
23	428	431	2	2	70	22	0	0	
24	0	0	0	0	0	0	0	0	
25	461	461	1	1	50	5	0	0	
26	0	0	0	0	0	0	0	0	
27	498	498	1	1	50	5	0	0	
28	0	0	0	0	0	0	0	0	
29	0	0	0	0	0	0	0	0	
30	0	0	0	0	0	0	0	0	
31	576	577	2	2	70	22	0	0	
32	604	604	1	1	50	5	0	0	

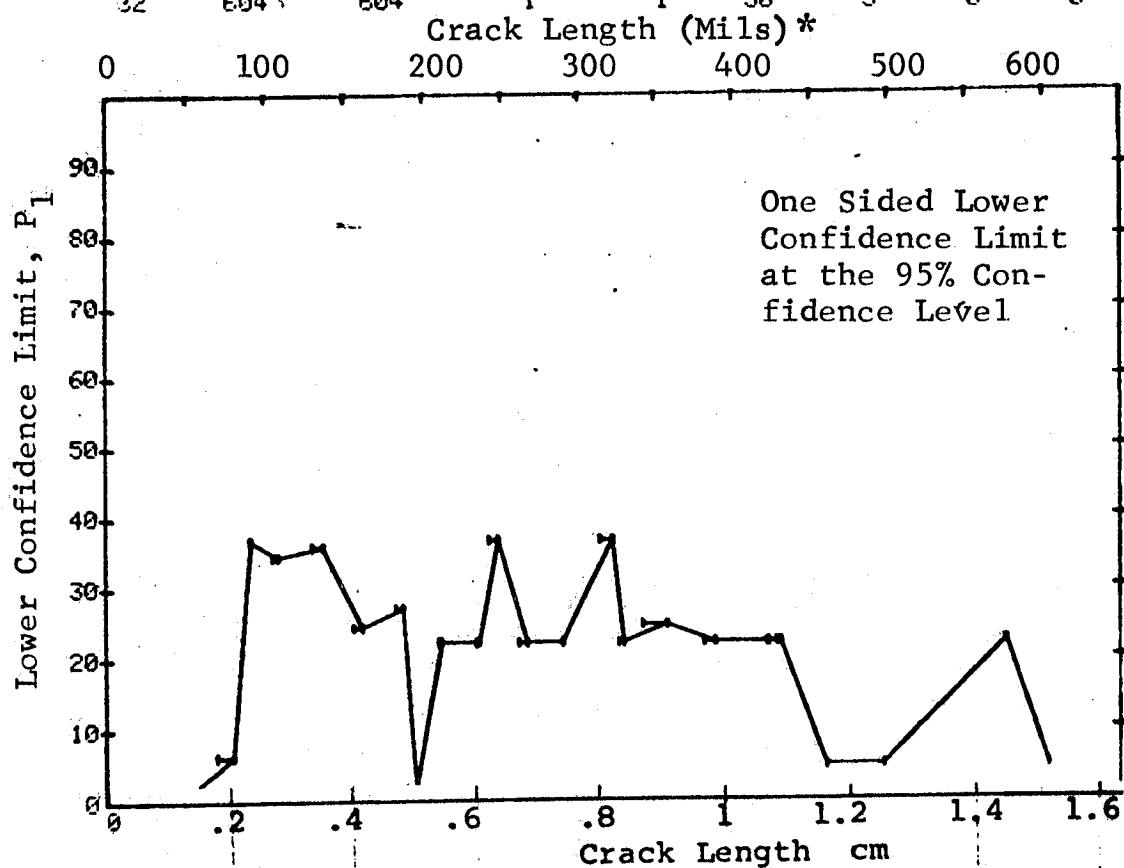


Figure D-54 Probability of Detection for 7075-T6511 Al Using Ultrasonic Shear Wave. Fatigue Cracks in Cylindrical Shell Specimens. Lab. Env..

(b) Optimum Probability Method of Data Cumulation

10-OCT-75		ULTRASONIC		N	TEST 2 (54)		95%	0 MISS	1 MISS
RANGE	MIN	LN	MAX LN		DET	50%			
1		52	* 53*	4	1	0	1	0	0
2		57	81	10	3	0	8	0	0
3		91	92	3	3	0	36	0	0
4		91	109	12	9	0	47	0	0
5		91	137	27	18	0	49	0	0
6		0	0	0	0	0	0	0	0
7		91	162	39	24	0	47	0	0
8		91	188	45	28	0	48	0	0
9		91	196	48	29	0	47	0	0
10		91	212	50	31	0	49	0	0
11		91	236	52	33	0	51	0	0
12	210		248	7	7	0	65	0	0
13	210		267	9	9	0	71	0	0
14	210		290	11	11	0	76	0	0
15	0		0	0	0	0	0	0	0
16	210		322	14	14	0	80	15	32
17	210		330	16	16	0	82	13	30
18	210		358	20	19	0	78	0	0
19	210		362	21	19	0	72	0	0
20	210		389	23	21	0	75	0	0
21	0		0	0	0	0	0	0	0
22	210		423	25	23	0	76	0	0
23	210		431	27	25	0	78	0	0
24	0		0	0	0	0	0	0	0
25	210		461	28	26	0	79	0	0
26	0		0	0	0	0	0	0	0
27	210		498	29	27	0	79	0	0
28	0		0	0	0	0	0	0	0
29	0		0	0	0	0	0	0	0
30	0		0	0	0	0	0	0	0
31	210		577	31	29	0	81	30	45
32	210		604	32	30	0	81	29	44

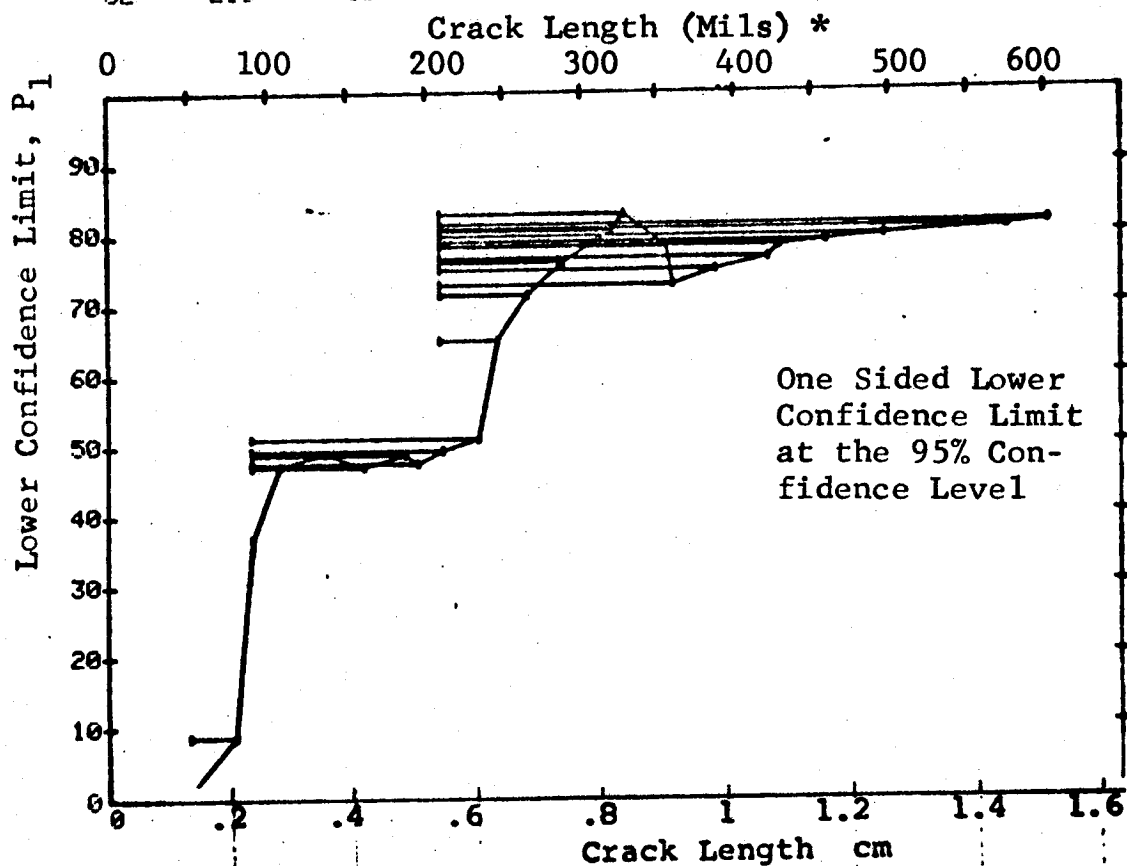


Figure D-54 (Continued)

(c) Overlapping Sixty Point Method of Data Cumulation

10-OCT-75		ULTRASONIC			TEST 3 (154)						
RANGE	MIN	LN	* MAX	LN *	N	DET	50%	95%	0 MISS	1 MISS	
1		0		0	0	0	0	0	0	0	
2		0		0	0	0	0	0	0	0	
3		0		0	0	0	0	0	0	0	
4		0		0	0	0	0	0	0	0	
5		0		0	0	0	0	0	0	0	
6		0		0	0	0	0	0	0	0	
7		0		0	0	0	0	0	0	0	
8		0		0	0	0	0	0	0	0	
9		0		0	0	0	0	0	0	0	
10		0		0	0	0	0	0	0	0	
11		0		0	0	0	0	0	0	0	
12		0		0	0	0	0	0	0	0	
13		0		0	0	0	0	0	0	0	
14		0		0	0	0	0	0	0	0	
15		0		0	0	0	0	0	0	0	
16		0		0	0	0	0	0	0	0	
17		0		0	0	0	0	0	0	0	
18		0		0	0	0	0	0	0	0	
19		0		0	0	0	0	0	0	0	
20		0		0	0	0	0	0	0	0	
21		0		0	0	0	0	0	0	0	
22		0		0	0	0	0	0	0	0	
23		0		0	0	0	0	0	0	0	
24		0		0	0	0	0	0	0	0	
25		0		0	0	0	0	0	0	0	
26		0		0	0	0	0	0	0	0	
27		0		0	0	0	0	0	0	0	
28		0		0	0	0	0	0	0	0	
29		0		0	0	0	0	0	0	0	
30		0		0	0	0	0	0	0	0	
31	52		190		57	32	55	44	0	0	
32	132		498		60	44	72	62	0	0	

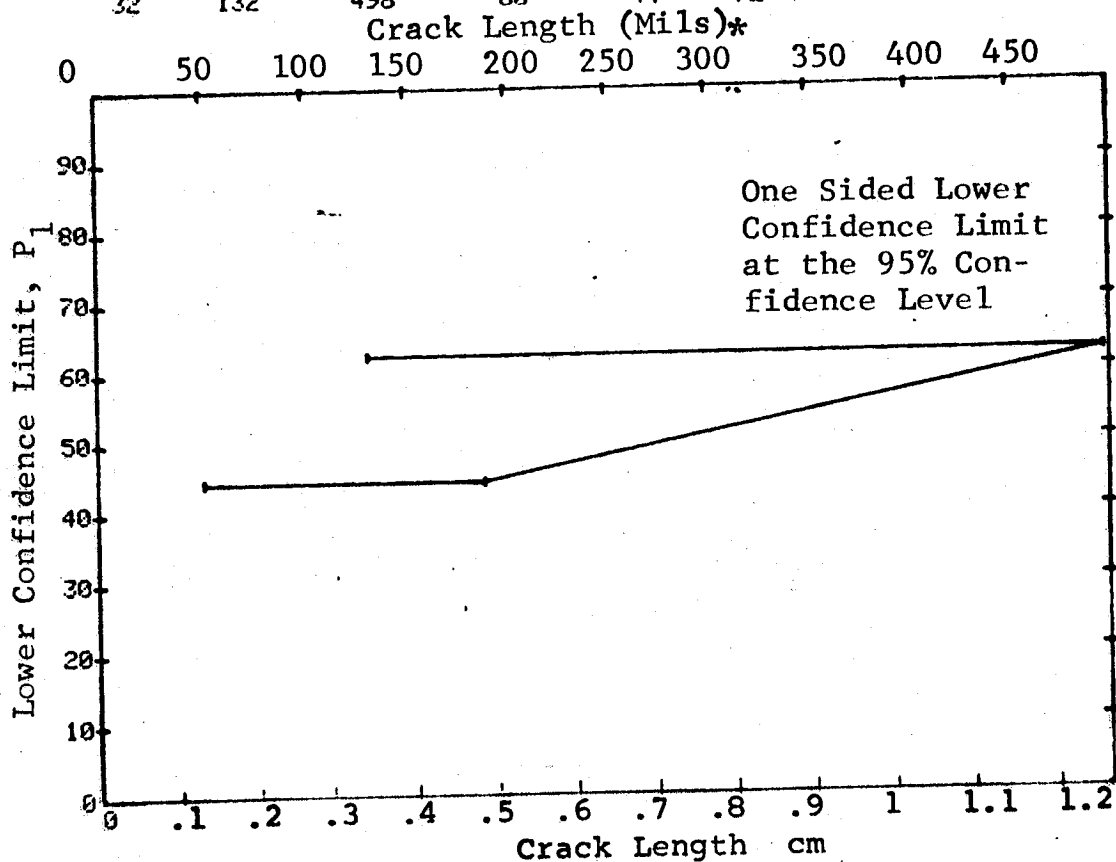


Figure D-54 (Concluded)

(a) Range Interval Method of Data Cumulation

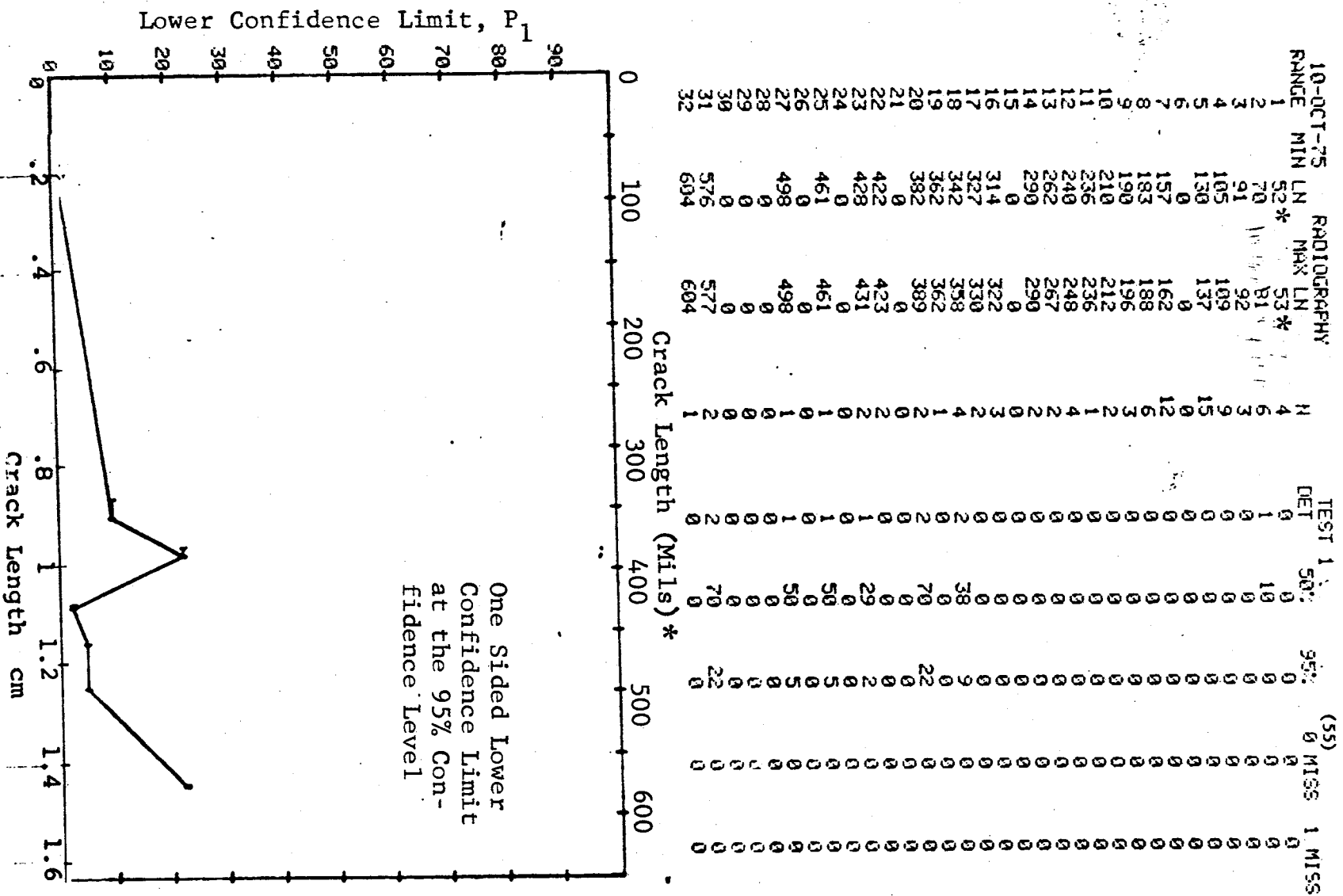


Figure D-55 Probability of Detection for 7075-T6511 Al Using X-ray. Fatigue Cracks in Cylindrical Shell. Lab. Env.

(b) Optimum Probability Method of Data Cumulation

10-OCT-75		RADIOGRAPHY		N	TEST 2		(55)		
RANGE	MIN	LN	* MAX LN		DET	50%	95%	0 MISS	1 MISS
1		52	53*	4	0	0	0	0	0
2		70	81	6	1	0	0	0	0
3		70	92	9	1	0	0	0	0
4		70	109	18	1	0	0	0	0
5		70	137	33	1	0	0	0	0
6		0	0	0	0	0	0	0	0
7		70	162	45	1	0	0	0	0
8		70	188	51	1	0	0	0	0
9		70	196	54	1	0	0	0	0
10		70	212	56	1	0	0	0	0
11		70	236	57	1	0	0	0	0
12		70	248	61	1	0	0	0	0
13		70	267	63	1	0	0	0	0
14		70	290	65	1	0	0	0	0
15		0	0	0	0	0	0	0	0
16		70	322	68	1	0	0	0	0
17		70	330	70	1	0	0	0	0
18	342		358	4	2	0	9	0	0
19	342		362	5	2	0	7	0	0
20	342		389	7	4	0	22	0	0
21	0		0	0	0	0	0	0	0
22	342		423	9	4	0	16	0	0
23	342		431	11	5	0	19	0	0
24	0		0	0	0	0	0	0	0
25	342		461	12	6	0	24	0	0
26	0		0	0	0	0	0	0	0
27	382		498	8	5	0	28	0	0
28	0		0	0	0	0	0	0	0
29	0		0	0	0	0	0	0	0
30	0		0	0	0	0	0	0	0
31	461		577	4	4	0	47	0	0
32	382		604	11	7	0	34	0	0

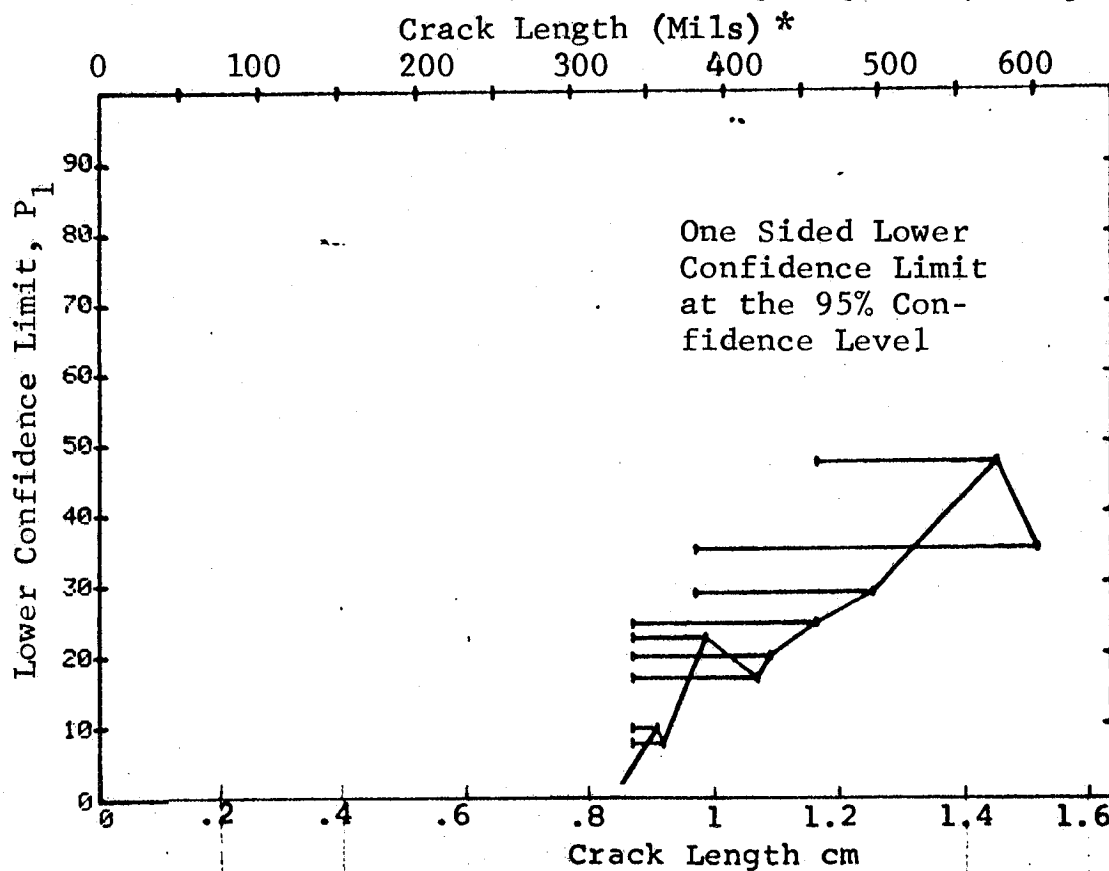


Figure D-55 (Continued)

(c) Overlapping Sixty Point Method of Data Cumulation

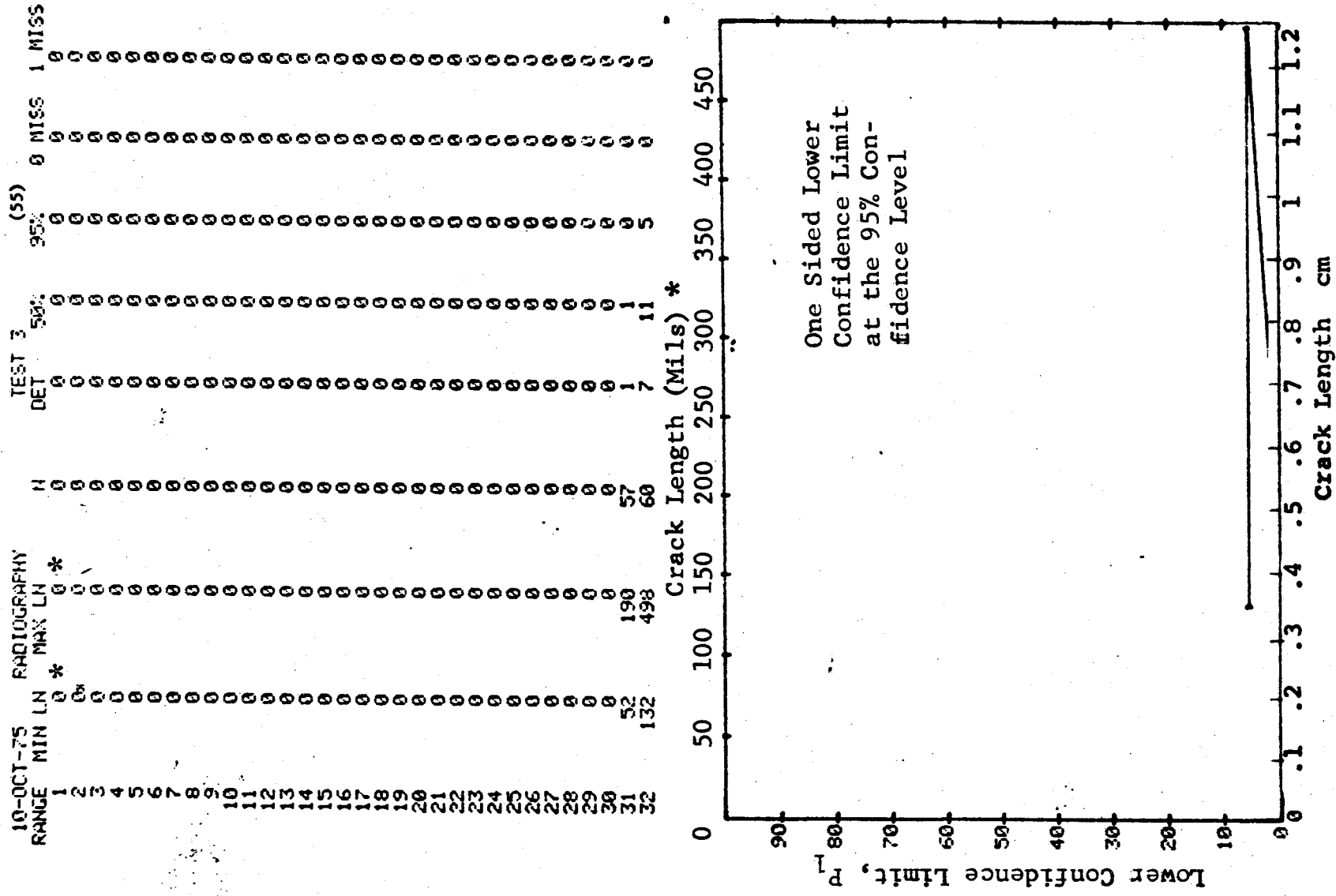


Figure D-55 (Concluded)

REPRODUCIBILITY OF THE
ORIGINAL PAGE IS POOR

(a) Range Interval Method of Data Cumulation

10-OCT-75		RADIOGRAPHY		N	TEST 1		(56)		0 MISS	1 MISS
RANGE	MIN LN	* MAX LN	*		DET	50%	95%			
1	70	70	*	1	0	0	0	0	0	0
2	0	0		0	0	0	0	0	0	0
3	100	105		4	0	0	0	0	0	0
4	120	120		2	0	0	0	0	0	0
5	130	140		11	0	0	0	0	0	0
6	150	150		2	0	0	0	0	0	0
7	157	158		5	0	0	0	0	0	0
8	170	170		1	0	0	0	0	0	0
9	184	190		3	0	0	0	0	0	0
10	200	200		2	0	0	0	0	0	0
11	212	215		2	0	0	0	0	0	0
12	236	236		7	0	0	0	0	0	0
13	0	0		0	0	0	0	0	0	0
14	262	264		4	1	15	1	0	0	0
15	0	0		0	0	0	0	0	0	0
16	288	292		5	0	0	0	0	0	0
17	0	0		0	0	0	0	0	0	0
18	314	315		3	0	0	0	0	0	0
19	0	0		0	0	0	0	0	0	0
20	337	344		5	1	12	1	0	0	0
21	0	0		0	0	0	0	0	0	0
22	368	368		1	0	0	0	0	0	0
23	0	0		0	0	0	0	0	0	0
24	394	394		2	0	0	0	0	0	0
25	420	420		1	0	0	0	0	0	0
26	0	0		0	0	0	0	0	0	0
27	446	446		1	0	0	0	0	0	0
28	0	0		0	0	0	0	0	0	0
29	472	473		2	1	29	2	0	0	0
30	0	0		0	0	0	0	0	0	0
31	499	499		1	1	50	5	0	0	0
32	526	526		1	1	50	5	0	0	0

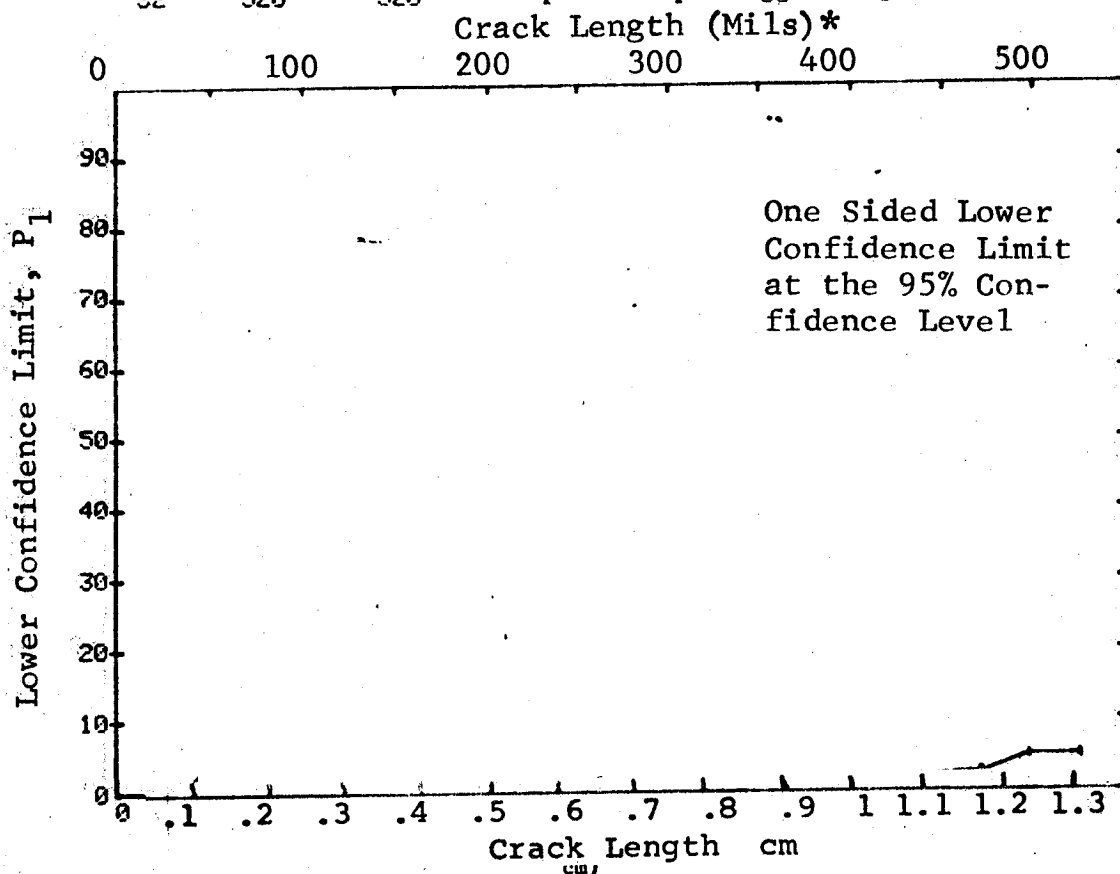


Figure D-56 Probability of Detection for 4330V Steel Using X-ray. Fatigue Cracks in Cylindrical Shell. Lab. Env.

(b) Optimum Probability Method of Data Cumulation

10-OCT-75			RADIOGRAPHY		N	TEST 2		(56)		
RANGE	MIN LN	LN	*MAX LN*	LN*		DET	50%	95%	0 MISS	1 MISS
1	70	70	70	70	1	0	0	0	0	0
2	0	0	0	0	0	0	0	0	0	0
3	100	105	105	105	4	0	0	0	0	0
4	120	120	120	120	2	0	0	0	0	0
5	130	140	140	140	11	0	0	0	0	0
6	150	150	150	150	2	0	0	0	0	0
7	157	158	158	158	5	0	0	0	0	0
8	170	170	170	170	1	0	0	0	0	0
9	184	190	190	190	3	0	0	0	0	0
10	200	200	200	200	2	0	0	0	0	0
11	212	215	215	215	2	0	0	0	0	0
12	236	236	236	236	7	0	0	0	0	0
13	0	0	0	0	0	0	0	0	0	0
14	262	264	264	264	4	1	0	1	0	0
15	0	0	0	0	0	0	0	0	0	0
16	262	292	292	292	9	1	0	0	0	0
17	0	0	0	0	0	0	0	0	0	0
18	262	315	315	315	12	1	0	0	0	0
19	0	0	0	0	0	0	0	0	0	0
20	262	344	344	344	17	2	0	2	0	0
21	0	0	0	0	0	0	0	0	0	0
22	262	368	368	368	18	2	0	2	0	0
23	0	0	0	0	0	0	0	0	0	0
24	262	394	394	394	20	2	0	1	0	0
25	262	420	420	420	21	2	0	1	0	0
26	0	0	0	0	0	0	0	0	0	0
27	262	446	446	446	22	2	0	1	0	0
28	0	0	0	0	0	0	0	0	0	0
29	262	473	473	473	24	3	0	3	0	0
30	0	0	0	0	0	0	0	0	0	0
31	472	499	499	499	3	2	0	13	0	0
32	472	526	526	526	4	3	0	24	0	0

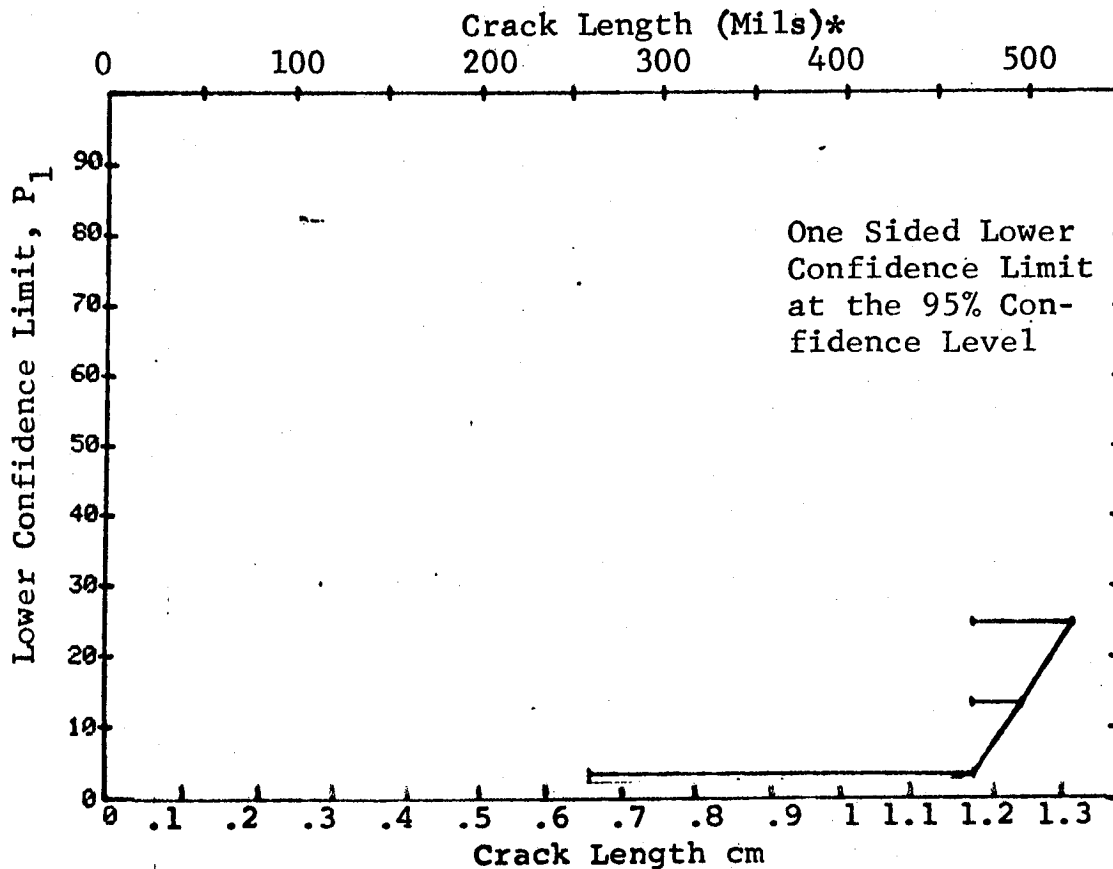


Figure D-56 (Continued)

(c) Overlapping Sixty Point Method of Data Cumulation

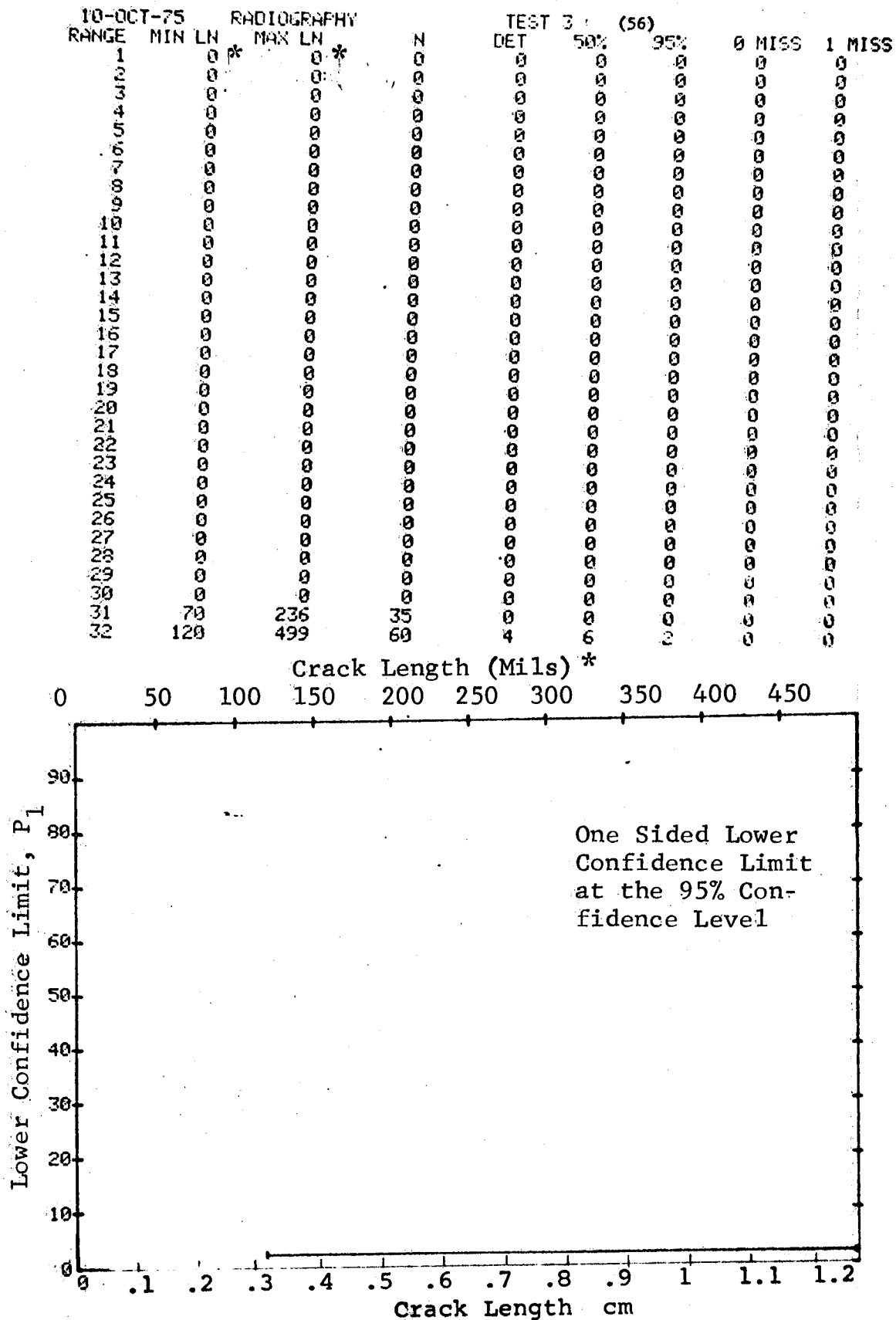


Figure D-56 (Concluded)

(a) Range Interval Method of Data Cumulation

17-OCT-75								(57)			
RANGE	MIN LH	MAX LH	*	N	DET	50%	95%	0 MISS	1 MISS	0 MISS	1 MISS
1	5	207	*	154	19	12	8	0	0	0	0
2	30	151		87	22	34	17	0	0	0	0
3	54	174		25	14	53	37	0	0	0	0
4	78	100		19	7	34	18	0	0	0	0
5	105	125		10	2	83	20	0	0	0	0
6	127	142		8	2	79	52	0	0	0	0
7	150	168		10	6	54	30	0	0	0	0
8	179	194		4	4	84	47	0	0	0	0
9	200	220		7	3	77	47	0	0	0	0
10	230	243		3	3	79	36	0	0	0	0
11	252	265		4	4	84	47	0	0	0	0
12	271	297		1	0	0	0	0	0	0	0
13	296	307		2	1	29	2	0	0	0	0
14	320	339		2	2	70	22	0	0	0	0
15	346	353		2	2	70	22	0	0	0	0
16	0	0		0	0	0	0	0	0	0	0
17	392	408		2	1	29	2	0	0	0	0
18	0	0		0	0	0	0	0	0	0	0
19	0	0		0	0	0	0	0	0	0	0
20	0	0		0	0	0	0	0	0	0	0
21	0	0		0	0	0	0	0	0	0	0
22	533	533		1	1	50	5	0	0	0	0
23	0	0		0	0	0	0	0	0	0	0
24	0	0		0	0	0	0	0	0	0	0
25	0	0		0	0	0	0	0	0	0	0
26	0	0		0	0	0	0	0	0	0	0
27	0	0		0	0	0	0	0	0	0	0
28	0	0		0	0	0	0	0	0	0	0
29	687	687		1	1	50	5	0	0	0	0
30	0	0		0	0	0	0	0	0	0	0
31	0	0		0	0	0	0	0	0	0	0
32	774	774		1	1	50	5	0	0	0	0

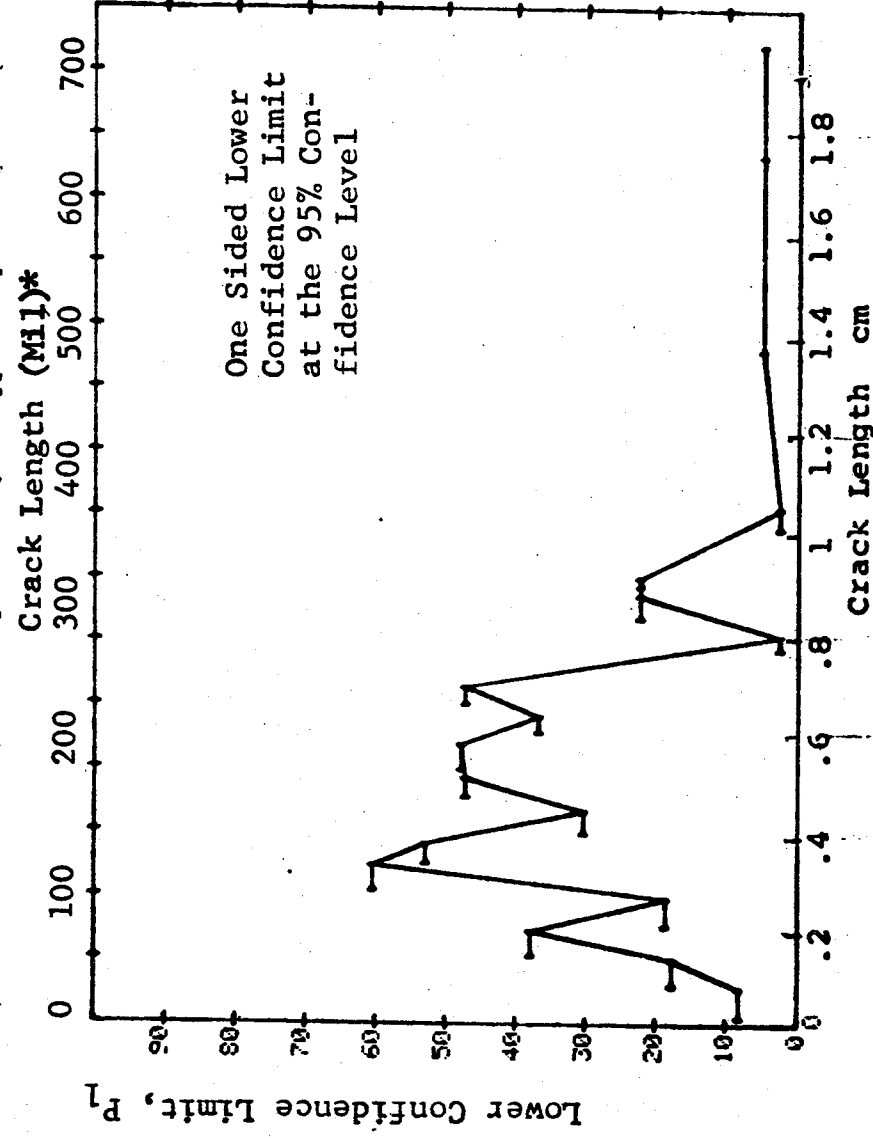


Figure D-57 Probability of Detection for 7178-T651 Al Using Eddy Current. Fatigue Cracks in Fastener Holes Measured by Team 2. Field Env.

(b) Optimum Probability Method of Data Cumulation

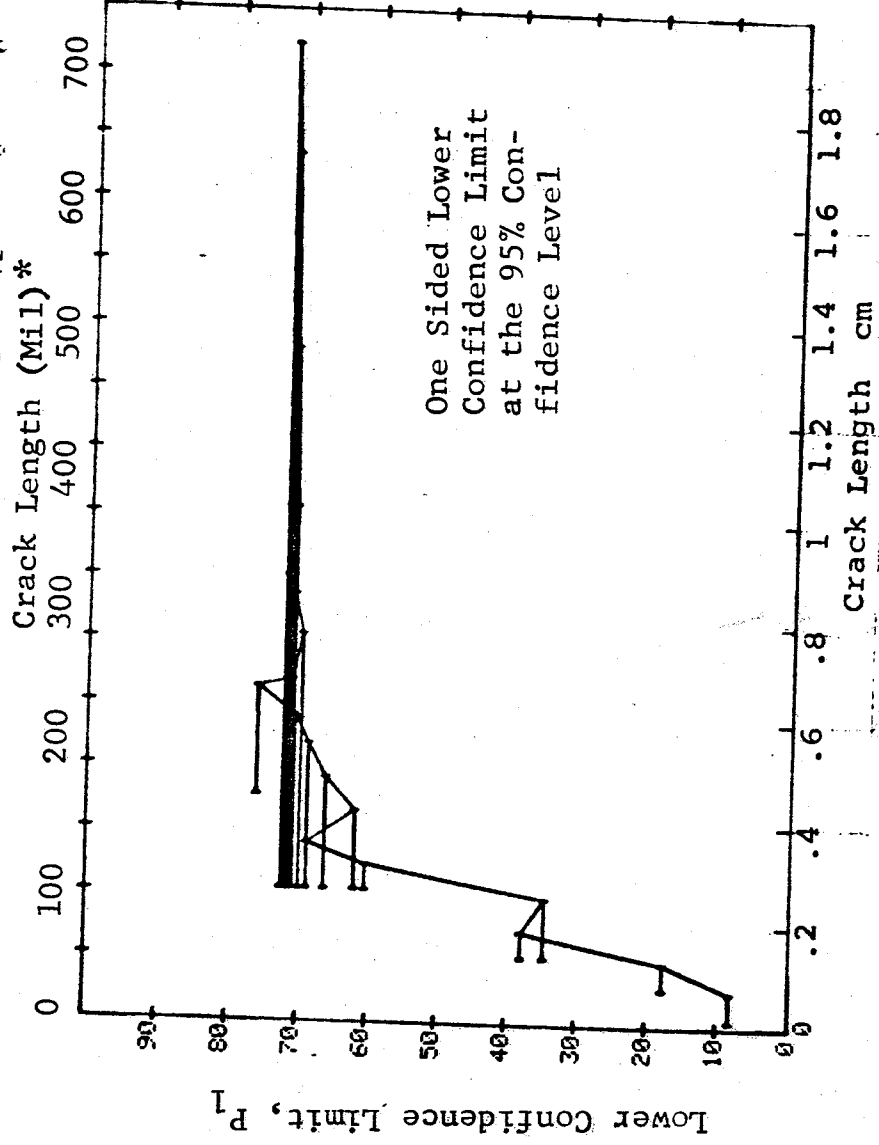
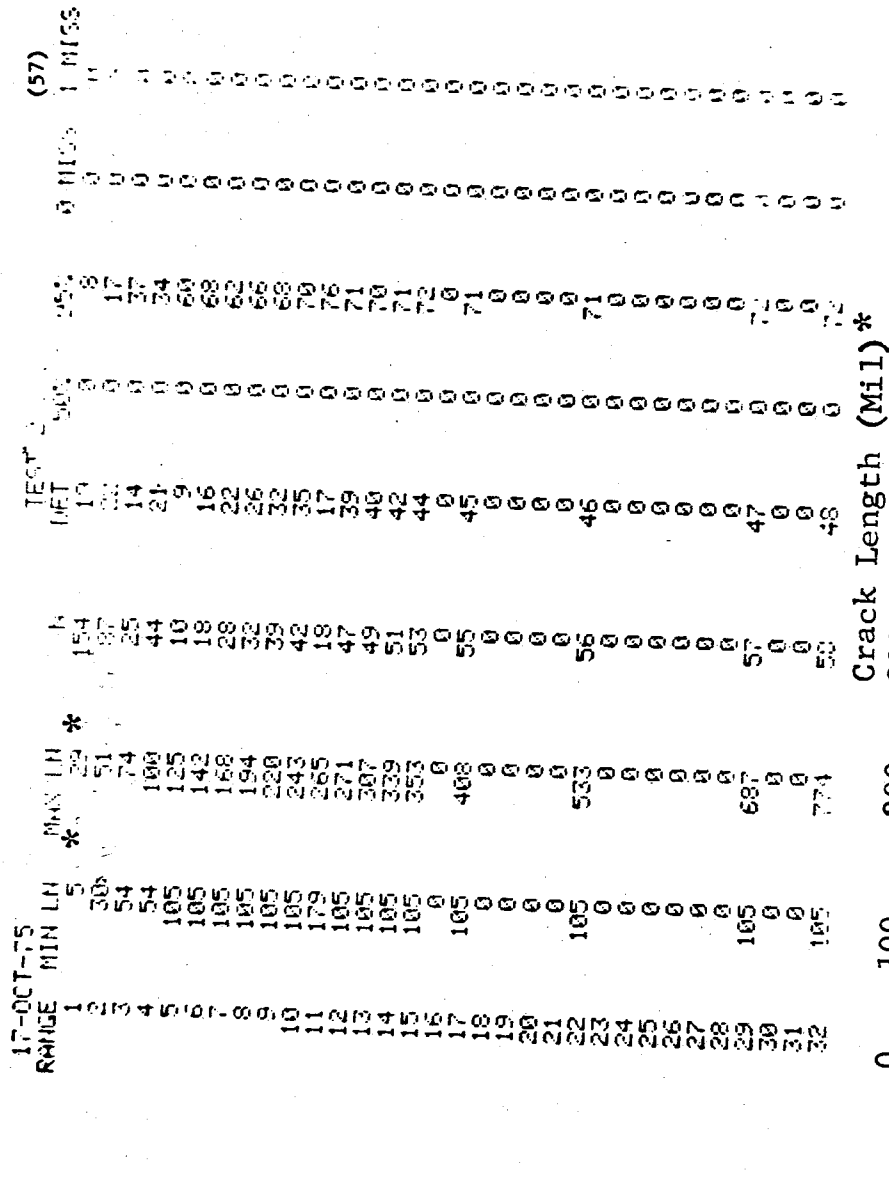


Figure D-57 (Continued)

(c) Overlapping Sixty Point Method of Data Cumulation

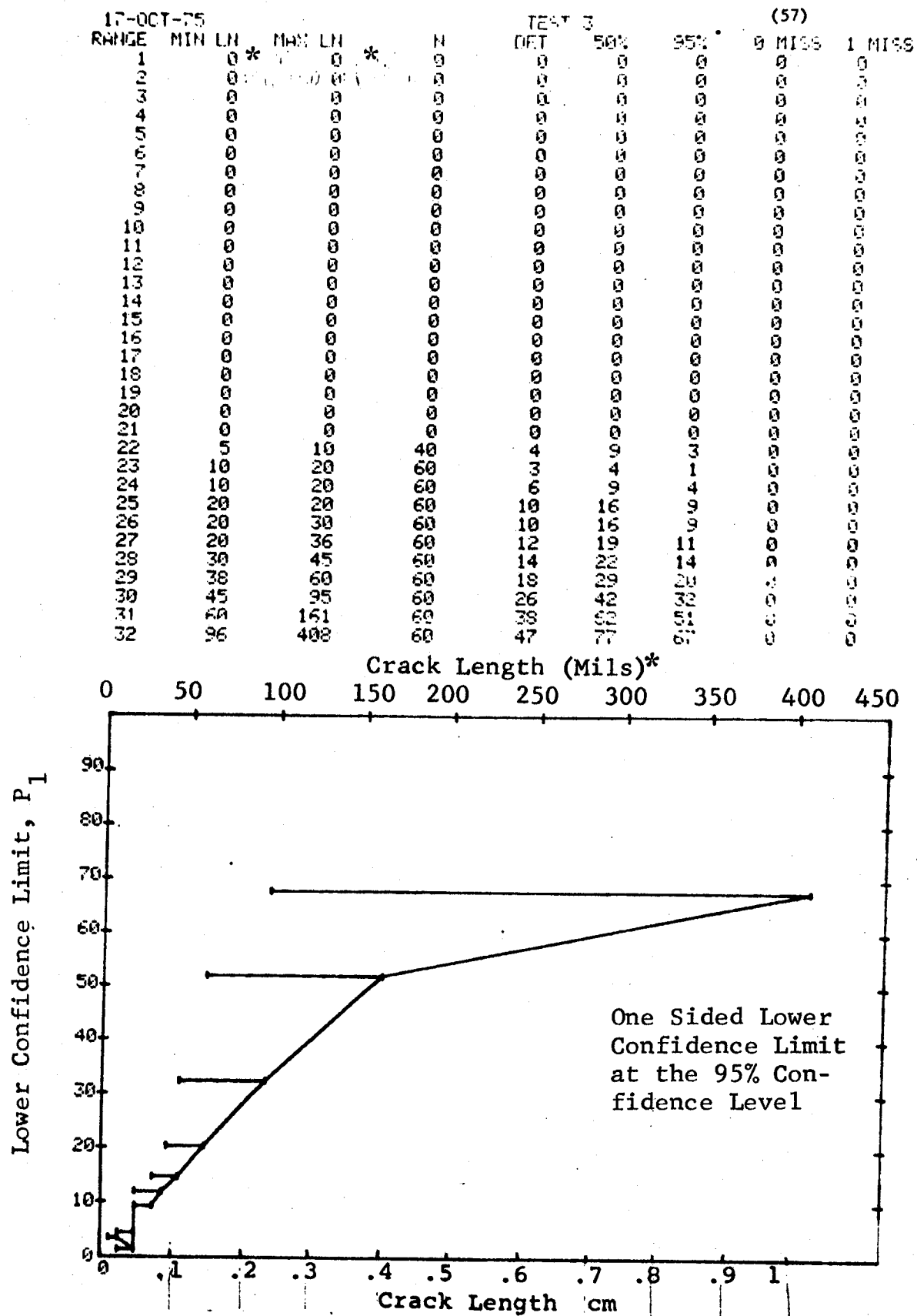


Figure D-57 (Concluded)

(a) Range Interval Method of Data Cumulation

17-OCT-75				POST 1				(58)			
RANGE	MIN LN	MAX LN	N	DET	50%	95%	0 MIN	0 MIN	0 MIN	0 MIN	0 MIN
1	5	5	150	4	2	0	0	0	0	0	0
2	30	30	30	4	1	1	0	0	0	0	0
3	54	54	23	3	1	1	0	0	0	0	0
4	78	100	26	3	13	4	0	0	0	0	0
5	105	125	10	3	25	0	0	0	0	0	0
6	127	142	7	1	9	0	0	0	0	0	0
7	150	169	9	2	17	4	0	0	0	0	0
8	179	194	5	0	0	0	0	0	0	0	0
9	208	220	5	3	50	18	0	0	0	0	0
10	230	243	4	0	0	0	0	0	0	0	0
11	252	265	4	0	0	0	0	0	0	0	0
12	271	280	4	0	61	24	0	0	0	0	0
13	296	307	6	0	0	0	0	0	0	0	0
14	320	339	3	1	20	1	0	0	0	0	0
15	346	353	3	0	0	0	0	0	0	0	0
16	0	0	0	1	20	2	0	0	0	0	0
17	392	408	3	0	0	0	0	0	0	0	0
18	0	0	0	0	0	0	0	0	0	0	0
19	0	0	0	0	0	0	0	0	0	0	0
20	0	0	0	0	0	0	0	0	0	0	0
21	0	0	0	0	0	0	0	0	0	0	0
22	533	533	1	0	0	0	0	0	0	0	0
23	0	0	0	0	0	0	0	0	0	0	0
24	0	0	0	0	0	0	0	0	0	0	0
25	0	0	0	0	0	0	0	0	0	0	0
26	0	0	0	0	0	0	0	0	0	0	0
27	0	0	0	0	0	0	0	0	0	0	0
28	0	0	0	0	0	0	0	0	0	0	0
29	687	687	1	0	0	0	0	0	0	0	0
30	0	0	0	0	0	0	0	0	0	0	0
31	0	0	0	0	0	0	0	0	0	0	0
32	774	774	1	1	50	5	0	0	0	0	0

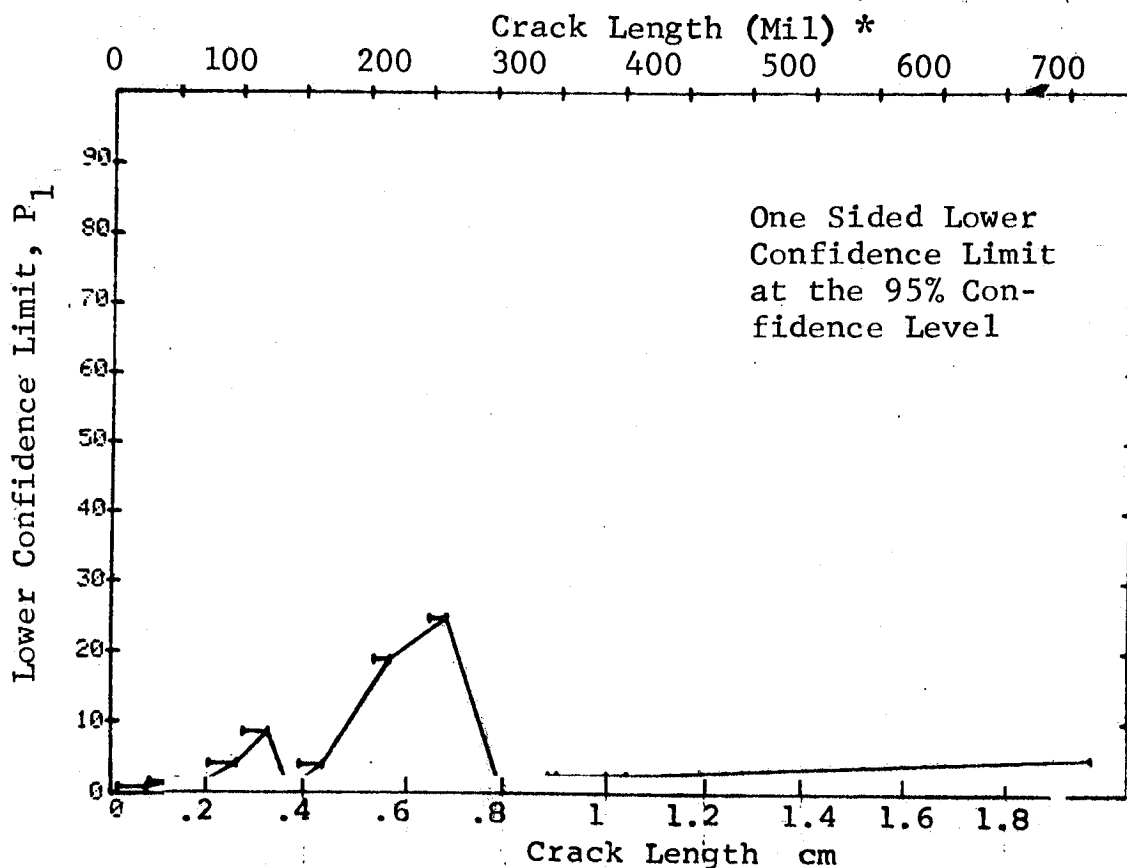


Figure D-58 Probability of Detection for 7178-T651 Al Using Eddy Current. Fatigue Cracks in Fastener Holes Measured by Team 4. Field Env.

(b) Optimum Probability Method of Data Cumulation

17-OCT-75

RANGE	MIN	IN	MAX	IN	MIN	IN	MAX	IN	(58)
1	5*	5*	150	1	0	0	0	0	0
2	5	0.51	143	2	0	0	1	0	0
3	30	74	109	3	0	0	2	0	0
4	54	100	43	4	0	0	4	0	0
5	78	125	30	5	0	0	6	0	0
6	78	142	37	6	0	0	9	0	0
7	78	162	46	7	0	0	10	0	0
8	78	184	51	8	0	0	9	0	0
9	208	220	5	9	0	0	12	0	0
10	105	243	40	10	0	0	12	0	0
11	252	265	4	11	0	0	24	0	0
12	208	280	15	12	0	0	19	0	0
13	208	307	18	13	0	0	19	0	0
14	208	339	20	14	0	0	17	0	0
15	208	353	22	15	0	0	19	0	0
16	0	0	0	16	0	0	0	0	0
17	208	408	24	17	0	0	21	0	0
18	0	0	0	18	0	0	0	0	0
19	0	0	0	19	0	0	0	0	0
20	0	0	0	20	0	0	0	0	0
21	0	0	0	21	0	0	0	0	0
22	208	537	25	22	0	0	20	0	0
23	0	0	0	23	0	0	0	0	0
24	0	0	0	24	0	0	0	0	0
25	0	0	0	25	0	0	0	0	0
26	0	0	0	26	0	0	0	0	0
27	0	0	0	27	0	0	0	0	0
28	0	0	0	28	0	0	0	0	0
29	208	687	26	29	0	0	17	0	0
30	0	0	0	30	0	0	0	0	0
31	0	0	0	31	0	0	0	0	0
32	208	774	27	32	0	0	21	0	0

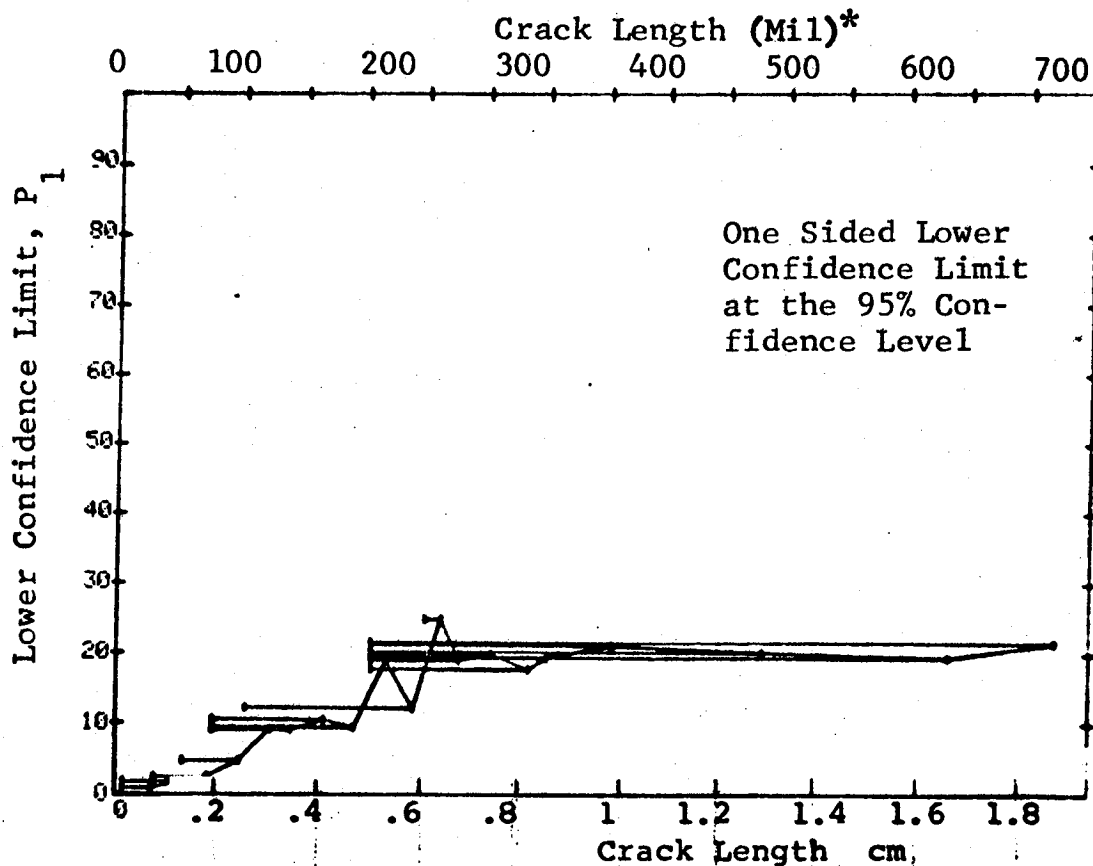
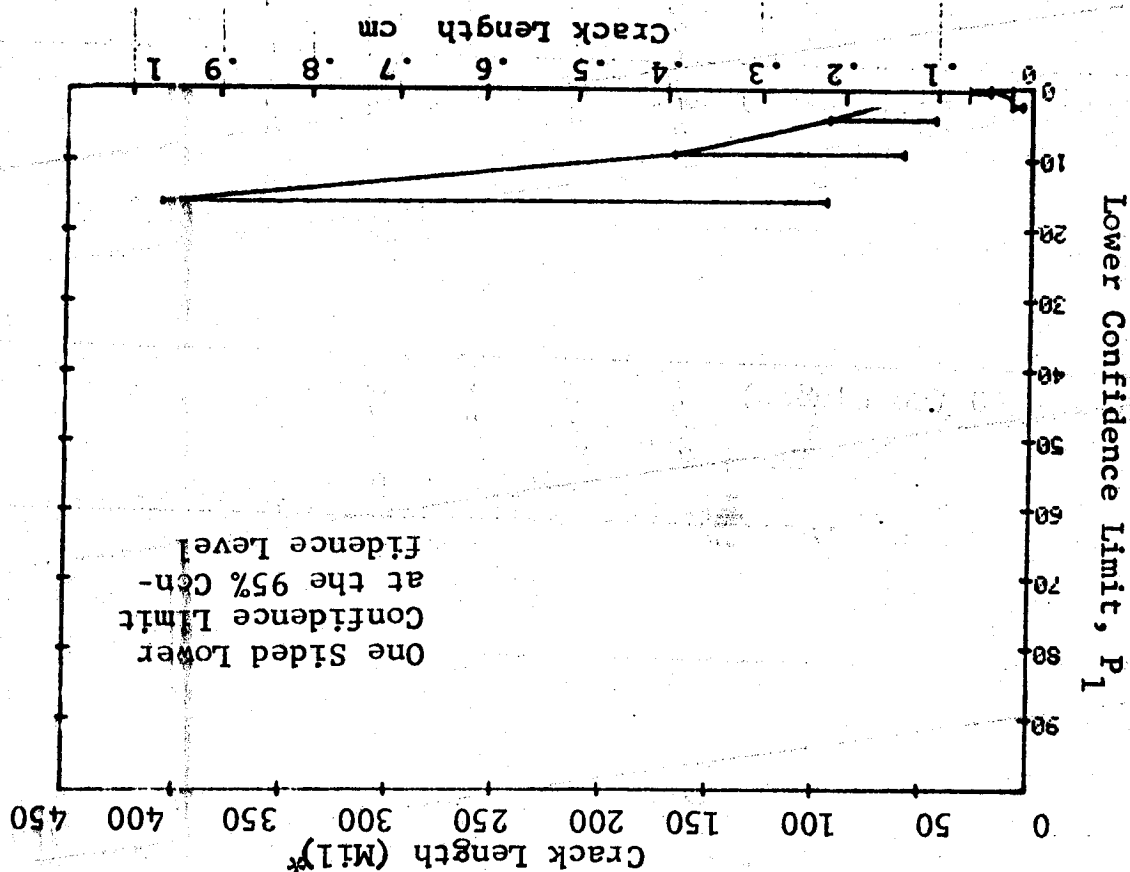


Figure D-58 (Continued)

Figure D-58 (Continued)



(c) Overlapping Sixty Point Method of Data Cumulation

(a) Range Interval Method of Data Cumulation

24-OCT-75	RANGE	MIN LN	* MAX LN	N	DET	50%	95%	ALL	0 MICS	(59)
1	27	26	895	82	9	7	0	0	0	0
2	51	50	517	109	21	18	0	0	0	0
3	78	74	150	59	39	32	0	0	0	0
4	99	97	85	32	37	28	0	0	0	0
5	124	120	64	33	50	40	0	0	0	0
6	150	142	53	27	50	38	0	0	0	0
7	179	169	48	35	51	39	0	0	0	0
8	200	194	21	13	59	41	0	0	0	0
9	220	218	26	17	63	47	0	0	0	0
10	252	243	21	14	64	46	0	0	0	0
11	271	265	19	16	81	64	0	0	0	0
12	296	280	17	4	50	22	0	0	0	0
13	320	307	14	10	67	45	0	0	0	0
14	346	339	10	3	25	8	0	0	0	0
15	392	353	10	8	74	49	0	0	0	0
16	0	0	0	0	0	0	0	0	0	0
17	0	408	9	7	71	45	0	0	0	0
18	0	0	0	0	0	0	0	0	0	0
19	0	0	0	0	0	0	0	0	0	0
20	500	0	0	0	0	0	0	0	0	0
21	533	0	2	2	70	22	0	0	0	0
22	607	0	0	0	0	0	0	0	0	0
23	0	533	4	2	38	9	0	0	0	0
24	0	0	0	0	0	0	0	0	0	0
25	0	0	0	0	0	0	0	0	0	0
26	0	607	1	0	0	0	0	0	0	0
27	0	0	0	0	0	0	0	0	0	0
28	0	0	0	0	0	0	0	0	0	0
29	687	687	4	3	61	24	0	0	0	0
30	0	0	0	0	0	0	0	0	0	0
31	0	0	0	0	0	0	0	0	0	0
32	774	774	5	5	57	54	0	0	0	0

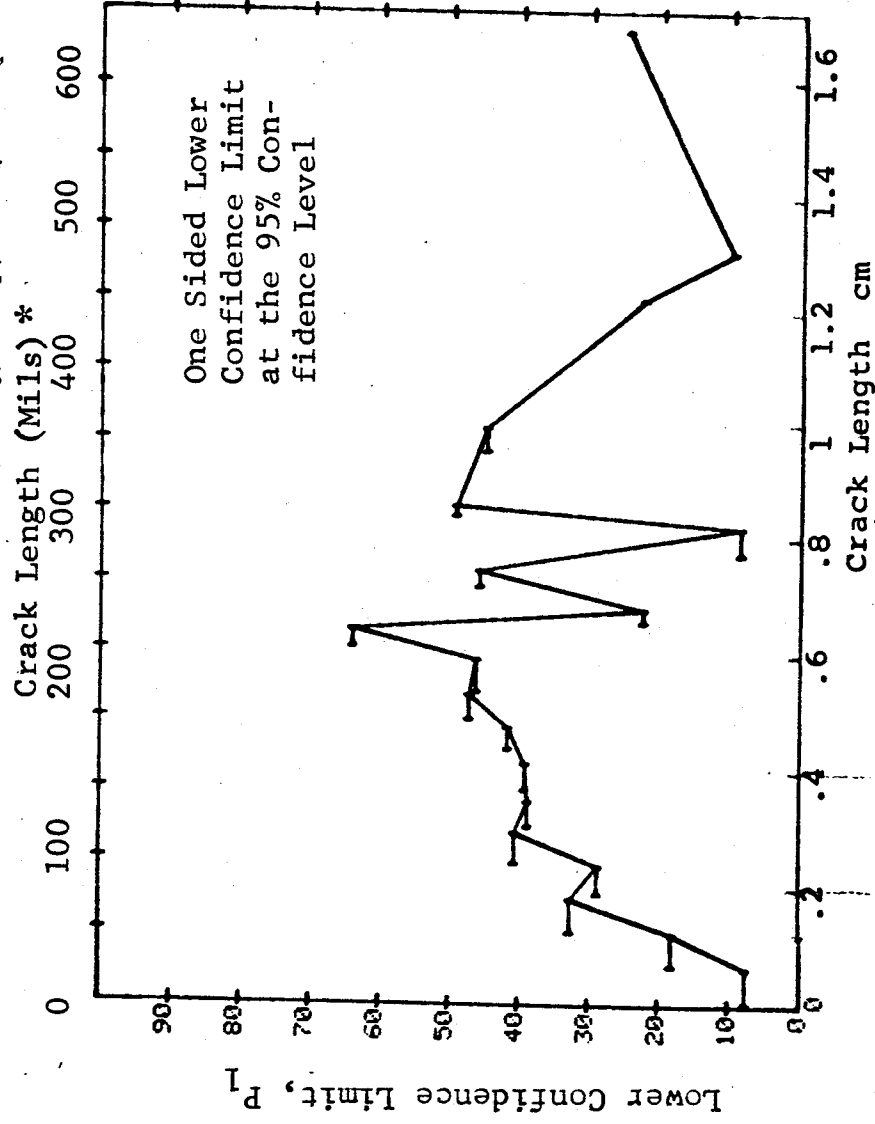


Figure D-59 Probability of Detection for 7178-T651 Al Using Eddy Current. Fatigue Cracks in Fastener Holes Measured by 5 Merged Teams. Field Env.

(b) Optimum Probability Method of Data Cumulation

24-OCT-75					TEST 2 (MERGE)					(59)	
RANGE	MIN	LN	MAX	LN	N	DET	50%	95%	0 MISS	MISS	MISS
1	2	*	26	*	895	82	0	7	0	0	0
2	27		50		517	109	0	18	0	0	0
3	51		74		150	59	0	32	0	0	0
4	51		97		235	91	0	33	0	0	0
5	99		120		64	33	0	40	0	0	0
6	124		142		53	27	0	38	0	0	0
7	124		169		101	52	0	42	0	0	0
8	124		194		122	65	0	45	0	0	0
9	179		218		47	30	0	50	0	0	0
10	179		243		68	44	0	54	0	0	0
11	252		265		19	16	0	64	0	0	0
12	200		280		73	51	0	59	0	0	0
13	252		307		40	30	0	61	0	0	0
14	179		339		118	77	0	57	0	0	0
15	200		353		107	72	0	59	0	0	0
16	0		0		0	0	0	0	0	0	0
17	200		408		116	79	0	60	0	0	0
18	0		0		0	0	0	0	0	0	0
19	0		0		0	0	0	0	0	0	0
20	0		0		0	0	0	0	0	0	0
21	346		500		21	17	0	61	0	0	0
22	0		0		0	0	0	0	0	0	0
23	200		533		122	83	0	60	0	0	0
24	0		0		0	0	0	0	0	0	0
25	0		0		0	0	0	0	0	0	0
26	200		607		123	83	0	59	0	0	0
27	0		0		0	0	0	0	0	0	0
28	0		0		0	0	0	0	0	0	0
29	200		687		127	86	0	60	0	0	0
30	0		0		0	0	0	0	0	0	0
31	0		0		0	0	0	0	0	0	0
32	346		774		35	27	0	62	0	0	0

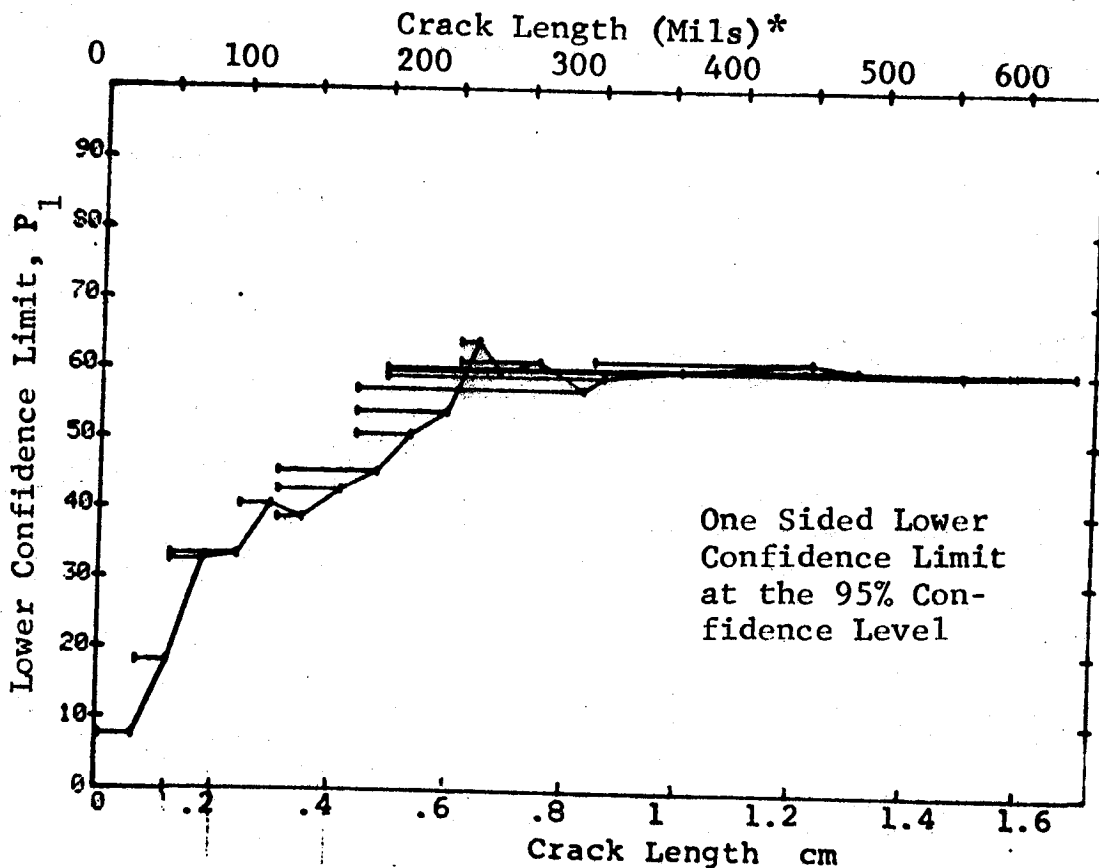


Figure D-59 (Continued)

(c) Overlapping Sixty Point Method of Data Cumulation

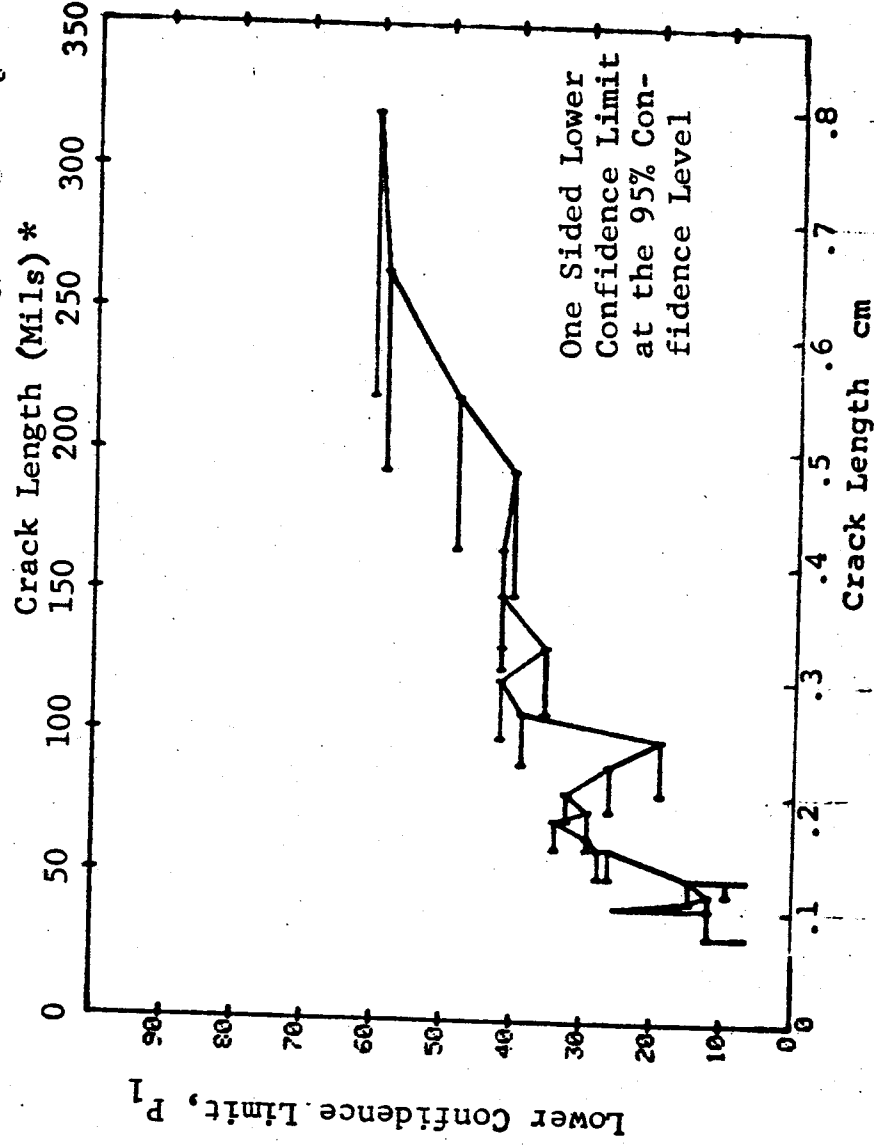
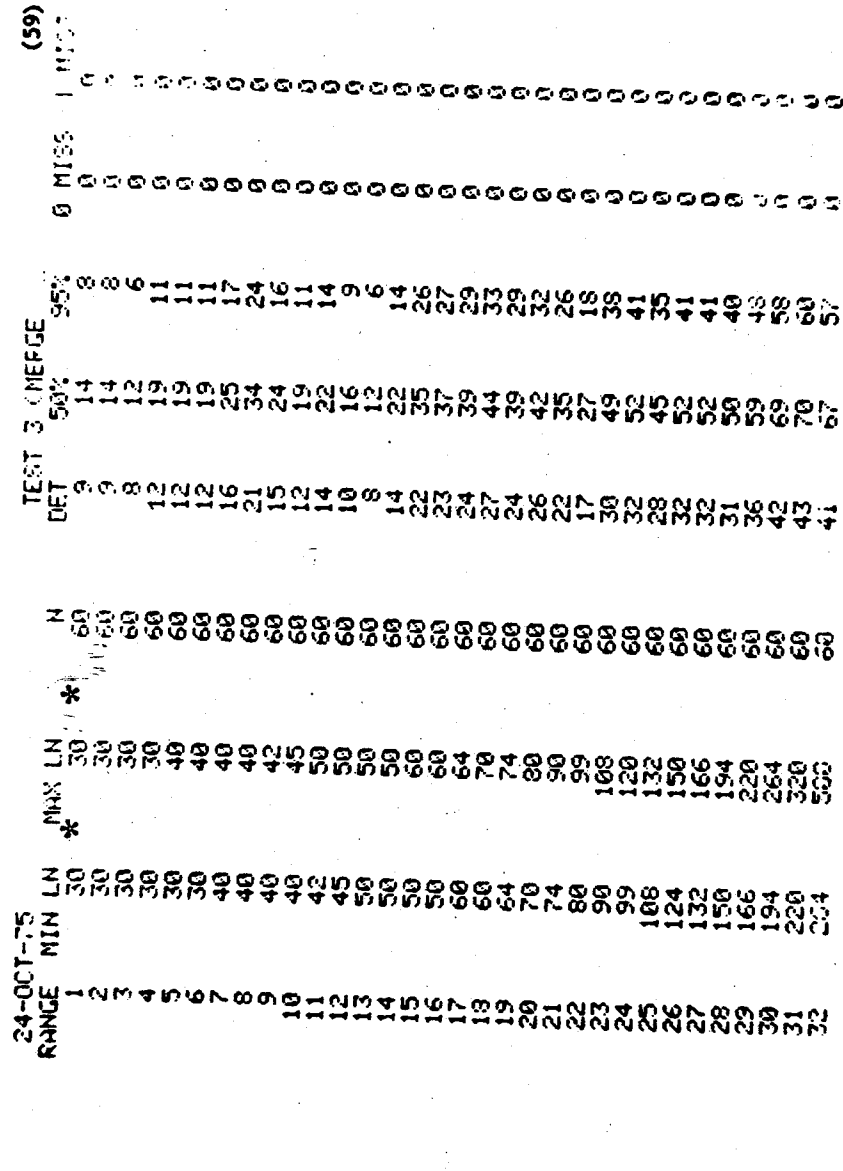


Figure D-59 (Concluded)

(a) Range Interval Method of Data Cumulation

24-OCT-75		PENETRANT		N	TEST 1		(60)	
RANGE	MIN LN	MAX LN	LN		DET	50%	95%	MISS
1	10 *	10 *	0	2	0	0	0	0
2	0	0	0	0	0	0	0	0
3	30	30	0	5	1	12	1	0
4	0	0	0	0	0	0	0	0
5	40	40	0	10	7	64	0	0
6	50	50	0	14	8	53	32	0
7	0	0	0	6	4	0	0	0
8	60	60	0	6	4	57	27	0
9	70	70	0	4	4	84	47	0
10	0	0	0	0	0	0	0	0
11	80	80	0	8	8	91	68	0
12	90	90	0	8	7	79	52	0
13	0	0	0	0	0	0	0	0
14	100	100	0	13	9	64	42	0
15	110	110	0	18	17	90	76	28
16	120	120	0	3	3	79	36	0
17	0	0	0	0	0	0	0	0
18	130	130	0	8	2	20	1	0
19	140	140	0	9	8	82	57	0
20	0	0	0	0	0	0	0	0
21	150	150	0	11	10	85	63	0
22	160	160	0	6	6	89	60	0
23	0	0	0	7	4	50	0	0
24	170	170	0	15	15	55	22	0
25	180	180	0	0	0	0	81	31
26	0	0	0	7	7	90	0	0
27	190	190	0	0	0	0	65	0
28	0	0	0	0	0	0	0	0
29	0	0	0	0	0	0	0	0
30	210	210	0	3	1	29	0	0
31	220	220	0	3	1	20	2	0
32	230	230	0	11	11	93	76	13

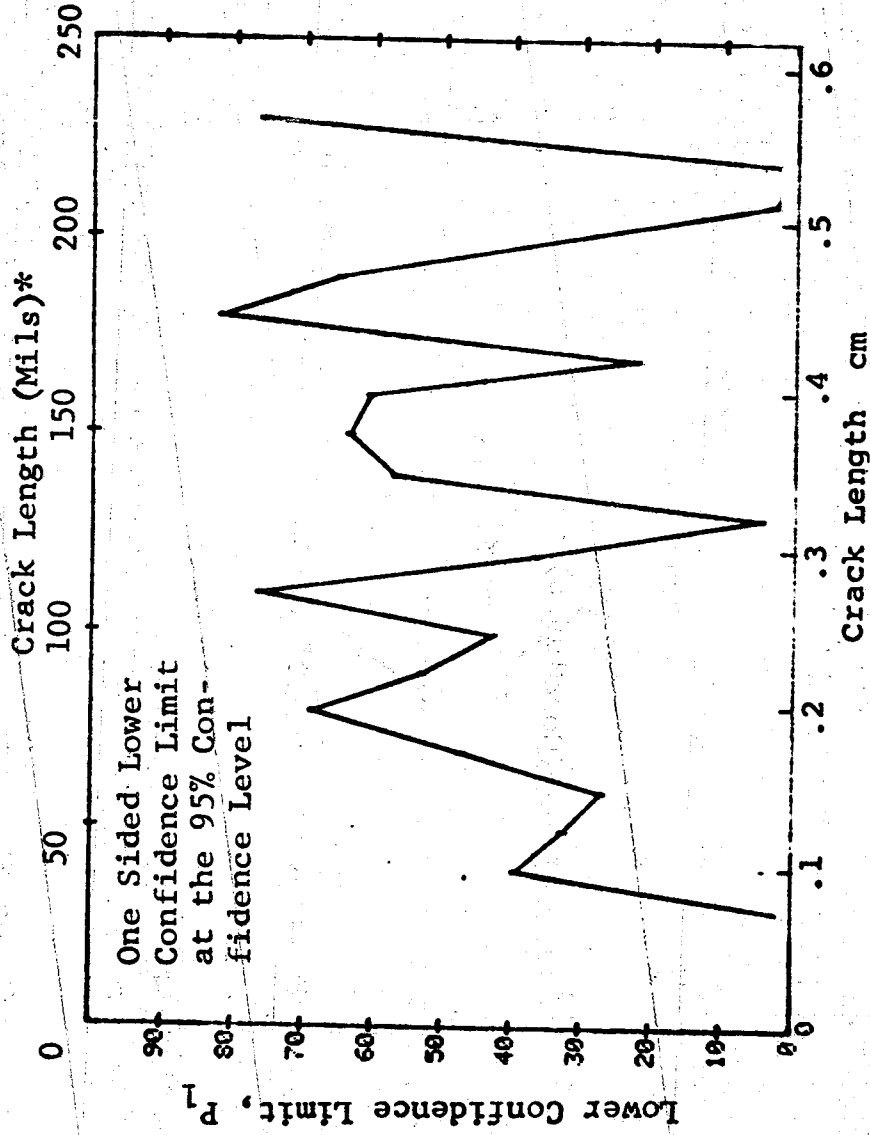


Figure D-60 Probability of Detection for 2024-T6 Al Using Liquid Penetrant. Compressed Notch Flaws in Tandem T Sections. Prod. Env.

(b) Optimum Probability Method of Data Cumulation

24-OCT-75 RANGE	MIN	LN	* MAX	LN	* PENETRANT	N	TEST 2 DET	50% 95%	(60)	0 MISS	1 MISS
1	10	10	10	10	10	2	0	0	0	0	0
2	30	30	30	30	30	0	0	0	0	0	0
3	0	0	0	0	0	5	1	0	1	0	0
4	0	0	0	0	0	0	0	0	0	0	0
5	40	40	40	40	40	10	7	0	0	0	0
6	40	40	40	40	40	24	15	0	39	0	0
7	0	0	0	0	0	0	0	0	43	0	0
8	40	40	40	40	40	30	19	0	46	0	0
9	40	40	40	40	40	34	23	0	52	0	0
10	0	0	0	0	0	0	12	0	0	0	0
11	70	70	70	70	70	12	19	0	77	0	0
12	70	70	70	70	70	20	0	0	78	0	0
13	0	0	0	0	0	0	28	0	70	0	0
14	70	70	70	70	70	33	45	0	78	0	0
15	70	70	70	70	70	51	20	0	79	0	0
16	110	110	110	110	110	21	0	0	0	0	0
17	0	0	0	0	0	0	50	0	70	0	0
18	70	70	70	70	70	62	58	0	72	0	0
19	70	70	70	70	70	71	0	0	0	0	0
20	0	0	0	0	0	0	68	0	74	0	0
21	70	70	70	70	70	82	24	0	77	0	0
22	140	140	140	140	140	26	0	0	0	0	0
23	0	0	0	0	0	0	78	0	74	0	0
24	70	70	70	70	70	95	15	0	81	0	0
25	180	180	180	180	180	15	0	0	0	0	0
26	0	0	0	0	0	0	22	0	87	0	0
27	180	180	180	180	180	22	0	0	0	0	0
28	0	0	0	0	0	0	0	0	0	0	0
29	0	0	0	0	0	0	23	0	0	0	0
30	180	180	180	180	180	24	52	0	81	0	0
31	140	140	140	140	140	50	35	0	77	0	0
32	180	180	180	180	180	38	0	0	80	38	51

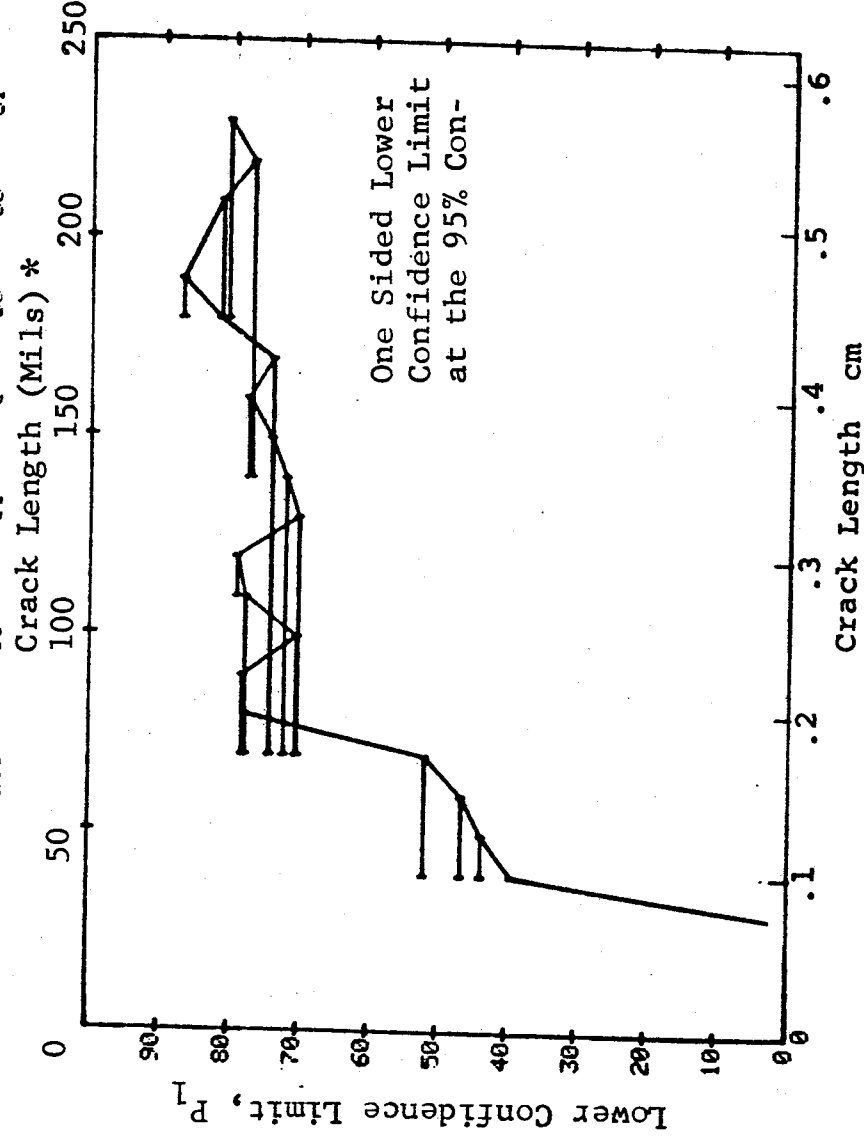


Figure D-60 (Continued)

(c) Overlapping Sixty Point Method of Data Cumulation

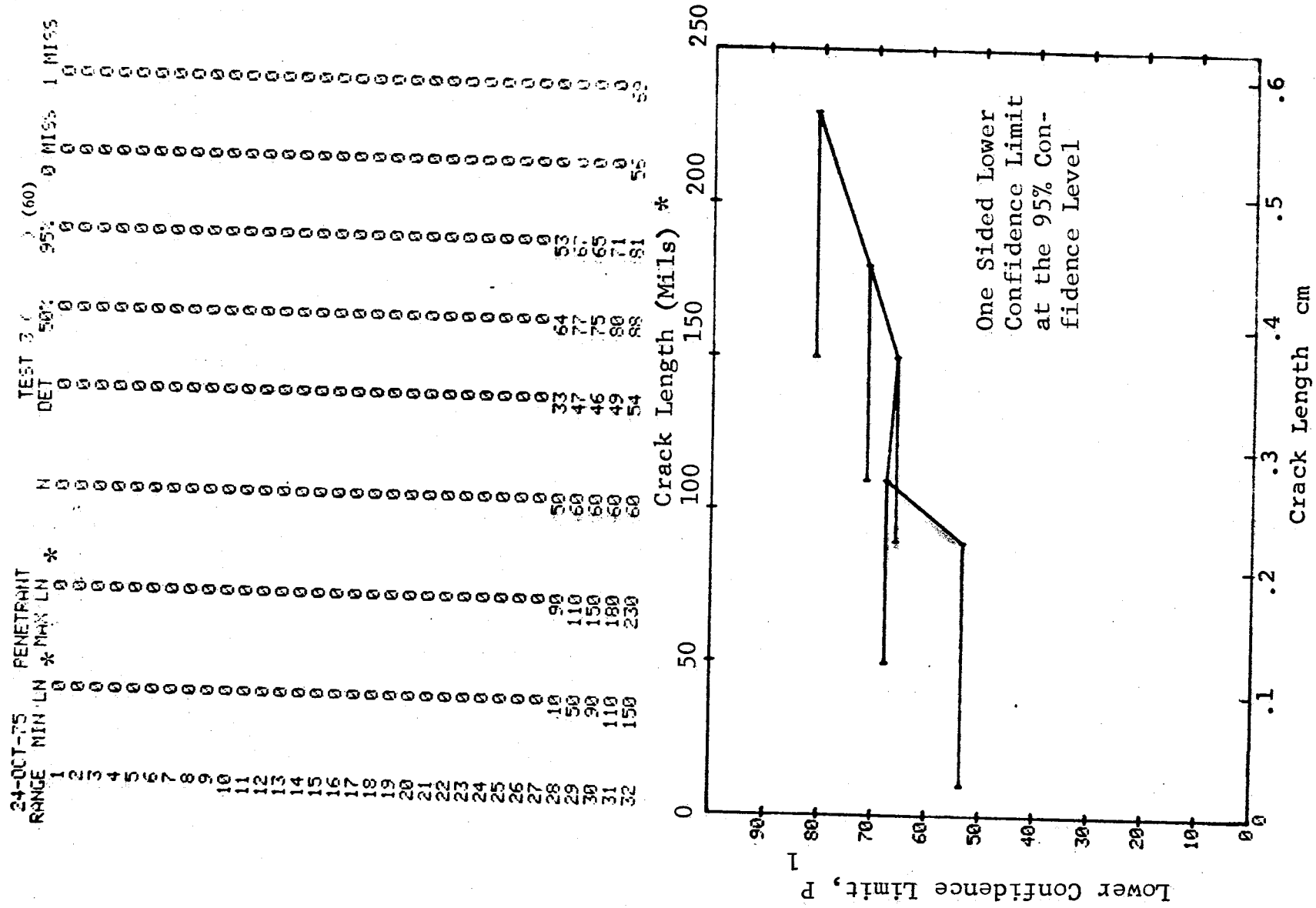


Figure D-60 (Concluded)

(a) Range Interval Method of Data Cumulation

24-OCT-75		PENETRAINT		N	TEST 1		(61)		0 MISS	1 MISS
RANGE	MIN LN	MAX LN			DET	50%	95%			
1	40	40	*	4	0	0	0	0	0	0
2	70	70	*	3	1	20	1	0	0	0
3	0	0		0	0	0	0	0	0	0
4	100	110		18	14	74	56	0	0	0
5	130	130		6	4	57	27	0	0	0
6	0	0		0	0	0	0	0	0	0
7	0	0		0	0	0	0	0	0	0
8	190	190		1	1	50	5	0	0	0
9	210	210		3	1	20	1	0	0	0
10	230	230		3	2	50	13	0	0	0
11	0	0		0	0	0	0	0	0	0
12	250	250		6	4	57	27	0	0	0
13	270	270		1	1	50	5	0	0	0
14	300	300		3	3	79	36	0	0	0
15	310	310		4	4	84	47	0	0	0
16	0	0		0	0	0	0	0	0	0
17	350	350		3	3	79	36	0	0	0
18	380	380		3	3	79	36	0	0	0
19	0	0		0	0	0	0	0	0	0
20	410	410		1	1	50	5	0	0	0
21	0	0		0	0	0	0	0	0	0
22	450	450		3	3	79	36	0	0	0
23	460	460		1	1	50	5	0	0	0
24	480	480		3	3	79	36	0	0	0
25	0	0		0	0	0	0	0	0	0
26	0	0		0	0	0	0	0	0	0
27	0	0		0	0	0	0	0	0	0
28	0	0		0	0	0	0	0	0	0
29	0	0		0	0	0	0	0	0	0
30	0	0		0	0	0	0	0	0	0
31	0	0		0	0	0	0	0	0	0
32	650	650		3	3	79	36	0	0	0

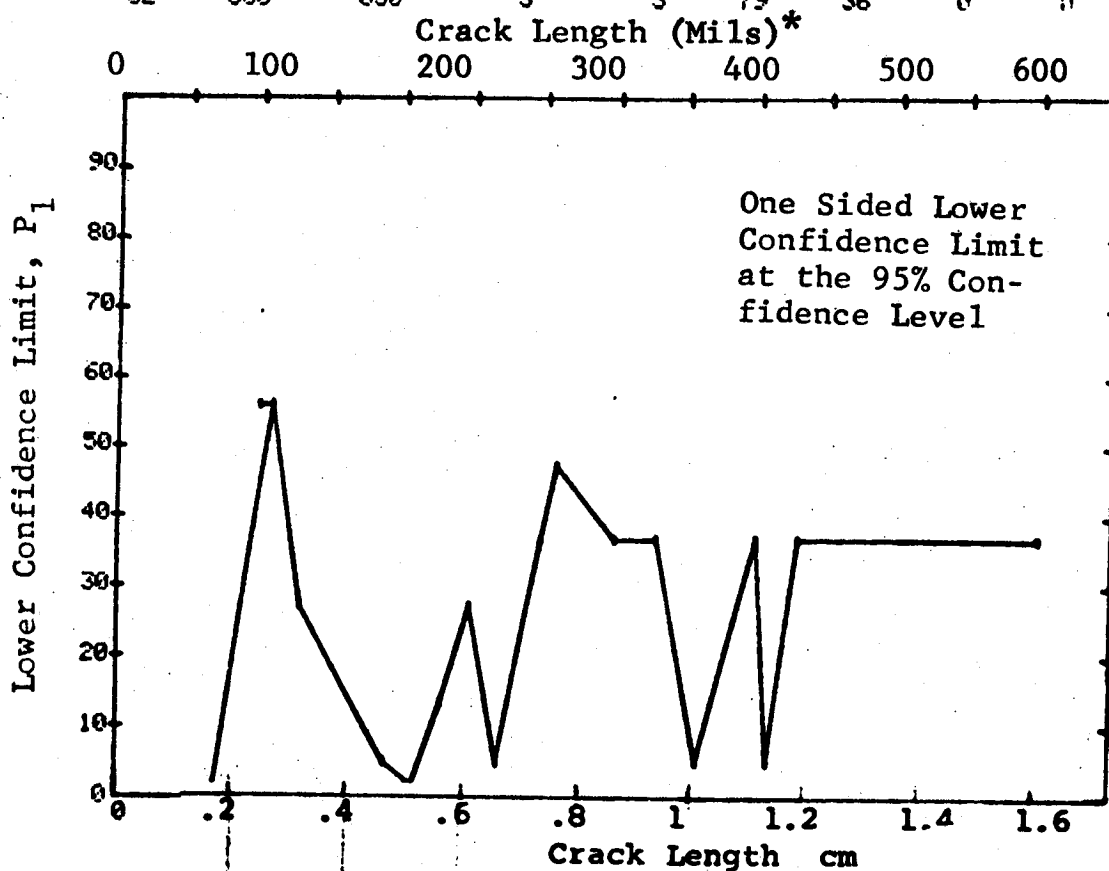


Figure D-61 Probability of Detection for 4340M Steel Using Liquid Penetrant. Compressed Notch Flaws in Solid Threaded Cylinder. Prod. Env.

(b) Optimum Probability Method of Data Cumulation

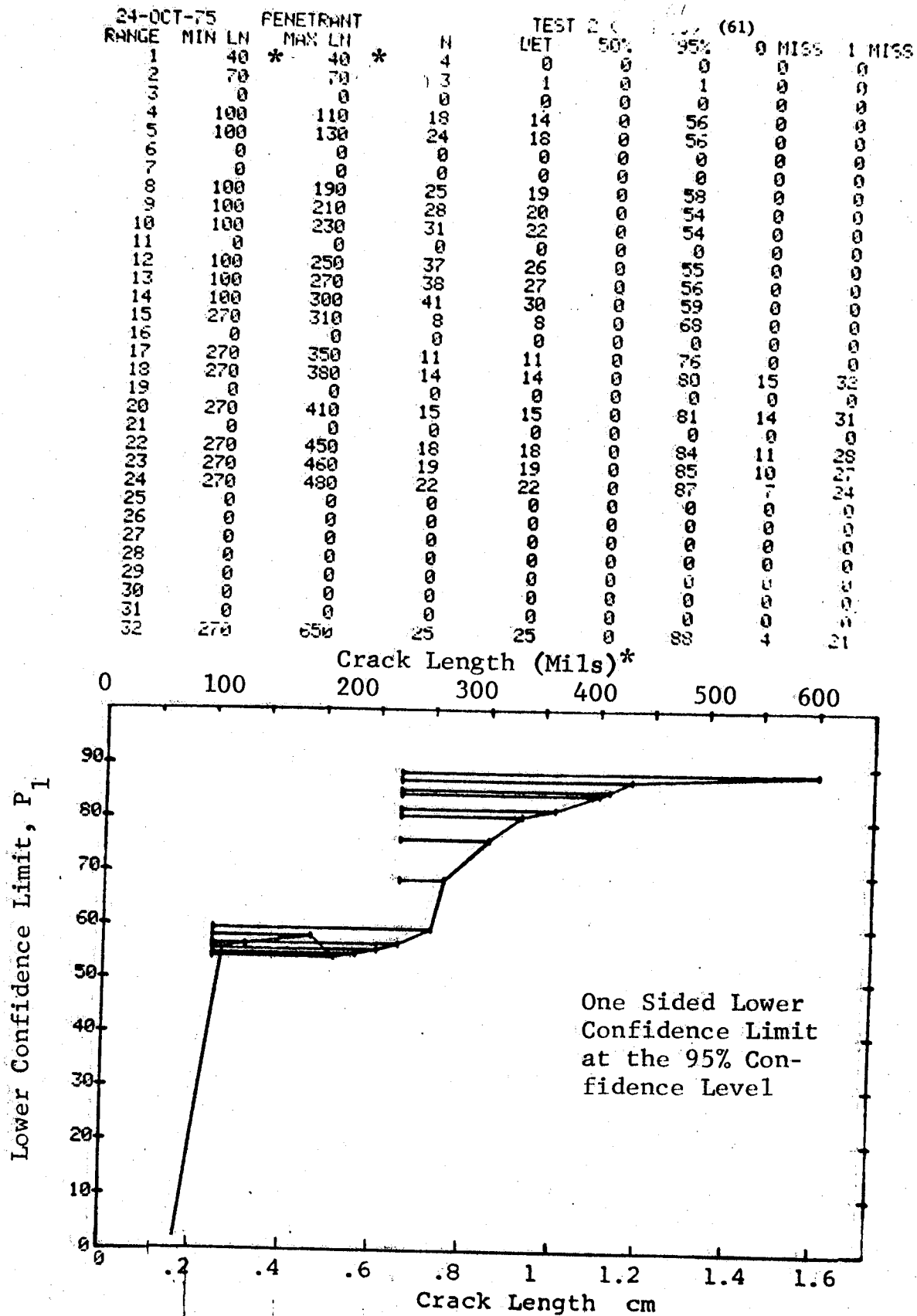


Figure D-61 (Continued)

(c) Overlapping Sixty Point Method of Data Cumulation

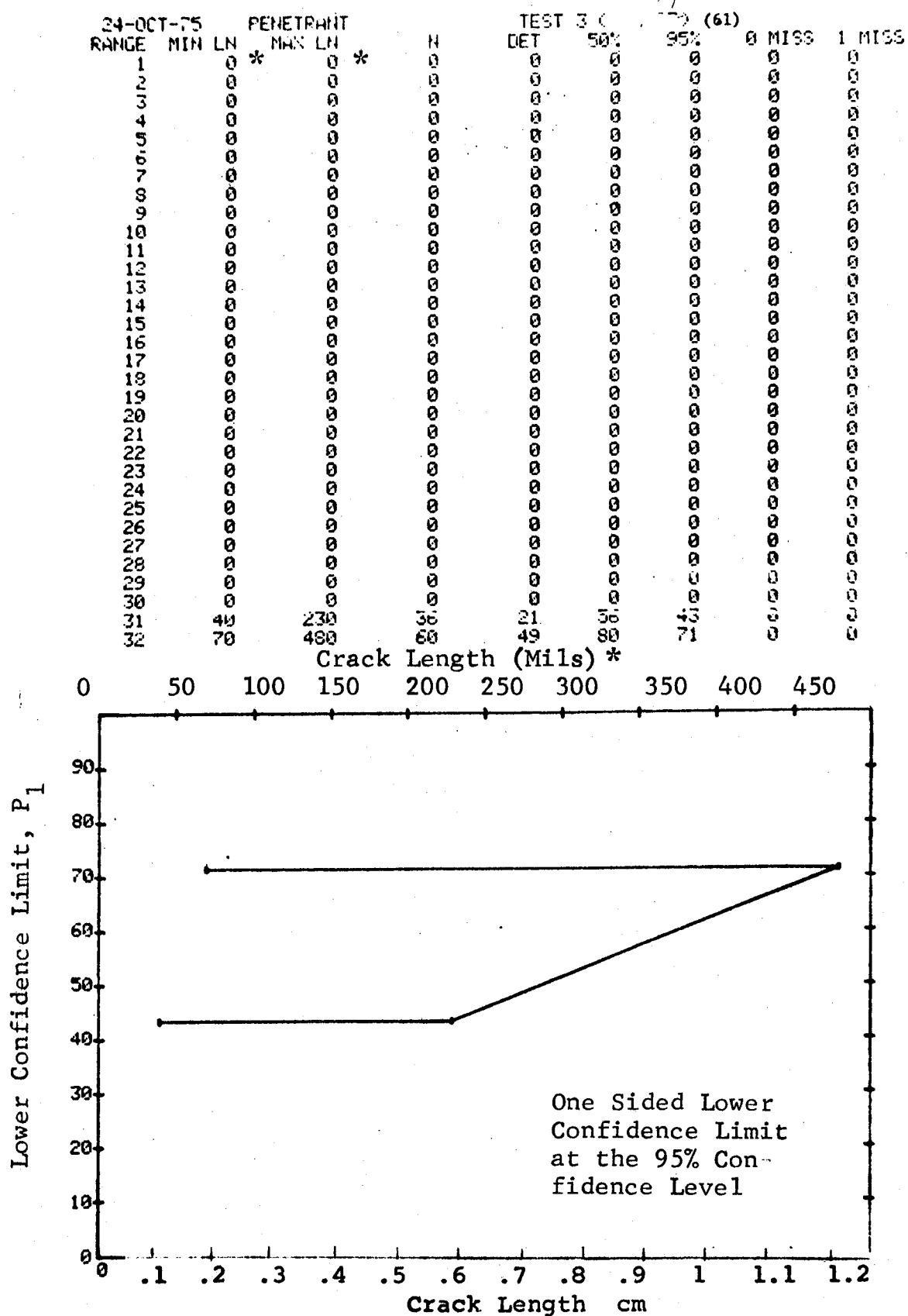


Figure D-61 (Concluded)

(a) Range Interval Method of Data Cumulation

24-OCT-75	PENETRANT		TEST 1		(62)			
RANGE	MIN LN	* MAX LN *	DET	50%	95%	0 MISS	1 MISS	
1	80	90	2	20	4	0	0	
2	0	0	0	0	0	0	0	
3	110	110	0	0	0	0	0	
4	120	120	0	0	0	0	0	
5	130	130	1	20	1	0	0	
6	140	140	0	0	0	0	0	
7	160	160	3	42	15	0	0	
8	0	0	1	20	1	0	0	
9	0	0	0	0	0	0	0	
10	0	0	0	0	0	0	0	
11	0	0	0	0	0	0	0	
12	0	0	0	0	0	0	0	
13	0	0	0	0	0	0	0	
14	0	0	0	0	0	0	0	
15	250	250	0	0	0	0	0	
16	270	270	1	29	2	0	0	
17	280	280	3	50	18	0	0	
18	0	0	1	29	2	0	0	
19	300	300	0	0	0	0	0	
20	310	310	2	50	13	0	0	
21	0	0	2	50	13	0	0	
22	0	0	0	0	0	0	0	
23	0	0	0	0	0	0	0	
24	0	0	0	0	0	0	0	
25	0	0	0	0	0	0	0	
26	0	0	0	0	0	0	0	
27	0	0	0	0	0	0	0	
28	0	0	0	0	0	0	0	
29	0	0	0	0	0	0	0	
30	0	0	0	0	0	0	0	
31	440	440	1	20	1	0	0	
32	450	460	3	50	18	0	0	

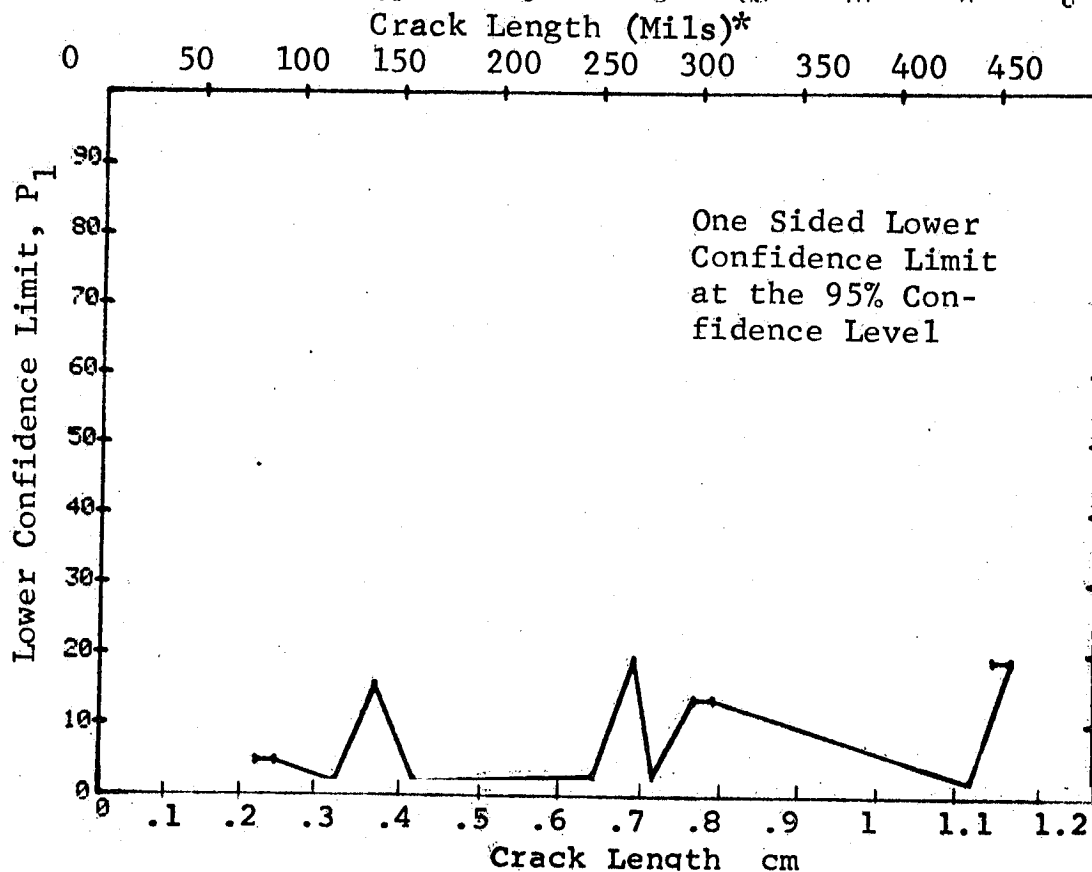


Figure D-62 Probability of Detection for 4340M Steel Using Liquid Penetrant. Compressed Notch Flaws in Hollow Cylinder. Prod. Env.

(b) Optimum Probability Method of Data Cumulation

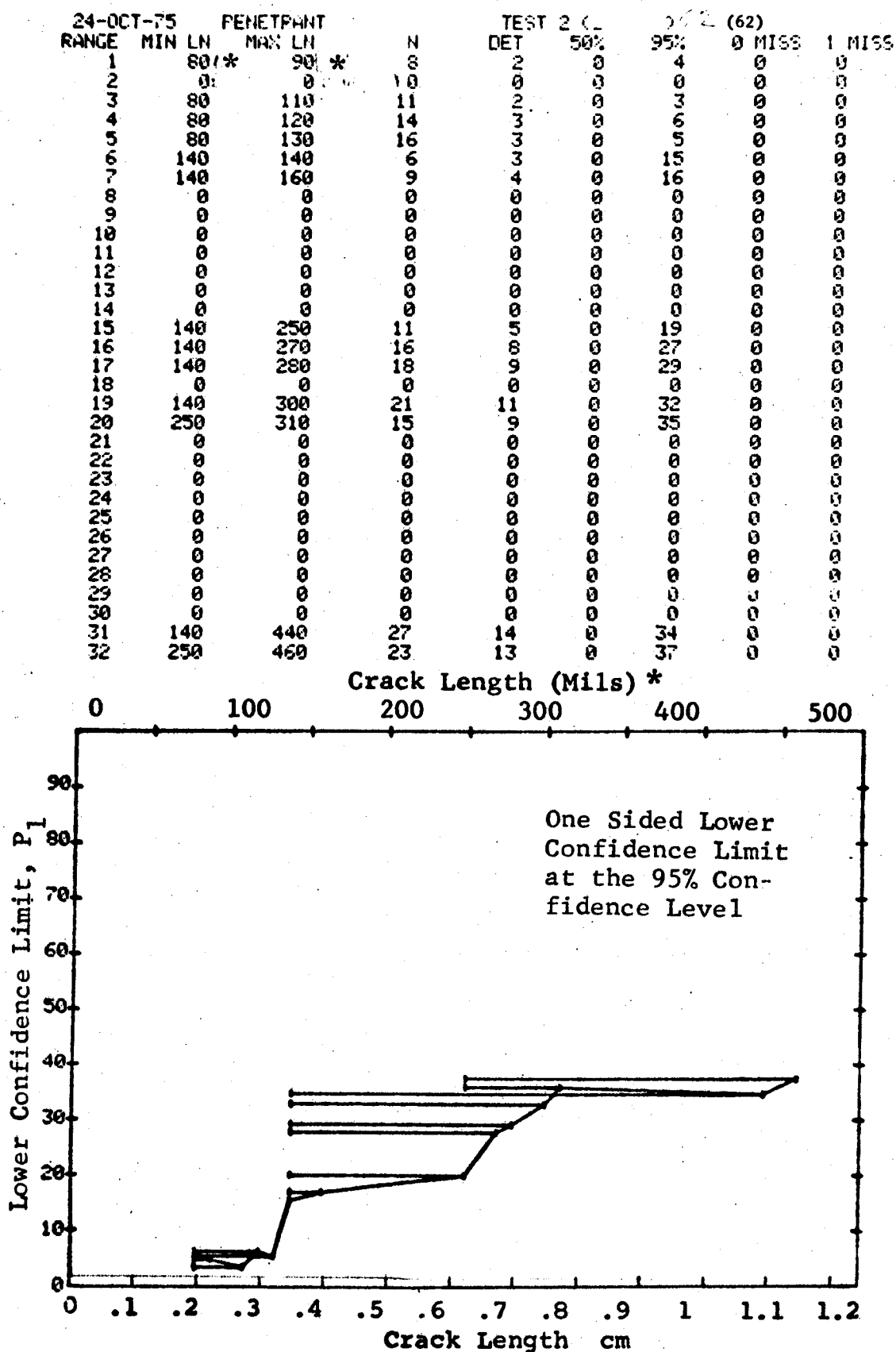


Figure D-62 (Continued)

(c) Overlapping Sixty Point Method of Data Cumulation

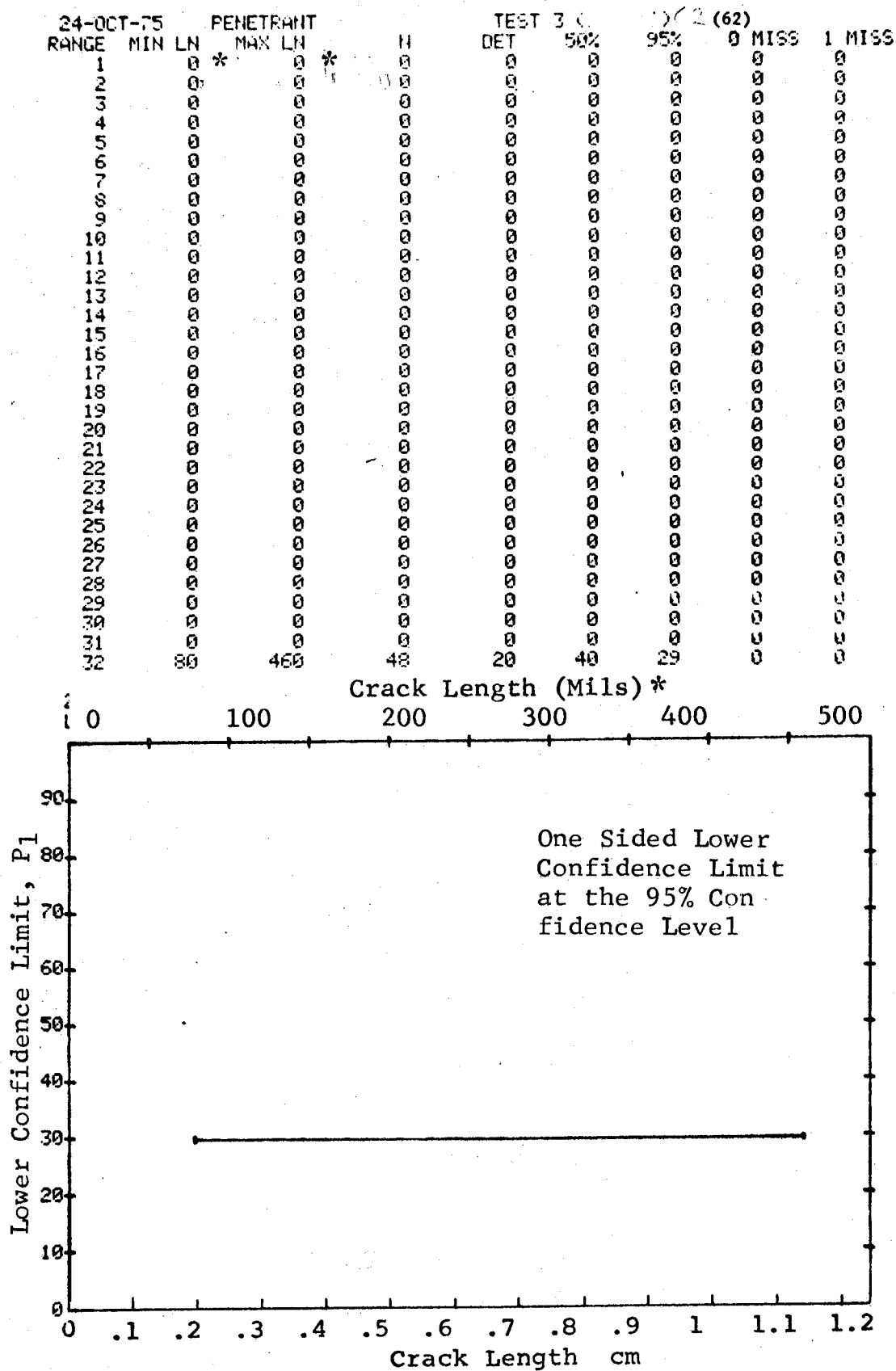


Figure D-62 (Concluded)

(a) Range Interval Method of Data Cumulation

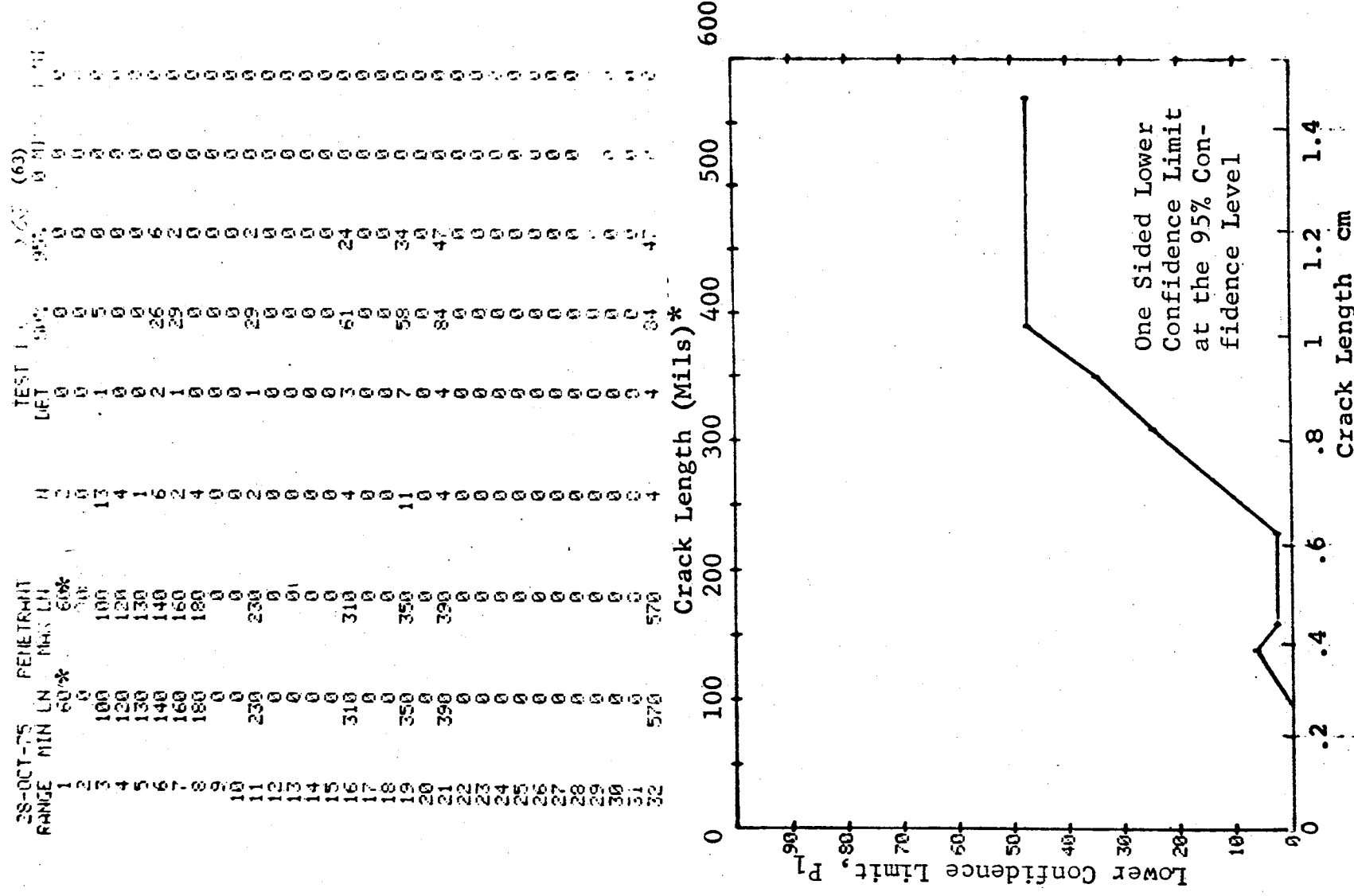


Figure D-63 Probability of Detection for 4340M Steel Using Liquid Penetrant. Compressed Notch Flaws in Filleted Hollow Cylinder. Prod. Env.

D-195

(b) Optimum Probability Method of Data Cumulation

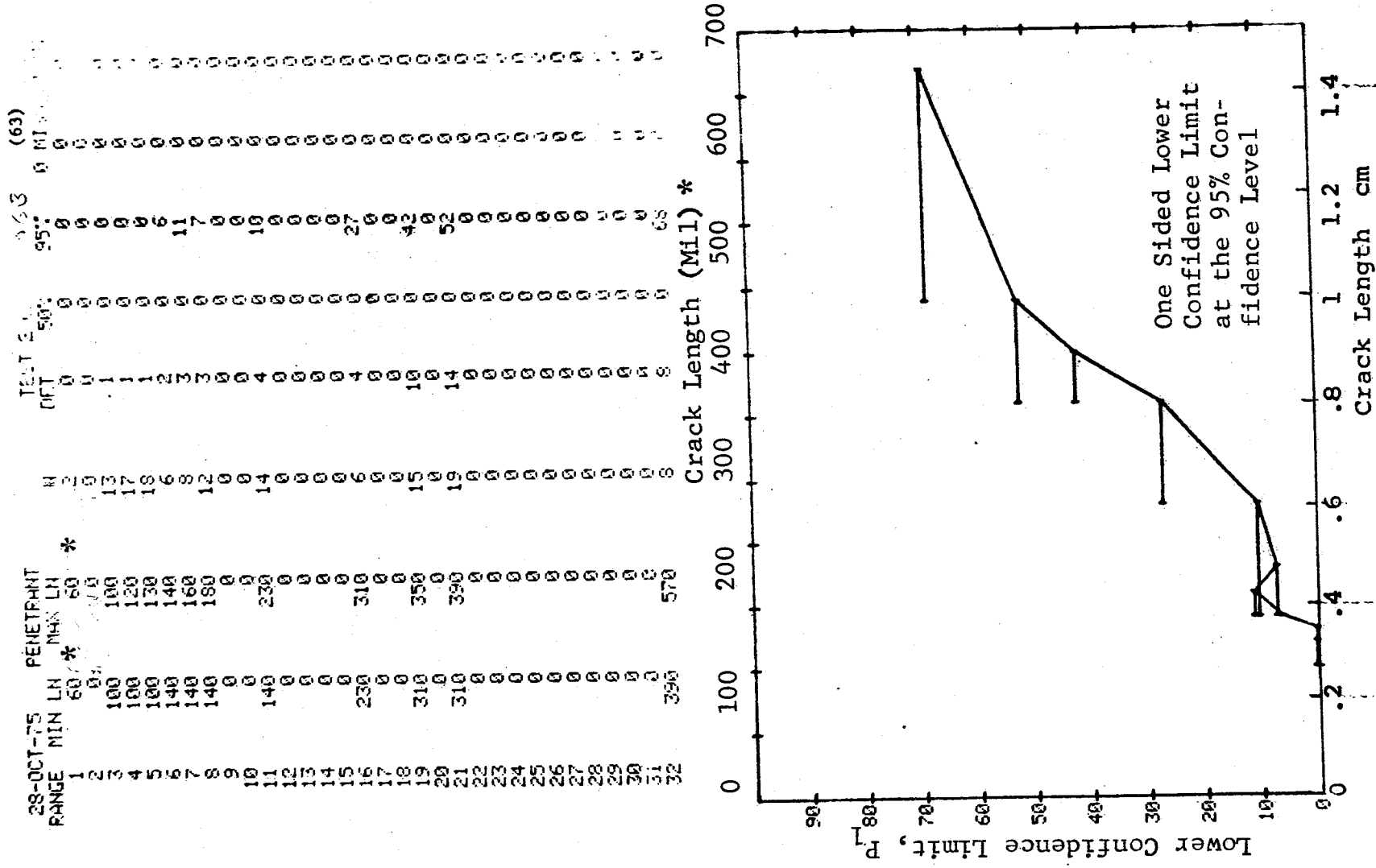


Figure D-63 (Continued)

(c) Overlapping Sixty Point Method of Data Cumulation

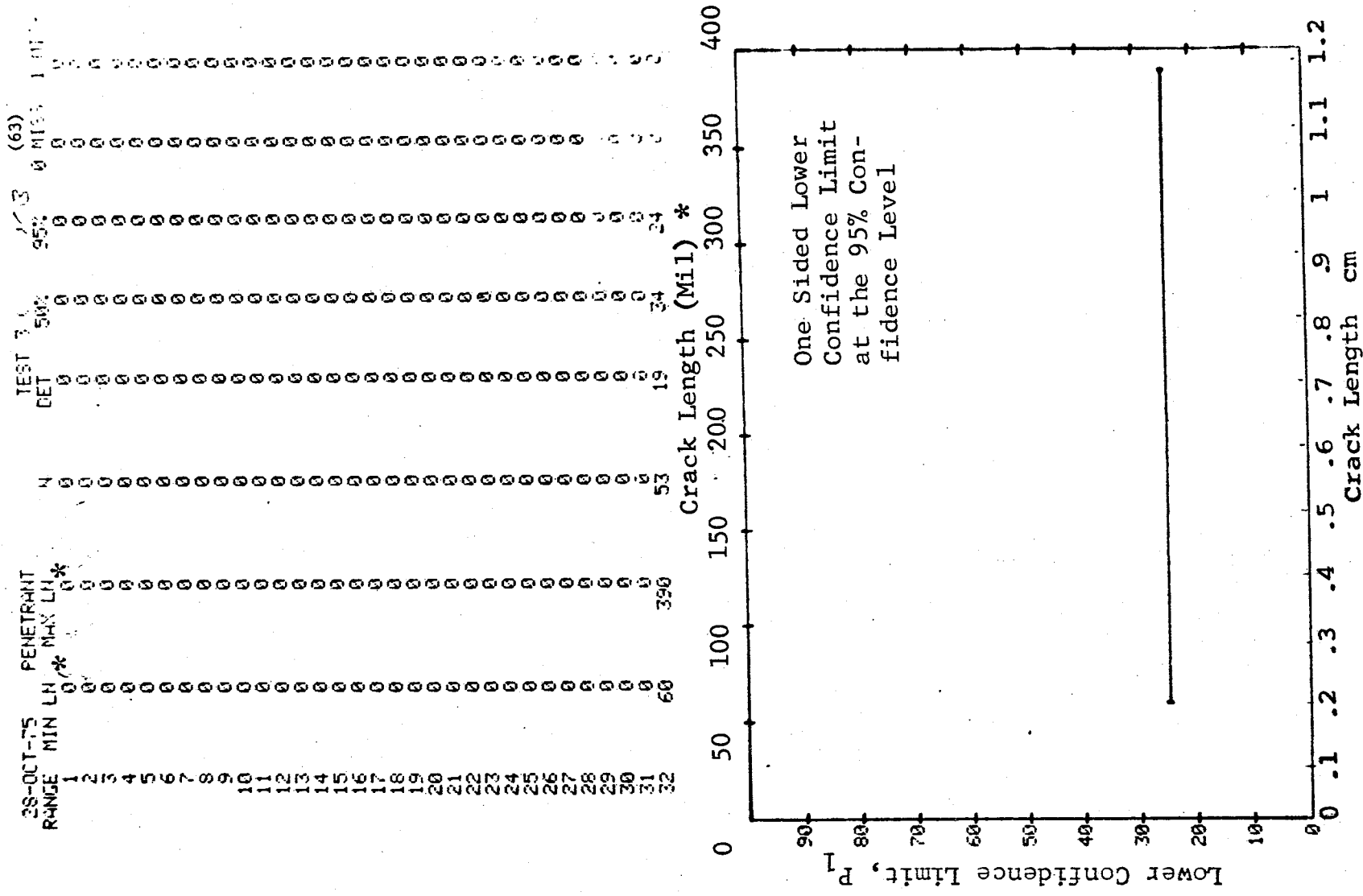


Figure D-63 (Concluded)

(a) Range Interval Method of Data Cumulation

24-OCT-75		PENETRANT		N	TEST 1		(64)		0 MICS	1 MISS
RANGE	MIN LN	* MAX LN	*		DET	50%	95%			
1	20	40	*	16	2	10	2	0	0	0
2	50	64		30	15	48	33	0	0	0
3	70	70		16	13	77	58	0	0	0
4	90	110		24	21	84	70	0	0	0
5	120	130		19	15	81	64	0	0	0
6	140	150		44	40	89	80	45	59	0
7	160	160		12	11	86	66	0	0	0
8	200	200		3	3	79	36	0	0	0
9	0	0		0	0	0	0	0	0	0
10	0	0		0	0	0	0	0	0	0
11	260	260		1	1	50	5	0	0	0
12	0	0		0	0	0	0	0	0	0
13	300	300		3	3	79	36	0	0	0
14	0	0		0	0	0	0	0	0	0
15	0	0		0	0	0	0	0	0	0
16	370	380		5	5	87	54	0	0	0
17	0	0		0	0	0	0	0	0	0
18	0	0		0	0	0	0	0	0	0
19	0	0		0	0	0	0	0	0	0
20	0	0		0	0	0	0	0	0	0
21	0	0		0	0	0	0	0	0	0
22	0	0		0	0	0	0	0	0	0
23	0	0		0	0	0	0	0	0	0
24	0	0		0	0	0	0	0	0	0
25	0	0		0	0	0	0	0	0	0
26	0	0		0	0	0	0	0	0	0
27	0	0		0	0	0	0	0	0	0
28	0	0		0	0	0	0	0	0	0
29	0	0		0	0	0	0	0	0	0
30	0	0		0	0	0	0	0	0	0
31	0	0		0	0	0	0	0	0	0
32	750	750		2	2	70	22	0	0	0

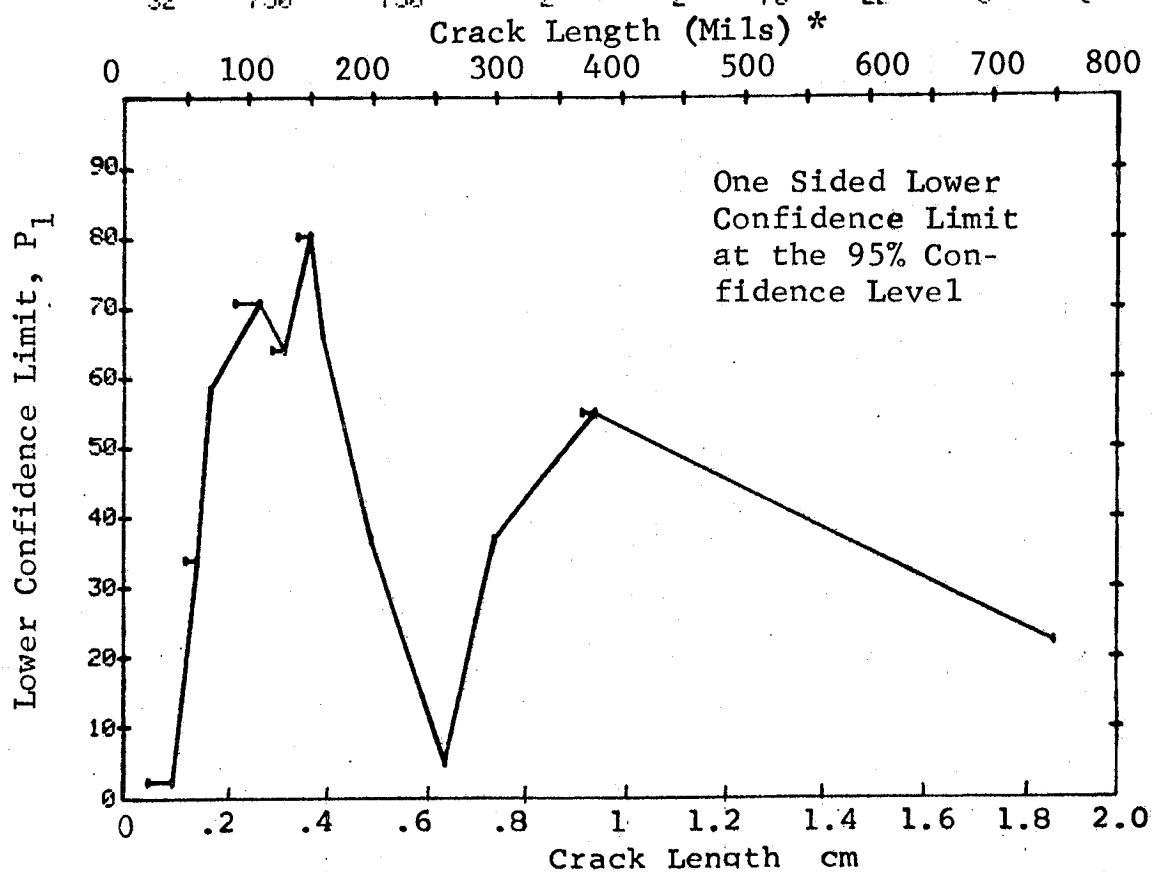


Figure D-64 Probability of Detection for 4340M Steel Using Liquid Penetrant. Compressed Notch Flaws in Solid Cylinder. Prod. Env.

(b) Optimum Probability Method of Data Cumulation

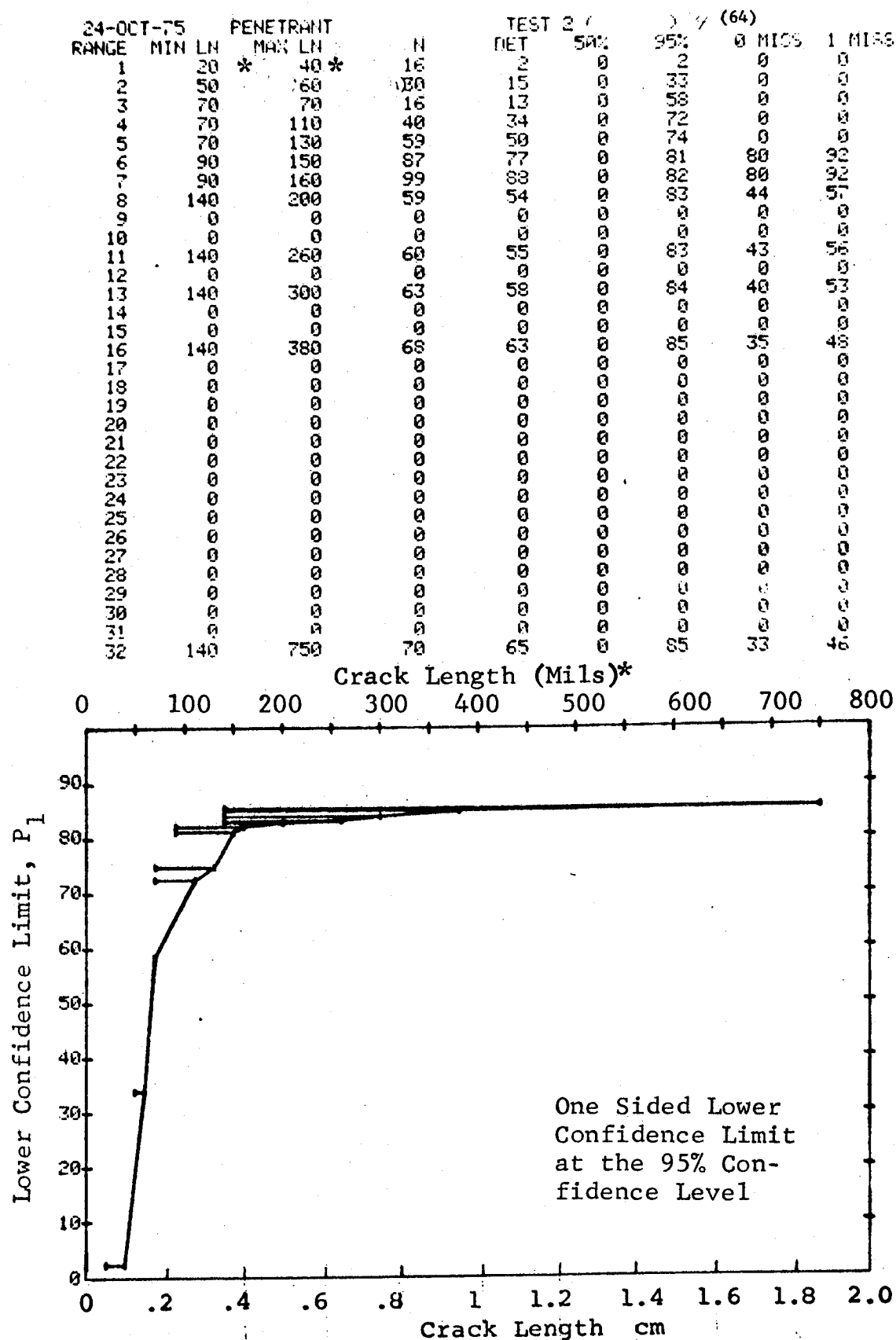


Figure D-64 (Continued)

(c) Overlapping Sixty Point Method of Data Cumulation

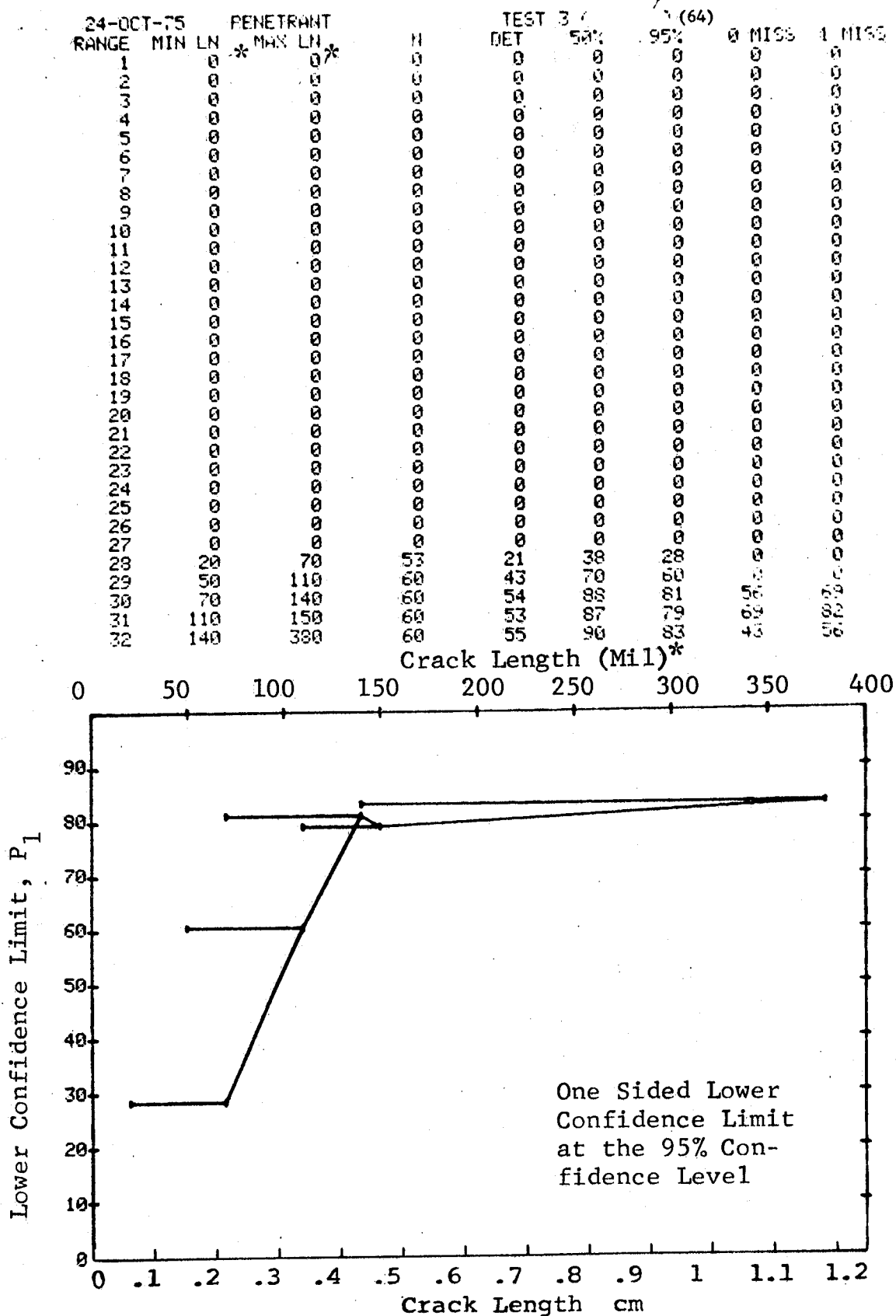


Figure D-64 (Concluded)

(a) Range Interval Method of Data Cumulation

24-OCT-75	PENETRANT		TEST 1		> 95%		(65)	1 MISS
RANGE	MIN	LN	DET	50%	95%	95%	0 MISS	1 MISS
1	10	10	1	10	0	0	0	0
2	10	10	0	0	0	0	0	0
3	30	30	3	79	36	0	0	0
4	0	0	0	0	0	0	0	0
5	40	40	11	93	76	0	18	35
6	50	50	32	92	92	0	27	42
7	0	0	0	0	0	0	17	34
8	60	60	12	94	77	0	0	0
9	70	70	2	70	22	0	0	0
10	0	0	0	0	0	0	0	0
11	80	80	9	92	71	0	0	0
12	90	90	14	95	80	0	15	32
13	0	0	0	0	0	0	0	0
14	100	100	1	50	57	0	7	24
15	110	110	22	96	22	0	0	0
16	120	120	0	70	22	0	0	0
17	0	0	0	0	0	0	0	0
18	130	130	5	55	28	0	0	0
19	140	140	7	90	65	0	0	0
20	0	0	0	0	0	0	0	0
21	150	150	18	96	84	0	11	28
22	160	160	2	70	22	0	0	0
23	0	0	0	0	0	0	0	0
24	170	170	11	93	76	0	18	35
25	180	180	11	93	76	0	18	35
26	0	0	0	0	0	0	0	0
27	190	190	1	50	5	0	0	0
28	0	0	0	0	0	0	0	0
29	0	0	0	0	0	0	0	0
30	210	210	3	79	36	0	0	0
31	220	220	2	70	22	0	0	0
32	230	230	0	91	68	0	0	0

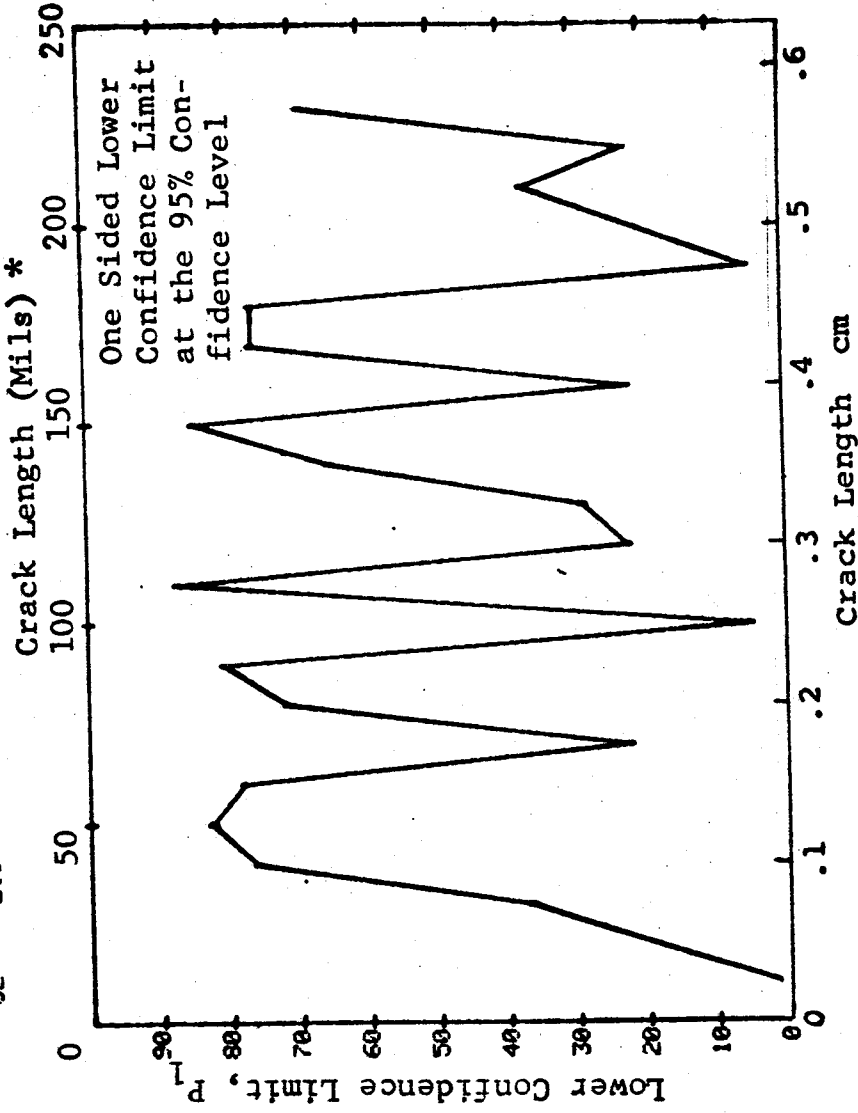


Figure D-65 Probability of Detection for 2024-T6 Al Using Liquid Penetrant. Compressed Notch Flaws in Tandem T Specimen. Lab. Env.

(b) Optimum Probability Method of Data Cumulation

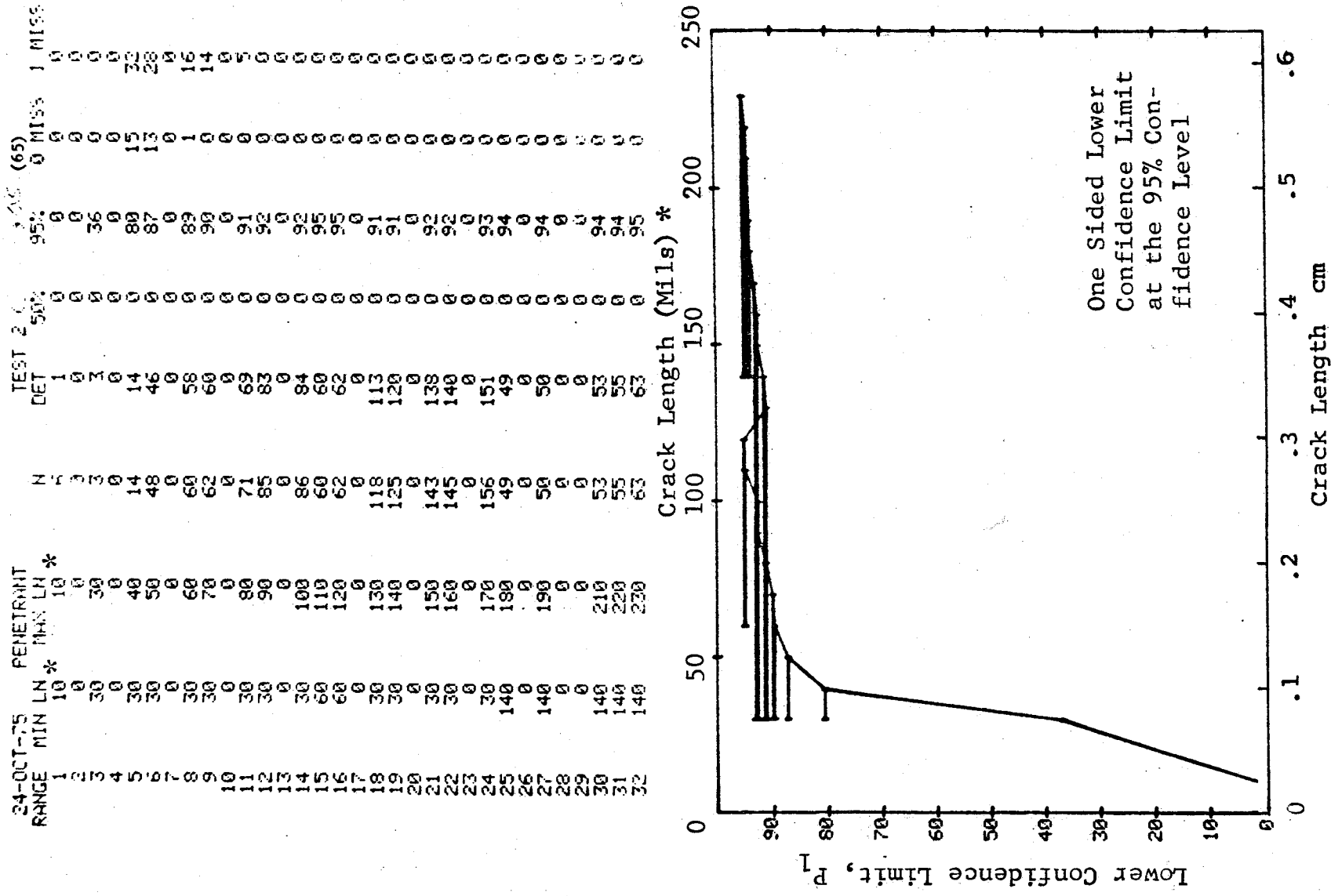


Figure D-65 (Continued)

(c) Overlapping Sixty Point Method of Data Cumulation

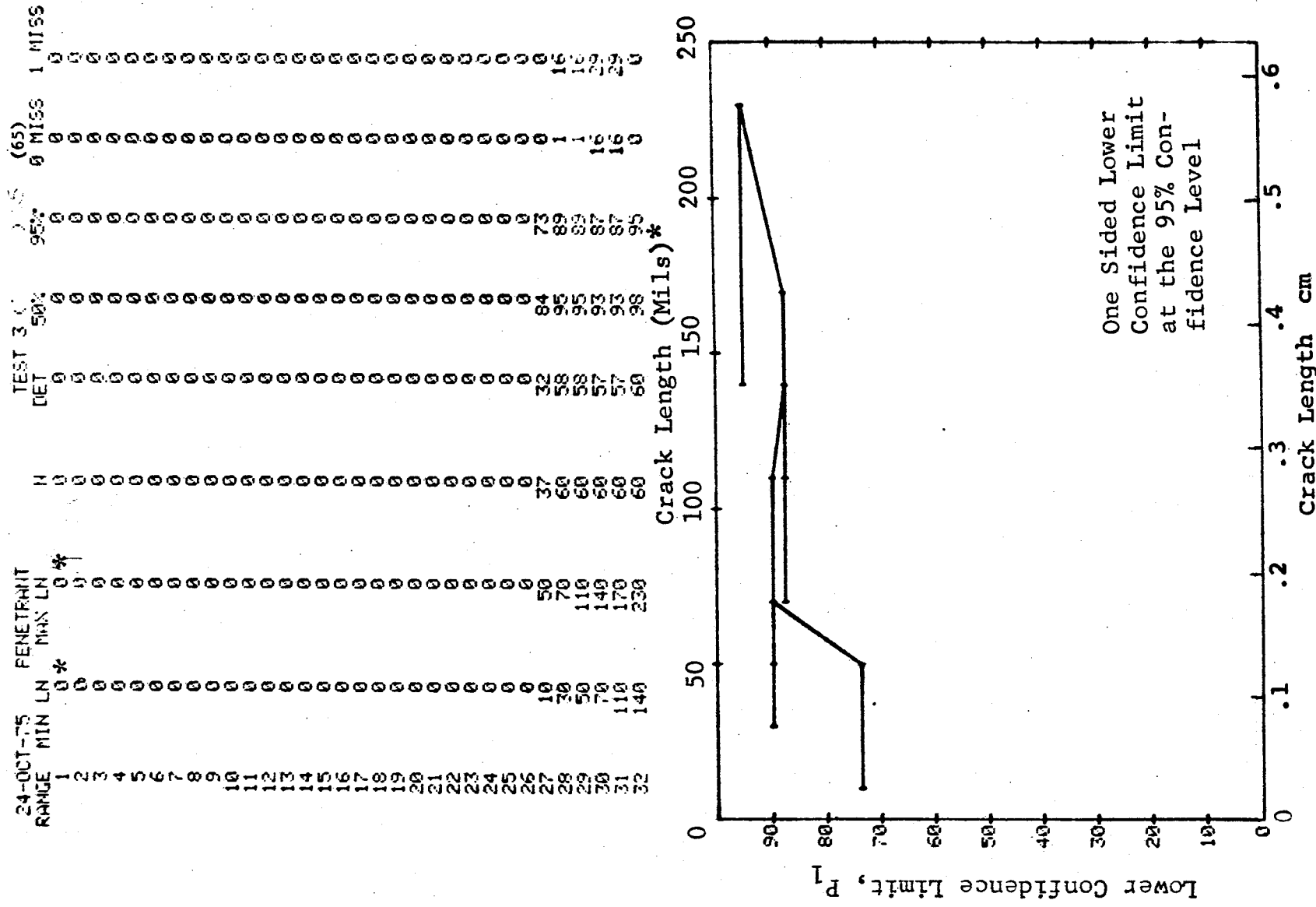


Figure D-65 (Concluded)

(a) Range Interval Method of Data Cumulation

27-OCT-75		PENETRANT		N	TEST 1		TEST 2 (66)		0 MISS	1 MISS
RANGE	MIN LN	* MAX LN *			DET	50%	95%			
1	40	40		4	4	84	47	0	0	0
2	70	70		4	4	84	47	0	0	0
3	0	0		0	0	0	0	0	0	0
4	100	110		29	25	84	71	0	0	0
5	130	130		16	16	95	82	13	30	0
6	0	0		0	0	0	0	0	0	0
7	0	0		0	0	0	0	0	0	0
8	190	190		4	4	84	47	0	0	0
9	210	210		4	4	84	47	0	0	0
10	230	230		5	5	87	54	0	0	0
11	0	0		0	0	0	0	0	0	0
12	250	250		5	5	87	54	0	0	0
13	270	270		4	4	84	47	0	0	0
14	300	300		4	4	84	47	0	0	0
15	310	310		4	4	84	47	0	0	0
16	340	340		4	4	84	47	0	0	0
17	350	350		4	4	84	47	0	0	0
18	380	380		4	4	84	47	0	0	0
19	0	0		0	0	0	0	0	0	0
20	410	410		4	4	84	47	0	0	0
21	0	0		0	0	0	0	0	0	0
22	450	450		5	5	87	54	0	0	0
23	460	460		4	4	84	47	0	0	0
24	480	480		4	4	84	47	0	0	0
25	0	0		0	0	0	0	0	0	0
26	0	0		0	0	0	0	0	0	0
27	0	0		0	0	0	0	0	0	0
28	0	0		0	0	0	0	0	0	0
29	0	0		0	0	0	0	0	0	0
30	0	0		0	0	0	0	0	0	0
31	0	0		0	0	0	0	0	0	0
32	650	650		4	4	84	47	0	0	0

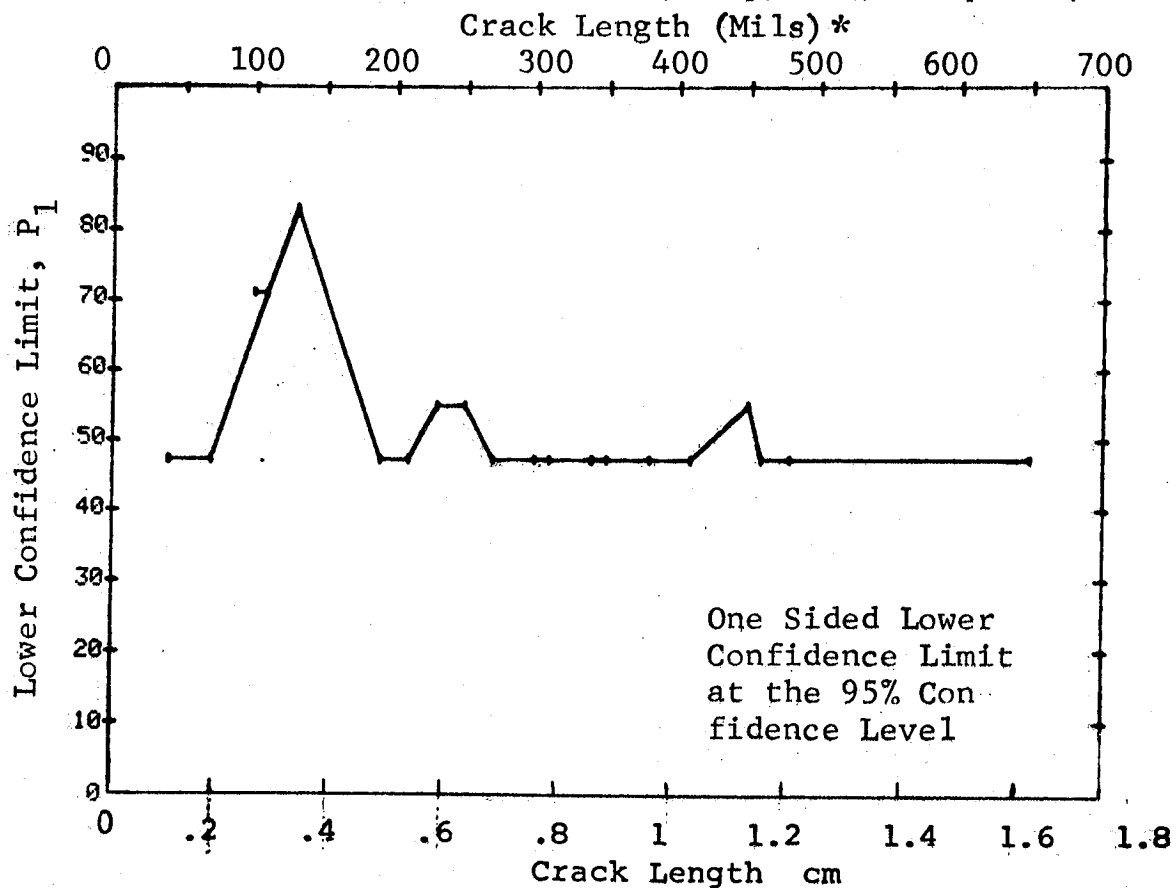


Figure D-66 Probability of Detection for 4340M Steel Using Liquid Penetrant. Compressed Notch Flaws in Solid Cylinder. Lab. Env.

(b) Optimum Probability Method of Data Cumulation

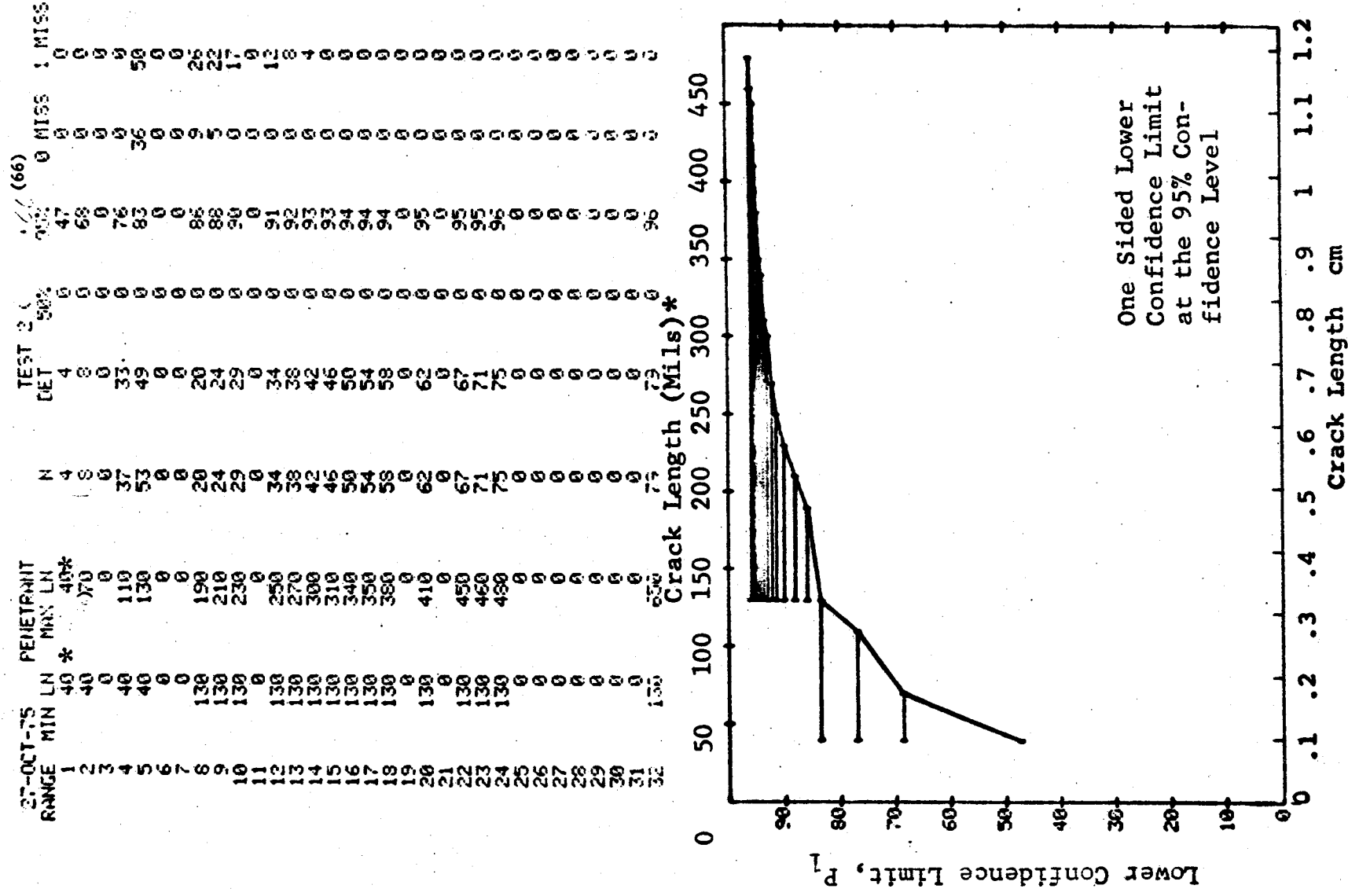


Figure D-66 (Continued)

(c) Overlapping Sixty Point Method of Data Cumulation

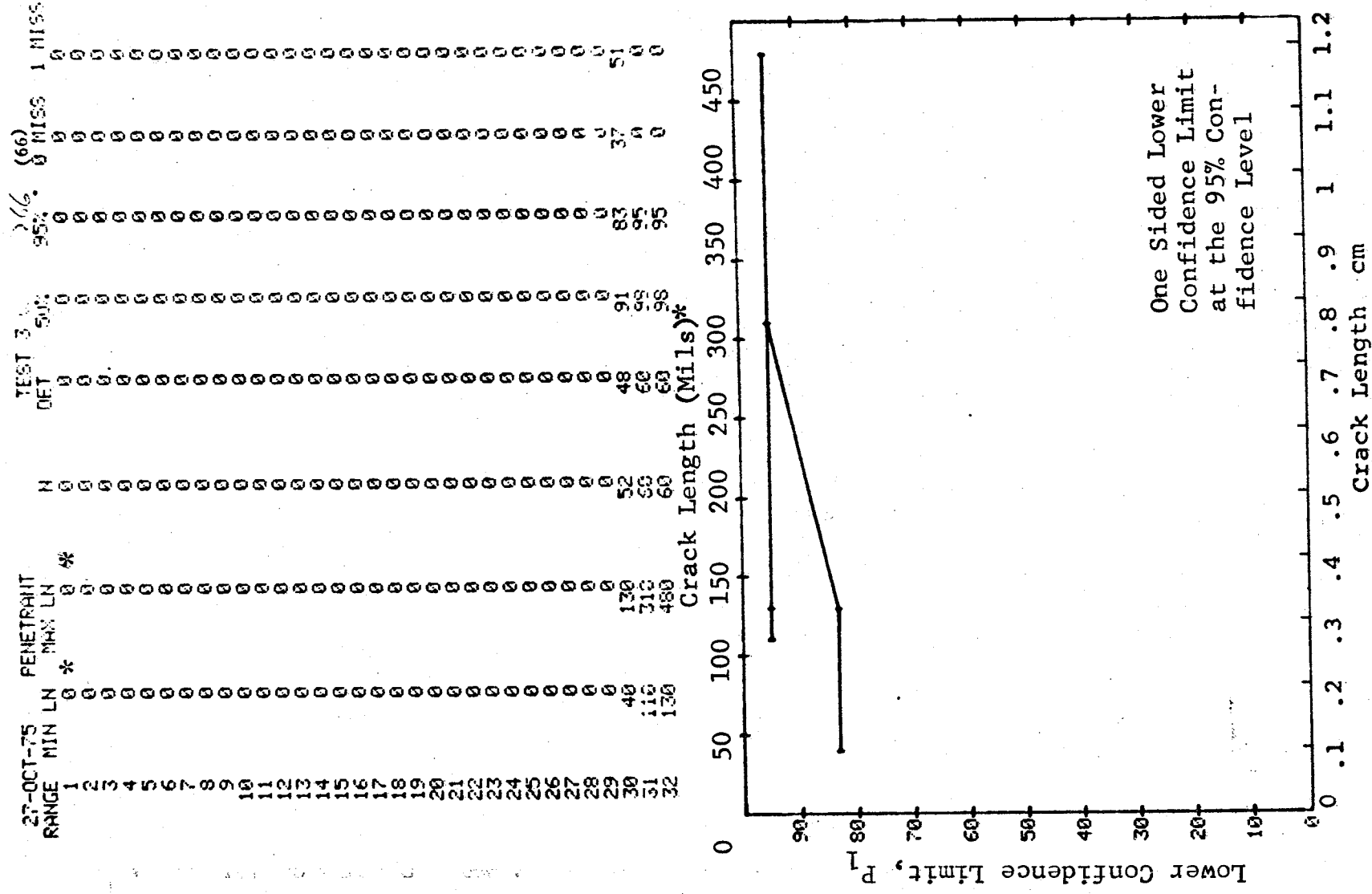


Figure D-66 (Concluded)

(a) Range Interval Method of Data Cumulation

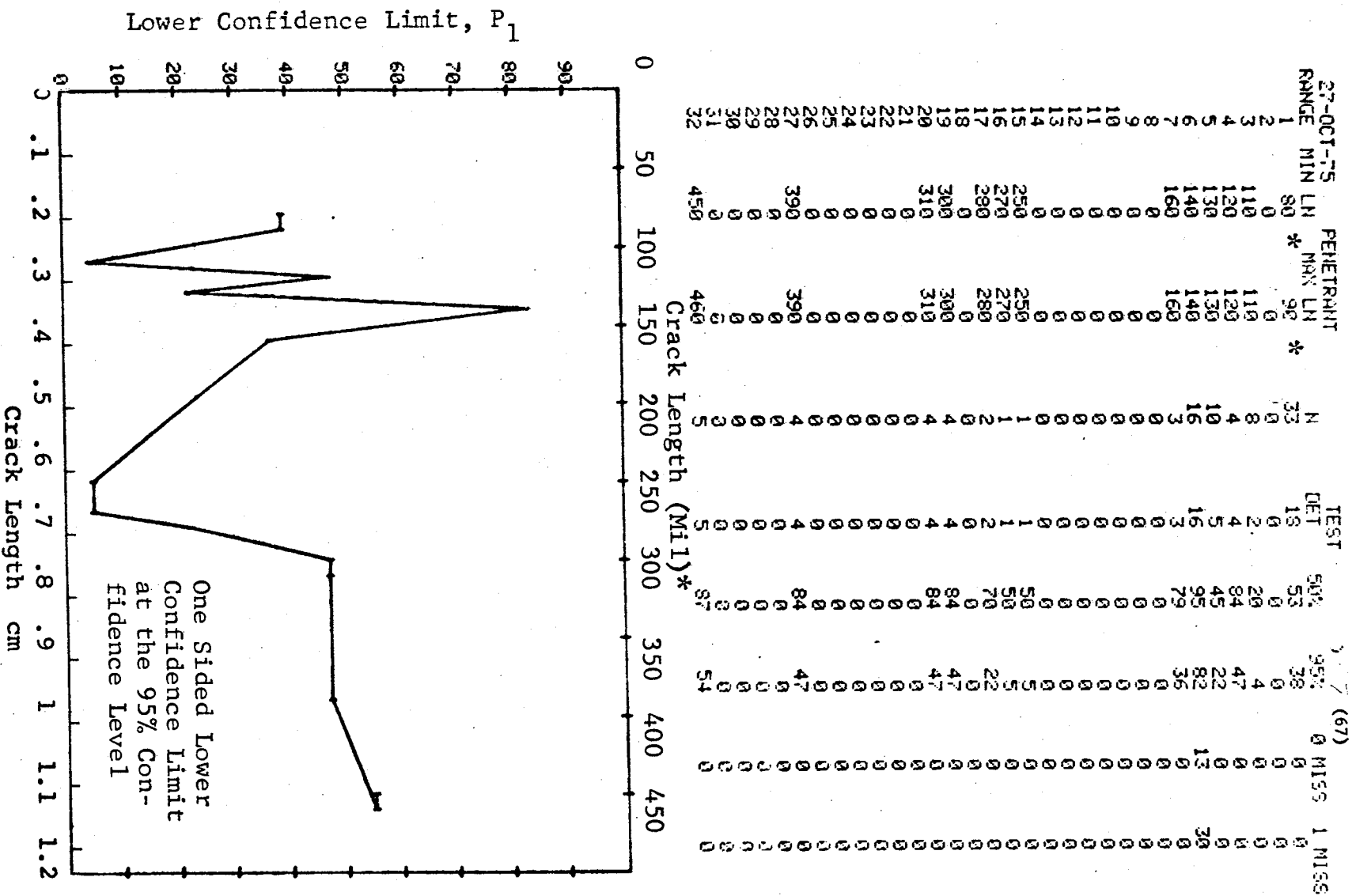


Figure D-67 Probability of Detection for 4340M Steel Using Liquid Penetrant. Compressed Notch Flaws in Hollow Cylinder. Lab. Env.

(b) Optimum Probability Method of Data Cumulation

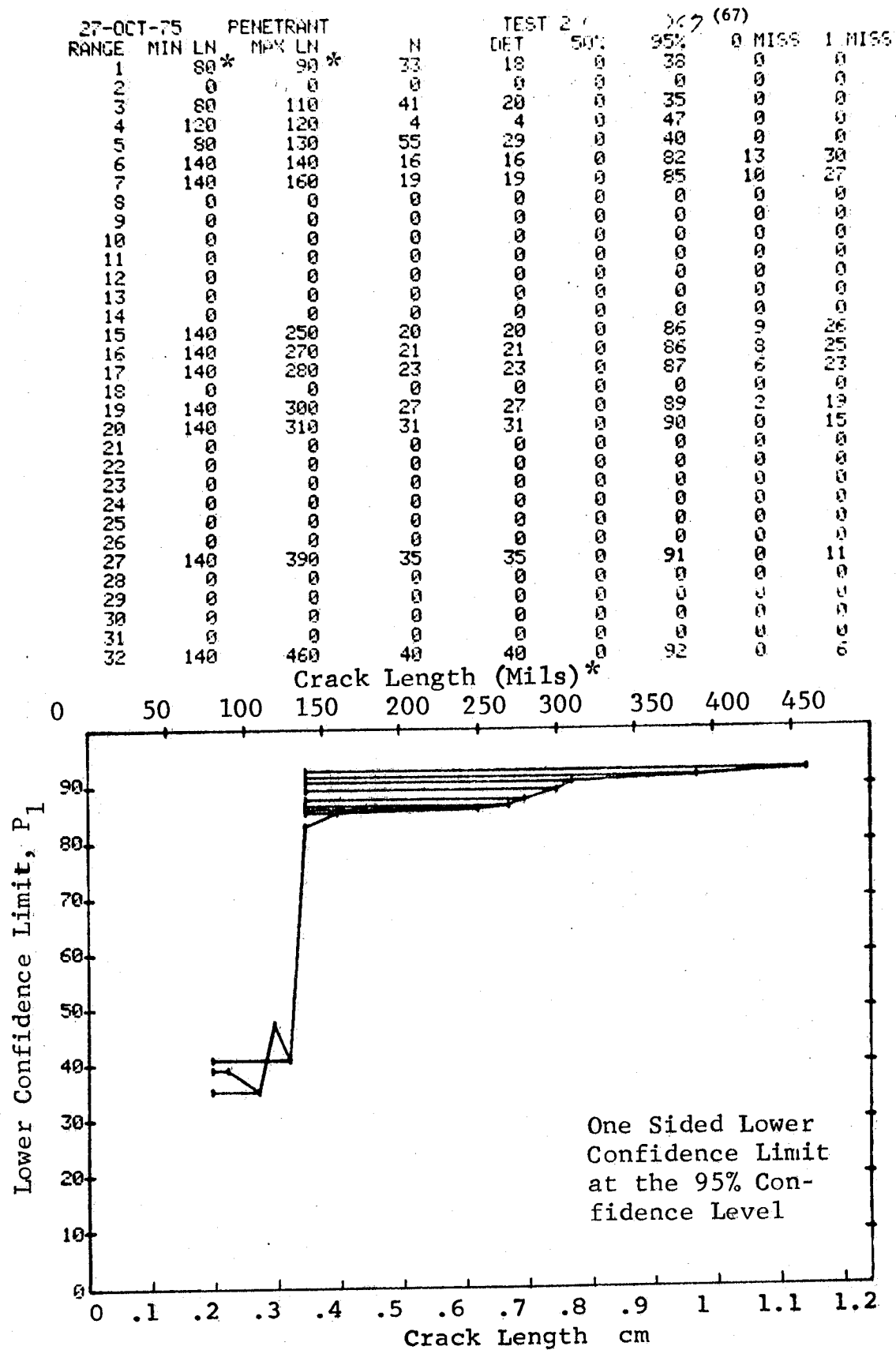


Figure D-67 (Continued)

(c) Overlapping Sixty Point Method of Data Cumulation

27-OCT-75		PENETRANT		TEST 3 (7 (67)		1 MISS	
RANGE	MIN LN	MAX LN	*	DET	50%	95%	0 MISS	0	1 MISS
1	0	0	*	0	0	0	0	0	0
2	0	0	0	0	0	0	0	0	0
3	0	0	0	0	0	0	0	0	0
4	0	0	0	0	0	0	0	0	0
5	0	0	0	0	0	0	0	0	0
6	0	0	0	0	0	0	0	0	0
7	0	0	0	0	0	0	0	0	0
8	0	0	0	0	0	0	0	0	0
9	0	0	0	0	0	0	0	0	0
10	0	0	0	0	0	0	0	0	0
11	0	0	0	0	0	0	0	0	0
12	0	0	0	0	0	0	0	0	0
13	0	0	0	0	0	0	0	0	0
14	0	0	0	0	0	0	0	0	0
15	0	0	0	0	0	0	0	0	0
16	0	0	0	0	0	0	0	0	0
17	0	0	0	0	0	0	0	0	0
18	0	0	0	0	0	0	0	0	0
19	0	0	0	0	0	0	0	0	0
20	0	0	0	0	0	0	0	0	0
21	0	0	0	0	0	0	0	0	0
22	0	0	0	0	0	0	0	0	0
23	0	0	0	0	0	0	0	0	0
24	0	0	0	0	0	0	0	0	0
25	0	0	0	0	0	0	0	0	0
26	0	0	0	0	0	0	0	0	0
27	0	0	0	0	0	0	0	0	0
28	0	0	0	0	0	0	0	0	0
29	0	0	0	0	0	0	0	0	0
30	80	110	0	0	0	0	0	0	0
31	80	140	0	20	55	41	0	0	0
32	110	450	0	49	62	51	0	0	0
				Crack Length (Mils)*					
				N					
				35					
				60					

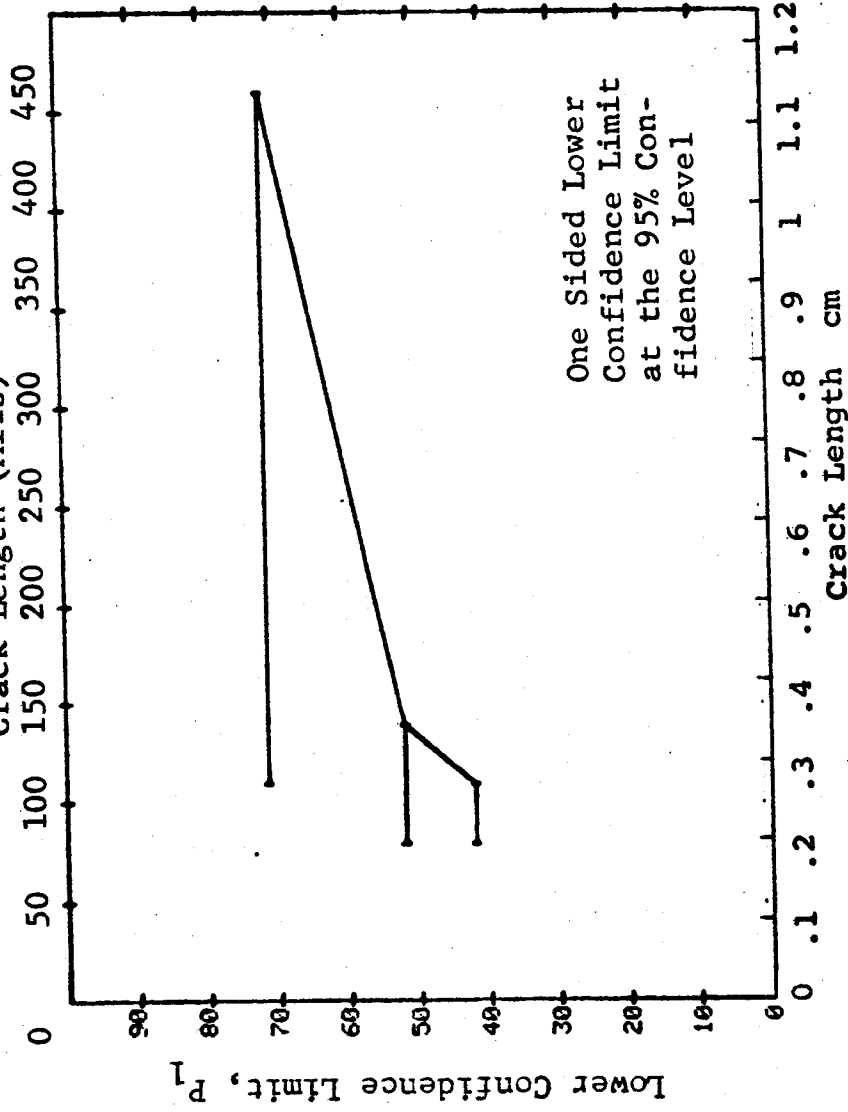


Figure D-67 (Concluded)

(a) Range Interval Method of Data Cumulation

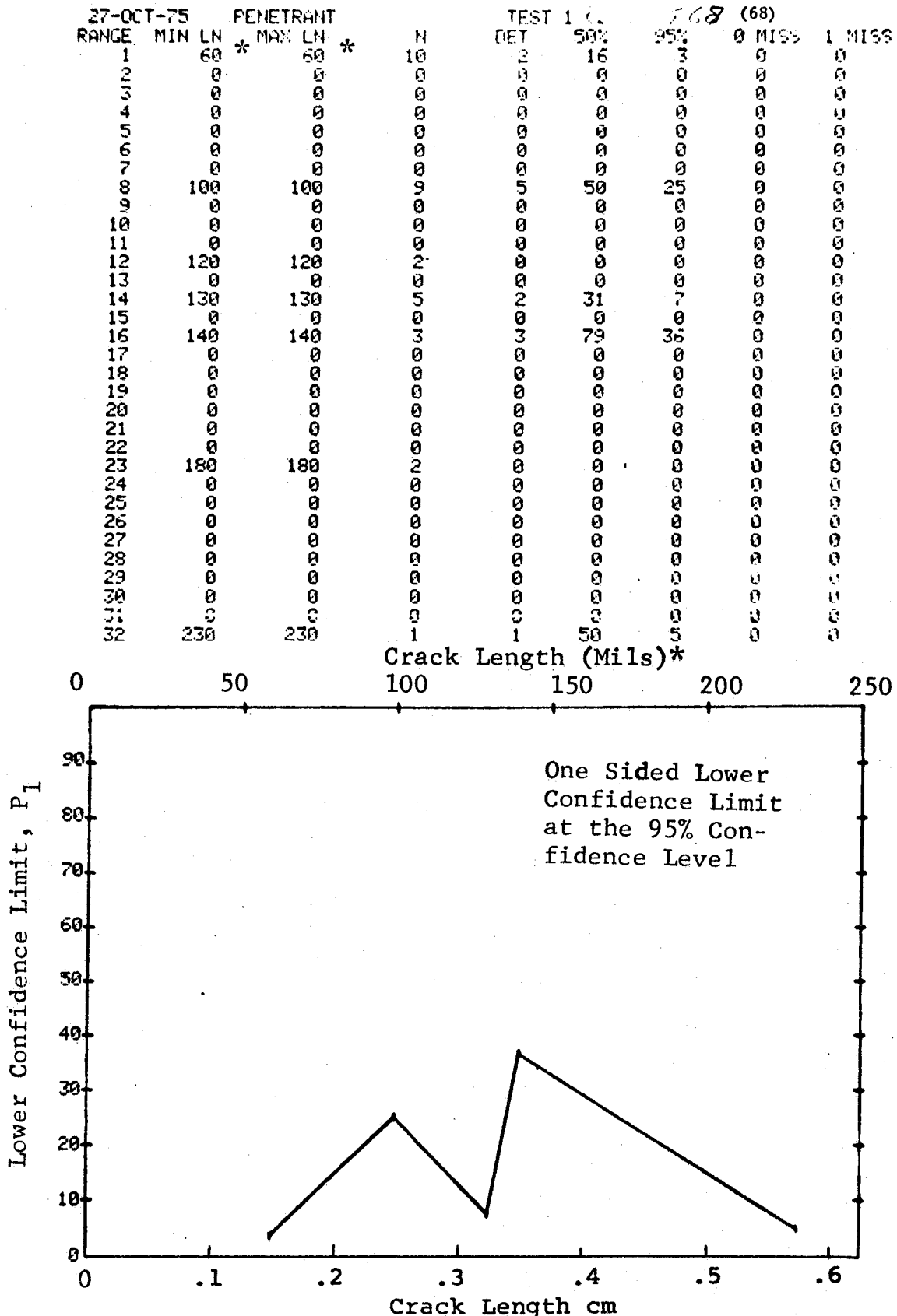


Figure D-68 Probability of Detection for 4340M Steel Using Liquid Penetrant. Compressed Notch Flaws in Filleted Hollow Cylinder. Lab. Env.

(b) Optimum Probability Method of Data Cumulation

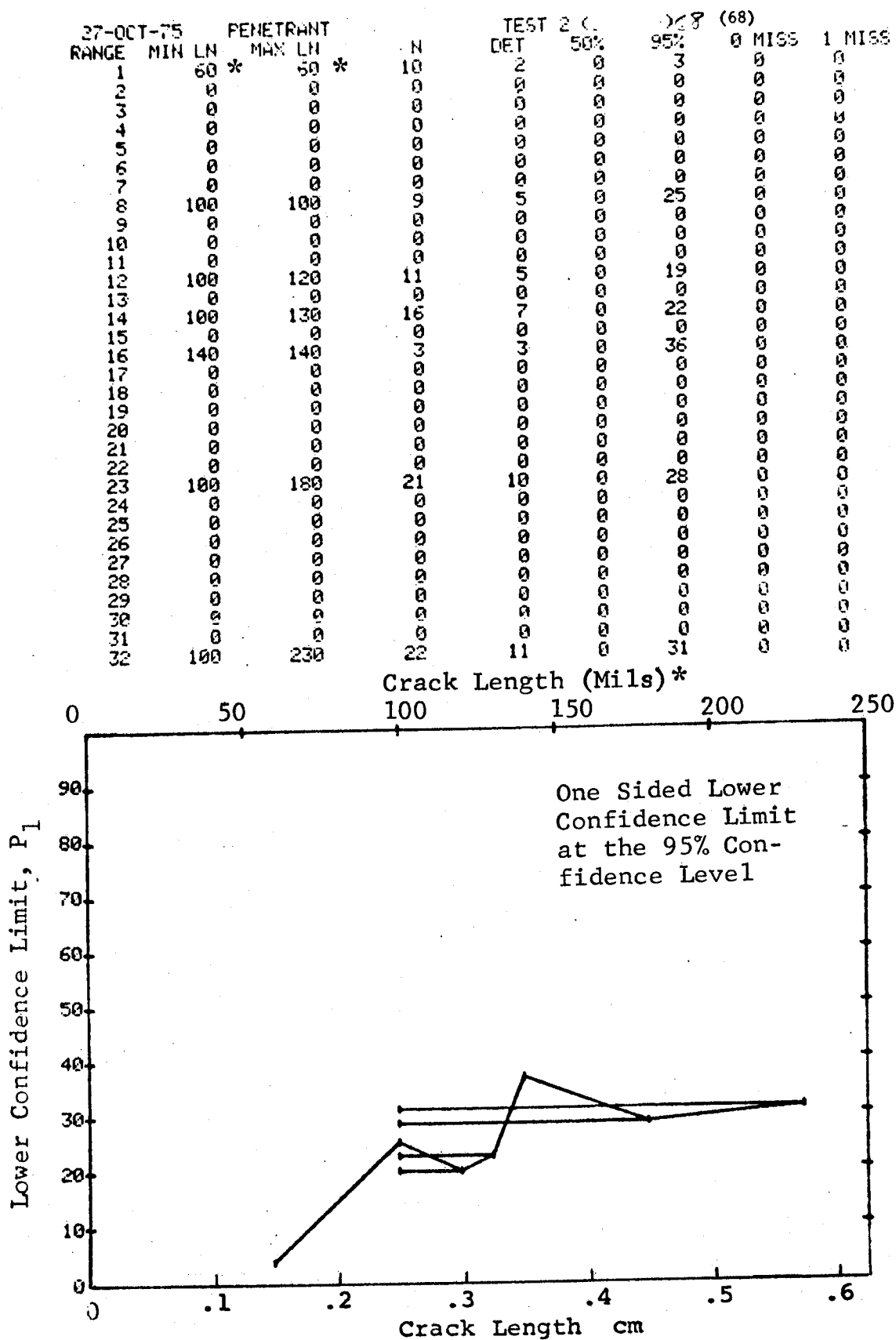


Figure D-68 (Continued)

(c) Overlapping Sixty Point Method of Data Cumulation

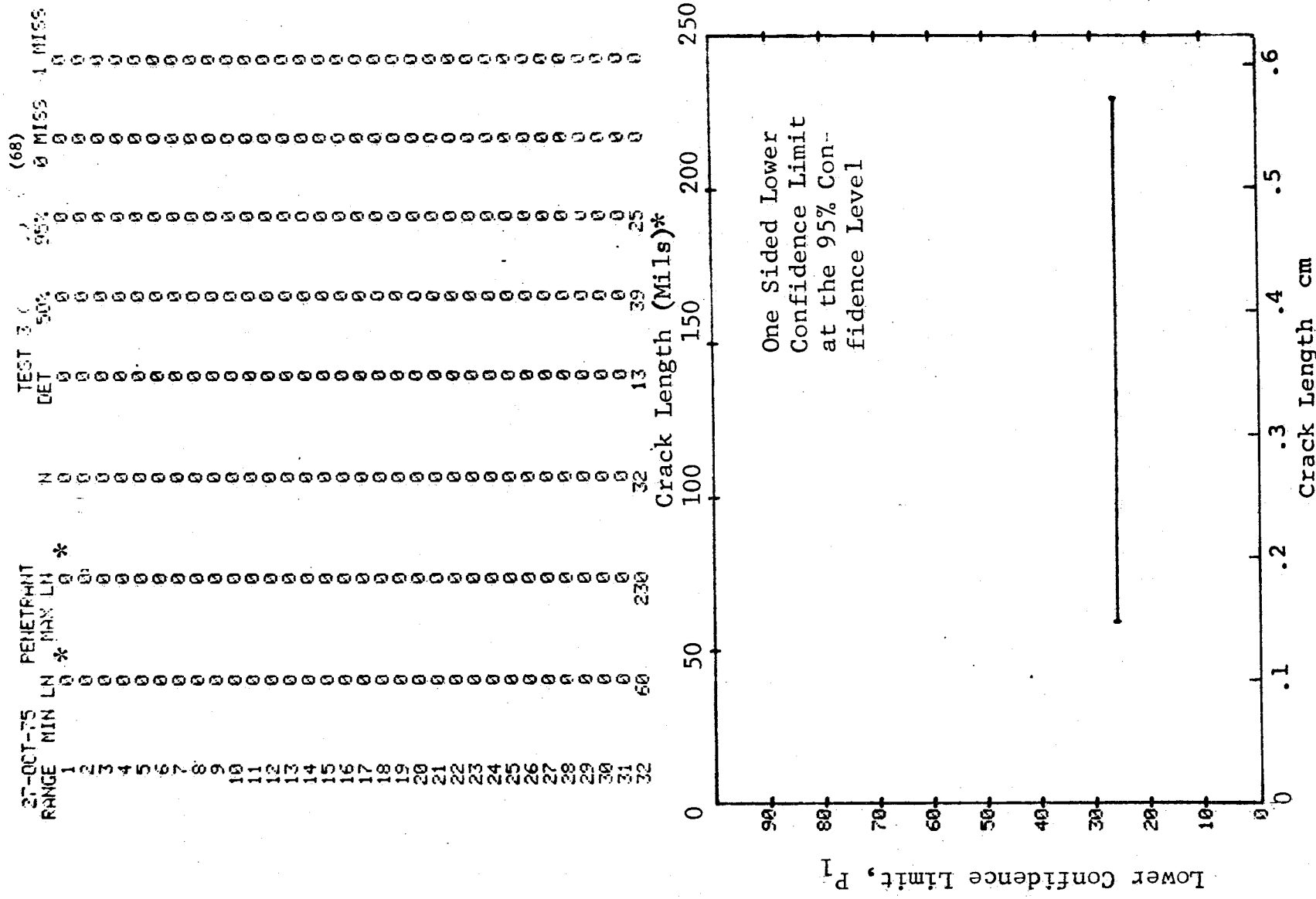


Figure D-68 (Concluded)

(a) Range Interval Method of Data Cumulation

27-OCT-75		PENETRANT		TEST AC		95% (69)		MISS	
RANGE	MIN LN *	MAX LN *	LN *	DET	50%	95%	95%	MISS	MISS
1	20	0	0	17	81	65	0	0	0
2	0	0	0	0	0	0	0	0	0
3	0	0	0	0	0	0	0	0	0
4	60	60	60	7	90	65	0	0	0
5	70	70	70	15	95	81	14	31	0
6	0	0	0	8	91	68	0	0	0
7	90	90	90	5	87	54	0	0	0
8	100	100	100	0	0	0	0	0	0
9	0	0	0	0	0	0	0	0	0
10	0	0	0	13	94	79	16	33	0
11	130	140	140	7	90	65	0	0	0
12	150	150	150	0	0	0	0	0	0
13	0	0	0	0	0	0	0	0	0
14	0	0	0	0	0	0	0	0	0
15	0	0	0	0	0	0	0	0	0
16	0	0	0	0	0	0	0	0	0
17	0	0	0	0	0	0	0	0	0
18	0	0	0	0	0	0	0	0	0
19	0	0	0	0	0	0	0	0	0
20	0	0	0	0	0	0	0	0	0
21	0	0	0	0	0	0	0	0	0
22	0	0	0	0	0	0	0	0	0
23	0	0	0	0	0	0	0	0	0
24	0	0	0	0	0	0	0	0	0
25	300	300	300	6	89	60	0	0	0
26	0	0	0	0	0	0	0	0	0
27	0	0	0	0	0	0	0	0	0
28	0	0	0	0	0	0	0	0	0
29	0	0	0	0	0	0	0	0	0
30	0	0	0	0	0	0	0	0	0
31	0	0	0	0	0	0	0	0	0
32	370	370	370	6	89	60	0	0	0

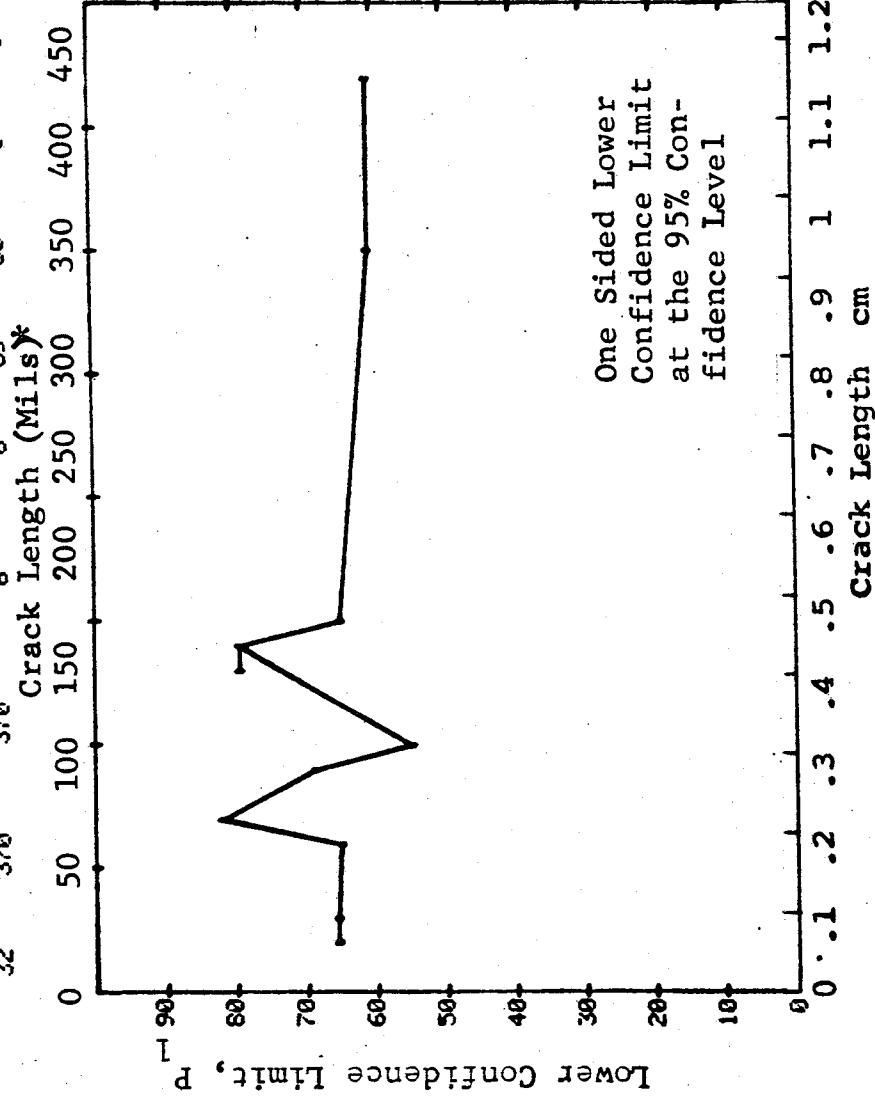


Figure D-69 Probability of Detection for 4340M Steel Using Liquid Penetrant. Compressed Notch Flaws in Filleted Solid Cylinder. Lab. Env. D-213

(b) Optimum Probability Method of Data Cumulation

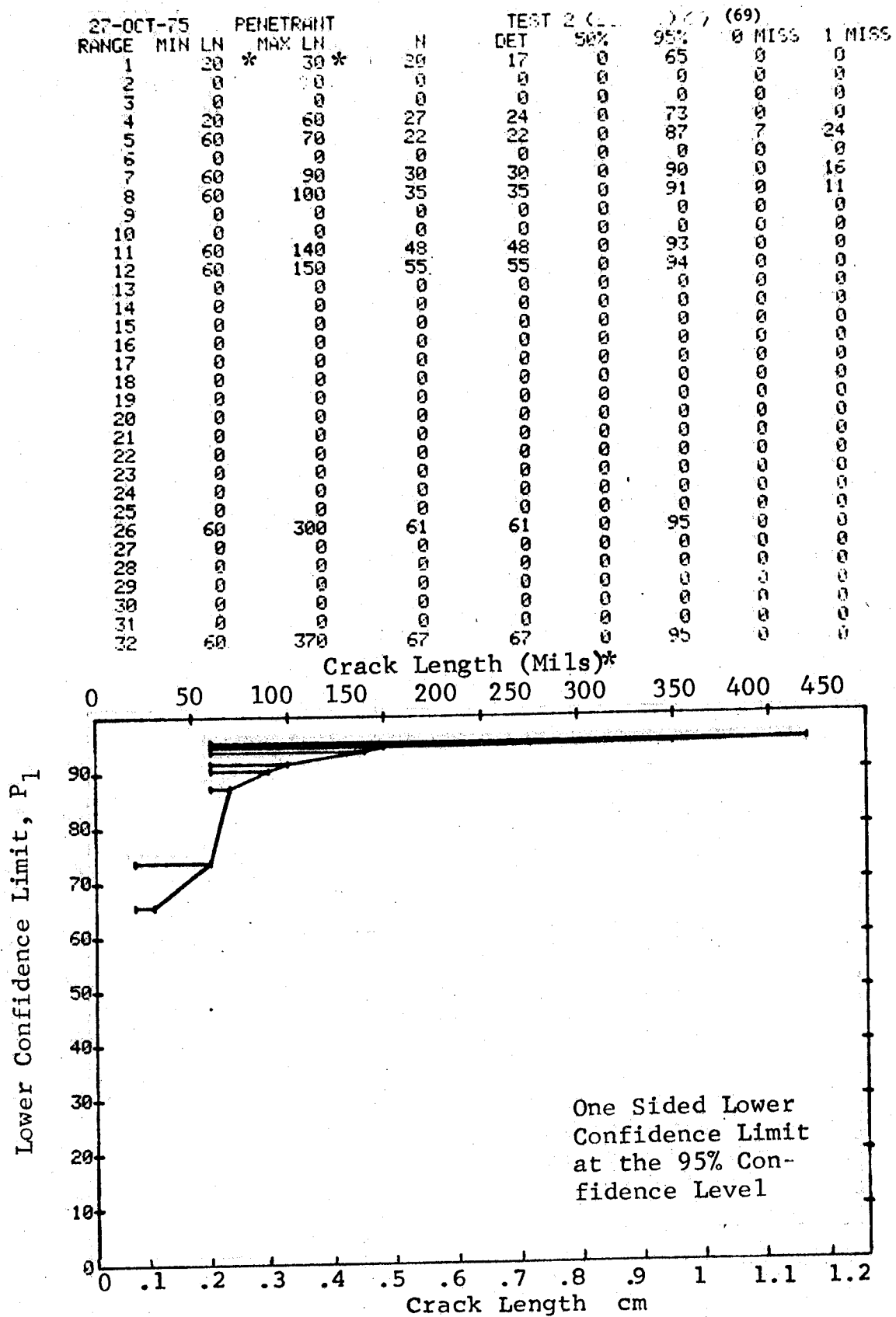


Figure D-69 (Continued)

(c) Overlapping Sixty Point Method of Data Cumulation

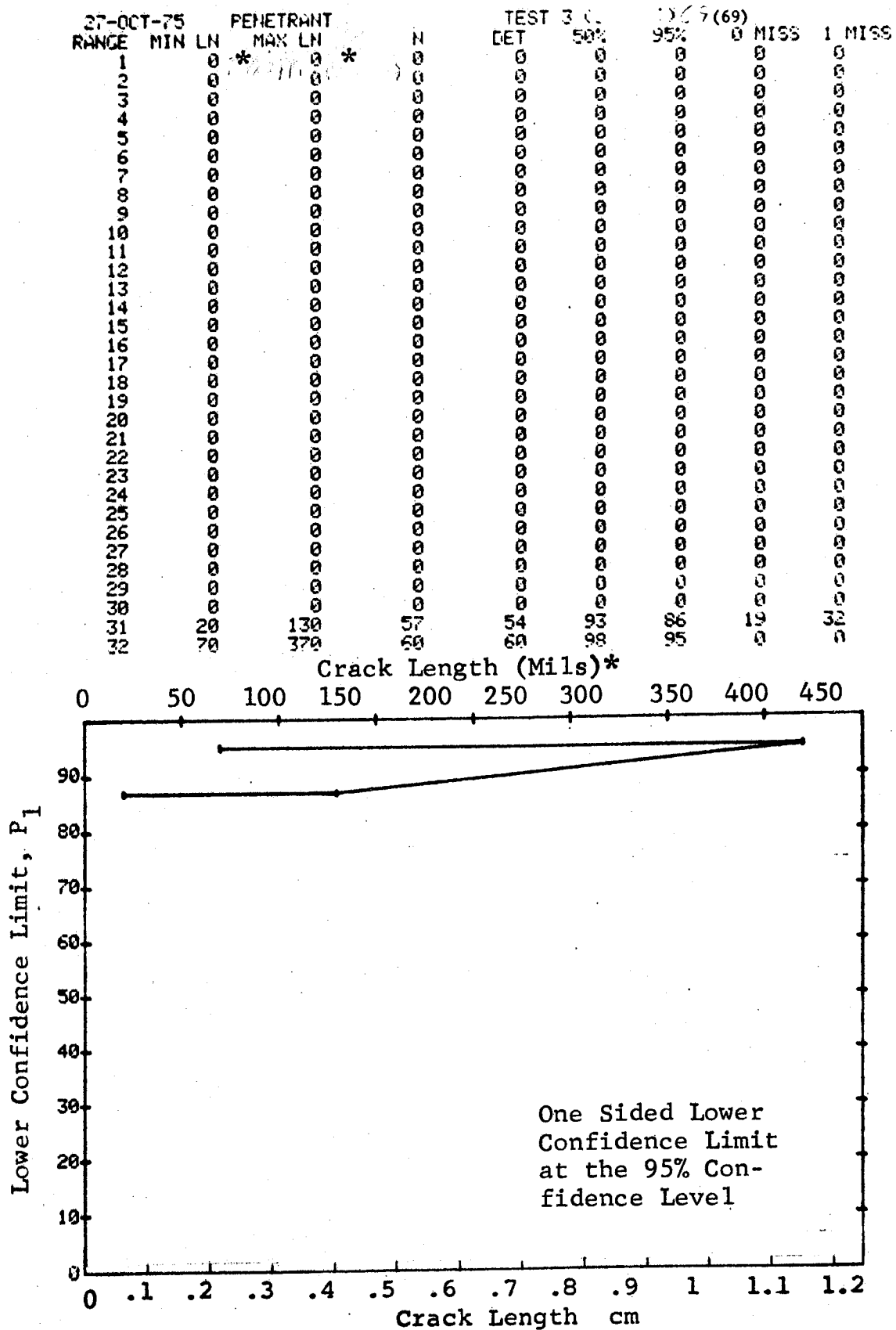


Figure D-69 (Concluded)

(a) Range Interval Method of Data Cumulation

27-OCT-75		PENETRANT		N	TEST 1 () 70 (70)				
RANGE	MIN LN	MAX LN			DET	50%	95%	0 MISS	1 MISS
1	30*	50*	22	6	25	12	0	0	0
2	60	70*	15	12	76	56	0	0	0
3	0	0	0	0	0	0	0	0	0
4	110	120	12	10	79	56	0	0	0
5	140	140	21	21	96	86	8	25	25
6	150	160	14	14	95	80	15	32	32
7	0	0	0	0	0	0	0	0	0
8	200	200	1	1	50	5	0	0	0
9	0	0	0	0	0	0	0	0	0
10	0	0	0	0	0	0	0	0	0
11	0	0	0	0	0	0	0	0	0
12	0	0	0	0	0	0	0	0	0
13	0	0	0	0	0	0	0	0	0
14	0	0	0	0	0	0	0	0	0
15	0	0	0	0	0	0	0	0	0
16	0	0	0	0	0	0	0	0	0
17	0	0	0	0	0	0	0	0	0
18	0	0	0	0	0	0	0	0	0
19	0	0	0	0	0	0	0	0	0
20	0	0	0	0	0	0	0	0	0
21	0	0	0	0	0	0	0	0	0
22	0	0	0	0	0	0	0	0	0
23	0	0	0	0	0	0	0	0	0
24	0	0	0	0	0	0	0	0	0
25	0	0	0	0	0	0	0	0	0
26	0	0	0	0	0	0	0	0	0
27	0	0	0	0	0	0	0	0	0
28	0	0	0	0	0	0	0	0	0
29	0	0	0	0	0	0	0	0	0
30	0	0	0	0	0	0	0	0	0
31	0	0	0	0	0	0	0	0	0
32	750	750	1	1	90	65	0	0	0

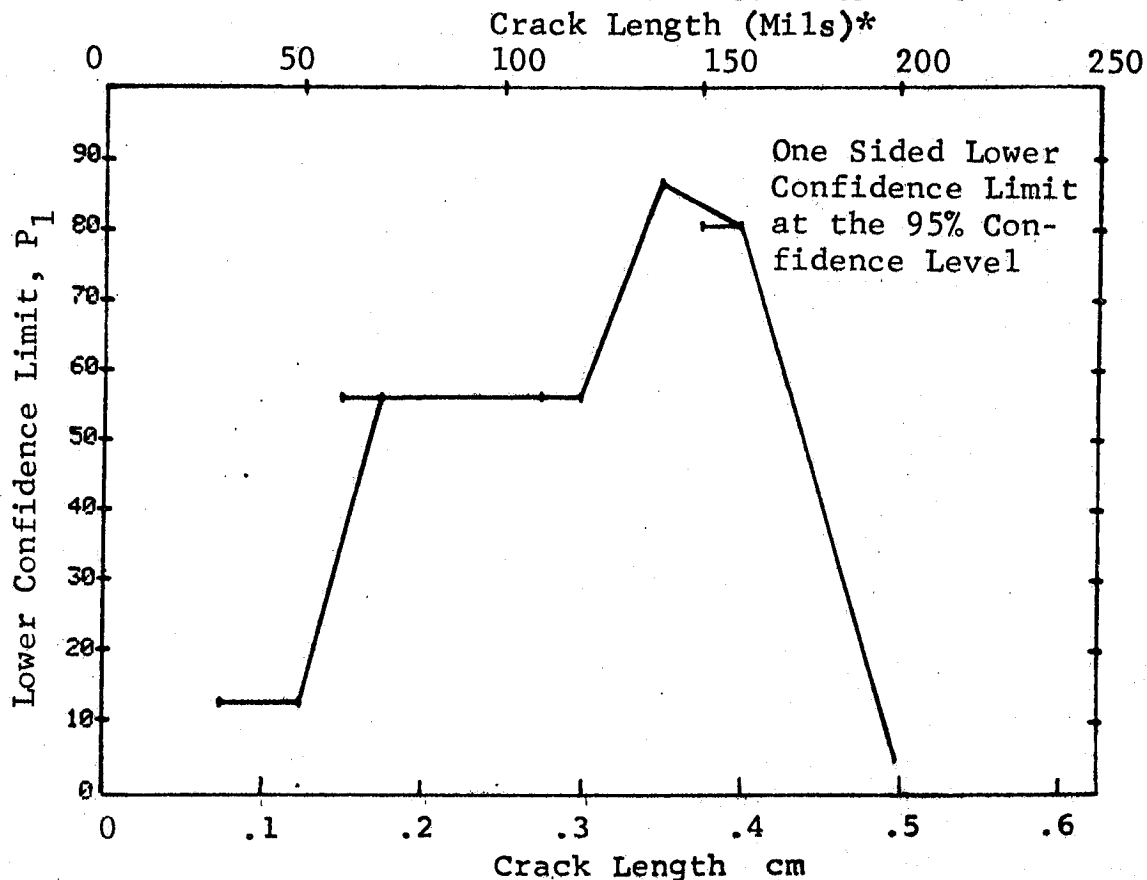


Figure D-70 Probability of Detection for 4340M Steel Using Liquid Penetrant. Compressed Notch Flaws in Filleted Solid Cylinder. Lab. Env.

(b) Optimum Probability Method of Data Cumulation

27-OCT-75	MIN	LN	MAX	LN	N	TEST 2	95%	(70)	MISS	MISS
RANGE	1	30	60	120	22	DET	12	0	0	1
	2	60	120	140	15		56	0	0	0
	3	0	0	0	0		64	0	0	0
	4	60	120	140	27		86	8	25	0
	5	140	160	0	21		91	0	11	0
	6	140	0	0	35		0	0	10	0
	7	140	0	0	36		92	0	0	0
	8	0	0	0	0		0	0	0	0
	9	0	0	0	0		0	0	0	0
	10	0	0	0	0		0	0	0	0
	11	0	0	0	0		0	0	0	0
	12	0	0	0	0		0	0	0	0
	13	0	0	0	0		0	0	0	0
	14	0	0	0	0		0	0	0	0
	15	0	0	0	0		0	0	0	0
	16	0	0	0	0		0	0	0	0
	17	0	0	0	0		0	0	0	0
	18	0	0	0	0		0	0	0	0
	19	0	0	0	0		0	0	0	0
	20	0	0	0	0		0	0	0	0
	21	0	0	0	0		0	0	0	0
	22	0	0	0	0		0	0	0	0
	23	0	0	0	0		0	0	0	0
	24	0	0	0	0		0	0	0	0
	25	0	0	0	0		0	0	0	0
	26	0	0	0	0		0	0	0	0
	27	0	0	0	0		0	0	0	0
	28	0	0	0	0		0	0	0	0
	29	0	0	0	0		0	0	0	0
	30	0	0	0	0		0	0	0	0
	31	0	0	0	0		0	0	0	0
	32	140	750	0	43		93	0	0	0

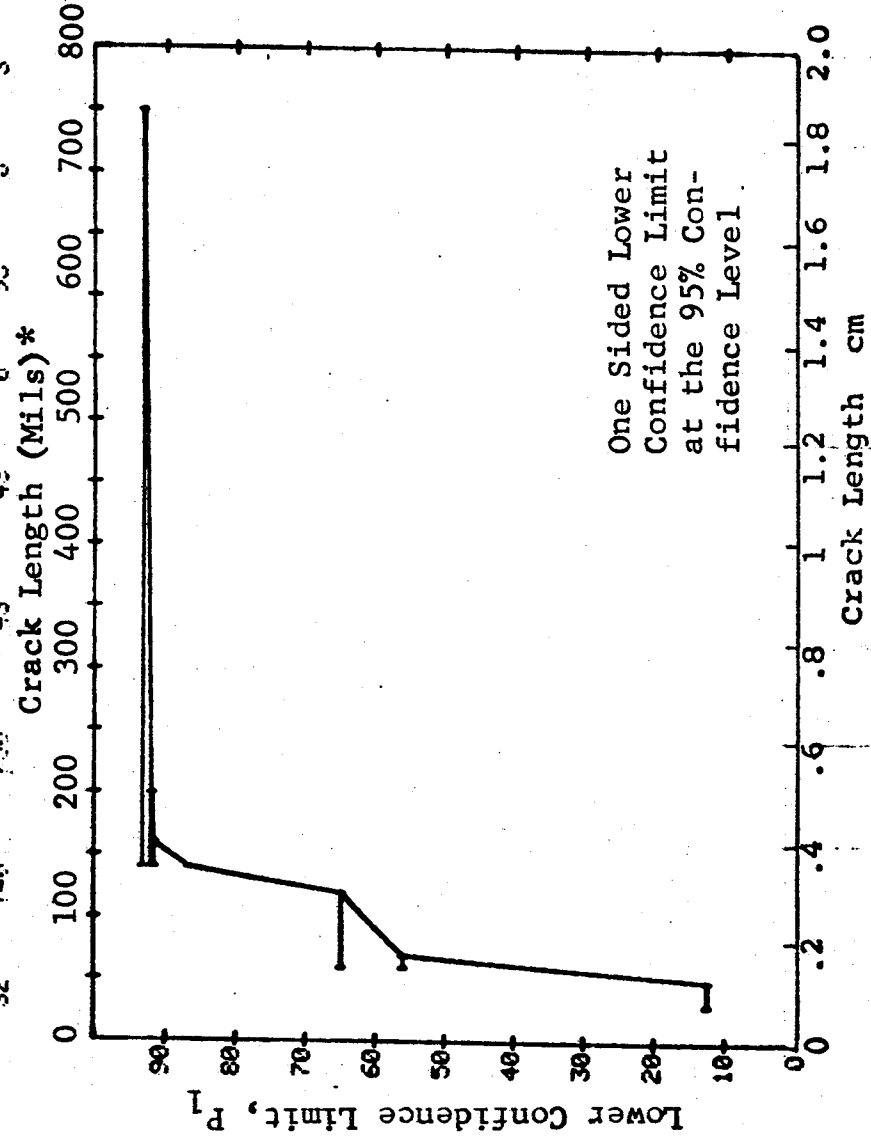


Figure D-70 (Continued)

(c) Overlapping Sixty Point Method of Data Cumulation

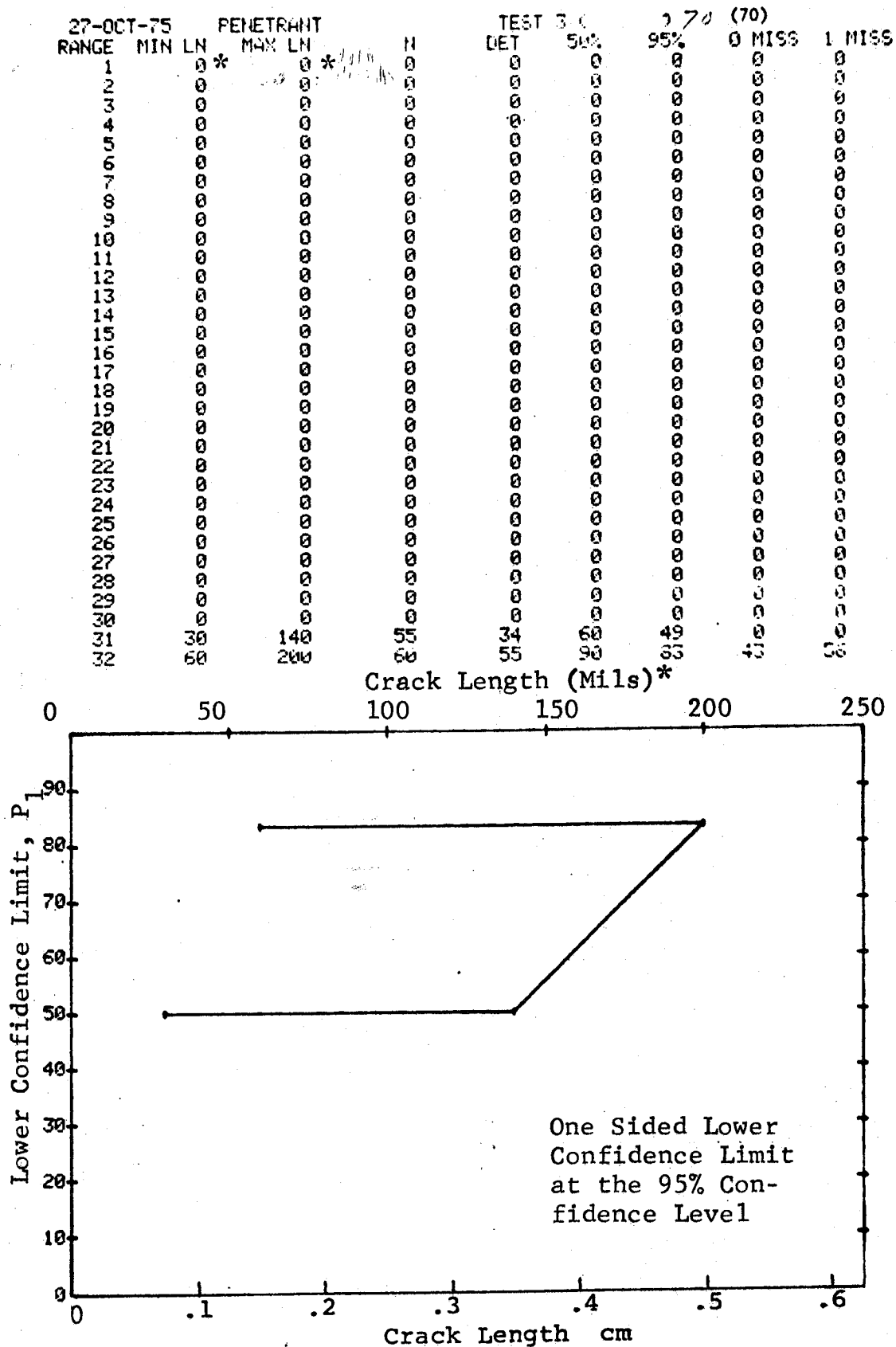


Figure D-70 (Concluded)

(a) Range Interval Method of Data Cumulation

27-OCT-75		ULTRASONIC		N	TEST 1		(71) 2/		0 MISS	1 MISS
RANGE	MIN LN*	MAX LN*			DET	50%	95%			
1	30	30		2	1	29	2		0	0
2	40	40		7	4	50	22		0	0
3	0	0		0	0	0	0		0	0
4	50	50		9	6	60	34		0	0
5	0	0		0	0	0	0		0	0
6	0	0		0	0	0	0		0	0
7	70	70		3	3	79	36		0	0
8	80	80		10	9	83	60		0	0
9	0	0		0	0	0	0		0	0
10	90	90		12	10	78	56		0	0
11	0	0		0	0	0	0		0	0
12	100	100		9	8	82	57		0	0
13	110	110		22	20	88	74		0	0
14	0	0		0	0	0	0		0	0
15	120	120		9	9	92	71		0	0
16	130	130		9	9	92	71		0	0
17	0	0		0	0	0	0		0	0
18	140	140		7	6	77	47		0	0
19	0	0		0	0	0	0		0	0
20	150	150		16	14	83	65		0	0
21	160	160		6	5	73	41		0	0
22	0	0		0	0	0	0		0	0
23	170	170		16	16	95	82	13	30	
24	180	180		8	8	91	68		0	0
25	0	0		0	0	0	0		0	0
26	190	190		4	4	84	47		0	0
27	0	0		0	0	0	0		0	0
28	0	0		0	0	0	0		0	0
29	210	210		2	2	70	22		0	0
30	0	0		0	0	0	0		0	0
31	220	220		9	9	92	71		0	0
32	230	230		19	9	85	60		0	0

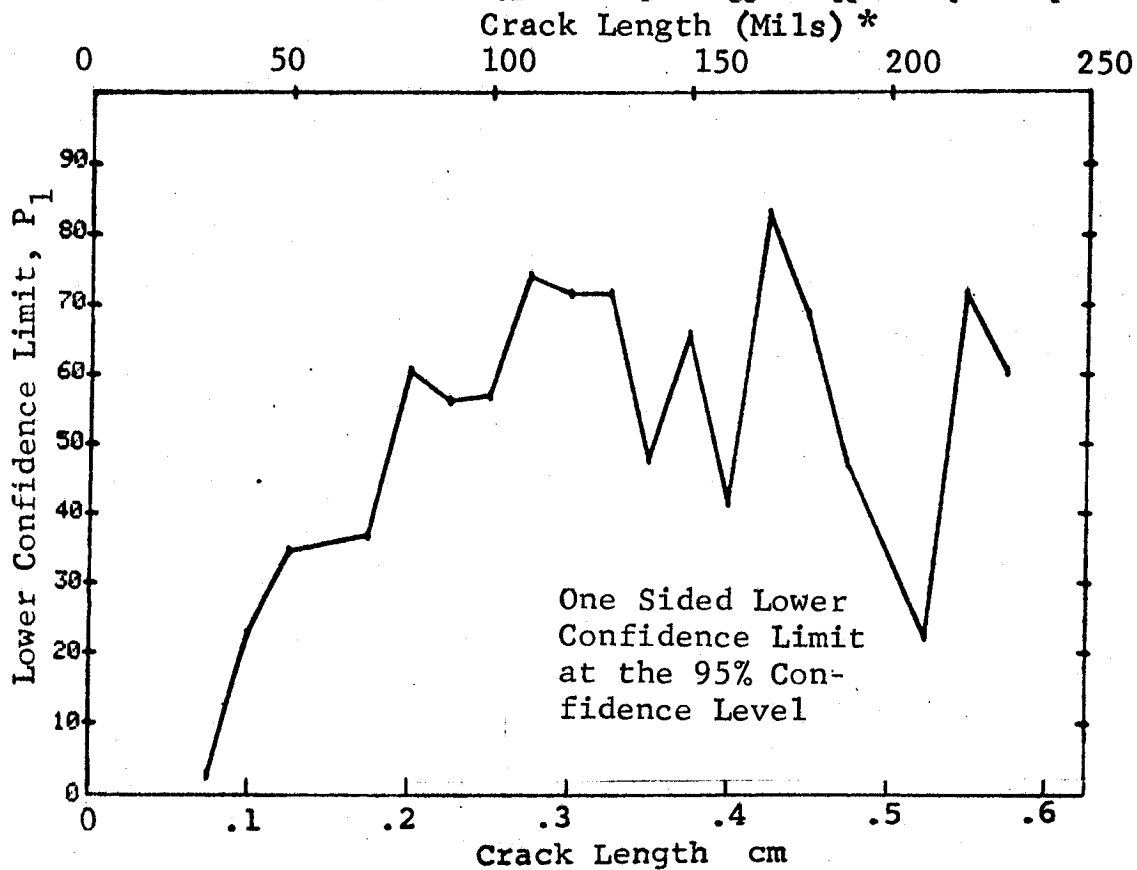


Figure D-71 Probability of Detection for 2024-T6 Al for Ultrasonic Shear and Surface Waves. Compressed Notch Flaws in Tandem T. Prod. Env.

(b) Optimum Probability Method of Data Cumulation

27-OCT-75		ULTRASONIC		N	TEST 2		27 (71)		MISS	
RANGE	MIN	LN	MAX		DET	50%	95%	0	MISS	1
1	30	30	30	2	1	0	25	0	0	0
2	30	30	30	3	5	0	0	0	0	0
3	30	30	30	0	0	0	0	0	0	0
4	30	30	30	18	11	0	39	0	0	0
5	30	30	30	0	0	0	0	0	0	0
6	30	30	30	0	0	0	0	0	0	0
7	30	30	30	0	0	0	0	0	0	0
8	30	30	30	12	9	0	47	0	0	0
9	30	30	30	13	12	0	68	0	0	0
10	30	30	30	0	0	0	0	0	0	0
11	30	30	30	25	22	0	71	0	0	0
12	30	30	30	0	0	0	0	0	0	0
13	30	30	30	34	30	0	75	0	0	0
14	30	30	30	56	50	0	79	0	0	0
15	30	30	30	0	0	0	0	0	0	0
16	30	30	30	65	59	0	82	0	0	0
17	30	30	30	40	38	0	85	0	0	0
18	30	30	30	0	0	0	0	0	0	0
19	30	30	30	56	52	0	84	0	0	0
20	30	30	30	0	0	0	0	0	0	0
21	30	30	30	97	88	0	84	0	0	0
22	30	30	30	103	93	0	0	0	0	0
23	30	30	30	0	0	0	0	0	0	0
24	30	30	30	85	79	0	86	0	0	0
25	30	30	30	24	24	0	88	0	0	0
26	30	30	30	0	0	0	0	0	0	0
27	30	30	30	28	28	0	89	0	0	0
28	30	30	30	0	0	0	0	0	0	0
29	30	30	30	0	0	0	0	0	0	0
30	30	30	30	30	30	0	90	0	0	0
31	30	30	30	0	0	0	0	0	0	0
32	30	30	30	39	39	0	92	0	0	0
33	30	30	30	49	48	0	90	0	0	0

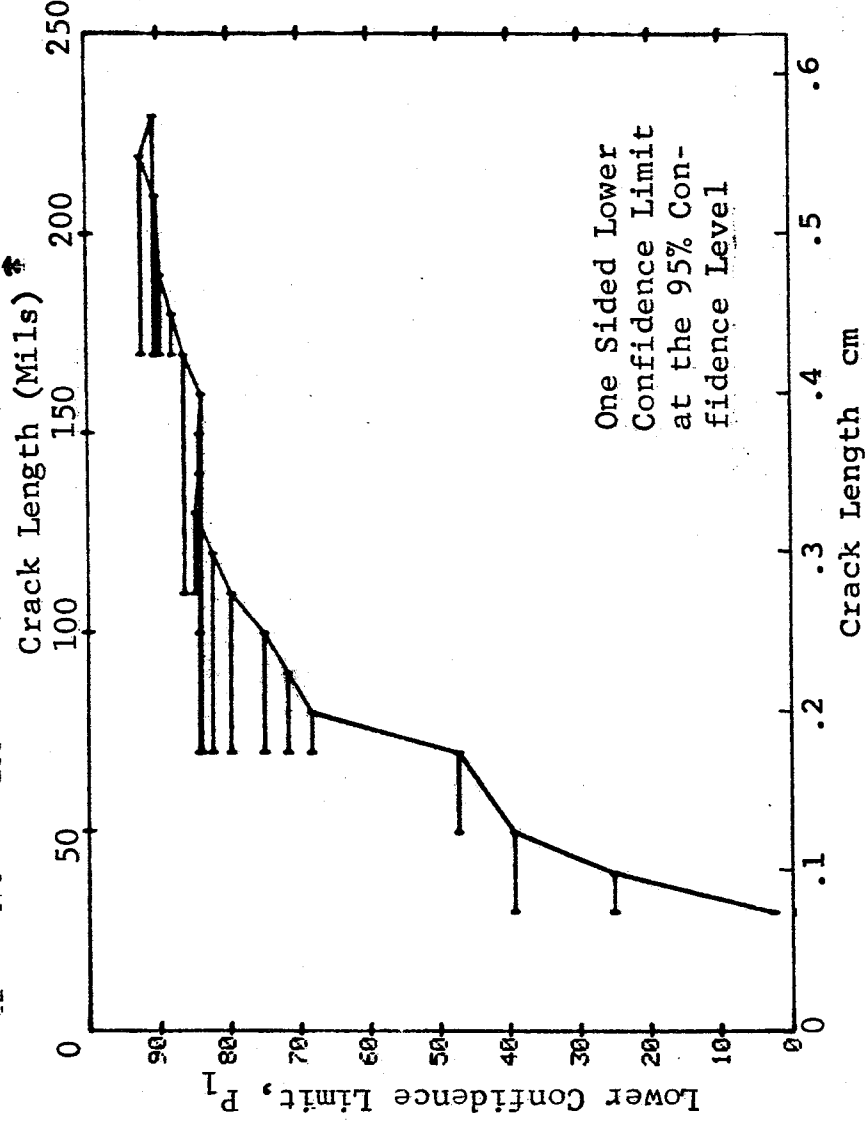


Figure D-70 (Continued)

(c) Overlapping Sixty Point Method of Data Cumulation

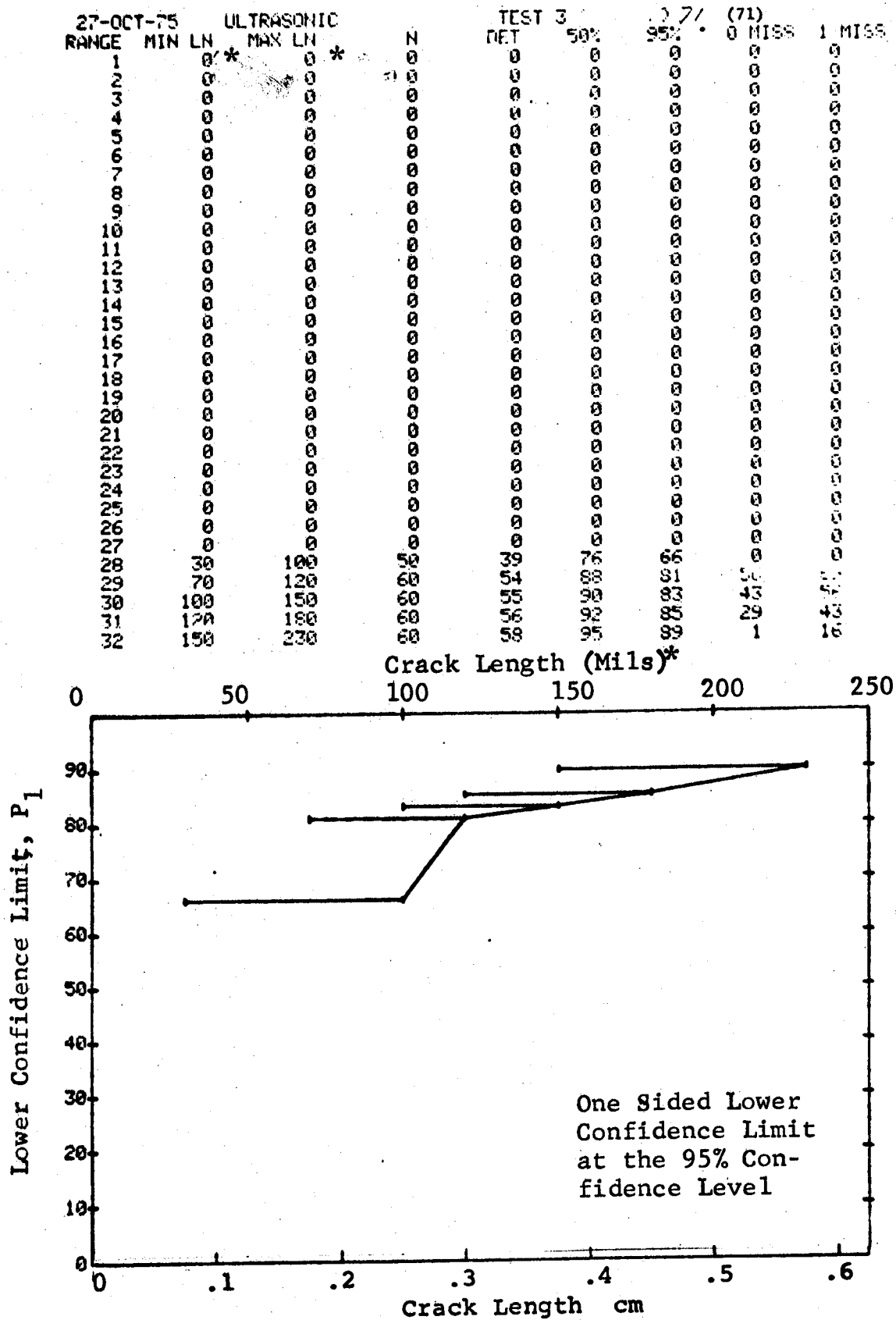


Figure D-71 (Concluded)

(a) Range Interval Method of Data Cumulation

27-OCT-75	ULTRASONIC		TEST 1 (72)		TEST 2 (72)		TEST 3 (72)	
RANGE	MIN LN	* MAX LN *	N	DET	50%	95%	0 MISS	1 MISS
1	40	* 40 *	2	0	0	0	0	0
2	70	70	1	0	0	0	0	0
3	0	0	0	0	0	0	0	0
4	100	110	11	0	14	3	0	0
5	130	130	4	1	15	1	0	0
6	0	0	0	0	0	0	0	0
7	0	0	0	0	0	0	0	0
8	190	190	1	1	50	5	0	0
9	210	210	1	0	0	0	0	0
10	230	230	2	2	70	22	0	0
11	0	0	0	0	0	0	0	0
12	250	250	3	3	79	36	0	0
13	0	0	0	0	0	0	0	0
14	300	300	2	2	70	22	0	0
15	310	310	2	2	70	22	0	0
16	0	0	0	0	0	0	0	0
17	350	350	2	2	70	22	0	0
18	380	380	2	2	70	22	0	0
19	0	0	0	0	0	0	0	0
20	0	0	0	0	0	0	0	0
21	0	0	0	0	0	0	0	0
22	450	450	2	2	70	22	0	0
23	460	460	1	1	50	5	0	0
24	480	480	2	2	70	22	0	0
25	0	0	0	0	0	0	0	0
26	0	0	0	0	0	0	0	0
27	0	0	0	0	0	0	0	0
28	0	0	0	0	0	0	0	0
29	0	0	0	0	0	0	0	0
30	0	0	0	0	0	0	0	0
31	0	0	0	0	0	0	0	0
32	650	650	2	2	70	22	0	0

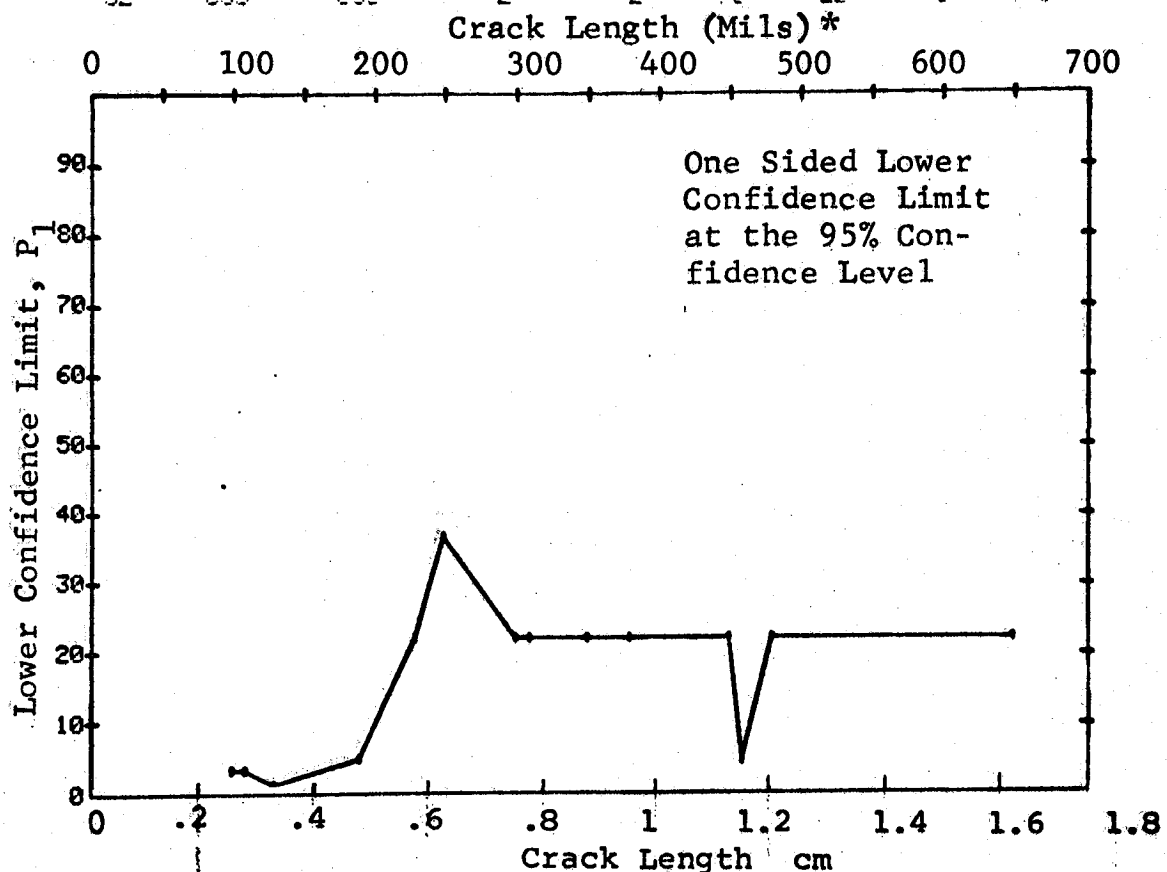


Figure D-72 Probability of Detection for 4340M Steel Using Ultrasonic Shear and Surface Waves. Compressed Notch Flaws in Solid Threaded Cylinder. Prod. Env.

(b) Optimum Probability Method of Data Cumulation

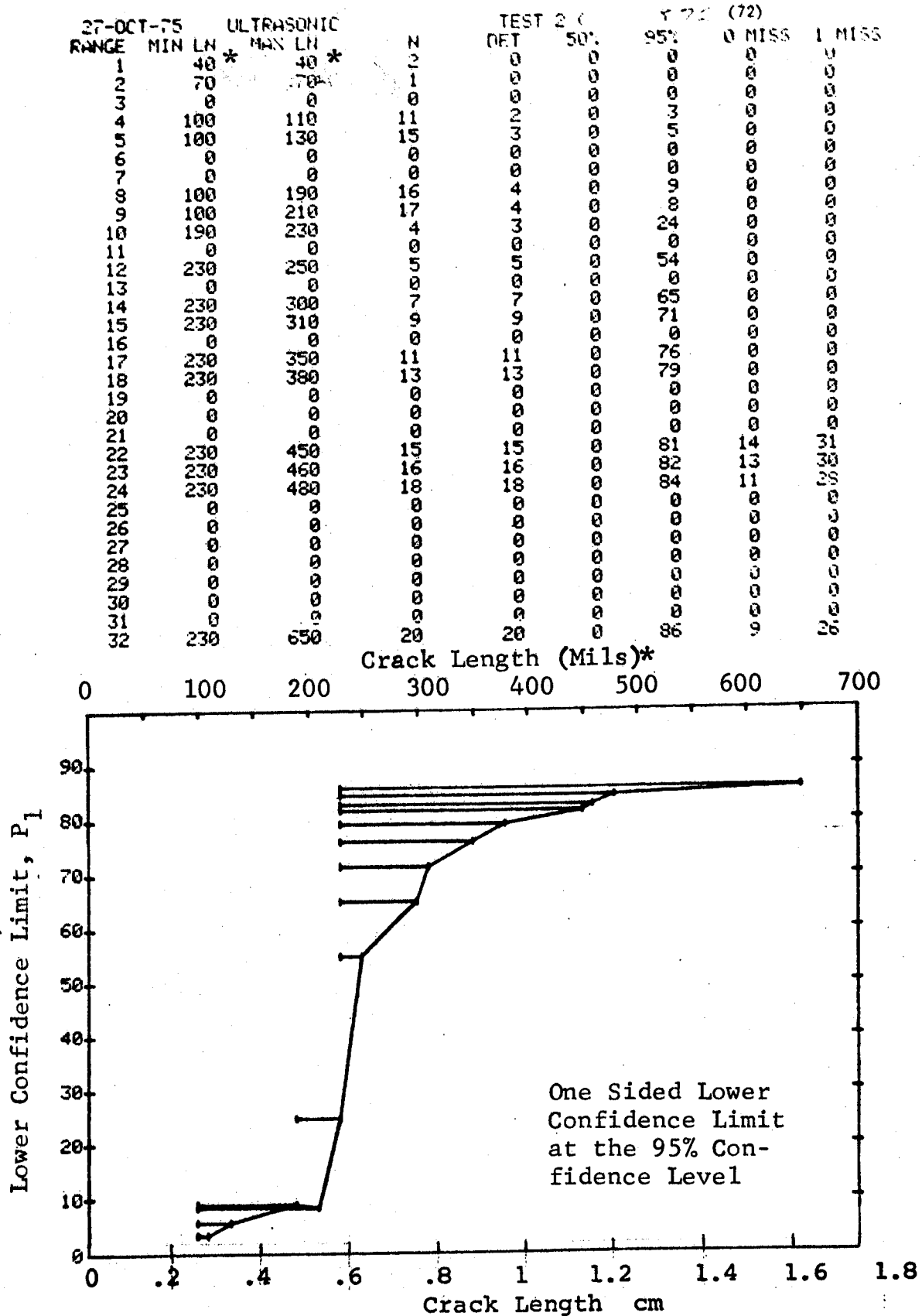


Figure D-72 (Continued)

(c) Overlapping Sixty Point Method of Data Cumulation

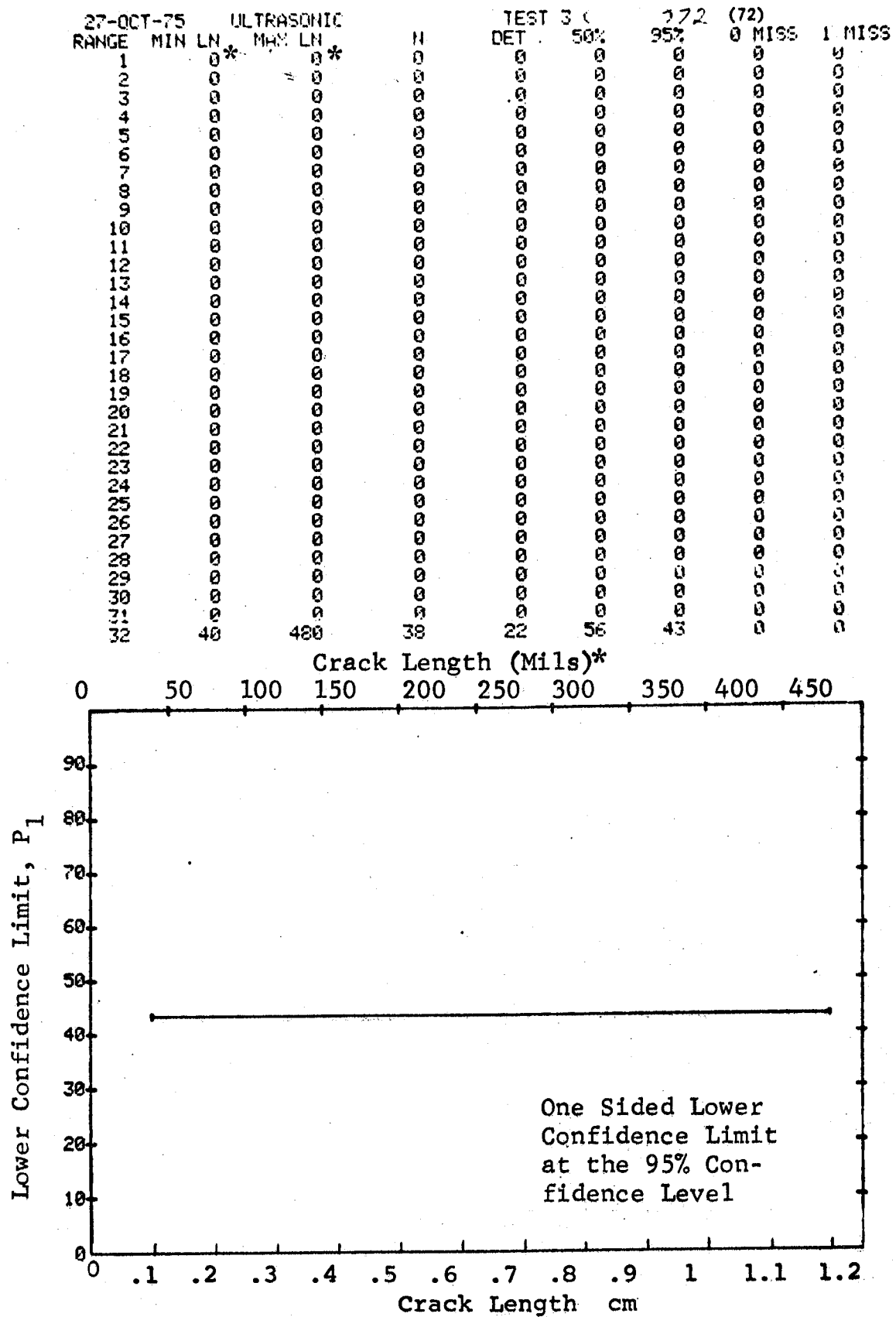


Figure D-72 (Concluded)

(a) Range Interval Method of Data Cumulation

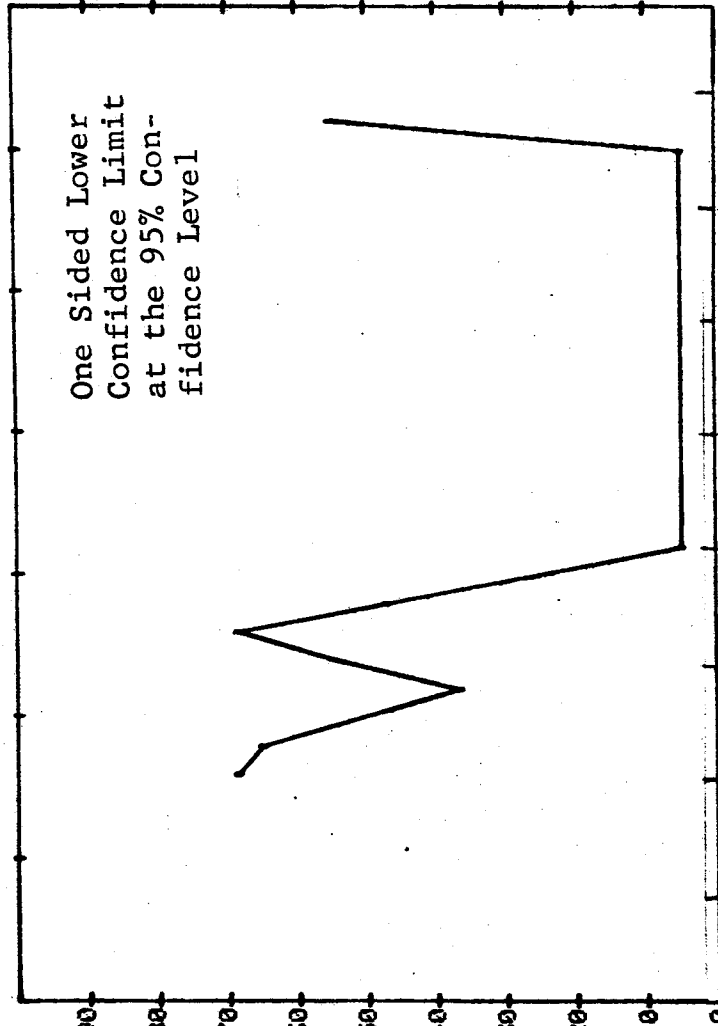
27-OCT-75 RANGE	ULTRASONIC		TEST #1 DET	95%		(73)
	MIN	LN *		50%	MISS	
1	1	80	8	91	0	0
2	2	90	7	90	0	0
3	3	0	0	0	0	0
4	4	0	0	0	0	0
5	5	110	3	79	0	0
6	6	120	5	87	0	0
7	7	130	8	91	0	0
8	8	0	0	0	0	0
9	9	140	4	84	0	0
10	10	0	0	0	0	0
11	11	0	0	0	0	0
12	12	160	1	50	0	0
13	13	0	0	0	0	0
14	14	0	0	0	0	0
15	15	0	0	0	0	0
16	16	0	0	0	0	0
17	17	0	0	0	0	0
18	18	0	0	0	0	0
19	19	0	0	0	0	0
20	20	0	0	0	0	0
21	21	0	0	0	0	0
22	22	0	0	0	0	0
23	23	0	0	0	0	0
24	24	0	0	0	0	0
25	25	0	0	0	0	0
26	26	0	0	0	0	0
27	27	0	0	0	0	0
28	28	0	0	0	0	0
29	29	0	0	0	0	0
30	30	0	0	0	0	0
31	31	300	1	50	0	0
32	32	310	5	97	54	0

Crack Length (Mils)*

0 50 100 150 200 250 300 350

One Sided Lower
Confidence Limit
at the 95% Con-
fidence Level

Lower Confidence Limit, P_1



Crack Length cm

Figure D-73 Probability of Detection for 4340M Steel Using Ultrasonic Shear and Surface Waves. Compressed Notch Flaws in Hollow Cylinder. Prod. Env.

(b) Optimum Probability Method of Data Cumulation

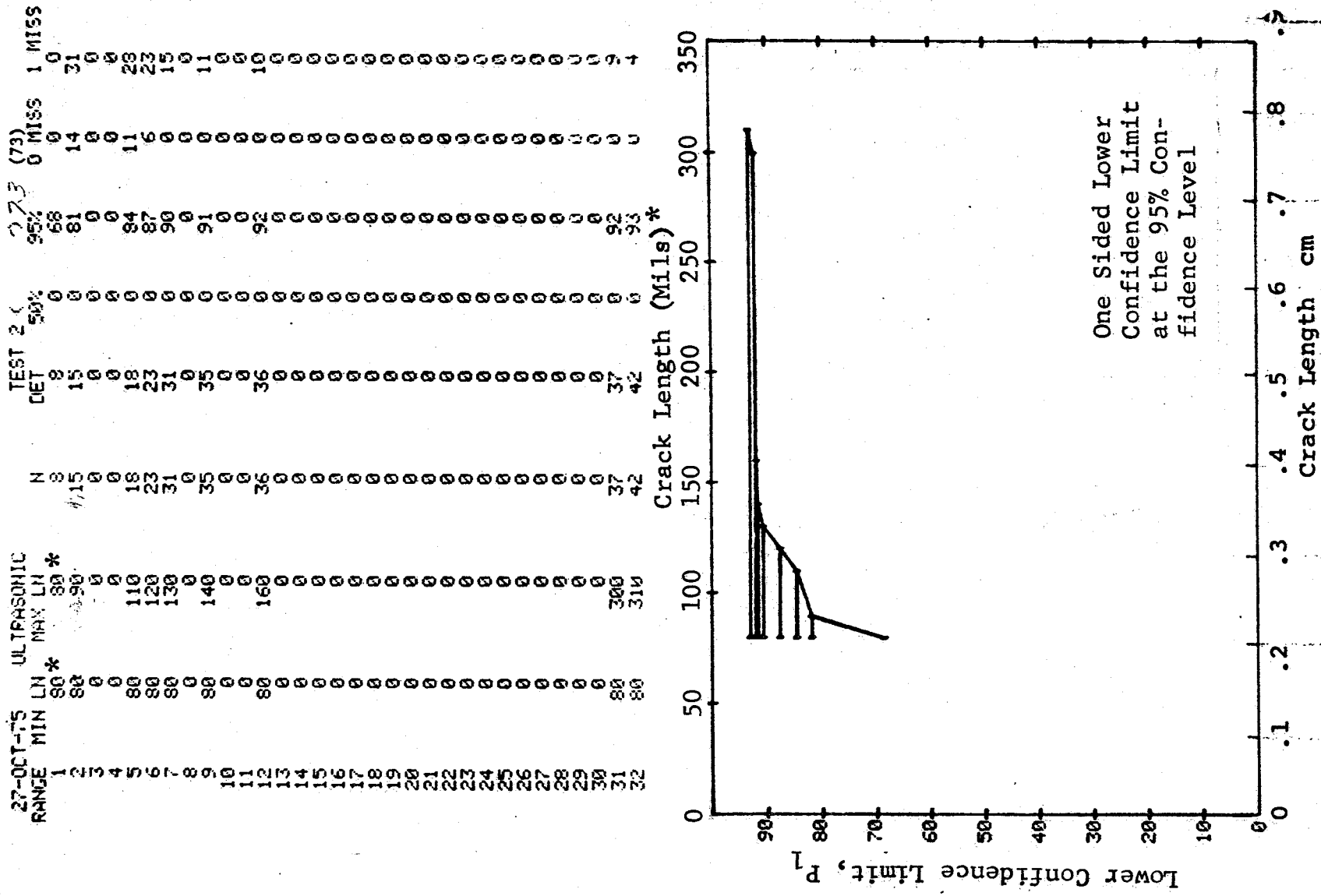


Figure D-73 (Continued)

(c) Overlapping Sixty Point Method of Data Cumulation

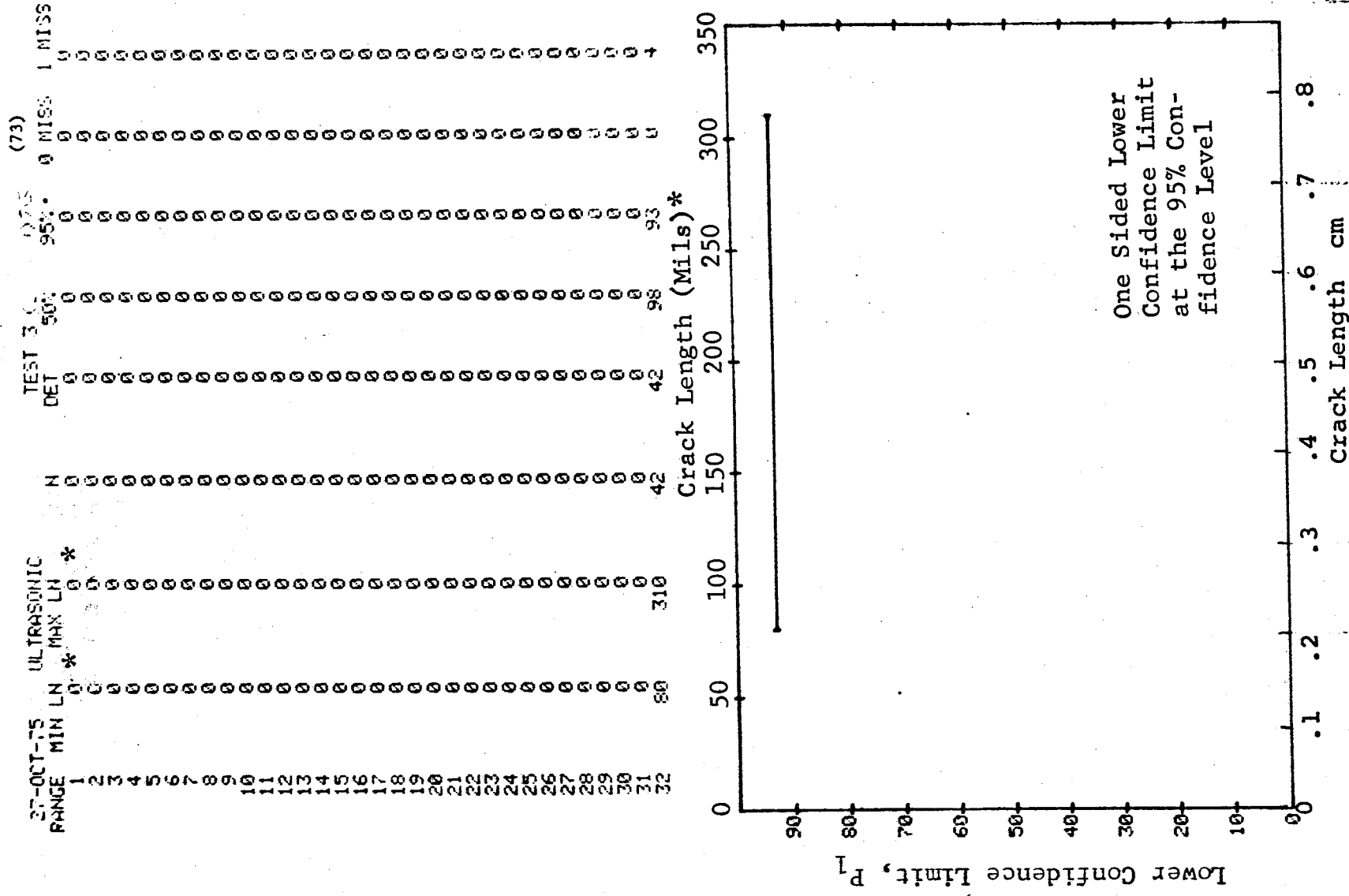


Figure D-73 (Concluded)

(a) Range Interval Method of Data Cumulation

27-OCT-75		ULTRASONIC		N	TEST 1		.077 (74)		0 MISS	1 MISS
RANGE	MIN	LN *	LN *		DET	50%	95%	95%		
1		60	60	12	10	78	56	0	0	0
2		0	0	0	0	0	0	0	0	0
3		0	0	0	0	0	0	0	0	0
4	100	100	100	23	22	92	80	23	38	0
5		0	0	0	0	0	0	0	0	0
6	120	120	120	6	6	89	60	0	0	0
7	130	130	130	5	5	87	54	0	0	0
8	140	140	140	5	5	87	54	0	0	0
9		0	0	0	0	0	0	0	0	0
10	160	160	160	3	2	50	13	0	0	0
11		0	0	0	0	0	0	0	0	0
12	180	180	180	6	6	89	60	0	0	0
13		0	0	0	0	0	0	0	0	0
14		0	0	0	0	0	0	0	0	0
15		0	0	0	0	0	0	0	0	0
16		0	0	0	0	0	0	0	0	0
17	230	230	230	1	1	50	5	0	0	0
18		0	0	0	0	0	0	0	0	0
19		0	0	0	0	0	0	0	0	0
20		0	0	0	0	0	0	0	0	0
21		0	0	0	0	0	0	0	0	0
22		0	0	0	0	0	0	0	0	0
23		0	0	0	0	0	0	0	0	0
24		0	0	0	0	0	0	0	0	0
25	310	310	310	1	1	50	5	0	0	0
26		0	0	0	0	0	0	0	0	0
27		0	0	0	0	0	0	0	0	0
28		0	0	0	0	0	0	0	0	0
29	350	350	350	2	2	70	2	0	0	0
30		0	0	0	0	0	0	0	0	0
31		0	0	0	0	0	0	0	0	0
32	390	390	390	1	1	50	5	0	0	0

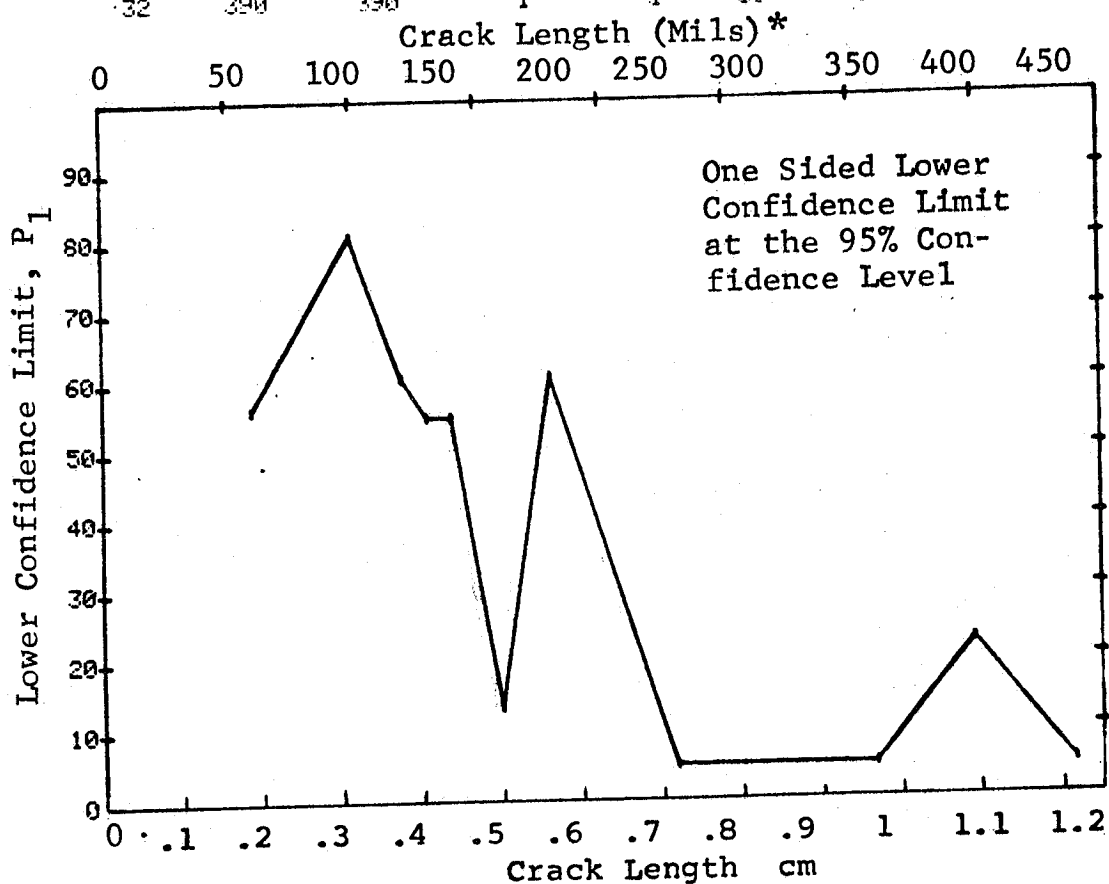


Figure D-74 Probability of Detection for 4340M Steel Using Ultrasonic Shear and Surface Waves. Compressed Notch Flaws in Filleted Hollow Cylinder. Prod. Env. REPRODUCIBILITY OF THE ORIGINAL PAGE IS POOR

(b) Optimum Probability Method of Data Cumulation

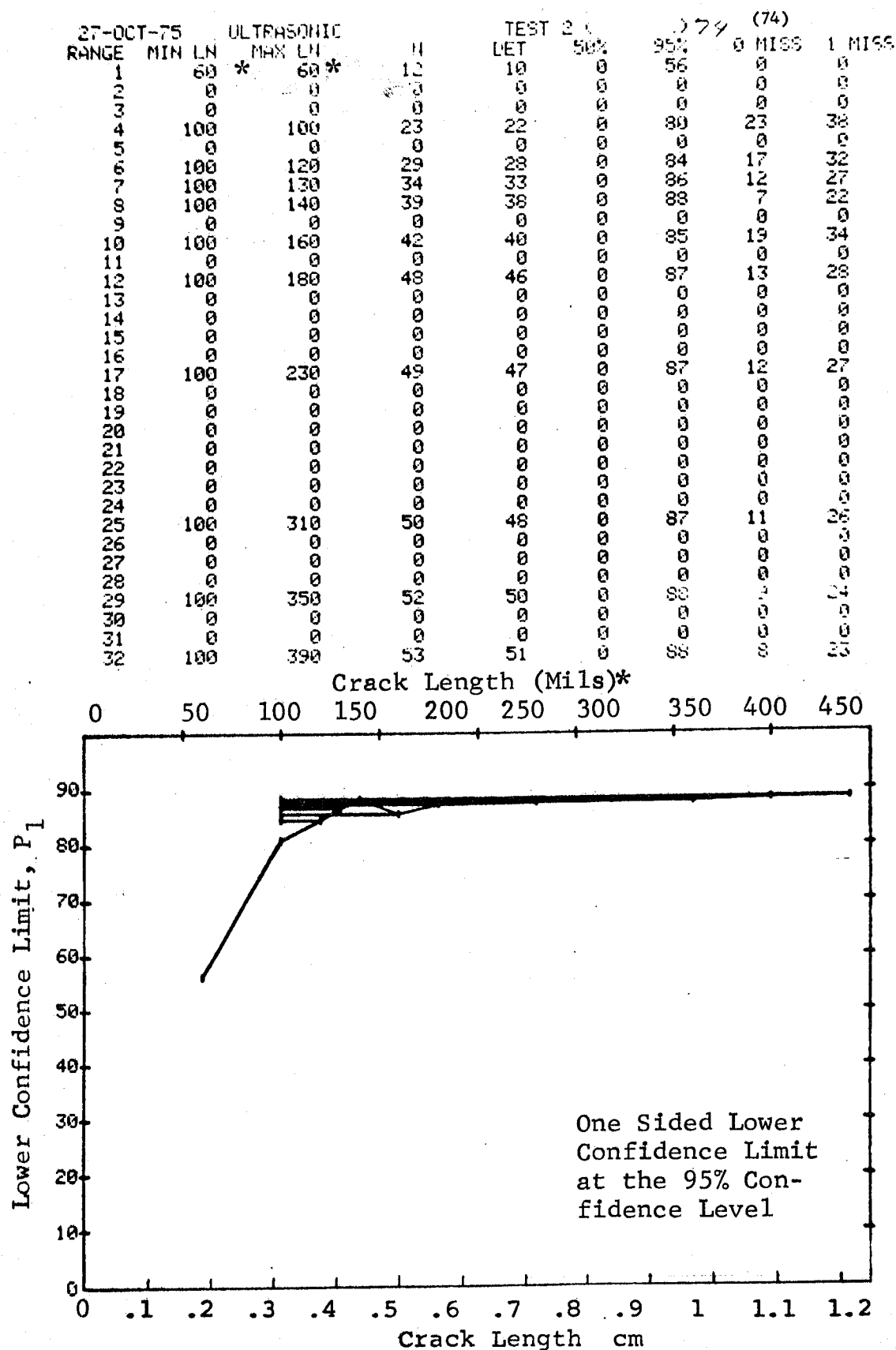


Figure D-74 (Continued)

(c) Overlapping Sixty Point Method of Data Cumulation

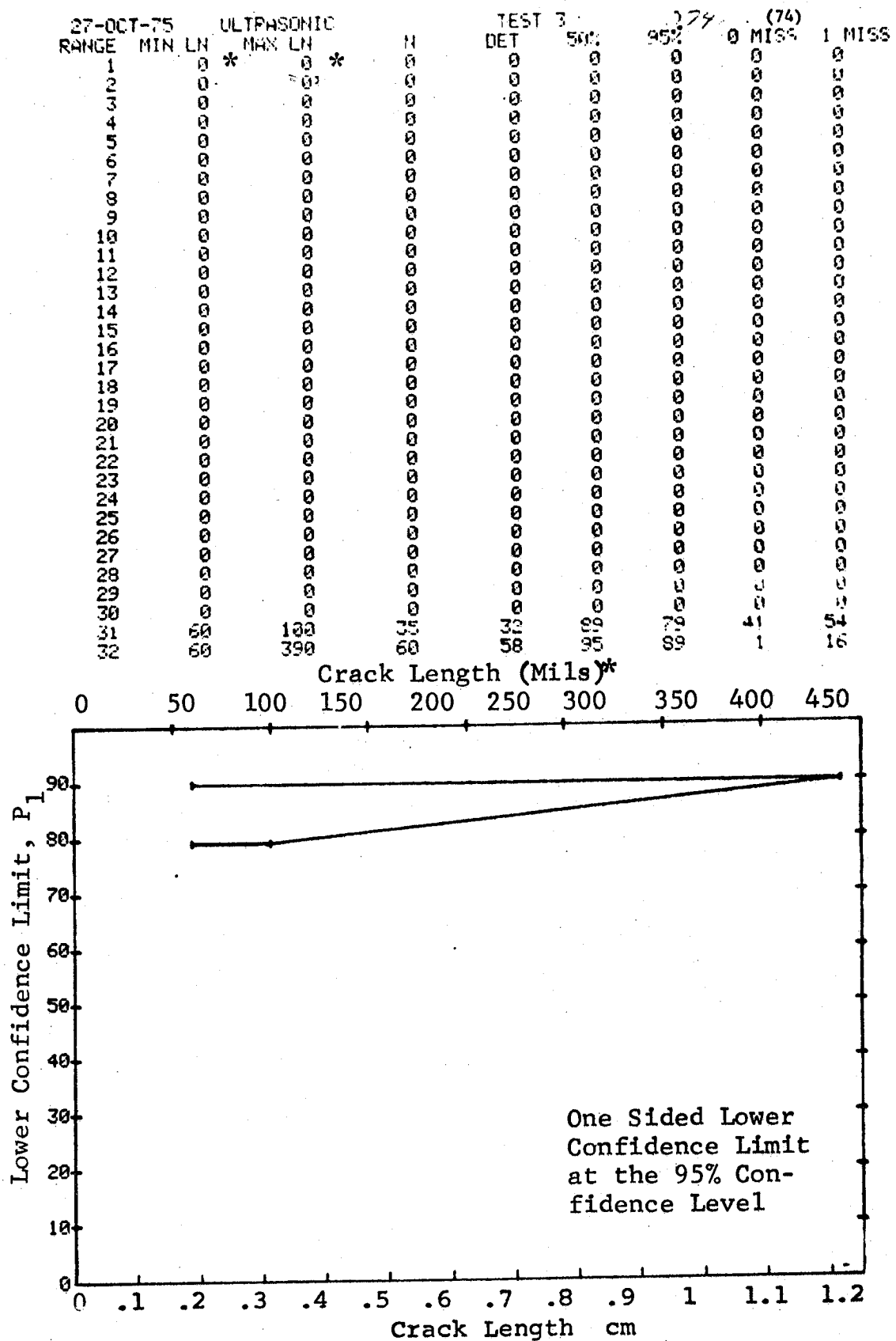


Figure D-74 (Concluded)

(a) Range Interval Method of Data Cumulation

27-OCT-75			ULTRASONIC			N	TEST 1 (75)			0 MISS	1 MISS
RANGE	MIN	LN	* MAX	LN	*		DET	50%	95%		
1		20		30		12	4	29	12	0	0
2		0		0		0	0	0	0	0	0
3		0		0		0	0	0	0	0	0
4		60		60		12	12	94	77	17	34
5		70		70		21	21	96	86	8	25
6		0		0		0	0	0	0	0	0
7		90		90		12	12	94	77	17	34
8		100		100		11	11	93	76	18	35
9		0		0		0	0	0	0	0	0
10		130		130		1	1	50	5	0	0
11		140		140		3	3	79	36	0	0
12		150		150		12	12	94	77	17	34
13		0		0		0	0	0	0	0	0
14		0		0		0	0	0	0	0	0
15		0		0		0	0	0	0	0	0
16		0		0		0	0	0	0	0	0
17		0		0		0	0	0	0	0	0
18		0		0		0	0	0	0	0	0
19		0		0		0	0	0	0	0	0
20		0		0		0	0	0	0	0	0
21		0		0		0	0	0	0	0	0
22		0		0		0	0	0	0	0	0
23		0		0		0	0	0	0	0	0
24		0		0		0	0	0	0	0	0
25		300		300		3	3	79	36	0	0
26		0		0		0	0	0	0	0	0
27		0		0		0	0	0	0	0	0
28		0		0		0	0	0	0	0	0
29		0		0		0	0	0	0	0	0
30		0		0		0	0	0	0	0	0
31		0		0		0	0	0	0	0	0
32		370		380		2	2	70	22	0	0

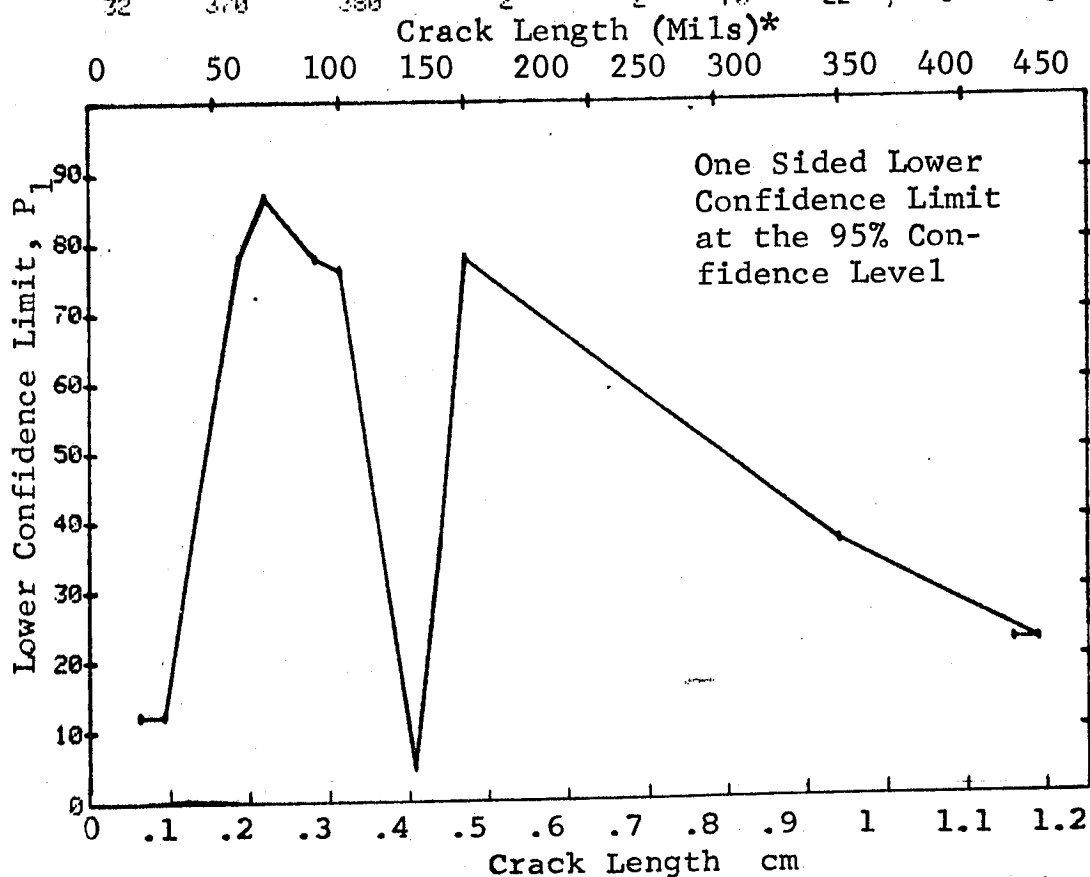


Figure D-75 Probability of Detection for 4340M Steel Using Ultrasonic Shear and Surface Waves. Compressed Notch Flaws in Filleted Solid Cylinder. Prod Env.

(b) Optimum Probability Method of Data Cumulation

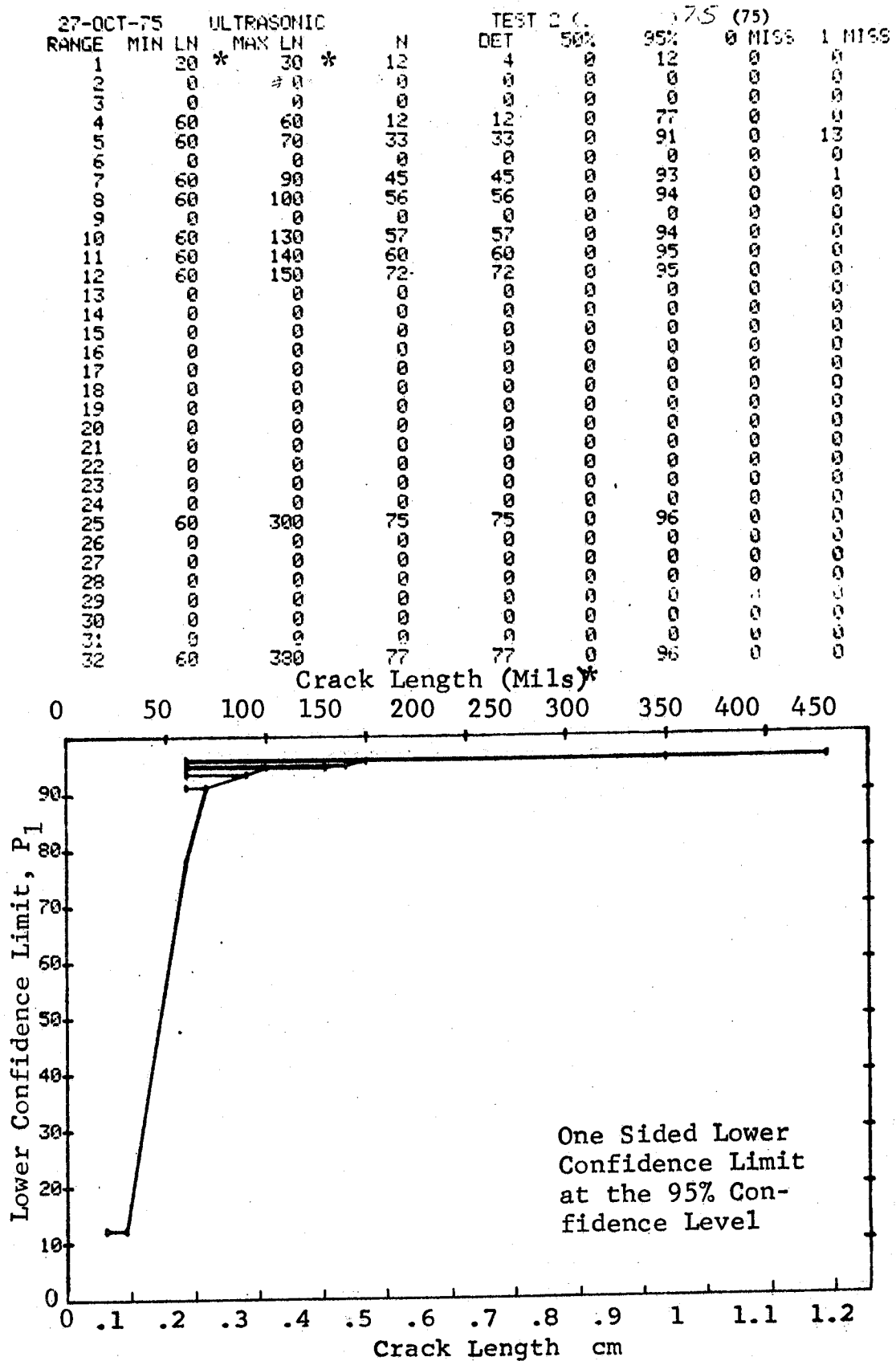


Figure D-75 (Continued)

(c) Overlapping Sixty Point Method of Data Cumulation

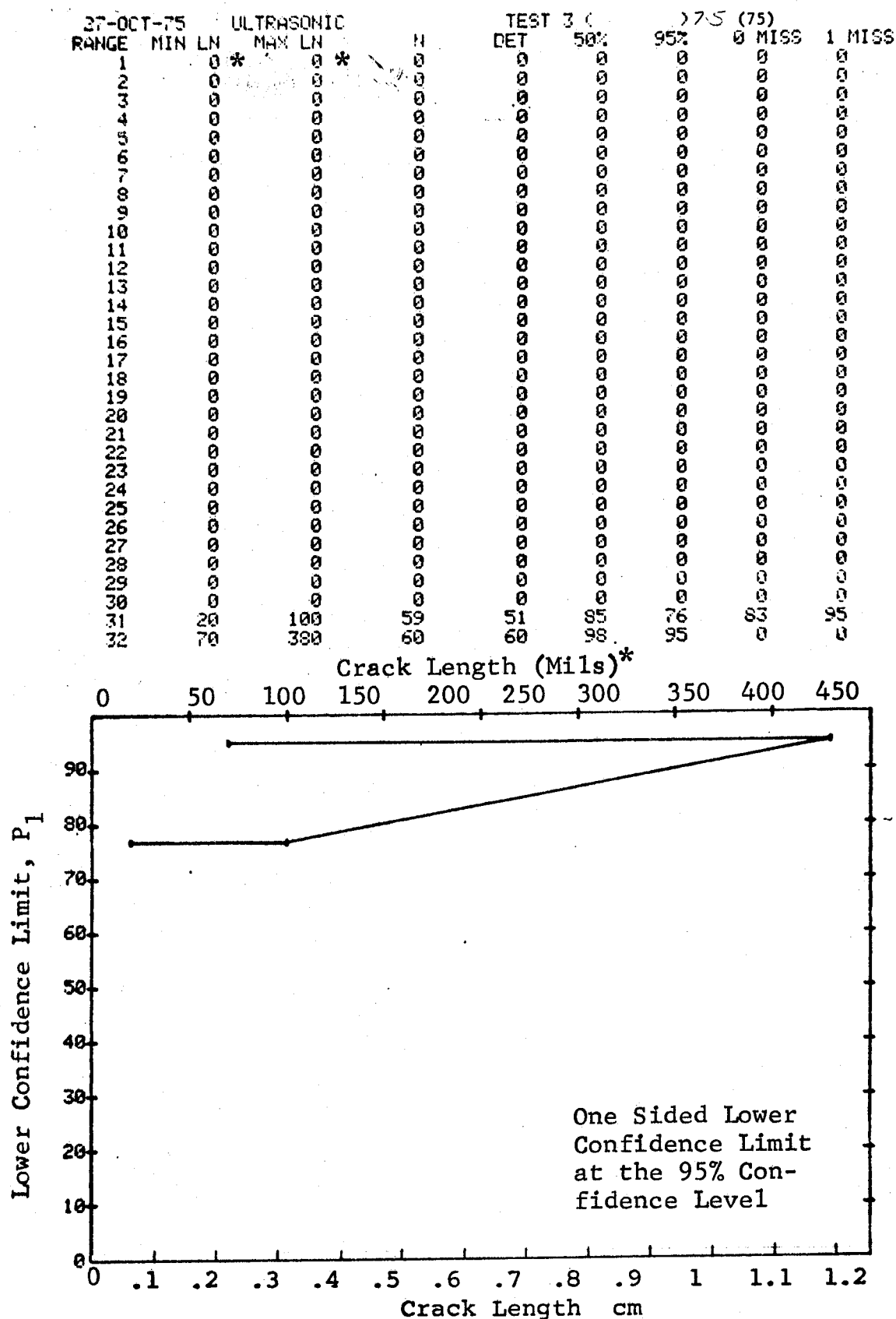


Figure D-75 (Concluded)

(a) Range Interval Method of Data Cumulation

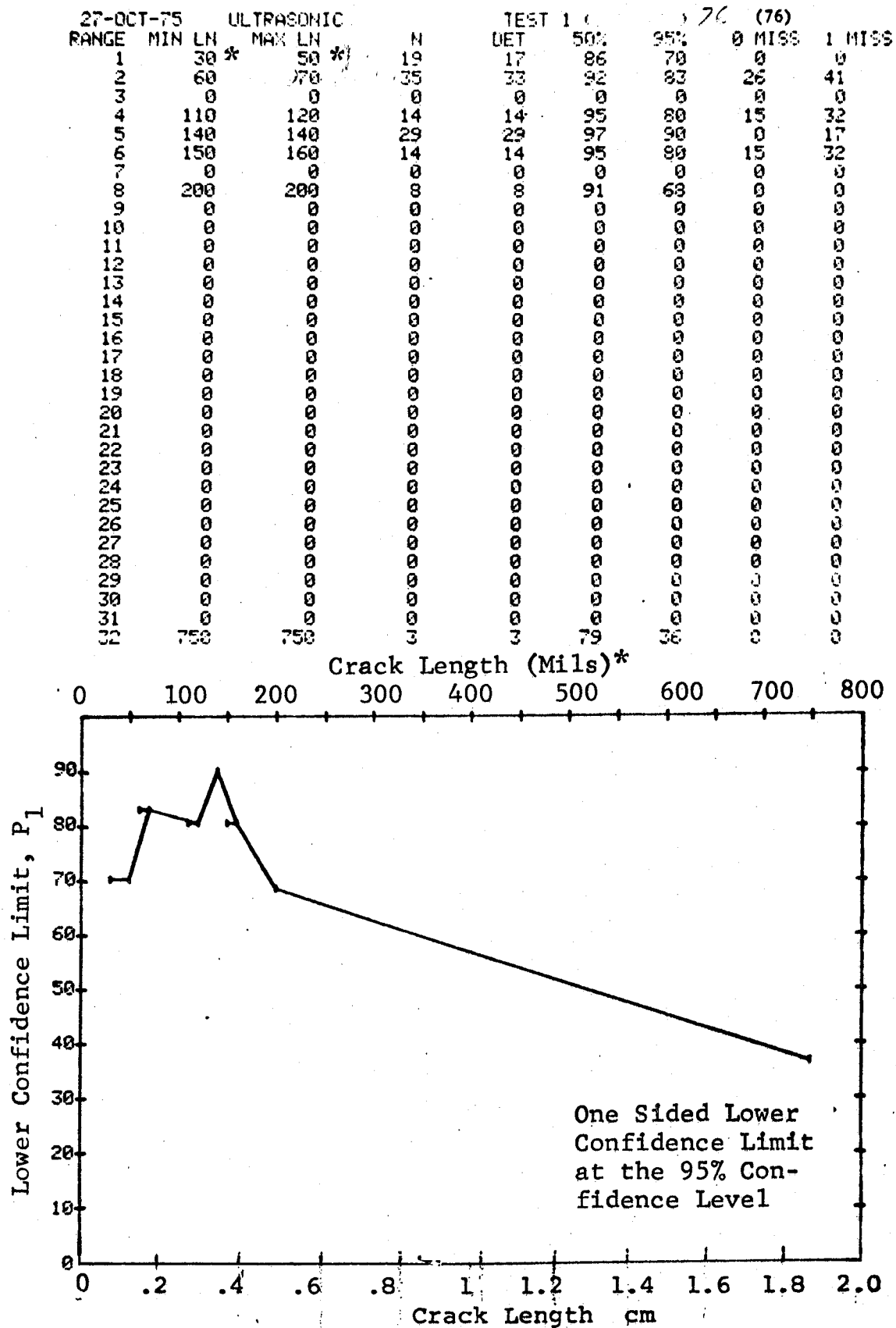


Figure D-76 Probability of Detection for 4340M Steel Using Ultrasonic Shear and Surface Waves. Compressed Notch Flaws in Filleted Solid Cylinder. Prod. Env.

(b) Optimum Probability Method of Data Cumulation

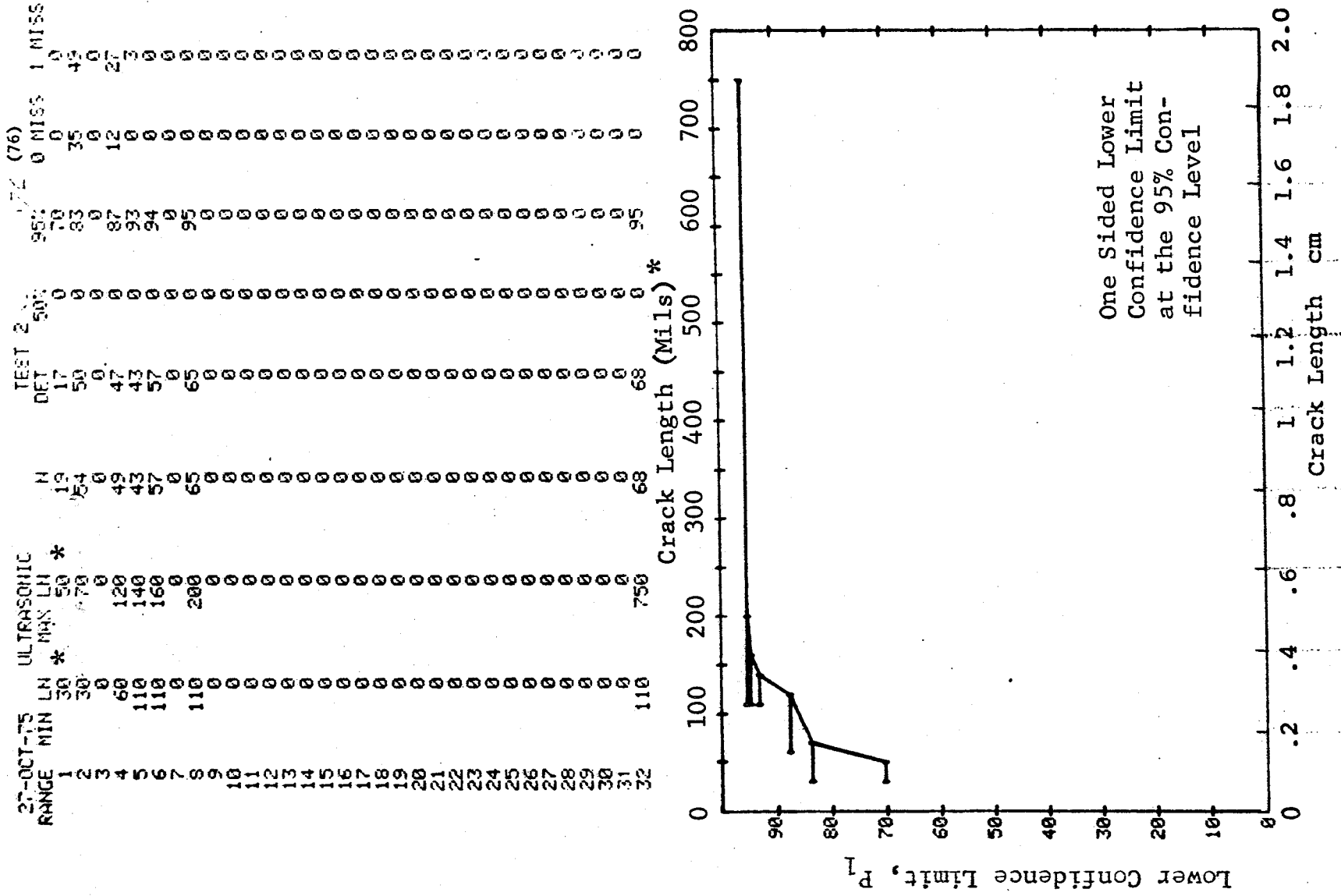


Figure D-76 (Continued)

(c) Overlapping Sixty Point Method of Data Cumulation

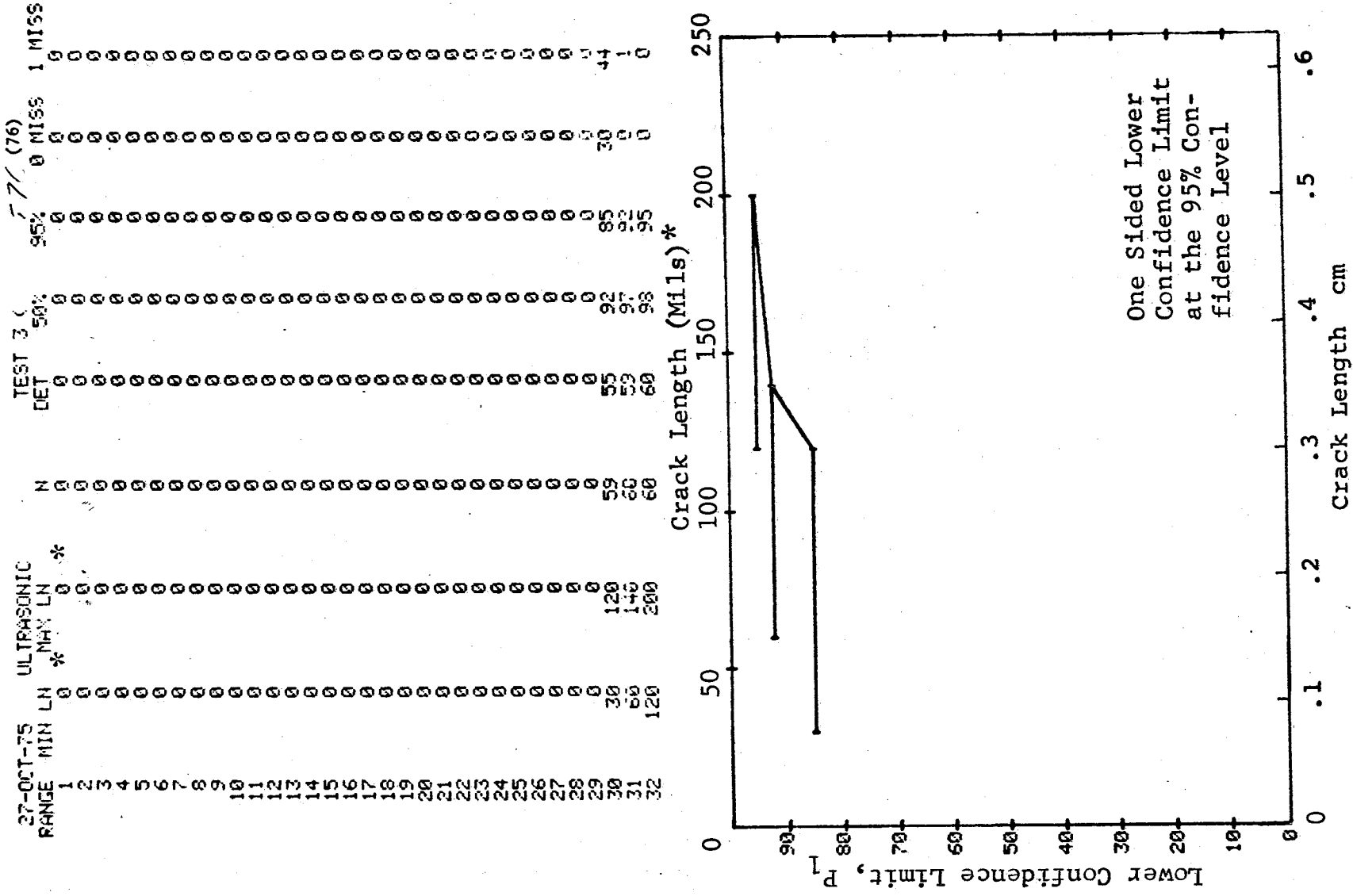


Figure D-76 (Concluded)

D-236

(a) Range Interval Method of Data Cumulation

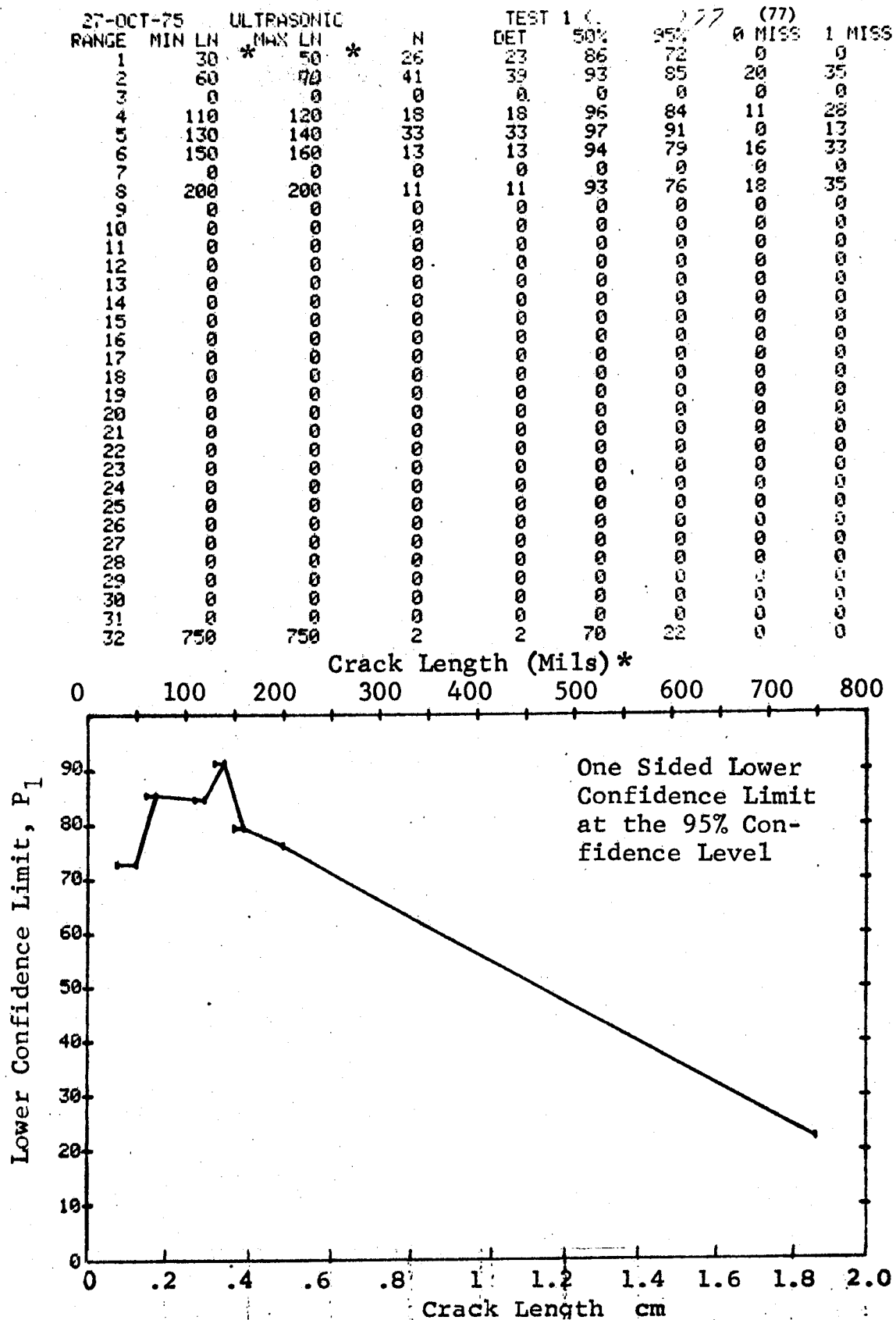


Figure D-77 Probability of Detection for 4340M Steel Using Ultrasonic Shear and Surface Waves, Compressed Notch Flaws in Filleted Solid Cylinder. Lab. Env. D-237

(b) Optimum Probability Method of Data Cumulation

27-OCT-75			ULTRASONIC		N	TEST 2 (77 (77)		MISS
RANGE	MIN	LN	LN	MAX		DET	50%	95%	0	
1	30	60	70	50	25	23	0	72	0	0
2	60	0	0	0	41	39	0	85	20	35
3	0	0	0	0	0	0	0	0	0	0
4	60	0	0	0	59	57	0	89	2	17
5	110	0	0	120	51	51	0	94	0	0
6	110	0	0	140	64	64	0	95	0	0
7	0	0	0	160	0	0	0	0	0	0
8	110	0	0	200	75	75	0	96	0	0
9	0	0	0	0	0	0	0	0	0	0
10	0	0	0	0	0	0	0	0	0	0
11	0	0	0	0	0	0	0	0	0	0
12	0	0	0	0	0	0	0	0	0	0
13	0	0	0	0	0	0	0	0	0	0
14	0	0	0	0	0	0	0	0	0	0
15	0	0	0	0	0	0	0	0	0	0
16	0	0	0	0	0	0	0	0	0	0
17	0	0	0	0	0	0	0	0	0	0
18	0	0	0	0	0	0	0	0	0	0
19	0	0	0	0	0	0	0	0	0	0
20	0	0	0	0	0	0	0	0	0	0
21	0	0	0	0	0	0	0	0	0	0
22	0	0	0	0	0	0	0	0	0	0
23	0	0	0	0	0	0	0	0	0	0
24	0	0	0	0	0	0	0	0	0	0
25	0	0	0	0	0	0	0	0	0	0
26	0	0	0	0	0	0	0	0	0	0
27	0	0	0	0	0	0	0	0	0	0
28	0	0	0	0	0	0	0	0	0	0
29	0	0	0	0	0	0	0	0	0	0
30	0	0	0	0	0	0	0	0	0	0
31	0	0	0	0	0	0	0	0	0	0
32	110	0	0	750	77	77	0	96	0	0

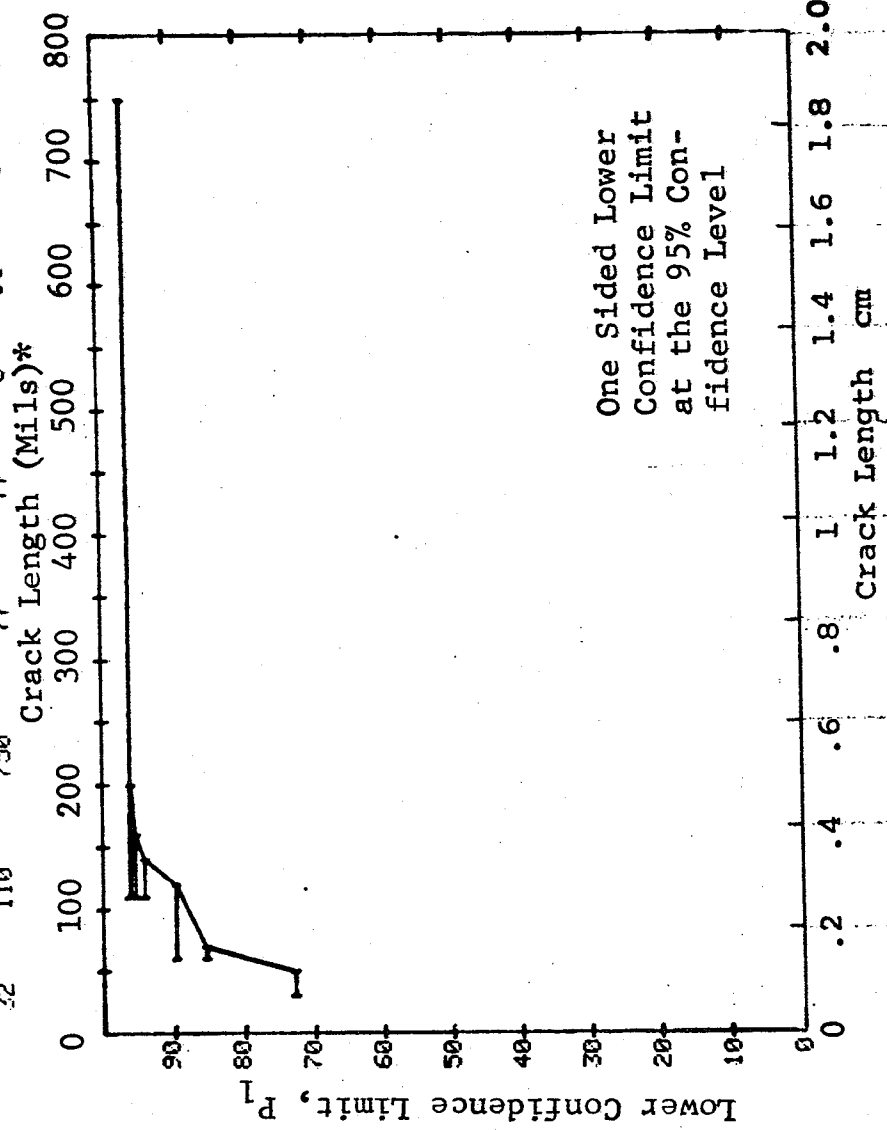


Figure D-77(Continued)

REPRODUCIBILITY OF THE
ORIGINAL PAGE IS POOR

(c) Overlapping Sixty Point Method of Data Cumulation

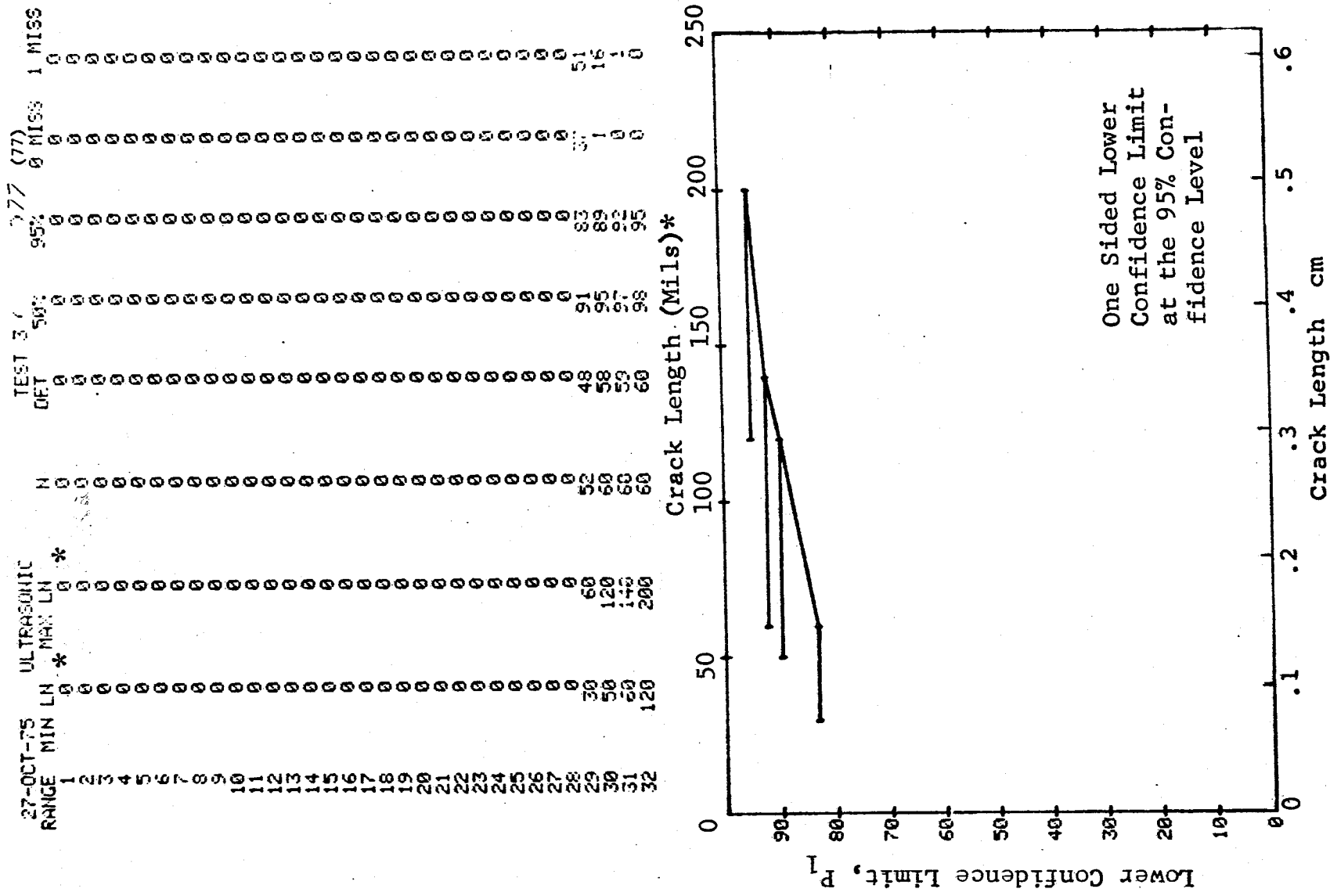


Figure D-77 (Concluded)

(a) Range Interval Method of Data Cumulation

27-OCT-75 RANGE	ULTRASONIC			H	TEST 1		95% MISS		(78)
	MIN	LN	MAX LN *		LET	50%	95%	MISS	
1	0	200	300	15	8	50	29	0	0
2	0	60	60	0	0	0	0	0	0
3	0	70	70	0	7	90	65	0	0
4	0	90	90	15	15	95	81	14	31
5	0	100	100	14	14	95	80	15	30
6	0	0	0	6	6	89	60	0	0
7	0	0	0	7	7	90	0	0	0
8	0	130	140	8	8	91	65	0	0
9	0	150	150	0	0	91	68	0	0
10	0	0	0	0	0	0	0	0	0
11	0	0	0	0	0	0	0	0	0
12	0	200	200	1	1	50	5	0	0
13	0	0	0	0	0	0	0	0	0
14	0	230	230	2	2	70	22	0	0
15	0	240	240	1	1	50	5	0	0
16	0	250	250	2	2	70	22	0	0
17	0	0	0	0	0	0	0	0	0
18	0	280	280	1	1	50	5	0	0
19	0	300	300	2	2	70	22	0	0
20	0	0	0	0	0	0	0	0	0
21	0	0	0	0	0	0	0	0	0
22	0	0	0	0	0	0	0	0	0
23	0	0	0	0	0	0	0	0	0
24	370	370	370	2	2	70	22	0	0
25	390	390	390	2	2	70	22	0	0
26	410	410	410	1	1	50	5	0	0
27	0	0	0	0	0	0	0	0	0
28	0	0	0	0	0	0	0	0	0
29	0	0	0	0	0	0	0	0	0
30	0	0	0	0	0	0	0	0	0
31	0	0	0	0	0	0	0	0	0
32	500	500	500	1	1	50	5	0	0

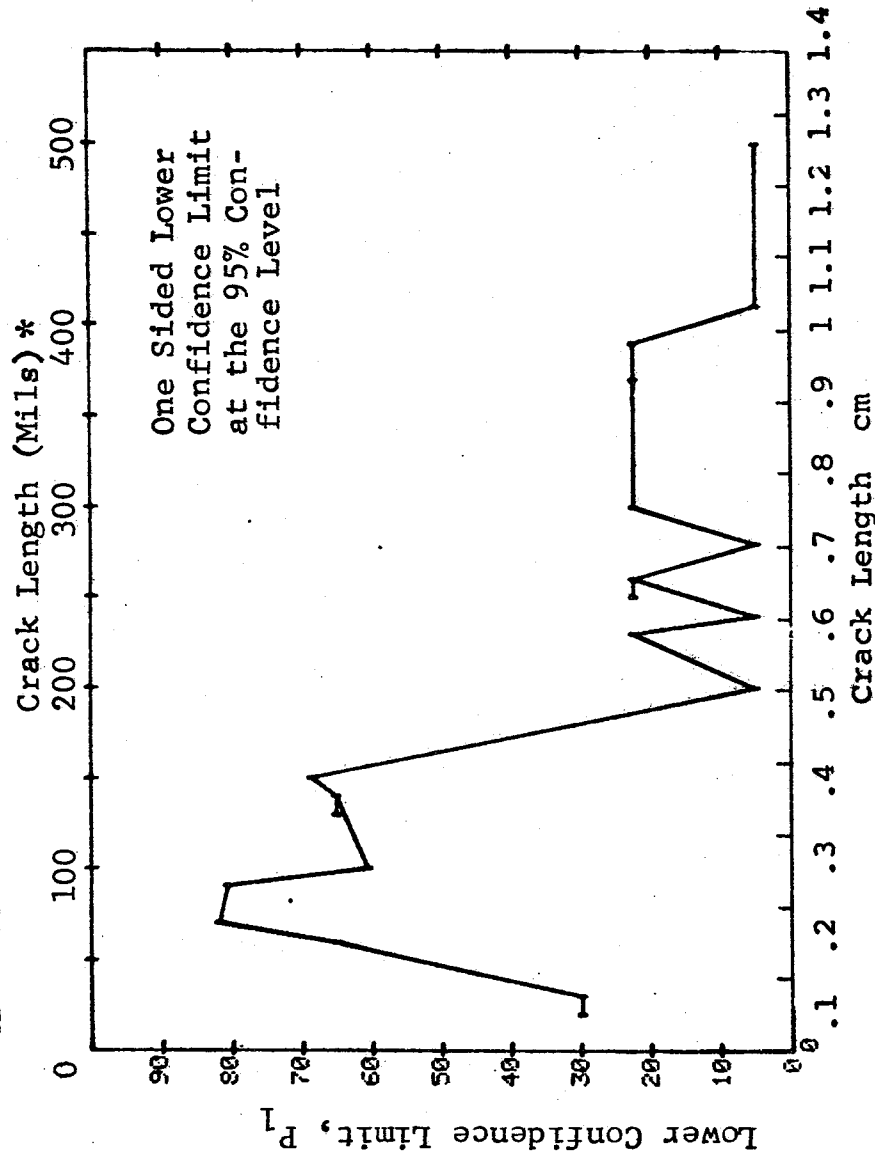


Figure D-78 Probability of Detection for 4340M Steel Using Ultrasonic Shear and Surface Waves. Compressed Notch Flaws in Filleted Solid Cylinder. Lab. Env. D-240

(b) Optimum Probability Method of Data Cumulation

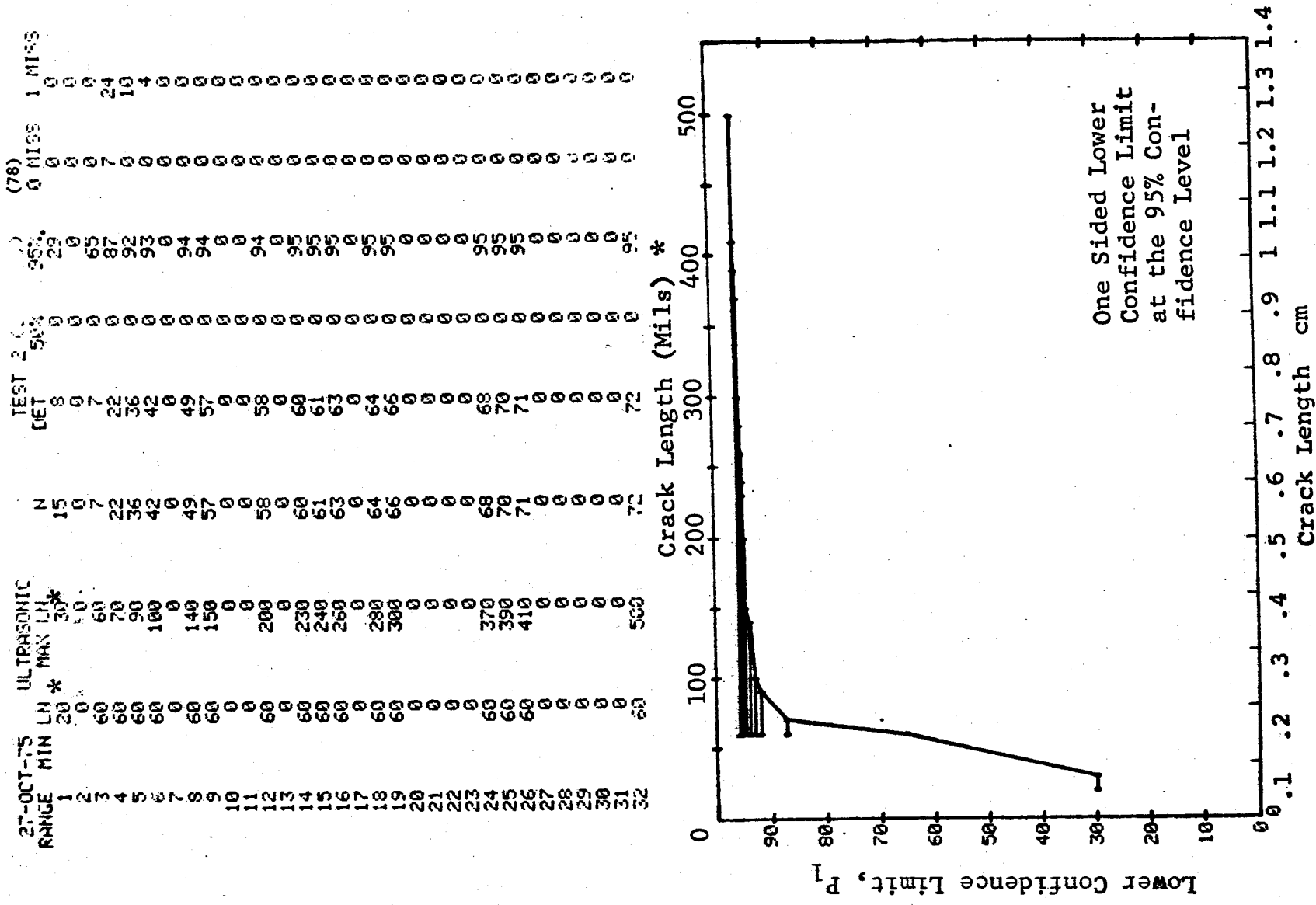


Figure D-78 (Continued)

(c) Overlapping Sixty Point Method of Data Cumulation

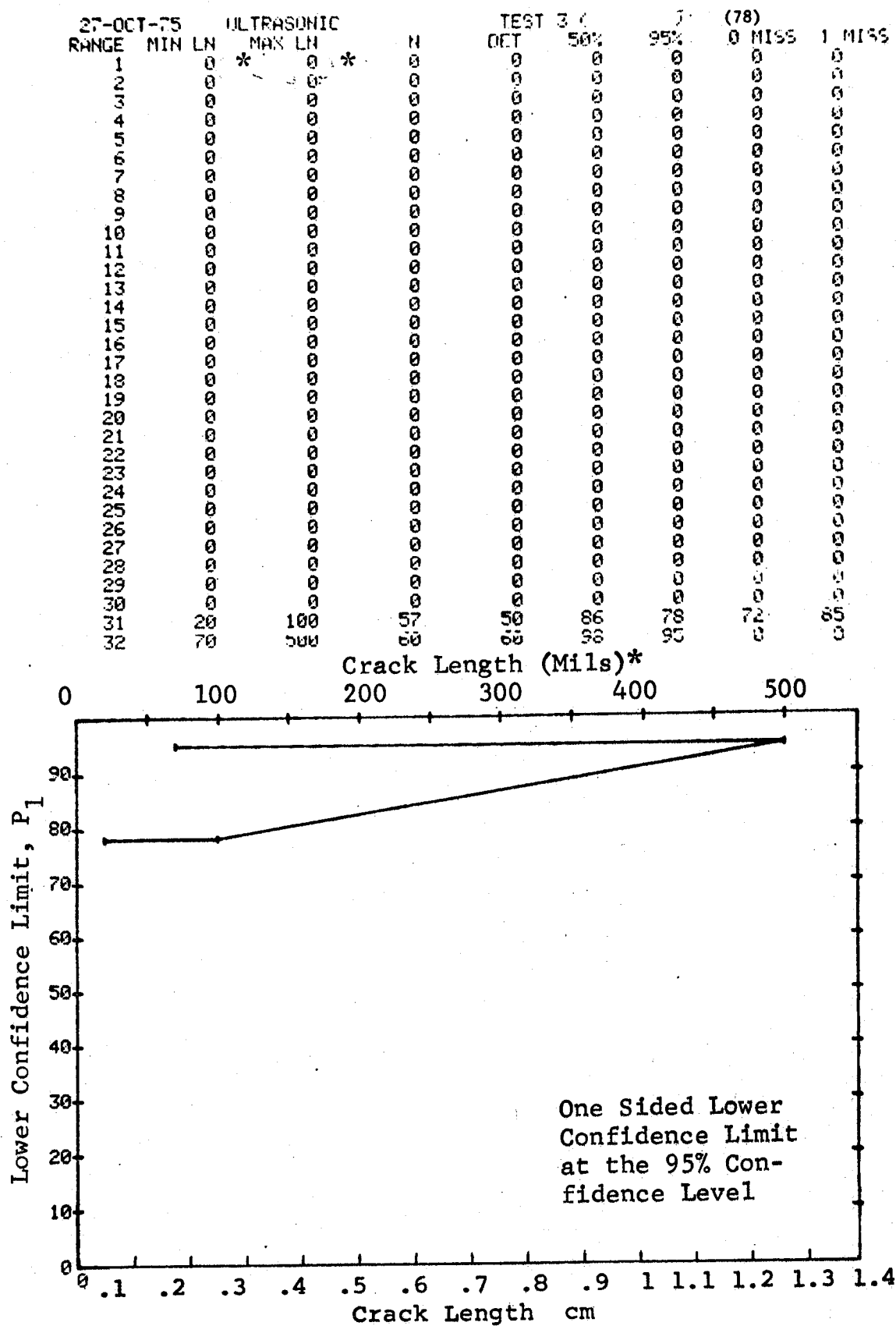


Figure D-78 (Concluded)

(a) Range Interval Method of Data Cumulation

27-OCT-75	ULTRASONIC	TEST 1	(79)	1 MISS
RANGE MIN LN*	MAX LN *	DET	95%	MISS
1 60	60	17	83	12
2 0	0	0	0	0
3 0	0	0	0	0
4 0	0	0	0	0
5 0	0	0	0	0
6 0	0	0	0	0
7 0	0	0	0	0
8 0	0	0	0	0
9 0	0	0	0	0
10 0	0	0	0	0
11 0	0	0	0	0
12 0	0	0	0	0
13 0	0	0	0	0
14 0	0	0	0	0
15 0	0	0	0	0
16 100	100	23	87	6
17 0	0	0	0	0
18 0	0	0	0	0
19 0	0	0	0	0
20 0	0	0	0	0
21 0	0	0	0	0
22 0	0	0	0	0
23 0	0	0	0	0
24 0	0	0	0	0
25 0	0	0	0	0
26 0	0	0	0	0
27 130	130	6	60	0
28 0	0	0	0	0
29 0	0	0	0	0
30 0	0	0	0	0
31 0	0	1	50	0
32 140	140	0	0	0

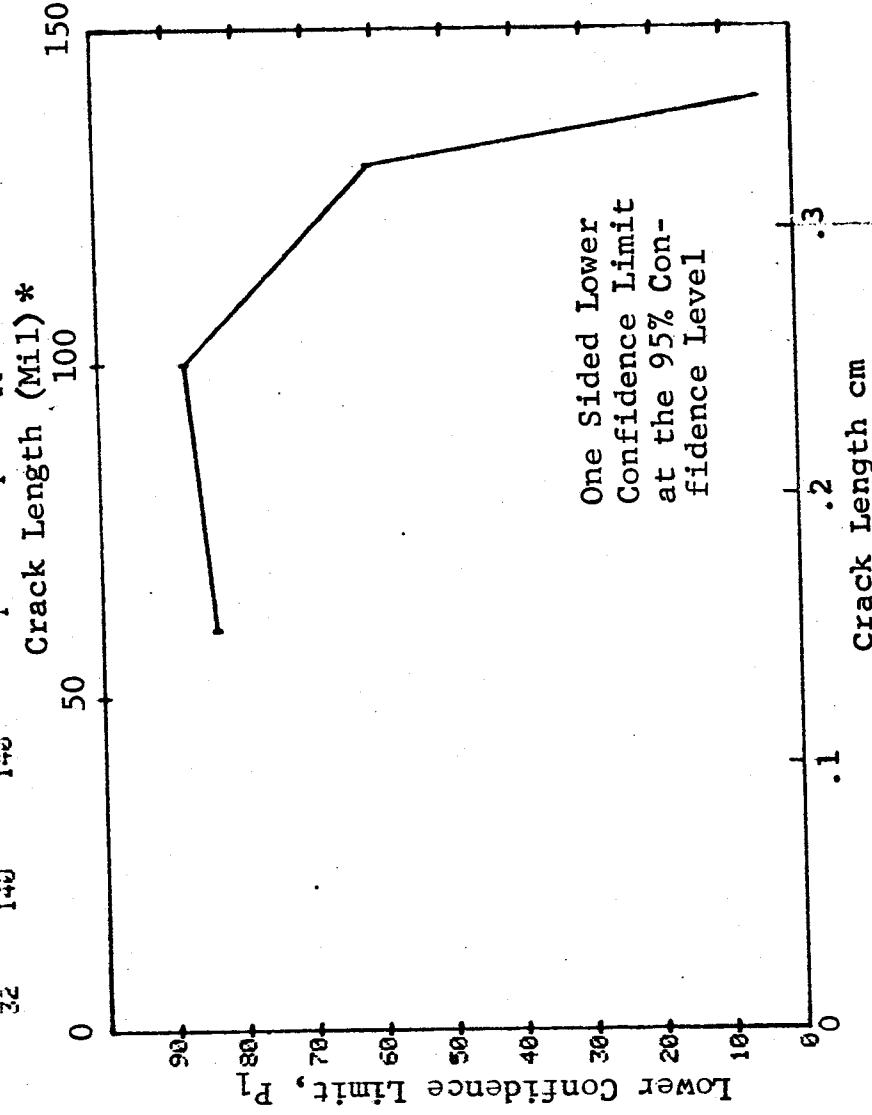


Figure D-79 Probability of Detection for 4340M Steel Using Ultrasonic Shear and Surface Waves. Compressed Notch Flaws in Hollow Cylinder. Lab. Env.

(b) Optimum Probability Method of Data Cumulation

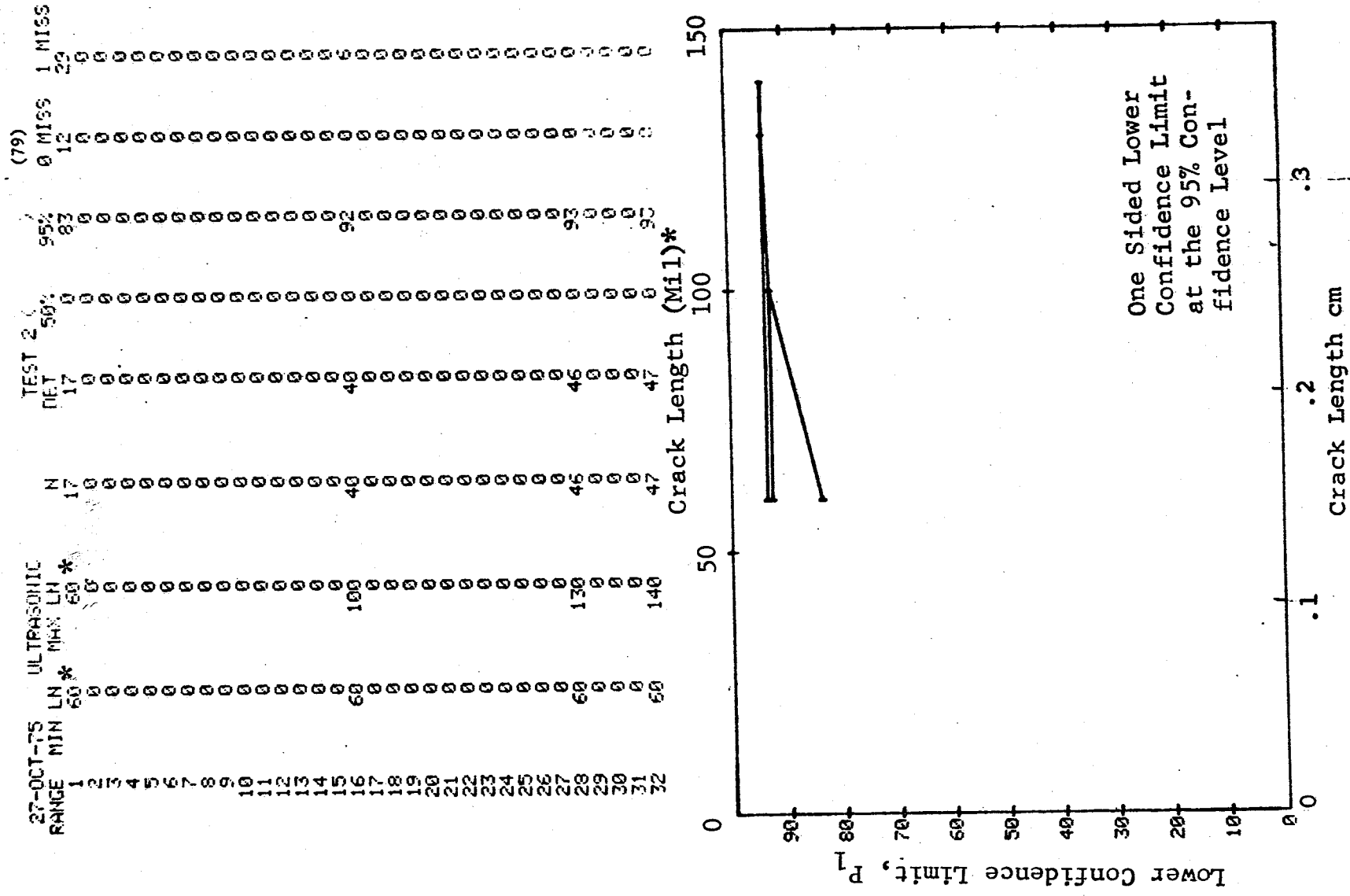


Figure D-79 (Continued)

(c) Overlapping Sixty Point Method of Data Cumulation

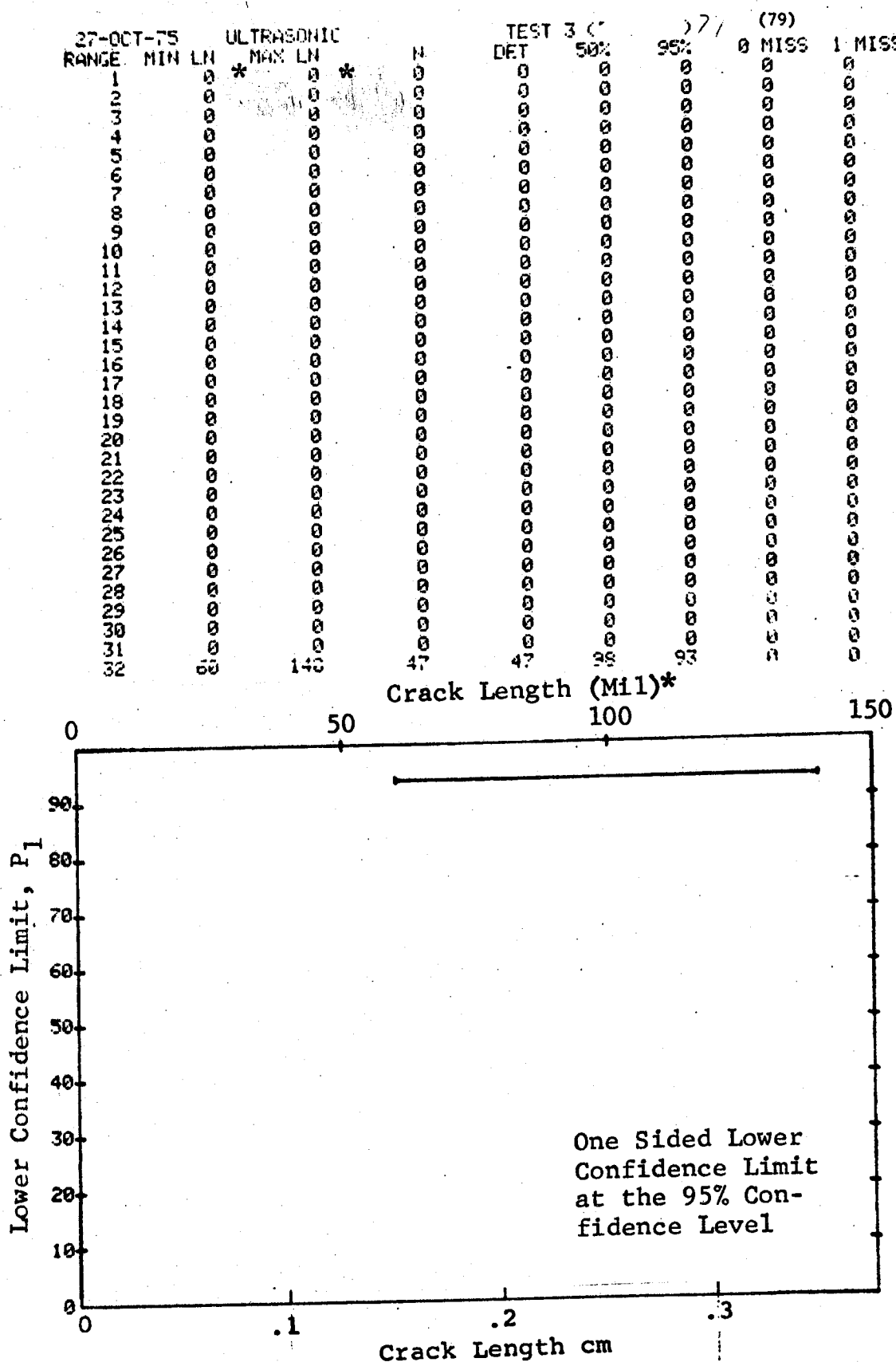


Figure D-79 (Concluded)

(a) Range Interval Method of Data Cumulation

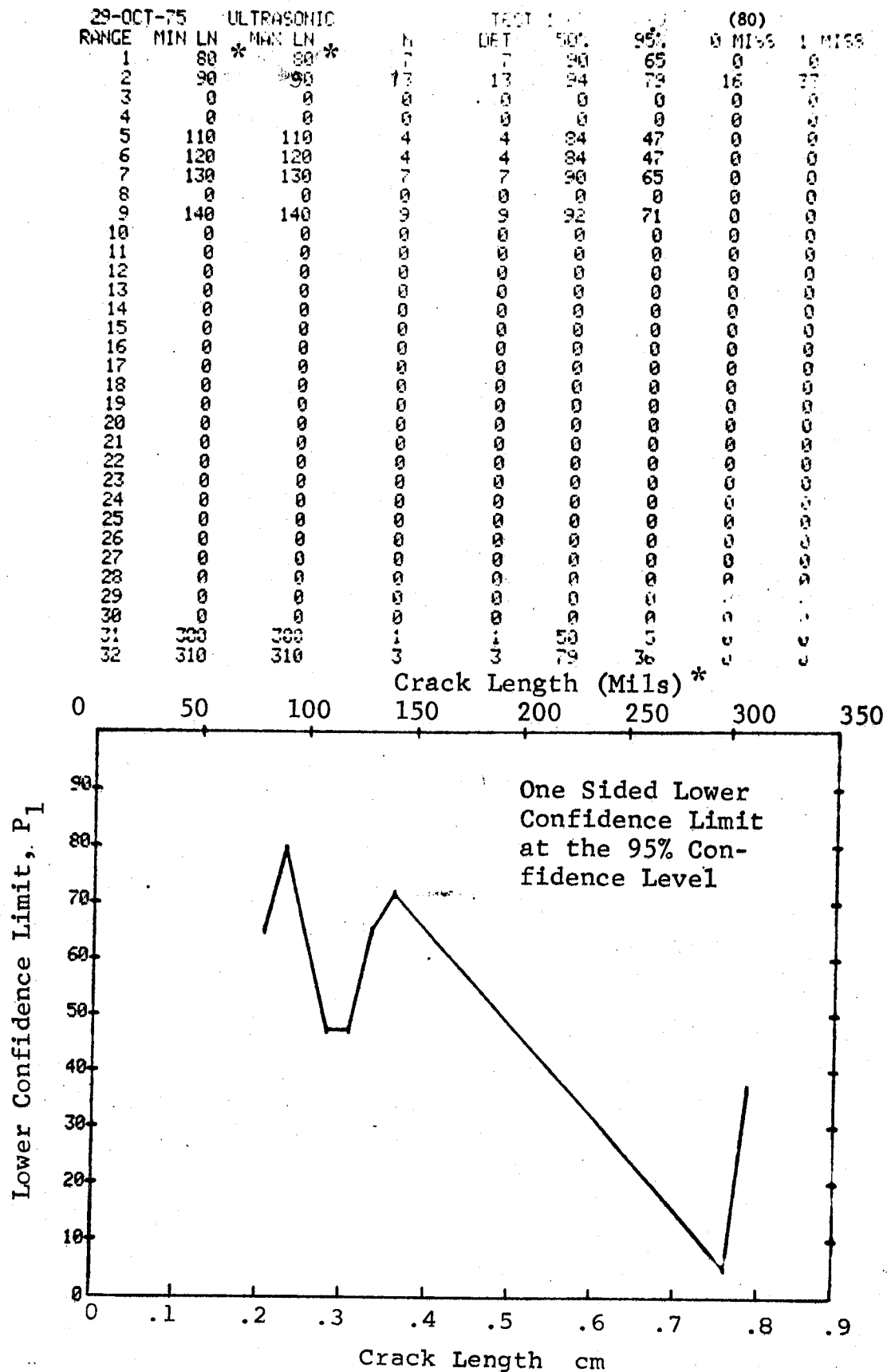


Figure D-80 Probability of Detection for 4340M Steel Using Ultrasonic Shear and Surface Waves. Compressed Notch Flaws in Filleted Hollow Cylinder. Lab. Env.

(b) Optimum Probability Method of Data Cumulation

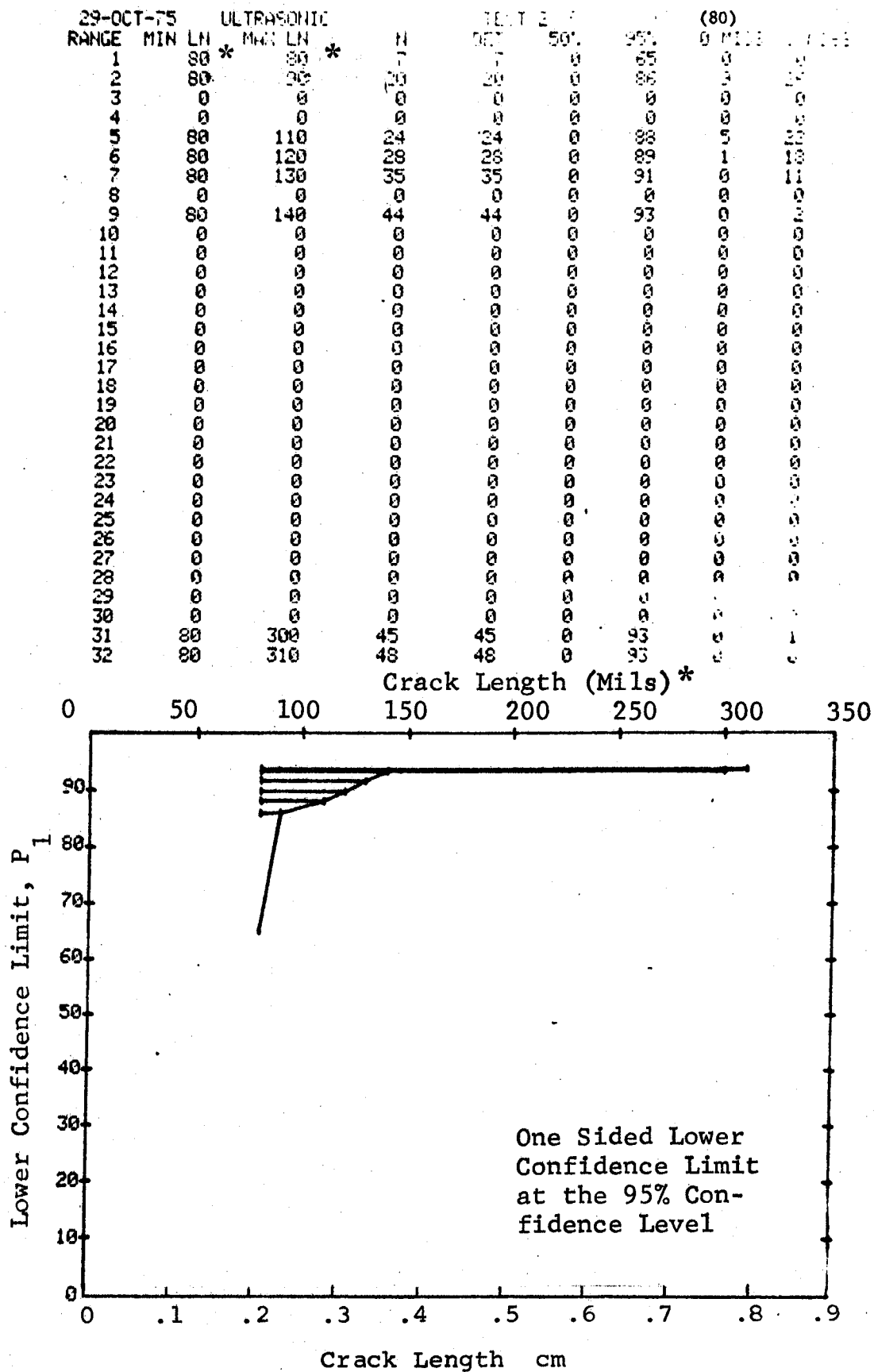


Figure D-80 (Continued)

(c) Overlapping Sixty Point Method of Data Cumulation

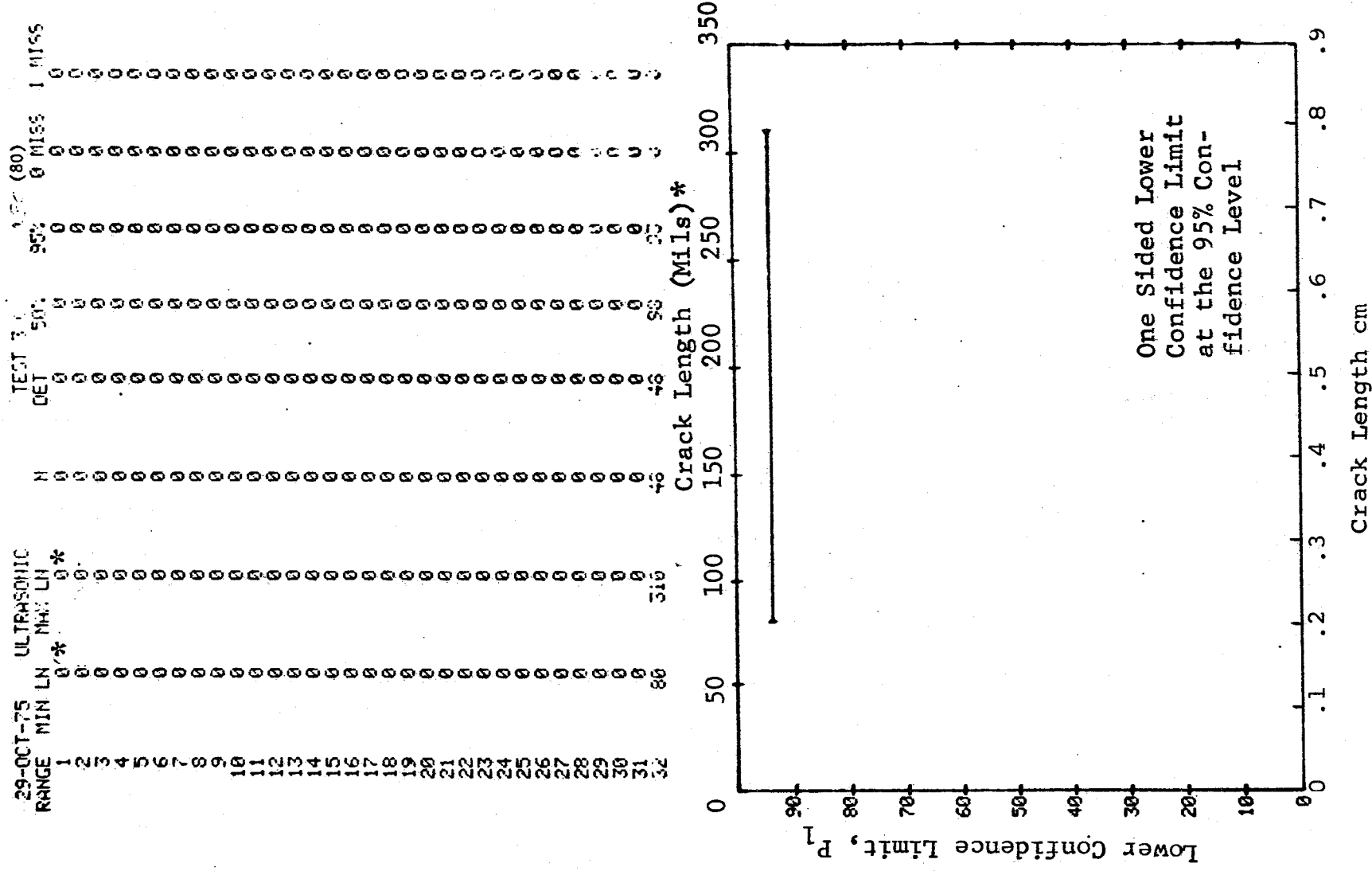


Figure D-80 (Concluded)

(a) Range Interval Method of Data Cumulation

27-OCT-75			ULTRASONIC		TEST 1		77(81)		1 MISS	
RANGE	MIN	LN	MAX	LN	DET	50%	95%	0 MISS	0 MISS	1 MISS
1	10	0	10*	0	4	57	27	0	0	0
2	30	0	30	0	0	0	0	0	0	0
3	40	0	40	0	0	0	0	0	0	0
4	50	0	50	0	0	0	0	0	0	0
5	60	0	60	0	8	67	43	0	0	0
6	70	0	70	0	11	50	32	0	0	0
7	80	0	80	0	0	0	0	0	0	0
8	90	0	90	0	7	58	34	0	0	0
9	100	0	100	0	6	89	60	0	0	0
10	110	0	110	0	0	0	0	0	0	0
11	120	0	120	0	0	0	0	0	0	0
12	130	0	130	0	0	0	0	0	0	0
13	140	0	140	0	7	90	65	0	0	0
14	150	0	150	0	10	72	50	0	0	0
15	160	0	160	0	0	0	0	0	0	0
16	170	0	170	0	9	92	71	0	0	0
17	180	0	180	0	19	83	68	0	0	0
18	190	0	190	0	1	29	2	0	0	0
19	200	0	200	0	0	0	0	0	0	0
20	210	0	210	0	9	92	71	0	0	0
21	220	0	220	0	8	74	49	0	0	0
22	230	0	230	0	0	0	0	0	0	0
23	240	0	240	0	21	96	86	0	0	0
24	250	0	250	0	4	84	47	0	0	0
25	260	0	260	0	0	0	0	0	0	0
26	270	0	270	0	8	91	68	0	0	0
27	280	0	280	0	12	94	77	0	0	0
28	290	0	290	0	5	87	54	0	0	0
29	300	0	300	0	0	0	0	0	0	0
30	310	0	310	0	0	0	0	0	0	0
31	320	0	320	0	1	50	5	0	0	0
32	330	0	330	0	2	70	22	0	0	0
33	340	0	340	0	3	76	33	0	0	0

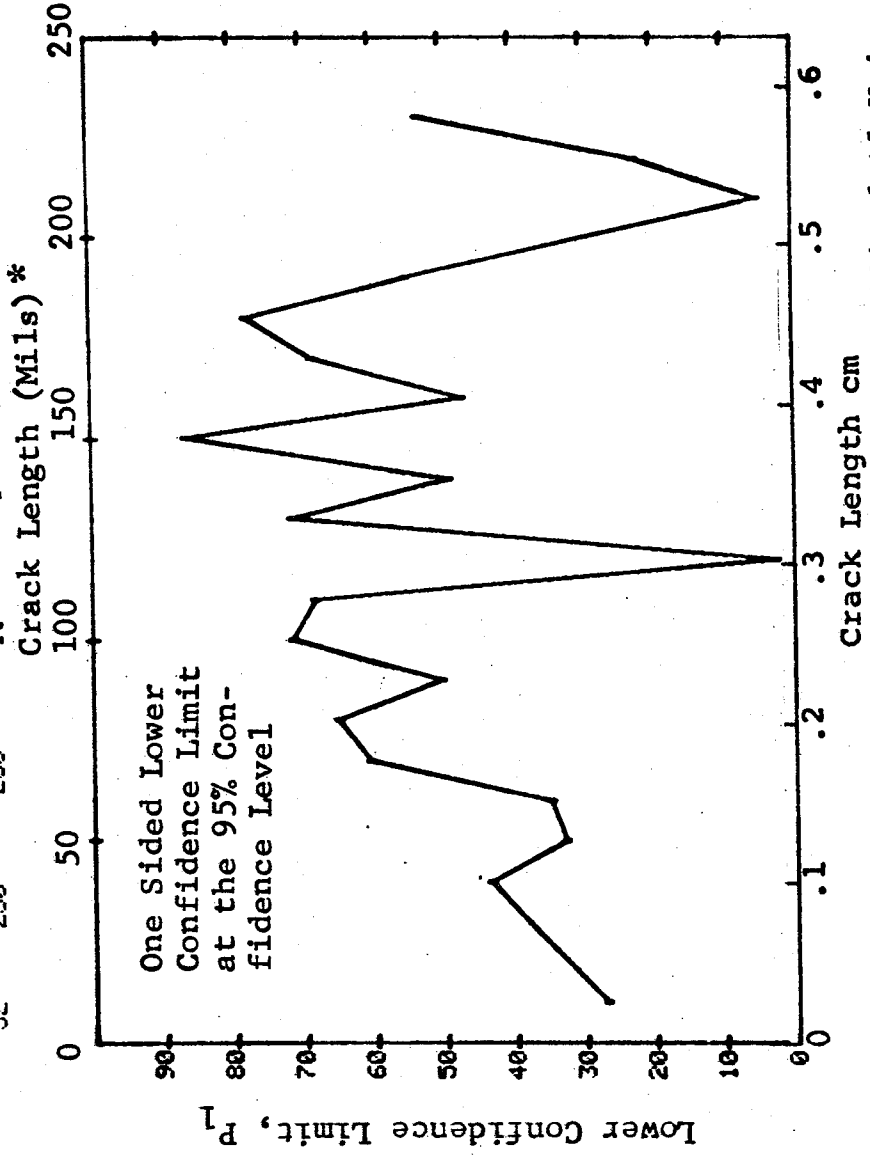


Figure D-81 Probability of Detection for 2024-T6 Al Using Ultrasonic Shear and Surface Waves. Compressed Notch Flaws in Tandem T Specimen. Lab. Env.

(b) Optimum Probability Method of Data Cumulation

27-OCT-75 RANGE	MIN	LN	ULTRASONIC 10*	MAX LN	10*	N	TEST 2 OFT	50%	35%	(81) MISS	MISS
1	10	0	0	0	0	6	4	0	35	0	0
2	10	0	0	0	0	0	0	0	27	0	0
3	10	0	0	30	0	0	0	0	0	0	0
4	10	0	0	0	0	9	4	0	16	0	0
5	40	0	0	0	0	0	0	0	0	0	0
6	40	0	0	40	0	11	8	0	43	0	0
7	40	0	0	50	0	32	19	0	43	0	0
8	40	0	0	0	0	0	0	0	0	0	0
9	70	0	0	60	0	43	26	0	46	0	0
10	70	0	0	70	0	6	6	0	60	0	0
11	70	0	0	0	0	0	0	0	0	0	0
12	70	0	0	90	0	13	13	0	79	0	0
13	70	0	0	0	0	26	23	0	72	0	0
14	70	0	0	0	0	0	0	0	0	0	0
15	70	0	0	100	0	35	32	0	79	0	0
16	70	0	0	110	0	57	51	0	80	0	0
17	70	0	0	120	0	59	52	0	78	0	0
18	70	0	0	0	0	0	0	0	0	0	0
19	70	0	0	130	0	68	61	0	81	0	0
20	70	0	0	140	0	78	69	0	80	0	0
21	150	0	0	0	0	0	0	0	0	0	0
22	150	0	0	150	0	21	21	0	86	0	0
23	150	0	0	160	0	25	25	0	88	0	0
24	150	0	0	0	0	0	0	0	0	0	0
25	150	0	0	170	0	33	33	0	91	0	0
26	150	0	0	180	0	45	45	0	93	0	0
27	150	0	0	190	0	0	0	0	0	0	0
28	150	0	0	0	0	50	50	0	94	0	0
29	150	0	0	0	0	0	0	0	0	0	0
30	150	0	0	210	0	0	0	0	0	0	0
31	150	0	0	220	0	51	51	0	94	0	0
32	150	0	0	230	0	53	53	0	94	0	0
						64	62	0	90	0	12

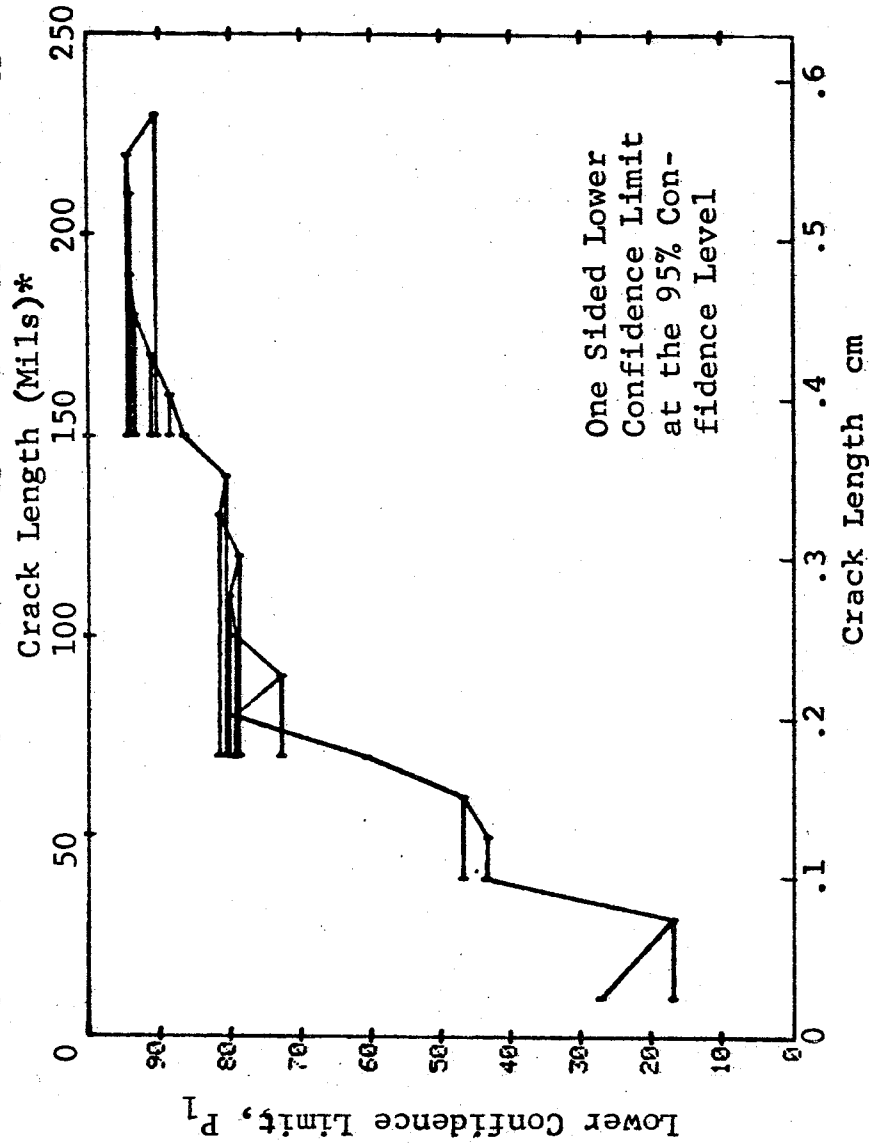


Figure D-81 (Continued)

(c) Overlapping Sixty Point Method of Data Cumulation

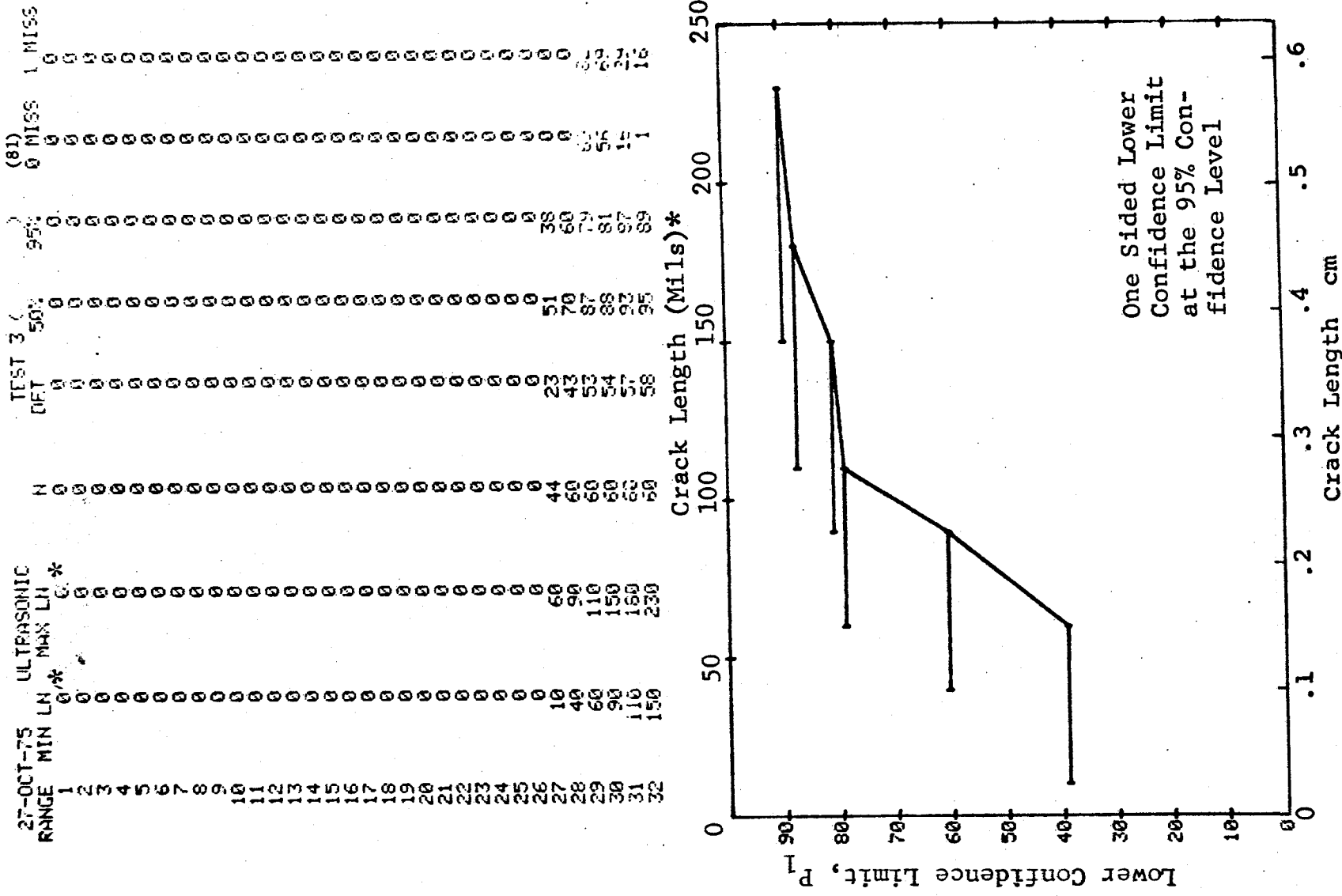


Figure D-81 (Concluded)

(a) Range Interval Method of Data Cumulation

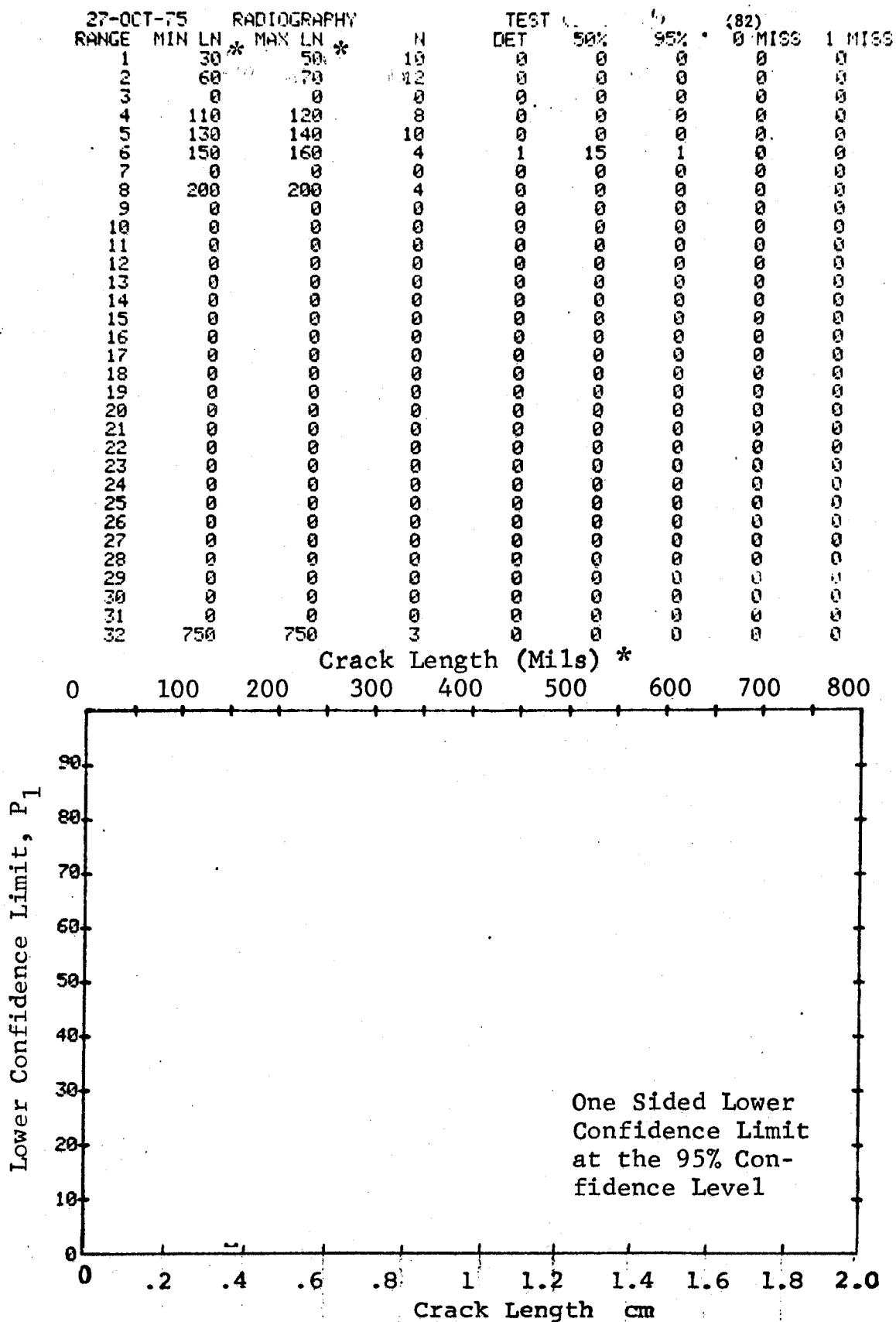


Figure D-82 Probability of Detection for 4340M Steel Using X-ray. Compressed Notch Flaws in Solid Cylinder. Prod. Env.

(b) Optimum Probability Method of Data Cumulation

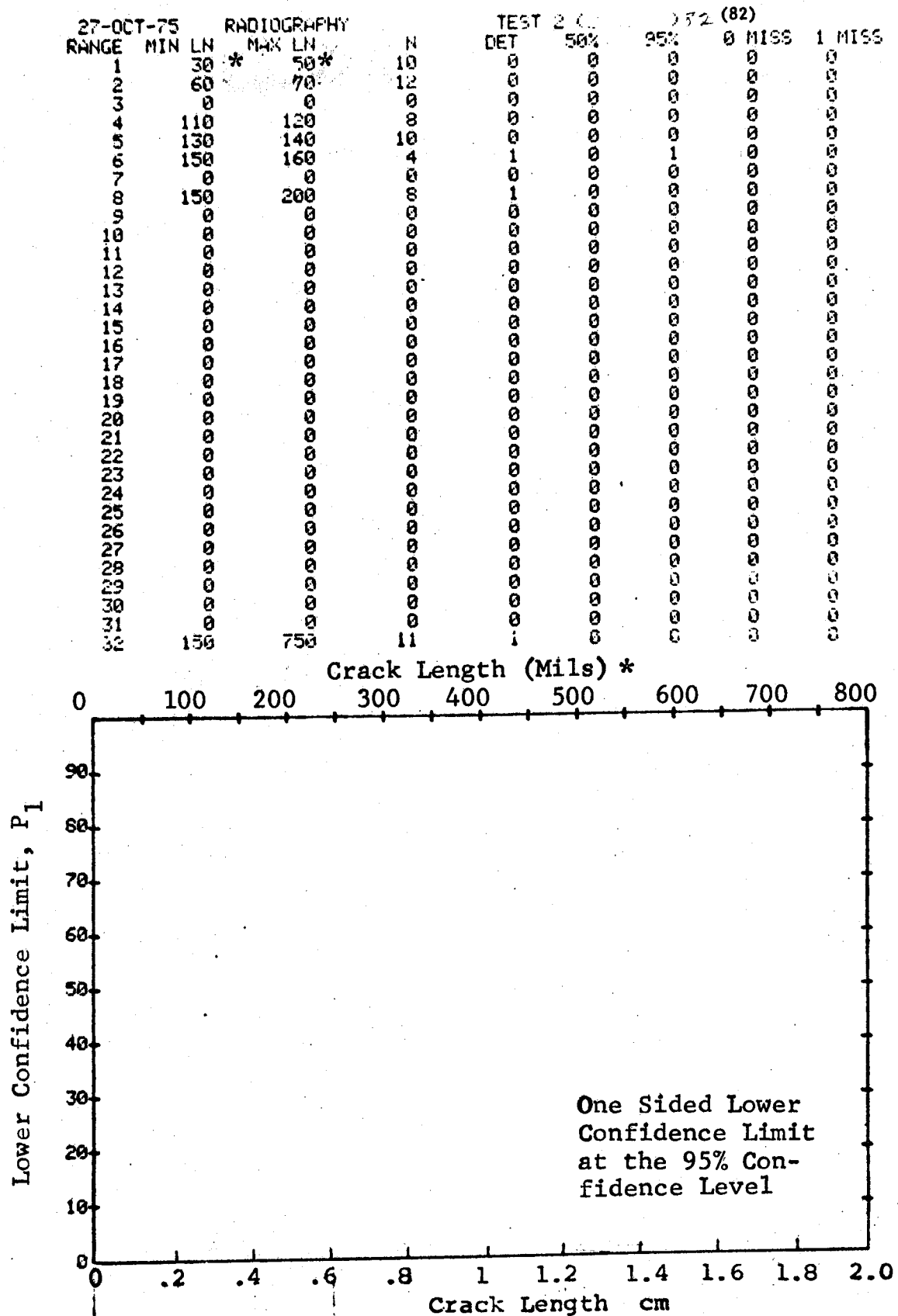


Figure D-82 (Continued)

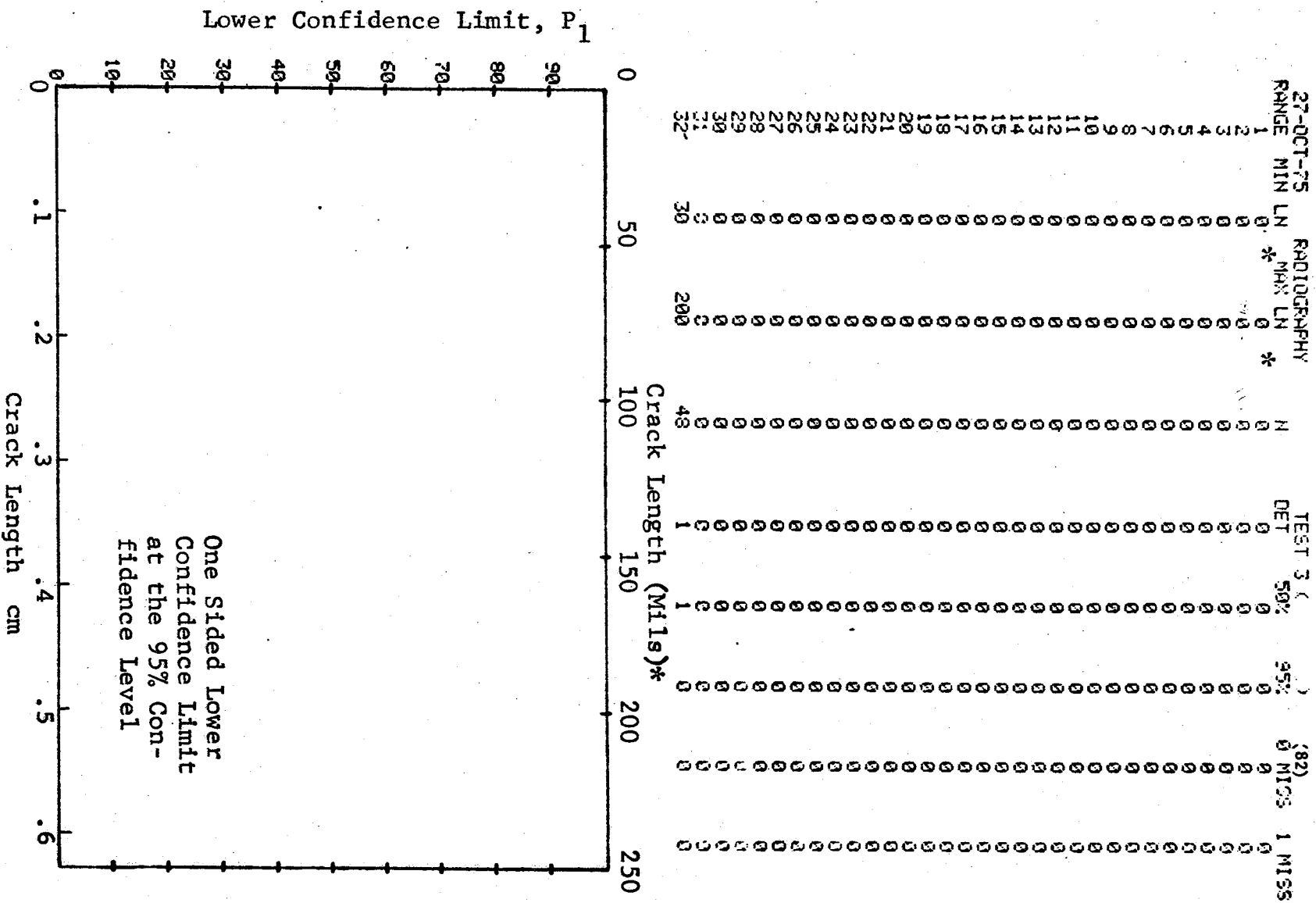


Figure D-82 (Concluded)

(a) Range Interval Method of Data Cumulation

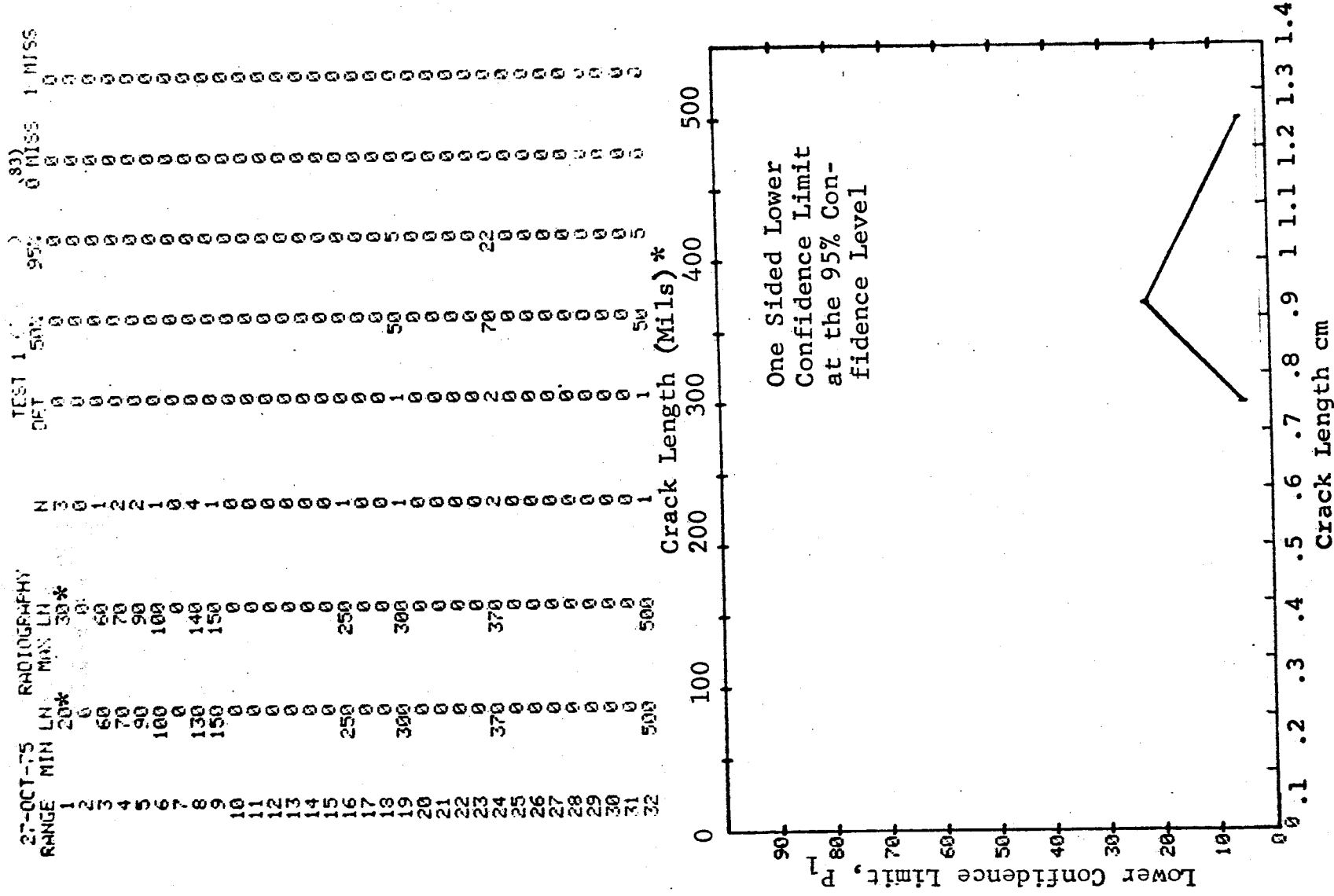


Figure D-83 Probability of Detection for 4340M Steel Using X-ray. Compressed Notch Flaws in Filleted Solid Cylinder. D-255 Prod. Env.

(b) Optimum Probability Method of Data Cumulation

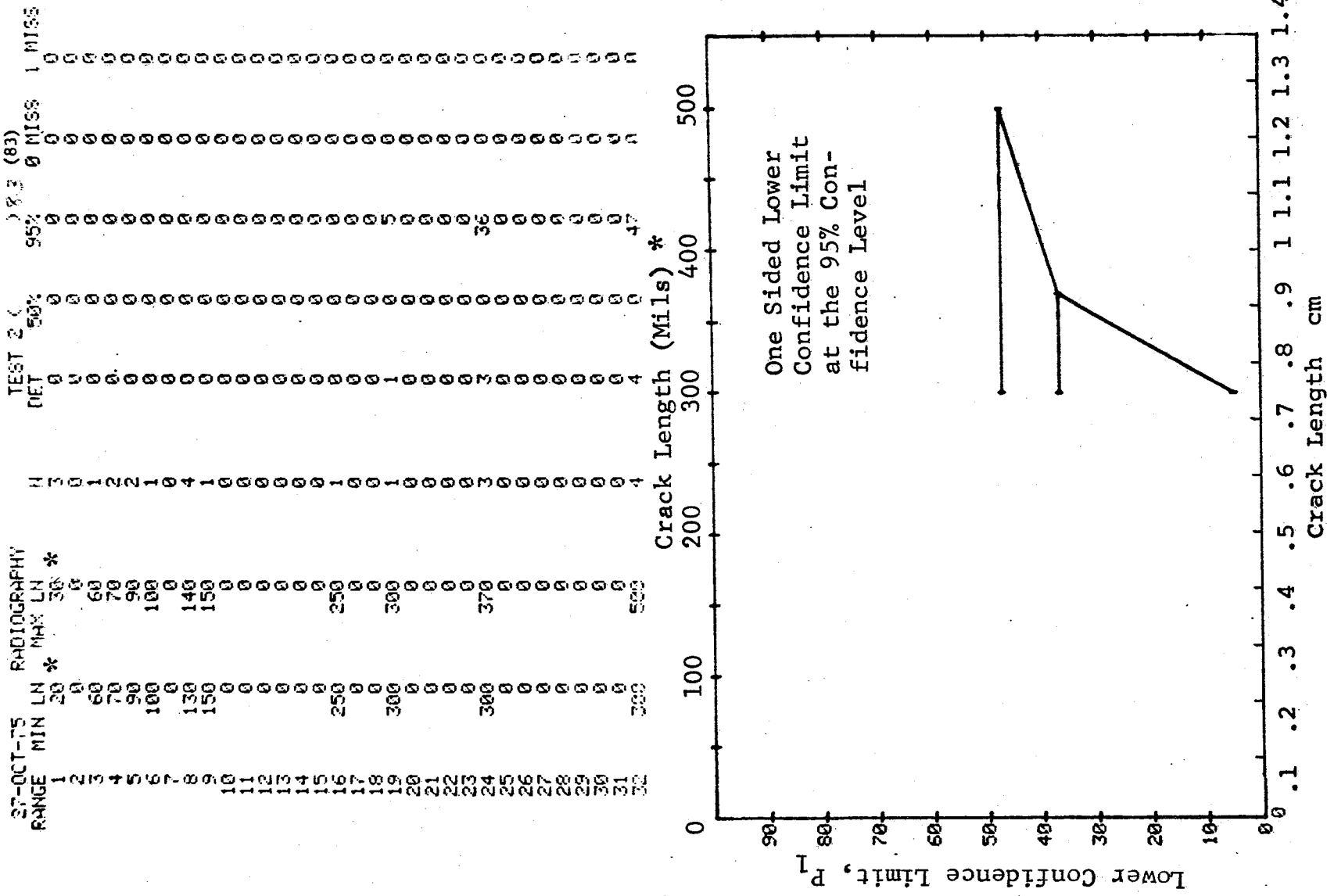


Figure D-83 (Continued)

REPRODUCIBILITY OF THE
ORIGINAL PAGE IS POOR

(c) Overlapping Sixty Point Method of Data Cumulation

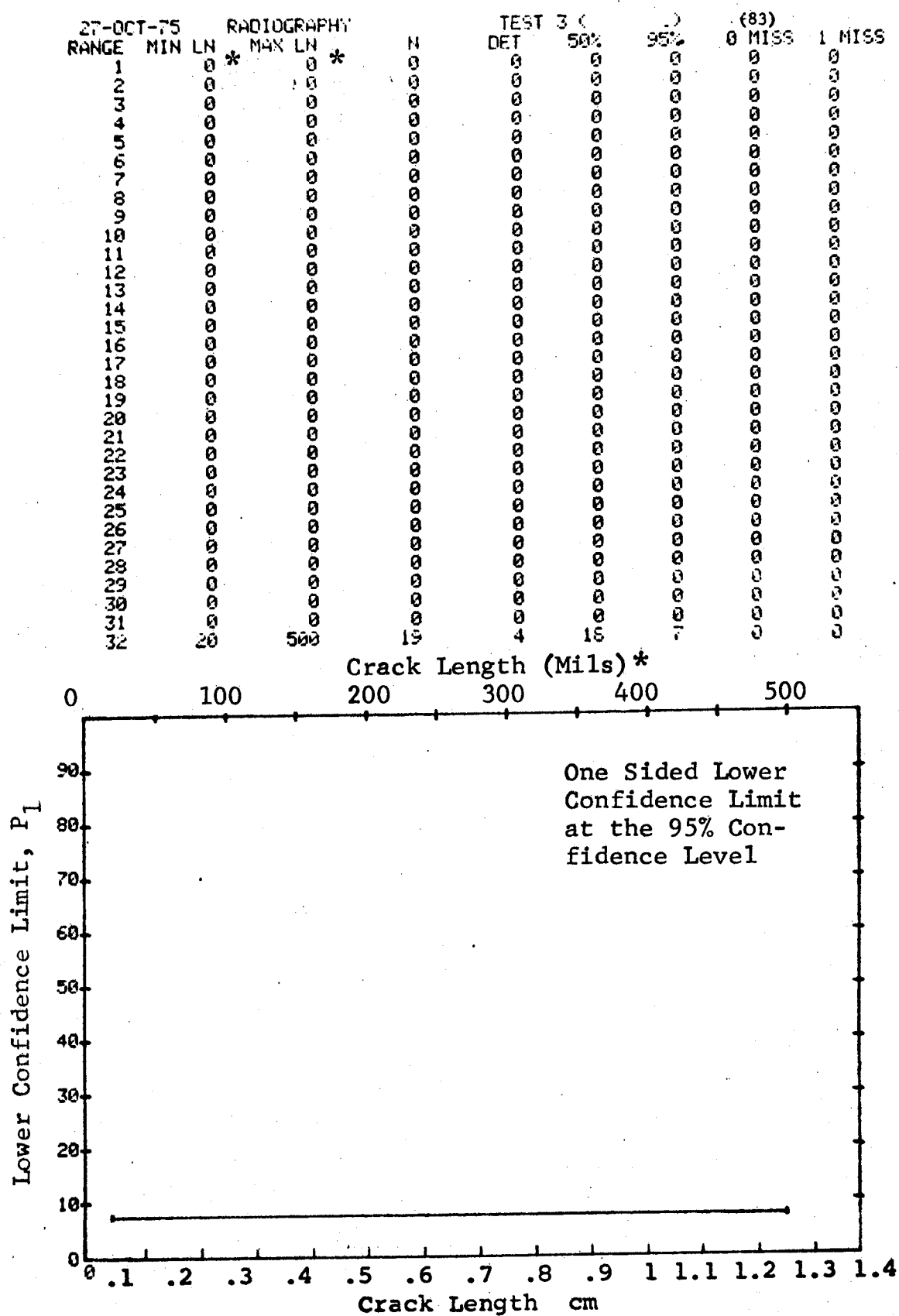


Figure D-83 (Concluded)

(a) Range Interval Method of Data Cumulation

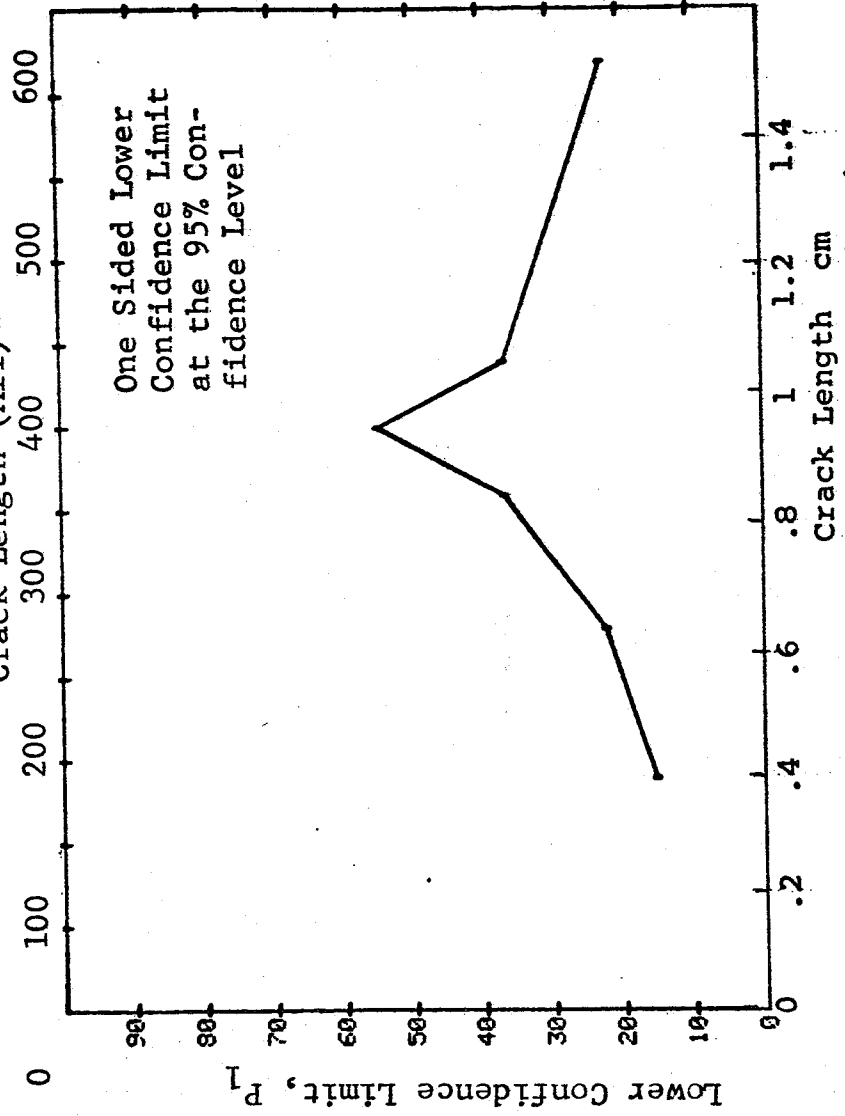
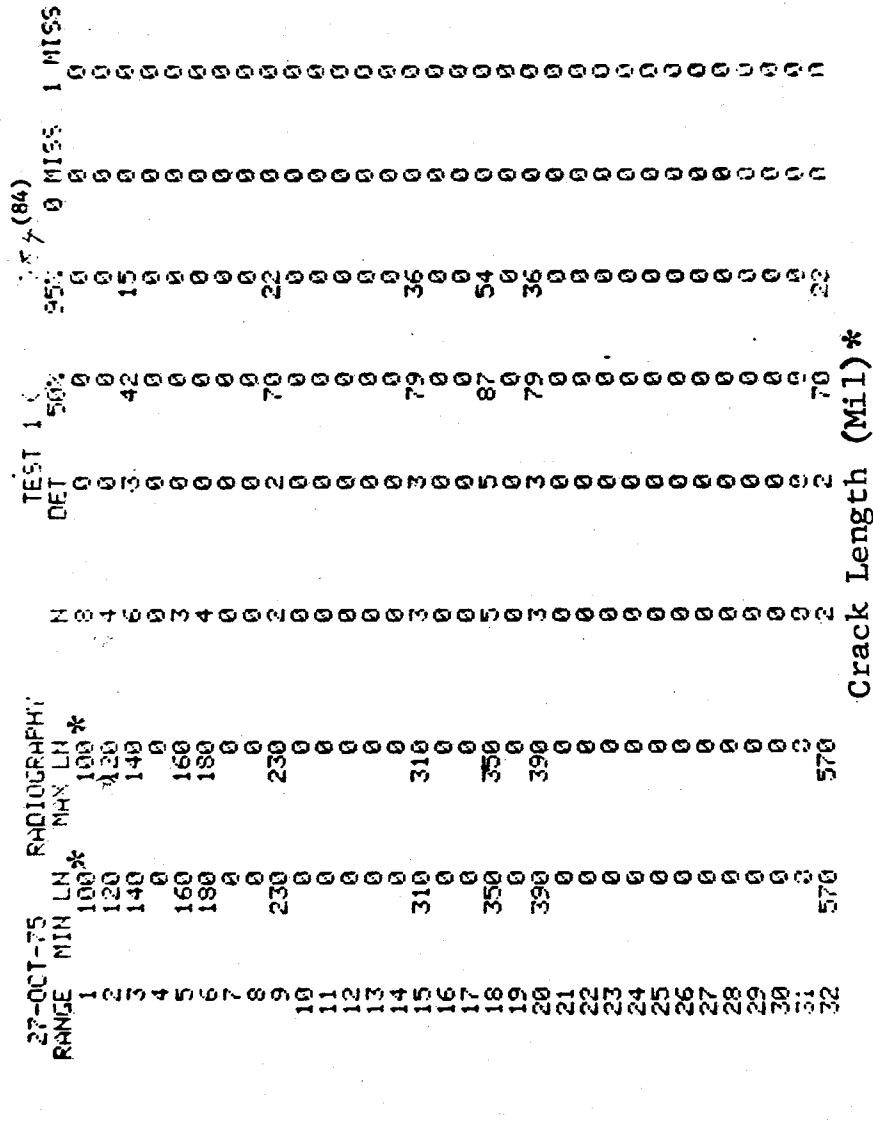


Figure D-84 Probability of Detection for 4340M Steel Using X-ray. Compressed Notch Flaws in Hollow Filleted Cylinder. Prod. Env. D-258

(b) Optimum Probability Method of Data Cumulation

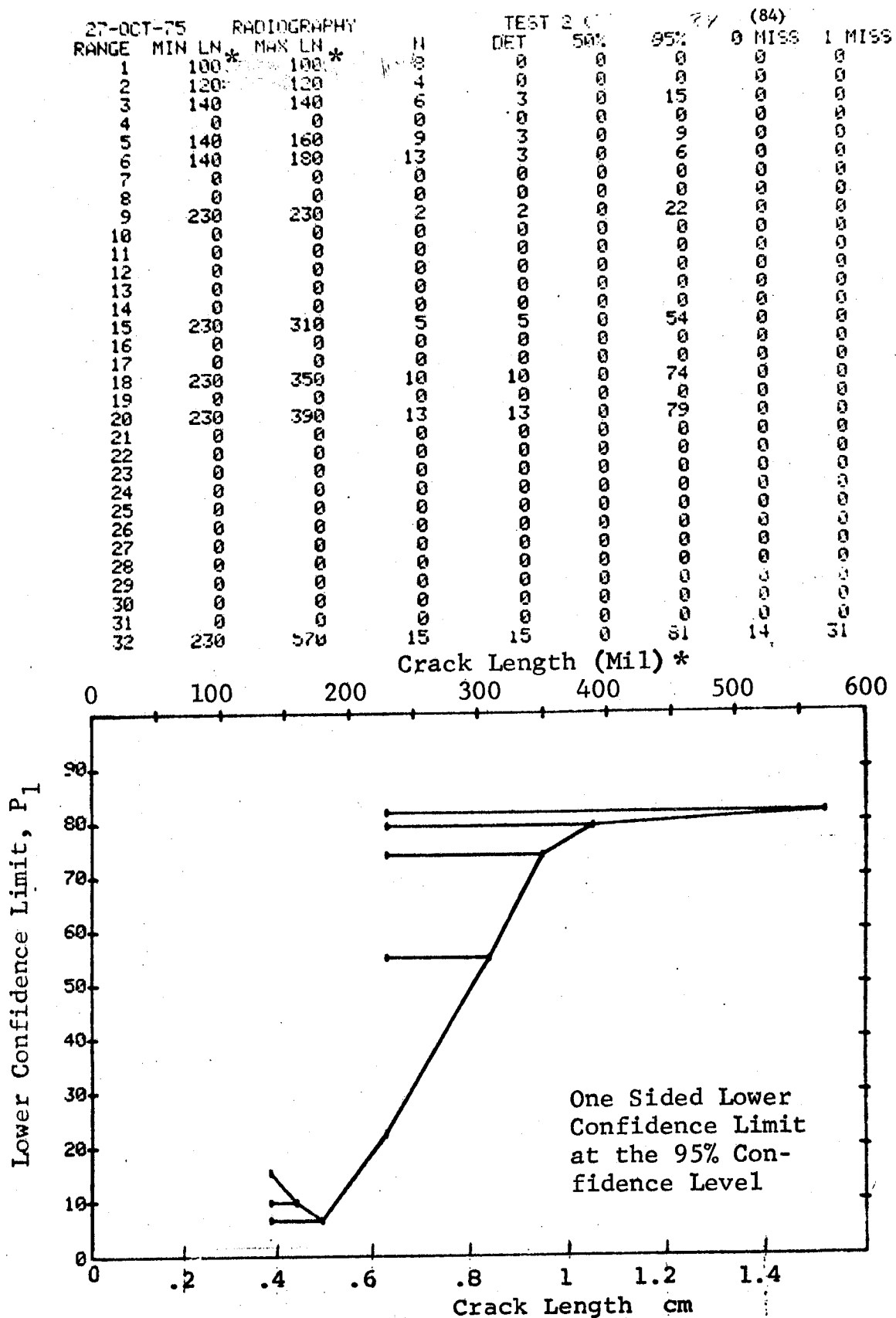


Figure D-84 (Continued)

(c) Overlapping Sixty Point Method of Data Cumulation

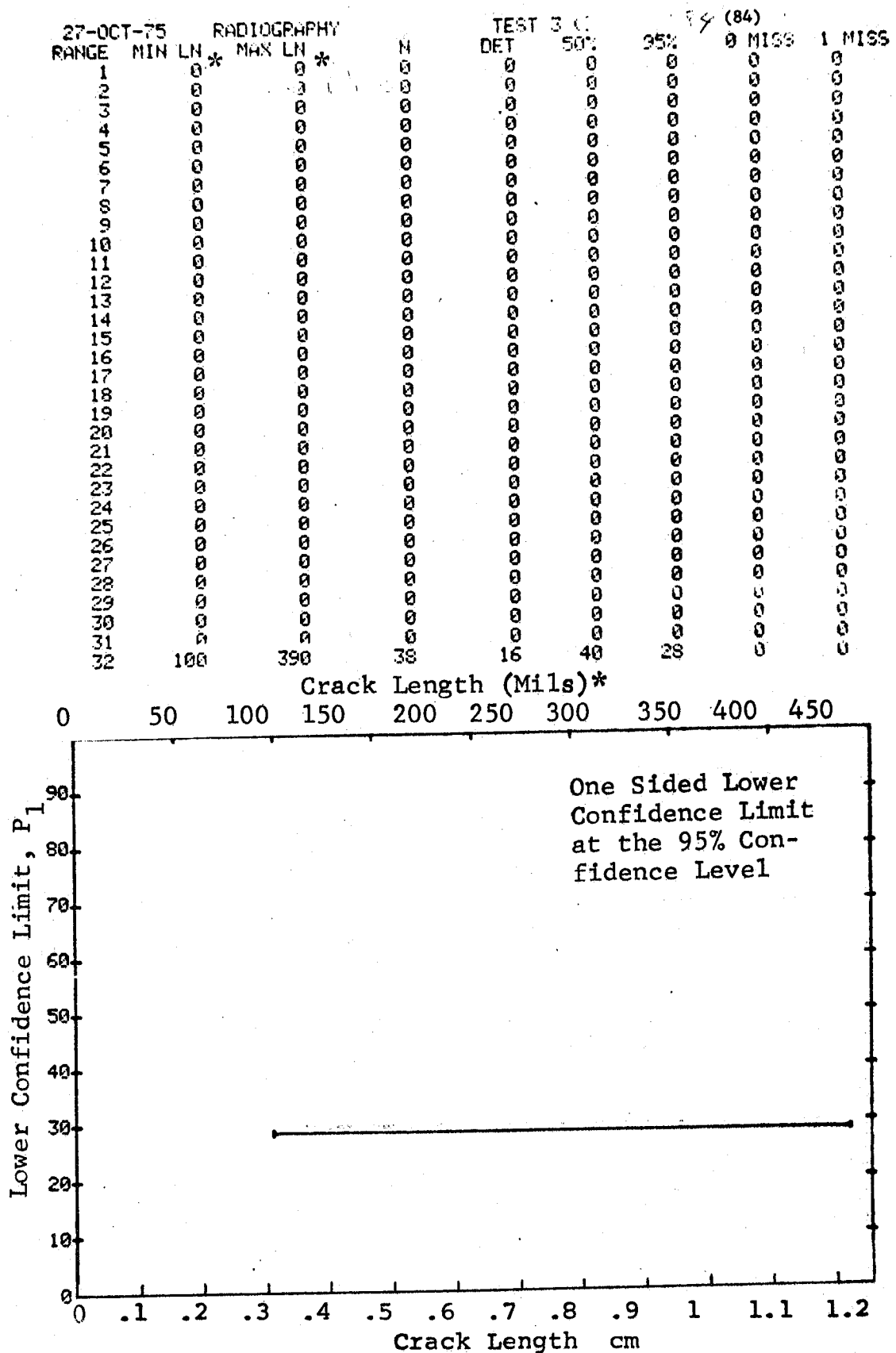


Figure D-84 (Concluded)

27-OCT-75		RADIOGRAPHY		N	TEST 1		P-25 (85)		
RANGE	MIN LN	MAX LN	90 *		DET	50%	95%	0 MISS	1 MISS
1	80	110	90	7	2	22	5	0	0
2	0	0	0	0	0	0	0	0	0
3	110	110	110	2	0	0	0	0	0
4	0	0	0	0	0	0	0	0	0
5	130	130	130	2	1	29	2	0	0
6	140	140	140	3	1	20	1	0	0
7	160	160	160	1	0	0	0	0	0
8	0	0	0	0	0	0	0	0	0
9	0	0	0	0	0	0	0	0	0
10	0	0	0	0	0	0	0	0	0
11	0	0	0	0	0	0	0	0	0
12	0	0	0	0	0	0	0	0	0
13	0	0	0	0	0	0	0	0	0
14	0	0	0	0	0	0	0	0	0
15	250	250	250	3	2	50	13	0	0
16	270	270	270	1	0	0	0	0	0
17	280	280	280	3	3	79	36	0	0
18	0	0	0	0	0	0	0	0	0
19	300	300	300	3	3	79	36	0	0
20	0	0	0	0	0	0	0	0	0
21	0	0	0	0	0	0	0	0	0
22	0	0	0	0	0	0	0	0	0
23	0	0	0	0	0	0	0	0	0
24	0	0	0	0	0	0	0	0	0
25	0	0	0	0	0	0	0	0	0
26	0	0	0	0	0	0	0	0	0
27	0	0	0	0	0	0	0	0	0
28	0	0	0	0	0	0	0	0	0
29	0	0	0	0	0	0	0	0	0
30	0	0	0	0	0	0	0	0	0
31	0	0	0	0	0	0	0	0	0
32	450	450	450	4	3	61	24	0	0

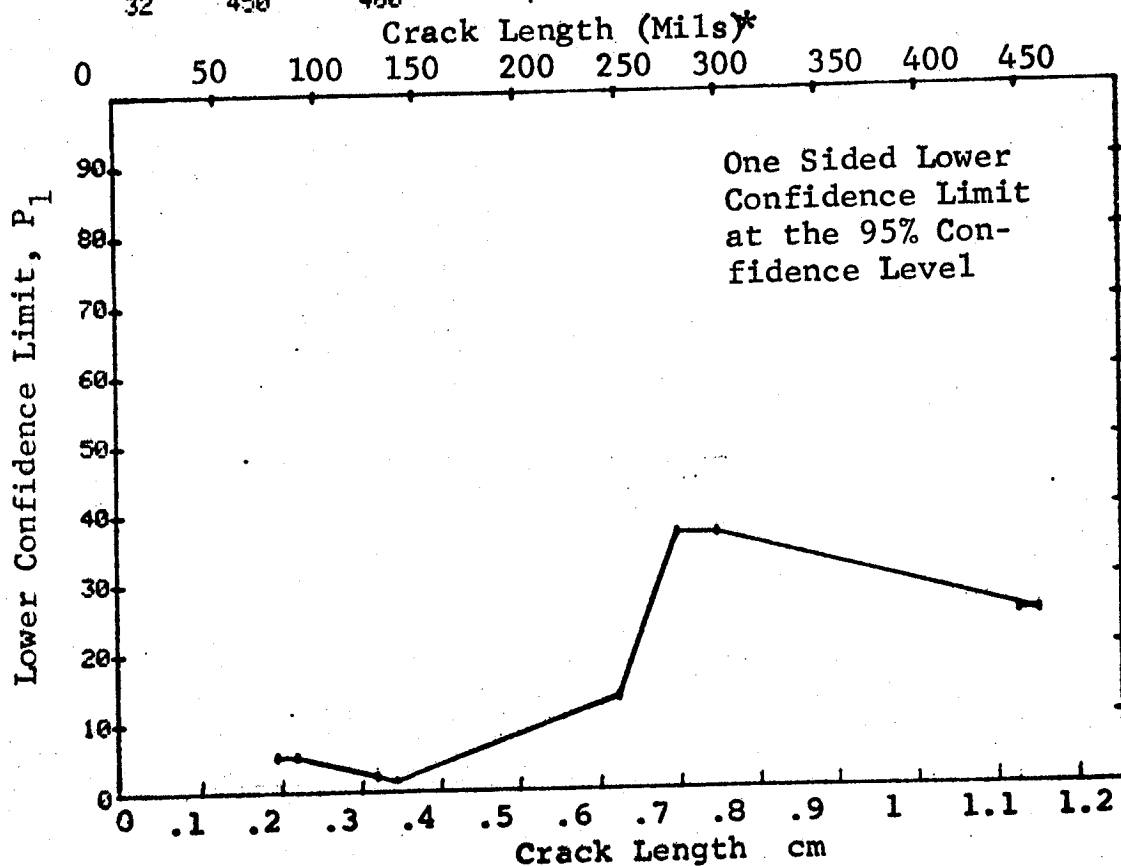


Figure D-85 Probability of Detection for 4340M Steel Using X-ray.
Compressed Notch Flaws in Hollow Filleted Cylinder.
Prod. Env.

(b) Optimum Probability Method of Data Cumulation

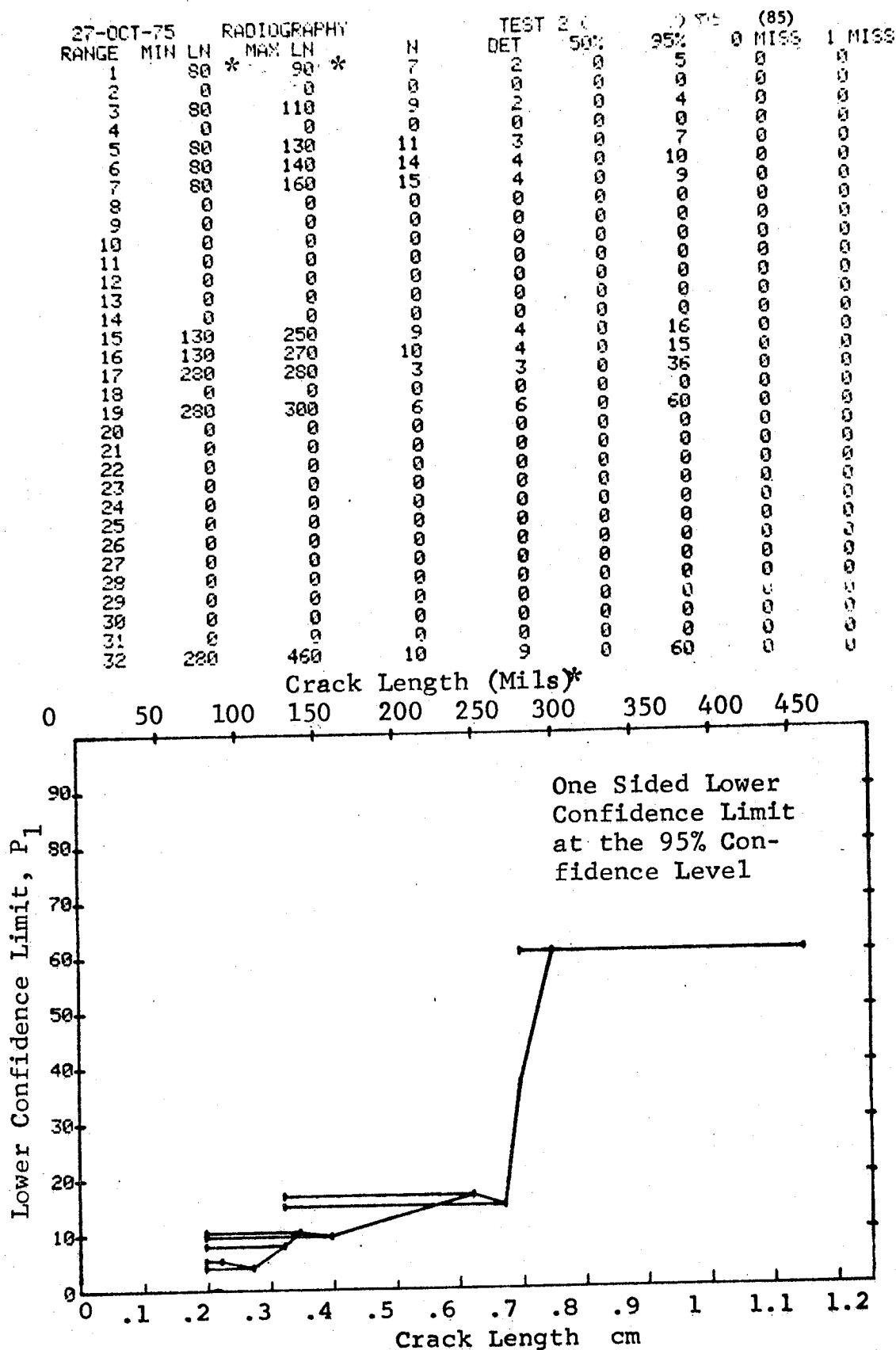


Figure D-85 (Continued)

(c) Overlapping Sixty Point Method of Data Cumulation

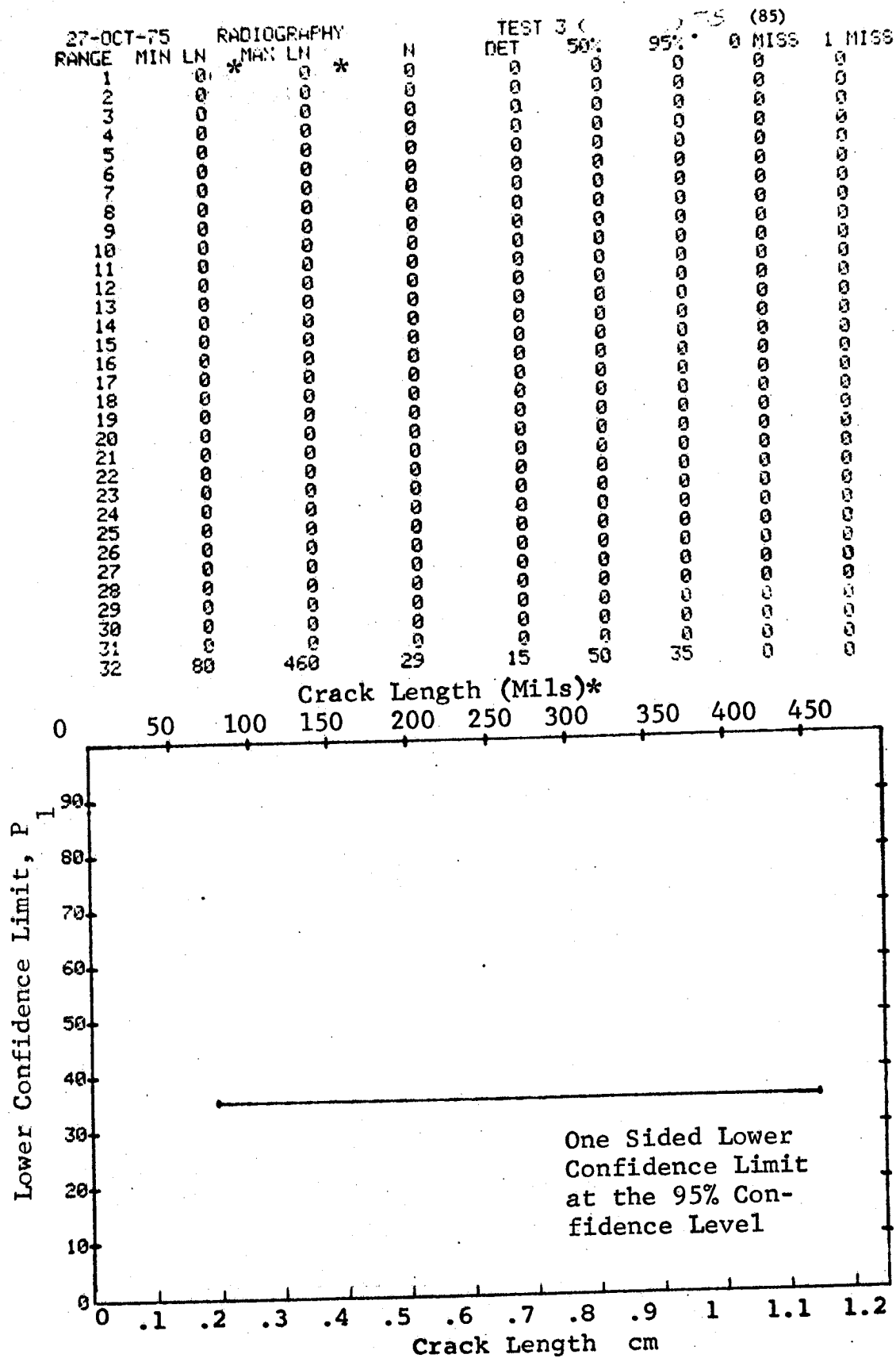


Figure D-85 (Concluded)

(a) Range Interval Method of Data Cumulation

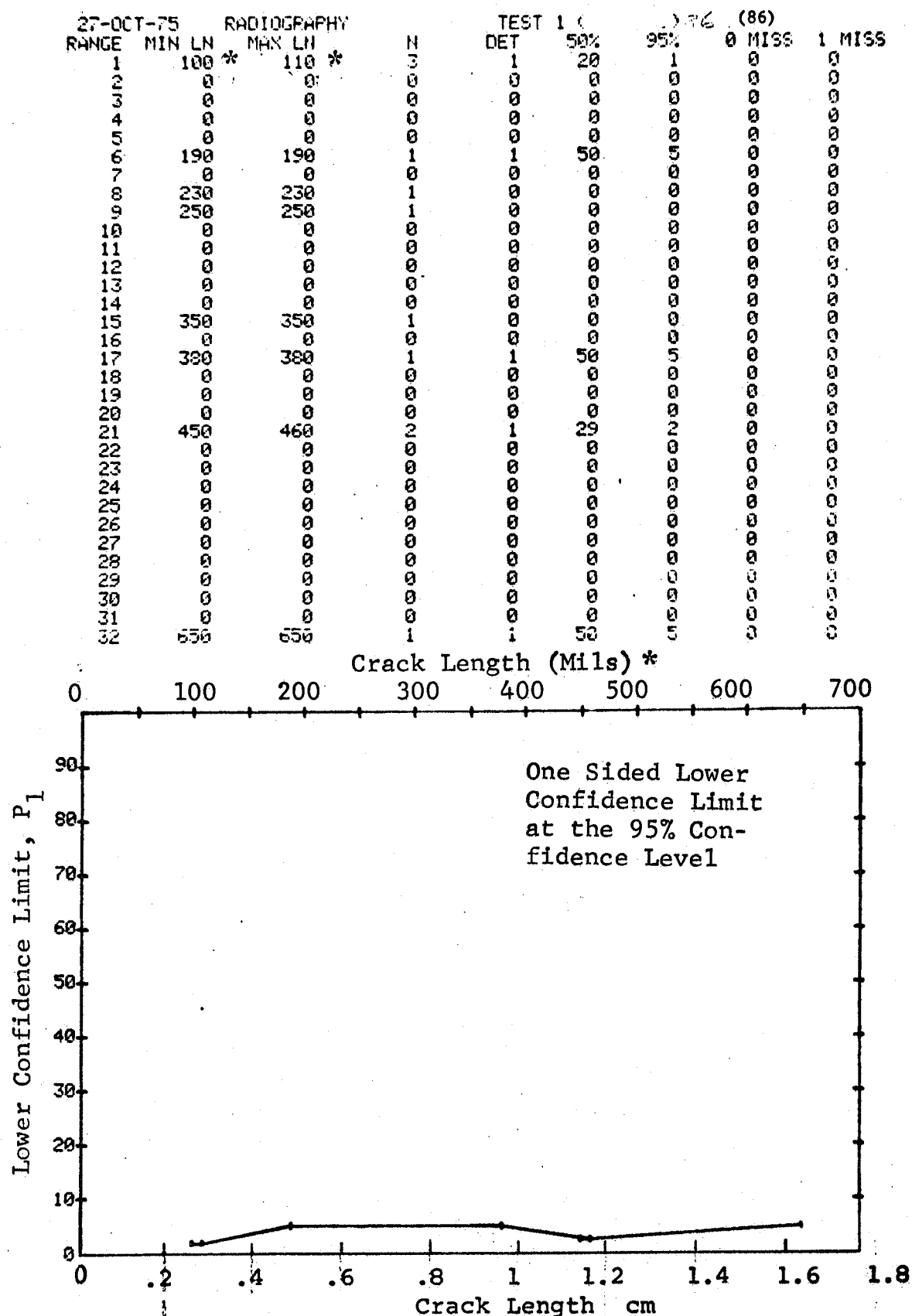


Figure D-86 Probability of Detection for 4340M Steel Using X-ray. Compressed Notch Flaws in Solid Threaded Cylinder. Prod. Env.

(b) Optimum Probability Method of Data Cumulation

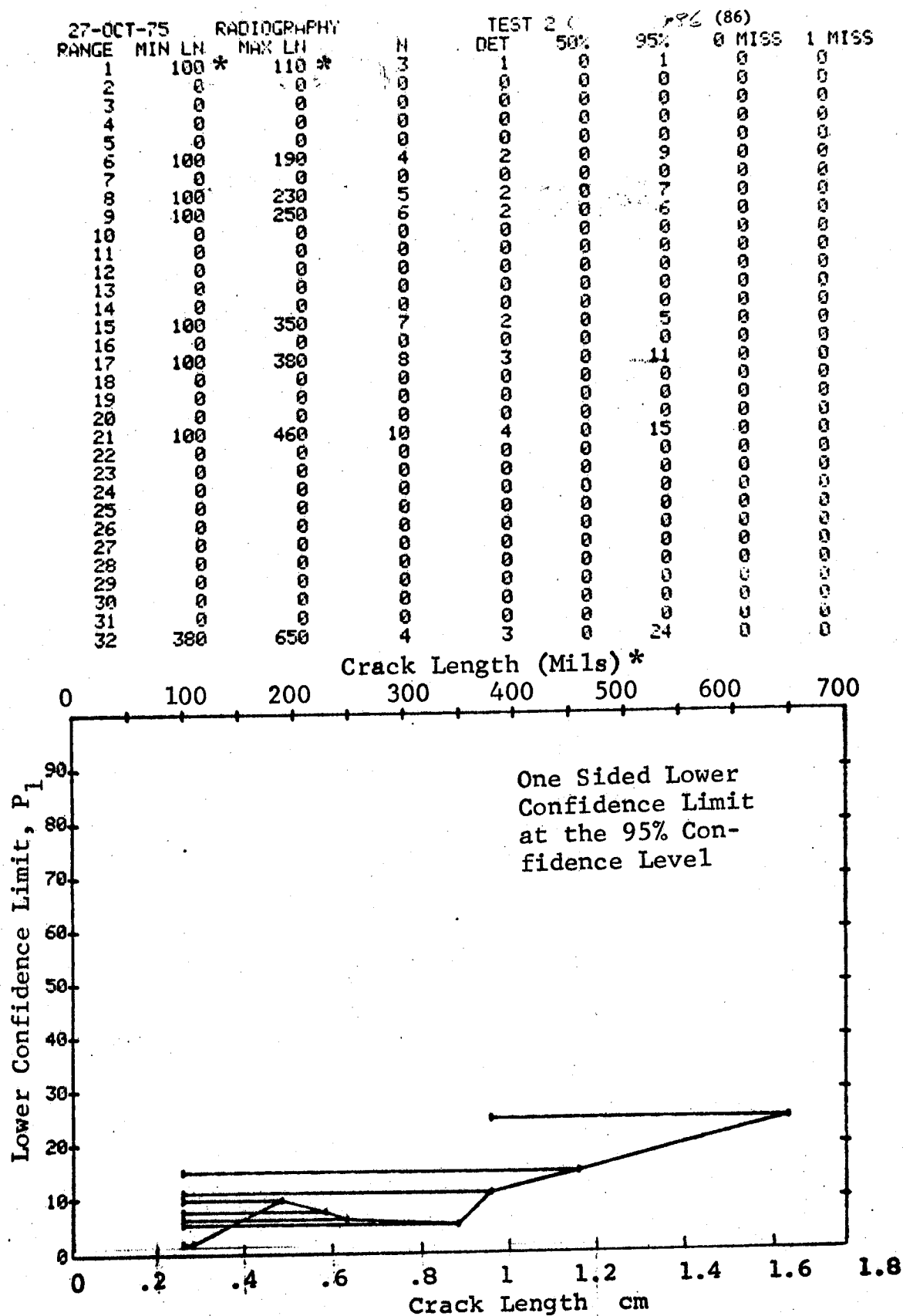


Figure D-86 (Continued)

(c) Overlapping Sixty Point Method of Data Cumulation

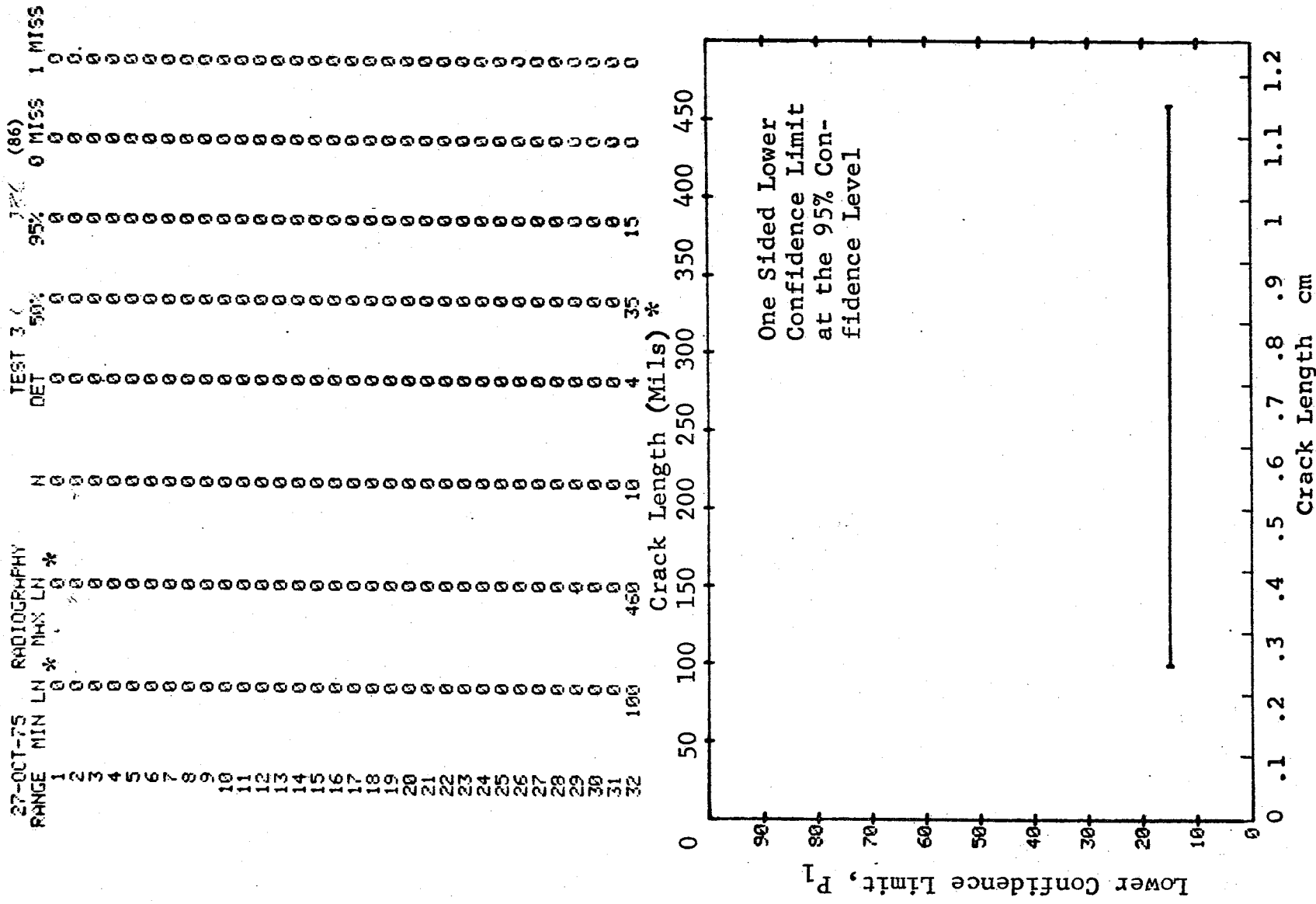


Figure D-86 (Concluded)

(a) Range Interval Method of Data Cumulation

27-OCT-75		RADIOGRAPHY		TEST 1		737 (87)	
RANGE	MIN LN	MAX LN	LN *	DET	50%	95%	MISS
1	10	10	0	0	0	0	0
2	30	30	0	0	0	0	0
3	40	40	0	3	79	36	0
4	50	50	0	0	0	0	0
5	60	60	0	0	0	0	0
6	70	70	0	6	60	34	0
7	80	80	0	17	86	70	0
8	90	90	0	0	0	0	0
9	100	100	0	8	91	68	0
10	110	110	0	1	50	5	0
11	120	120	0	0	0	0	0
12	130	130	0	4	57	27	0
13	140	140	0	4	68	34	0
14	150	150	0	4	0	0	0
15	160	160	0	2	38	9	0
16	170	170	0	6	77	47	0
17	180	180	0	3	79	36	0
18	190	190	0	0	0	0	0
19	200	200	0	4	84	47	0
20	210	210	0	1	29	2	0
21	220	220	0	0	92	71	0
22	230	230	0	9	0	0	0
23	240	240	0	0	0	0	0
24	250	250	0	5	87	54	0
25	260	260	0	8	82	57	0
26	270	270	0	0	0	0	0
27	280	280	0	0	0	0	0
28	290	290	0	0	0	0	0
29	300	300	0	0	0	0	0
30	310	310	0	0	0	0	0
31	320	320	0	3	79	36	0
32	330	330	0	4	68	34	0

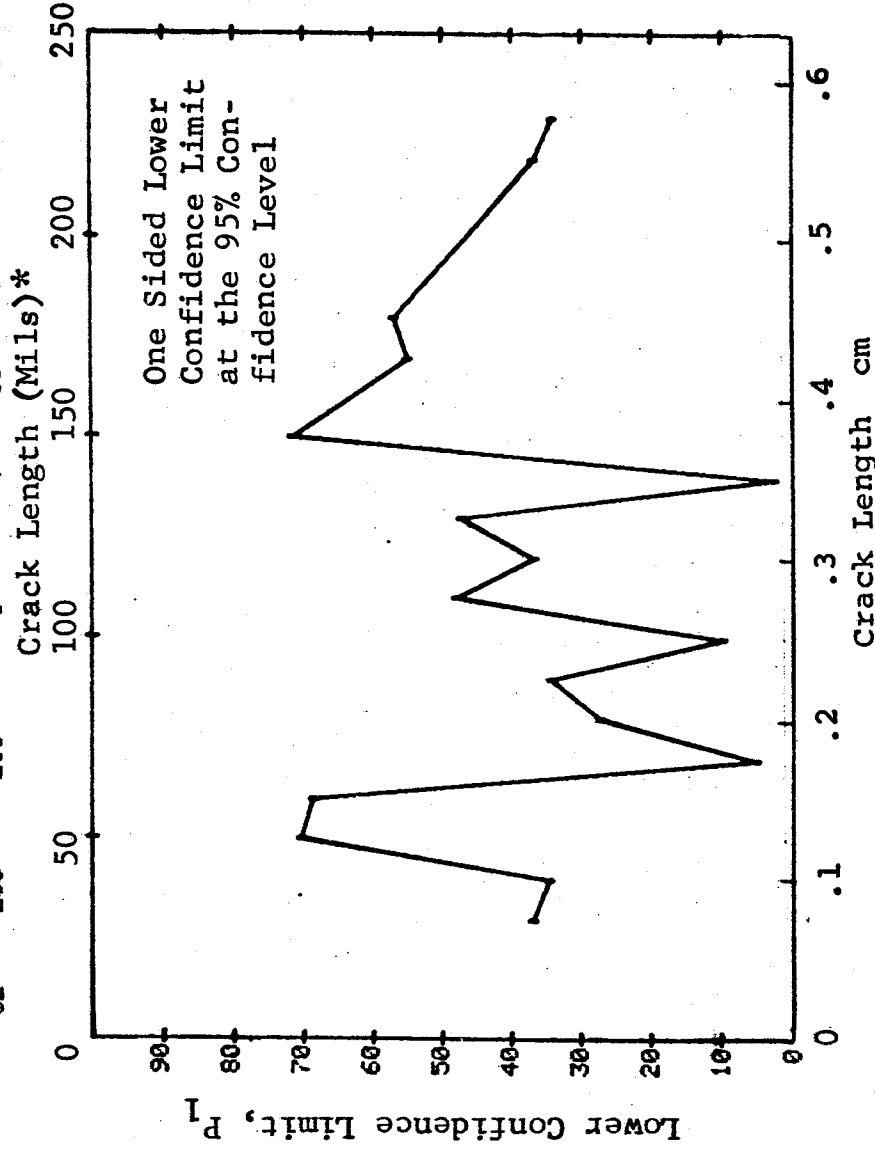


Figure D-87 Probability of Detection for 2024-T6 Al Using X-ray. Compressed Notch Flaws in Tandem-T Specimen. Prod. Env.

(b) Optimum Probability Method of Data Cumulation

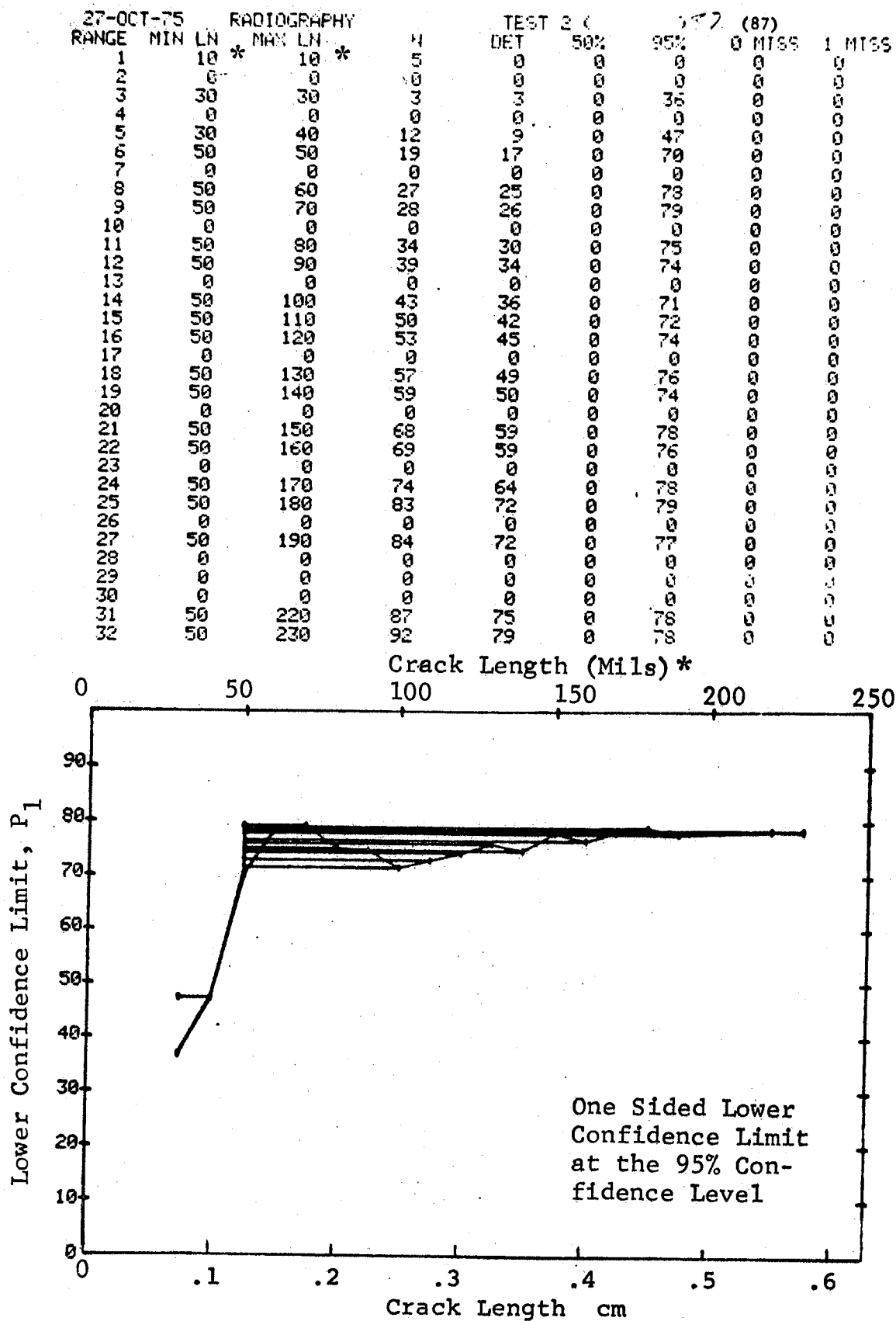


Figure D-87 (Continued)

(c) Overlapping Sixty Point Method of Data Cumulation

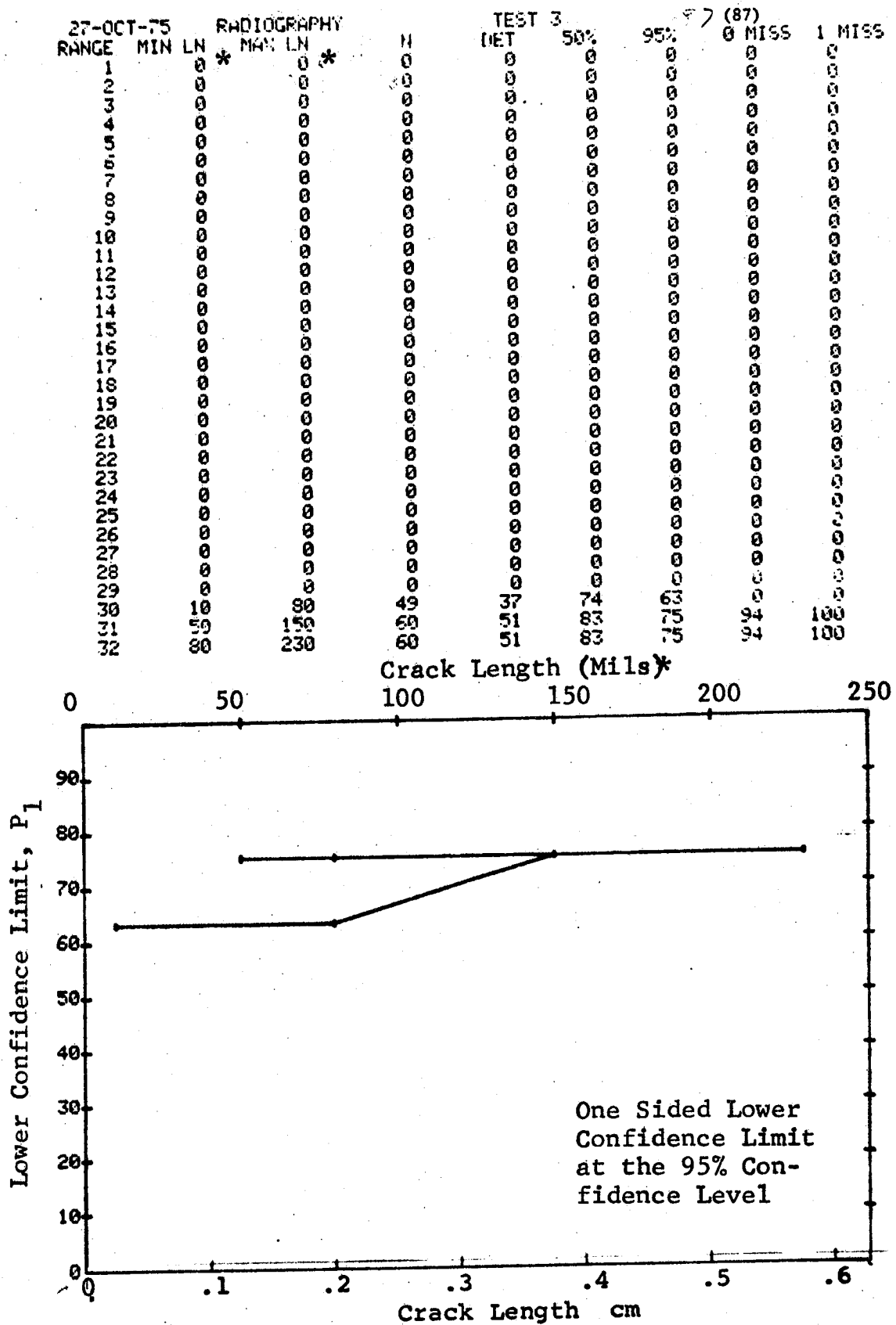


Figure D-87 (Concluded)

(a) Range Interval Method of Data Cumulation

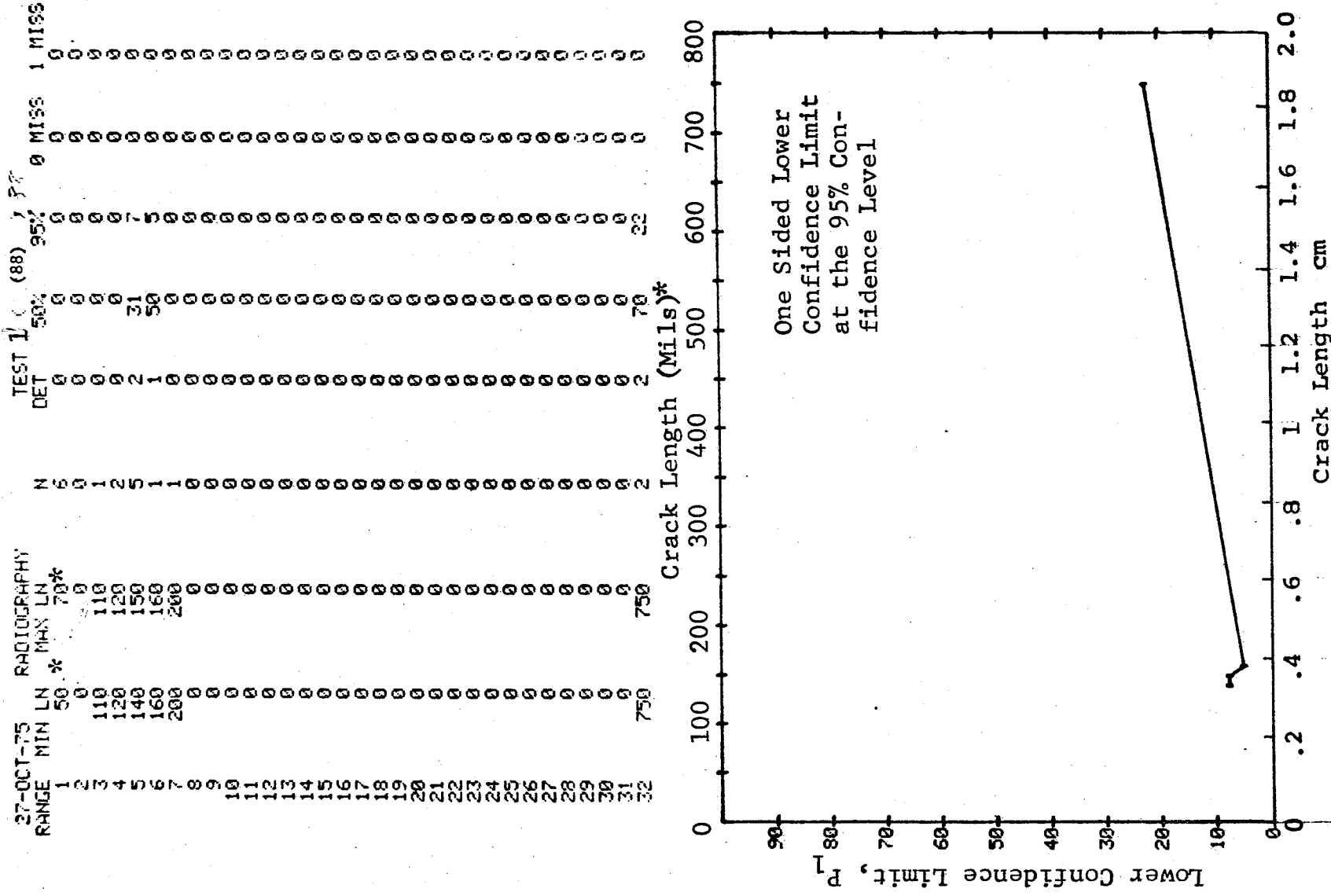


Figure D-88 Probability of Detection for 4340M Steel Using X-ray.
Compressed Notch Flaws in Solid Cylinder. Lab. Env.

(b) Optimum Probability Method of Data Cumulation

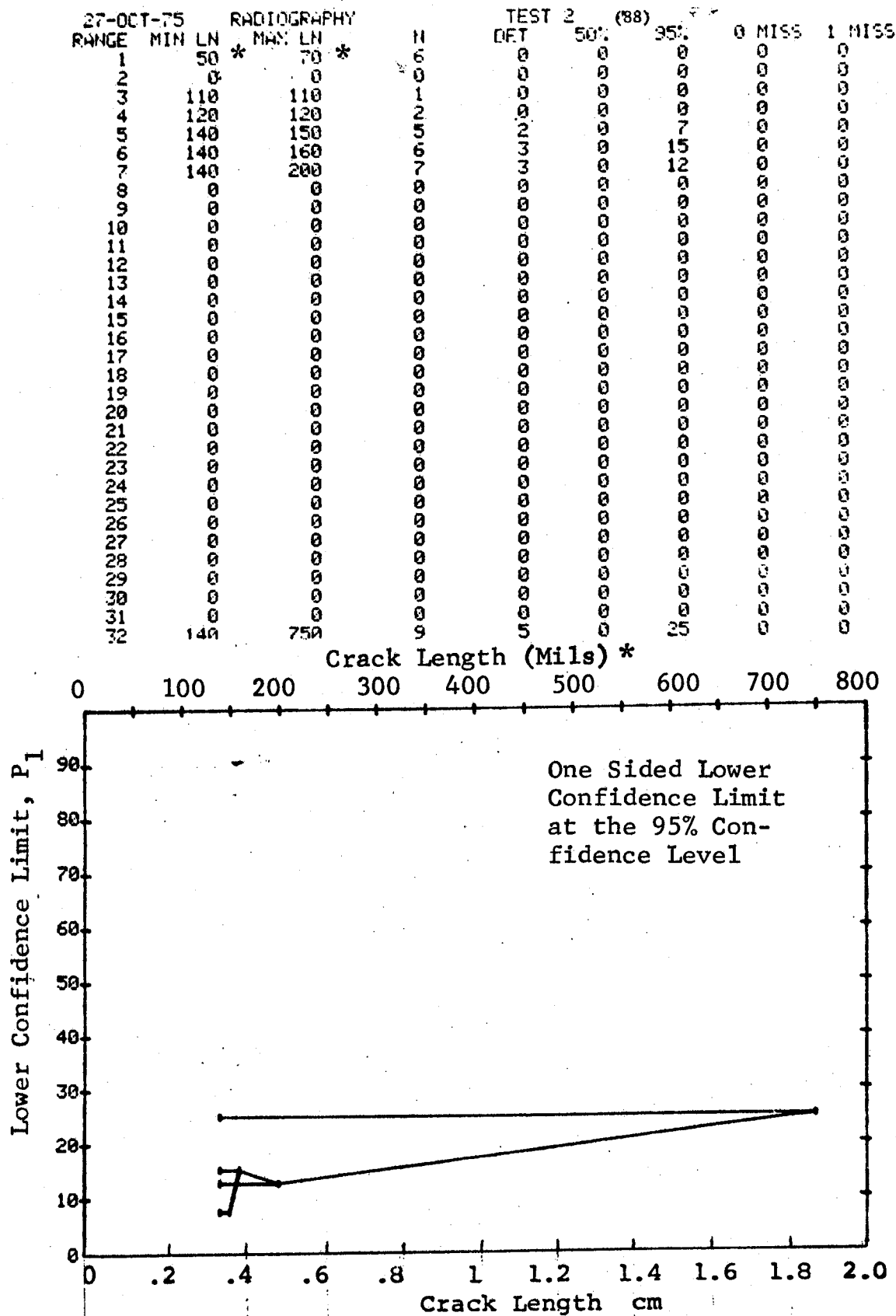


Figure D-88 (Continued)

(c) Overlapping Sixty Point Method of Data Cumulation

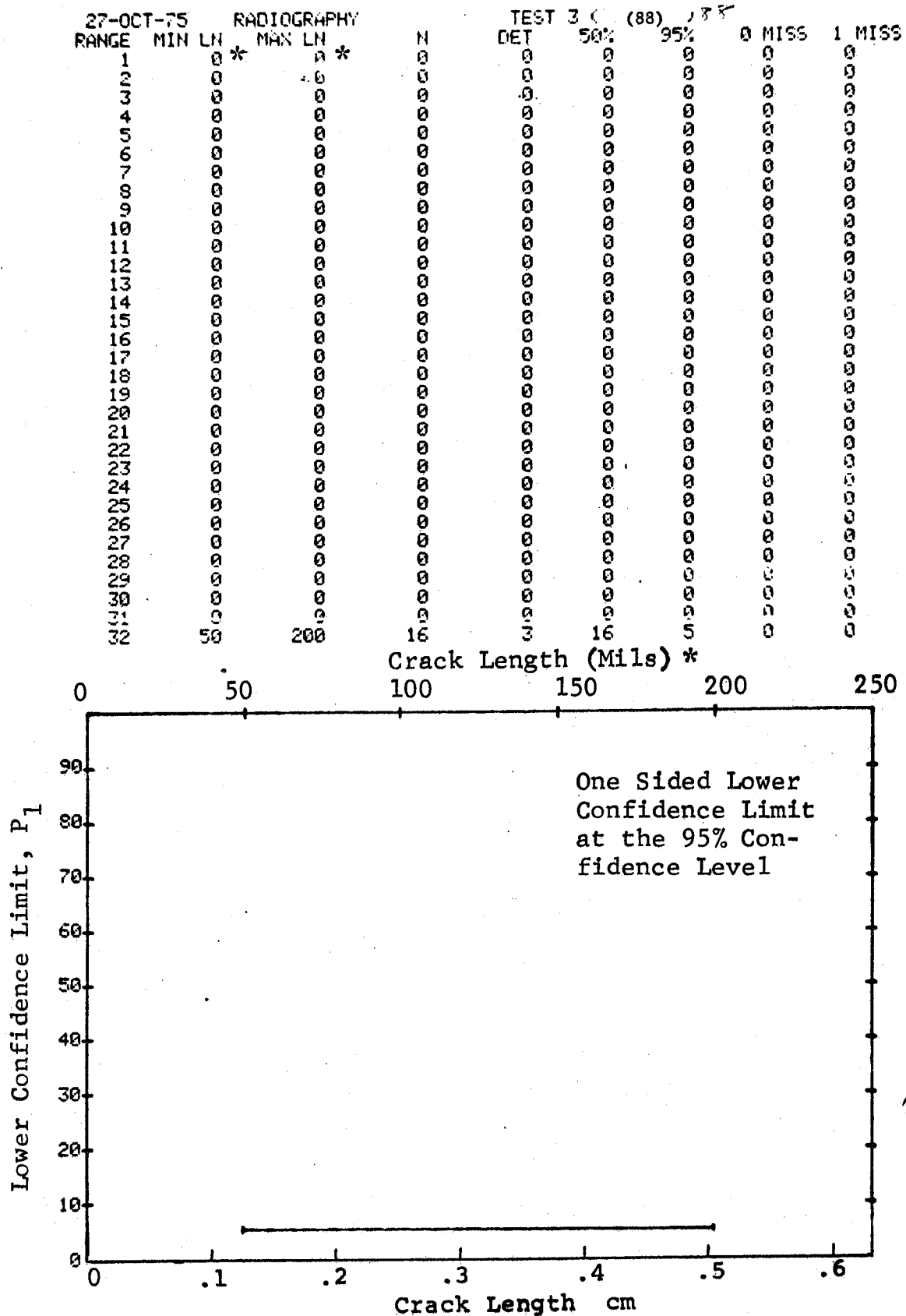


Figure D-88 (Concluded)

(a) Range Interval Method of Data Cumulation

27-OCT-75 RANGE	MIN	LN	MAX	LN	RADIOGRAPHY	N	TEST 1 C DET	50%	(89) 95%	MISS	MISS
1	0	0	0	0	0	1	1	50	5	0	0
2	0	0	0	0	0	0	0	0	0	0	0
3	0	0	0	0	0	0	0	0	0	0	0
4	0	0	0	0	0	0	0	0	0	0	0
5	0	0	0	0	0	0	0	0	0	0	0
6	140	0	0	0	0	1	1	50	5	0	0
7	160	0	0	0	0	0	0	0	0	0	0
8	180	0	0	0	0	1	1	50	5	0	0
9	180	0	0	0	0	0	0	0	0	0	0
10	0	0	0	0	0	1	1	50	5	0	0
11	0	0	0	0	0	0	0	0	0	0	0
12	0	0	0	0	0	0	0	0	0	0	0
13	0	0	0	0	0	0	0	0	0	0	0
14	0	0	0	0	0	0	0	0	0	0	0
15	250	0	0	0	0	1	1	50	5	0	0
16	270	0	0	0	0	0	0	0	0	0	0
17	280	0	0	0	0	1	1	50	5	0	0
18	300	0	0	0	0	2	2	70	22	0	0
19	0	0	0	0	0	1	1	50	5	0	0
20	0	0	0	0	0	0	0	0	0	0	0
21	0	0	0	0	0	0	0	0	0	0	0
22	0	0	0	0	0	0	0	0	0	0	0
23	0	0	0	0	0	0	0	0	0	0	0
24	0	0	0	0	0	0	0	0	0	0	0
25	0	0	0	0	0	0	0	0	0	0	0
26	390	0	0	0	0	2	2	70	22	0	0
27	0	0	0	0	0	0	0	0	0	0	0
28	0	0	0	0	0	0	0	0	0	0	0
29	0	0	0	0	0	0	0	0	0	0	0
30	440	0	0	0	0	0	0	0	0	0	0
31	450	0	0	0	0	1	1	50	5	0	0
32	460	0	0	0	0	4	4	84	47	0	0

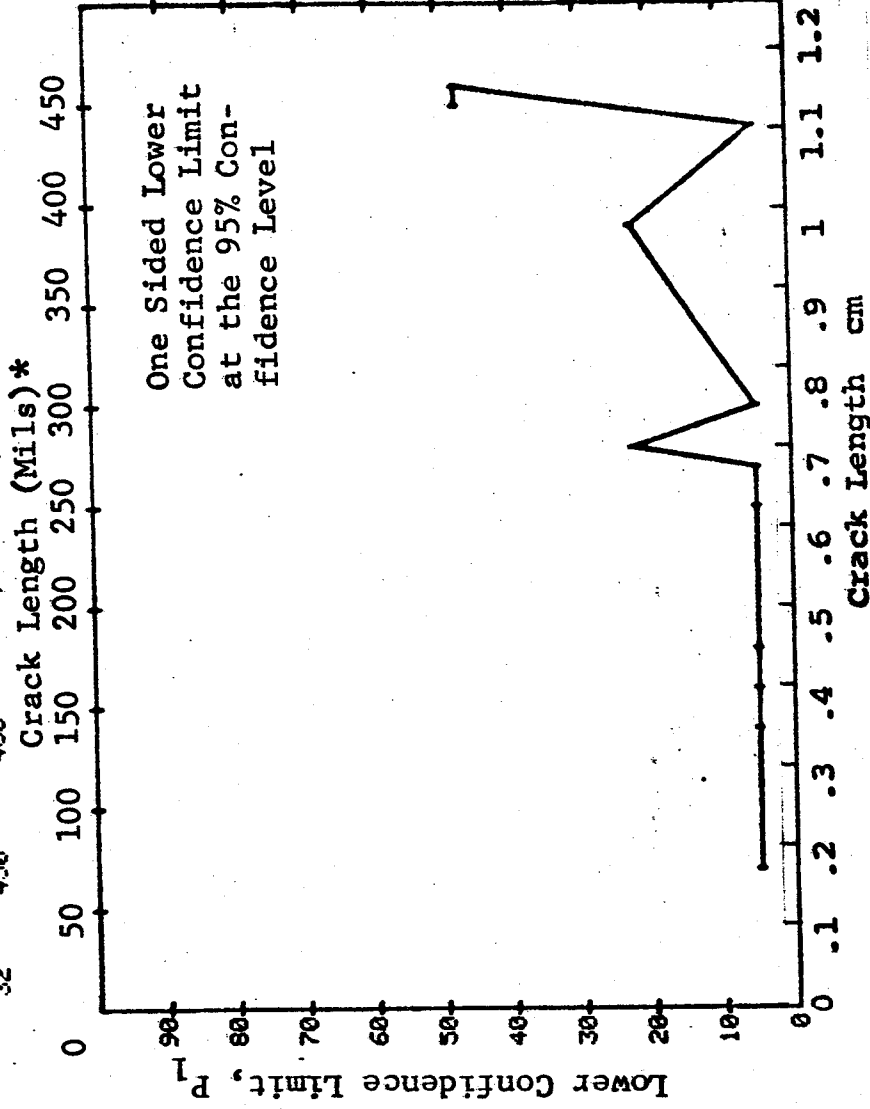


Figure D-89 Probability of Detection for 4340M Steel Using X-ray.
Compressed Notch Flaws in Hollow Filleted Cylinder.
Lab. Env. D-273

(b) Optimum Probability Method of Data Cumulation

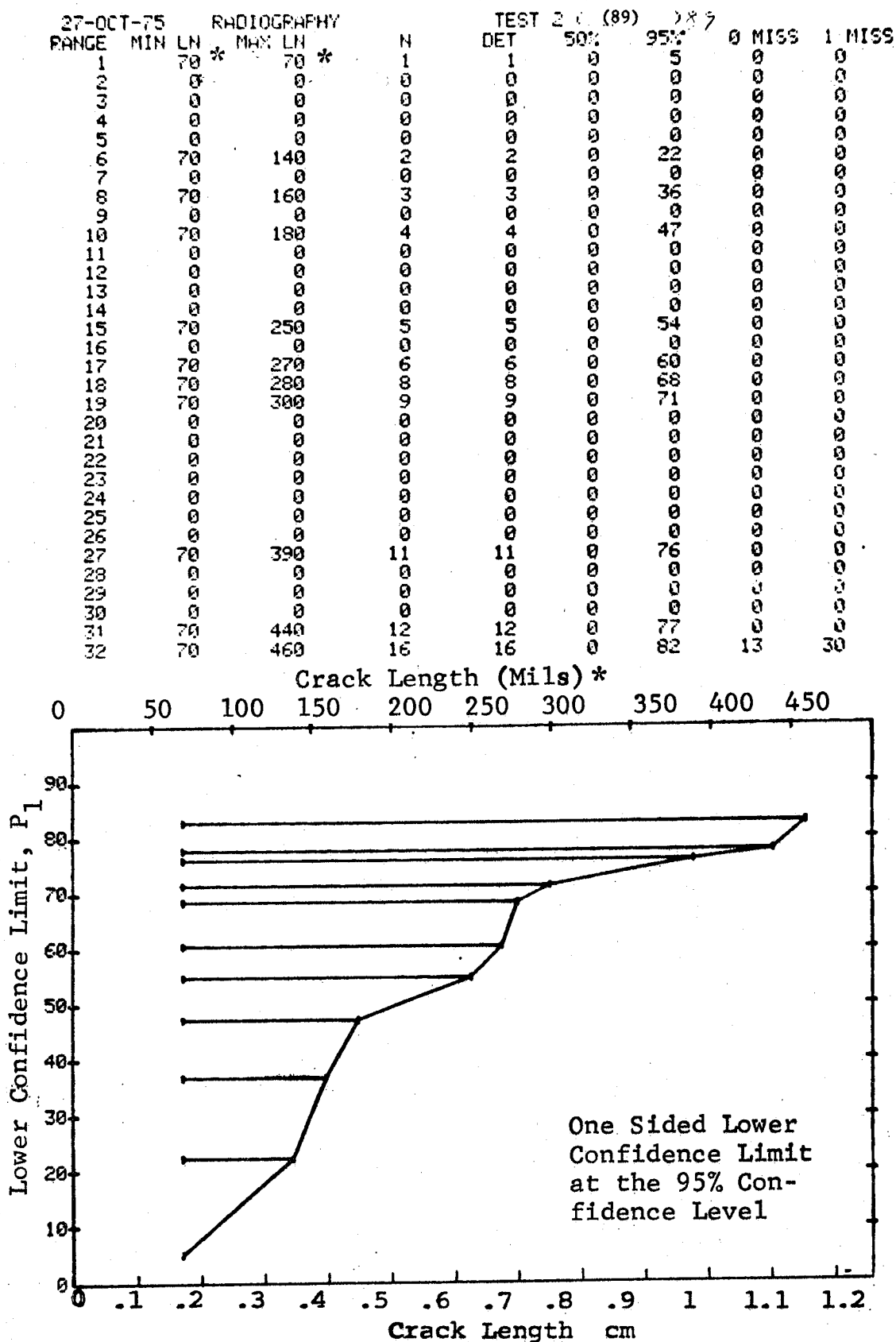


Figure D-89 (Continued)

(c) Overlapping Sixty Point Method of Data Cumulation

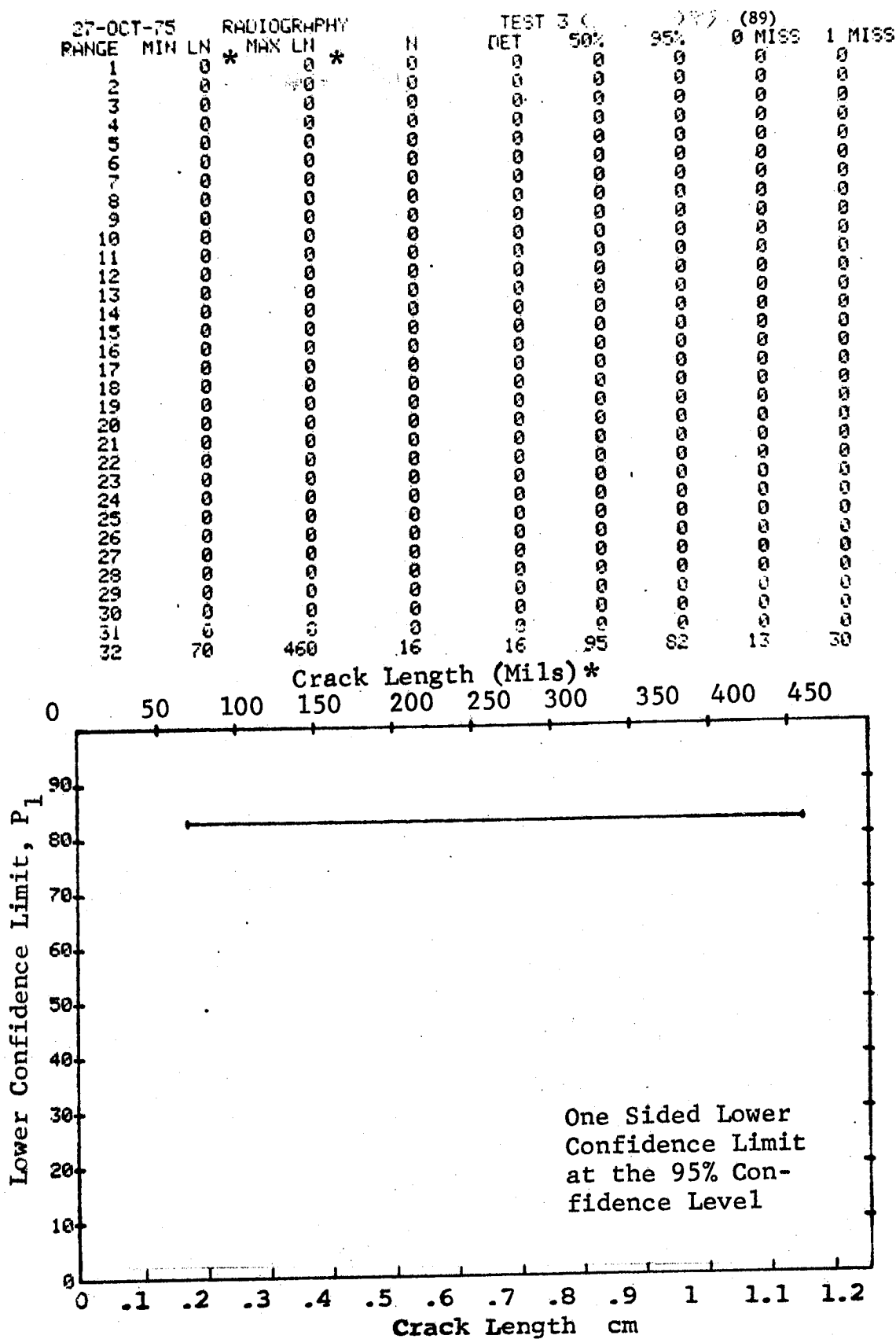


Figure D-89 (Concluded)

(a) Range Interval Method of Data Cumulation

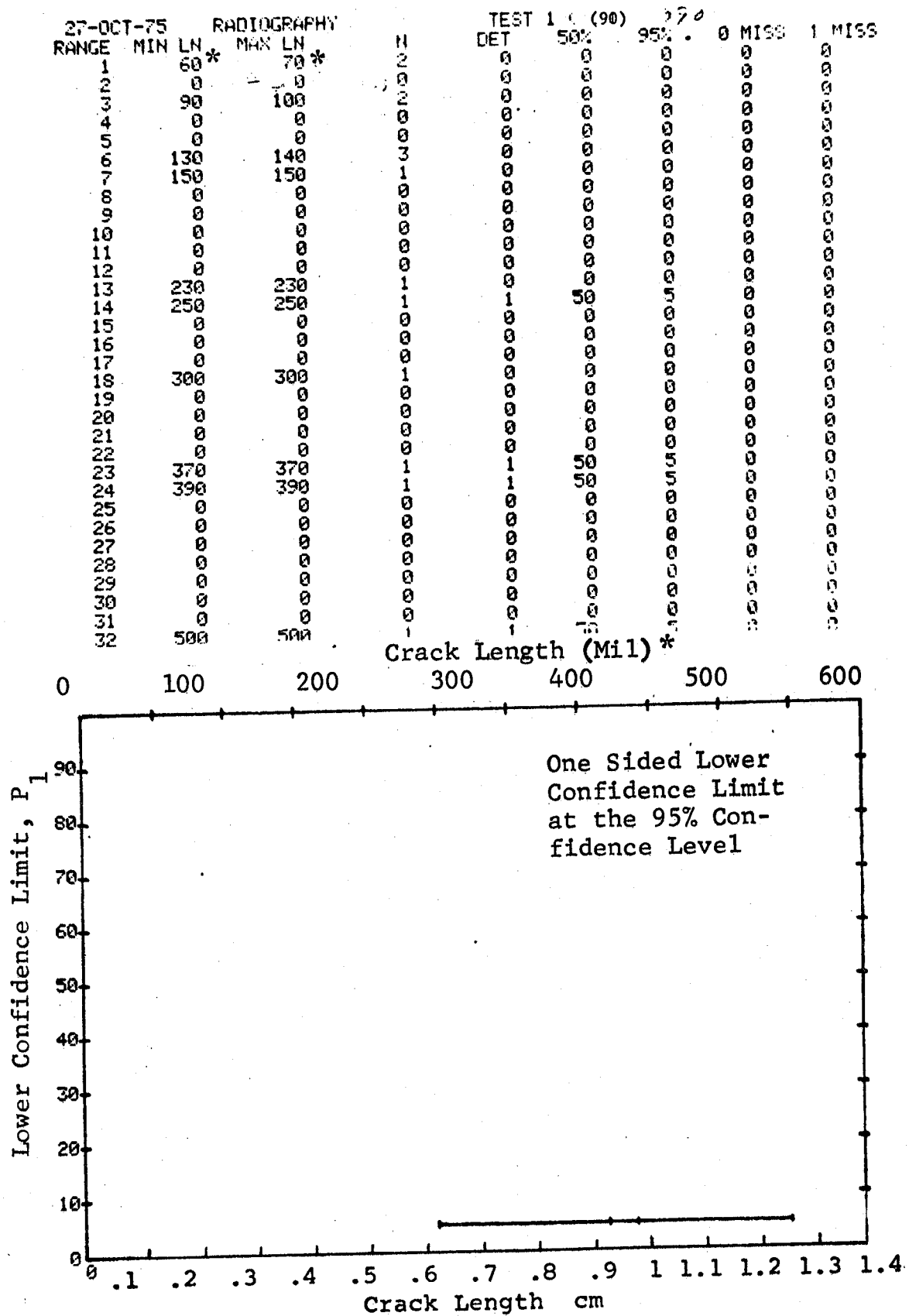


Figure D-90 Probability of Detection for 4340M Steel Using X-ray. Compressed Notch Flaws in Solid Filleted Cylinder. Lab. Env.

(b) Optimum Probability Method of Data Cumulation

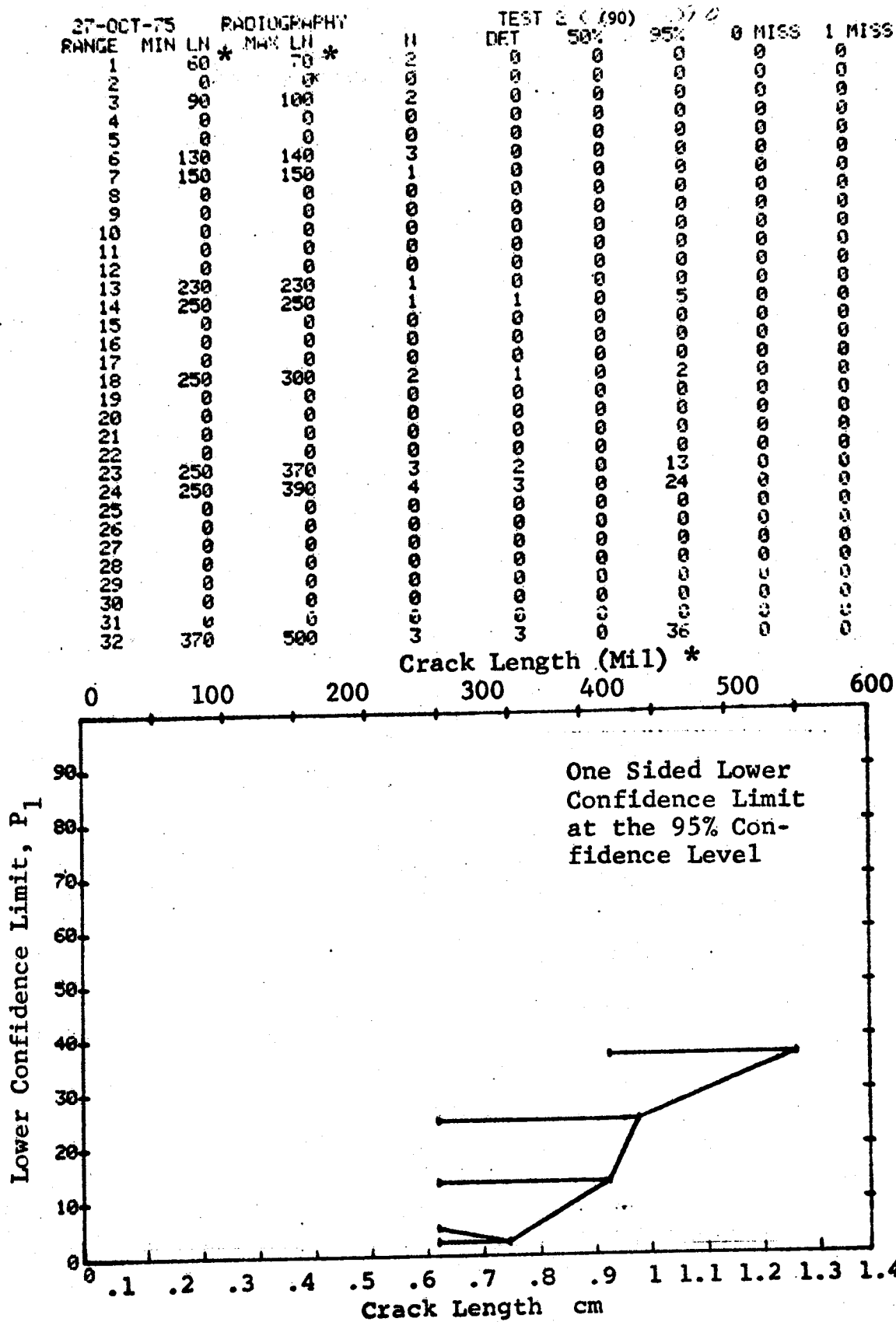


Figure D-90 (Continued)

(c) Overlapping Sixty Point Method of Data Cumulation

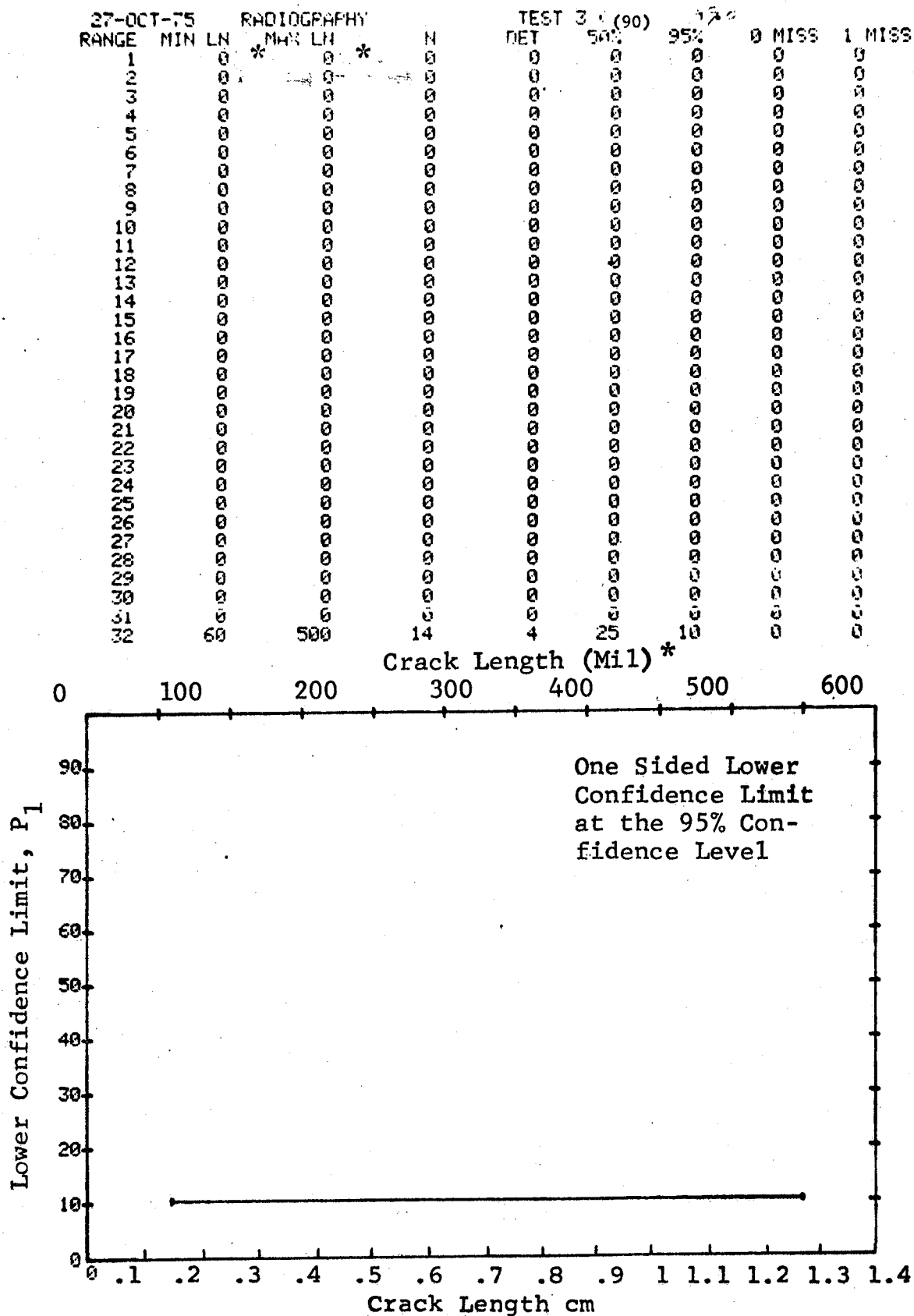


Figure D-90 (Concluded)

(a) Range Interval Method of Data Cumulation

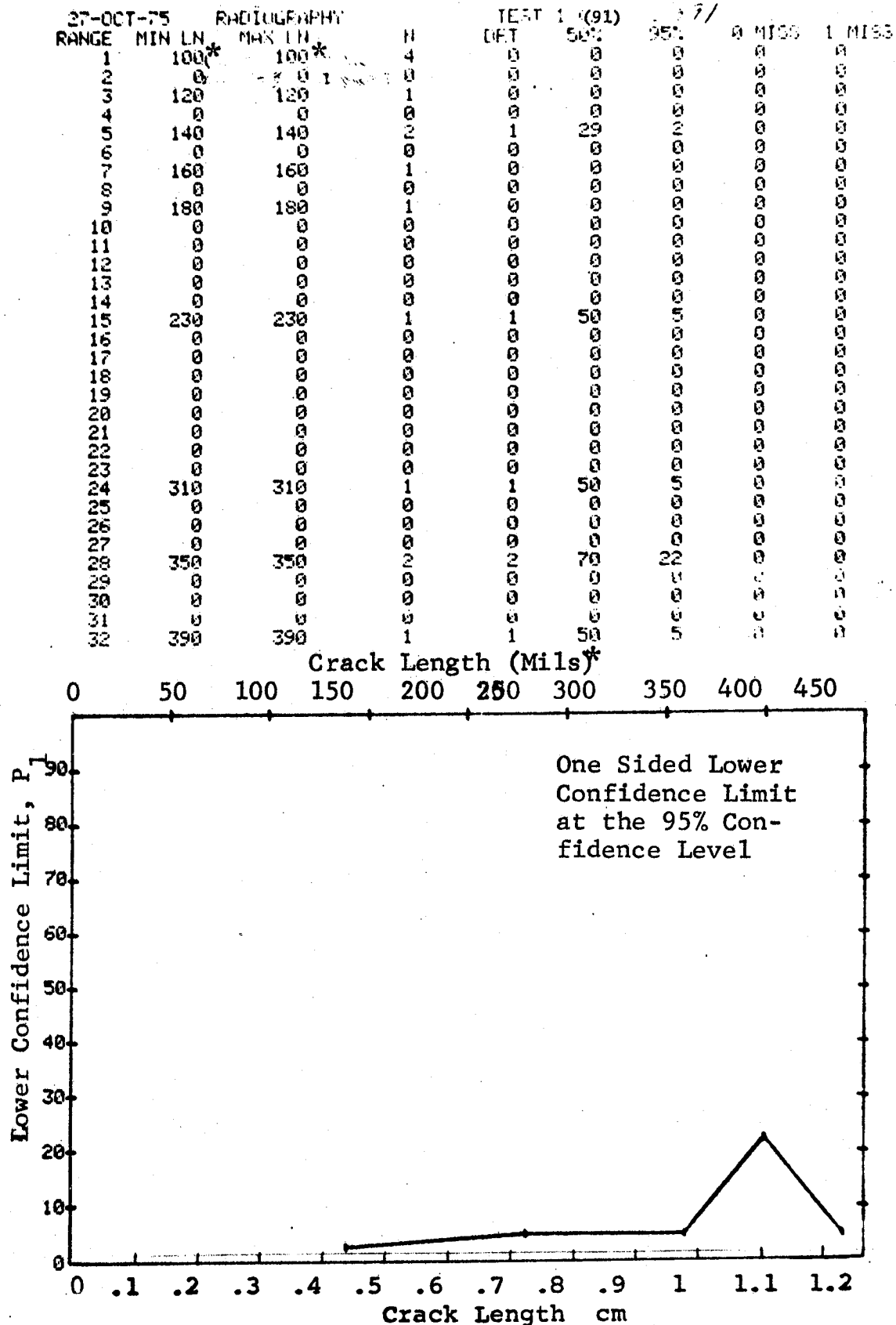


Figure D-91 Probability of Detection for 4340M Steel Using X-ray. Compressed Notch Flaws in Hollow Filleted Cylinder. Lab. Inv.

(b) Optimum Probability Method of Data Cumulation

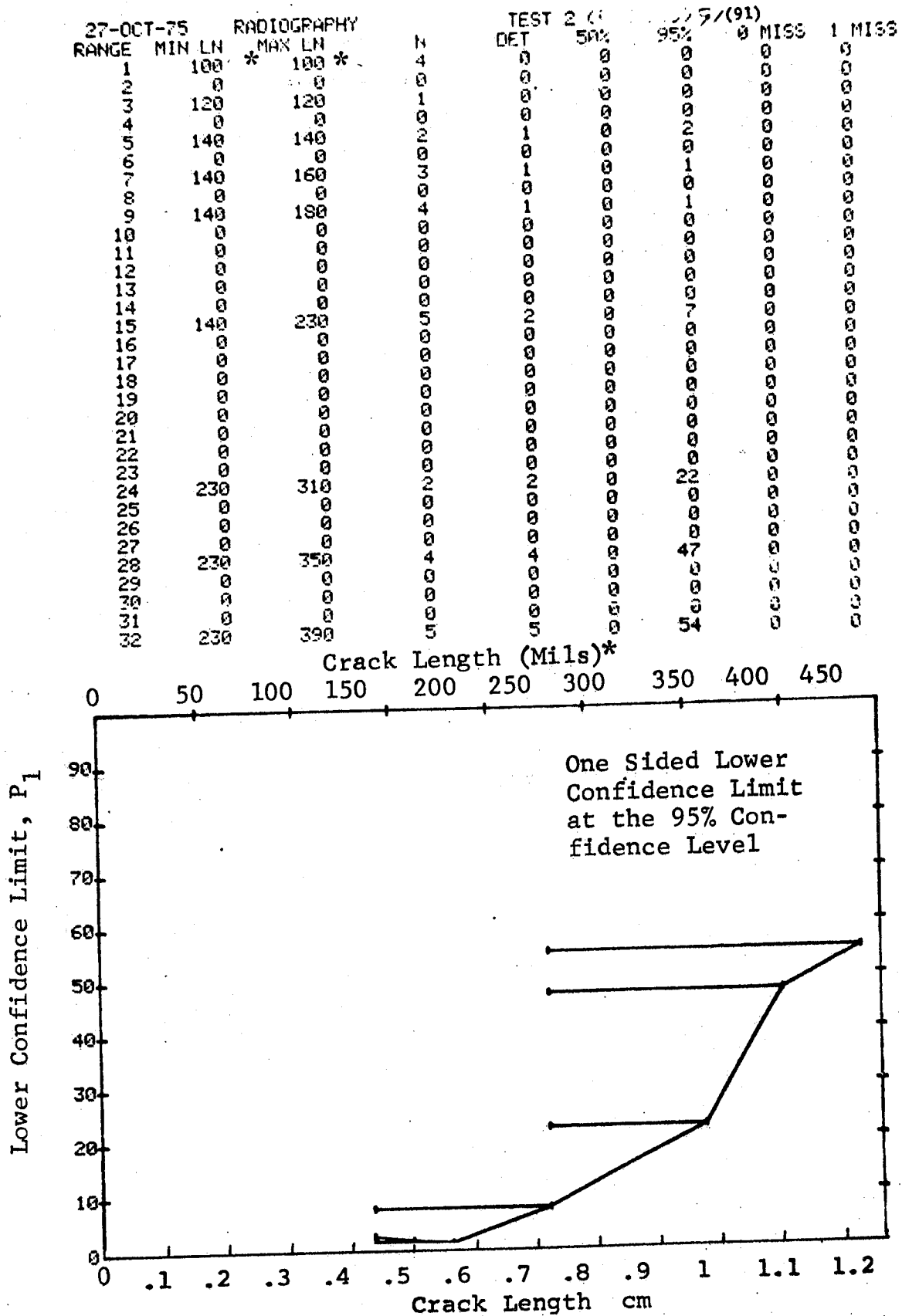


Figure D-91. (Continued).

(c) Overlapping Sixty Point Method of Data Cumulation

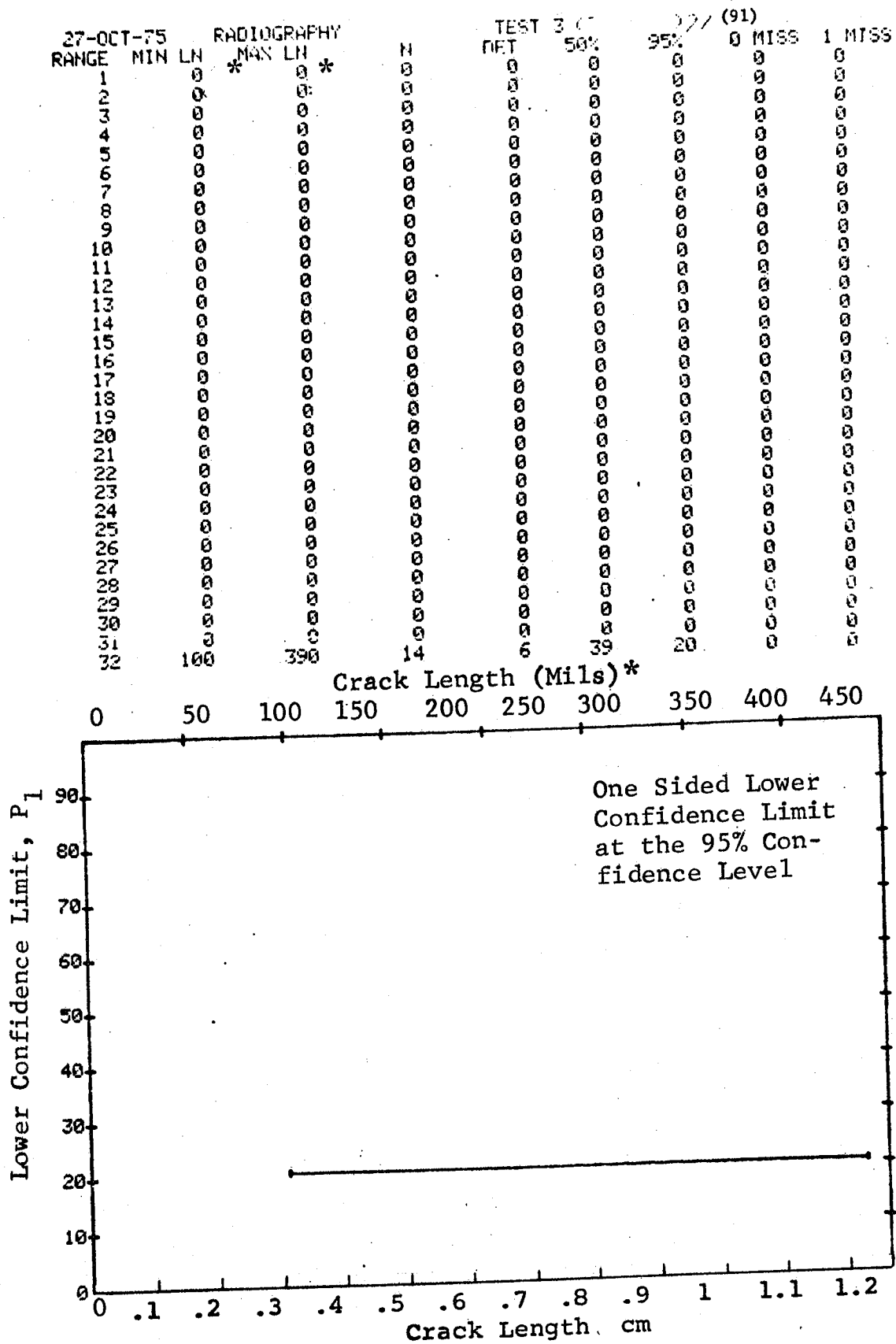


Figure D-91 (Concluded)

(a) Range Interval Method of Data Cumulation

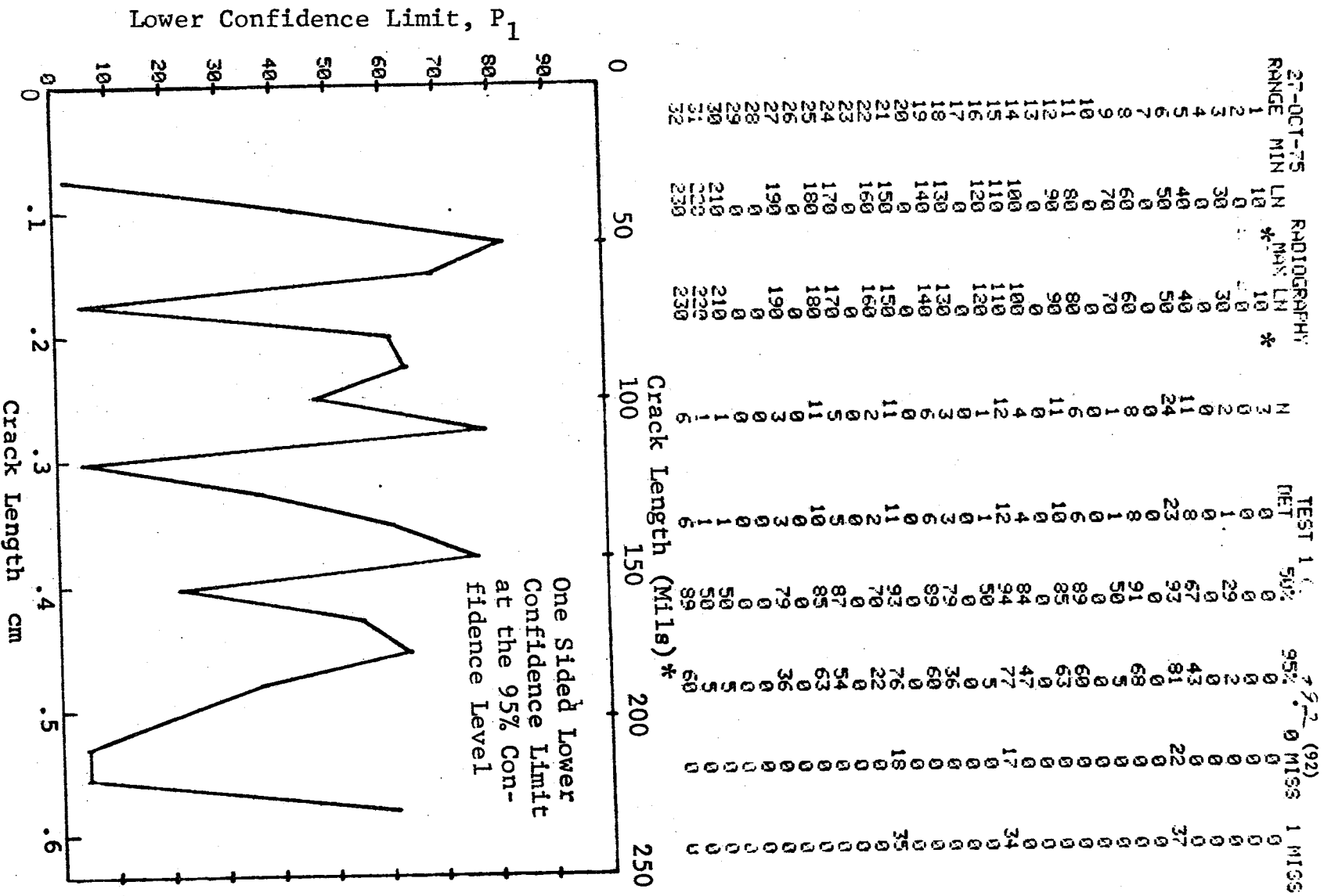


Figure D-92 Probability of Detection for 2024-T6 Al Using X-ray.
Compressed Notch Flaws in Tandem T Specimen. Lab. Env.

(b) Optimum Probability Method of Data Cumulation

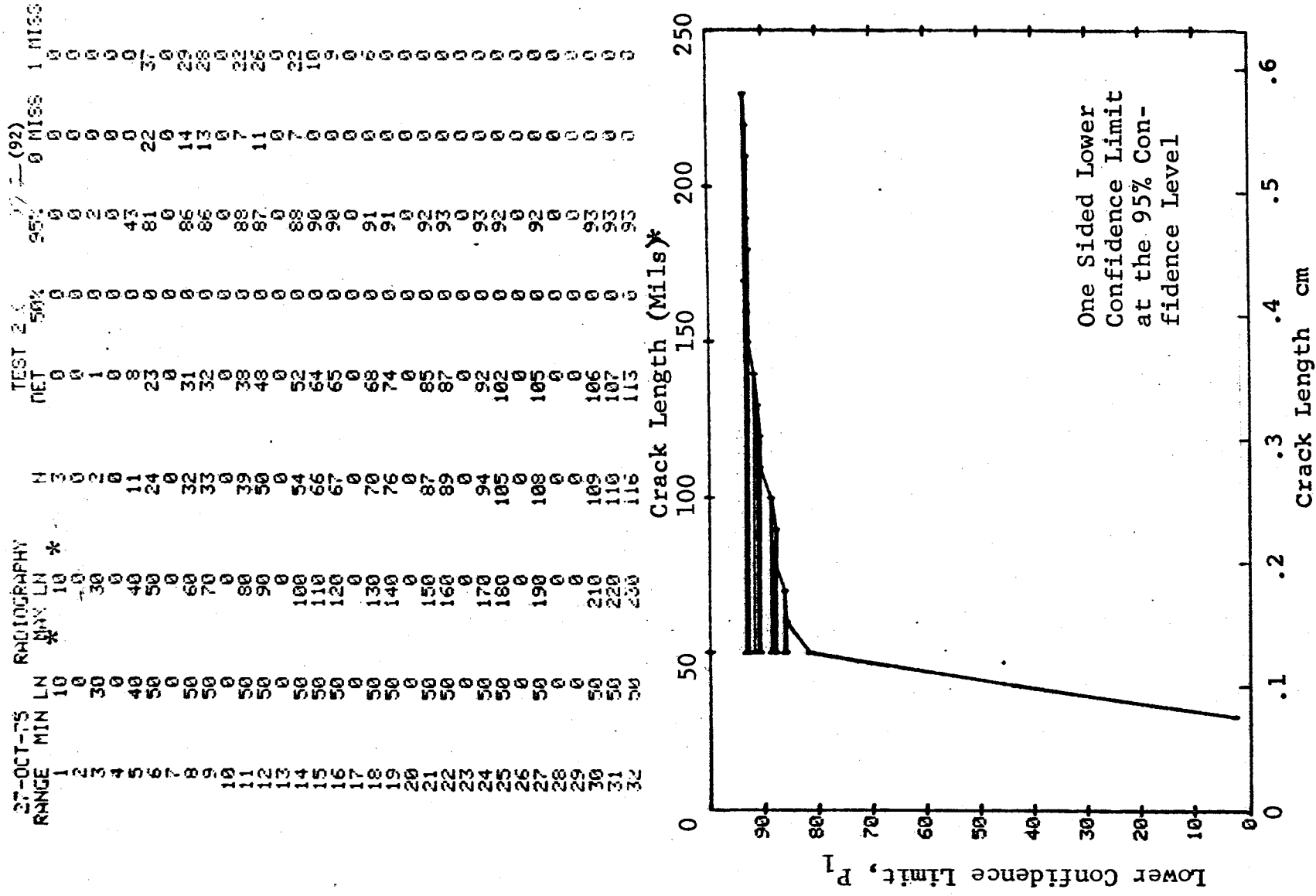


Figure D-92 (Continued)

(c) Overlapping Sixty Point Method of Data Cumulation

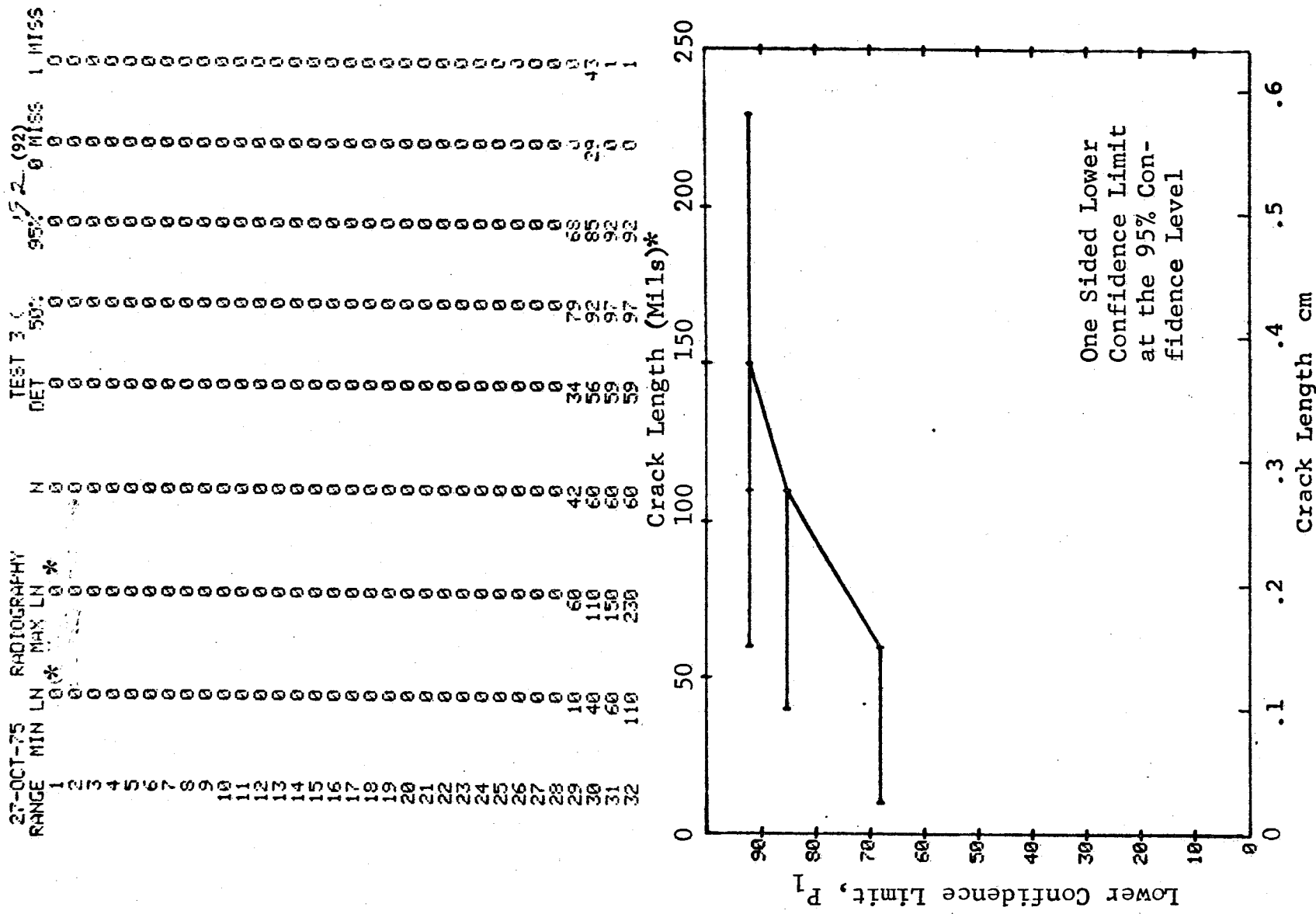


Figure D-92 (Concluded)

(a) Range Interval Method of Data Cumulation

27-OCT-75	MAGNETIC PARTICLE		TEST/	(93)	MISS	MISS
RANGE	MIN	LN	MAX	LN	DET	50%
1	30	*	50	30	15	72
2	60		70	27	26	93
3	0		0	0	0	0
4	110		120	23	23	97
5	130		140	34	34	97
6	150		160	23	23	97
7	0		0	0	0	0
8	200		200	5	5	87
9	0		0	0	0	0
10	0		0	0	0	0
11	0		0	0	0	0
12	0		0	0	0	0
13	0		0	0	0	0
14	0		0	0	0	0
15	0		0	0	0	0
16	0		0	0	0	0
17	0		0	0	0	0
18	0		0	0	0	0
19	0		0	0	0	0
20	0		0	0	0	0
21	0		0	0	0	0
22	0		0	0	0	0
23	0		0	0	0	0
24	0		0	0	0	0
25	0		0	0	0	0
26	0		0	0	0	0
27	0		0	0	0	0
28	0		0	0	0	0
29	0		0	0	0	0
30	0		0	0	0	0
31	0		0	0	0	0
32	0		0	0	0	0

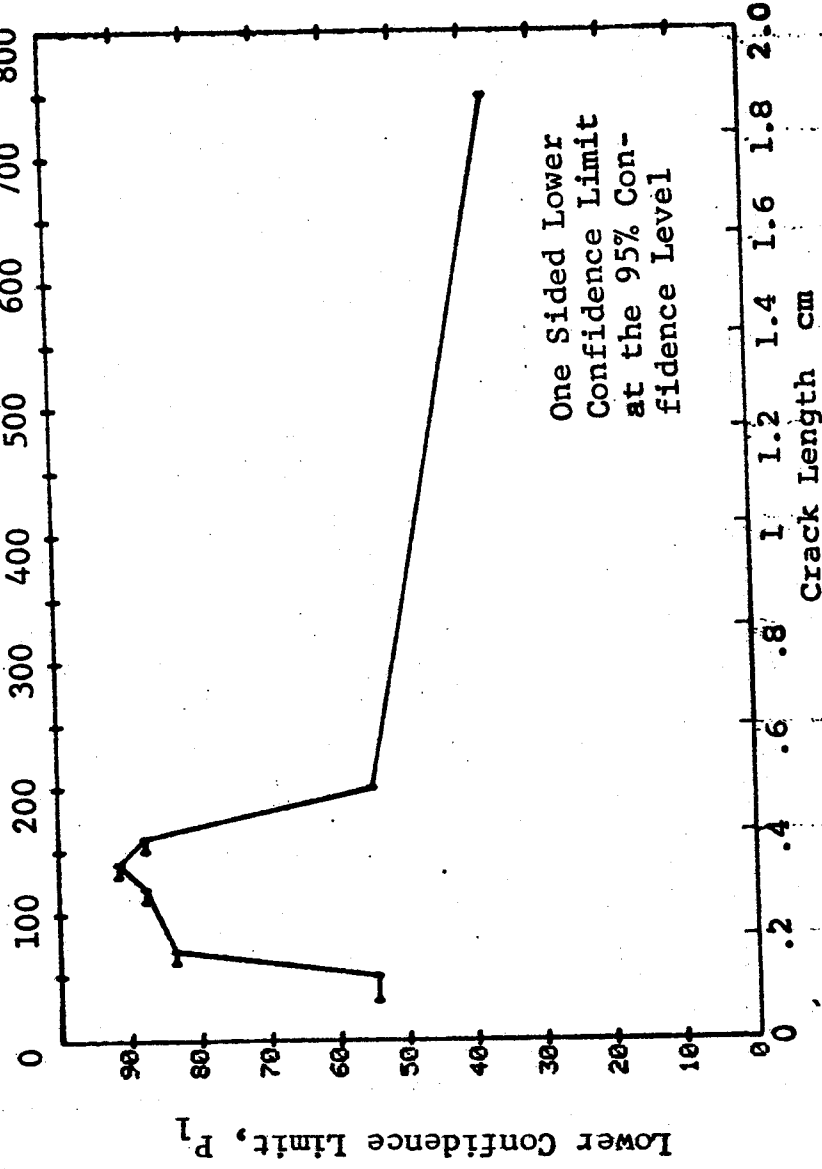


Figure D-93 Probability of Detection for 4340M Steel Using Magnetic Particles. Compressed Notch Flaws in Solid Cylinder. Prod. Env. D-285

(b) Optimum Probability Method of Data Cumulation

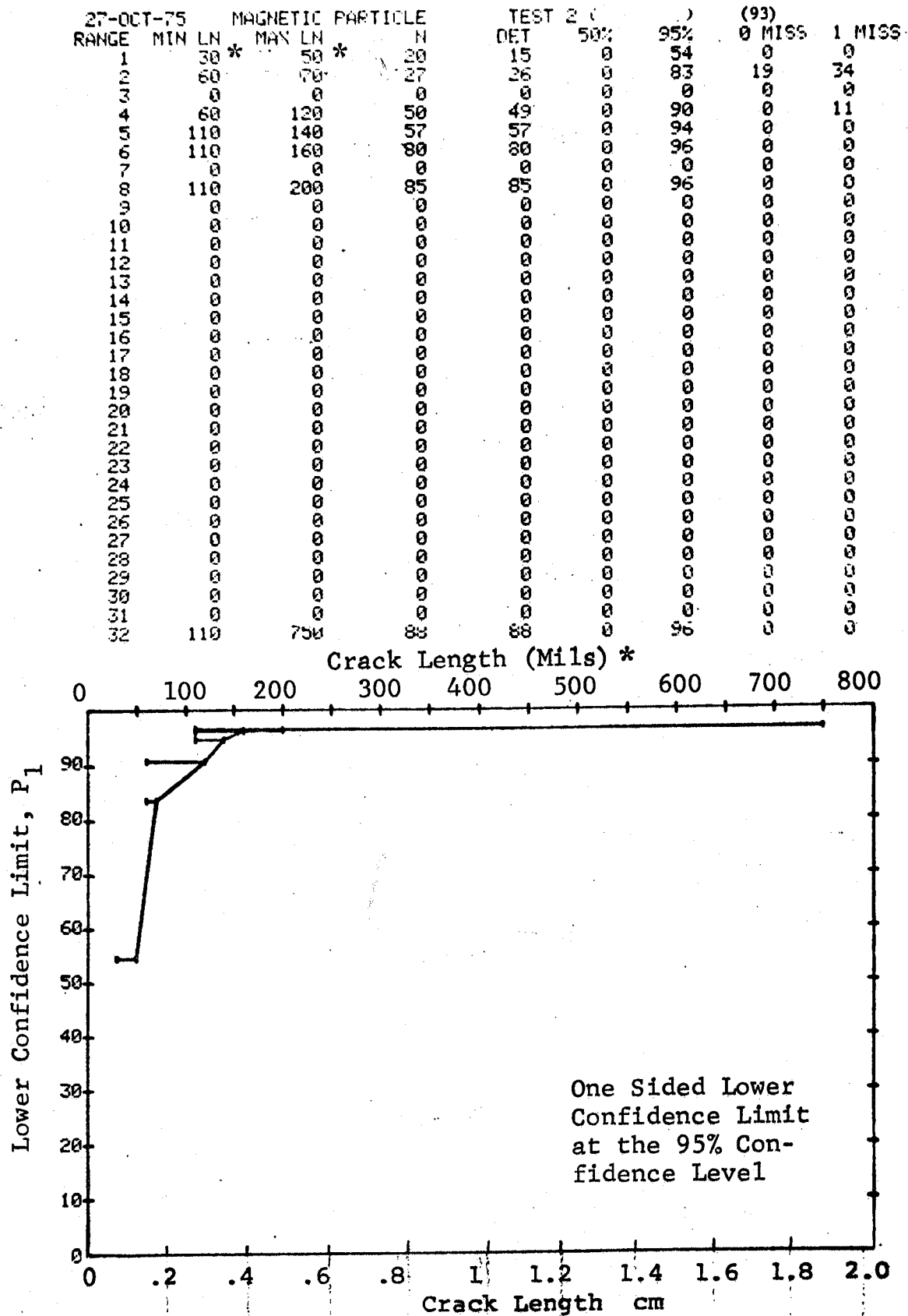


Figure D-93 (Continued)

(c) Overlapping Sixty Point Method of Data Cumulation

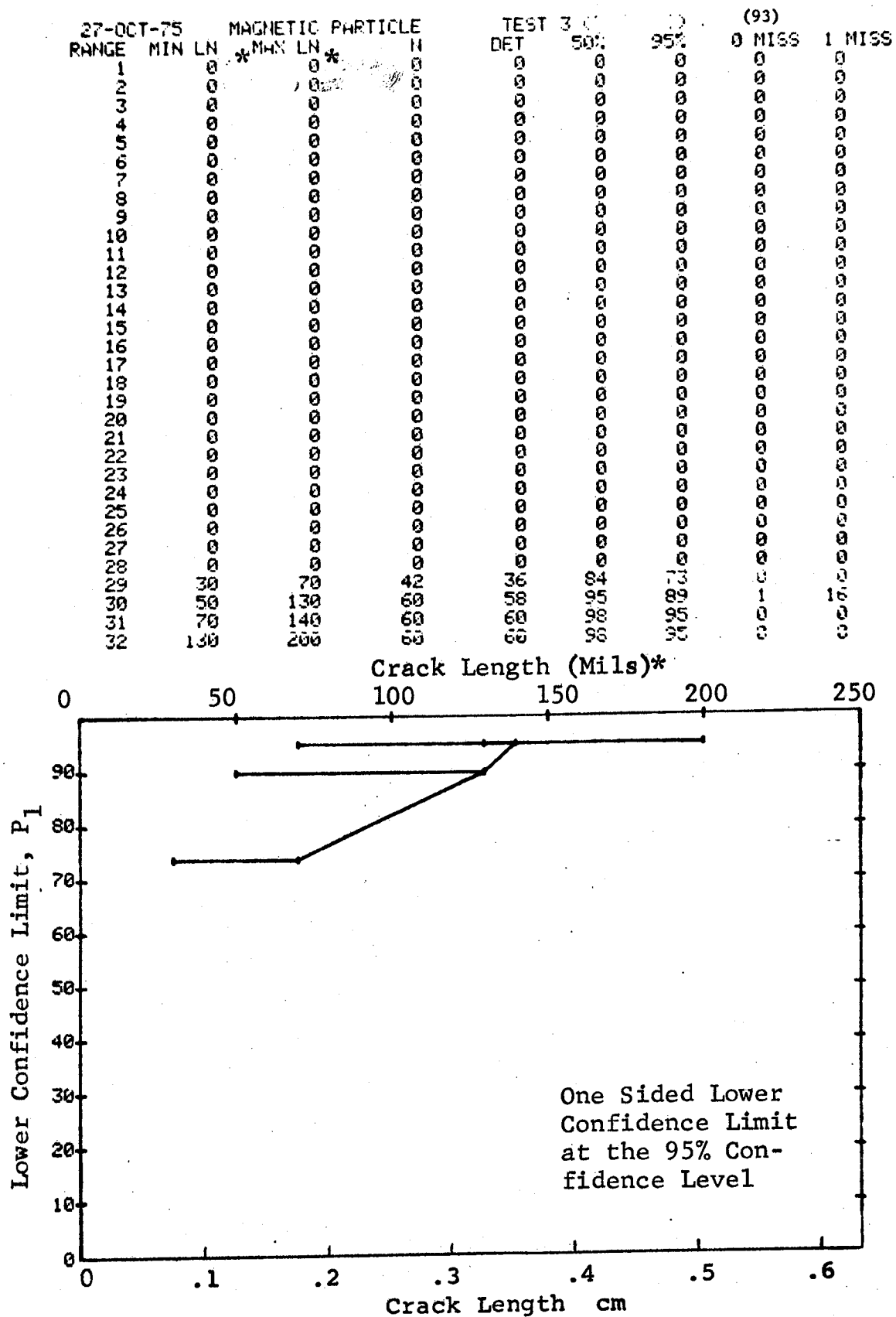


Figure D-93 (Concluded)

(a) Range Interval Method of Data Cumulation

27-OCT-75				MAGNETIC PARTICLE			TEST 1			(94)	
RANGE	MIN	LN	* MAX LN *	N	DET	50%	95%	0 MISS	1 MISS		
1	20	0	30	13	3	20	6	0	0		
2	0	0	0	0	0	0	0	0	0		
3	0	0	0	0	0	0	0	0	0		
4	60	0	60	9	9	92	71	0	0		
5	70	0	70	16	15	89	73	0	0		
6	0	0	0	0	0	0	0	0	0		
7	90	0	90	11	11	93	76	18	35		
8	100	0	100	8	8	91	68	0	0		
9	0	0	0	0	0	0	0	0	0		
10	130	0	130	4	4	84	47	0	0		
11	140	0	140	7	7	90	65	0	0		
12	150	0	150	9	9	92	71	0	0		
13	0	0	0	0	0	0	0	0	0		
14	0	0	0	0	0	0	0	0	0		
15	0	0	0	0	0	0	0	0	0		
16	0	0	0	0	0	0	0	0	0		
17	0	0	0	0	0	0	0	0	0		
18	0	0	0	0	0	0	0	0	0		
19	0	0	0	0	0	0	0	0	0		
20	0	0	0	0	0	0	0	0	0		
21	0	0	0	0	0	0	0	0	0		
22	260	0	260	2	2	70	22	0	0		
23	0	0	0	0	0	0	0	0	0		
24	0	0	0	0	0	0	0	0	0		
25	300	0	300	5	5	87	54	0	0		
26	0	0	0	0	0	0	0	0	0		
27	0	0	0	0	0	0	0	0	0		
28	0	0	0	0	0	0	0	0	0		
29	0	0	0	0	0	0	0	0	0		
30	0	0	0	0	0	0	0	0	0		
31	0	0	0	0	0	0	0	0	0		
32	370	0	380	5	5	87	54	0	0		

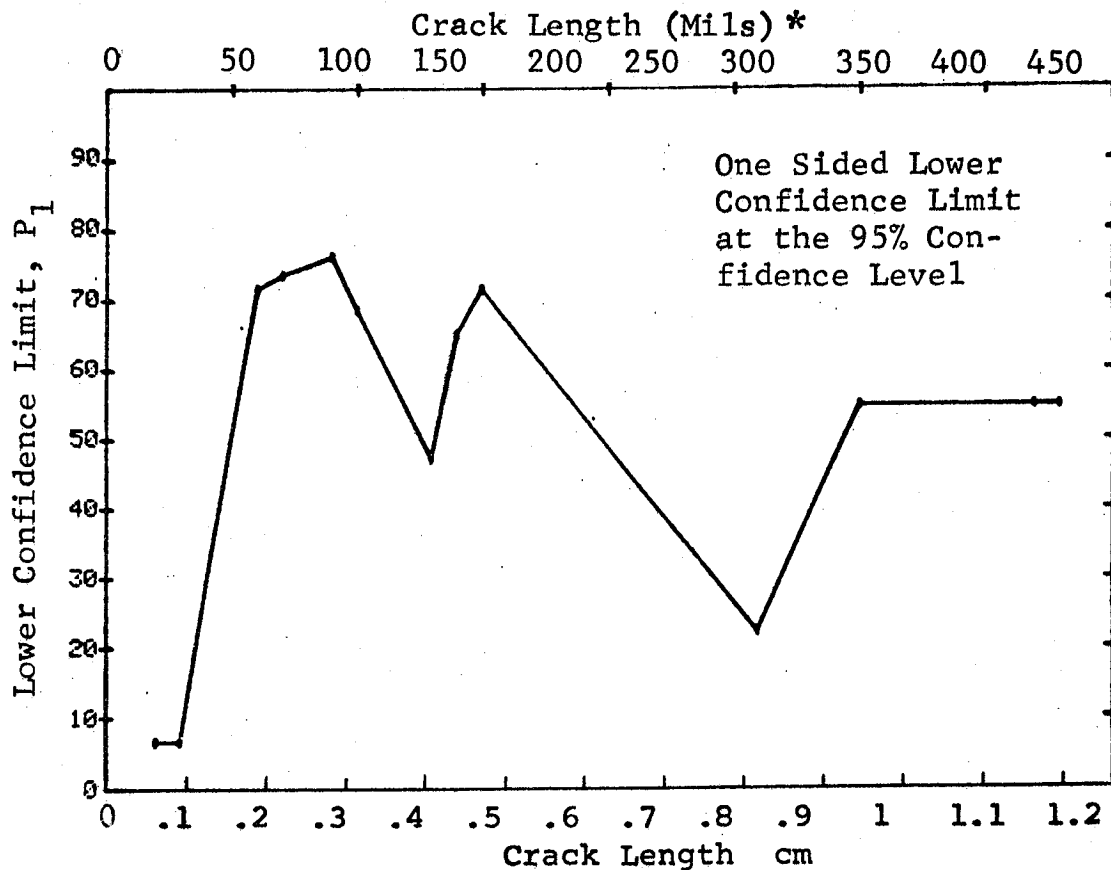


Figure D-94 Probability of Detection for 4340M Steel Using Magnetic Particles. Compressed Notch Flaws in Hollow Filleted Cylinder. Prod. Env.

(b) Optimum Probability Method of Data Cumulation

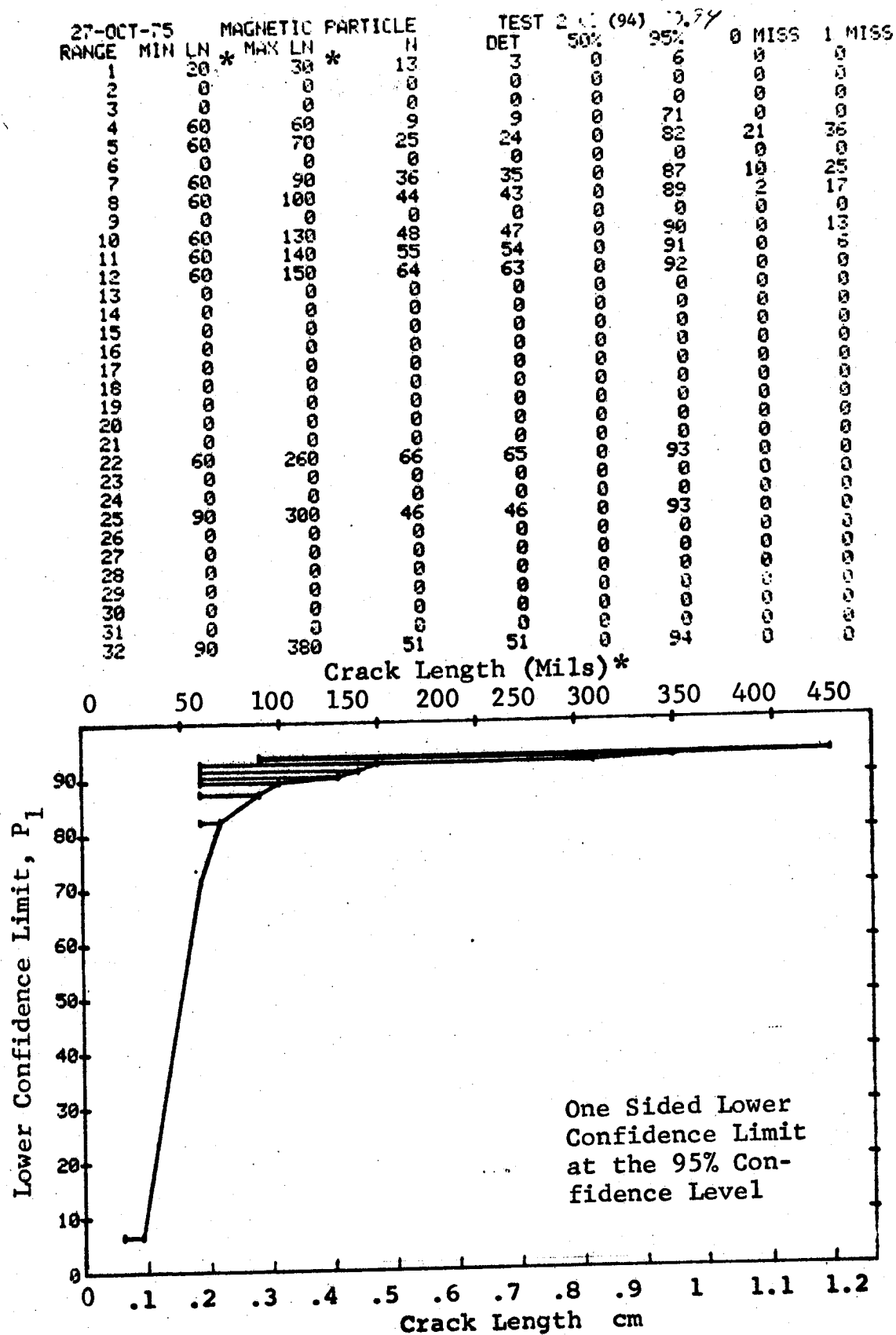


Figure D-94 (Continued)

(c) Overlapping Sixty Point Method of Data Cumulation

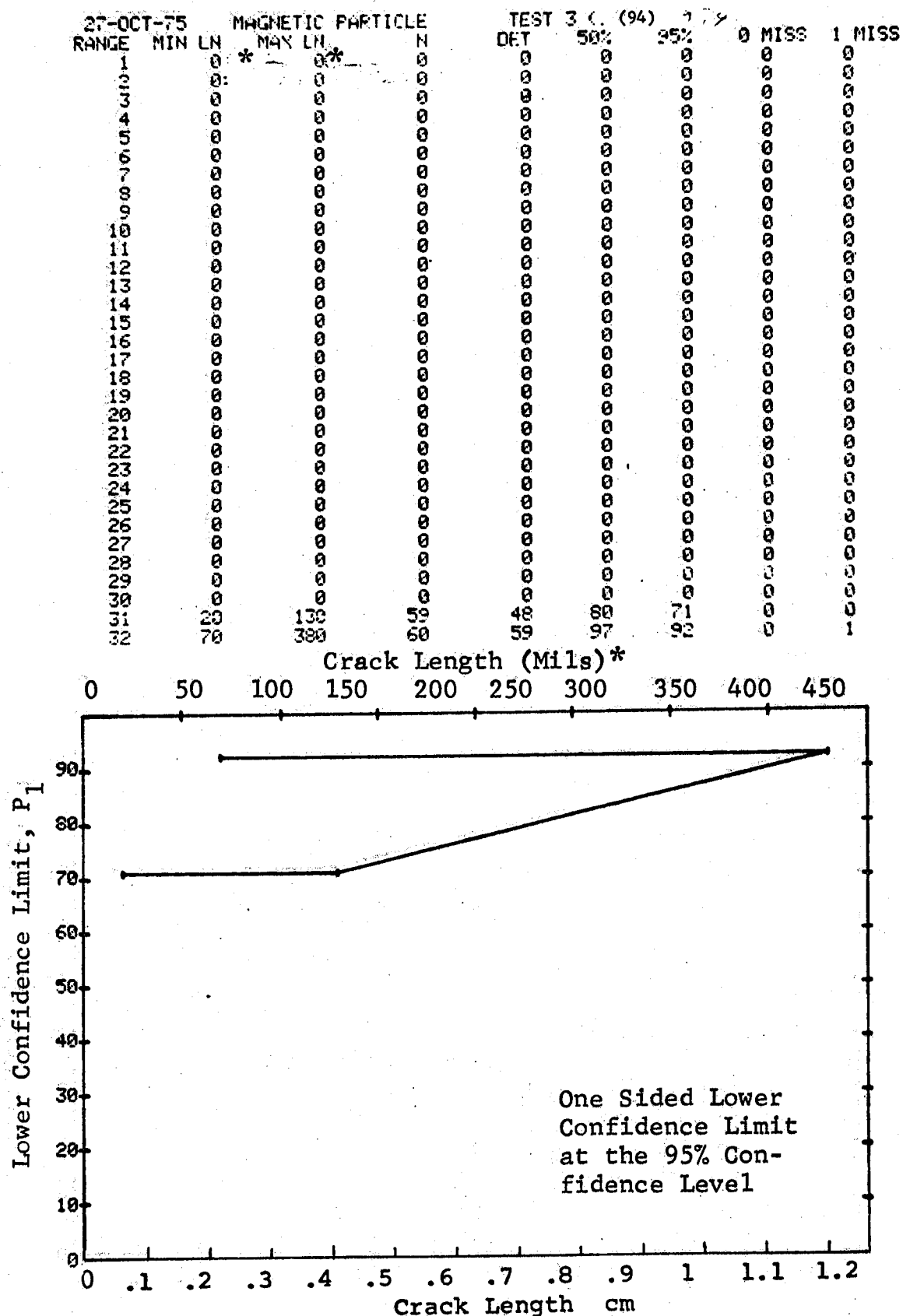


Figure D-94 (Concluded)

(a) Range Interval Method of Data Cumulation

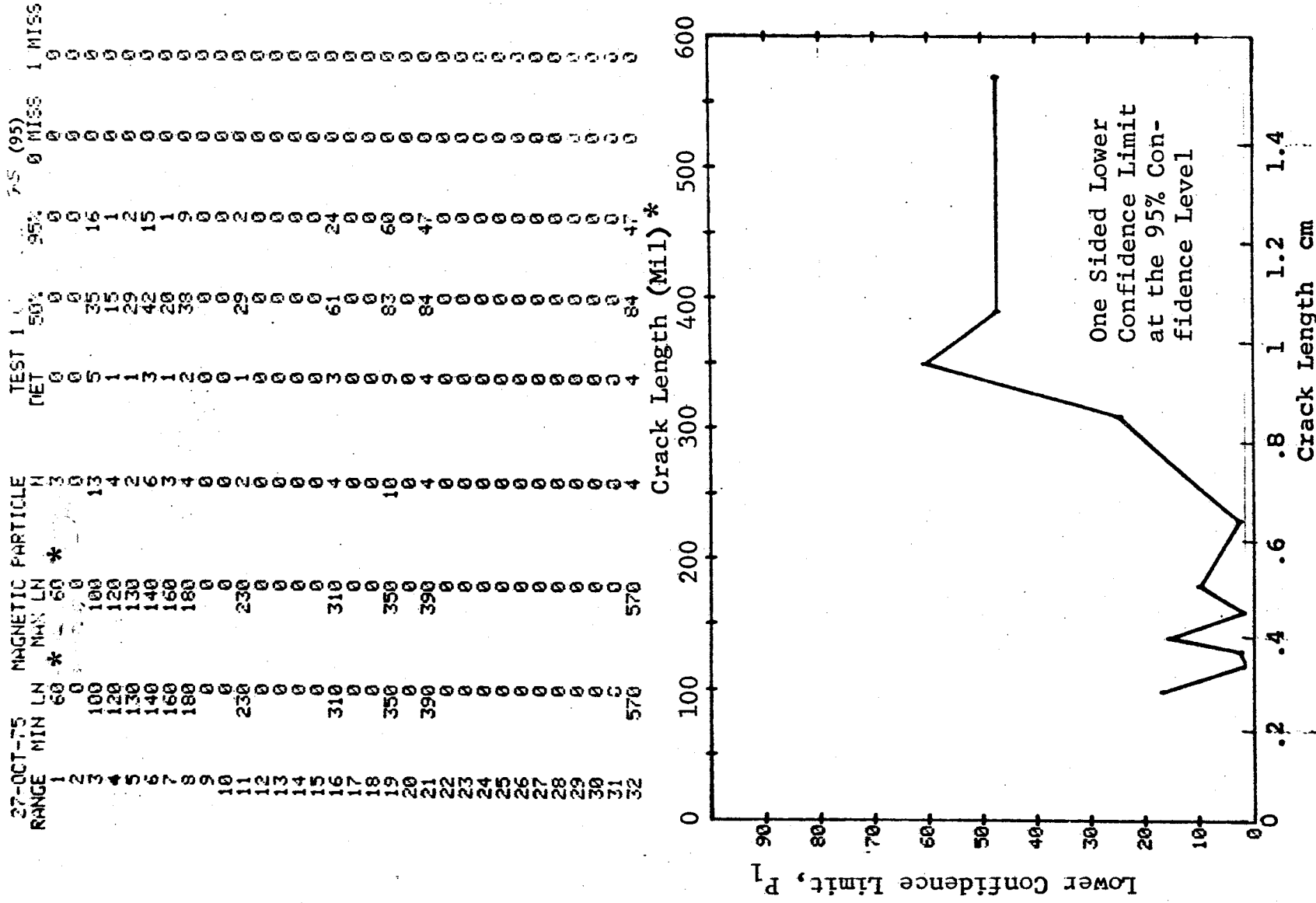


Figure D-95 Probability of Detection for 4340M Steel Using Magnetic Particles. Compressed Notch Flaws in Hollow Filleted Cylinder.
Prod. Env. D-291

(b) Optimum Probability Method of Data Cumulation

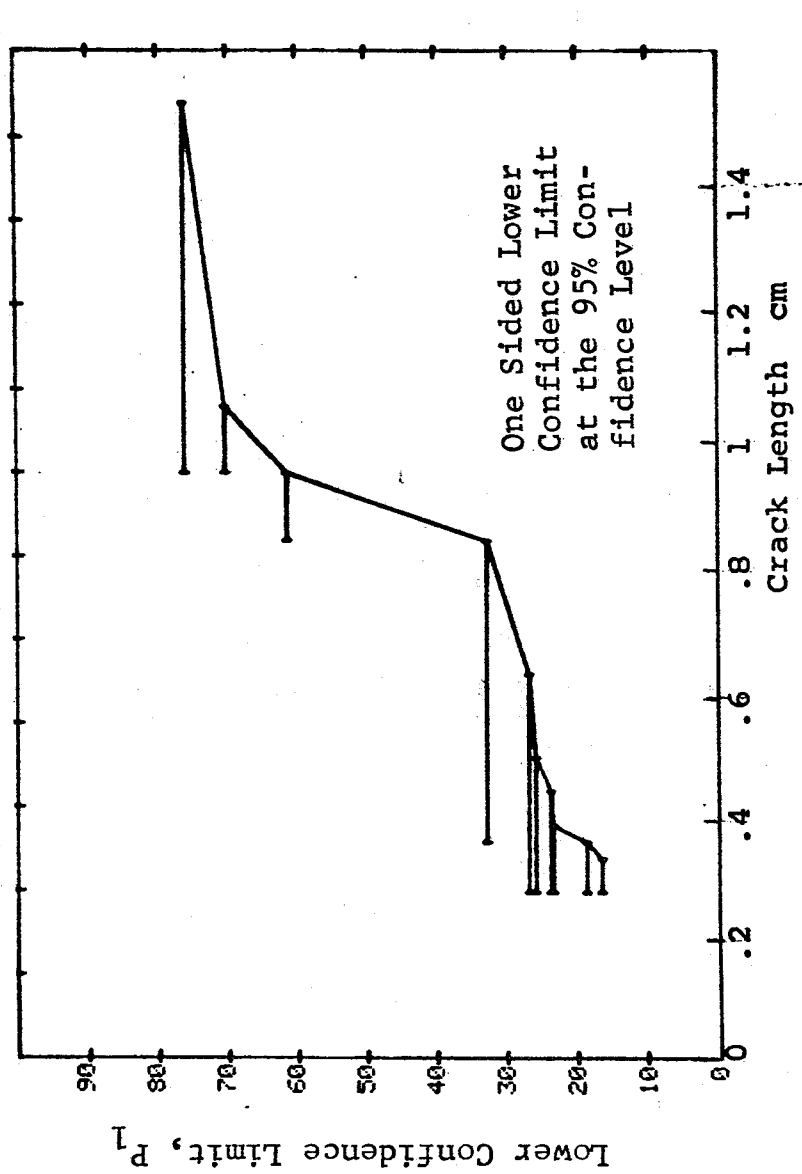
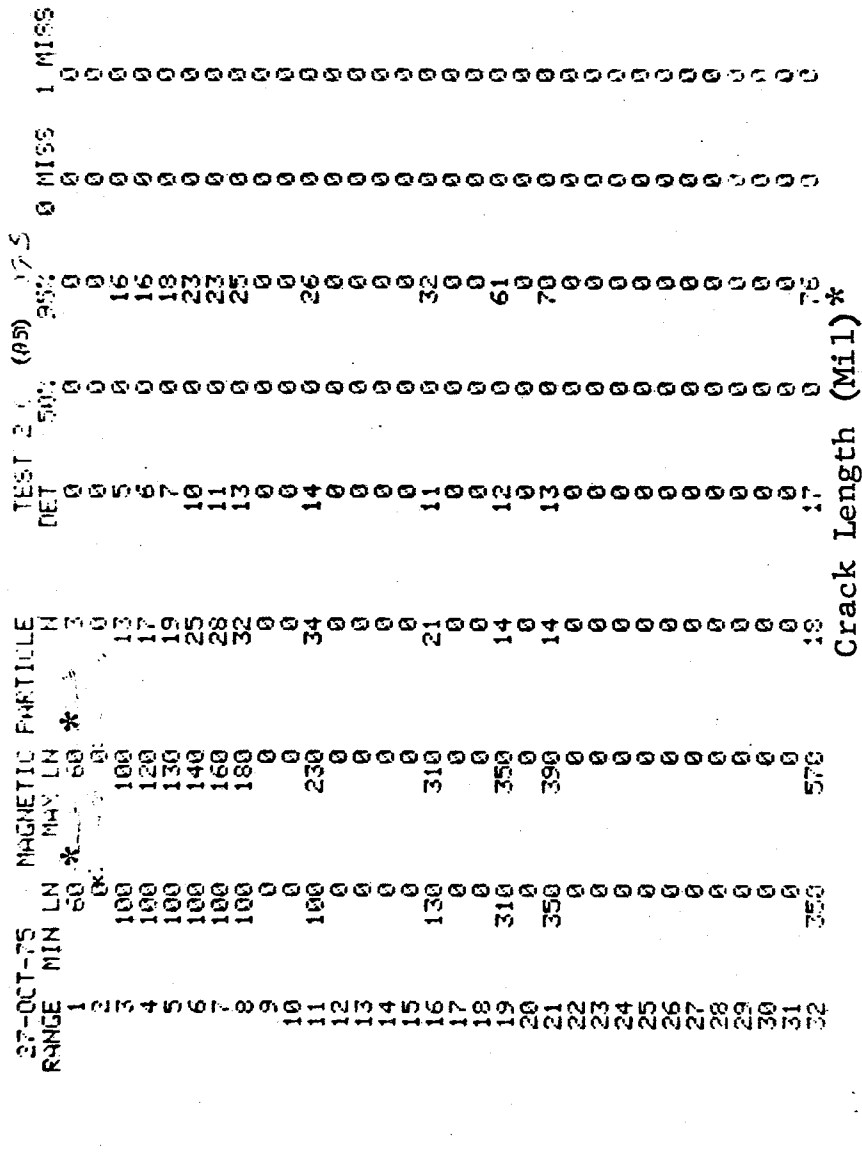


Figure D-95 (Continued)

(c) Overlapping Sixty Point Method of Data Cumulation

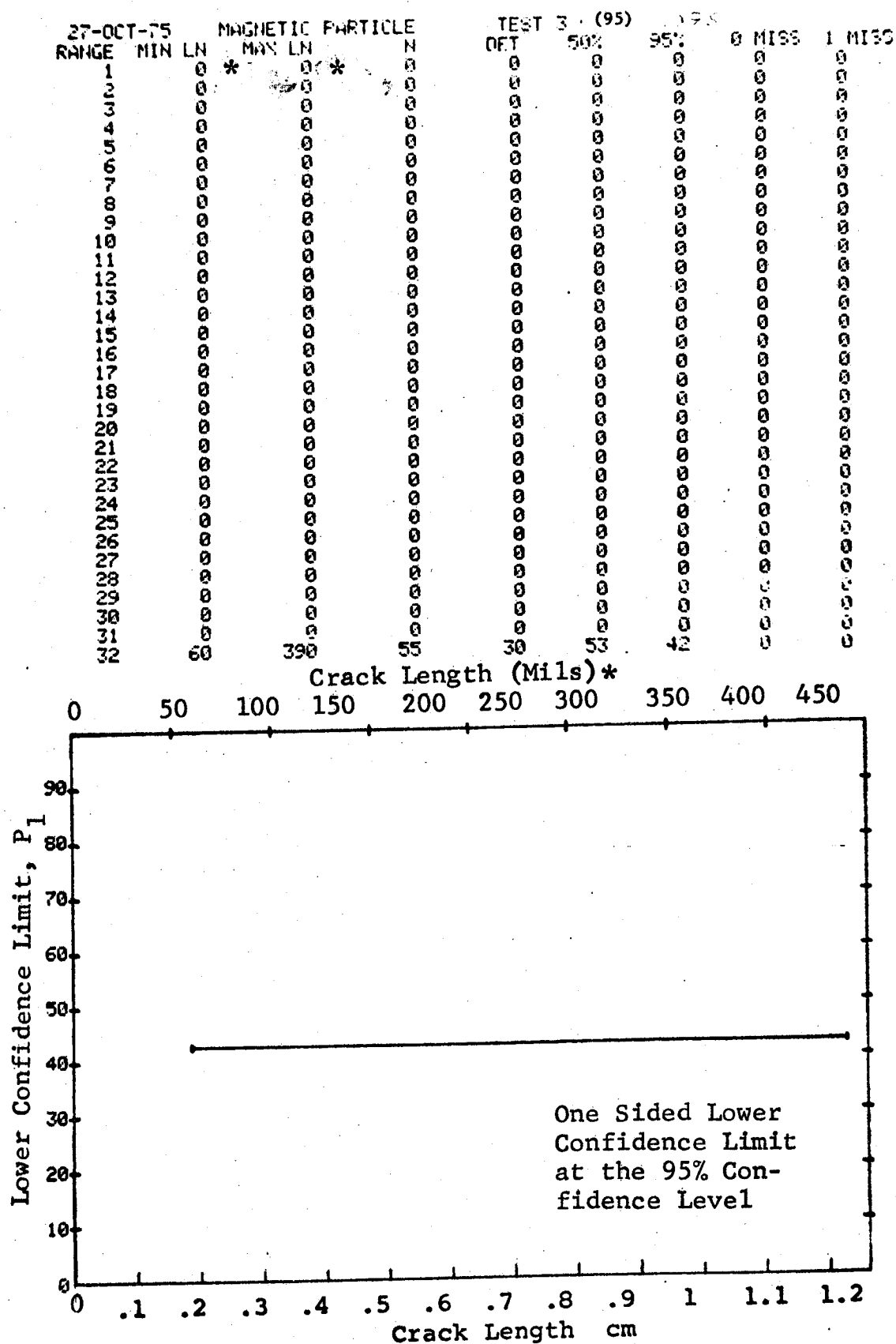


Figure D-95 (Concluded)

(a) Range Interval Method of Data Cumulation

28-OCT-75			MAGNETIC PARTICLE			TEST 1			(96)		
RANGE	MIN	LN	MAX	LN	N	DET	50%	95%	0	MISS	1
1	80	*	90	*	10	2	16	3	0	0	0
2	0		0		0	0	0	0	0	0	0
3	110		110		4	0	0	0	0	0	0
4	120		120		3	2	50	13	0	0	0
5	130		130		3	0	0	0	0	0	0
6	140		140		8	1	8	0	0	0	0
7	160		160		3	1	20	1	0	0	0
8	0		0		0	0	0	0	0	0	0
9	0		0		0	0	0	0	0	0	0
10	0		0		0	0	0	0	0	0	0
11	0		0		0	0	0	0	0	0	0
12	0		0		0	0	0	0	0	0	0
13	0		0		0	0	0	0	0	0	0
14	0		0		0	0	0	0	0	0	0
15	250		250		2	1	29	2	0	0	0
16	270		270		5	2	31	2	0	0	0
17	280		280		2	1	29	2	0	0	0
18	0		0		0	0	0	0	0	0	0
19	300		300		3	2	50	13	0	0	0
20	310		310		3	2	50	13	0	0	0
21	0		0		0	0	0	0	0	0	0
22	0		0		0	0	0	0	0	0	0
23	0		0		0	0	0	0	0	0	0
24	0		0		0	0	0	0	0	0	0
25	0		0		0	0	0	0	0	0	0
26	0		0		0	0	0	0	0	0	0
27	0		0		0	0	0	0	0	0	0
28	0		0		0	0	0	0	0	0	0
29	0		0		0	0	0	0	0	0	0
30	0		0		0	0	0	0	0	0	0
31	440		440		3	3	70	30	0	0	0
32	450		450		5	2	31	10	0	0	0

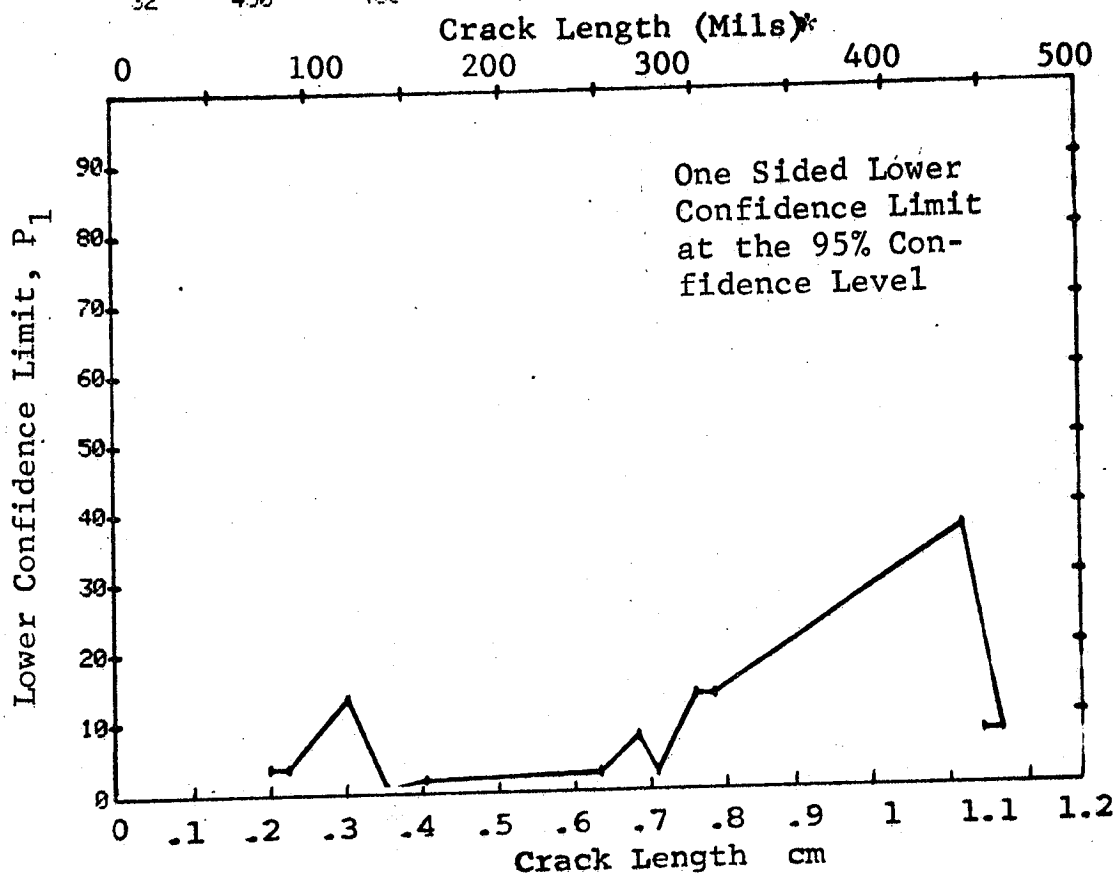


Figure D-96 Probability of Detection for 4340M Steel Using Magnetic Particles. Compressed Notch Flaws in Hollow Filleted Cylinder Prod. Env. D-294

(b) Optimum Probability Method of Data Cumulation

28-OCT-75			MAGNETIC PARTICLE			TEST 2 (96)				
RANGE	MIN	LN	MAX	LN	N	DET	50%	95%	0 MISS	1 MISS
1		80 *	90 *		10	2	0	3	0	0
2		0	0		10	0	0	0	0	0
3		80	110		14	2	0	2	0	0
4	120	120	120		3	2	0	13	0	0
5	80	130	130		20	4	0	7	0	0
6	80	140	140		28	5	0	7	0	0
7	80	160	160		31	6	0	8	0	0
8	0	0	0		0	0	0	0	0	0
9	0	0	0		0	0	0	0	0	0
10	0	0	0		0	0	0	0	0	0
11	0	0	0		0	0	0	0	0	0
12	0	0	0		0	0	0	0	0	0
13	0	0	0		0	0	0	0	0	0
14	0	0	0		0	0	0	0	0	0
15	120	250	250		19	5	0	10	0	0
16	160	270	270		10	4	0	15	0	0
17	160	280	280		12	5	0	18	0	0
18	0	0	0		0	0	0	0	0	0
19	250	300	300		12	6	0	24	0	0
20	250	310	310		15	8	0	29	0	0
21	0	0	0		0	0	0	0	0	0
22	0	0	0		0	0	0	0	0	0
23	0	0	0		0	0	0	0	0	0
24	0	0	0		0	0	0	0	0	0
25	0	0	0		0	0	0	0	0	0
26	0	0	0		0	0	0	0	0	0
27	0	0	0		0	0	0	0	0	0
28	0	0	0		0	0	0	0	0	0
29	0	0	0		0	0	0	0	0	0
30	0	0	0		0	0	0	0	0	0
31	300	440	440		9	7	0	45	0	0
32	300	460	460		14	9	0	39	0	0

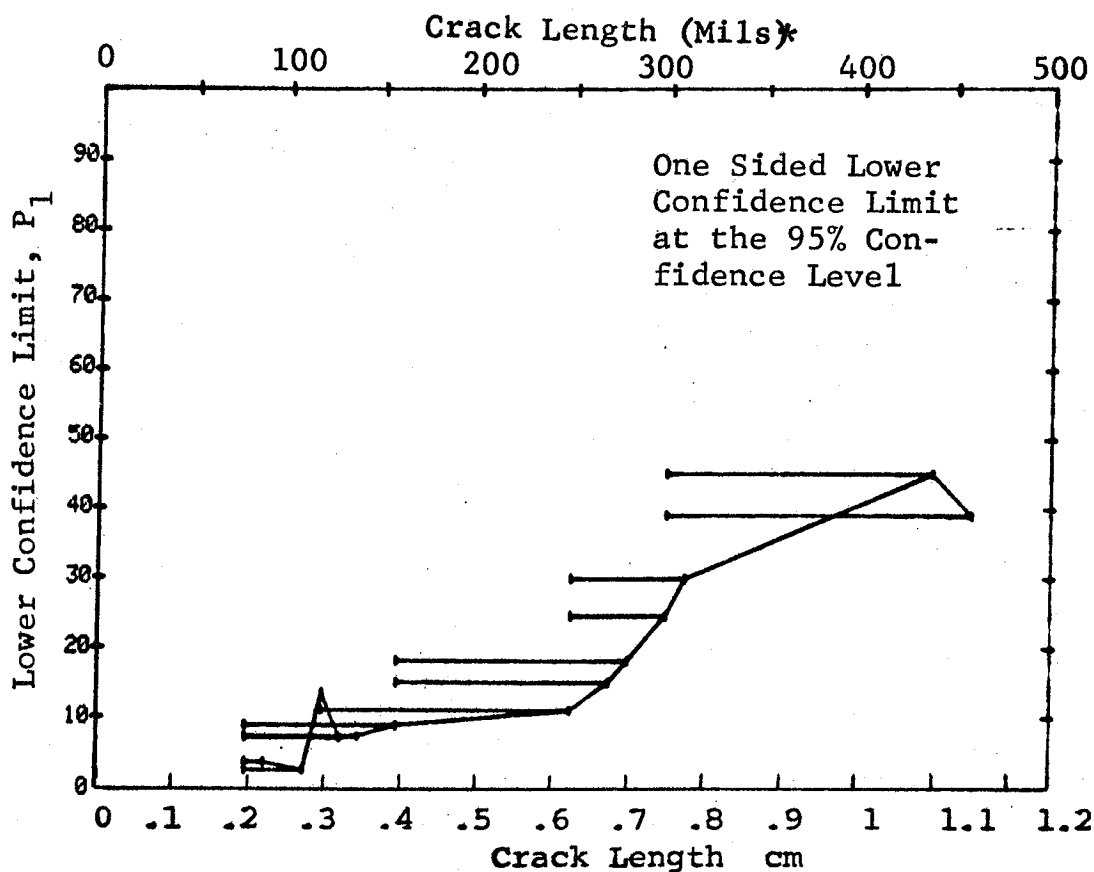


Figure D-96 (Continued)

(c) Overlapping Sixty Point Method of Data Cumulation

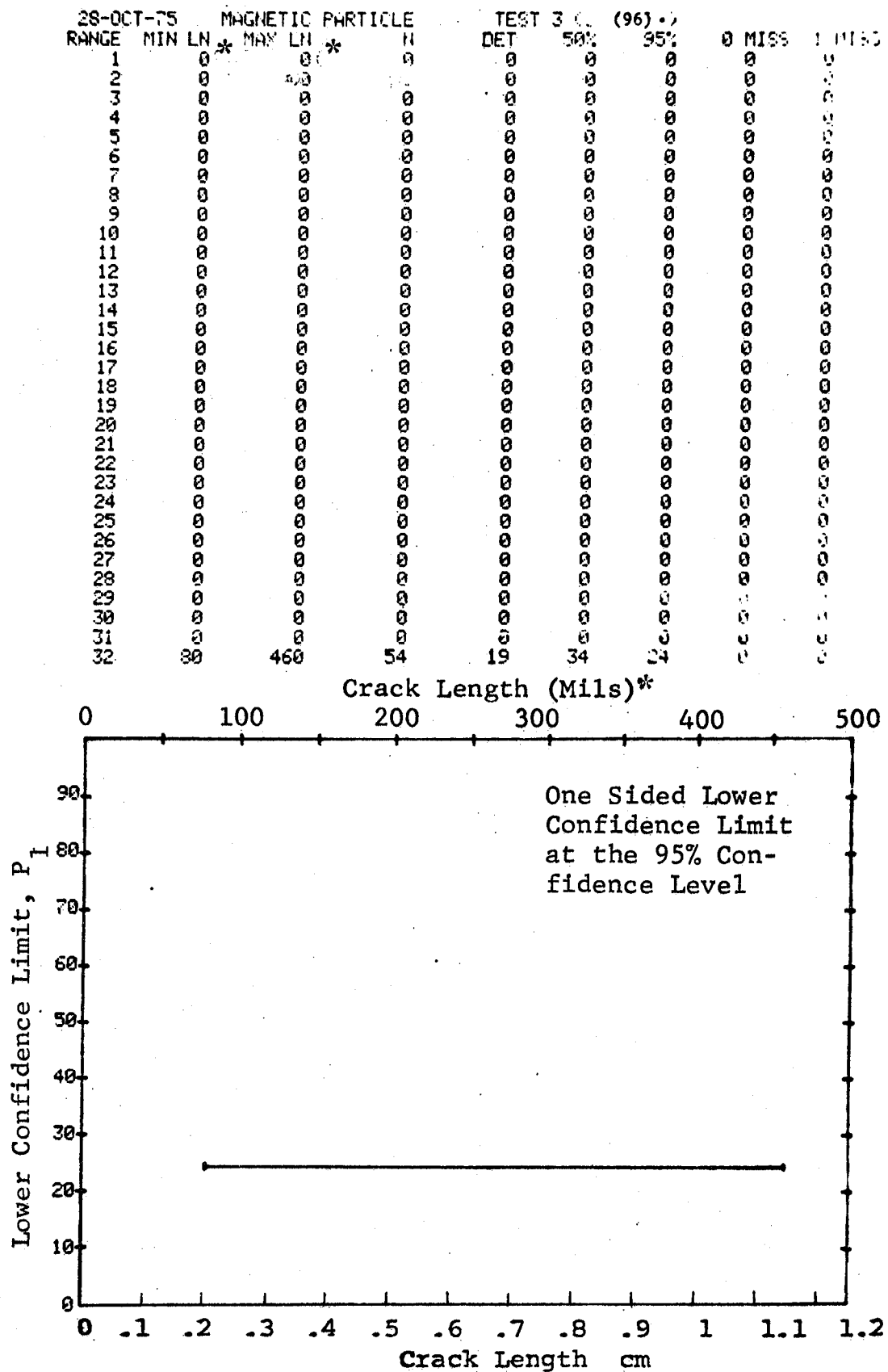


Figure D-96 (Concluded)

(a) Range Interval Method of Data Cumulation

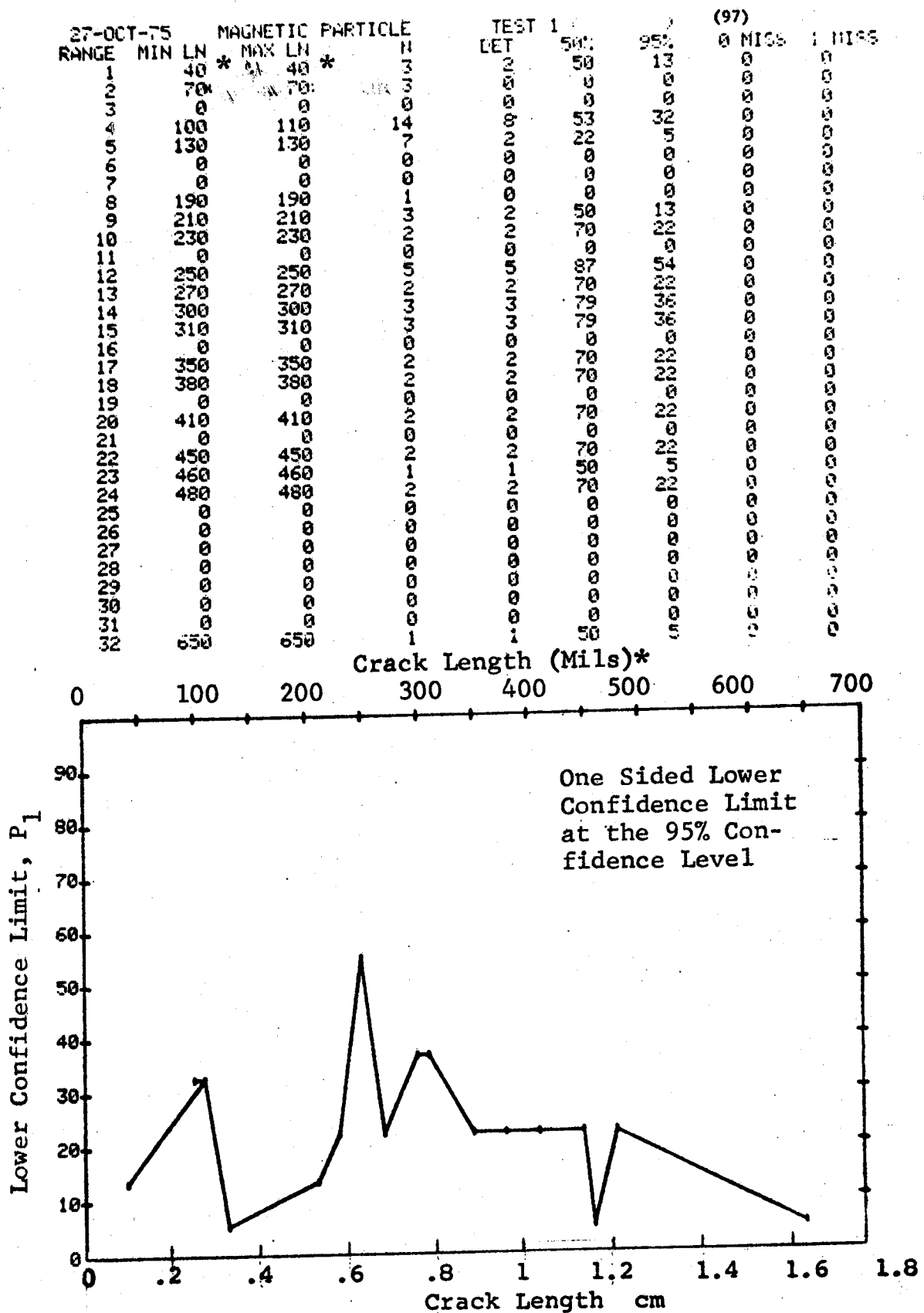


Figure D-97 Probability of Detection for 4340M Steel Using Magnetic Particles. Compressed Notch Flaws in Solid Threaded Cylinder. Prod. Env.

(b) Optimum Probability Method of Data Cumulation

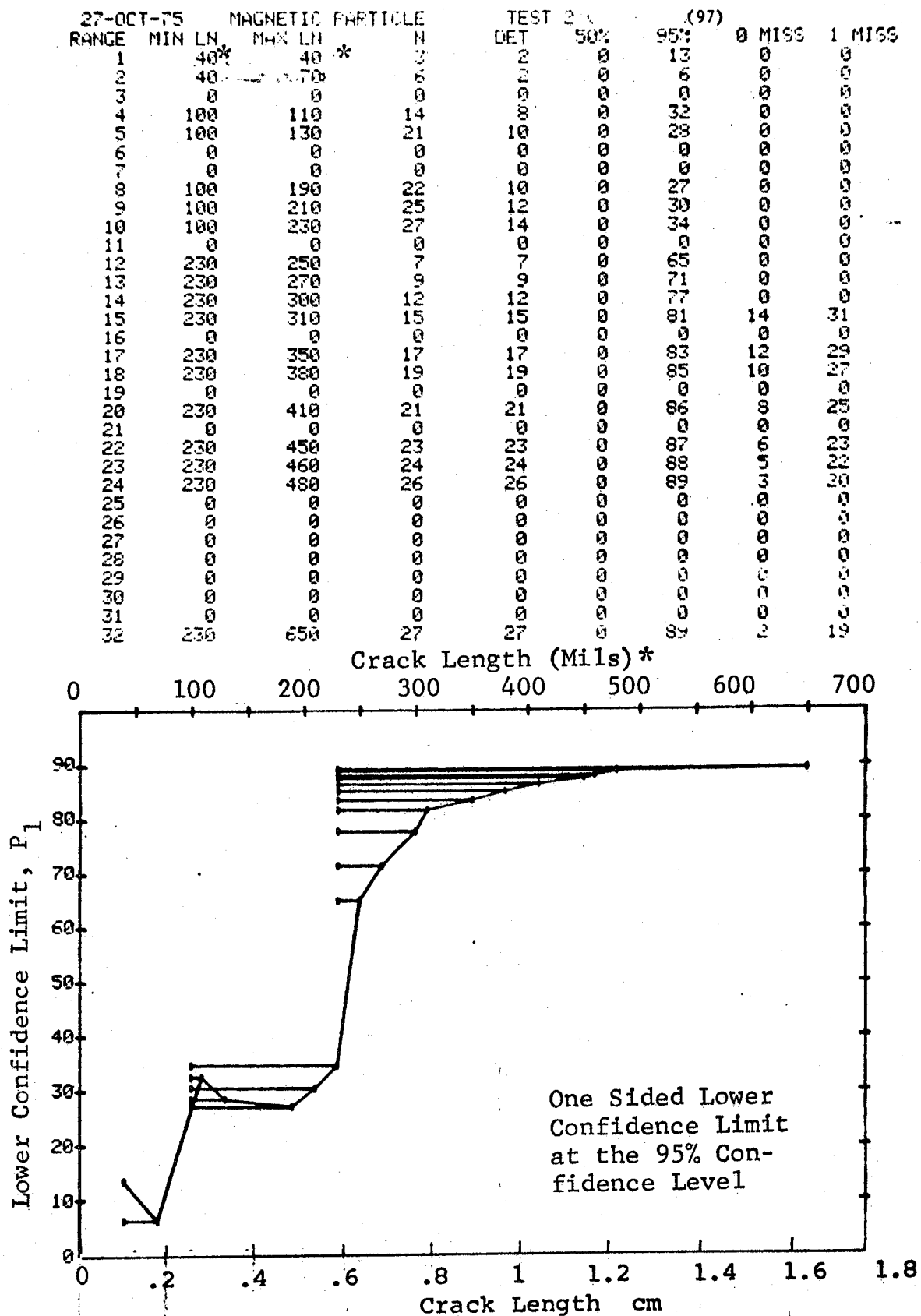


Figure D-97 (Continued)

(c) Overlapping Sixty Point Method of Data Cumulation

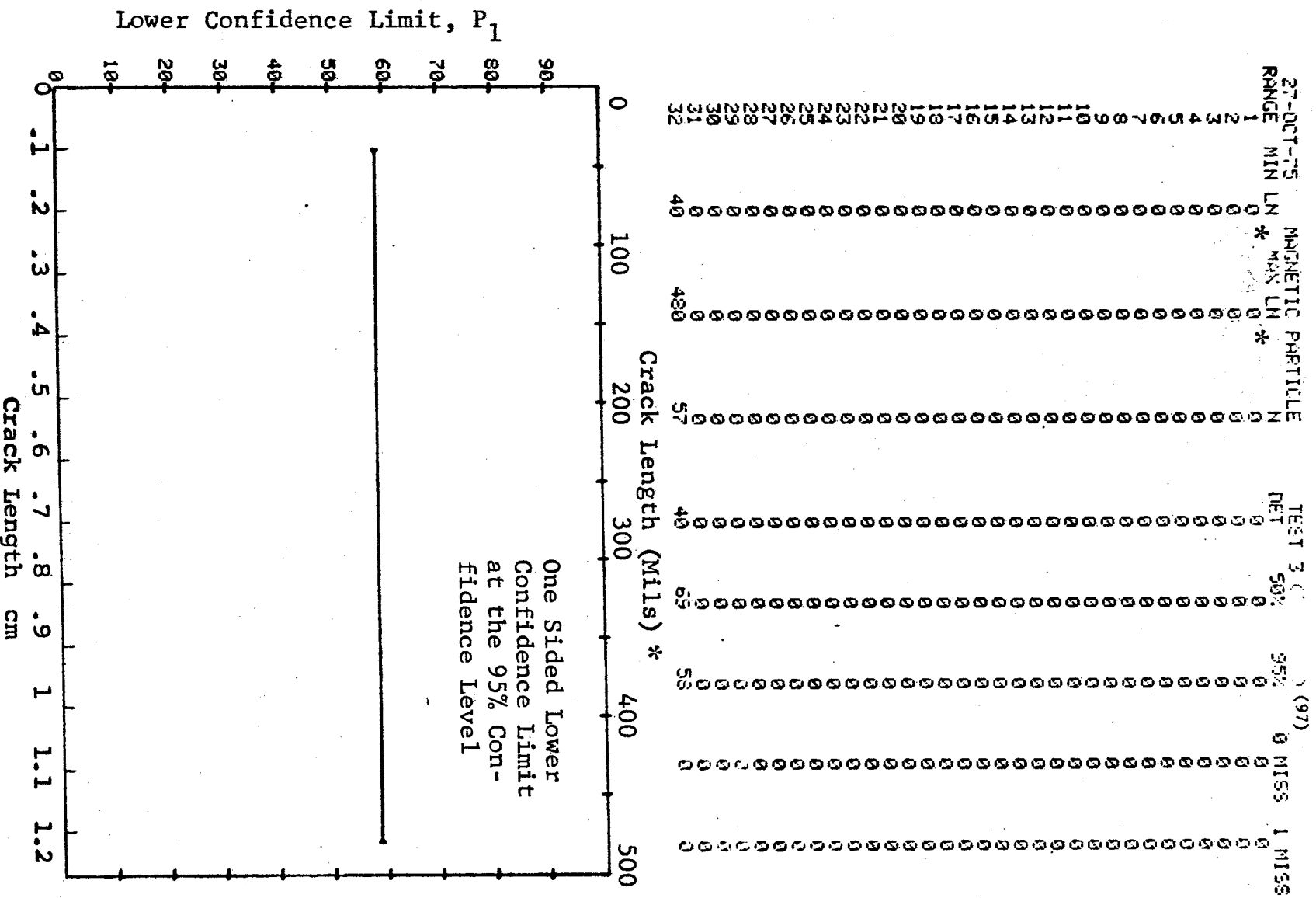


Figure D-97(Concluded)

(a) Range Interval Method of Data Cumulation

28-OCT-75		MAGNETIC PARTICLE		TEST 1		(98)	
RANGE	MIN LN *	MAX LN *	N	DET	95%	0 MISS	1 MISS
1	30	50	31	24	50	0	0
2	60	70	27	27	75	0	0
3	0	0	0	0	97	2	10
4	110	120	0	25	0	4	21
5	130	140	25	38	97	0	0
6	150	160	38	13	98	0	8
7	0	0	13	0	94	16	33
8	200	200	0	0	79	0	0
9	0	0	3	3	0	0	0
10	0	0	0	0	0	0	0
11	0	0	0	0	0	0	0
12	0	0	0	0	0	0	0
13	0	0	0	0	0	0	0
14	0	0	0	0	0	0	0
15	0	0	0	0	0	0	0
16	0	0	0	0	0	0	0
17	0	0	0	0	0	0	0
18	0	0	0	0	0	0	0
19	0	0	0	0	0	0	0
20	0	0	0	0	0	0	0
21	0	0	0	0	0	0	0
22	0	0	0	0	0	0	0
23	0	0	0	0	0	0	0
24	0	0	0	0	0	0	0
25	0	0	0	0	0	0	0
26	0	0	0	0	0	0	0
27	0	0	0	0	0	0	0
28	0	0	0	0	0	0	0
29	0	0	0	0	0	0	0
30	0	0	0	0	0	0	0
31	0	0	0	0	0	0	0
32	750	750	0	0	89	0	0

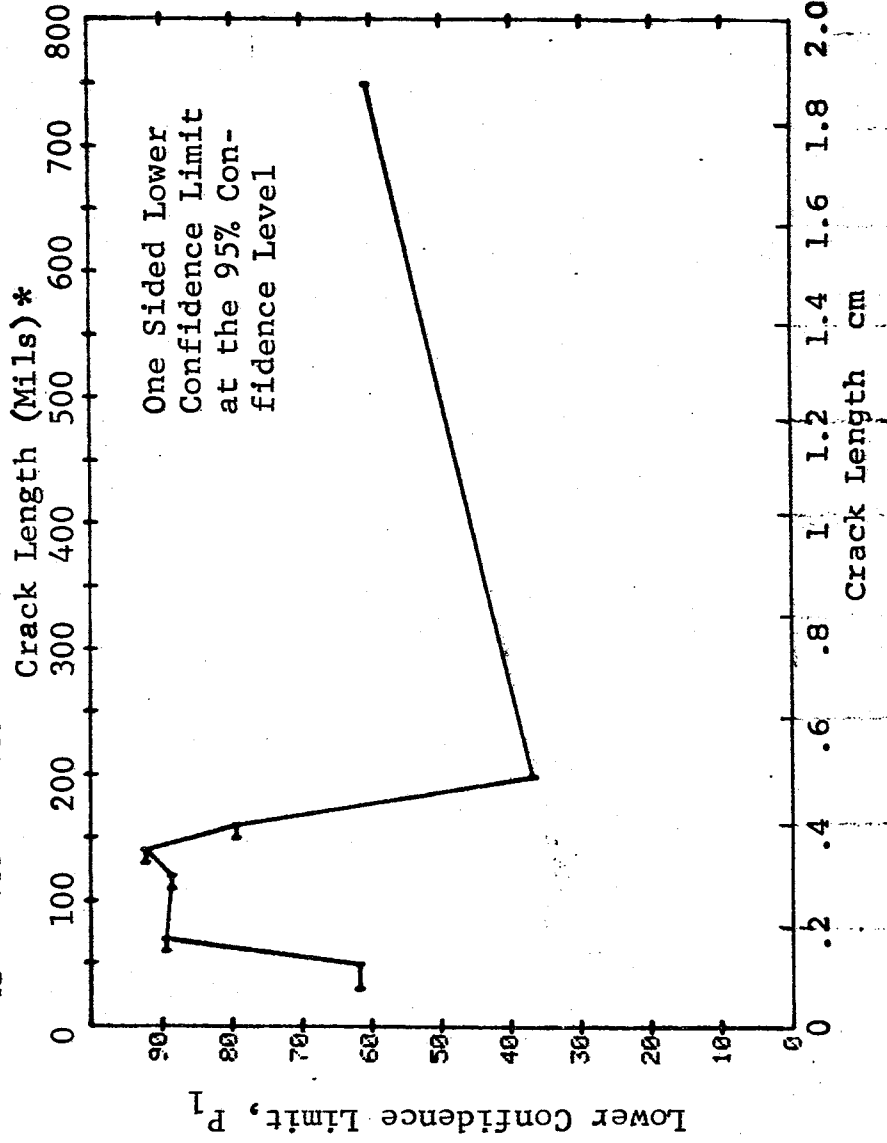


Figure D-98 Probability of Detection for 4340M Steel Using Magnetic Particles. Compressed Notch Flaws in Solid Cylinder. Lab. Env.

(b) Optimum Probability Method of Data Cumulation

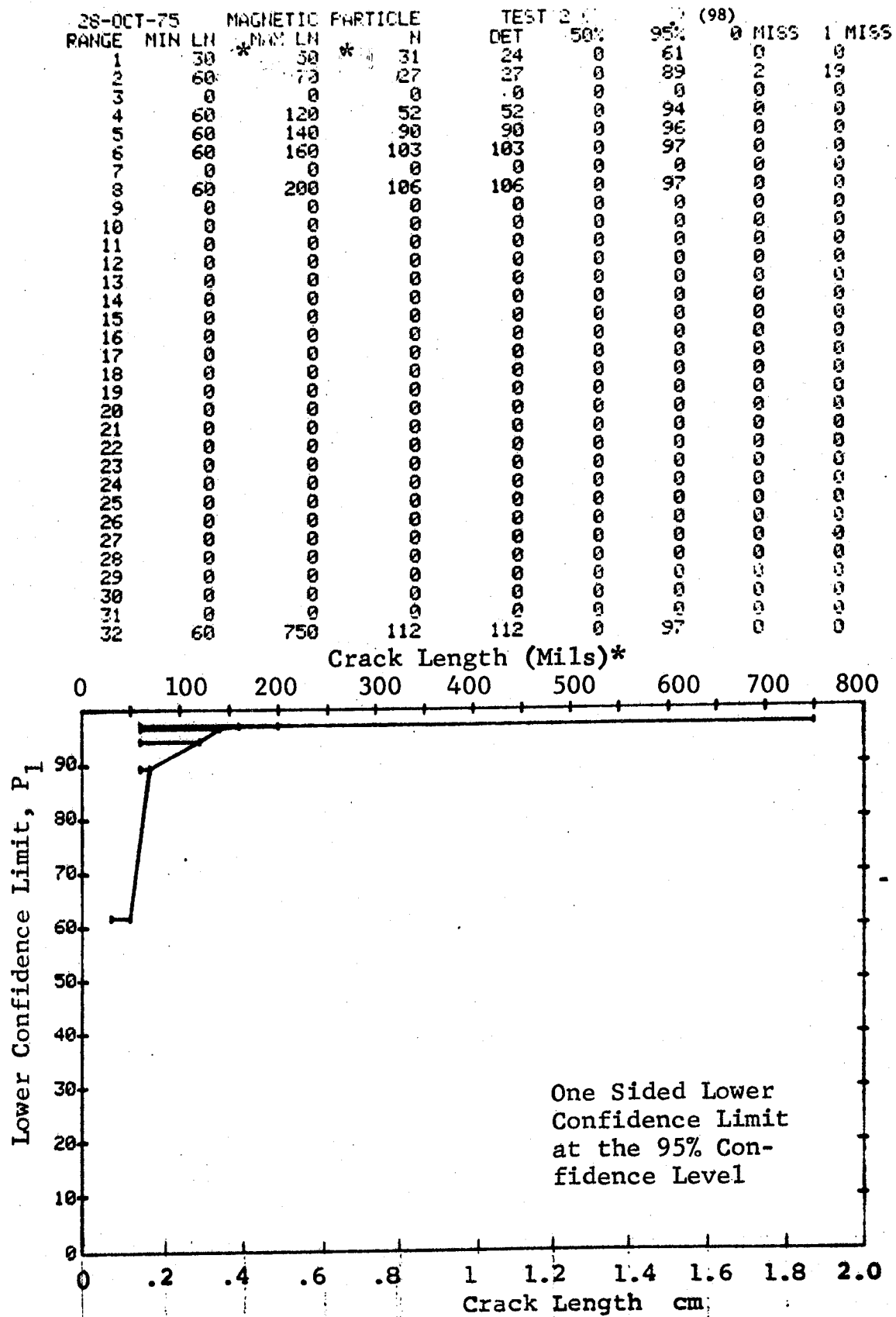


Figure D-98 (Continued)

(c) Overlapping Sixty Point Method of Data Cumulation

28-OCT-75	MAGNETIC PARTICLE		TEST 3		MISS	
RANGE	MIN	LN	MAX	LN	MISS	MISS
1	0	0	0	0	0	0
2	0	0	0	0	0	0
3	0	0	0	0	0	0
4	0	0	0	0	0	0
5	0	0	0	0	0	0
6	0	0	0	0	0	0
7	0	0	0	0	0	0
8	0	0	0	0	0	0
9	0	0	0	0	0	0
10	0	0	0	0	0	0
11	0	0	0	0	0	0
12	0	0	0	0	0	0
13	0	0	0	0	0	0
14	0	0	0	0	0	0
15	0	0	0	0	0	0
16	0	0	0	0	0	0
17	0	0	0	0	0	0
18	0	0	0	0	0	0
19	0	0	0	0	0	0
20	0	0	0	0	0	0
21	0	0	0	0	0	0
22	0	0	0	0	0	0
23	0	0	0	0	0	0
24	0	0	0	0	0	0
25	0	0	0	0	0	0
26	0	0	0	0	0	0
27	0	0	0	0	0	0
28	30	0	0	0	0	0
29	50	0	0	0	0	0
30	60	0	0	0	0	0
31	60	0	0	0	0	0
32	120	0	0	0	0	0

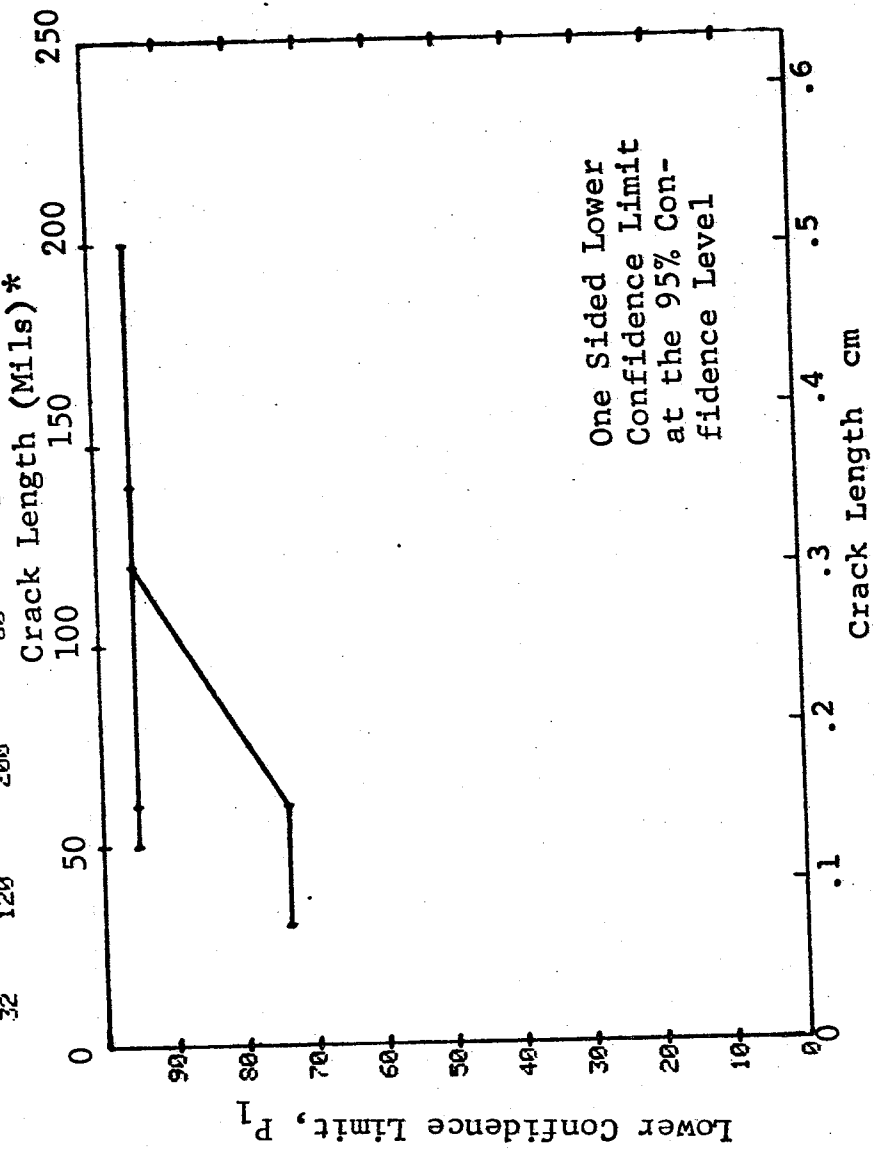


Figure D-98 (Concluded)

(a) Range Interval Method of Data Cumulation

28-OCT-75		MAGNETIC PARTICLE		TEST 1		(99)		MISS		MISS	
RANGE	MIN LN	* MAX LN	* N	DET	50%	95%	0	MISS	1	MISS	
1	90	90	119	19	96	86	0	9	26		
2	0	0	8	0	96	85	0	10	27		
3	0	0	0	0	0	0	0	0	0		
4	110	110	12	6	67	40	0	0	0		
5	120	130	12	12	94	77	0	17	34		
6	140	140	16	16	95	82	0	13	30		
7	0	0	2	2	0	0	0	0	0		
8	160	160	0	0	70	22	0	0	0		
9	0	0	0	0	0	0	0	0	0		
10	180	180	0	0	92	71	0	0	0		
11	0	0	0	0	0	0	0	0	0		
12	0	0	0	0	0	0	0	0	0		
13	0	0	0	0	0	0	0	0	0		
14	0	0	0	0	0	0	0	0	0		
15	250	250	1	0	50	5	0	0	0		
16	0	0	1	1	0	0	0	0	0		
17	270	270	2	2	70	22	0	0	0		
18	280	280	1	1	50	5	0	0	0		
19	300	300	11	11	93	76	0	18	75		
20	310	310	0	0	0	0	0	0	0		
21	0	0	0	0	0	0	0	0	0		
22	0	0	0	0	0	0	0	0	0		
23	0	0	0	0	0	0	0	0	0		
24	0	0	0	0	0	0	0	0	0		
25	0	0	0	0	0	0	0	0	0		
26	0	0	0	0	0	0	0	0	0		
27	390	390	1	1	50	5	0	0	0		
28	0	0	0	0	0	0	0	0	0		
29	0	0	0	0	0	0	0	0	0		
30	0	0	0	0	0	0	0	0	0		
31	0	0	0	0	0	0	0	0	0		
32	450	460	3	3	79	36	0	0	0		

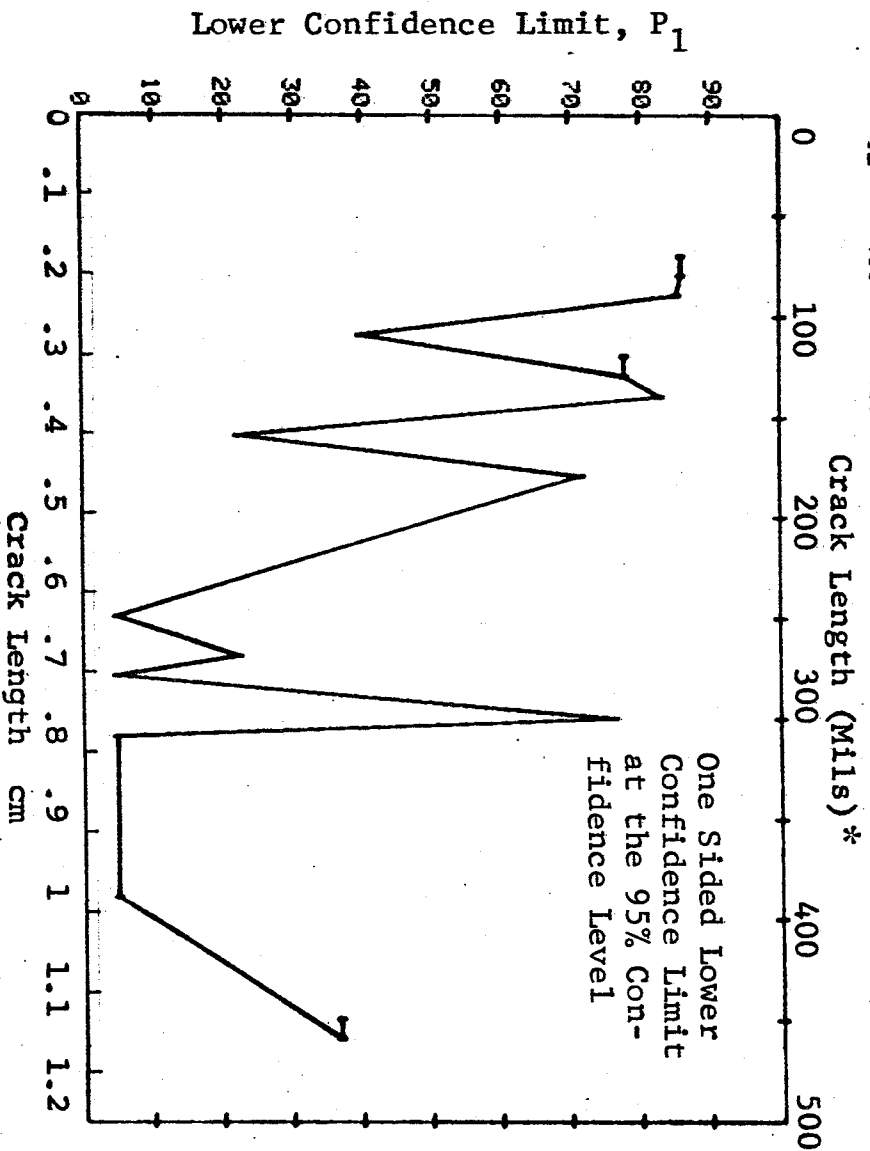


Figure D-99 Probability of Detection for 4340M Steel Using Magnetic Particles. Compressed Notch Flaws in Hollow Filleted Cylinder. Lab. Env.

(b) Optimum Probability Method of Data Cumulation

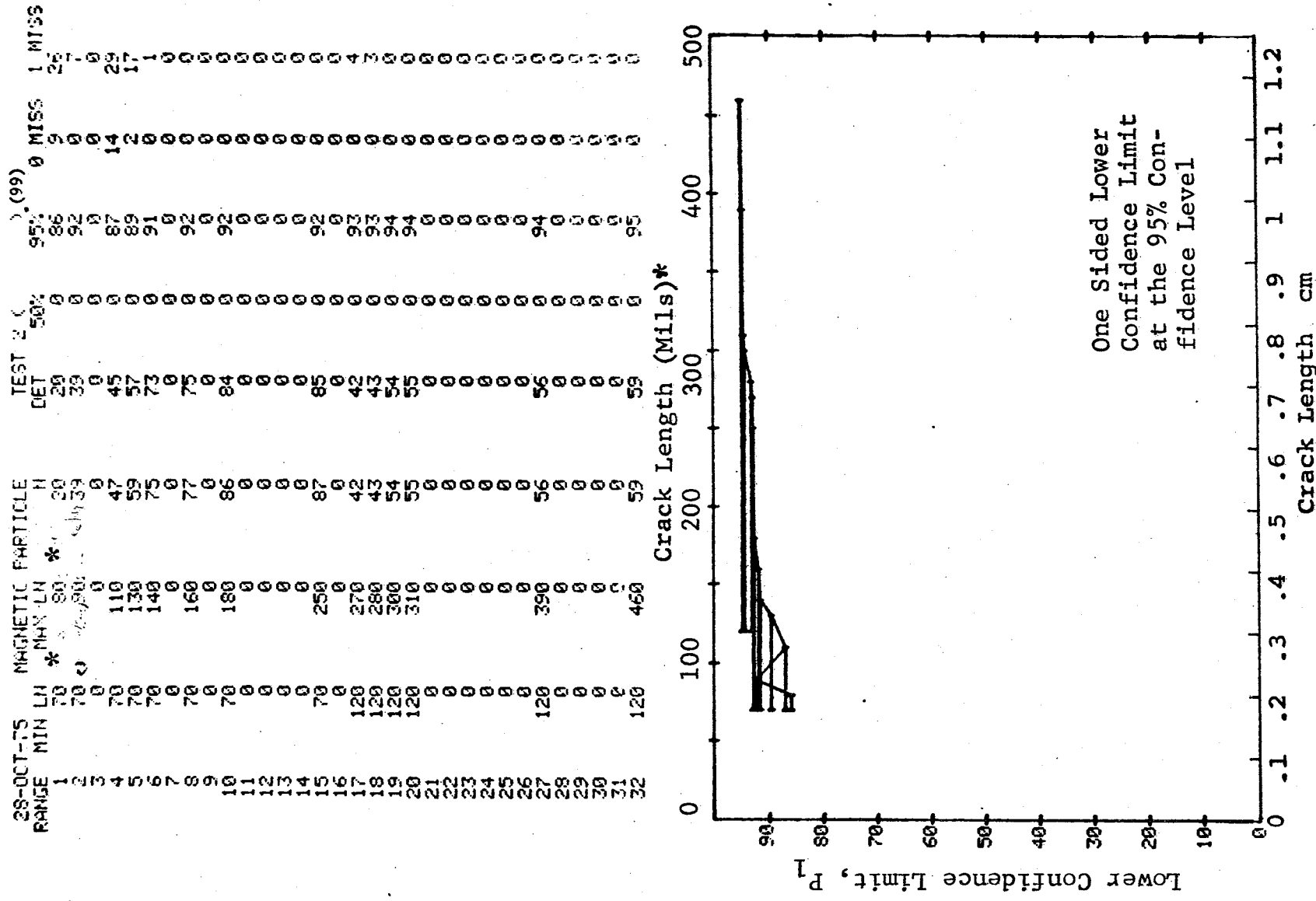


Figure D-99 (Continued)

(c) Overlapping Sixty Point Method of Data Cumulation

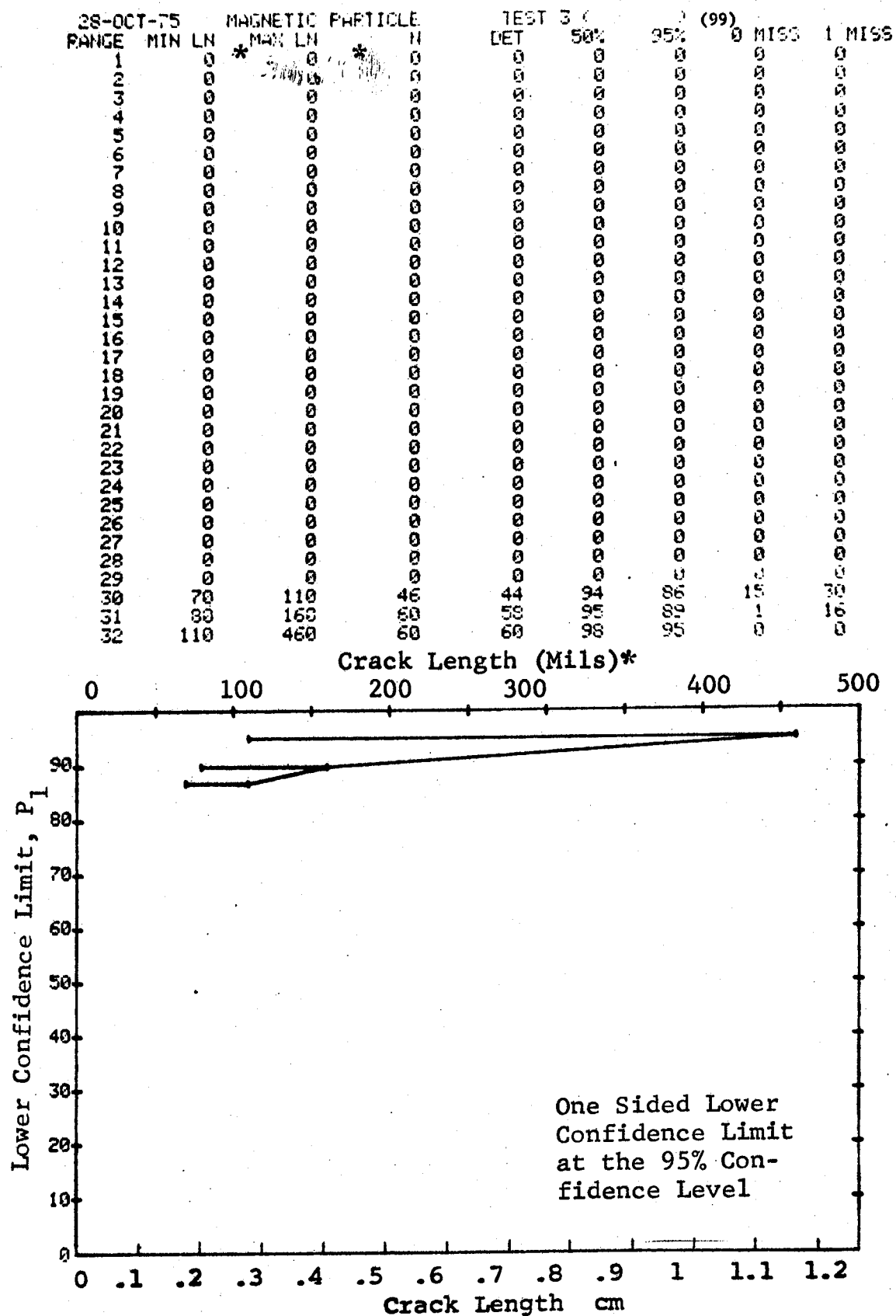


Figure D-99 (Concluded)

(a) Range Interval Method of Data Cumulation

28-OCT-75		MAGNETIC PARTICLE		TEST 1 (DET)		95% (100)		MISS	
RANGE	MIN LN	* MAX LN	* H	DET	50%	95%	0	MISS	1 MISS
1	40	70	1	1	50	5	0	0	0
2	70	100	1	0	0	0	0	0	0
3	100	130	0	0	0	0	0	0	0
4	130	160	7	3	36	12	0	0	0
5	160	190	4	1	15	1	0	0	0
6	190	220	0	0	0	0	0	0	0
7	220	250	0	0	0	0	0	0	0
8	250	280	1	1	50	0	0	0	0
9	280	310	1	1	50	0	0	0	0
10	310	340	1	1	50	0	0	0	0
11	340	370	0	0	0	0	0	0	0
12	370	400	2	2	70	23	0	0	0
13	400	430	1	1	50	5	0	0	0
14	430	460	1	1	50	5	0	0	0
15	460	490	1	1	50	5	0	0	0
16	490	520	0	0	0	0	0	0	0
17	520	550	1	1	50	5	0	0	0
18	550	580	1	1	50	5	0	0	0
19	580	610	0	0	0	0	0	0	0
20	610	640	1	1	50	5	0	0	0
21	640	670	0	0	0	0	0	0	0
22	670	700	1	1	50	5	0	0	0
23	700	730	1	1	50	5	0	0	0
24	730	760	1	1	50	5	0	0	0
25	760	790	0	0	0	0	0	0	0
26	790	820	0	0	0	0	0	0	0
27	820	850	0	0	0	0	0	0	0
28	850	880	0	0	0	0	0	0	0
29	880	910	0	0	0	0	0	0	0
30	910	940	0	0	0	0	0	0	0
31	940	970	0	0	0	0	0	0	0
32	970	1000	1	1	50	5	0	0	0

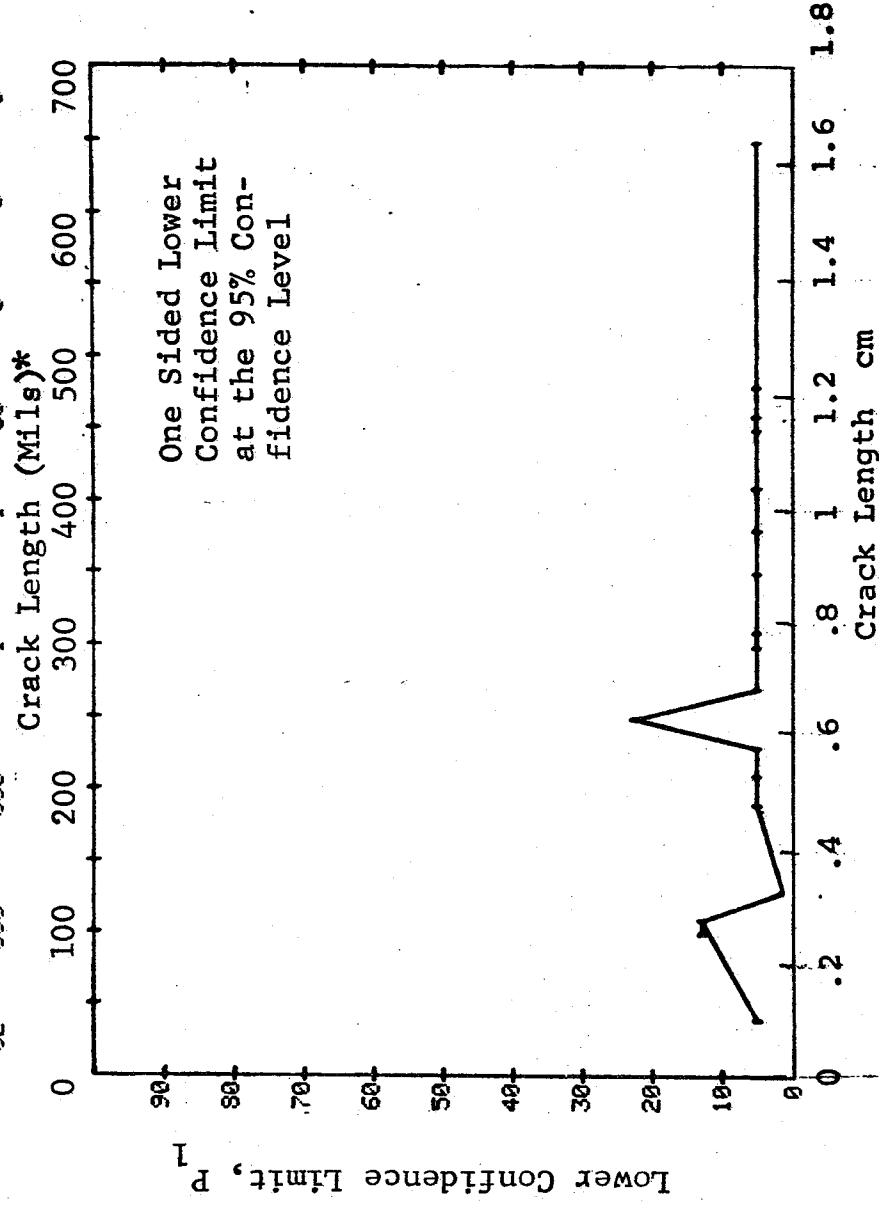


Figure D-100 Probability of Detection for 4340M Steel Using Magnetic Particles. Compressed Notch Flaws in Solid Threaded Cylinder. Lab. Env.

(b) Optimum Probability Method of Data Cumulation

28-OCT-75		MAGNETIC PARTICLE			TEST 2 (100)					
RANGE	MIN	LN *	MAX	LN *	H	DET	50%	95%	0 MISS	1 MISS
1	40	0	40	0	1	1	0	5	0	0
2	40	0	70	0	2	1	0	2	0	0
3	0	0	0	0	0	0	0	0	0	0
4	40	0	110	0	9	4	0	16	0	0
5	40	0	130	0	13	5	0	16	0	0
6	0	0	0	0	0	0	0	0	0	0
7	0	0	0	0	0	0	0	0	0	0
8	40	0	190	0	14	6	0	20	0	0
9	40	0	210	0	15	7	0	24	0	0
10	190	0	230	0	3	3	0	36	0	0
11	0	0	0	0	0	0	0	0	0	0
12	190	0	250	0	5	5	0	54	0	0
13	190	0	270	0	6	6	0	60	0	0
14	190	0	300	0	7	7	0	65	0	0
15	190	0	310	0	8	8	0	68	0	0
16	0	0	0	0	0	0	0	0	0	0
17	190	0	350	0	9	9	0	71	0	0
18	190	0	380	0	10	10	0	74	0	0
19	0	0	0	0	0	0	0	0	0	0
20	190	0	410	0	11	11	0	76	0	0
21	0	0	0	0	0	0	0	0	0	0
22	190	0	450	0	12	12	0	77	0	0
23	190	0	460	0	13	13	0	79	0	0
24	190	0	480	0	14	14	0	80	15	32
25	0	0	0	0	0	0	0	0	0	0
26	0	0	0	0	0	0	0	0	0	0
27	0	0	0	0	0	0	0	0	0	0
28	0	0	0	0	0	0	0	0	0	0
29	0	0	0	0	0	0	0	0	0	0
30	0	0	0	0	0	0	0	0	0	0
31	0	0	0	0	0	0	0	0	0	0
32	190	0	650	0	15	15	0	81	14	31

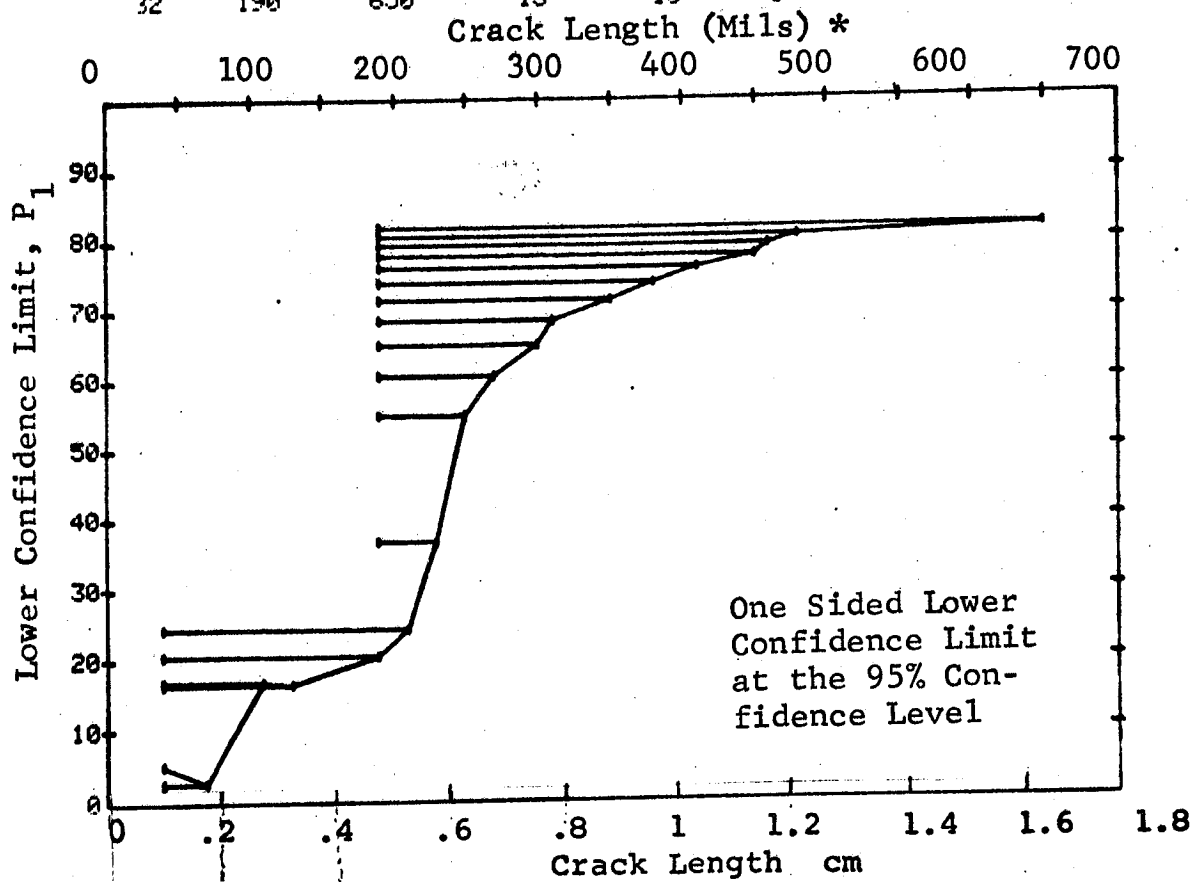


Figure D-100 (Continued)

(c) Overlapping Sixty Point Method of Data Cumulation

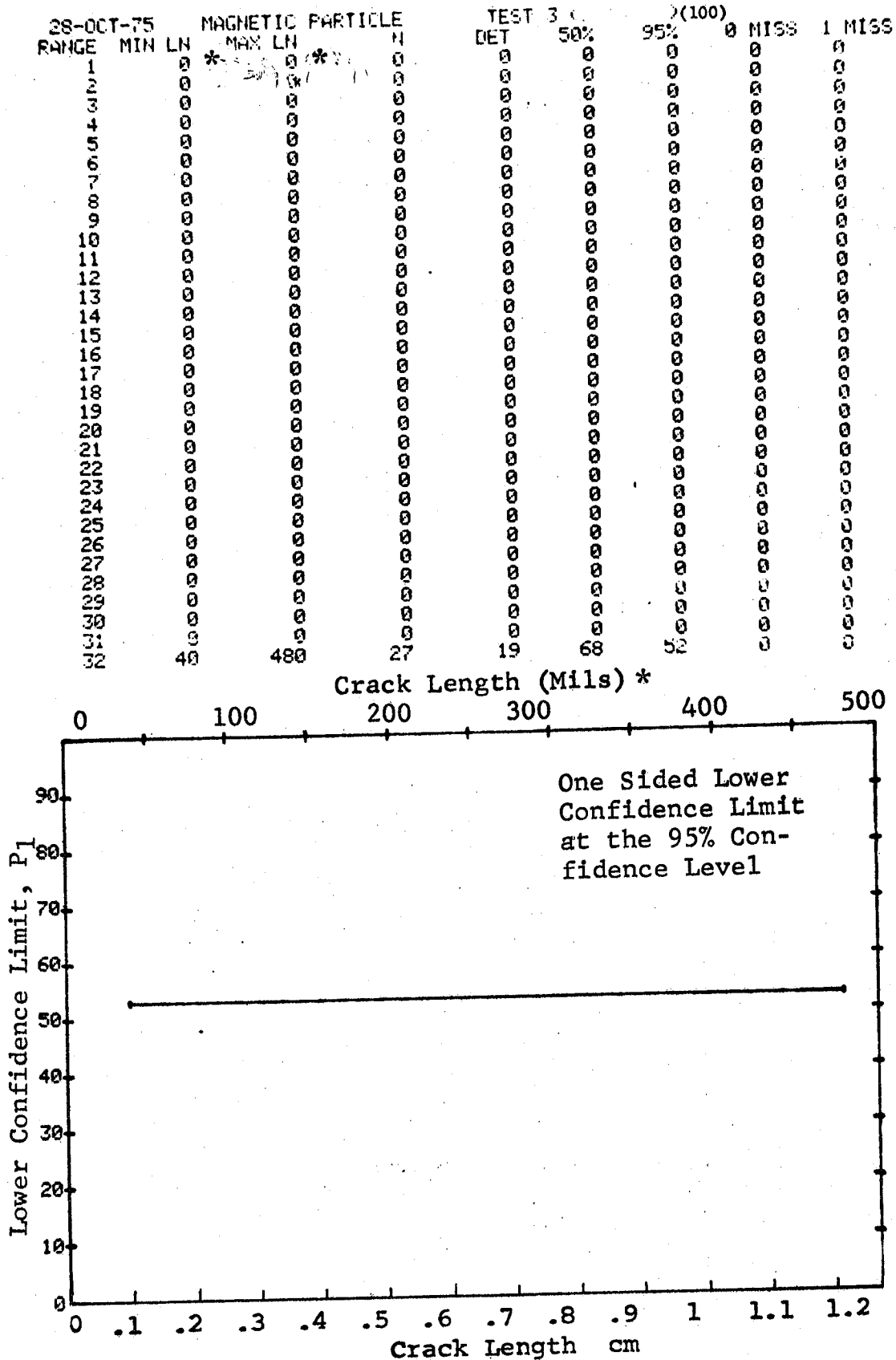


Figure D-100 (Concluded)

(a) Range Interval Method of Data Cumulation

35-OCT-75	MAGNETIC PARTICLE		TEST 1	(101)	
RANGE	MIN LN	MAX LN	DET	95%	MISS
1	20	30	16	50	0
2	0	0	0	0	0
3	60	60	11	76	13
4	70	70	13	84	11
5	90	90	13	79	16
6	100	100	10	74	0
7	0	0	0	0	0
8	130	140	25	83	20
9	150	150	12	68	0
10	0	0	0	0	0
11	0	0	0	0	0
12	200	200	2	22	0
13	0	0	0	0	0
14	230	230	3	36	0
15	240	240	2	22	0
16	250	260	4	47	0
17	0	0	0	0	0
18	280	280	2	22	0
19	300	300	10	74	0
20	0	0	0	0	0
21	0	0	0	0	0
22	0	0	0	0	0
23	0	0	0	0	0
24	370	380	11	93	18
25	390	390	4	84	0
26	410	410	2	70	0
27	0	0	0	0	0
28	0	0	0	0	0
29	0	0	0	0	0
30	0	0	0	0	0
31	0	0	0	0	0
32	500	500	2	70	0

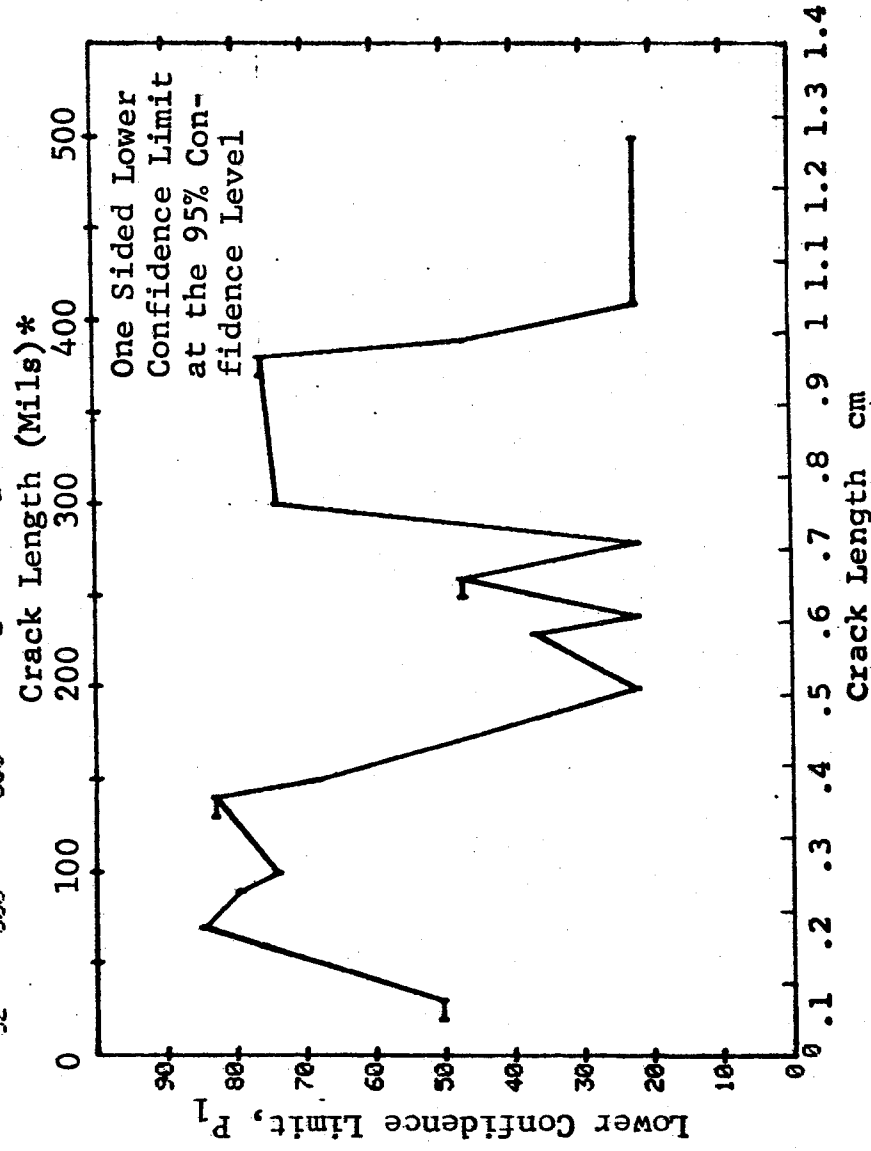


Figure D-101 Probability of Detection for 4340M Steel Using Magnetic Particles. Compressed Notch Flaws in Solid Filleted Cylinder. Lab. Env.

(b) Optimum Probability Method of Data Cumulation

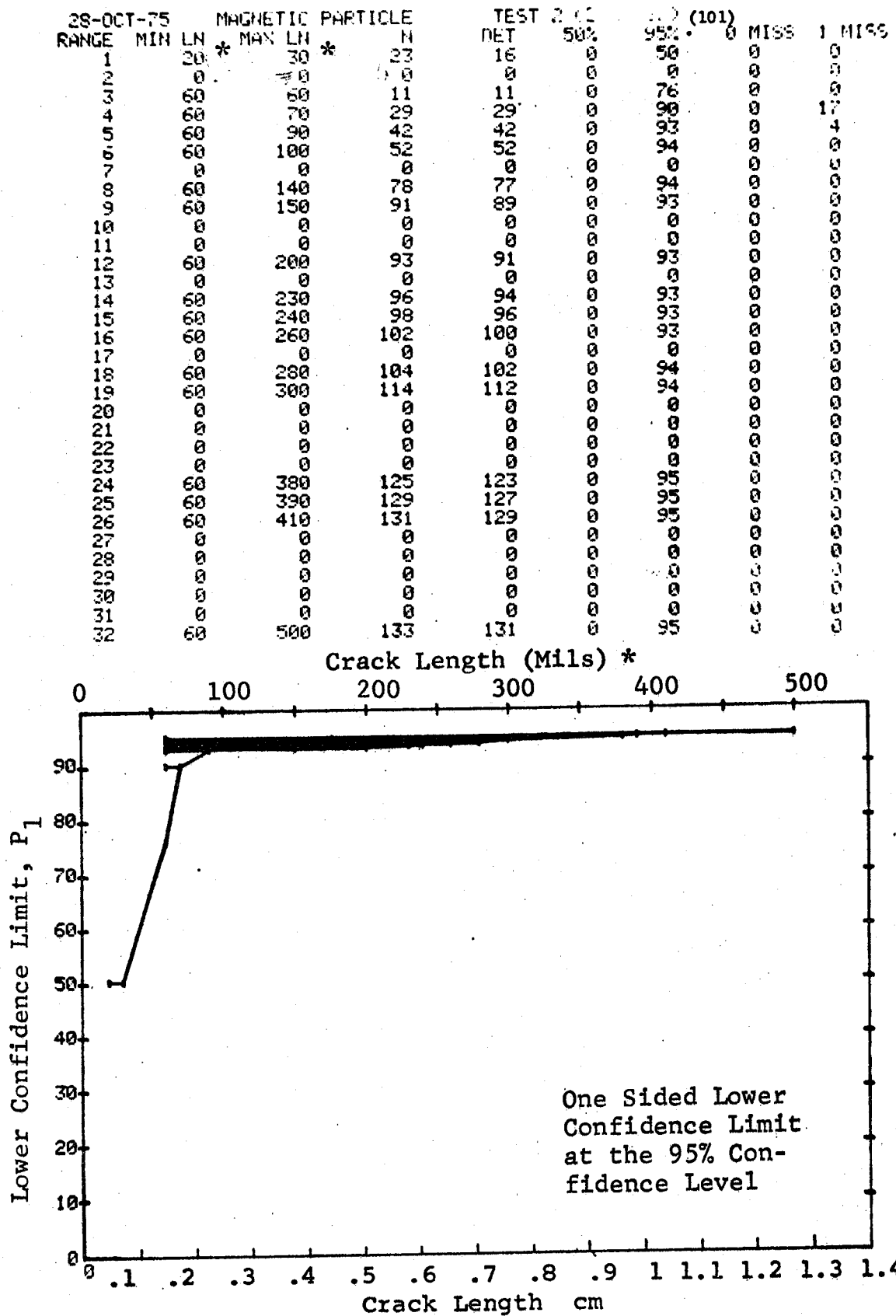


Figure D-101 (Continued)

(c) Overlapping Sixty Point Method of Data Cumulation

28-OCT-75	MAGNETIC PARTICLE		TEST 3		(101)	MISS		MISS
RANGE	MIN	LN	MAX	LN	DET	50%	95%	1 MISS
1	0	0	0	0	0	0	0	0
2	0	0	0	0	0	0	0	0
3	0	0	0	0	0	0	0	0
4	0	0	0	0	0	0	0	0
5	0	0	0	0	0	0	0	0
6	0	0	0	0	0	0	0	0
7	0	0	0	0	0	0	0	0
8	0	0	0	0	0	0	0	0
9	0	0	0	0	0	0	0	0
10	0	0	0	0	0	0	0	0
11	0	0	0	0	0	0	0	0
12	0	0	0	0	0	0	0	0
13	0	0	0	0	0	0	0	0
14	0	0	0	0	0	0	0	0
15	0	0	0	0	0	0	0	0
16	0	0	0	0	0	0	0	0
17	0	0	0	0	0	0	0	0
18	0	0	0	0	0	0	0	0
19	0	0	0	0	0	0	0	0
20	0	0	0	0	0	0	0	0
21	0	0	0	0	0	0	0	0
22	0	0	0	0	0	0	0	0
23	0	0	0	0	0	0	0	0
24	0	0	0	0	0	0	0	0
25	0	0	0	0	0	0	0	0
26	0	0	0	0	0	0	0	0
27	0	0	0	0	0	0	0	0
28	20	20	70	0	29	78	66	62
29	20	20	100	36	53	87	67	62
30	70	140	200	60	59	97	93	1
31	100	200	300	60	59	97	93	0
32	140	500	500	60	59	97	93	1

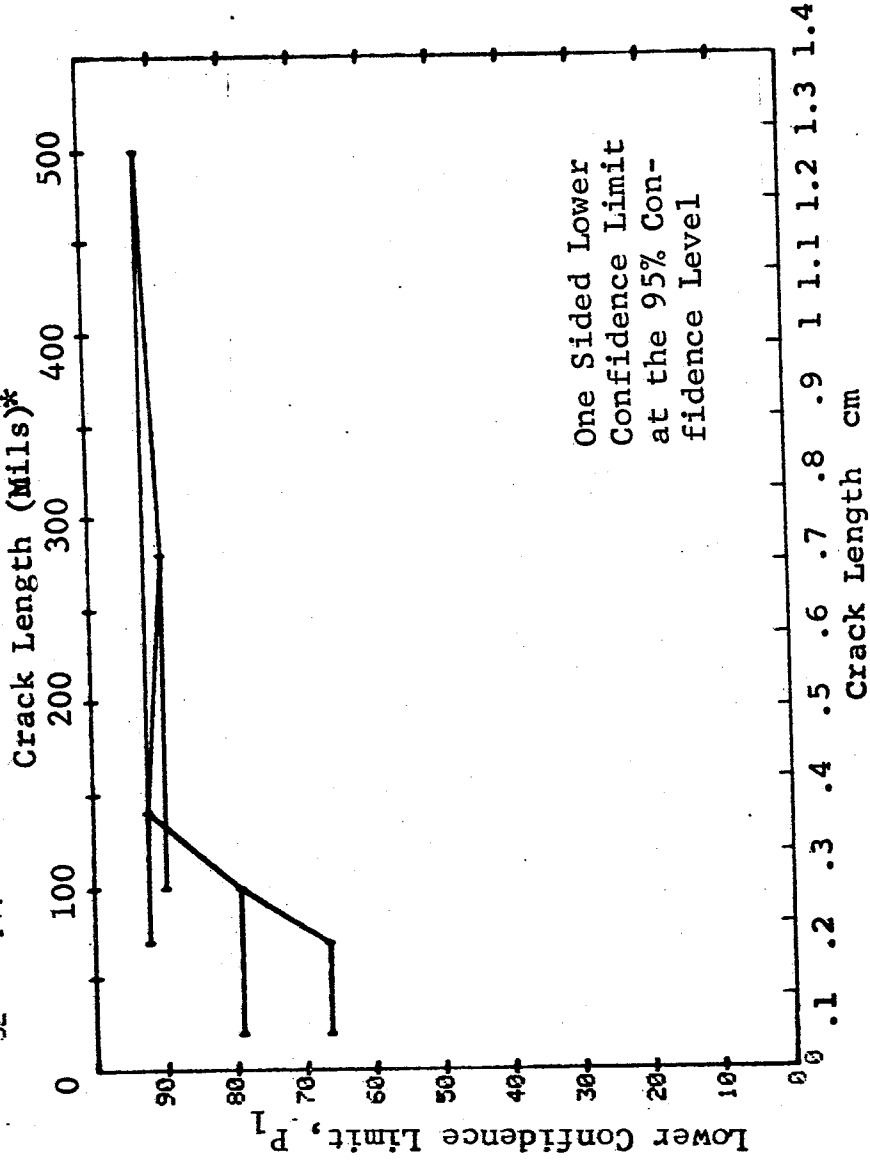


Figure D-101 (Concluded)

(a) Range Interval Method of Data Cumulation

28-OCT-75	MAGNETIC PARTICLE	TEST 1	(102)	MISS
RANGE	MIN LN *	DET	95%	MISS
1	60	17	96	29
2	90	1	50	0
3	90	17	96	29
4	100	2	70	0
5	120	9	92	0
6	130	8	91	0
7	140	2	70	0
8	170	2	70	0
9	180	0	0	0
10	0	0	0	0
11	230	3	79	0
12	0	0	0	0
13	0	0	0	0
14	0	0	0	0
15	0	0	0	0
16	310	1	50	0
17	0	0	0	0
18	0	0	0	0
19	350	4	84	0
20	0	0	0	0
21	390	1	50	0
22	0	0	0	0
23	0	0	0	0
24	0	0	0	0
25	0	0	0	0
26	0	0	0	0
27	0	0	0	0
28	0	0	0	0
29	0	0	0	0
30	0	0	0	0
31	0	0	0	0
32	570	1	50	0

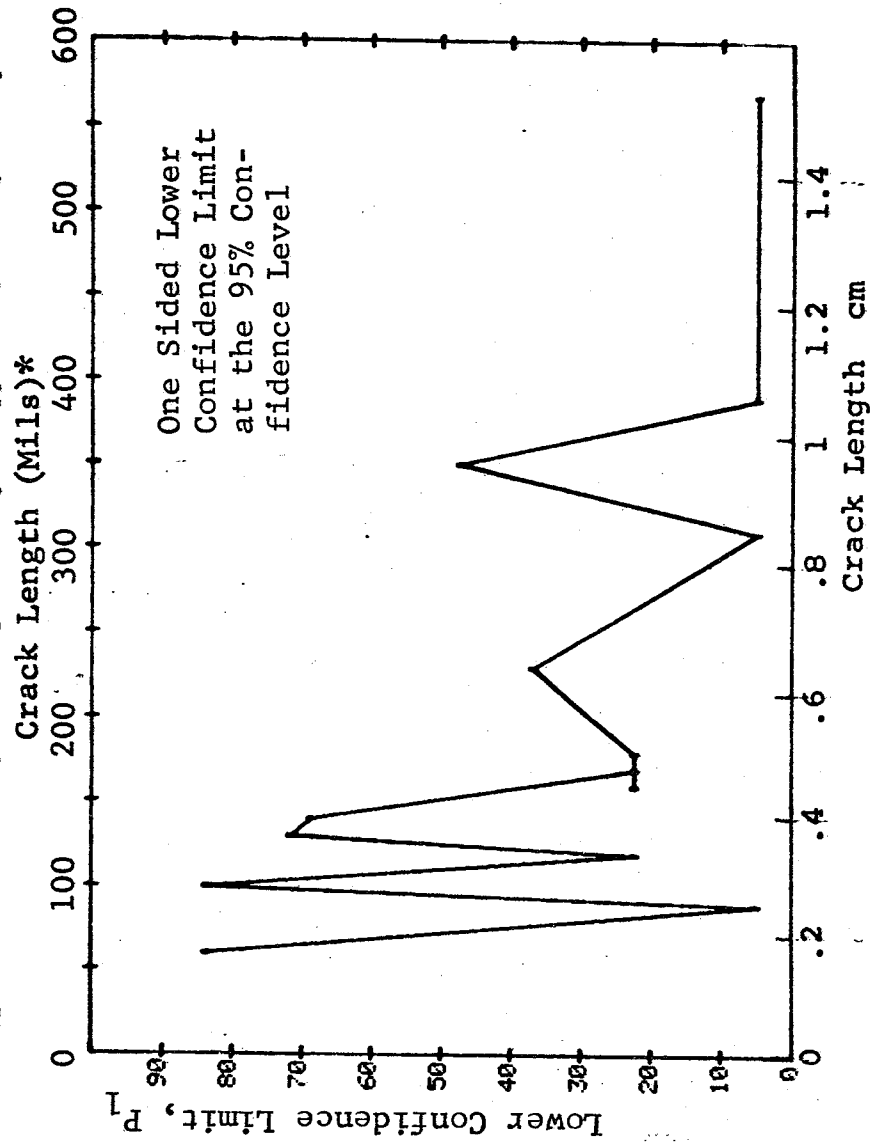


Figure D-102 Probability of Detection for 4340M Steel Using Magnetic Particles. Compressed Notch Flaws in Hollow Cylinder. Lab. Env.

(b) Optimum Probability Method of Data Cumulation

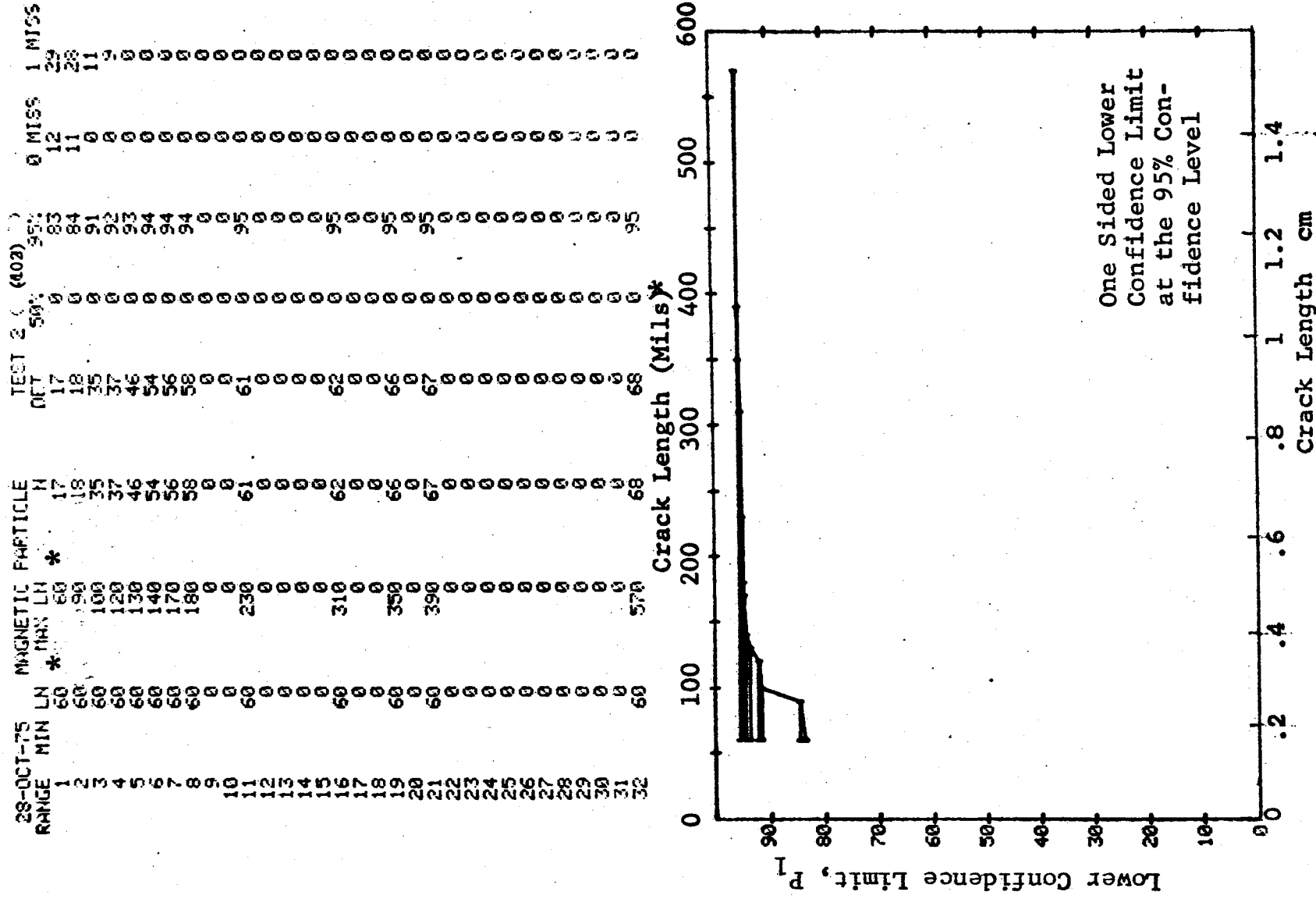


Figure D-102 (Continued)

(c) Overlapping Sixty Point Method of Data Cumulation

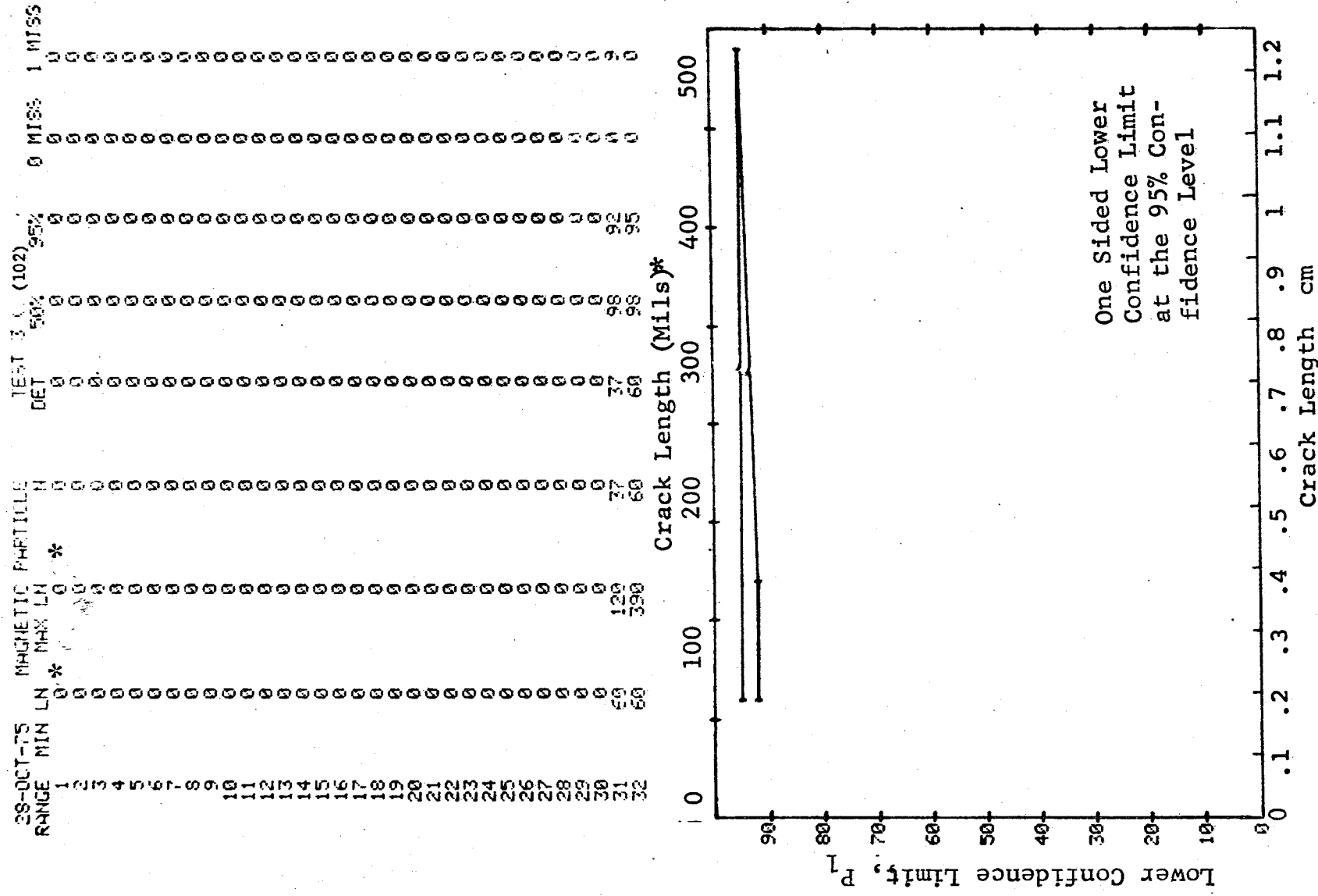


Figure D-102 (Concluded)

(a) Range Interval Method of Data Cumulation

28-OCT-75	EDDY CURRENT	TEST 1	DET	50%	95%	0 MISS	1 MISS
RANGE	MIN LN	MAX LN	*				
1	30	50	12	54	37	0	0
2	60	70	11	69	48	0	0
3	0	0	10	0	0	0	0
4	110	120	17	96	83	12	23
5	130	140	21	92	80	24	33
6	150	160	12	94	77	17	34
7	0	0	0	0	0	0	0
8	200	200	0	70	22	0	0
9	0	0	2	0	0	0	0
10	0	0	0	0	0	0	0
11	0	0	0	0	0	0	0
12	0	0	0	0	0	0	0
13	0	0	0	0	0	0	0
14	0	0	0	0	0	0	0
15	0	0	0	0	0	0	0
16	0	0	0	0	0	0	0
17	0	0	0	0	0	0	0
18	0	0	0	0	0	0	0
19	0	0	0	0	0	0	0
20	0	0	0	0	0	0	0
21	0	0	0	0	0	0	0
22	0	0	0	0	0	0	0
23	0	0	0	0	0	0	0
24	0	0	0	0	0	0	0
25	0	0	0	0	0	0	0
26	0	0	0	0	0	0	0
27	0	0	0	0	0	0	0
28	0	0	0	0	0	0	0
29	0	0	0	0	0	0	0
30	0	0	0	0	0	0	0
31	0	0	0	0	0	0	0
32	750	750	4	84	47	0	0

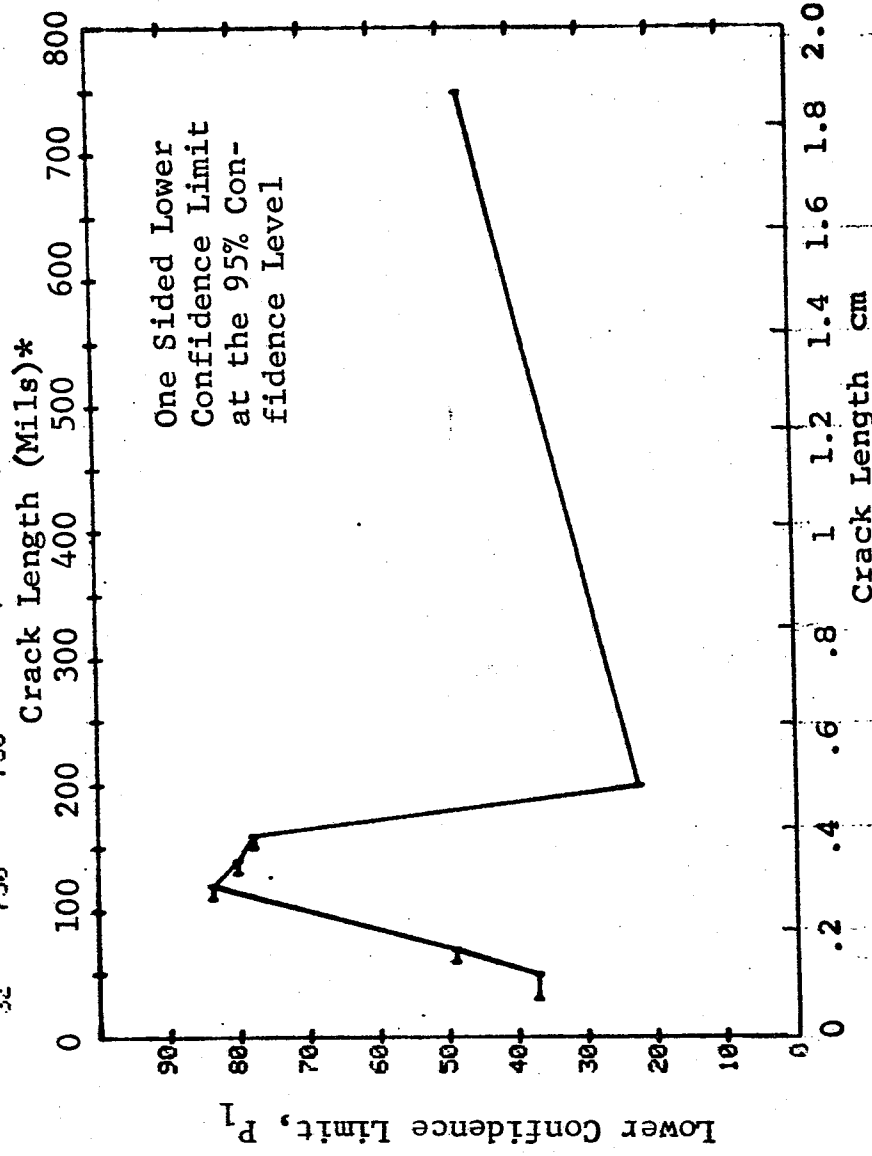


Figure D-103 Probability of Detection for 4340M Steel Using Eddy Current. Compressed Notch Flaws in Solid Cylinder. Prod. Env.

(b) Optimum Probability Method off Data Cumulation

28-OCT-75		EDDY CURRENT		TEST 2 (103)					
RANGE	MIN LN	* MAX LN *	N	DET	50%	95%	0 MISS	1 MISS	
1	30	50	21	12	0	37	0	0	
2	60	70	15	11	0	48	0	0	
3	0	0	0	0	0	0	0	0	
4	110	120	17	17	0	83	12	29	
5	110	140	39	38	0	88	7	23	
6	110	160	51	50	0	91	0	10	
7	0	0	0	0	0	0	0	0	
8	110	200	53	52	0	91	0	0	
9	0	0	0	0	0	0	0	0	
10	0	0	0	0	0	0	0	0	
11	0	0	0	0	0	0	0	0	
12	0	0	0	0	0	0	0	0	
13	0	0	0	0	0	0	0	0	
14	0	0	0	0	0	0	0	0	
15	0	0	0	0	0	0	0	0	
16	0	0	0	0	0	0	0	0	
17	0	0	0	0	0	0	0	0	
18	0	0	0	0	0	0	0	0	
19	0	0	0	0	0	0	0	0	
20	0	0	0	0	0	0	0	0	
21	0	0	0	0	0	0	0	0	
22	0	0	0	0	0	0	0	0	
23	0	0	0	0	0	0	0	0	
24	0	0	0	0	0	0	0	0	
25	0	0	0	0	0	0	0	0	
26	0	0	0	0	0	0	0	0	
27	0	0	0	0	0	0	0	0	
28	0	0	0	0	0	0	0	0	
29	0	0	0	0	0	0	0	0	
30	0	0	0	0	0	0	0	0	
31	0	0	0	0	0	0	0	0	
32	110	750	57	56	0	91	0	4	

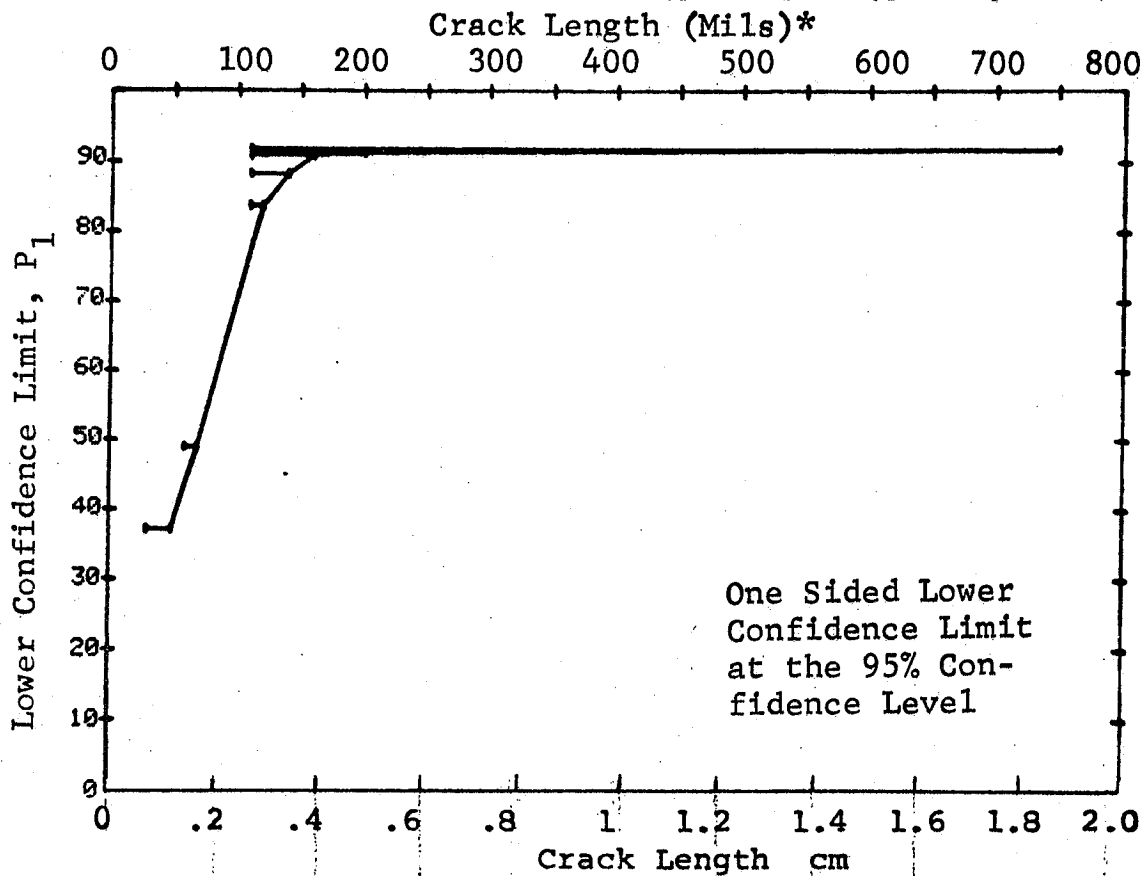


Figure D-103 (Continued)

(c) Overlapping Sixty Point Method of Data Cumulation

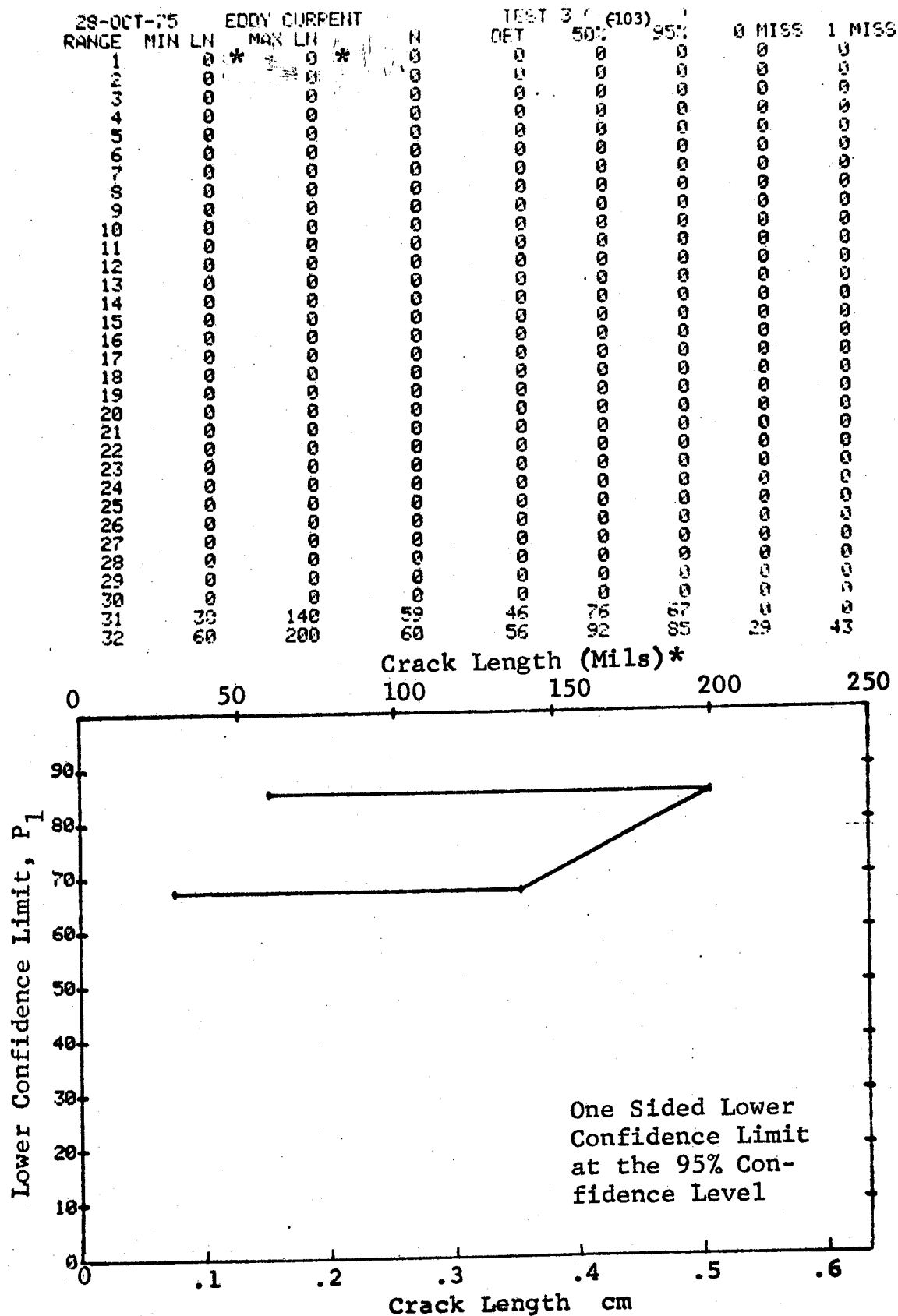


Figure D-103 (Concluded)

(a) Range Interval Method of Data Cumulation

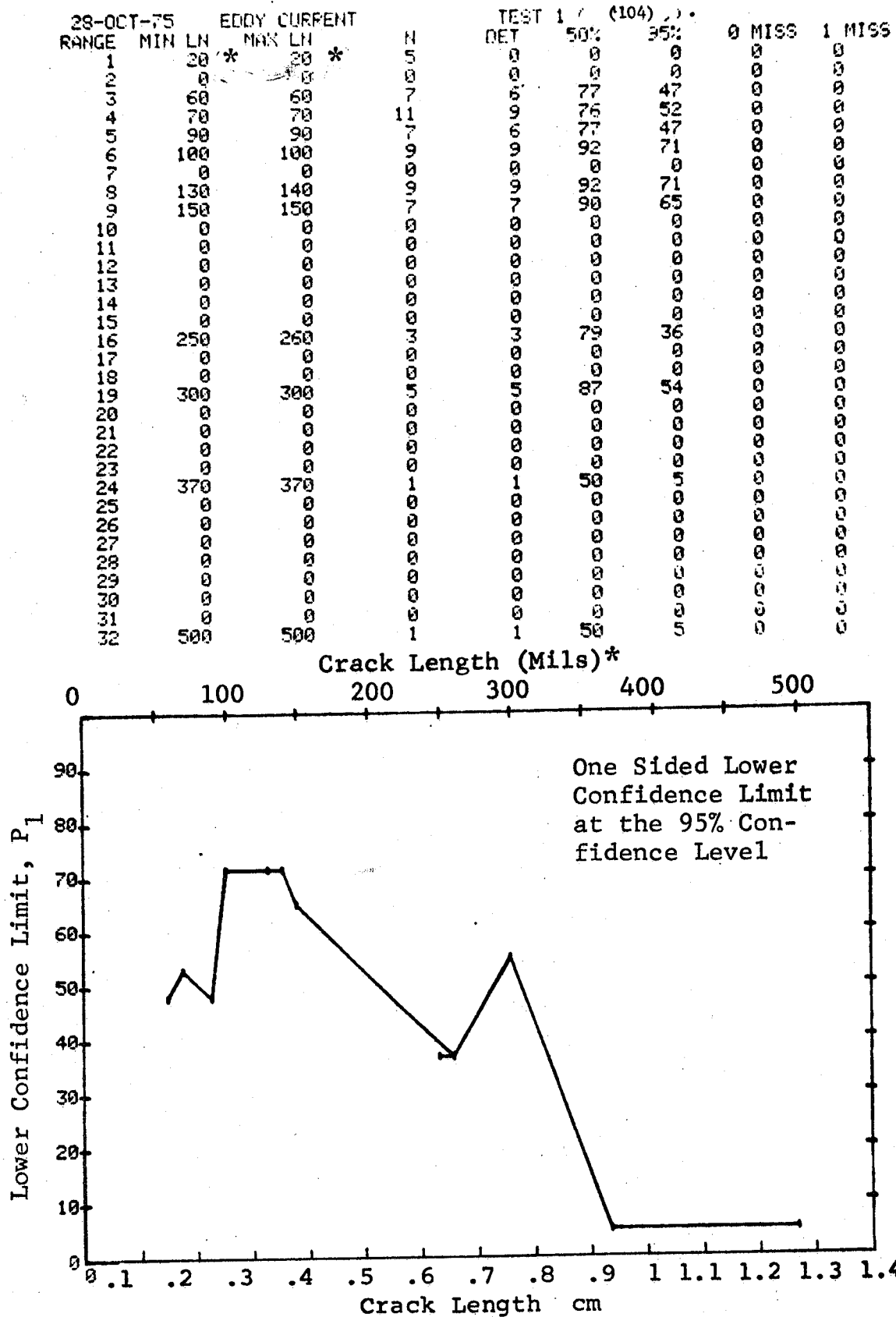


Figure D-104 Probability of Detection for 4340M Steel Using Eddy Current. Compressed Notch Flaws in Solid Filleted Cylinder. Prod. Env.

(b) Optimum Probability Method of Data Cumulation

28-OCT-75		EDDY CURRENT		N	TEST 2 (104)			0 MISS	1 MISS
RANGE	MIN LN	MAX LN *			DEF	50%	95%		
1	20	20	5	0	0	0	0	0	0
2	0	0	0	0	0	0	0	0	0
3	60	60	7	6	0	47	0	0	0
4	60	70	18	15	0	62	0	0	0
5	60	90	25	21	0	66	0	0	0
6	60	100	34	30	0	75	0	0	0
7	0	0	0	0	0	0	0	0	0
8	100	140	18	18	0	84	11	28	0
9	100	150	25	25	0	88	4	21	0
10	0	0	0	0	0	0	0	0	0
11	0	0	0	0	0	0	0	0	0
12	0	0	0	0	0	0	0	0	0
13	0	0	0	0	0	0	0	0	0
14	0	0	0	0	0	0	0	0	0
15	0	0	0	0	0	0	0	0	0
16	100	260	28	28	0	89	1	18	0
17	0	0	0	0	0	0	0	0	0
18	0	0	0	0	0	0	0	0	0
19	100	300	33	33	0	91	0	13	0
20	0	0	0	0	0	0	0	0	0
21	0	0	0	0	0	0	0	0	0
22	0	0	0	0	0	0	0	0	0
23	0	0	0	0	0	0	0	0	0
24	100	370	34	34	0	91	0	12	0
25	0	0	0	0	0	0	0	0	0
26	0	0	0	0	0	0	0	0	0
27	0	0	0	0	0	0	0	0	0
28	0	0	0	0	0	0	0	0	0
29	0	0	0	0	0	0	0	0	0
30	0	0	0	0	0	0	0	0	0
31	0	0	0	0	0	0	0	0	0
32	100	500	35	35	0	91	0	11	0

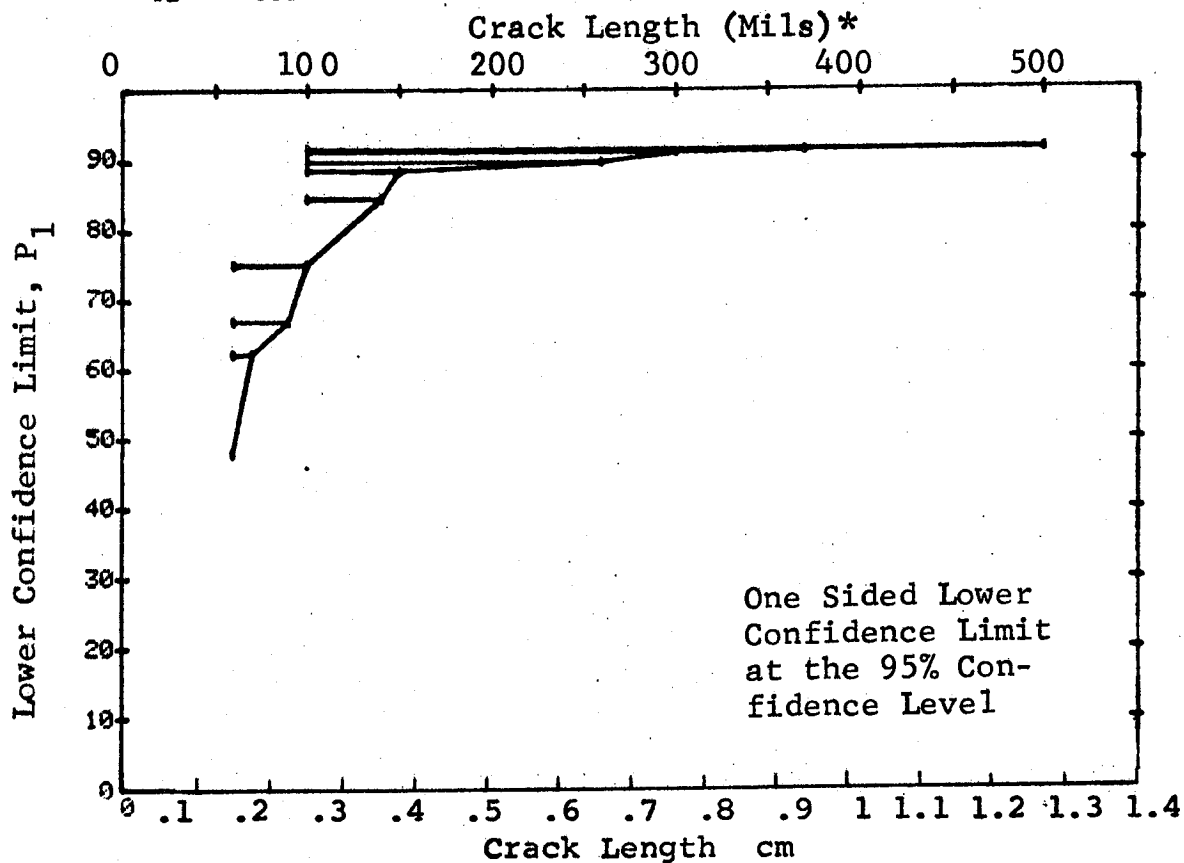


Figure D-104 (Continued)

(c) Overlapping Sixty Point Method of Data Cumulation

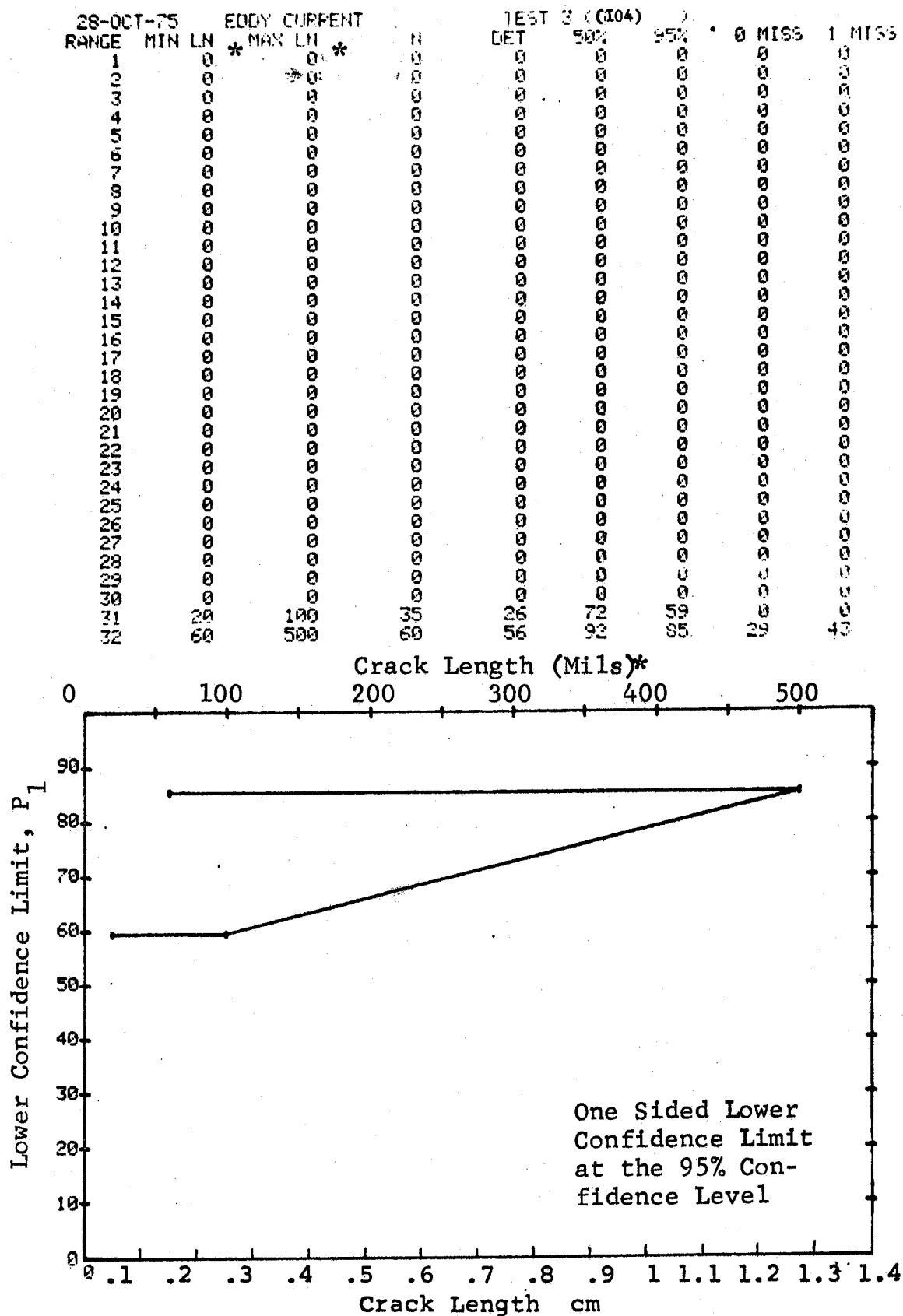


Figure D-104 (Concluded)

(a) Range Interval Method of Data Cumulation

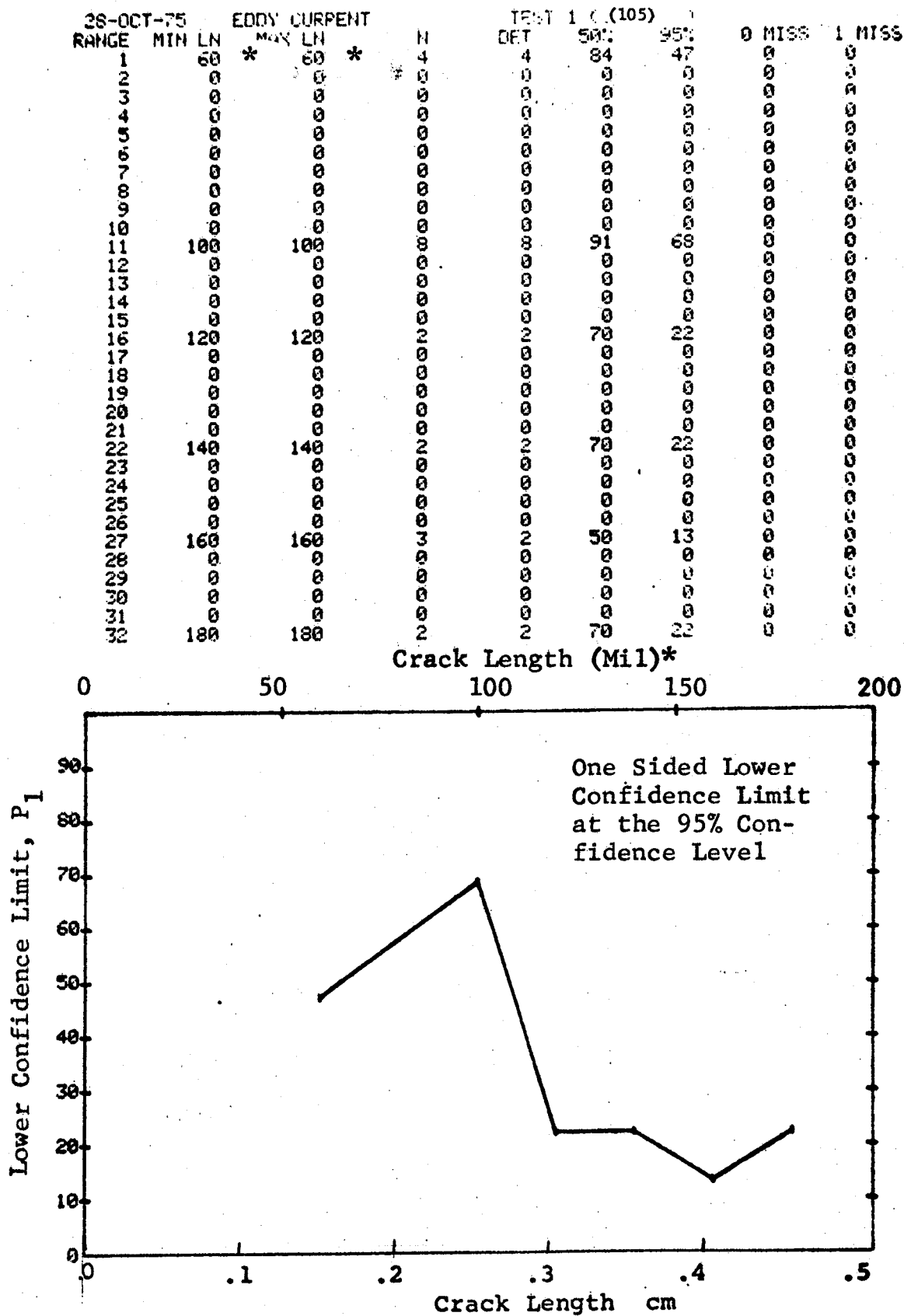


Figure D-105 Probability of Detection for 4340M Steel Using Eddy Current. Compressed Notch Flaws in Hollow Cylinder. Prod. Env.

(b) Optimum Probability Method of Data Cumulation

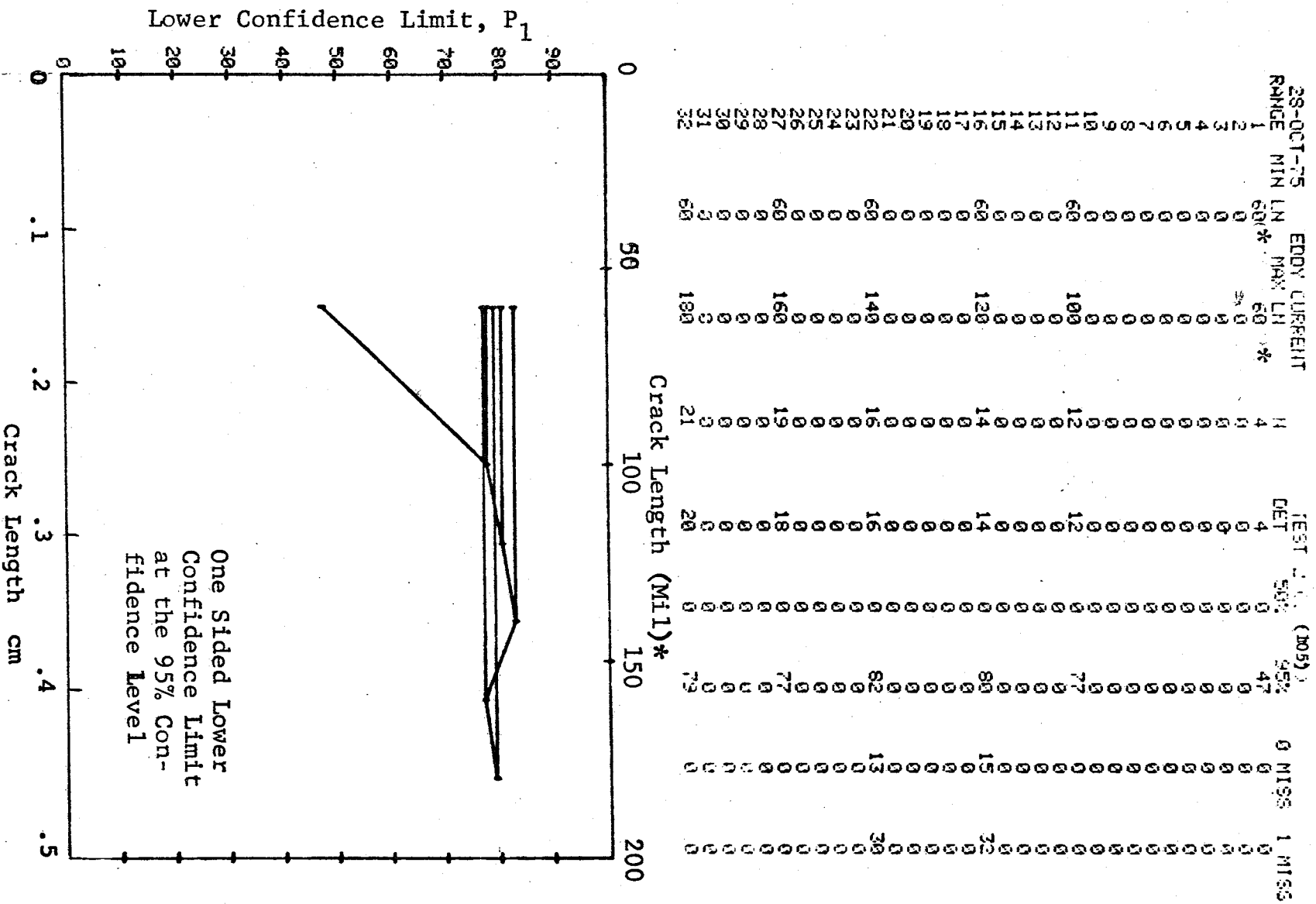


Figure D-105 (Continued)

(c) Overlapping Sixty Point Method of Data Cumulation

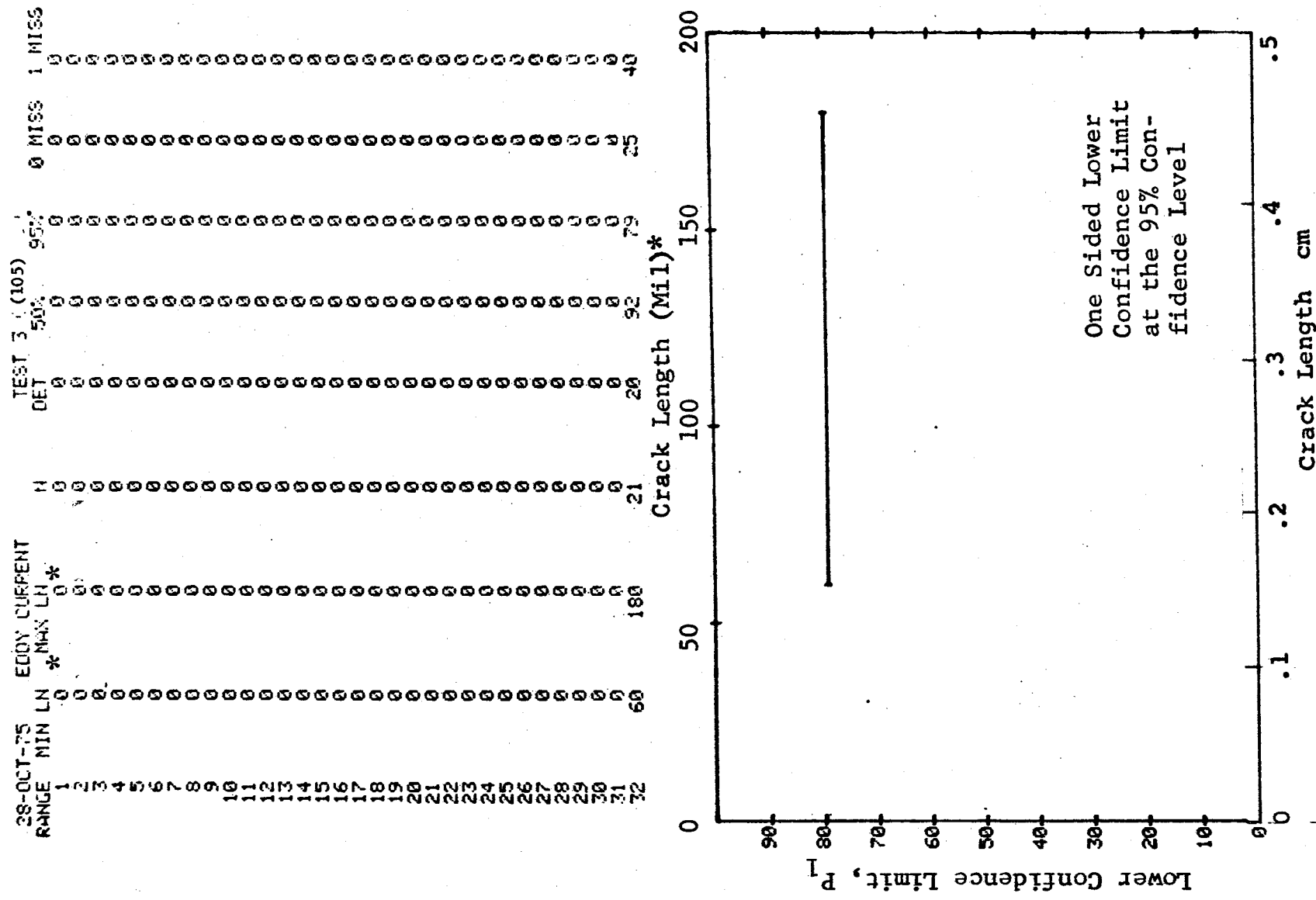


Figure D-105 (Concluded)

(a) Range Interval Method of Data Cumulation

28-OCT-75		EDDY CURRENT		N	TEST 1 (106)		0 MISS	1 MISS
RANGE	MIN LN	* MAX LN *			DET	50%		
1	90	90	*	1	1	50	5	0
2	90	90		0	0	91	68	0
3	0	0		0	0	0	0	0
4	0	0		0	0	0	0	0
5	110	110		4	4	84	47	0
6	120	120		1	1	50	5	0
7	0	0		0	0	0	0	0
8	130	130		1	1	50	5	0
9	140	140		7	7	90	65	0
10	0	0		0	0	0	0	0
11	0	0		0	0	0	0	0
12	0	0		0	0	0	0	0
13	0	0		0	0	0	0	0
14	0	0		0	0	0	0	0
15	0	0		0	0	0	0	0
16	0	0		0	0	0	0	0
17	0	0		0	0	0	0	0
18	0	0		0	0	0	0	0
19	0	0		0	0	0	0	0
20	0	0		0	0	0	0	0
21	0	0		0	0	0	0	0
22	0	0		0	0	0	0	0
23	0	0		0	0	0	0	0
24	0	0		0	0	0	0	0
25	0	0		0	0	0	0	0
26	0	0		0	0	0	0	0
27	0	0		0	0	0	0	0
28	0	0		0	0	0	0	0
29	0	0		0	0	0	0	0
30	0	0		0	0	0	0	0
31	0	0		0	0	0	0	0
32	300	300		3	3	79	36	0

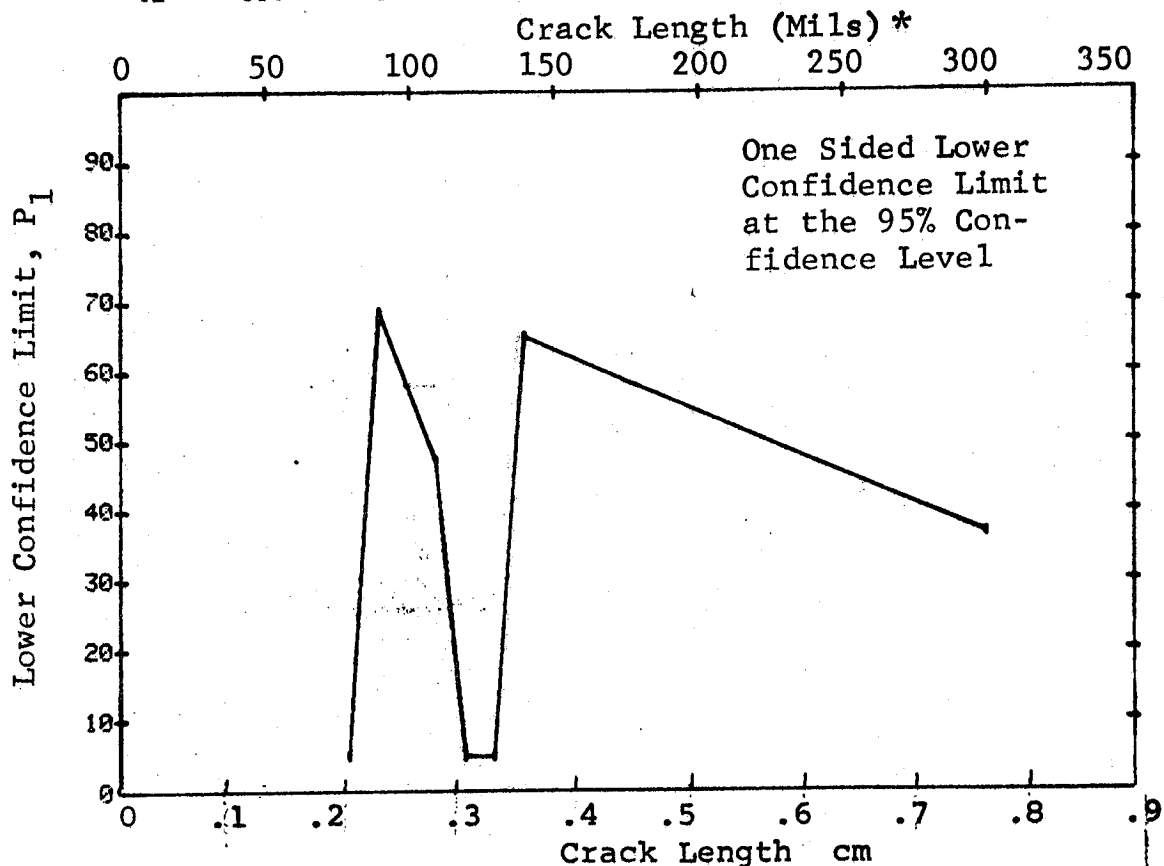


Figure D-106 Probability of Detection for 4340M Steel Using Eddy Current Compressed Notch Flaws in Hollow Cylinder. Prod. Env.

(b) Optimum Probability Method of Data Cumulation

28-OCT-75			EDDY CURRENT			TEST 2 (106)			0 MISS 1 MISS		
RANGE	MIN	LN	LN	MIN	LN	DET	500	950	0	MISS	1 MISS
1	80	80	80	80	80	1	0	5	0	0	0
2	80	80	80	80	80	9	0	71	0	0	0
3	80	80	80	80	80	0	0	0	0	0	0
4	80	80	80	80	80	0	0	0	0	0	0
5	80	80	80	80	80	0	0	0	0	0	0
6	80	80	80	80	80	13	0	79	0	0	0
7	80	80	80	80	80	14	0	80	15	0	32
8	80	80	80	80	80	15	0	81	14	0	0
9	80	80	80	80	80	22	0	87	17	0	24
10	80	80	80	80	80	0	0	0	0	0	0
11	80	80	80	80	80	0	0	0	0	0	0
12	80	80	80	80	80	0	0	0	0	0	0
13	80	80	80	80	80	0	0	0	0	0	0
14	80	80	80	80	80	0	0	0	0	0	0
15	80	80	80	80	80	0	0	0	0	0	0
16	80	80	80	80	80	0	0	0	0	0	0
17	80	80	80	80	80	0	0	0	0	0	0
18	80	80	80	80	80	0	0	0	0	0	0
19	80	80	80	80	80	0	0	0	0	0	0
20	80	80	80	80	80	0	0	0	0	0	0
21	80	80	80	80	80	0	0	0	0	0	0
22	80	80	80	80	80	0	0	0	0	0	0
23	80	80	80	80	80	0	0	0	0	0	0
24	80	80	80	80	80	0	0	0	0	0	0
25	80	80	80	80	80	0	0	0	0	0	0
26	80	80	80	80	80	0	0	0	0	0	0
27	80	80	80	80	80	0	0	0	0	0	0
28	80	80	80	80	80	0	0	0	0	0	0
29	80	80	80	80	80	0	0	0	0	0	0
30	80	80	80	80	80	0	0	0	0	0	0
31	80	80	80	80	80	0	0	0	0	0	0
32	80	80	80	80	80	25	0	88	1	0	21

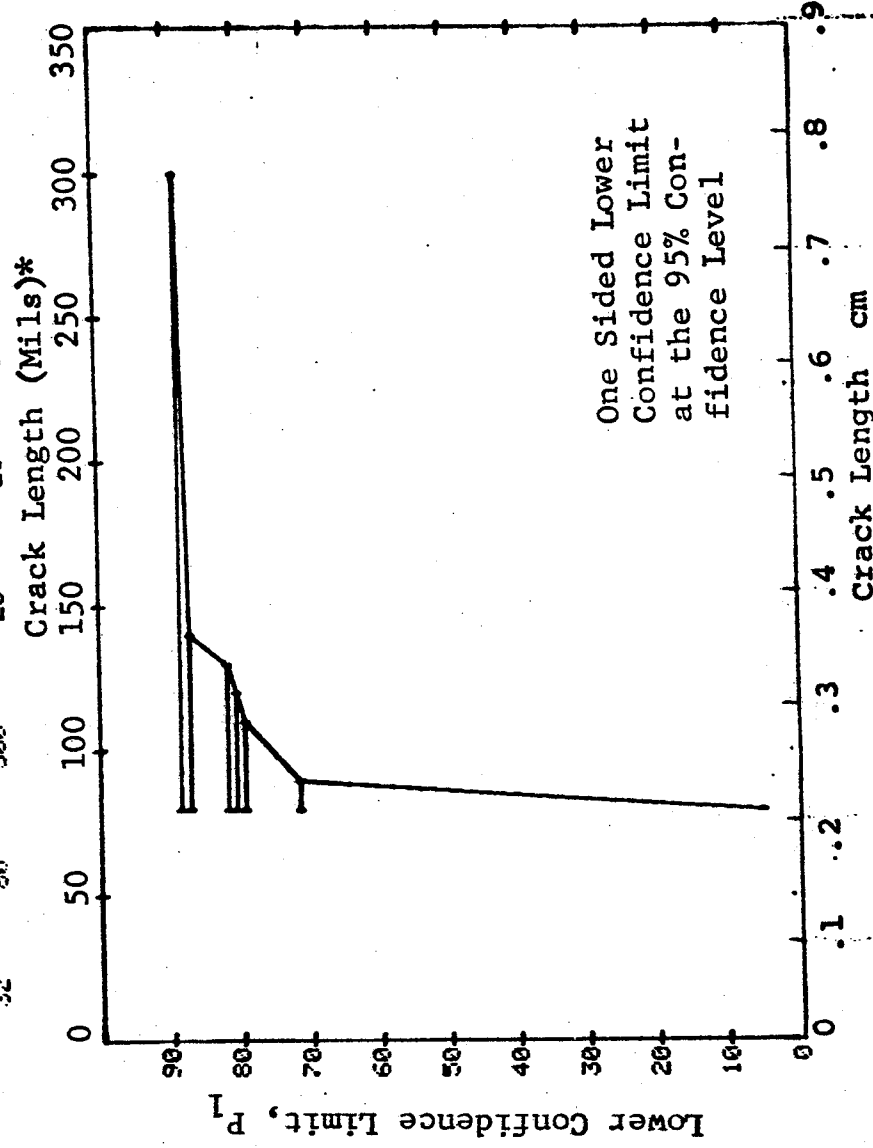


Figure D-106 (Continued)

(c) Overlapping Sixty Point Method of Data Cumulation

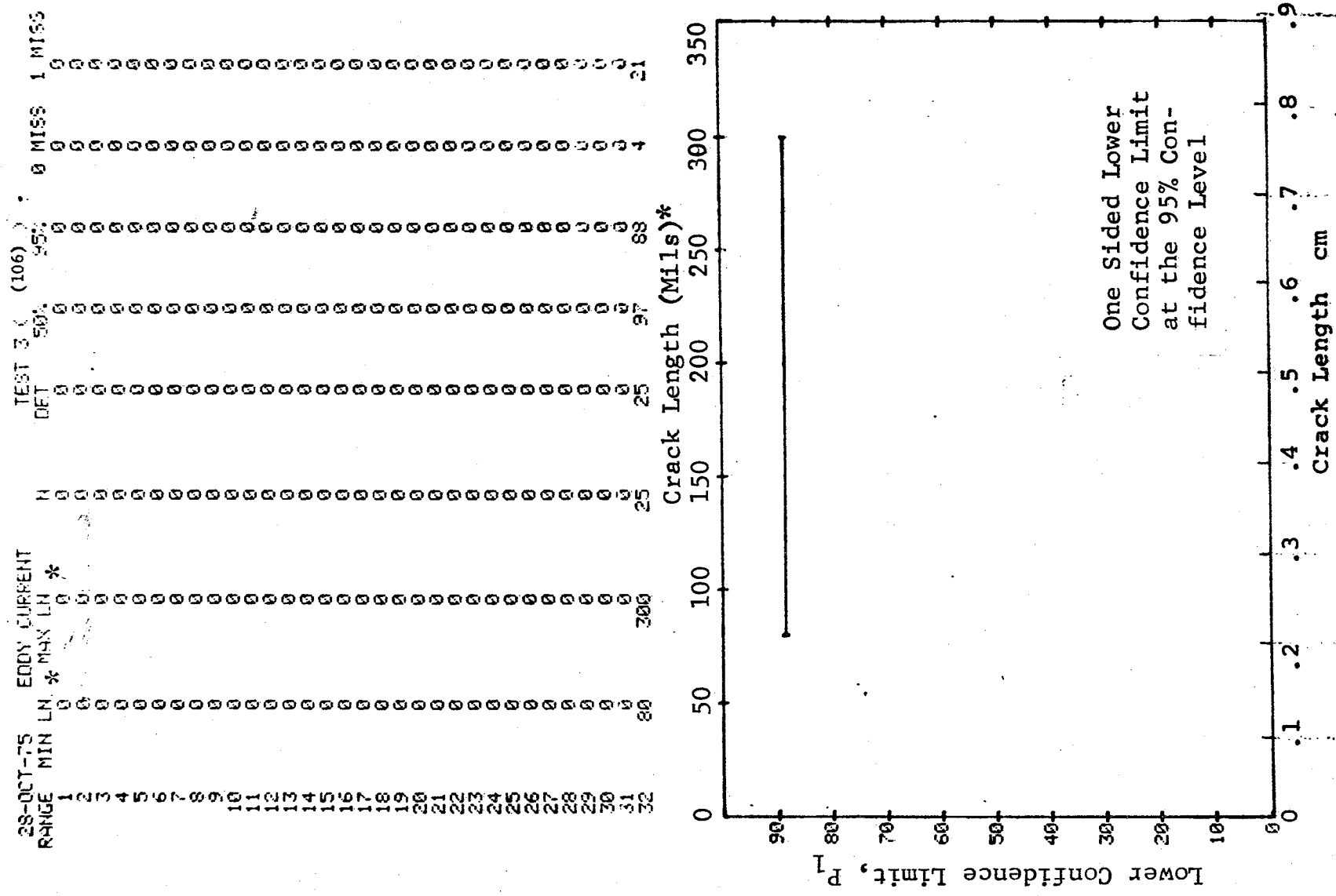


Figure D-106 (Concluded)

(a) Range Interval Method of Data Cumulation

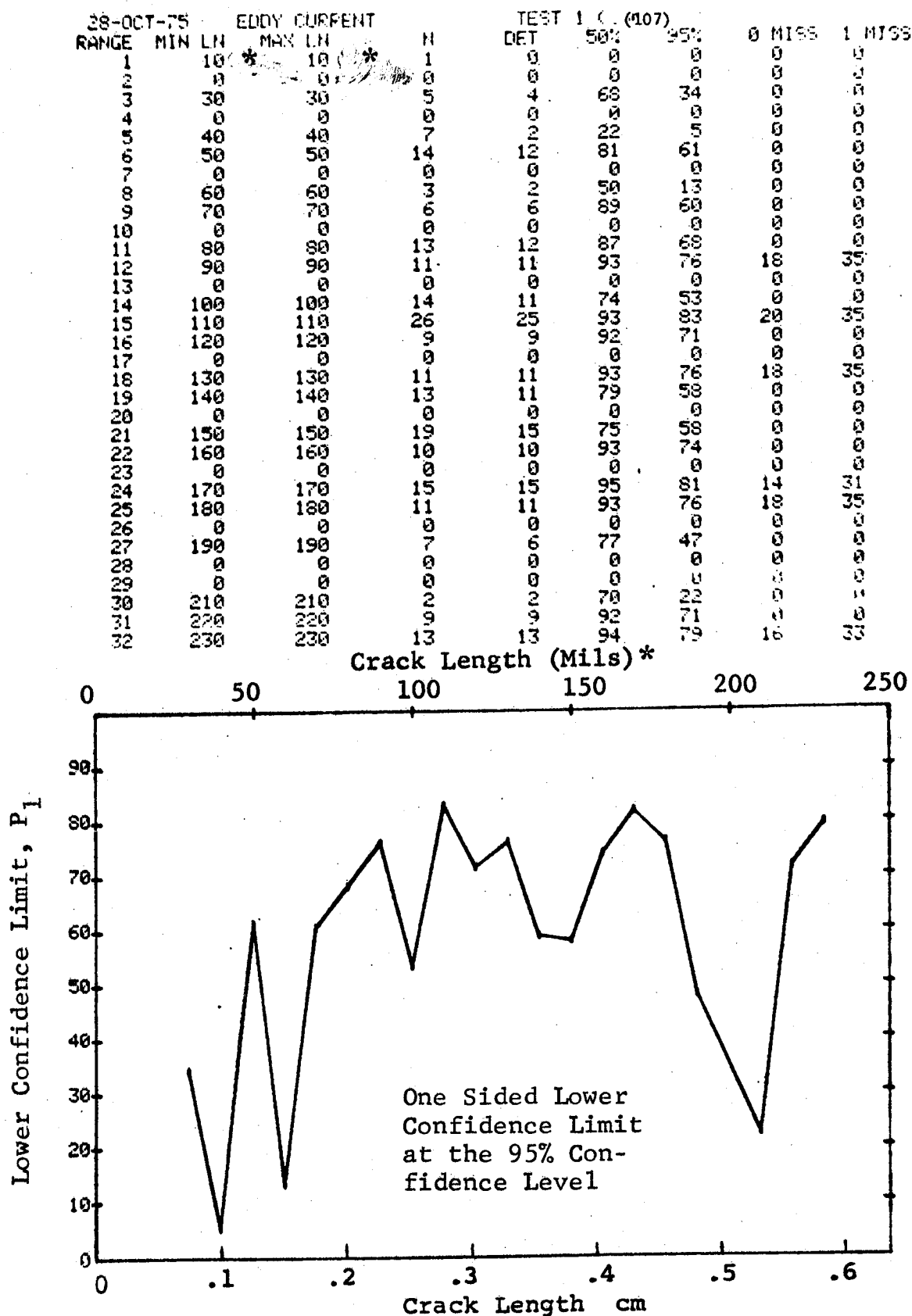


Figure D-107 Probability of Detection for 2024-T6 Al Using Eddy Current. Compressed Notch Flaws in Tandem T Specimens. Production Environment.

(b) Optimum Probability Method of Data Cumulation

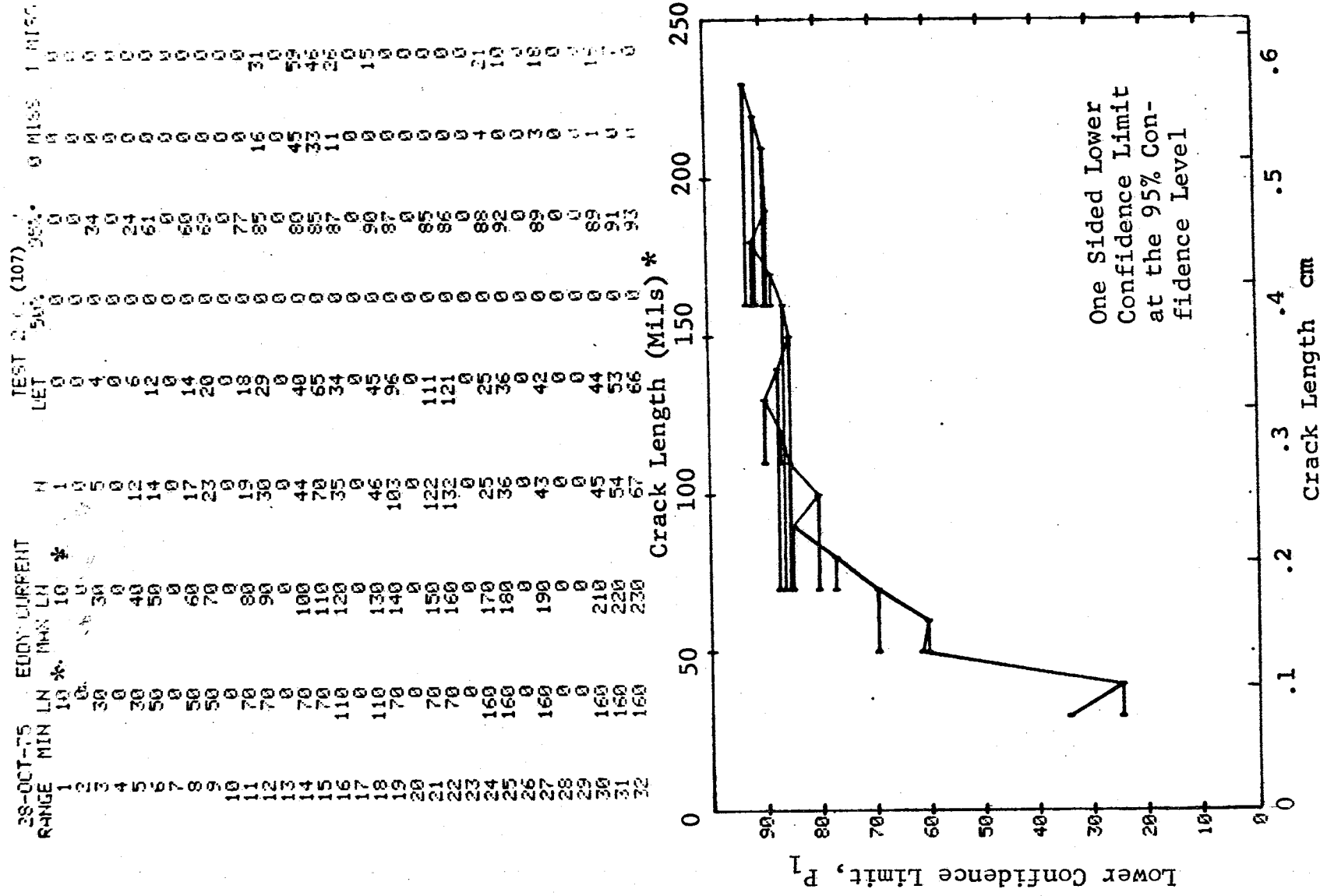


Figure D-107 (Continued)

(c) Overlapping Sixty Point Method of Data Cumulation

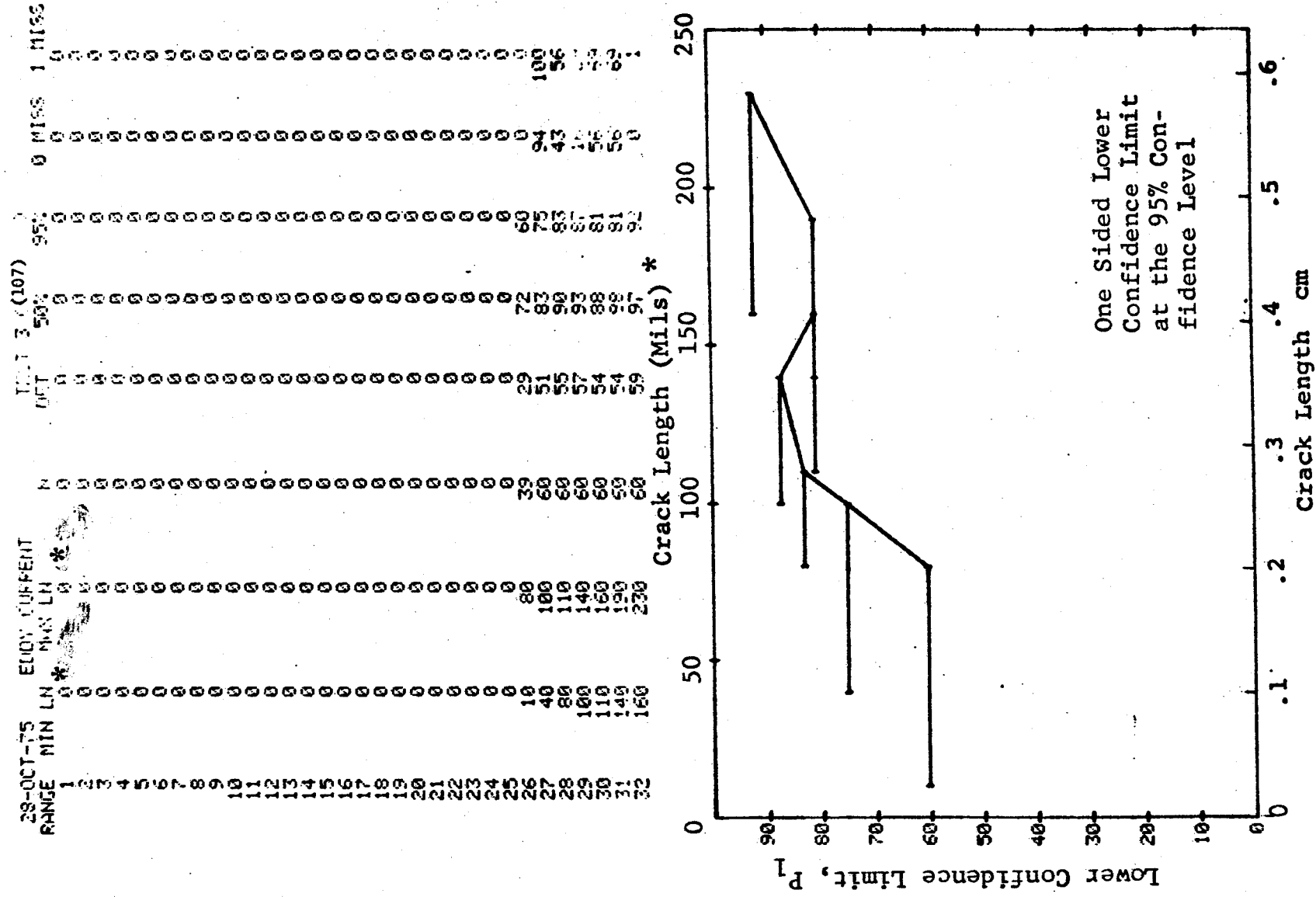


Figure D-107 (Concluded)

(a) Range Interval Method of Data Cumulation

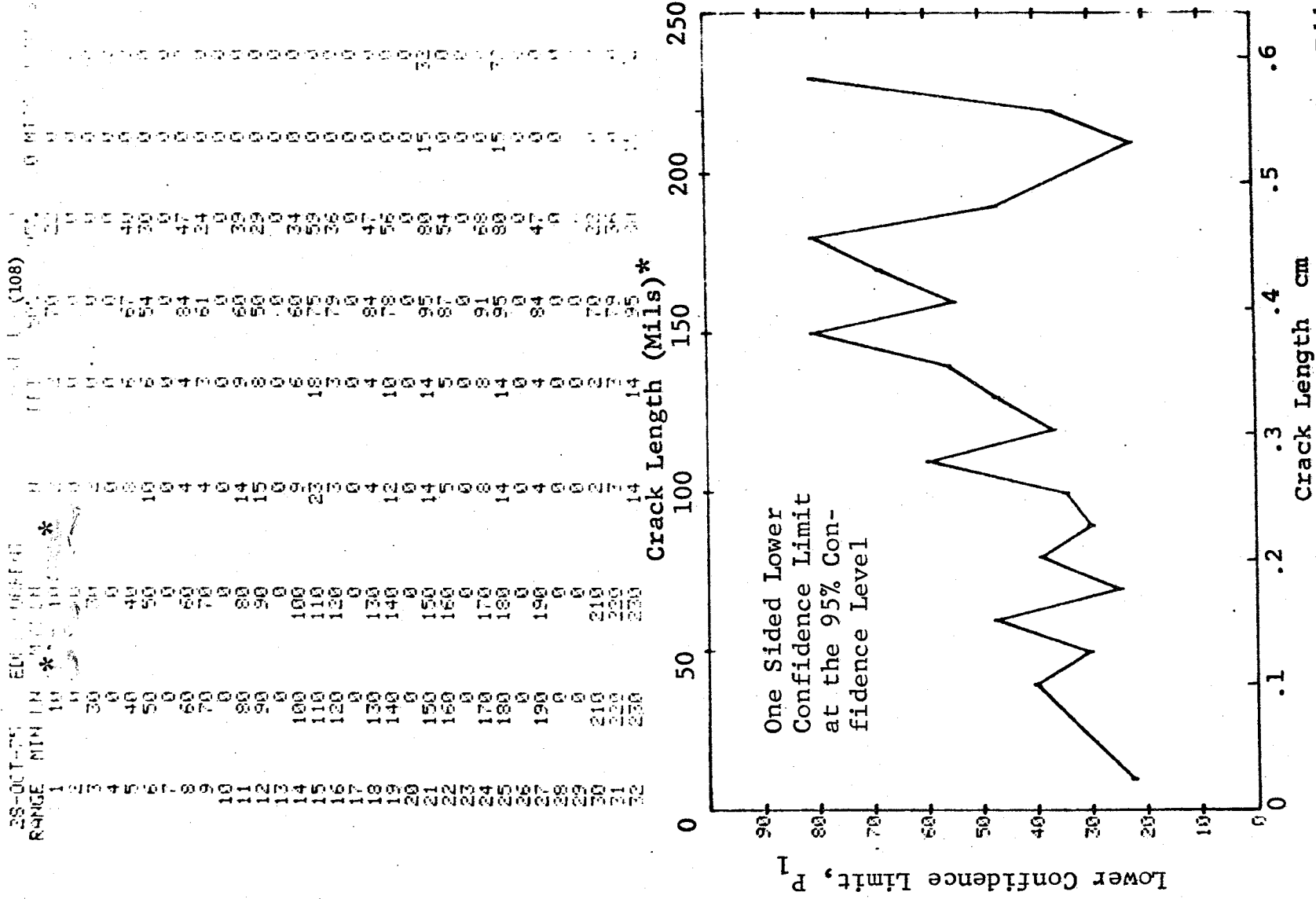


Figure D-108 Probability of Detection for 2024-T6 A1 Using Eddy Current. Compressed Notch Flaws in Tandem T Specimen. Laboratory Environment.

(b) Optimum Probability Method of Data Cumulation

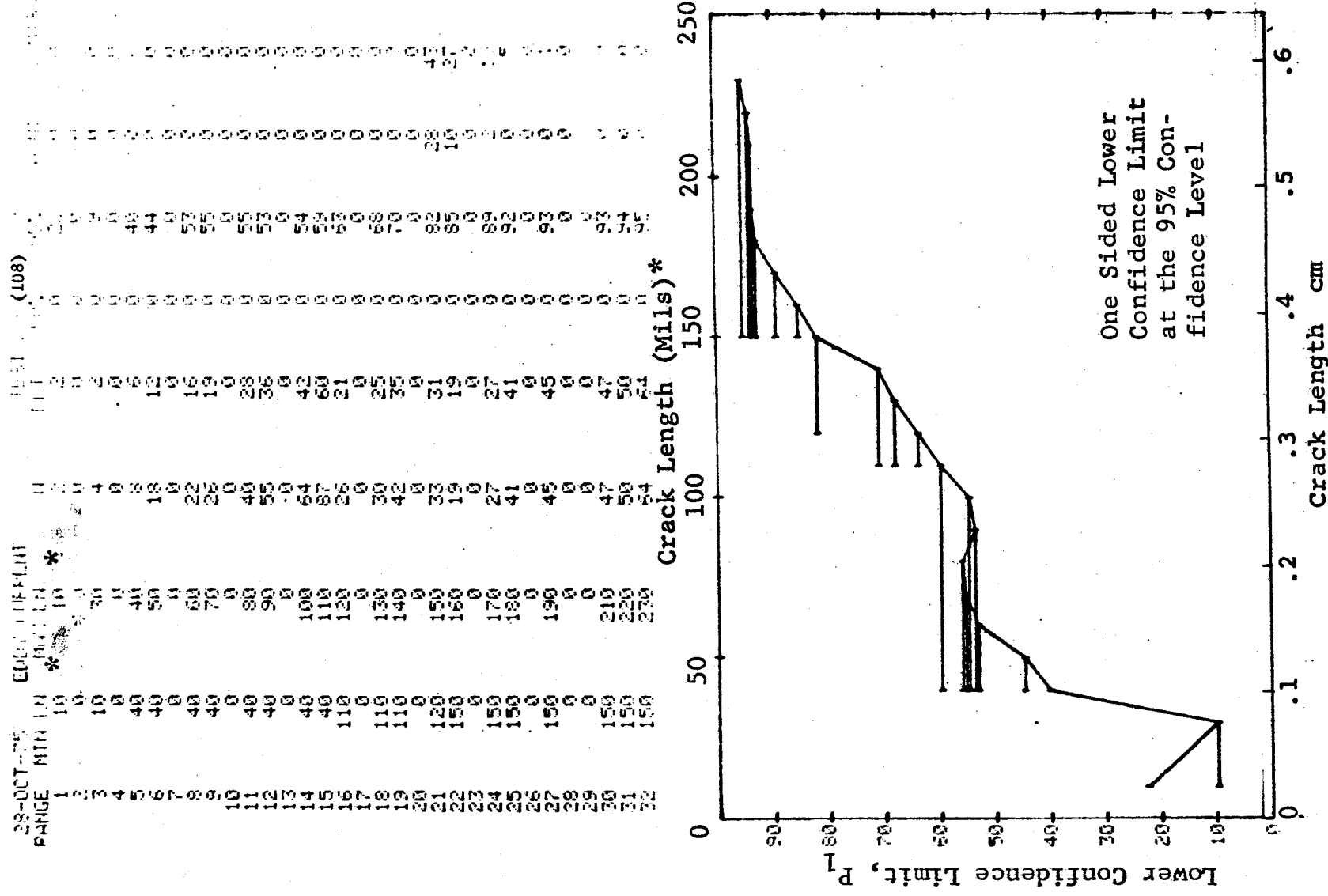


Figure D-108. (Continued)

REPRODUCIBILITY OF THE
ORIGINAL PAGE IS POOR

D-331

(c) Overlapping Sixty Point Method of Data Cumulation

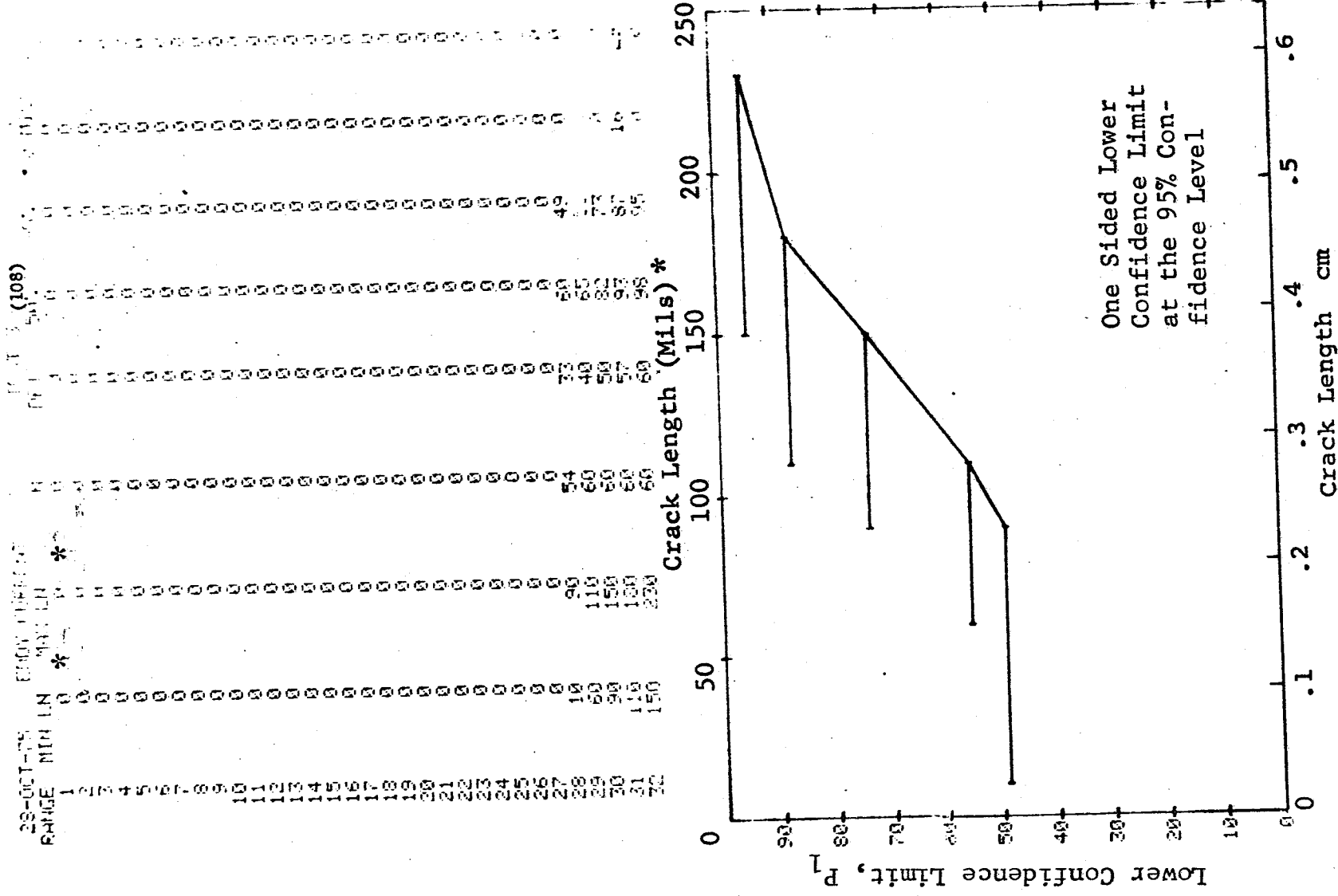


Figure D-108 (Concluded)

(a) Range Interval Method of Data Cumulation

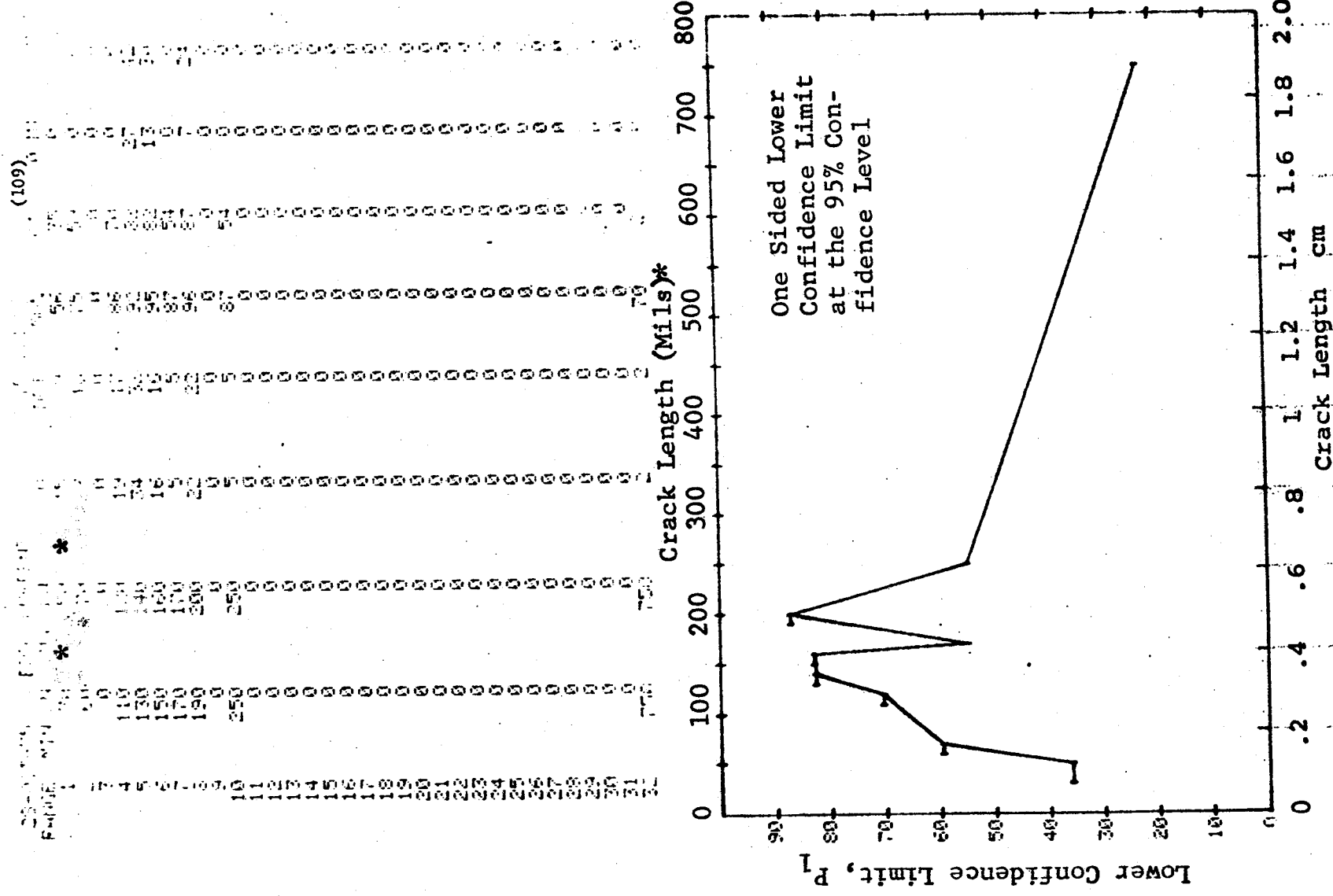
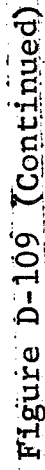
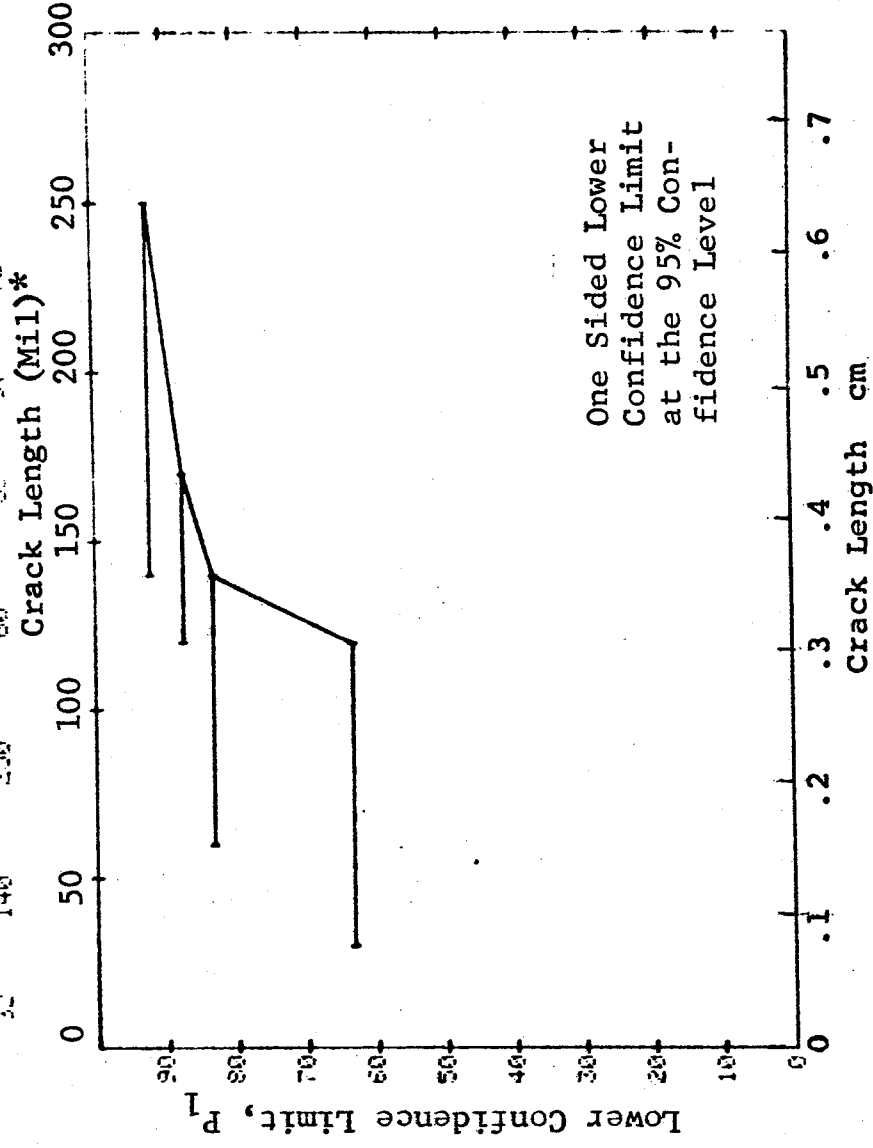


Figure D-109 Probability of Detection for 4340M Steel Using Eddy Current. Compressed Notch Flaws in Solid Cylinder. Laboratory Environment.

[illegible]

[illegible]

D-335

(a) Range Interval Method of Data Cumulation

28-OCT-75	EDDY CURRENT	TEST 1	TEST 2
RANGE MIN LN	MAX LN	IFT	IFT
1 100 0	0	50	95
2 100 0	0	71	45
3 100 0	0	94	79
4 100 0	0	93	0
5 100 0	0	93	74
6 100 0	0	93	34
7 100 0	0	97	90
8 100 0	0	0	54
9 100 0	0	87	0
10 100 0	0	50	5
11 100 0	0	0	0
12 100 0	0	0	0
13 100 0	0	0	0
14 100 0	0	0	0
15 100 0	0	0	0
16 100 0	0	0	0
17 100 0	0	0	0
18 100 0	0	0	0
19 100 0	0	0	0
20 100 0	0	0	0
21 100 0	0	0	0
22 100 0	0	0	0
23 100 0	0	0	0
24 100 0	0	0	0
25 100 0	0	0	0
26 100 0	0	0	0
27 100 0	0	0	0
28 100 0	0	0	0
29 100 0	0	0	0
30 100 0	0	0	0
31 100 0	0	0	0
32 100 0	0	0	0

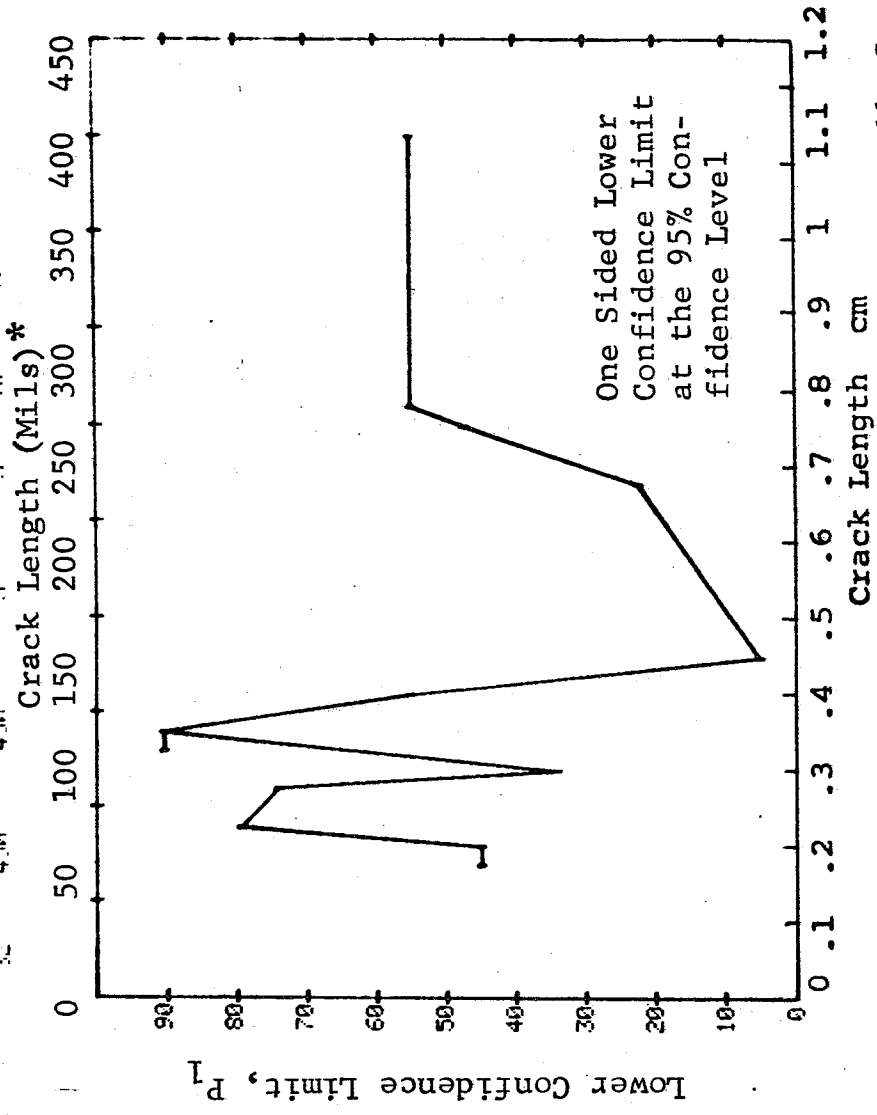


Figure D-110 Probability of Detection for 4340M Steel Using Eddy Current. Compressed Notch Flaws in Hollow Filleted Cylinder. Laboratory Environment. D-336

(b) Optimum Probability Method of Data Cumulation

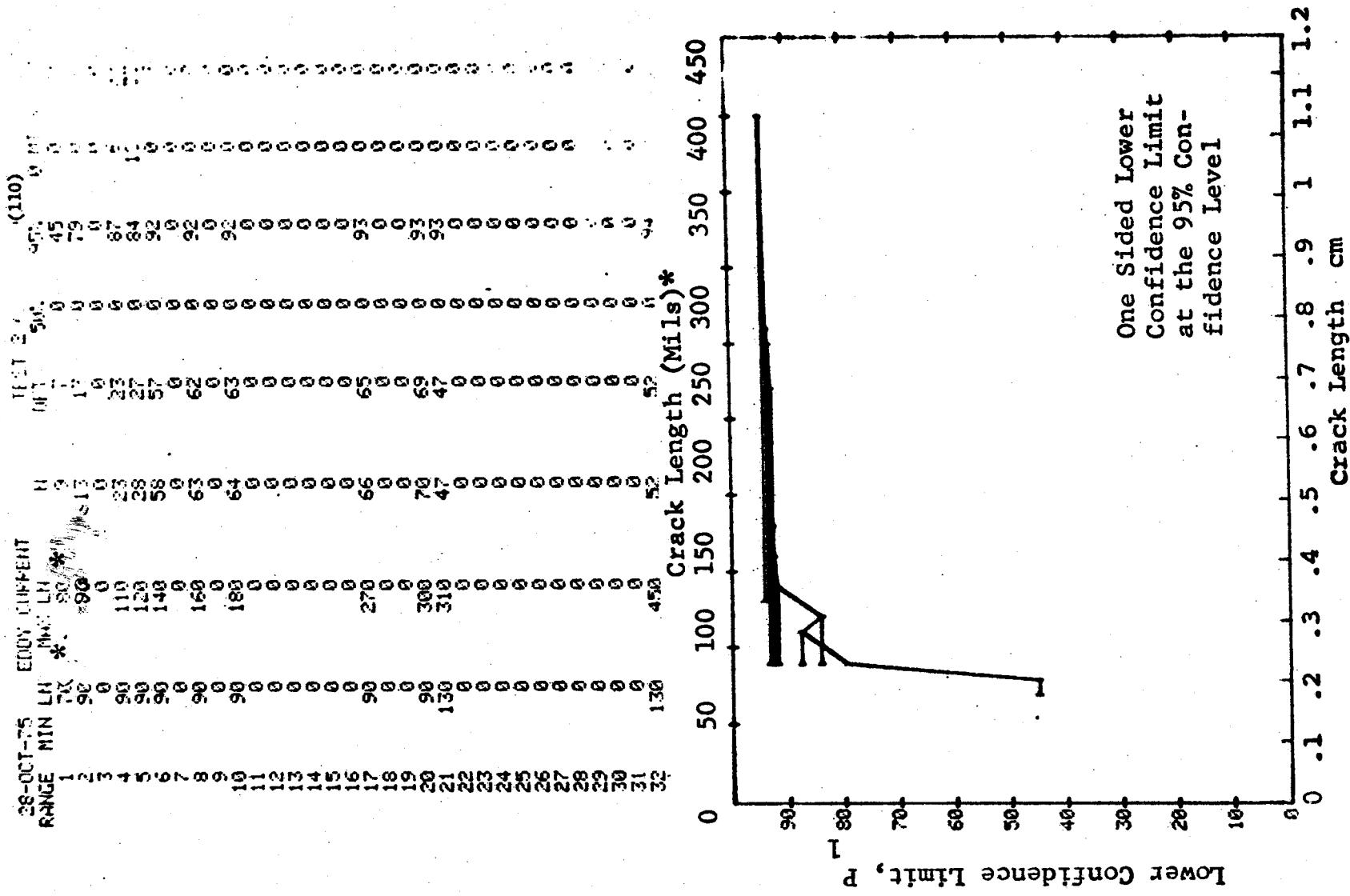


Figure D-110 (Continued)

(c) Overlapping Sixty Point Method of Data Cumulation

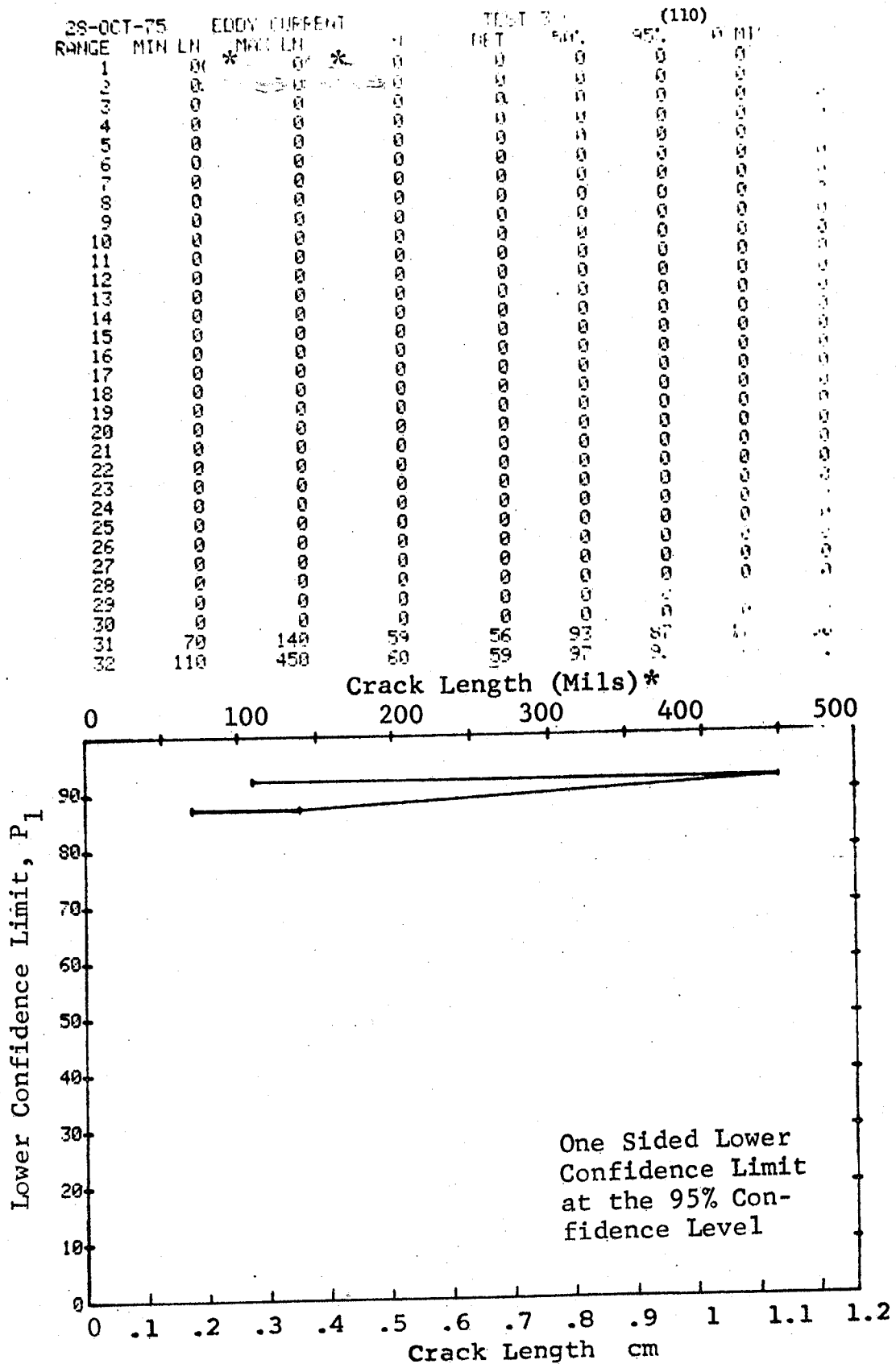


Figure D-110 (Concluded)

(a) Range Interval Method of Data Cumulation

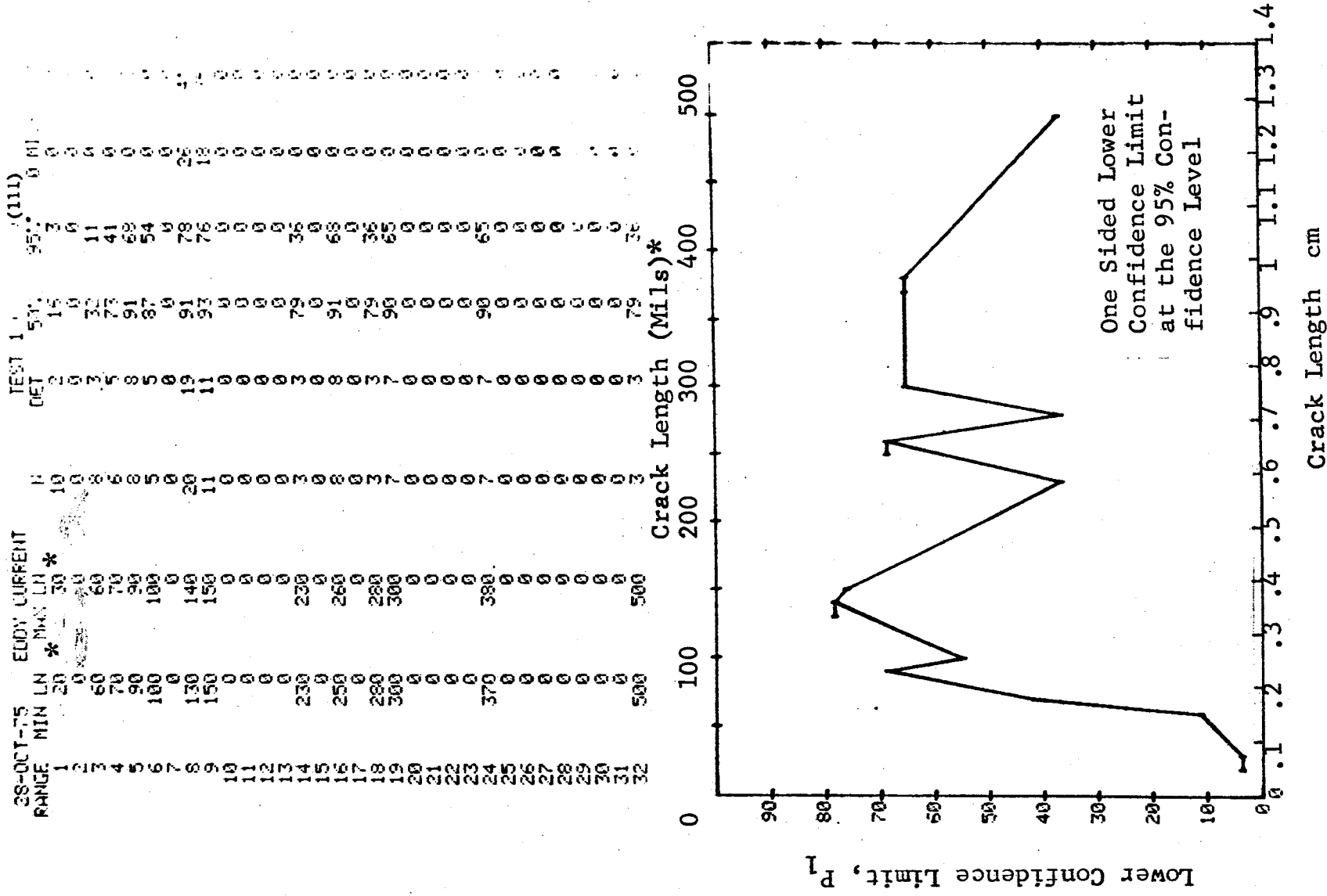


Figure D-111 Probability of Detection for 4340M Steel Using Eddy Current. Compressed Notch Flaws in Solid Filleted Cylinder. Laboratory Environment

(b) Optimum Probability Method of Data Cumulation

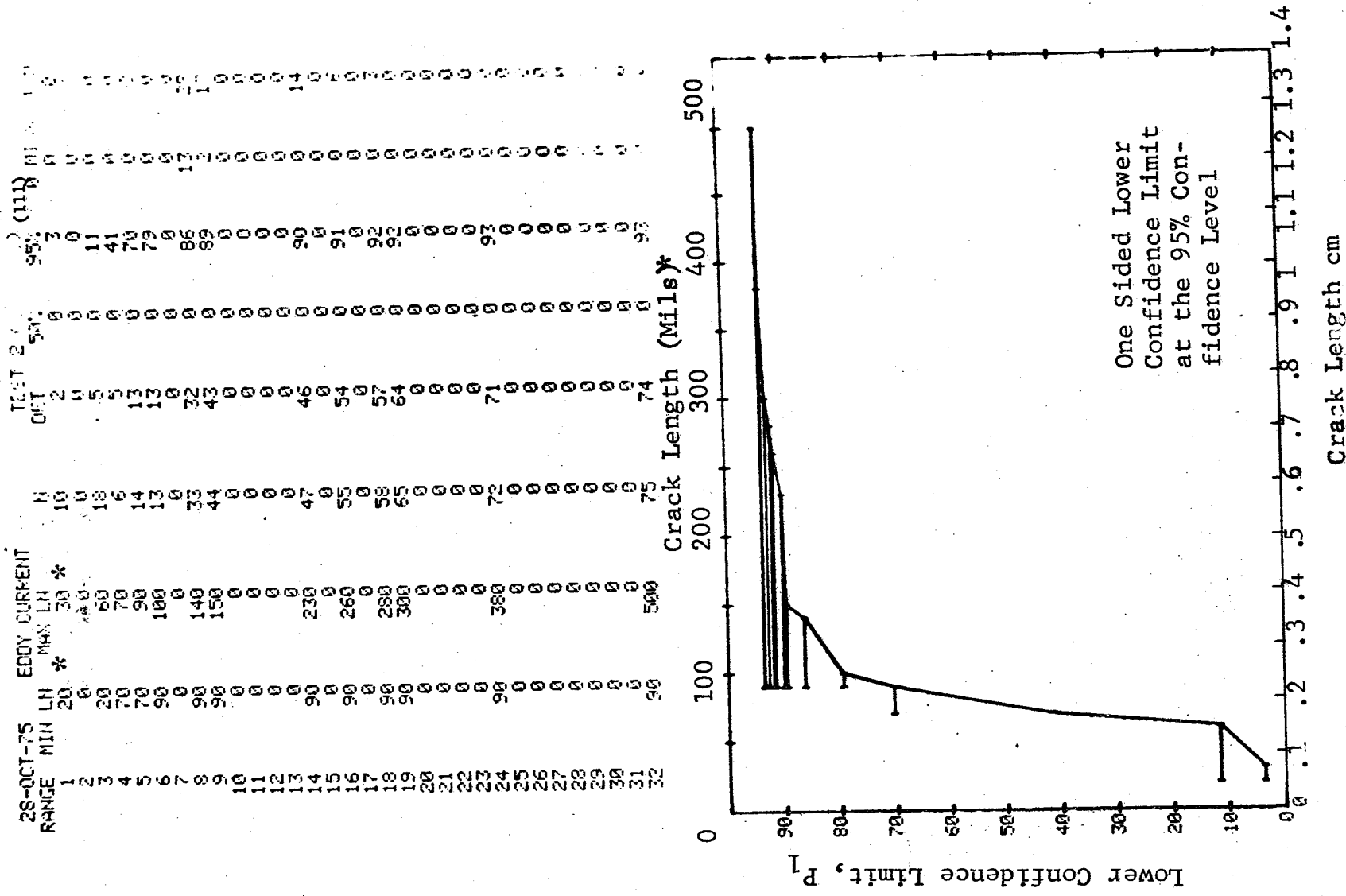


Figure D-111 (Continued)

(c) Overlapping Sixty Point Method of Data Cumulation

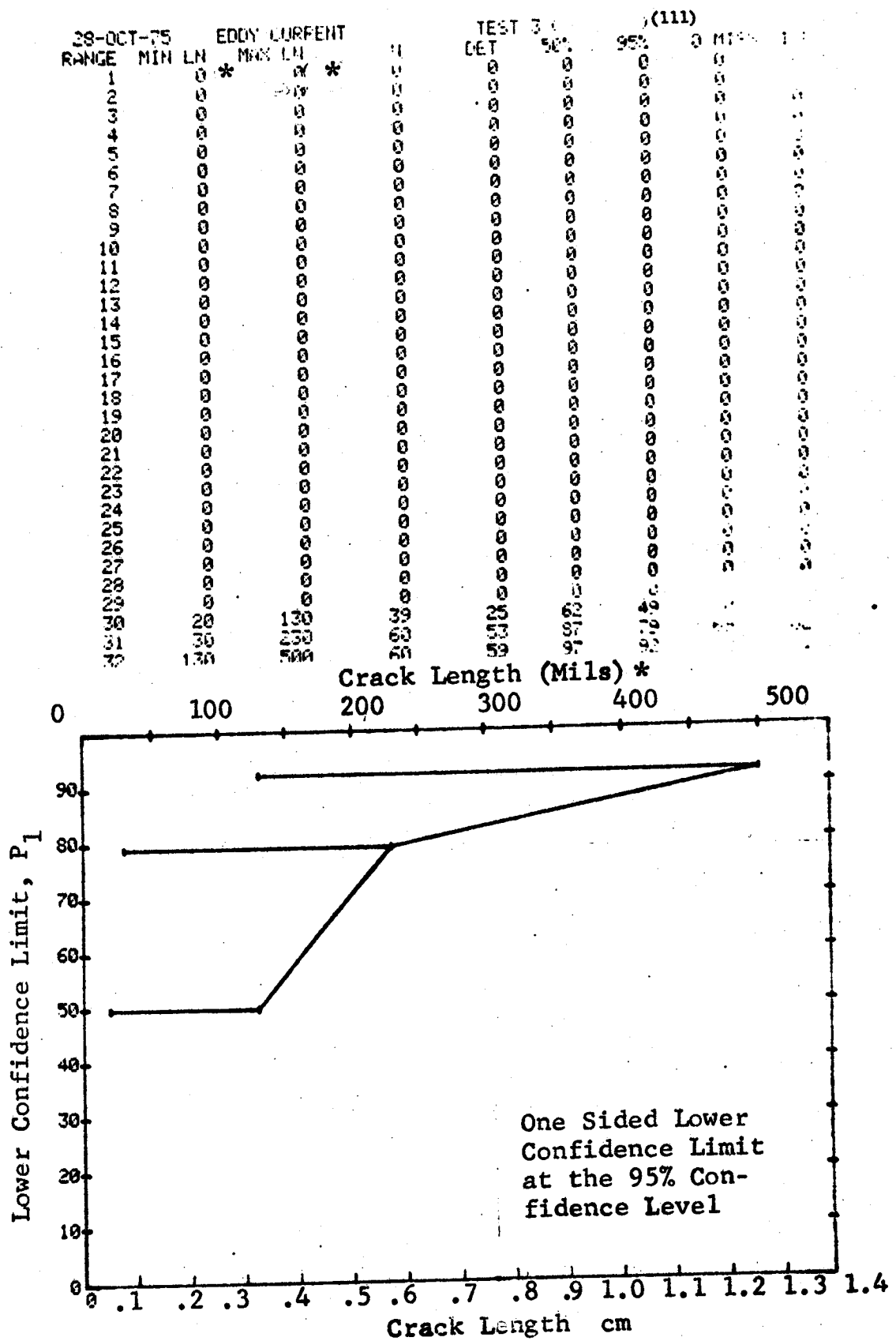


Figure D-111 (Concluded)

(a) Range Interval Method of Data Cumulation

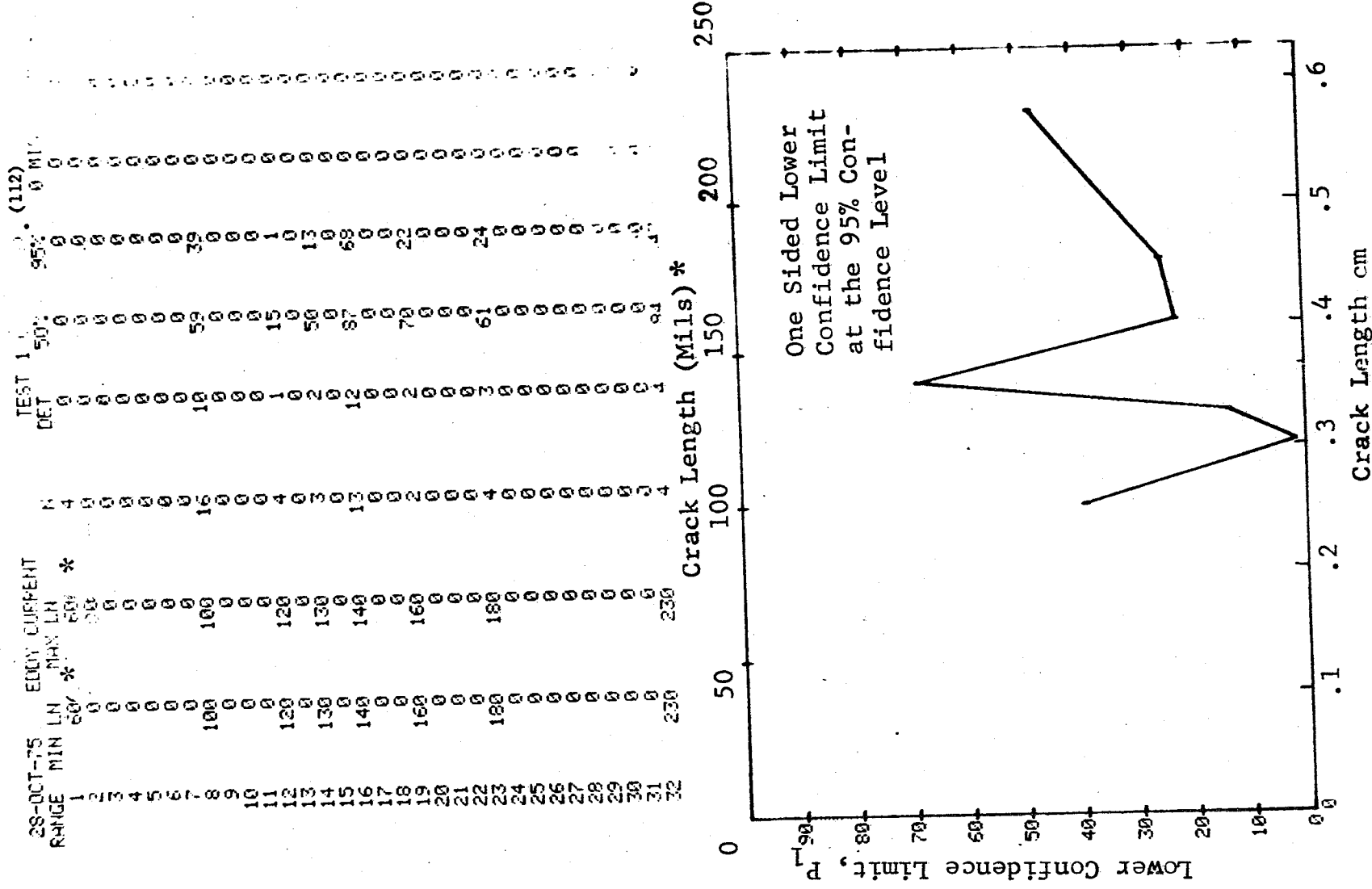


Figure D-112 Probability of Detection for 4340M Steel Using Eddy Current. Compressed Notch Flaws in Hollow Cylinder. Laboratory Environment.

D-342

REPRODUCIBILITY OF THE
ORIGINAL PAGE IS POOR

(b) Optimum Probability Method of Data Cumulation

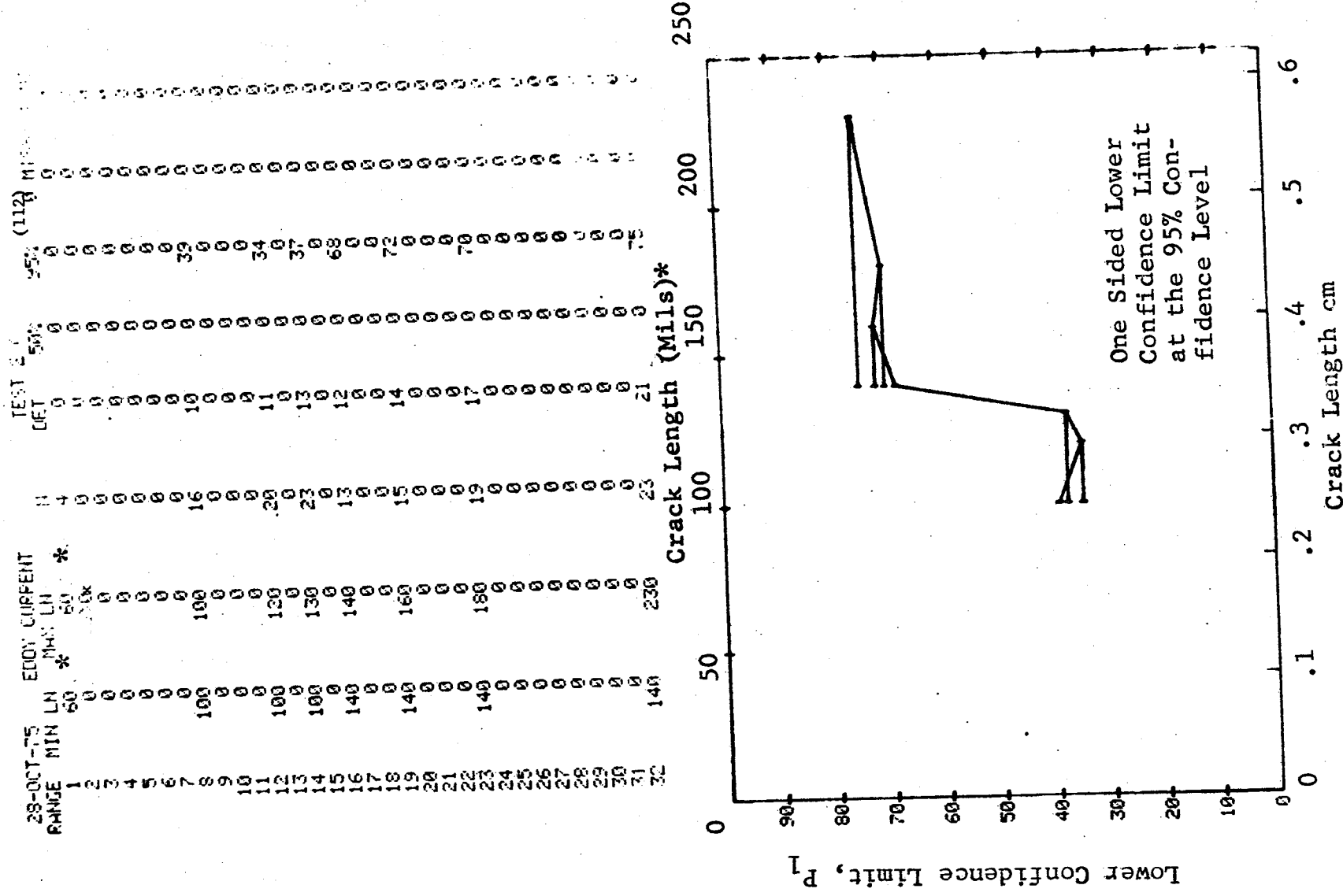
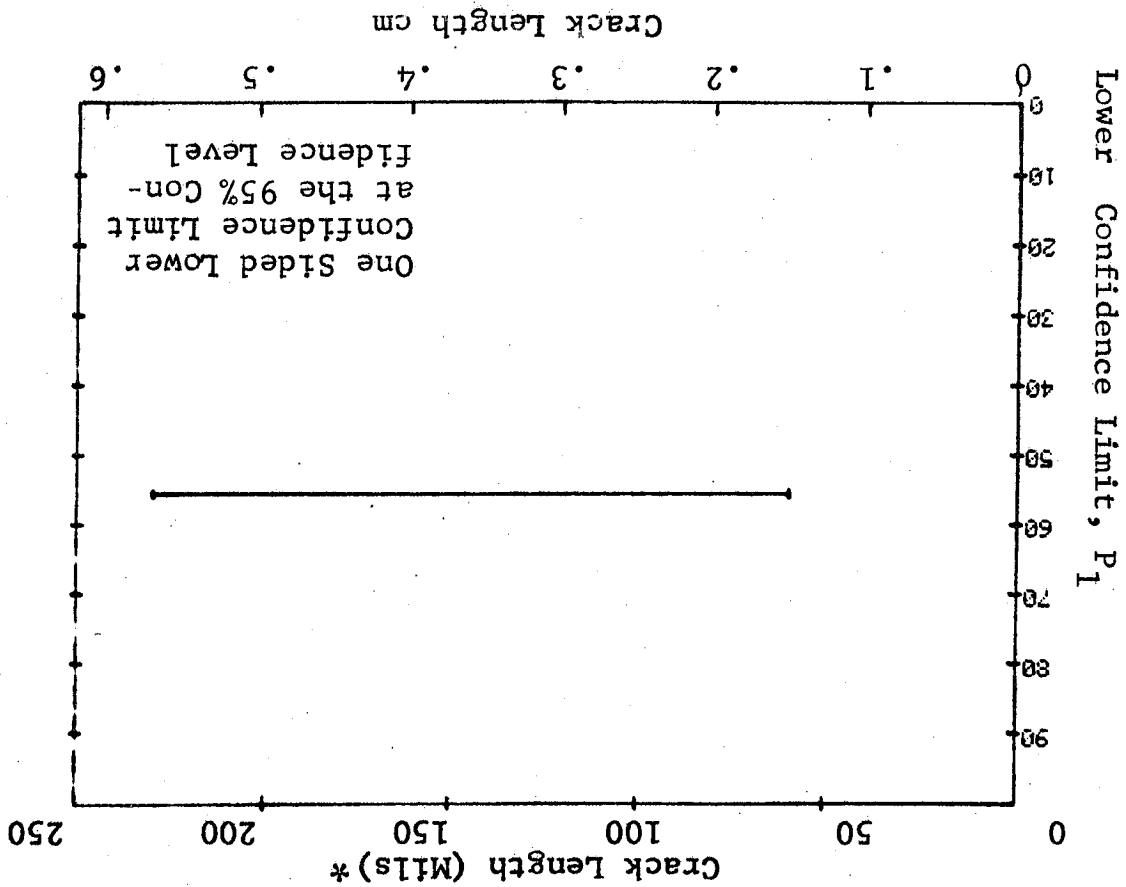


Figure D-112 (Continued)

Figure D-112 (Concluded)



(c) Overlapping Sixty Point Method of Data Cumulation

DISTRIBUTION LIST

Contract NAS3-18907
Final Contractor Report

NASA-Lewis Research Center
Cleveland, OH 44135

Attn: *T. Gulko, MS 49-3

*R.L. Davies, MS 106-1

*N.T. Saunders, MS 105-1

*Audit Branch, MS 500-303

*S.J. Klima, MS 106-1

(22 copies)

*J.E. Dilley, MS 500-313

G.T. Smith, MS 49-3

W.F. Brown, MS 105-1

Library, MS 60-3

(2 copies)

Technology Utilization, MS 3-9

Report Control, MS 5-5

R.W. Hall, MS 49-1

National Aeronautics and Space Administration
Washington, DC 20546

Attn: RW/G.C. Deutsch

RWS/ M. Salkind

Library

MHQ/G. Eriksen

MQ/P. Wood

National Aeronautics and Space Administration
George C. Marshall Space Flight Center
Marshall Space Flight Center, AL 35812

Attn: J. M. Knadler, III, Code EH13

R. C. Crockett, Code EI44

Library

National Aeronautics and Space Administration
Lyndon B. Johnson Space Center
Houston, TX 77058

Attn: ES-5/R.E. Johnson

ES-5/W.L. Castner

Library

National Aeronautics and Space Administration
Langley Research Center
Hampton, VA 23365

Attn: R.W. Leonard, MS 188

Library

76 1747

D-345
REPRODUCIBILITY OF THE
ORIGINAL PAGE IS POOR

National Aeronautics and Space Administration
John F. Kennedy Space Center
Kennedy Space Center, FL 32899
Attn: R. Sannicandro, DB-SED-4
Library

National Aeronautics and Space Administration
Goddard Space Flight Center
Greenbelt, MD 20771
Attn: Library

Jet Propulsion Laboratory
4800 Oak Grove Drive
Pasadena, CA 91103
Attn: Library

U. S. Air Force
Wright Patterson AFB, OH 45433
Attn: T.D. Cooper, AFML/MXA
M.J. Garrick, AMRL/HE
N. Tupper, AFEDL/FBA
W.R. Luebben, AFLC/MAUT
D. Fournay, AFML/LLP

Scientific and Technical Information Facility
Box 8757
Baltimore-Washington Int. Airport
Baltimore, MD 21240
Attn: NASA Representative (6 copies)

Lockheed Georgia Company
Marietta, GA 30063
Attn: W.H. Lewis, D/73-30, Z-285

TRW Inc.
23555 Euclid Ave.
Cleveland, OH 44117
Attn: I.M. Matay TM-2966

North American Rockwell
Quality Assurance
12214 Lakewood Boulevard
Downey, CA 90241
Attn: C.R. Bishop

U. S. Air Force
Hq. SAAMA/MMEW-4
Kelly Air Force Base, TX 78241
Attn: B.W. Boisvert

Pratt & Whitney Aircraft
P. O. Box 2691
West Palm Beach, FL 33402
Attn: C. Biddle

D-346

McDonnell Douglas Corp.
P.O. Box 516
St. Louis, MO 63166
Attn: R. J. Roehrs

Pratt & Whitney Aircraft
East Hartford, CT
Attn: F. Vick

Lockheed-California Company
Dept. 74-44, Bldg. 243, Plant 2
Burbank, CA 91503
Attn: D.E. Pettit

Rockwell International
Los Angeles Division
Los Angeles, CA
Attn: E. L. Caustin

Martin-Marietta Corporation
P.O. Box 179
Denver, CO 80201
Attn: W. Rummel, MS 1620

LTV Aerospace Division
P.O. Box 5907
Dallas, TX 75222
Attn: B.W. Staff

Naval Air Development Center
Warminster, PA 18974
Attn: F.S. Williams, Code 302

Northrop Corporation
A/C Division
3901 West Broadway
Hawthorne, CA 90250
Attn: W.R. Sturrock, 7620/23

Fairchild Republic Company
Quality Assurance Laboratory
Bldg. 32
Farmingdale, NY 11735
Attn: R. Brousseau

Grumman Aerospace Corp.
Q.C.A.D.
Bethpage, NY 11714
Attn: S. Chance

Systems Research Laboratory
2800 Indian Ripple Road
Dayton, OH 45440
Attn: W. Dirkes

D-347

Army Materials & Mechanics Research Center
Mechanics of Materials
Watertown, MA 02172
Attn: G. A. Darcy

General American Research Division
7449 North Natchez Avenue
Niles, IL 60642
Attn: W. Lichodziejewski

U. S. Air Force
Tinker AFB
Oklahoma City, OK 73145
Attn: M. Mizell, ALC/MMET

Boeing Commercial Airplane Company
P.O. Box 3707
Seattle, WA 98124
Attn: H. Southworth, MS 73-05

Rockwell International
Science Center
1049 Camino Dos Rios
Thousand Oaks, CA 91360
Attn: D. Thompson

U. S. Air Force
Hill AFB
Ogden, UT 84401
Attn: C. Thomson, ALC/MMET

General Electric Company
Aircraft Engine Group
Evendale, OH 45215
Attn: H. Truscott, M/L M-87
R. Wagner

National Bureau of Standards
Materials Building, Rm. B354
Washington, DC 20234
Attn: H. Berger

Transportation Systems Center
Kendall Square
Cambridge, MA 02142
Attn: J. Litant

Sandia Laboratories
Dept. 9350
Albuquerque, NM 87115
Attn: F.W. Neilsen

D-348

National Science Foundation
Division of Materials Research
1800 G Street, N.W.
Washington, DC 20550
Attn: J. R. Lane

NASA-Ames Research Center
Moffett Field, CA 94035
Attn: R. Hampton, MS213-4

Shannon Luminous Materials Company
Tracer-Tech Division
7356 Santa Monica Blvd.
Los Angeles, CA 90046
Attn: J.R. Alburger

Martin Marietta
P. O. Box 29304
New Orleans, LA 70189
Attn: V. Clisham

Bucyrus-Erie Company
Construction Machinery
Milwaukee, WI
Attn: K.V. Johnson

Babcock & Wilcox Company
Hwy. 69 S
Mt. Vernon, IN 47620
Attn: P.J. Kovach

Schlumberger Well Services
P.O. Box 2175
Houston, TX 77001
Attn: E. Moser

Wyman-Gordon Company
14600 S. Wood Street
Harvey, IL 60426
Attn: J. Sekerka

Combustion Engineering
911 West Main Street
Chattanooga, TN 37401
Attn: R.M. Stone

Office of The Secretary of Transportation
Office of Pipeline Safety
Washington, DC 20590
Attn: J.C. Caldwell

Westinghouse Electric Corporation
Gas Turbine Engine Division
Building A 603
Philadelphia, PA 19113
Attn: T. Sherlock

D-349

DOCUMENT RELEASE AUTHORIZATION

NASA Scientific and Technical Information Facility P.O. Box 8757, Balt/Wash International Airport, Maryland 21240		Control No. _____ Date: _____		
D E S C R I P T I O N	TITLE: Assessment of NDE Reliability Data			
	AUTHOR(S): B. G. W. Yee, F. H. Chang, J. C. Couchman, G. H. Lemon, and P. F. Packman			
	ORIGINATING ORGANIZATION: General Dynamics, Fort Worth Division		COGNIZANT, NASA CENTER NASA Lewis Research Center Mail Stop 106-1 21000 Brookpark Rd. Cleveland, OH 44135	
	CONTRACT NO: NAS3-18907			
	SECURITY CLASSIFICATION: U			
	TITLE: _____ DOCUMENT: _____			
	REPORT NO: _____			
	DATE: _____			
NASA CR NO 134991		WORK UNIT NO: YHG6780	NASA TECHNICAL MONITOR S. J. Klima	OFFICE CODE 5532
NASA TMX NO: _____				
THE FOLLOWING TO BE COMPLETED BY THE RESPONSIBLE NASA PROGRAM OFFICER OR HIS DESIGNEE				
(Further information is available in SP-7034 entitled R & D Reporting Guidance for Technical Monitoring of NASA Contracts)				
I. Document may be processed into the NASA Information System as follows:				
<input checked="" type="checkbox"/> May be announced in STAR (or CSTAR if a limited availability is checked below)				
<input type="checkbox"/> May not be announced (The attached letter may be consulted for information pertaining to the NASA non-announcement series)				
<input type="checkbox"/> May not be entered into the System because _____				
(Provide a brief statement to be quoted in answering requests for the referenced document)				
II. Document may be made available as checked below:				
<input checked="" type="checkbox"/> Publicly Available				
<input type="checkbox"/> Classified but Unlimited to Security Qualified Requesters				
<input type="checkbox"/> U.S. Government Agencies and Contractors Only				
<input type="checkbox"/> U.S. Government Agencies Only				
<input type="checkbox"/> U.S. Government Agencies, NASA and NASA Contractors Only				
<input type="checkbox"/> NASA and NASA Contractors Only				
<input type="checkbox"/> NASA Headquarters and Centers Only				
<input type="checkbox"/> Other Limitations (Specify) _____				
Signature (Program Officer or Designee):		Office Code: 5532		Date Signed:
		Telephone No: 216/433-4000 X357		
MAILING LABEL Use open window envelope or Clip out and paste		TO: NASA Scientific and Technical Information Facility Attn: Accessioning Department P.O. Box 8757 Balt/Wash International Airport Maryland 21240		

